LONG-TERM CONSEQUENCES OF SEPSIS AND SEVERE TRAUMA ON INNATE AND ADAPTIVE IMMUNITY

EDITED BY: Florian Uhle, Vladimir Badovinac and Thomas Griffith
PUBLISHED IN: Frontiers in Immunology

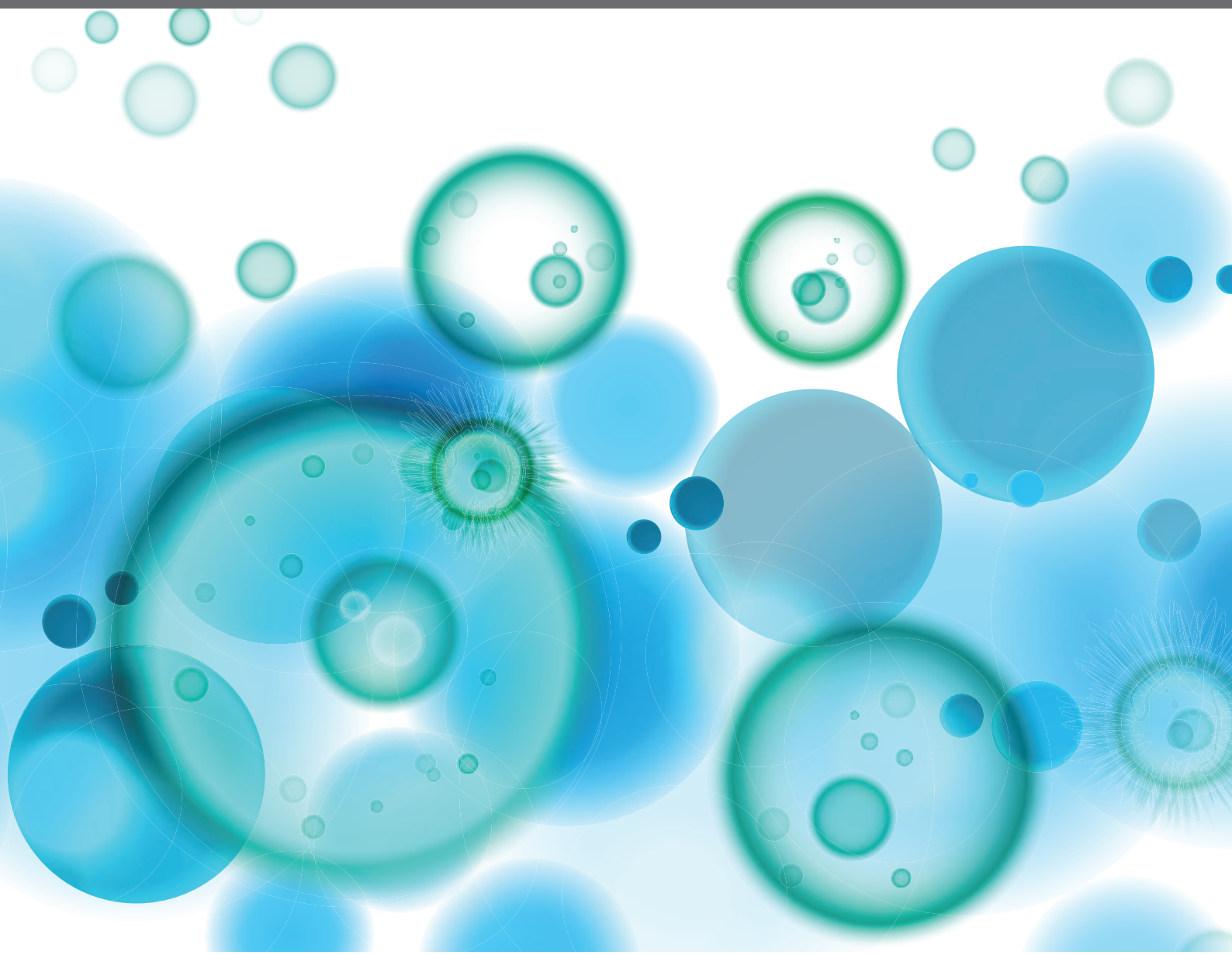

frontiers Research Topics

frontiers

ISSN 1664-8714
ISBN 978-2-88974-176-2
DOI 10.3389/978-2-88974-176-2

About Frontiers

Frontiers is more than just an open-access publisher of scholarly articles: it is a pioneering approach to the world of academia, radically improving the way scholarly research is managed. The grand vision of Frontiers is a world where all people have an equal opportunity to seek, share and generate knowledge. Frontiers provides immediate and permanent online open access to all its publications, but this alone is not enough to realize our grand goals.

Frontiers Journal Series

The Frontiers Journal Series is a multi-tier and interdisciplinary set of open-access, online journals, promising a paradigm shift from the current review, selection and dissemination processes in academic publishing. All Frontiers journals are driven by researchers for researchers; therefore, they constitute a service to the scholarly community. At the same time, the Frontiers Journal Series operates on a revolutionary invention, the tiered publishing system, initially addressing specific communities of scholars, and gradually climbing up to broader public understanding, thus serving the interests of the lay society, too.

Dedication to Quality

Each Frontiers article is a landmark of the highest quality, thanks to genuinely collaborative interactions between authors and review editors, who include some of the world's best academicians. Research must be certified by peers before entering a stream of knowledge that may eventually reach the public - and shape society; therefore, Frontiers only applies the most rigorous and unbiased reviews.
Frontiers revolutionizes research publishing by freely delivering the most outstanding research, evaluated with no bias from both the academic and social point of view. By applying the most advanced information technologies, Frontiers is catapulting scholarly publishing into a new generation.

What are Frontiers Research Topics?

Frontiers Research Topics are very popular trademarks of the Frontiers Journals Series: they are collections of at least ten articles, all centered on a particular subject. With their unique mix of varied contributions from Original Research to Review Articles, Frontiers Research Topics unify the most influential researchers, the latest key findings and historical advances in a hot research area! Find out more on how to host your own Frontiers Research Topic or contribute to one as an author by contacting the Frontiers Editorial Office: frontiersin.org/about/contact

LONG-TERM CONSEQUENCES OF SEPSIS AND SEVERE TRAUMA ON INNATE AND ADAPTIVE IMMUNITY

Topic Editors:
Florian Uhle, Heidelberg University Hospital, Germany
Vladimir Badovinac, The University of Iowa, United States
Thomas Griffith, University of Minnesota Twin Cities, United States

Citation: Uhle, F., Badovinac, V., Griffith, T., eds. (2022). Long-term Consequences of Sepsis and Severe Trauma on Innate and Adaptive Immunity. Lausanne: Frontiers Media SA. doi: 10.3389/978-2-88974-176-2

Table of Contents

05 ***Endothelial HSPA12B Exerts Protection Against Sepsis-Induced Severe Cardiomyopathy via Suppression of Adhesion Molecule Expression by miR-126***
Xia Zhang, Xiaohui Wang, Min Fan, Fei Tu, Kun Yang, Tuanzhu Ha, Li Liu, John Kalbfleisch, David Williams and Chuanfu Li

21 ***Antibody Production in Murine Polymicrobial Sepsis—Kinetics and Key Players***
Oliver Nicolai, Christian Pötschke, Katrin Schmoeckel, Murthy N. Darisipudi, Julia van der Linde, Dina Raafat and Barbara M. Bröker

32 ***Sepsis Triggers a Late Expansion of Functionally Impaired Tissue-Vascular Inflammatory Monocytes During Clinical Recovery***
Camille Baudesson de Chanville, Benjamin Glenn Chousterman, Pauline Hamon, Marie Laviron, Noelline Guillou, Pierre Louis Loyher, Aida Meghraoui-Kheddar, Sandrine Barthelemy, Philippe Deterre, Alexandre Boissonnas and Christophe Combadière

47 ***Increased Plasma Levels of Mitochondrial DNA and Normal Inflammasome Gene Expression in Monocytes Characterize Patients With Septic Shock Due to Multidrug Resistant Bacteria***
Stefano Busani, Sara De Biasi, Milena Nasi, Annamaria Paolini, Sophie Venturelli, Martina Tosi, Massimo Girardis and Andrea Cossarizza

54 ***Distinct Neutrophil Populations in the Spleen During PICS***
Satarupa Sengupta, Charles C. Caldwell and Vanessa Nomellini

64 ***The Metabolic Basis of Immune Dysfunction Following Sepsis and Trauma***
Margaret A. McBride, Allison M. Owen, Cody L. Stothers, Antonio Hernandez, Liming Luan, Katherine R. Burelbach, Tazeen K. Patil, Julia K. Bohannon, Edward R. Sherwood and Naeem K. Patil

85 ***Identification of Unique mRNA and miRNA Expression Patterns in Bone Marrow Hematopoietic Stem and Progenitor Cells After Trauma in Older Adults***
Dijoia B. Darden, Julie A. Stortz, McKenzie K. Hollen, Michael C. Cox, Camille G. Apple, Russell B. Hawkins, Jaimar C. Rincon, Maria-Cecilia Lopez, Zhongkai Wang, Eduardo Navarro, Jennifer E. Hagen, Hari K. Parvataneni, Maigan A. Brusko, Michael Kladde, Rhonda Bacher, Babette A. Brumback, Scott C. Brakenridge, Henry V. Baker, Christopher R. Cogle, Alicia M. Mohr and Philip A. Efron

98 ***An Inverse Relationship Between c-Kit/CD117 and mTOR Confers NK Cell Dysregulation Late After Severe Injury***
Björn Bösken, Monika Hepner-Schefczyk, Sonja Vonderhagen, Marcel Dudda and Stefanie B. Flohé

109 **Agaricus brasiliensis *Mushroom Protects Against Sepsis by Alleviating Oxidative and Inflammatory Response***
Kely Campos Navegantes-Lima, Valter Vinicius Silva Monteiro, Silvia Leticia de França Gaspar, Ana Ligia de Brito Oliveira, Juliana Pinheiro de Oliveira, Jordano Ferreira Reis, Rafaelli de Souza Gomes, Caroline Azulay Rodrigues, Herta Stutz, Vanessa Sovrani, Alessandra Peres, Pedro Roosevelt Torres Romão and Marta Chagas Monteiro

123 ***CD4 T Cell Responses and the Sepsis-Induced Immunoparalysis State***
Matthew D. Martin, Vladimir P. Badovinac and Thomas S. Griffith

134 ***Pediatric Burn Survivors Have Long-Term Immune Dysfunction With Diminished Vaccine Response***
Blair Z. Johnson, Sonia McAlister, Helen M. McGuire, Vetrichevvel Palanivelu, Andrew Stevenson, Peter Richmond, Debra J. Palmer, Jessica Metcalfe, Susan L. Prescott, Fiona M. Wood, Barbara Fazekas de St Groth, Matthew D. Linden, Mark W. Fear and Vanessa S. Fear

149 ***Corrigendum: Pediatric Burn Survivors Have Long-Term Immune Dysfunction With Diminished Vaccine Response***
Blair Z. Johnson, Sonia McAlister, Helen M. McGuire, Vetrichevvel Palanivelu, Andrew Stevenson, Peter Richmond, Debra J. Palmer, Jessica Metcalfe, Susan L. Prescott, Fiona M. Wood, Barbara Fazekas de St Groth, Matthew D. Linden, Mark W. Fear and Vanessa S. Fear

150 ***Oxidation-Specific Epitopes (OSEs) Dominate the B Cell Response in Murine Polymicrobial Sepsis***
Oliver Nicolai, Christian Pötschke, Dina Raafat, Julia van der Linde, Sandra Quosdorf, Anna Laqua, Claus-Dieter Heidecke, Claudia Berek, Murthy N. Darisipudi, Christoph J. Binder and Barbara M. Bröker

163 ***mTORC1 Is Not Principally Involved in the Induction of Human Endotoxin Tolerance***
Kristin Ludwig, Ralf A. Husain and Ignacio Rubio

175 ***CD4 T Follicular Helper Cells Prevent Depletion of Follicular B Cells in Response to Cecal Ligation and Puncture***
Matthew D. Taylor, Mariana R. Brewer, Ana Nedeljkovic-Kurepa, Yihe Yang, Kalpana S. Reddy, Mabel N. Abraham, Betsy J. Barnes and Clifford S. Deutschman

186 ***Polymicrobial Sepsis Impairs Antigen-Specific Memory CD4 T Cell-Mediated Immunity***
Frances V. Sjaastad, Tamara A. Kucaba, Thamotharampillai Dileepan, Whitney Swanson, Cody Dail, Javier Cabrera-Perez, Katherine A. Murphy, Vladimir P. Badovinac and Thomas S. Griffith

frontiers in Immunology

ORIGINAL RESEARCH
published: 29 April 2020
doi: 10.3389/fimmu.2020.00566

Endothelial HSPA12B Exerts Protection Against Sepsis-Induced Severe Cardiomyopathy via Suppression of Adhesion Molecule Expression by miR-126

*Xia Zhang[1], Xiaohui Wang[1], Min Fan[1,2], Fei Tu[1,2], Kun Yang[1,2], Tuanzhu Ha[1,2], Li Liu[3], John Kalbfleisch[2,4], David Williams[1,2] and Chuanfu Li[1,2]**

[1] Department of Surgery, James H. Quillen College of Medicine, East Tennessee State University, Johnson City, TN, United States, [2] The Center of Excellence in Inflammation, Infectious Disease and Immunity, James H. Quillen College of Medicine, East Tennessee State University, Johnson City, TN, United States, [3] Department of Geriatrics, The First Affiliated Hospital of Nanjing Medical University, Nanjing, China, [4] Biometry and Medical Computing, James H. Quillen College of Medicine, East Tennessee State University, Johnson City, TN, United States

Heat shock protein A12B (HSPA12B) is predominately expressed in endothelial cells (ECs) and has been reported to protect against cardiac dysfunction from endotoxemia or myocardial infarction. This study investigated the mechanisms by which endothelial HSPA12B protects polymicrobial sepsis–induced cardiomyopathy. Wild-type (WT) and endothelial HSPA12B knockout (HSPA12B$^{-/-}$) mice were subjected to polymicrobial sepsis induced by cecal ligation and puncture (CLP). Cecal ligation and puncture sepsis accelerated mortality and caused severe cardiac dysfunction in HSPA12B$^{-/-}$ mice compared with WT septic mice. The levels of adhesion molecules and the infiltrated immune cells in the myocardium of HSPA12B$^{-/-}$ septic mice were markedly greater than in WT septic mice. The levels of microRNA-126 (miR-126), which targets adhesion molecules, in serum exosomes from HSPA12B$^{-/-}$ septic mice were significantly lower than in WT septic mice. Transfection of ECs with adenovirus expressing HSPA12B significantly increased miR-126 levels. Increased miR-126 levels in ECs prevented LPS-stimulated expression of adhesion molecules. *In vivo* delivery of miR-126 carried by exosomes into the myocardium of HSPA12B$^{-/-}$ mice significantly attenuated CLP sepsis increased levels of adhesion molecules, and improved CLP sepsis–induced cardiac dysfunction. The data suggest that HSPA12B protects against sepsis-induced severe cardiomyopathy via regulating miR-126 expression which targets adhesion molecules, thus decreasing the accumulation of immune cells in the myocardium.

Keywords: endothelial HSPA12B, polymicrobial sepsis, cardiomyopathy, exosomes, microRNAs, endothelial adhesion molecules

OPEN ACCESS

Edited by:
Vladimir Badovinac, The University of Iowa, United States

Reviewed by:
Claudio Canetti, Federal University of Rio de Janeiro, Brazil
Hansjörg Hauser, Helmholtz Association of German Research Centers (HZ), Germany

***Correspondence:**
Chuanfu Li
Li@etsu.edu

Specialty section:
This article was submitted to Inflammation, a section of the journal Frontiers in Immunology

Received: *12 December 2019*
Accepted: *12 March 2020*
Published: *29 April 2020*

Citation:
Zhang X, Wang X, Fan M, Tu F, Yang K, Ha T, Liu L, Kalbfleisch J, Williams D and Li C (2020) Endothelial HSPA12B Exerts Protection Against Sepsis-Induced Severe Cardiomyopathy via Suppression of Adhesion Molecule Expression by miR-126. Front. Immunol. 11:566. doi: 10.3389/fimmu.2020.00566

INTRODUCTION

Sepsis is defined as a life-threatening organ dysfunction caused by a dysregulated host innate and inflammatory responses to the infection (1). In the United States, the mortality rates of sepsis is 28.3%, which is higher than other disease in intensive care units (2). Cardiovascular dysfunction is a major complication associated with sepsis-induced morbidity and mortality [7;9].

Cardiomyopathy is present in >40% of sepsis patients (3, 4) and is associated with mortality rates of up to 70% (3, 4). Despite the severity of this condition, the mechanisms that mediate septic cardiomyopathy remain unclear.

Endothelial cell (EC) dysfunction contributes to multiple organ damage and high morbidity and mortality in sepsis/septic shock (5). Increasing evidence shows that ECs actively participate in both innate and adaptive immune responses (6, 7) via pattern recognition receptors, including Toll-like receptors (8). Pathogen-associated molecular patterns, such as LPS or endogenous ligands, generated during sepsis/septic shock stimulate EC activation. Activated ECs have upregulated expression of chemokines and adhesion molecules, which attract and promote immune cell infiltration and inflammatory response, resulting in organ injury (9). Therefore, preservation of endothelial function is an important approach for attenuating sepsis-induced outcomes.

HSPA12B is the newest member of the HSP70 family of proteins (10). It is predominantly expressed in ECs (11, 12) and is essential for angiogenesis (12). Stegall et al. have demonstrated that endothelial HSPA12B is involved in angiogenesis through the turnover of a known angiogenesis regulator, a kinase anchoring protein 12 (AKAP12), resulting in upregulation of VEGF expression (12). Hu et al. (11) reported the endothelial HSPA12B is involved in regulating EC function. Knockdown of HSPA12B by small interfering RNAs in human umbilical vein ECs (HUVECs) interfered with wound healing, EC migration, and tube formation. In contrast, overexpression of HSPA12B enhanced migration of ECs and accelerated wound healing (11). We have reported that transgenic mice overexpressing HSPA12B (HSPA12B Tg) exhibit protection against myocardial ischemic injury and attenuate LPS-induced cardiac dysfunction (13). HSPA12B has been reported to preserve EC function (14, 15). However, the mechanisms by which HSPA12B preserves EC function during sepsis are still unknown.

MicroRNAs (miRs) have been identified as novel regulators of gene expression at the posttranscriptional level by binding to target messenger RNAs (16, 17). Recent evidence suggests that miRs play a critical role in sepsis/septic shock–induced innate immune and inflammatory responses (16, 17). MicroRNA-126 (miR-126) is predominantly expressed in ECs (18) and has been reported to regulate the progression of angiogenesis (19) and the expression of vascular cell adhesion molecule 1 (VCAM-1) (20). MicroRNA-126 is also involved in regulation of survival and function of plasmacytoid dendritic cells via the VEGFR2 pathway (21), indicating that miR-126 may regulate innate immune responses. However, the role of miR-126 in sepsis-induced cardiomyopathy has not been investigated.

The present study has shown that endothelial-specific HSPA12B exerts a protective effect on sepsis-induced cardiomyopathy. We demonstrated that EC HSPA12B could regulate miR-126 expression, which targets adhesion molecules, resulting in decreases in the accumulation of immune cells in the myocardium, thus attenuating sepsis-induced cardiac dysfunction.

MATERIALS AND METHODS

Animals

Male C57BL/6 mice were obtained from Jackson Laboratory. Endothelial cell–specific HSPA12B knockout ($HSPA12B^{-/-}$) mice were generated as described below. Wild-type (WT) and $HSPA12B^{-/-}$ mice were maintained in the Division of Laboratory Animal Resources, East Tennessee State University (ETSU). The experiments outlined in this article conform to the Guide for the Care and Use of Laboratory Animals published by the National Institutes of Health (NIH Publication, eighth edition, 2011). The animal care and experimental protocols were approved by the ETSU Committee on Animal Care.

Generation of EC-Specific HSPA12B Knockout Mice

The knockout targeting strategy is outlined in **Supplementary Figure S1**. LoxP sites flanking exon 2 were introduced using a recombineering-based approach for making linearized targeting construct. The targeting construct contained PGK-driven Neo cassette and MC1 promoter–driven HSV-TK cassette, allowing for positive and negative selection. The right and the left arm loxP knockin were confirmed by genomic Southern blot with (*Eco*RI and probe A) and *Sal*I digestion of polymerase chain reaction (PCR) product by external and internal primer (5′-TCTGTGTCTGCCTGTGTTCTGT and 5′-TAGTCTGCATTCGGAGGCAAGT). The successful homologous recombination clones were subsequently transfected with pCre-Pac for excision by Cre to generate targeted alleles.

Endothelial-specific HSPA12B knockout mice were generated by cross-breeding the conditionally targeted HSPA12B mice with C57BL/6.Cg-Tg (Tek-cre) strain, which carries Cre recombinase under the control of the Tek promoter. Genotypes for the specific deletions were confirmed by PCR analysis of floxed allele (HspA12B-cko-1: gaagcaagcatattcatctcattactattc; HspA12B-cko-2: gcttgctcaaaagtgatggttgctc. 151 bp for knockout and 191 bp for WT mice), HSPA12B deletion (HspA12B-cko-1: gaagcaagcatattcatctcattactattc; HspA12B-cko-4: taaagcctacactcagatgagagcag, 240-bp product for deletion and > 2 kB or no product for WT control), and for Cre gene expression. Western blot and immunohistochemistry were also performed to identify endothelial-specific deficiency of HSPA12B.

Immunofluorescence Staining

Immunohistochemistry was performed as described previously (22, 23). Briefly, the heart sections were stained with primary antibodies that are specific rabbit anti-HSPA12B and rat anti-CD31 (PECAM-1) (1:100) overnight at 4°C. The tissue sections were then incubated with secondary antibody Alexa Fluor-488 goat anti-rabbit immunoglobulin G (IgG) (H + L) (green; Thermo Fisher Scientific, Waltham, MA, United States) and Alexa Fluor-555 goat anti-rat IgG (H + L) (red) (Thermo Fisher Scientific) for 1 h at room temperature. The slides were examined with a fluorescent microscope at a magnification of 40×.

Cecal Ligation and Puncture Polymicrobial Sepsis Model

Cecal ligation and puncture (CLP) was performed to induce polymicrobial sepsis in mice as previously described (22, 23). Briefly, the mice were anesthetized by isoflurane (induced by 5.0% and maintained by 1.5%). A midline incision was made on the anterior abdomen, and the cecum was exposed and ligated with a 4-0 suture. Two punctures were made through the cecum with an 18-gauge needle, and feces were extruded from the holes. The abdomen was then closed in two layers. Sham surgically operated mice served as the surgery control group. Immediately following surgery, a single dose of resuscitative fluid (lactated Ringer's solution, 50 mL/kg body weight) was administered by subcutaneous injection (22, 23).

Echocardiography

Transthoracic two-dimensional M-mode echocardiogram was obtained using a Toshiba Aplio 80 Imaging System (Toshiba Medical Systems, Tochigi, Japan) equipped with a 12-MHz linear transducer as described previously (22). M-mode tracings were used to measure LV end-systolic diameter and LV end-diastolic diameter. Percent fractional shortening (% FS) and ejection fraction (EF %) were calculated as described previously (22, 24).

Accumulation of Neutrophils and Macrophages in the Myocardium

Accumulation of immune cells in heart tissues was examined with antineutrophil elastase antibody (Abcam, Cambridge, United Kingdom) and antimacrophage antibody F4/80 (1:50 dilution; Santa Cruz Biotechnology, Santa Cruz, CA, United States), separately (22, 23). Three samples from each group were evaluated, counterstained with hematoxylin, and examined with bright-field microscopy. Four different areas of each section were evaluated. The results are expressed as the numbers of neutrophils or macrophages per field examined with bright field microscope (40×).

Myeloperoxidase Activity Assay

Myeloperoxidase (MPO) activity was measured using an MPO fluorometric Detection kit (Assay Designs Inc., Ann Arbor, MI, United States) according to the manufacturers' instructions.

Immunohistochemistry Staining

Immunohistochemistry was performed as described previously (22, 23). Briefly, heart tissues were immersion-fixed in 4% buffered paraformaldehyde, embedded in paraffin, and cut at 5-μm sections. The sections were stained with specific goat anti-intercellular adhesion molecule 1 (ICAM-1, 1:50 dilution; Santa Cruz Biotechnology) and rabbit anti-VCAM-1 (1:50 dilution, Santa Cruz Biotechnology), respectively, and treated with the ABC staining system (Santa Cruz Biotechnology) according to the instructions of the manufacturer. Three slides from each block were evaluated, counterstained with hematoxylin, and examined with bright field microscope (40×). Four different areas of each section were evaluated.

Electrophoretic Mobility Shift Assay

Nuclear proteins were isolated from heart samples as previously described (22, 23). Nuclear factor κB (NF-κB) binding activity was performed using a LightShift Chemiluminescent EMSA (electrophoretic mobility shift assay) kit (Thermo Fisher Scientific) as described previously (22, 25) in a 20-μL binding reaction mixture containing 1× binding buffer, 50 ng poly dI:dC, 20 fmol of double-stranded NF-κB consensus oligonucleotide that was end-labeled with biotin, 15 μg nuclear proteins. The binding reaction mixture was incubated at room temperature for 20 min and analyzed by electrophoresis and then transferred to a nylon membrane. The biotin end-labeled DNA was detected using the streptavidin–horseradish peroxidase conjugate and the chemiluminescent substrate (22, 25).

Enzyme-Linked Immunosorbent Assay for Cytokine Assay

The levels of cytokines [tumor necrosis factor α (TNFα), interleukin 6 (IL-6)] in cell-free supernatants were measured by enzyme-linked immunosorbent assay development kits (Peprotech, Rocky Hill, NJ, United States) according to manufacturers' instructions as described previously (22, 23).

Western Blot

Western blot was performed as described previously (22, 23). Briefly, the cellular proteins were separated by sodium dodecyl sulfate–polyacrylamide gel electrophoresis and transferred onto Hybond ECL membranes (Amersham Pharmacia, Piscataway, NJ, United States). The ECL membranes were incubated with the appropriate primary antibodies (anti–VCAM-1 and anti–ICAM1 from Santa Cruz Biotechnology; anti-CD63, anti-CD81, from System Biosciences, Palo Alto, CA, United States; anti-GAPDH from Meridian Life Science, Inc., Memphis, TN, United States, respectively. Anti-HspA12B is a kind gift from Dr. Han Zhihua) followed by incubation with peroxidase-conjugated secondary antibodies (Cell Signaling Technology, Inc., Danvers, MA, United States) and analysis by the ECL system (Amersham Pharmacia). The signals were quantified using the G: Box gel imaging system by Syngene (Syngene, USA, Fredrick, MD, United States).

Isolation of Exosomes

Ten hours after CLP, the blood was collected from the experimental mice followed by centrifugation at 5,400 revolutions/min (rpm) for 15 min at 18°C. The supernatant was collected and added with ExoQuick exosome precipitation solution (63 μL/250 μL plasma, ExoQ5A-1; SBI, Palo Alto, CA, United states) according to manufacturer's instruction.

Isolation of RNA From Exosomes

Total RNA was extracted from the exosomes using Trizol (RN190; Molecular Research Center, Cincinnati, OH, United States) according to manufacturer's instructions. Approximately 10 ng of total RNA was applied to examination of miRNA levels as described previously (26).

Quantitative PCR Assay of MiRNAs

MicroRNAs were isolated from heart tissues or exosomes using the mirVana miR isolation kit (Ambion, Austin, TX, United States) as described previously (27). MicroRNA levels were quantified by quantitative PCR (qPCR) using specific Taqman assays (Applied Biosystems, Foster City, CA, United States) and specific primers (Applied Biosystems, primer identification numbers: 002228 for hsa–miR-126-3p and 001973 for snRU6). The levels of miRs were quantified with the $2(^{-}\Delta\Delta ct)$ relative quantification method that was normalized to the U6 small nucleolar RNA (snRU6).

Treatment of ECs With Exosomes

Exosomes were isolated from sham and septic mice using ExoQuickTC exosome precipitation solution (ExoQ5A-1; SBI). Human umbilical vein ECs were treated with exosomes (5 μg/mL) diluted in conditional medium, which was exosome-free medium prepared by centrifugation at 120,000 rpm for 18 h at 4°C. After treatment, HUVECs were collected for analysis of adhesion molecules ICAM-1 and VCAM-1 by Western blot (22, 23).

Transfection of MiRNA Mimics Into ECs

Human umbilical vein ECs (1×10^6) in six-well plates were transfected with 40 nmol of miR-126 mimics (Ambion), anti–miR-126 mimics (Exiqon) and miR-scrambled control (Exiqon), respectively by Lipofectamine 2000 (Thermo Fisher Scientific). Twenty-four hours after transfection, the cells were treated with LPS (1 μg/mL) for 24 h. The cells were harvested for analysis of adhesion molecules (VCAM-1 and ICAM-1) by Western blot.

Preparation of Exosomal miR-126

Bone marrow stromal cells (BMSCs) were isolated from HSPA12B$^{-/-}$ and WT mice as described previously (28). Briefly, mice were euthanized, and bone marrow was isolated by flushing the femur and tibia with Dulbecco modified Eagle medium (DMEM) using a 25-gauge 0.5-inch needle (BD, San Jose, CA, United States). The bone marrow was dissociated by syringe. Cell mixture was cultured in DMEM supplemented with 10% fetal bovine serum (FBS) (HyClone; Thermo Fisher Scientific), glutamine (2 mM), and penicillin/streptomycin (50 U/mL and 50 mg/mL; Sigma-Aldrich, St. Louis, MO, United States). After incubation at 37°C with 5% CO_2, non-adherent cells were removed carefully by two washes with phosphate-buffered saline (PBS), and fresh medium was replaced. The medium was changed every other day. Cells at the fourth to seventh generation were transfected with 40 nmol/L hsa–miR-126 mimics (MC12841; Ambion), hsa–miR-126 inhibitor (MH12841; Ambion), or Cy3 dye–labeled miR-scrambled control (AM17010; Ambion), using Lipofectamine 2000 transfection reagent (Thermo Fisher Scientific) according to the manufacturer's protocol. Twenty-four hours after transfection, supernatants were harvested for exosome isolation using Exoquick-TC Exosome Precipitation Solution (SBI) according to the manufacturer's protocol.

In vivo Delivery of Exosomal miR-126 Into Mouse Hearts

Mice were transfected with exosomes loaded with miR-126 or exosomes loaded with miR-control through the right carotid artery as described previously (27, 29). Briefly, mice were intubated and mechanically ventilated. The anesthesia was induced by 5% isoflurane and maintained by 1.5% isoflurane driven by 100% oxygen. Body temperature was maintained at 37°C by surface water heating. An incision was made in the middle of the neck, and the right common carotid artery was carefully exposed. A microcatheter was introduced into the isolated common carotid artery and positioned into the aortic root. Exosomes (10 μg diluted in 100 μL PBS) loaded with miR-126 or loaded with miR-Con were injected through the microcatheter immediately after the induction of polymicrobial sepsis. The microcatheter was gently removed, and the common carotid artery was tightened before the skin was closed (22, 23).

Statistical Analysis

The data are expressed as mean ± SE. Comparisons of data between groups were made using one-way analysis of variance, and Tukey procedure for multiple-range tests was performed. The log-rank test was used to compare group survival trends. Probability levels of 0.05 or smaller were used to indicate statistical significance.

RESULTS

EC-Specific Deficiency of HSPA12B (HSPA12B$^{-/-}$) Results in Increased Mortality in Polymicrobial Sepsis

We first examined the expression of HSPA12B in the myocardium. As shown in **Figure 1A**, HSPA12B is specifically expressed on cardiac ECs as evidenced by positive immunofluorescent staining of HSPA12B on ECs in the myocardium from WT mice but not from HSPA12B$^{-/-}$ mice. Western blot analysis shows the high levels of myocardial HSPA12B in WT mice but not in HSPA12B$^{-/-}$ mice (**Figure 1B**). **Figure 1C** shows that EC HSPA12B deficiency accelerates mortality of CLP septic mice. The time to 50% mortality in WT septic mice was 56 h, and 100% occurred at 100 h after induction of CLP-sepsis. In HSPA12B$^{-/-}$ septic mice, however, the time to 50% mortality was 40 h. The mortality reached to 100% was 60 h after induction of CLP sepsis ($P < 0.01$). These data indicate that EC HSPA12B plays a role in reducing the mortality associated with polymicrobial sepsis.

Endothelial HSPA12B Deficiency Results in Worsened Cardiac Dysfunction in Polymicrobial Sepsis

Cardiomyopathy is a major consequence of sepsis and contributes to mobility and mortality (30). **Figures 1D,E** show that CLP sepsis markedly decreased the values of EF% (34.3%) and % FS (42.8%) in WT septic mice and 48.2

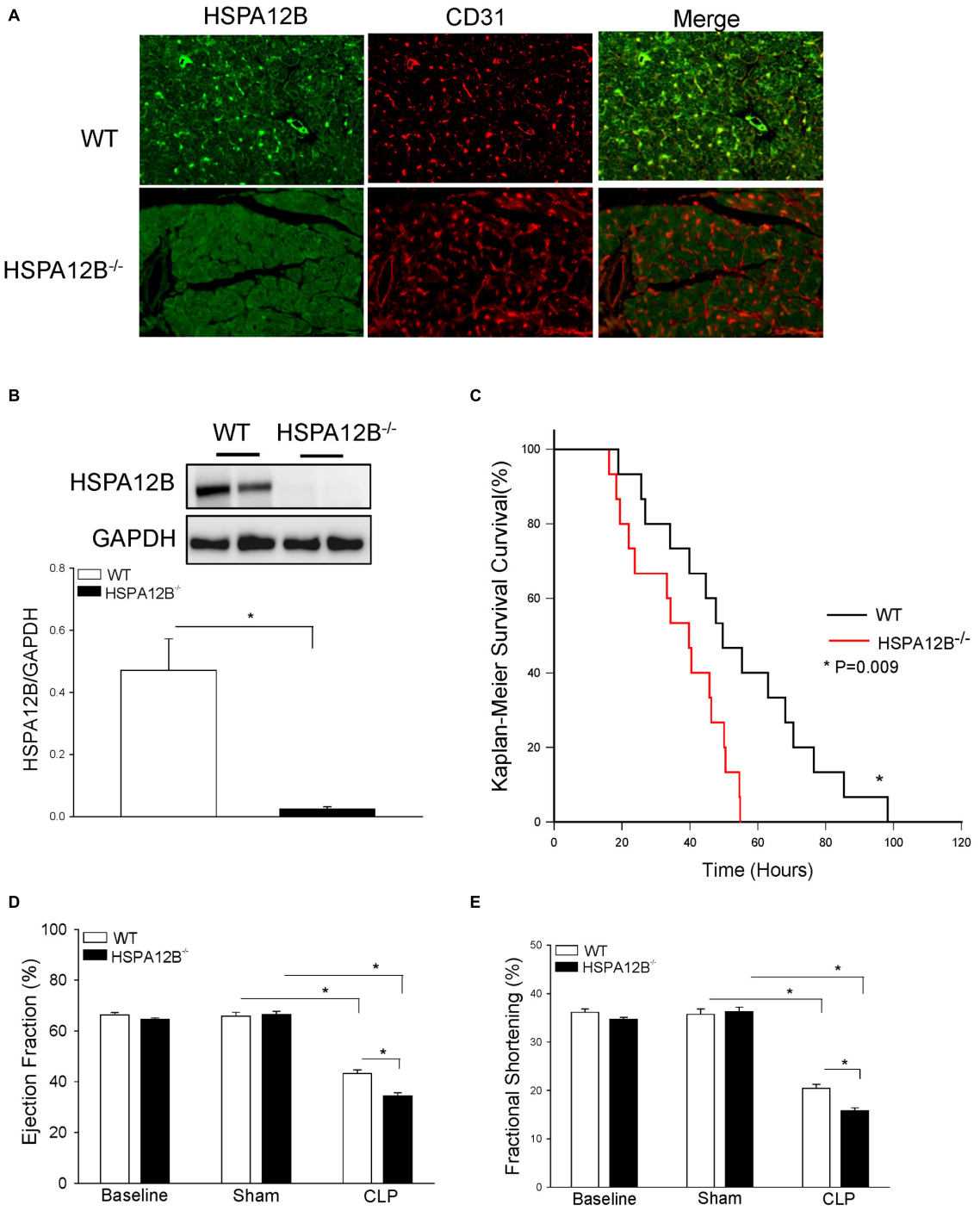

FIGURE 1 | Endothelial-specific deficiency of HSPA12B results in increased mortality and worsened cardiac dysfunction in polymicrobial sepsis. **(A,B)** HSPA12B is expressed in the ECs of WT myocardium but not in HSPA12B$^{-/-}$ mice. **(A)** Heart tissues from WT and HSPA12B$^{-/-}$ mice were sectioned and subjected to immunostaining with anti-CD31 (EC marker) and anti-HSPA12B. There is a negative staining of HSPA12B in the myocardium of HSPA12B$^{-/-}$ mice. The immunofluorescent staining was examined with fluorescent microscope (40×). **(B)** Western blot analysis of HSPA12B expression in the myocardium of WT and HSPA12B$^{-/-}$ mice. **(C)** Sepsis increases the mortality of HSPA12B$^{-/-}$ mice. Wild-type and HSPA12B$^{-/-}$ mice were subjected to CLP sepsis. Sham surgical operation served as sham control. The survival rate was closely monitored up to 5 days (n = 15–16/group). **(D,E)** Cardiac function was examined by echocardiography before and 6 h after CLP (n = 6–13/group). Cecal ligation and puncture sepsis markedly decreases ejection fraction (EF %) and fractional shortening (FS %) in WT mice. However, the values of EF % and FS % in HSPA12B$^{-/-}$ septic mice were further decreased compared with WT septic mice. **(D)** (EF %) and **(E)** (FS %). *P < 0.05 compared with indicated group.

and 56.5% in HSPA12B$^{-/-}$ septic mice, when compared with the respective sham controls. HSPA12B$^{-/-}$ septic mice exhibited a lower EF% (20.5%) and FS% (22.8%) than in WT septic mice. There was no significant difference in the baseline values of EF% and %FS between WT and HSPA12B$^{-/-}$ mice. These data indicate that EC HSPA12B plays an important role in the regulation of cardiac function during polymicrobial sepsis.

Inflammatory Cells Are Increased in the Myocardium of HSPA12B$^{-/-}$ Septic Mice

Increased accumulation of inflammatory cells, including neutrophils and macrophages, in the myocardium contributes to septic cardiomyopathy (22). **Figure 2A** shows that CLP sepsis markedly increased the numbers of neutrophils (9.3 ± 0.66 vs. 1.8 ± 0.22) and MPO activity (89.9%) in the myocardium of WT mice, when compared with WT sham controls. In contrast, neutrophil accumulation in the myocardium and myocardial MPO activity in HSPA12B$^{-/-}$ septic mice was significantly 72 and 88% greater than in WT septic mice. Cecal ligation and puncture sepsis also significantly increased the numbers of macrophages (15.6 ± 1.01 vs. 2.6 ± 0.0.36) in the myocardium of WT mice compared with sham control (**Figure 2B**). In HSPA12B$^{-/-}$ septic mice, macrophage accumulation in the myocardium was markedly 57.9% higher than in WT septic mice. The data indicate that EC HSPA12B could attenuate infiltration of immune cells into the myocardium during polymicrobial sepsis.

Increased Myocardial NF-κB Activation and Serum Inflammatory Cytokine Levels in HSPA12B$^{-/-}$ Septic Mice

Nuclear factor κB is an important transcription factor that regulates inflammatory cytokine production (31). Proinflammatory cytokines have been demonstrated to play a role in cardiovascular dysfunction during sepsis/septic shock (32). **Figure 2C** shows that myocardial NF-κB binding activity was markedly increased 36.8% in WT septic mice and 82.3% in HSPA12B$^{-/-}$ septic mice, when compared with the respective sham controls. Cecal ligation and puncture sepsis also significantly increased the serum levels of TNFα (**Figure 2D**) and IL-6 (**Figure 2E**) in WT septic mice. However, the levels of serum TNFα and IL-6 in HSPA12B$^{-/-}$ septic mice were markedly 243 and 223% greater than in WT septic mice (**Figures 2D,E**). The data indicate that EC HSPA12B plays a role in the regulation of NF-κB activation and proinflammatory cytokine production during polymicrobial sepsis.

HSPA12B$^{-/-}$ Results in Increased Expression of Adhesion Molecules Following Polymicrobial Sepsis

Increased expression of adhesion molecules on ECs promotes the infiltration of inflammatory cells into the myocardium (33). **Figures 2F,G** show that CLP sepsis increased the immunostaining of VCAM-1 (F) and ICAM-1 (G) in the myocardium of WT mice. However, there is more positive immunostaining for VCAM-1 and ICAM-1 in the myocardium from HSPA12B$^{-/-}$ septic mice than in WT septic mice. Western blot analysis shows that CLP sepsis markedly increased the levels of myocardial VCAM-1 (**Figure 2H**) and ICAM-1 (**Figure 2I**) in WT mice. The levels of myocardial VCAM-1 and ICAM-1 in HSPA12B$^{-/-}$ septic mice were further increased 173 and 191%, respectively, when compared with WT septic mice. The data suggest that HSPA12B is involved in the regulation of adhesion molecule expression on ECs, which ultimately facilitate the infiltration of inflammatory cells into the myocardium following polymicrobial sepsis.

Increased HSPA12B Levels Suppress LPS-Induced VCAM-1 and ICAM-1 Expression in ECs

To further investigate the role HSPA12B in the regulation of adhesion molecule expression during polymicrobial sepsis, we performed *in vitro* experiments. Endothelial cells (HUVECs) were transfected with adenovirus expressing HSPA12B (Ad-HSPA12B) or Ad-GFP (**Figure 3A**). Twenty-four hours after transfection, the cells were stimulated with LPS (1 μg/mL) for 24 h. Confocal microscope examination shows that LPS stimulation increased ICAM-1 expression as evidenced by showing more immunofluorescent staining of ICAM-1 in LPS-stimulated ECs (**Figure 3B**). Western blot analysis also shows that LPS stimulation markedly increased the expression of VCAM-1 (**Figure 3C**) and ICAM-1 (**Figure 3D**), when compared with untreated control. However, both immunostaining and Western blot analysis show that increased HSPA12B expression by Ad-HSPA12B transfection markedly suppressed LPS-stimulated expression of VCAM-1 and ICAM-1. The data suggest that HSPA12B may prevent upregulation of adhesion molecule expression in ECs during sepsis.

HSPA12B Upregulates MiRNA-126 Expression in ECs

MicroRNA-126 is predominantly expressed in ECs and suppresses adhesion molecule expression (18, 20). We examined whether HSPA12B suppressed LPS-induced adhesion molecule expression is mediated via upregulation of miR-126 expression in ECs. We transfected HUVECs with Ad-HSPA12B or Ad-GFP, which served as vector control. Twenty-four hours after transfection, the cells were stimulated with LPS. The levels of miR-126 were measured by qPCR. As shown in **Figure 4**, LPS stimulation increased the levels of miR-126 (A) and HSPA12B (B) in ECs. Interestingly, LPS stimulation further increased expression of miR-126 and HSPA12B after the cells were transfected by Ad-HSPA12B. The data indicate that HSPA12B is involved in the regulation of miR-126 expression in ECs following LPS challenge.

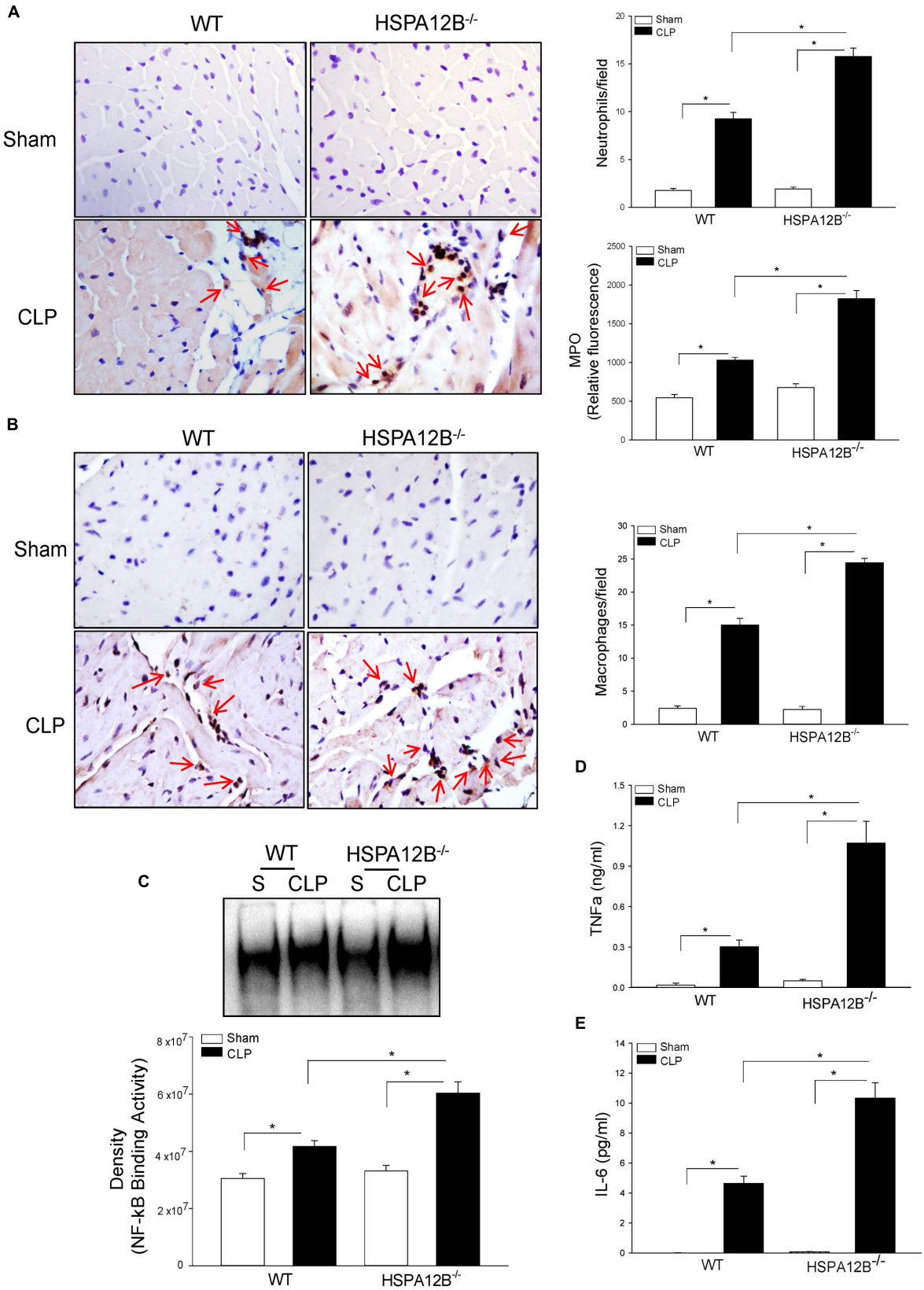

FIGURE 2 | Continued

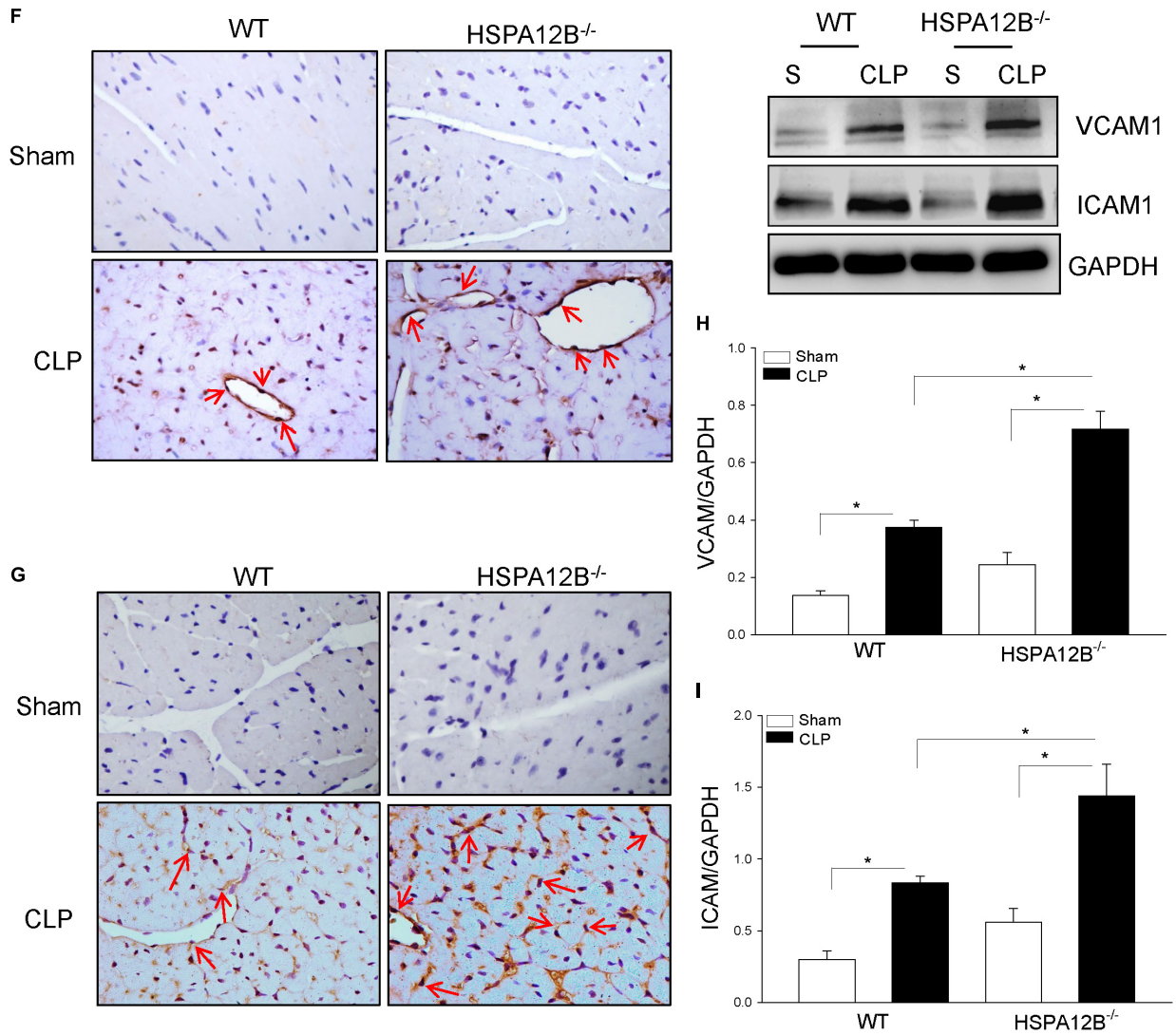

FIGURE 2 | Increased accumulation of immune cells and NF-κB binding activity in the myocardium of HSPA12B$^{-/-}$ septic mice. Wild-type and HSPA12B$^{-/-}$ mice were subjected to CLP sepsis or sham surgical operation. Heart tissues were harvested 6 h after CLP. **(A)** The accumulation of neutrophils in heart tissues was examined by immunohistochemistry with antineutrophil antibody and MPO activity (n = 6–8/group). **(B)** Macrophages in the heart tissues were examined by antimacrophage antibody F4/80. The positive staining of neutrophils and macrophages are dark brown color marked with red arrows. **(C)** Myocardial NF-κB binding activity in WT and HSPA12B$^{-/-}$ septic mice was performed with EMSA (n = 6–8/group). **(D,E)** Serum cytokine TNFα **(D)** and IL-6 **(E)** levels were measured by EMSA kits (n = 4–8/group). **(F–I)** Increased expression of adhesion molecules in the myocardium of WT and HSPA12B$^{-/-}$ septic mice. Heart tissues were harvested 6 h after CLP, sectioned, and subjected to immunohistochemistry staining with anti–VCAM-1 **(F)** and anti–ICAM-1 **(G)** antibodies. **(H,I)** Western blot analysis of VCAM-1 **(H)** and ICAM1 **(I)** levels in the heart tissues. n = 4–8/group. *P < 0.05 compared with indicated groups. The immunohistochemistry staining was examined with bright field microscope (40×).

MiR-126 Suppresses LPS-Increased Adhesion Molecule Expression in ECs

We then examined whether increased miR-126 levels will suppress LPS-stimulated adhesion molecule expression in ECs. We transfected ECs with miR-126 mimics or miR-control mimics 24 h before the cells were stimulated with LPS. **Figure 4C** shows a high efficiency of the miRNA transfection into ECs. Transfection of ECs with miR-126 mimics prevented LPS-stimulated the expression of VCAM-1 (**Figure 4D**) and ICAM-1 (**Figure 4E**). Antagomir-126 or miR-control mimics transfection did not alter LPS-stimulated increases in the expression of adhesion molecules. The data suggest that miR-126 targets adhesion molecule expression in ECs.

Decreased Levels of miR-126 Levels in Serum Exosomes From HSPA12B$^{-/-}$ Septic Mice

To investigate whether increased adhesion molecule expression in the myocardium from HSPA12B$^{-/-}$ septic mice will be associated with miR-126 levels, we collected serum from WT

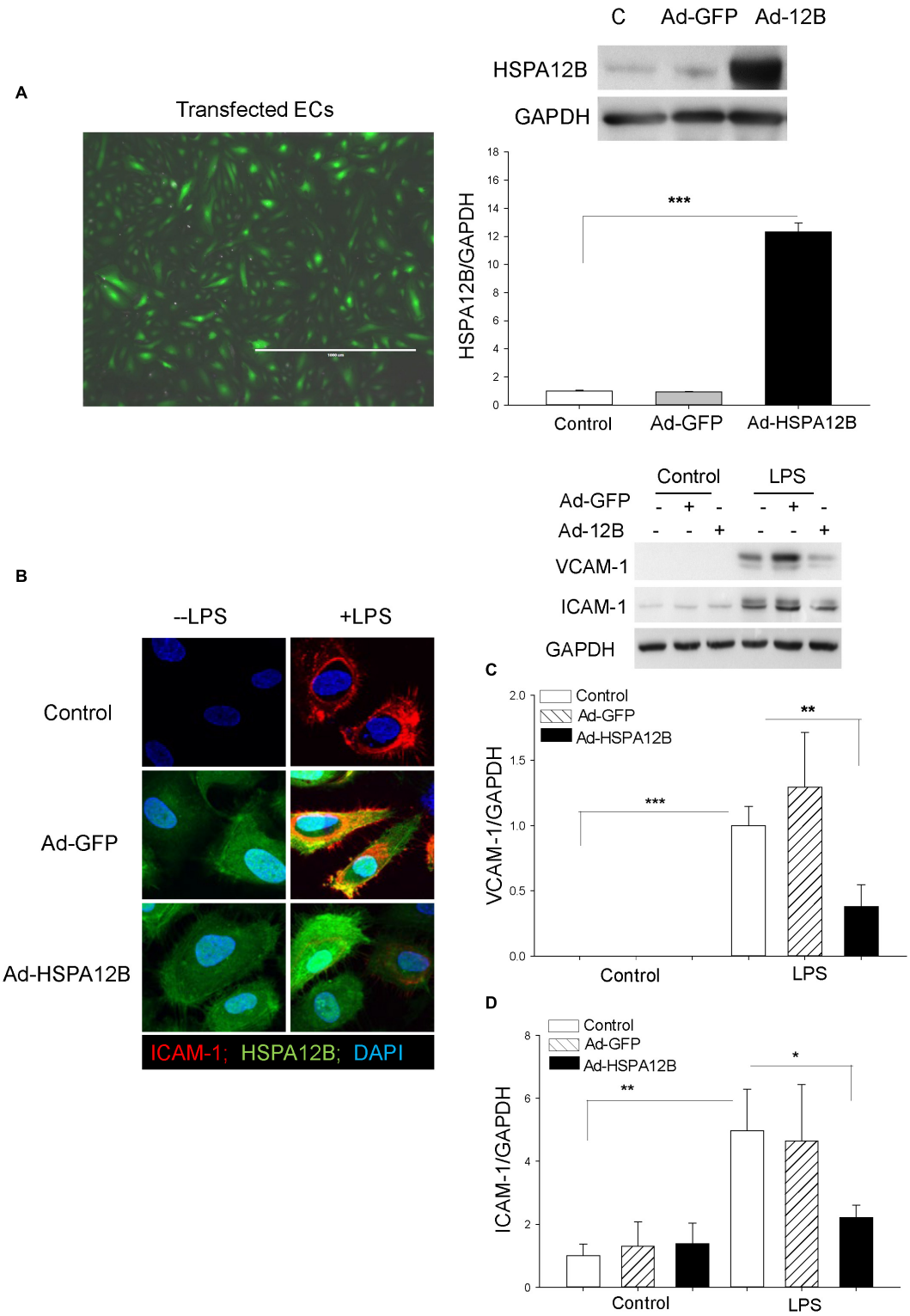

FIGURE 3 | HSPA12B attenuates LPS-induced expression of adhesion molecules in ECs. Endothelial cells (HUVECs) were transfected with adenovirus-expressing HSPA12B (Ad-HSPA12B) or Ad-GFP 24 h before the cells were stimulated with LPS. **(A)** Green color indicates Ad-HSPA12B transfected into the HUVECs. Western blot shows that transfection of HUVECs with Ad-HSPA12B increased the levels of HSPA12B. **(B)** Confocal microscopy examination (66×) shows that Ad-HSPA12B transfection attenuates LPS-induced ICAM-1 (red color) expression in HUVECs. Green color indicates HSPA12B; blue color indicates nucleus stained with DAPI. **(C,D)** Western blot shows that Ad-HSPA12B transfection significantly suppressed LPS-induced VCAM-1 **(C)** and ICAM-1 **(D)** expression in HUVECs. n = 3/groups. $^{*}P < 0.05$; $^{**}P < 0.01$; $^{***}P < 0.001$ compared with indicated groups.

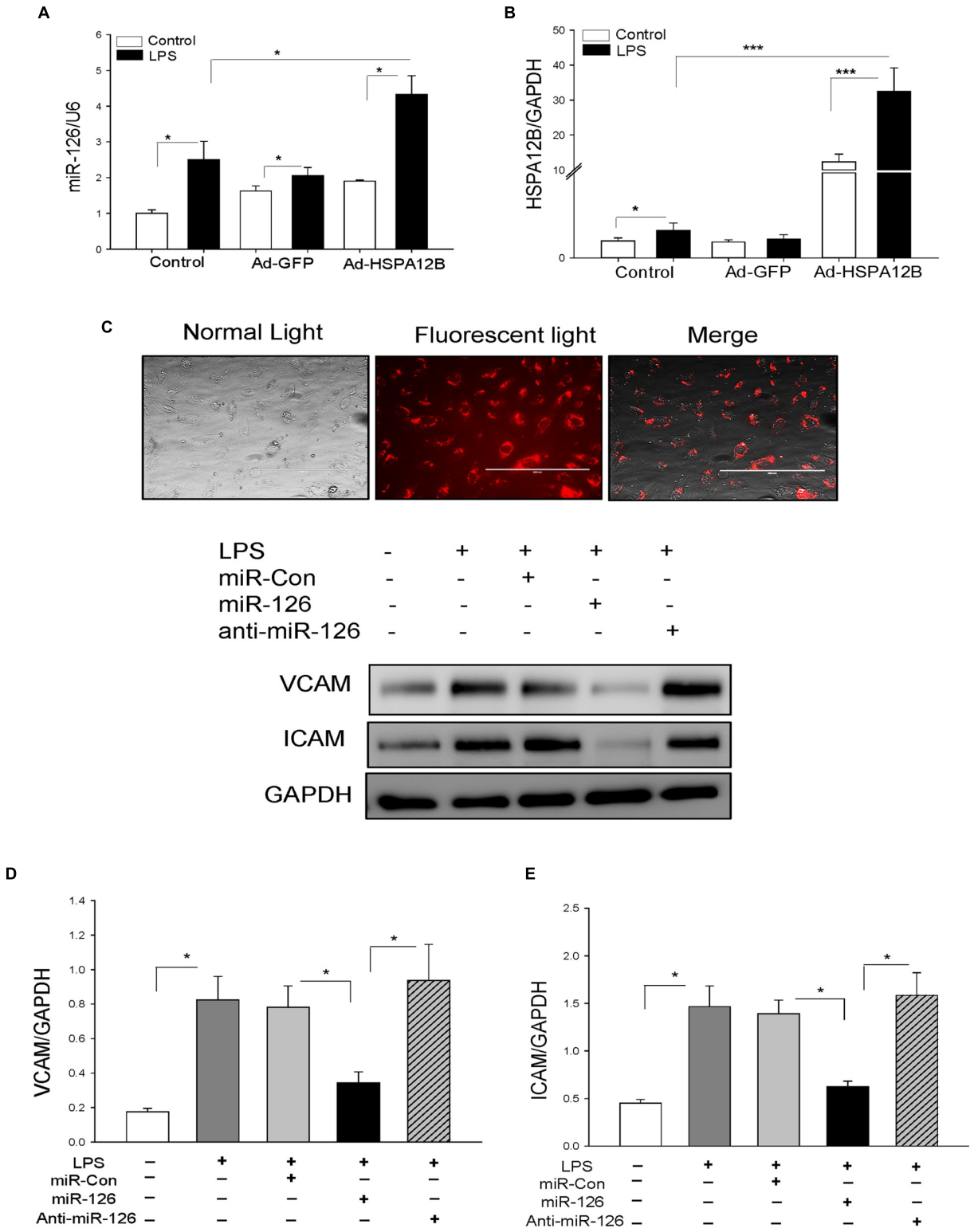

FIGURE 4 | Transfection of endothelial cells with miR-126 mimics prevented LPS-induced expression of adhesion molecule expression. Endothelial cells (HUVECs) were transfected with 40 nmol of microRNAs (scrambled miR-control, miR-126 mimics, or anti–miR-126) by Lipofectamine 2000. Twenty-four hours after transfection, the cells were treated with LPS (1 μg/mL) for 6 h. **(A)** miR-126 levels and **(B)** HSPA12B expression. **(C)** Transfection of miR-126 mimics (red color) into endothelial cells. Transfection of miR-126 mimics suppresses LPS-induced expression of VCAM-1 **(D)** and ICAM1 **(E)** in endothelial cells. $n = 3$–4/group. $^*P < 0.05$ compared with indicated groups.

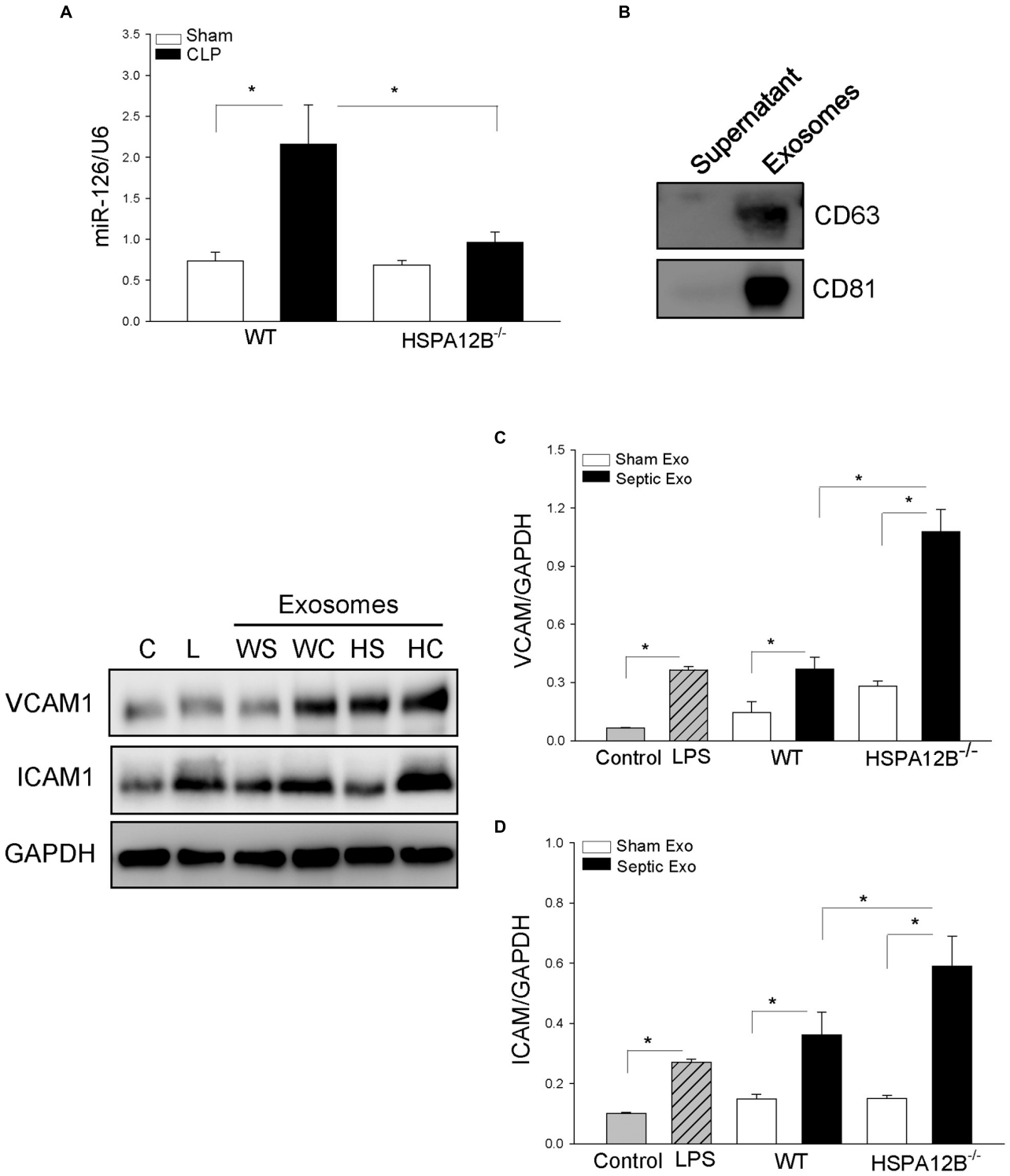

FIGURE 5 | Serum exosomes from HSPA12B$^{-/-}$ septic mice increased expression of adhesion molecules in endothelial cells. Wild-type and HSPA12B$^{-/-}$ mice were subjected to CLP sepsis or sham surgical operation. Ten hours after CLP, blood was collected for the isolation of serum exosomes with ExoQuick exosome isolation kit. **(A)** miR-126 levels in the isolated serum exosomes were examined by qPCR. **(B)** Exosome markers (CD63 and CD81). **(C)** Endothelial cells (HUVEC) were treated with isolated exosomes for 12 h. The cells were harvested for analysis of VCAM-1 **(C)** and ICAM1 **(D)** by Western blot (n = 4–6/group). C, control; L, LPS; WS, WT sham; WC, WT CLP; HS, HSPA12B$^{-/-}$ sham; HC, HSPA12B$^{-/-}$ CLP; Exo, exosomes. *$P < 0.05$ compared with indicated groups.

and HSPA12B$^{-/-}$ sham and septic mice, isolated exosomes, and examined miR-126 levels with qPCR. As shown in **Figure 5A**, CLP sepsis markedly increased the levels of miR-126 in exosomes from WT mice but not from HSPA12B$^{-/-}$ mice. The levels of miR-126 in HSPA12B$^{-/-}$ septic exosomes were significantly lower than in WT septic exosomes. The data indicate that lower levels of miR-126 in HSPA12B$^{-/-}$ septic exosomes may be responsible for increased expression of adhesion molecules and accumulation of immune cells in the myocardium of HSPA12B$^{-/-}$ septic mice.

HSPA12B$^{-/-}$ Septic Exosomes Enhance the Expression of Adhesion Molecules on *ECs*

To investigate the role of HSPA12B$^{-/-}$ septic exosomes in adhesion molecule expression on ECs, we collected blood and isolated serum exosomes from WT and HSPA12B$^{-/-}$ mice. We then treated ECs with the isolated exosomes and examined the levels of adhesion molecules. **Figure 5B** shows exosome markers (CD63 and CD81) in the isolated exosomes. **Figures 5C,D** shows that treatment of ECs with WT septic exosomes markedly increased 87.2% VCAM-1C and 157.3% ICAM-1D levels, when compared with the WT sham exosome-treated group. However, treatment of ECs with HSPA12B$^{-/-}$ septic exosomes resulted in greater levels of VCAM-1 and ICAM-1, when compared with WT septic exosome treatment. The levels of VCAM-1 and ICAM-1 in the HSPA12B$^{-/-}$ septic exosomes group were 75.1 and 78.9% greater than in WT septic exosome-treated cells. The data suggest that lower levels of miR-126 in the exosomes from HSPA12B$^{-/-}$ septic mice may be responsible for increased adhesion molecule expression in the myocardium during polymicrobial sepsis.

Delivery of miR-126 Carried by Exosomes Suppressed Adhesion Molecule Expression in the Myocardium From HSPA12B$^{-/-}$ Septic Mice

To further investigate the role of exosomal miR-126 in the regulation of adhesion molecule expression, we isolated BMSCs from HSPA12B$^{-/-}$ mice, transfected BMSCs with miR-126 mimics or miR-control mimics, and isolated exosomes from cultured medium. **Figure 6A** shows that miR-126 levels in the exosomes were significantly greater than in the exosomes loaded with miR-control. We delivered the exosomal miR-126 or exosomal miR-control into the myocardium through the right carotid artery (27, 29) immediately after induction of CLP in HSPA12B$^{-/-}$ mice. Twenty-four hours after delivery, we collected blood and measured serum levels of miR-126 levels by qPCR. **Figure 6B** shows that delivery of exosomal miR-126 markedly increased the serum miR-126 levels (178%) in HSPA12B$^{-/-}$ septic mice compared with delivery of exosomal miR-control. Immunostaining shows that delivery of exosomal miR-126 prevented sepsis-increased expression of VCAM-1 and ICAM-1 (**Figure 6C**). Western blot analysis shows that exosomal miR-126 transfection markedly prevented sepsis-induced increases in VACM-1 (**Figure 6D**) and ICAM-1 (**Figure 6E**) levels in the myocardium. We also analyzed the effect of delivery of exosomal miR-126 on sepsis-induced accumulation of immune cell in the myocardium. As shown in **Figure 6F**, delivery of exosomal miR-126 significantly decreased sepsis-induced accumulation of neutrophil (**Figure 6G**) and macrophage (**Figure 6H**) in the myocardium from HSPA12B$^{-/-}$ septic mice. The data clearly suggest that decreased miR-126 levels could be responsible for increased expression of adhesion molecules and immune cell accumulation in the myocardium in HSPA12B$^{-/-}$ septic mice.

Delivery of Exosomal miR-126 Improved Cardiac Function in HSPA12B$^{-/-}$ Septic Mice

We then examined whether suppression of adhesion molecule expression and reduced accumulation of immune cells in the myocardium by exosomal miR-126 will improve cardiac function in HSPA12B$^{-/-}$ septic mice. **Figures 6I,J** show that delivery of exosomal miR-126 into the myocardium of HSPA12B$^{-/-}$ septic mice significantly increased the values of EF% (47.8%) and %FS (61.2%) respectively, when compared with the exosomal miR-control group. The data demonstrated that miR-126 plays an important role in cardiac function by suppressing adhesion molecule expression during polymicrobial sepsis.

DISCUSSION

The present study has shown that EC-specific HSAP12B exerts a protective role in polymicrobial sepsis–induced cardiomyopathy. There are several important findings in the present study. First, deficiency of endothelial-specific HSPA12B (HSPA12B$^{-/-}$) results in severe cardiac dysfunction and poor survival outcome following polymicrobial sepsis, suggesting that endothelial HSP12B serves a protective role in cardiac function in sepsis. Second, endothelial HSPA12B deficiency promotes the increased expression of adhesion molecules and leads to accumulation of immune cells in the myocardium. This indicates that HSPA12B is involved in controlling adhesion molecule expression and immune cell infiltration into the myocardium following CLP sepsis. Third, the serum exosomes isolated from HSPA12B$^{-/-}$ septic mice contain lower levels of miR-126 when compared with the exosomes from WT septic mice. MicroRNA-126 specifically targets adhesion molecules (20). Therefore, it is possible that lower levels of miR-126 may be responsible for increased adhesion molecule expression and accumulation of immune cells in the myocardium. Finally, we loaded miR-126 onto exosomes derived from HSPA12B$^{-/-}$ BMSCs, delivered into the myocardium of HSPA12B$^{-/-}$ septic mice, and observed that transfection of miR-126 carried by exosomes significantly improves cardiac function of HSPA12B$^{-/-}$ septic mice by suppressing the expression of adhesion molecules and decreasing the infiltration of inflammatory cells into the myocardium. The

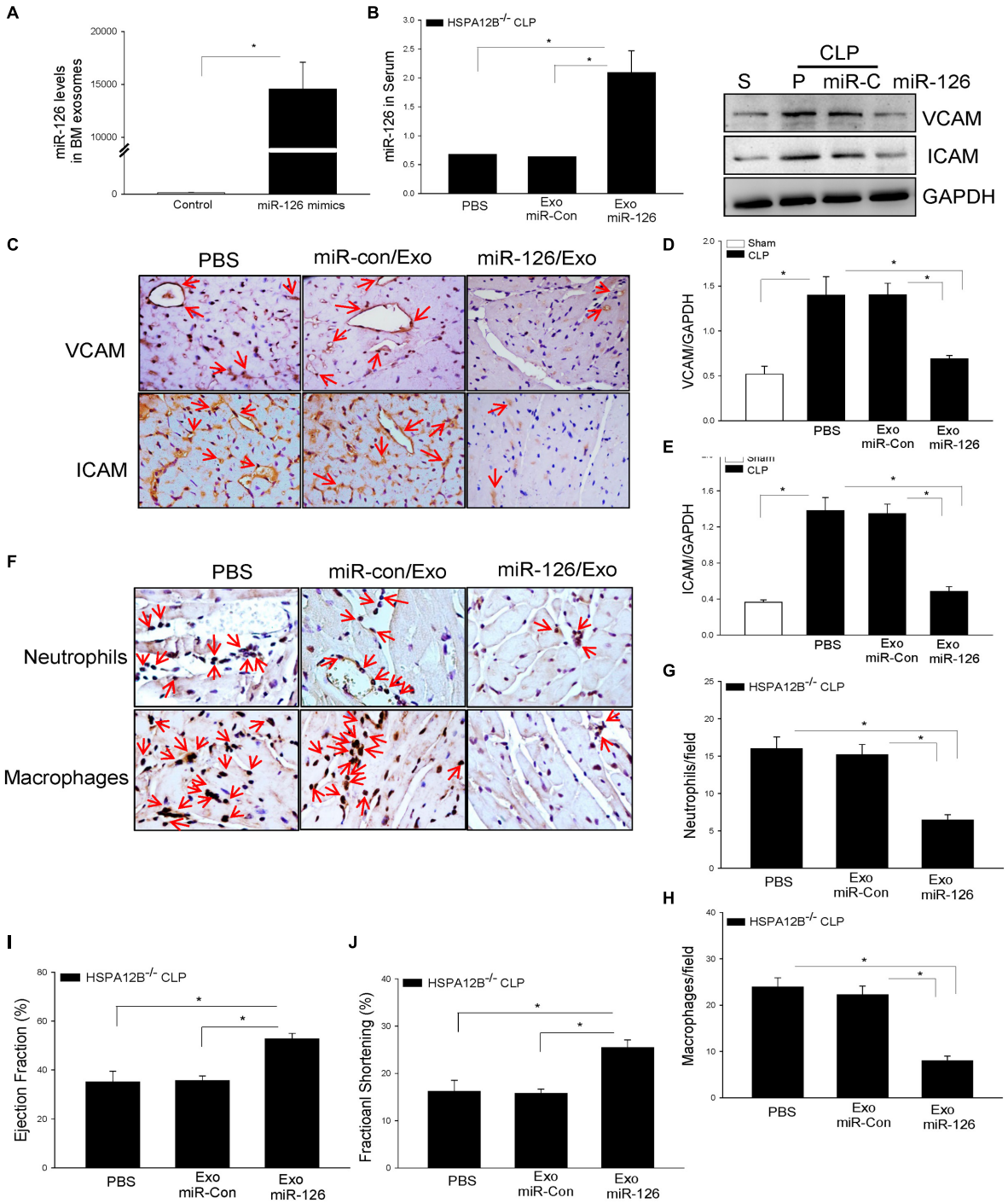

FIGURE 6 | MicroRNA-126 carried by exosomes derived from bone marrow stromal cells suppressed adhesion molecule expression in the myocardium of HSPA12B$^{-/-}$ septic mice. Bone marrow stromal cells (BMSCs) were isolated from HSPA12B$^{-/-}$ mice and transfected with 40 nmol/L scrambled miR-control or miR-126 mimics at the fourth to seventh generation. Twenty-four hours after transfection, exosomes were isolated from supernatants. **(A)** The levels of miR-126 in exosomes were examined qPCR. (B) HSPA12B$^{-/-}$ mice were transfected with exosomes loaded with miR-126 mimic or scrambled miR-control through the right carotid artery immediately before induction of CLP sepsis. Serum miR-126 levels were examined by qPCR 6 h after CLP. **(C)** VCAM-1 and ICAM1 expressions in the heart tissues were examined by immunohistochemistry staining with anti–VCAM-1 and anti–ICAM-1 antibodies. **(D,E)** Western blot analysis of VCAM-1 and ICAM1 levels in the myocardium of HSP12B$^{-/-}$ septic mice (n = 6–9/group). **(F)** The accumulation of neutrophils and macrophages in the myocardium was examined by immunohistochemistry with antineutrophil elastase antibody and antimacrophage antibody F4/80. **(G,H)** miR-126 carried by exosomes decreased the numbers of neutrophils **(G)** and macrophages **(H)** in the myocardium of HSPA12B$^{-/-}$ septic mice. **(I,J)** miR-126 carried by exosomes improves cardiac function (EF %, FS %) measured by echocardiography. n = 6–9/group for Western blot and n = 3/group for immunohistochemistry. *$P < 0.05$ compared with indicated groups. The immunohistochemistry staining was examined with bright field microscope (40×).

data suggest that endothelial miR-126 plays an important role in HSPA12B regulation of adhesion molecule expression during polymicrobial sepsis.

It is well known that EC dysfunction contributes to the pathophysiology of sepsis/septic shock and multiple organ dysfunction (34). Biomarkers of EC dysfunction have been concentrated on ICAMs. Increased expression of adhesion molecules, such as ICAM-1 and VCAM-1, has been shown to recruit neutrophils and macrophages into the myocardium, leading to cardiac dysfunction in sepsis (35, 36). Activated macrophages also release chemokines to attract neutrophils into the myocardium (35). We have previously reported that polymicrobial sepsis (22) and endotoxemia (13) significantly increased the expression of adhesion molecules, resulting in accumulation of neutrophils and macrophages in the myocardium. Therefore, suppression of adhesion molecule expression could be an important approach for the attenuation of sepsis-induced cardiomyopathy. Indeed, we observed in our previous studies that transgenic mice with EC-specific expression of HSPA12B show a significant attenuation of endotoxin-increased adhesion molecule expression and cardiac dysfunction through activation of PI3K/Akt signaling (13). However, the precise mechanisms by which HSPA12B is required for EC function are still unsolved.

We observed in the present study that HSPA12B$^{-/-}$ septic mice exhibit higher levels of adhesion molecules and greater immune cell accumulation in the myocardium than in WT septic mice. Our observation is consistent with previous studies showing HSPA12B is essential for EC functioning during sepsis/septic shock (13). Increased expression of ICAM-1 and VCAM-1 facilities the recruitment of macrophages and neutrophils into the myocardium, leading to inflammatory response in sepsis (35, 36). We observed that myocardial NF-κB binding activity and serum inflammatory cytokine levels, such as TNFα and IL-6, in HSPA12B$^{-/-}$ septic mice were markedly greater than in WT septic mice. This suggests that endothelial HSPA12B may play a role in not only regulating adhesion molecule expression but also controlling NF-κB mediated inflammatory cytokine production in polymicrobial sepsis.

To investigate how EC deficiency of HSPA12B increased adhesion molecule expression and the accumulation of immune cells in the myocardium following polymicrobial sepsis, we examined the effects of serum exosomes isolated from experimental mice on adhesion molecule expression in ECs *in vitro*. Exosomes are membranous nanovesicles (30–100 nm), which arise inside many cells from endosomal compartments called multivesicular bodies (37). Recent evidence demonstrated that exosomes play a critical role in cell-to-cell communication and serve as a novel vehicle for transferring proteins and/or miRs (37–39) from one cell to another through membrane fusion with the target cells, by binding with specific receptors at the cell surface of target cells, or endocytotic internalization. Exosomes are also shown to play a key role in host immunity to pathogens during infection (40). Interestingly, we found that treatment of ECs with exosomes that were isolated from HSPA12B$^{-/-}$ septic mice significantly increased the expression of VCAM-1 and ICAM1, when compared with WT septic exosomes. Our observations suggest that exosomes isolated from septic mice play a critical role in mediating EC dysfunction during sepsis.

At present, we do not understand which cells released exosomes into the serum in response to polymicrobial sepsis/shock. We also do not understand which compositions in the septic exosomes will be responsible for causing EC dysfunction. Interestingly, we observed that the levels of miR-126 in HSPA12B$^{-/-}$ septic exosomes were significantly lower than in WT septic exosomes. MicroRNA-126 is predominately expressed in ECs (18), targets adhesion molecules (20), and regulates angiogenesis (19). Lower levels of miR-126 in the exosomes may be responsible for the higher levels of myocardial adhesion molecules of HSPA12B$^{-/-}$ septic mice. To evaluate our hypothesis, we treated ECs with exosomes that were isolated from septic mice and observed that the levels of adhesion molecules in HSPA12B$^{-/-}$ septic exosome-treated ECs were significantly greater than in the effect of WT septic exosomes. To confirm our observation, we transfected ECs with miR-126 mimics before the cells were treated with LPS and observed that transfection miR-126 markedly suppresses LPS-induced increases in the expression of adhesion molecules.

Our *in vitro* data indicate that suppression of adhesion molecule expression by miR-126 mimics may decrease the infiltration of inflammatory cells into the myocardium and result in attenuation of cardiac function *in vivo* following polymicrobial sepsis. To test this hypothesis, we isolated BMSCs from HSPA12B$^{-/-}$ mice, transfected BMSCs with miR-126 mimics and isolated exosomes derived from BMSCs. We then delivered miR-126 carried by exosomes into the myocardium immediately after induction of polymicrobial sepsis. We observed that delivery of miR-126 carried by exosomes significantly improved cardiac function in HSPA12B$^{-/-}$ septic mice. Importantly, delivery of exosomes loaded with miR-126 attenuated sepsis-induced expression of adhesion molecules and accumulation of macrophages and neutrophils in the myocardium of HSPA12B$^{-/-}$ mice. At the moment, we do not understand the mechanisms by which endothelial-specific deficiency of HSPA12B results in lower levels of miR-126 in serum exosomes. However, our data suggest that targeting adhesion molecules is an important approach for maintenance of EC function and attenuation of inflammatory cell infiltration in the myocardium during polymicrobial sepsis. Exosomes loaded with miR-126 could be a novel approach for this purpose.

DATA AVAILABILITY STATEMENT

All datasets generated for this study are included in the article/**Supplementary Material**.

ETHICS STATEMENT

The animal study was reviewed and approved the ETSU University Committee on Animal Care.

AUTHOR CONTRIBUTIONS

XZ performed experiments and wrote the manuscript. XW performed the miR-126 experiments. MF performed the miR and adhesion molecule expression experiments. FT and KY performed the in vitro experiments. TH performed the gene type identification experiments. LL interpreted the data and contributed to the discussion. JK was involved in the data statistical analysis. DW was involved in the data discussion and preparation of the manuscript. CL was involved in the experimental design, data interpretation, and preparation of the manuscript.

FUNDING

This work was supported in part by the National Institutes of Health grants HL071837 (CL), GM083016 (CL and DW), GM53522 (DW), and C06RR0306551.

SUPPLEMENTARY MATERIAL

The Supplementary Material for this article can be found online at: https://www.frontiersin.org/articles/10.3389/fimmu.2020.00566/full#supplementary-material

FIGURE S1 | The targeting strategy for the development of Flox/Flox mice.

REFERENCES

1. Singer M, Deutschman CS, Seymour CW, Shankar-Hari M, Annane D, Bauer M, et al. The third international consensus definitions for sepsis and septic shock (Sepsis-3). *JAMA*. (2016) 315:801–10. doi: 10.1001/jama.2016.0287
2. Mayr FB, Yende S, Angus DC. Epidemiology of severe sepsis. *Virulence*. (2014) 5:4–11. doi: 10.4161/viru.27372
3. Celes MRN, Prado CM, Rossi MA. Sepsis: going to the heart of the matter. *Pathobiology*. (2013) 80:70–86. doi: 10.1159/000341640
4. Parrillo JE, Parker MM, Natanson C, Suffredini AF, Danner RL, Cunnion RE, et al. Septic shock in humans: advances in the understanding of pathogenesis, cardiovascular dysfunction, and therapy. *Ann Intern Med*. (1990) 113:227–42.
5. Aird WC. The role of the endothelium in severe sepsis and multiple organ dysfunction syndrome. *Blood*. (2003) 101:3765–77. doi: 10.1182/blood-2002-06-1887
6. Khakpour S, Wilhelmsen K, Hellman J. Vascular endothelial cell Toll-like receptor pathways in sepsis. *Innate Immun*. (2015) 21:827–46. doi: 10.1177/1753425915606525
7. Mai J, Virtue A, Shen J, Wang H, Yang X-F. An evolving new paradigm: endothelial cells – conditional innate immune cells. *J Hematol Oncol*. (2013) 6:61. doi: 10.1186/1756-8722-6-61
8. Pryshchep O, Ma-Krupa W, Younge BR, Goronzy JJ, Weyand CM. Vessel-specific Toll-like receptor profiles in human medium and large arteries. *Circulation*. (2008) 118:1276–84. doi: 10.1161/CIRCULATIONAHA.108.789172
9. Rao RM, Yang L, Garcia-Cardena G, Lusinskas FW. Endothelial-dependent mechanisms of leukocyte recruitment to the vascular wall. *Circ Res*. (2007) 101:234–47. doi: 10.1161/CIRCRESAHA.107.151860b
10. Han Z, Truong QA, Park S, Breslow JL. Two Hsp70 family members expressed in atherosclerotic lesions. *Proc Natl Aad Sci USA*. (2003) 100:1256–61. doi: 10.1073/pnas.252764399
11. Hu G, Tang J, Zhang B, Lin Y, Hanai J, Galloway J, et al. A novel endothelial-specific heat shock protein HspA12B is required in both zebrafish development and endothelial functions in vitro. *J Cell Sci*. (2006) 119:4117–2126. doi: 10.1242/jcs.03179
12. Steagall RJ, Rusinol AE, Truong QA, Han Z. HSPA12B is predominantly expressed in endothelial cells and required for angiogenesis. *Arterioscler Thromb Vasc Biol*. (2006) 26:2012–8. doi: 10.1161/01.ATV.0000235720.61091.c7
13. Zhou H, Qian J, Li C, Li J, Zhang X, Ding Z, et al. Attenuation of cardiac dysfunction by HSPA12B in endotoxin-induced sepsis in mice through a PI3K-dependent mechanism. *Cardiovasc Res*. (2011) 89:109–18. doi: 10.1093/cvr/cvq268
14. Chen Y, Wang L, Kang Q, Zhang X, Yu G, Wan X, et al. Heat shock protein A12B protects vascular endothelial cells against sepsis-induced acute lung injury in mice. *Cell Physiol Biochem*. (2017) 42:1156–68. doi: 10.1159/000477308
15. Kang Q, Chen Y, Zhang X, Yu G, Wan X, Wang J, et al. Heat shock protein A12B protects against sepsis-induced impairment in vascular endothelial permeability. *Sci Direct*. (2016) 2016:87–94. doi: 10.1016/j.jss.2015.12.034
16. Sheedy FJ, O'Neill LAJ. Adding fuel to fire: microRNAs as a new class of mediators of inflammation. *Ann Rheum Dis*. (2008) 67(Suppl. 3):iii50–5. doi: 10.1136/ard.2008.100289
17. Taganov KD, Boldin MP, Baltimore D. MicroRNAs and immunity: tiny players in a big field. *Immunity*. (2007) 26:133–7. doi: 10.1016/j.immuni.2007.02.005
18. Jansen F, Yang X, Hoelscher M, Cattelan A, Schmitz T, Proebsting S, et al. Endothelial microparticle-mediated transfer of MicroRNA-126 promotes vascular endothelial cell repair via SPRED1 and is abrogated in glucose-damaged endothelial microparticles. *Circulation*. (2013) 128:2026–38. doi: 10.1161/CIRCULATIONAHA.113.001720
19. Wang S, Aurora AB, Johnson BA, Qi X, McAnally J, Hill JA, et al. The endothelial-specific microRNA miR-126 governs vascular integrity and angiogenesis. *Dev Cell*. (2008) 15:261–71. doi: 10.1016/j.devcel.2008.07.002
20. Harris TA, Yamakuchi M, Ferlito M, Mendell JT, Lowenstein CJ. MicroRNA-126 regulates endothelial expression of vascular cell adhesion molecule 1. *Proc Natl Aad Sci USA*. (2008) 105:1516–21. doi: 10.1073/pnas.0707493105
21. Agudo J, Ruzo A, Tung N, Salmon H, Leboeuf M, Hashimoto D, et al. The miR-126-VEGFR2 axis controls the innate response to pathogen-associated nucleic acids. *Nat Immunol*. (2014) 15:54–62. doi: 10.1038/ni.2767
22. Gao M, Ha T, Zhang X, Liu L, Wang X, Kelley J, et al. Toll-like receptor 3 plays a central role in cardiac dysfunction during polymicrobial sepsis. *Crit Care Med*. (2012) 40:2390–9. doi: 10.1097/CCM.0b013e3182535aeb
23. Gao M, Ha T, Zhang X, Wang X, Liu L, Kalbfleisch J, et al. The toll-like receptor 9 ligand, CpG-oligodeoxynucleotide, attenuates cardiac dysfunction in polymicrobial sepsis, involving activation of both phosphoinositide 3 kinase/AKT and and extracellular-signal-related signaling. *J Infect Dis*. (2013) 207:1471–9. doi: 10.1093/infdis/jit036
24. Ha T, Lu C, Liu L, Hua F, Hu Y, Kelley J, et al. TLR2 ligands attenuate cardiac dysfunction in polymicrobial sepsis via a phosphoinositide-3-kinase dependent mechanism. *Am J Physiol Heart Circ Physiol*. (2010) 298:H984–91. doi: 10.1152/ajpheart.01109.2009
25. Williams DL, Ha T, Li C, Kalbfleisch JH, Schweitzer J, Vogt W I, et al. Modulation of tissue toll-like receptor 2 and 4 during the early phases of polymicrobial sepsis correlates with mortality. *Crit.Care Med*. (2003) 31:1808–18. doi: 10.1097/01.CCM.0000069343.27691.F3
26. Gao M, Wang X, Zhang X, Ha T, Ma H, Liu L, et al. Attenuation of cardiac dysfunction in polymicrobial sepsis by MicroRNA-146a is mediated via targeting of IRAK1 and TRAF6 expression. *J Immunol*. (2015) 195:672–82. doi: 10.4049/jimmunol.1403155

27. Wang X, Ha T, Liu L, Zou J, Zhang X, Kalbfleisch J, et al. Increased expression of microRNA-164a decreases myocardial ischemia/reperfusion injury. *Cardiovas Res*. (2013) 97:432–42. doi: 10.1093/cvr/cvu044
28. Soleimani M, Nadri S. A protocol for isolation and culture of mesenchymal stem cells from mouse bone marrow. *Nat Protoc*. (2009) 4:102–6. doi: 10.1038/nprot.2008.221
29. Wang X, Ha T, Zou J, Ren D, Liu L, Zhang X, et al. MicroRNA-125b protects against myocardial ischaemia/reperfusion injury via targeting p53-mediated apoptotic signalling and TRAF6. *Cardiovasc Res*. (2014) 102(14 A.D.):385–95.
30. Fernandes CJ Jr., de Assuncao MSC. Myocardial dysfunction in sepsis: a large, unsolved puzzle. *Crit Care Res Pract*. (2012) 2012:896430.
31. Medzhitov R, Horng T. Transcriptional control of the inflammatory response. *Nat Rev Immunol*. (2009) 9:692–703. doi: 10.1038/nri2634
32. Schulte W, Bernhagen J, Bucala R. Cytokines in sepsis: potent immunoregulators and potential therapeutics targets–an updated view. *Med Inflamm*. (2013) 2013:165974. doi: 10.1155/2013/165974
33. Golias C, Tsoutsi E, Matziridis A, Makridis P, Batistatou A, Charalabopoulos K. Review. Leukocyte and endothelial cell adhesion molecules in inflammation focusing on inflammatory heart disease. *In vivo*. (2007) 21:757–69.
34. Boisrame-Helms J, Kremer H, Schini-Kerth V, Meziani F. Endothelial dysfunction in sepsis. *Curr Vasc Pharmacol*. (2013) 11:150–60.
35. Cavaillon J-M, Adib-Conquy M. Monocytes/macrophages and sepsis. *Crit Care Med*. (2005) 33:S506–9. doi: 10.1097/01.ccm.0000185502.21012.37
36. Raeburn CD, Calkins CM, Zimmerman MA, Song Y, Ao L, Banerjee A, et al. ICAM-1 and VCAM-1 mediate endotoxemic myocardial dysfunction independent of neutrophil accumulation. *Am J Physiol Regulatory Integrative Comp Physiol*. (2002) 283:R477–86. doi: 10.1152/ajpregu.00034.2002
37. Camussi G, Derigibus MC, Bruno S, Cantaluppi V, Biancone L. Exosomes/microvesicles as a mechanism of cell-to-cell communication. *Kidney Int*. (2010) 78:838–48. doi: 10.1038/ki.2010.278
38. Alexander M, Hu R, Runtsch MC, Kagele DA, Mosbruger TL, Tolmachova T, et al. Exosome-delivered microRNAs modulate the inflammatory response to endotoxin. *Nat Commun*. (2015) 6:7321. doi: 10.1038/ncomms8321
39. Valadi H, Ekstrom K, Bossios A, Sjostrand M, Lee JJ, Lotvall JO. Exosome-mediated transfer of mRNAs and microRNAs is a novel mechanism of genetic exchange between cells. *Nat Cell Biol*. (2007) 9:654–9. doi: 10.1038/ncb1596
40. Schorey JS, Cheng Y, Singh PP, Smith VL. Exosomes and other extracellular vesicles in host-pathogen interactions. *EMBO Rep*. (2015) 16:24–43. doi: 10.15252/embr.201439363

Conflict of Interest: The authors declare that the research was conducted in the absence of any commercial or financial relationships that could be construed as a potential conflict of interest.

frontiers in Immunology

ORIGINAL RESEARCH
published: 30 April 2020
doi: 10.3389/fimmu.2020.00828

Antibody Production in Murine Polymicrobial Sepsis—Kinetics and Key Players

Oliver Nicolai[1†‡], Christian Pötschke[1†‡], Katrin Schmoeckel[1‡], Murthy N. Darisipudi[1], Julia van der Linde[2], Dina Raafat[1,3] and Barbara M. Bröker[1]*

[1] Immunology Department, Institute of Immunology and Transfusion Medicine, University Medicine Greifswald, Greifswald, Germany, [2] Department of General Surgery, Visceral, Thoracic and Vascular Surgery, University Medicine Greifswald, Greifswald, Germany, [3] Department of Microbiology and Immunology, Faculty of Pharmacy, Alexandria University, Alexandria, Egypt

Although antigen-specific priming of antibody responses is impaired during sepsis, there is nevertheless a strong increase in IgM and IgG serum concentrations. Using colon ascendens stent peritonitis (CASP), a mouse model of polymicrobial abdominal sepsis, we observed substantial increases in IgM as well as IgG of all subclasses, starting at day 3 and peaking 2 weeks after sepsis induction. The dominant source of antibody-secreting cells was by far the spleen, with a minor contribution of the mesenteric lymph nodes. Remarkably, sepsis induction in splenectomized mice did not change the dynamics of the serum IgM/IgG reaction, indicating that the marginal zone B cells, which almost exclusively reside in the spleen, are dispensable in such a setting. Hence, in systemic bacterial infection, the function of the spleen as dominant niche of antibody-producing cells can be compensated by extra-splenic B cell populations as well as other lymphoid organs. Depletion of CD4+ T cells did not affect the IgM response, while it impaired IgG generation of all subclasses with the exception of IgG3. Taken together, our data demonstrate that the robust class-switched antibody response in sepsis encompasses both T cell-dependent and -independent components.

Keywords: sepsis, splenectomy, T cell, antibody-secreting cells, IgM, IgG

OPEN ACCESS

Edited by:
Florian Uhle, Heidelberg University Hospital, Germany

Reviewed by:
Sergio Iván Valdés-Ferrer, Salvador Zubirán National Institute of Medical Sciences and Nutrition (INCMNSZ), Mexico
Sangeeta S. Chavan, Feinstein Institute for Medical Research, United States

***Correspondence:**
Barbara M. Bröker
broeker@uni-greifswald.de

† These authors have contributed equally to this work

‡ Present address:
Oliver Nicolai, Z.A.S. Zentral Archiv Service GmbH, Neubrandenburg, Germany
Christian Pötschke, Salutas Pharma GmbH, Barleben, Germany
Katrin Schmoeckel, CHEPLAPHARM Arzneimittel GmbH, Greifswald, Germany

Specialty section:
This article was submitted to Inflammation, a section of the journal Frontiers in Immunology

Received: *14 February 2020*
Accepted: *14 April 2020*
Published: *30 April 2020*

Citation:
Nicolai O, Pötschke C, Schmoeckel K, Darisipudi MN, van der Linde J, Raafat D and Bröker BM (2020) Antibody Production in Murine Polymicrobial Sepsis—Kinetics and Key Players. Front. Immunol. 11:828. doi: 10.3389/fimmu.2020.00828

INTRODUCTION

Sepsis is still associated with astoundingly high morbidity and mortality despite improvements in intensive care (1–5). A systemic hyper-inflammatory phase (systemic inflammatory response syndrome, SIRS) is followed or accompanied by a compensatory anti-inflammatory response (compensatory anti-inflammatory response syndrome, CARS), with the risk of lethal (secondary) infections (6, 7). During the initial hyper-inflammatory phase, 40–50% of the T and B cell populations as well as innate immune cells go into apoptosis (8). Antigen presentation and T cell proliferation are impaired in the subsequent hypo-inflammatory phase, with a concomitant increase in concentrations of stress-induced anti-inflammatory glucocorticoids. These aforementioned effects, together with a Th2 cytokine bias, impair an effective immune response against primary or secondary infections (9–16). This explains the fact that mortality from sepsis mostly occurs during this later phase (17, 18).

It is well-documented that the antigen-specific B cell response in sepsis is strongly reduced (19–22). For example, Mohr et al. have shown an impaired primary B cell response against defined

antigens (22). However, they have also observed an unspecific increase of serum IgM and IgG concentrations after cecal ligation and puncture, a commonly used mouse model of sepsis (22). However, details of the B cell response in sepsis that could explain that discrepancy are largely unknown (21, 23).

During an antigen-driven T cell-dependent (TD) immunoreaction against protein antigens, follicular B cells, which belong to the group of B-2 cells, are activated via the B cell receptor. With the help of activated T cells, they start to differentiate and form germinal centers, where class switch and somatic hypermutation take place. By the end of this process, affinity-matured plasma cells have developed that continuously secrete antibodies (24).

On the other hand, microbial components, which are systemically disseminated during sepsis, can activate B cells in a T cell-independent (TI) manner. For instance, TI-2 antigens (e.g., polysaccharides) crosslink B cell receptors and initiate a strong and long-lasting antigen-specific primary response (25). TI-1 antigens (e.g., lipopolysaccharide, LPS and bacterial DNA, CpG) activate B cells independent from the B cell receptor via toll-like receptors (TLRs), thereby inducing proliferation and antibody secretion (26, 27). In addition, TLR ligation itself can induce class switch recombination (28–31).

Though all naive and memory B cells in the mouse constitutively express TLRs (32–35), there are mainly two B cell subtypes, namely B-1 and marginal zone (MZ) B cells, which differentiate into antibody-secreting cells (ASC) soon after TLR-activation (34). Their antibody repertoire is restricted, polyreactive and lacking somatic hypermutation (36–38). These antibodies are produced to bridge the time gap until the adaptive response has sufficiently matured.

B-1 cells differ in their mode of activation, development, specificities and locations from follicular B cells. Their main reservoir are the pleural and peritoneal cavities, where they can be further subdivided based on their CD5 expression into B-1a (CD5+) and B-1b (CD5-) cells. In addition, they can be found in small proportions in all lymphoid organs and are prone to TI responses. They are selected during development based on a certain strength of self-binding. In strong contrast to follicular B cells, their BCR engagement does not lead to activation. They are able to switch to all IgG subclasses *in vitro*, whereas *in vivo* they produce natural antibodies mainly of the IgM, IgG3 and IgA isotype [reviewed extensively in (24, 38, 39)].

MZ B cells are located close to the marginal sinus in the murine spleen (40, 41), where they have direct access to blood-borne antigens (42, 43). Although they have the capacity to generate TD and TI responses (44–46), their main function is the TI response against blood pathogens. They differentiate very early into IgM- or IgG-secreting cells (43).

Follicular B cells (or B-2 cells) react only moderately or weakly to TI-1 antigens (34, 47, 48), but are classically the main producers of T cell-dependent, class-switched and hypermutated antibodies, which are produced in response to an antigen-specific TD response. They are found in peripheral lymphoid organs but also in the peritoneal cavity (PC) (49, 50).

In the present study, we set out to examine B cell reactions and antibody secretion in polymicrobial abdominal sepsis, with the aim of explaining disparities in research findings. For that purpose, we used two murine models for sepsis induction: (i) fecal-induced peritonitis (FIP): intraperitoneal (*i.p.*) injection of pooled cecal content of donor mice into recipient mice (51–53); (ii) colon ascendens stent peritonitis (CASP): continuous leakage of own gut content over a certain time, which mimics the clinical setting (54, 55). Whether splenic follicular or MZ B cells have a key role in the humoral response in sepsis was examined by explanting the spleen parallel to sepsis induction. In addition, CD4+ T cells were depleted before sepsis induction to determine the portion of the T cell-dependent and -independent humoral response.

MATERIALS AND METHODS

Animal Experiments and Ethics Statement

Female C57BL/6 wild type (WT) mice were housed in a conventional, temperature-controlled animal facility (Central service and Research Institute for experimental animals of the University Medicine Greifswald) with a 12-h light and dark cycle, and provided with food and water *ad-libitum*. All animal experiments were performed in accordance with the German Animal Welfare Act (Deutsches Tierschutzgesetz) and the Federation of Laboratory Animal Science Associations (FELASA). The animal research protocol was approved by the animal ethics committee of the responsible local animal protection authority (LALLF, State Office for Agriculture, Food Safety and Fisheries Mecklenburg-Western Pomerania; numbers LALLF M-V/TSD/7221.3-1.1-052/07 and LALLF M-V/TSD/7221.3-1.2-013/09). All efforts were made to minimize animal suffering.

Colon Ascendens Stent Peritonitis (CASP)

Colon ascendens stent peritonitis (CASP) surgery was performed as described before (54, 56). Briefly, mice were anesthetized with *i.p.* Ketamin (Ketanest, Parke-Davis GmbH, Berlin) and Xylazin (Rompun, Bayer Health Care, Leverkusen), 100/10 μg per g body weight, respectively. The abdomen was opened through a small incision and a 18G stent (Ohmeda AB, Helsingborg, Sweden) was implanted into their colon ascendens. After surgery, all animals were carefully monitored every 6 h (h) until the end of the experiment. Control animals received sham operations, without stent implantation. Animals were euthanized 10 or 14 days following CASP surgery.

Fecal-Induced Peritonitis (FIP)

Sepsis was induced by introducing feces into the peritoneum using the method described by Wang et al. (57). In brief, littermates were anesthetized and euthanized. Fecal content (FC) was collected by cutting the *Ampulla ceci* and squeezing out the content. FC was homogenized in PBS to a final concentration of 100 mg/mL. The recipients received 7.25×10^5 CFU *i.p.*, whereas control animals were treated with PBS instead. At certain time points after sepsis induction (days 1, 3, 7, 14, 28, as well as at 12 weeks), animals were euthanized and the splenocytes isolated.

Splenectomy

Following anesthesia, a midline laparotomy was performed. The cranial-dorsal and caudal-ventral spleen blood vessels were ligated with Mariderm 7/0, after applying yasergil-clips, and cut. The spleen was subsequently explanted.

Antibody Assay

Mice were anesthetized, and blood was collected via the retrobulbar venous plexus using a microhematocrit capillary. Serum was collected after centrifugation of the coagulated blood at 16,000 × *g* for 10 min. Total serum IgM and IgG concentrations in murine serum were measured with the Milliplex® Mouse Immunoglobulin Isotyping Immunoassay (Millipore, MA, USA) according to the manufacturer's instructions. The samples were measured with the Luminex® 200 System (Bio-Rad Laboratories, Munich). Concentrations were calculated with the BioPlex Manager 5.0 software based on a provided standard.

Enzyme Linked Immuno Spot Assay (ELISpot)

On assigned days, mice were euthanized under deep anesthesia and then spleen, mesenteric lymph nodes (MLN), femur and omentum were harvested for the preparation of single-cell suspensions. For spleen and MLN, 70 μm cell strainers (Sigma-Aldrich) were used. Bone marrow cells were prepared by flushing the femur with 10 mL cold PBS containing 5% fetal bovine serum (5% FBS/PBS). Cells were washed with cold 5% FBS/PBS (250 × *g*, 6 min, 4°C), and erythrocytes were lysed with sterile filtered ammonium chloride-buffer followed by another washing step.

A single-cell suspension of omentum was prepared by collagenase and DNAseI digestion (Roche Diagnostics GmbH, Mannheim, Germany). Briefly, the omentum was washed with PBS containing 5 mM EDTA for 1 min to get rid of the attached cells, followed by washing in HBSS containing 10% FBS and 0.01 M HEPES. The omentum was then cut into small pieces with a sterile scissor and incubated in 500 μL digestion buffer (PBS, 10% FBS, 0.01 M HEPES, 1.5 mg/mL collagenase D, 2 mg/mL DNAseI) for 30 min at 37°C with constant shaking (500 rpm). The resulting tissue was then mashed through a 70 μm cell strainer and washed twice in HBSS containing 10% FBS and 0.01 M HEPES (500 × *g*, 5 min, 4°C). The last step was then repeated with a 30 μm cell strainer.

All cells were resuspended in cold culture media (RPMI1640 supplemented with 50 μM 2-mercaptoethanol, 100 U/mL penicillin/streptomycin, 2 mM glutamine, 1 mM sodium pyruvate, 0.2% D-glucose, and 1% non-essential amino acids). The numbers of DAPI-negative and CD45-positive cells were determined as described in the flow cytometry section. The numbers of IgM- and IgG-secreting cells were determined using a mouse IgM and IgG ELISpotPLUS kit (Mabtech AB, Nacka Strand, Sweden). ELISpot was performed according to the manufacturer's instructions for *in vivo* activated cells (no additional activation required). Cells, titrated to 5,000–50,000 per well, were seeded in triplicates and incubated at 37°C for 16 h.

Spots were imaged using an ELISPOT plate reader (ImmunoSpot S5 Versa, Cellular Technology Limited) and counted using the Immunospot 5.0.3 Professional software (Cellular Technology Limited).

The number of ASCs per organ was calculated as follows:

cells per organ (BM only one femur) / cell number seeded × number of spots counted.

TABLE 1 | Antibodies used for B cell characterization.

Specificity	Fluorochrome	Isotype	Clone	Provider	Final conc. [μg/mL]
B220	APC-A780	Rat IgG2a, κ	RA3-6B2	eBioscience	1
CD21	FITC	Rat IgG2b, κ	7G6	BD	10
CD23	PE	Rat IgG2a	B3B4	eBioscience	2
CD69	APC	Hamster IgG1	H1.2F3	BD	2
CD73	PE	Rat IgG2a, κ	TY/23	BD	4
CD95	PE-Cy7	Hamster IgG2	Jo2	BD	2
GL7	Alexa647	Rat IgM, κ	GL7	eBioscience	2
IgD	Horizon V450	Rat IgG2a, κ	11.26c2a	BD	5
IgM	PE-Cy7	Rat IgG2a, κ	R6-60.2	BD	10
CD45	FITC	Rat IgG2b, κ	30-F11	BioLegend	10

TABLE 2 | Isotype controls.

Isotype	Fluorochrome	Clone	Provider	Final conc. [μg/mL]
Hamster IgG	APC	eBio299Arm	eBioscience	2
Hamster IgG2	PE-Cy7	B81-3	BD	2
Rat IgM, κ	Alexa647	RTK2118	BioLegend	5
Rat IgG2b	FITC		eBioscience	5
Rat IgG2a, κ	PE	R35-95	BD	4-8

TABLE 3 | Definition of B cell populations.

Population	Marker	References	Gating
Follicular B cells	B220+ IgM+ IgD+ CD21int CD23+	(58, 59)	**Supplementary Figure 1A**
Marginal zone B cells	B220+ IgMhi IgDlo CD21+++ CD23-	(60)	**Supplementary Figure 1A**
Germinal center B cells	B220+ GL7+ CD95hi CD73int	(61)	**Supplementary Figure 1B**

Flow Cytometry

B cells were characterized using specific antibodies listed in **Table 1**, together with the necessary isotype controls (**Table 2**). B cell subpopulations were phenotypically defined according to the criteria listed in **Table 3**. Spleen cell suspensions were obtained as described before (62). Cell numbers were determined using BD TruCOUNT™ beads. One million cells were incubated with 2 μL Fc-Block for 15 min at 4°C. Then, 50 μL of the appropriate antibody-cocktail was added and incubated for further 30 min at 4°C. After washing (300 × *g*, 6 min) with FACS-buffer (BD FACSFlow Sheath Fluid, 2% FBS, 0.02% sodium azide), the pellet was resuspended in FACS-buffer and analyzed on a BD LSRII flow cytometer.

Depletion of CD4+ T Cells

For the depletion of CD4+ T cells, 150 μg rat anti-mouse CD4 mAb (GK1.5, in-house) was injected *i.p.* 1 and 3 days before CASP surgery. This efficiently depleted CD4+ cells without affecting CD8+ T lymphocytes (**Supplementary Figure 2**) as shown by FACS analysis using antibodies listed in

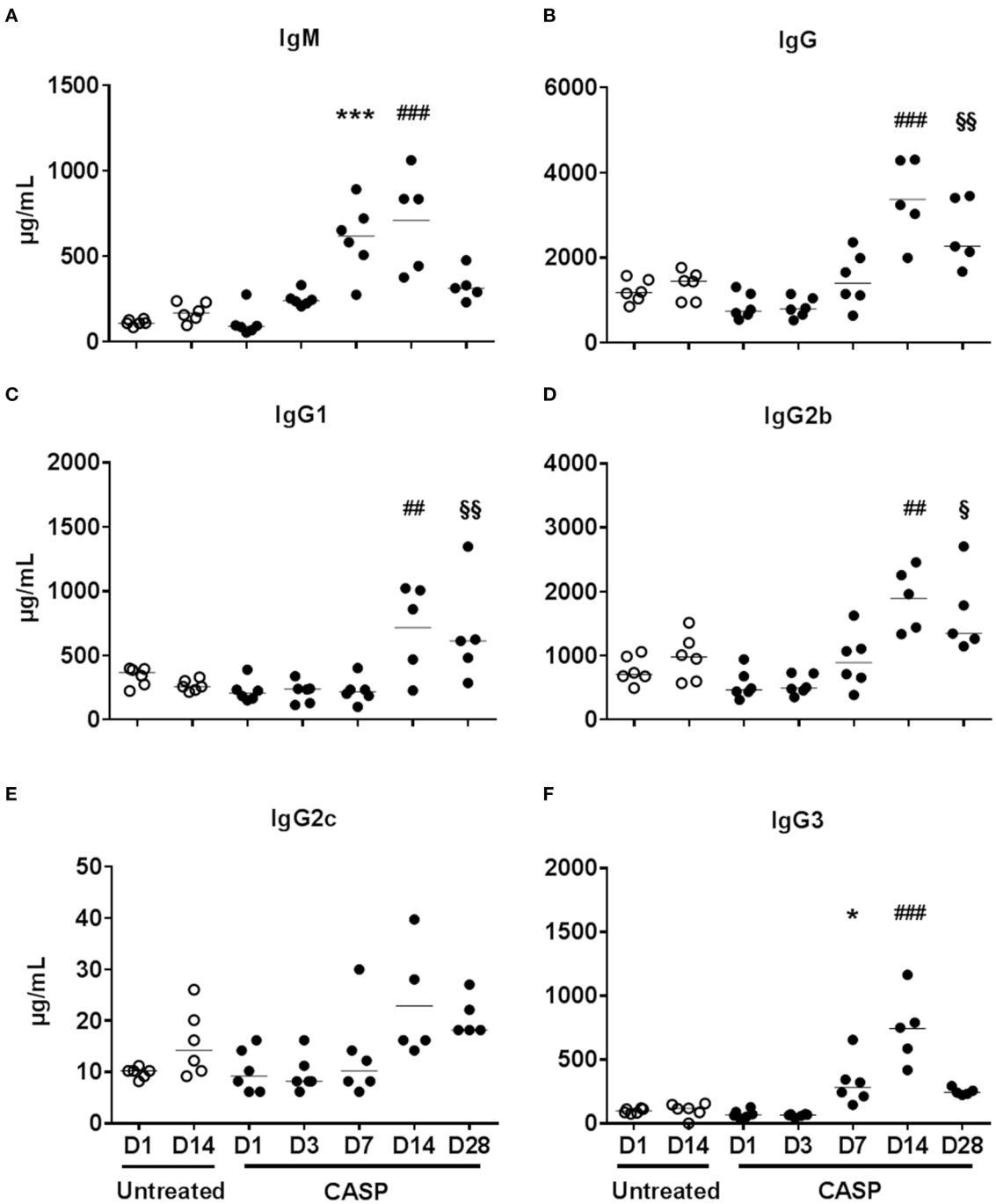

FIGURE 1 | Serum immunoglobulin concentrations during the course of sepsis. Sepsis was induced by CASP-operation in female C57BL/6 mice. Untreated animals served as controls. At the indicated time points animals were anesthetized and blood was collected. Serum IgM **(A)** and IgG **(B)** concentrations, as well as the concentrations of all IgG-subtypes (C-F), were measured by Luminex®-technology. One of two similar experiments is shown here. We used the One Way ANOVA and Bonferroni *post hoc* test for selected pairs for statistical evaluation, and the mean is depicted in this figure. Significances are shown as number of symbols. one symbol $p < 0.05$; two symbols $p < 0.01$; three symbols $p < 0.001$. (*) CASP D7 vs. untreated D1, ($^{\#}$) CASP D14 vs. untreated D14, ($^{\$}$) CASP D28 vs. untreated D14; N = 5-6/group. The 95% confidence intervals of the differences of means are given in **Supplementary Tables 1**, **2**.

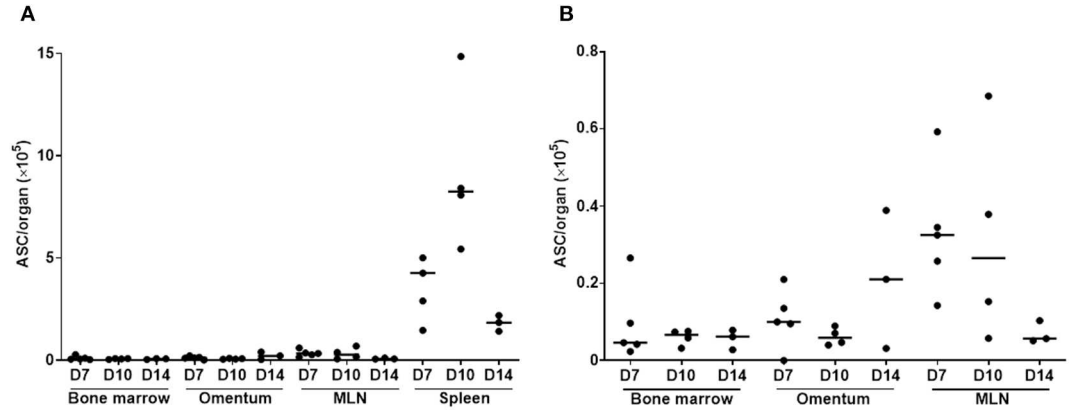

FIGURE 2 | Antibody-secreting cells in lymphoid organs after sepsis. Sepsis was induced by CASP-operation in female C57BL/6 mice. At the indicated time points bone marrow, omentum, mesenteric lymph nodes (MLN) and spleen were harvested and cells isolated. Antibody-secreting cells (ASC, sum of IgM and IgG) per organ were measured with an ELISpot, and the median is depicted **(A)**. ASC/organ values below 1×10^5 for bone marrow, omentum and MLN are separately shown **(B)**. $N = 3$–5.

Supplementary Table 3. Control mice received PBS instead. 14 days after depletion, the CD4 population in depleted, non-septic control mice had recovered to 40% compared with the non-depleted controls (own unpublished data).

Statistical Analysis

Statistical analyses were performed using GraphPad Prism 6 for Windows (GraphPad Software, CA, USA). Data were assessed for significant differences using One-Way ANOVA with Bonferroni correction (Bonferroni *post-hoc* test) for selected pairs. $P < 0.05$ were considered significant.

RESULTS

Strong Increase in Serum Immunoglobulin Concentrations After Sepsis

During the course of sepsis, serum immunoglobulin (Ig) concentrations increased, reflecting B cell-activation and differentiation (**Figure 1**). In CASP, the IgM-serum concentration increased from 111.5 ± 17.71 μg/mL (CI 95%: 92.9–130; untreated d1) to 710.2 ± 291.1 μg/mL (CI 95%: 349–1,072) 14 days later (**Figure 1A**). At the same time the IgG-serum concentrations peaked at 3,372 ± 966.8 μg/mL (CI 95%: 2,171–4,572) at 14 days, compared to levels at day 1 [untreated day 1: 1,216 ± 270.6 μg/mL (CI 95%: 932–1,500)] (**Figure 1B**). This increase was distributed among all IgG-subtypes (**Figures 1C–F**), indicating at least partially T cell-dependent processes. These dynamics have also been observed in two other abdominal sepsis models (cecal ligation and puncture (CLP) and FIP, data not shown).

The Spleen Is the Main Source of IgM- and IgG-Secreting Cells After Sepsis

Next, the source of the strong antibody reaction to sepsis was determined. Abdominal sepsis starts in the PC and is characterized by the systemic dissemination of pathogens and their products. Thus, both local and systemic immune responses are expected to take place. Locally, the parathymic lymph nodes are draining the PC (49, 63). They increase in size after sepsis induction but still have a much lower cell count compared to the spleen, ruling out a major contribution to the serum Ig response. Furthermore, the omentum and its lymph follicle-like structures, the so-called milky spots, have been ascribed a role in lymphocyte migration to and from the PC (49, 64, 65), while the mesenteric lymph nodes (MLN), an accumulation of relatively large lymph nodes in the PC, drain the gut and are probably not directly involved in the immune cell migration to or out of the PC. On the other hand, a systemic immune reaction will take place in the spleen due to the hematogenous spread of microbial compounds. Finally, the bone marrow might be involved as a source of immature as well as memory B cells, and a niche of long-lived plasma cells (66–68). ELISpot analyses clearly revealed the highest amount of ASCs in the spleen. At the peak of the response, namely 10 days after sepsis induction, around 10^6 ASCs were counted in the spleens of septic animals. In addition, the MLNs seem to make a contribution to the antibody response, but the means differ by more than 20-fold (**Figures 2A,B**). In accordance with this, splenic follicular B cells, marginal zone B cells as well as germinal center B cells were rapidly activated in sepsis induced by FIP (within 24 h). The latter remained activated over a period of 12 weeks (**Supplementary Figure 3**).

Spleen Cells, Including Marginal Zone B Cells, Are Not Necessary for the Production of Antibodies After Sepsis

Although we detected B cell activation and germinal center formation in the spleen, together with the majority of ASCs, it turned out that this organ was superfluous with regard to the observed strong increase of immunoglobulins after sepsis. To determine the input of splenic B cells to the overall humoral response, we splenectomized mice in parallel to CASP induction. Fourteen days later, there were no major changes in IgM or

IgG serum concentrations as compared to the animals that received only CASP (**Figure 3**). Moreover, the lack of spleen had no effect on the induced IgG subclasses in the septic immune response (**Supplementary Figure 4**). The ostensible IgG-increase following splenectomy and CASP compared to CASP-only is due to three animals whose IgG2b concentrations increased strongly (**Figure 3** and **Supplementary Figure 4**).

The Antibody-Response After Sepsis Is Partially T Cell-Dependent

The generation of germinal centers as well as the strong increase in serum concentrations of all IgG subclasses makes a case for an antigen-driven TD Ig response in sepsis. Depleting CD4+ cells with an antibody (Gk1.5) prior to sepsis induction (**Supplementary Figure 2**) had no influence on IgM secretion (**Figure 4A**), but led to reduced serum IgG concentrations 14 days after CASP (**Figure 4B**). This supports the notion of a TD component in the B cell response. Interestingly, the decrease in serum IgG concentrations was absolute for IgG1 (returning to background levels), intermediate for IgG2b and IgG2c, but only in tendency for IgG3 (**Figures 4C–F**). Therefore, class switch in sepsis is evidently not exclusively dependent on T cells, but additionally driven by T cell-independent processes/antigens.

DISCUSSION

While battling invading pathogens, the systemic immune response causes collateral damage to the host, impairing life-securing homeostasis. Compensatory anti-inflammatory mechanisms and the necessary apoptotic loss of immune effector cells lead to immunosuppression, culminating in immunoparalysis (7, 8, 10, 12, 69, 70). It was hence assumed that the antibody response would also be impaired (70, 71). We have shown that serum IgM as well as IgG concentrations start to increase three to seven days after sepsis induction. The IgG increase was distributed among all IgG-subclasses, with the strongest relative increase observed for IgG3. IgG1, IgG2b, and IgG3 reached similar absolute serum concentrations of 1-2 mg/mL. The robust increase in serum Ig appears to be a general phenomenon in sepsis. Mohr et al. observed a similar increase 10 days after CLP (22), and our group obtained analogous results in a mouse model of FIP (data not shown). Brunner et al. have detected increased serum IgG concentrations in septic patients as early as 48 h after diagnosis (72).

An important role has been attributed to the spleen in the early defense against bacterial dissemination in the blood. Phagocytosis, endotoxin detoxification and antibody production are the main effector mechanisms. Especially MZ B cells carry TI responses (43, 73–75) and were deemed essential for successful pathogen eradication (42, 76). In accordance with this, the spleen was the main source of ASCs in our sepsis model, with a minor contribution of the MLNs. Moreover, we have shown an early activation of follicular and MZ B cells in the spleen, corroborating the results of other research groups (77). In accordance with what was observed by Kelly-Scumpia et al. (77), germinal centers were

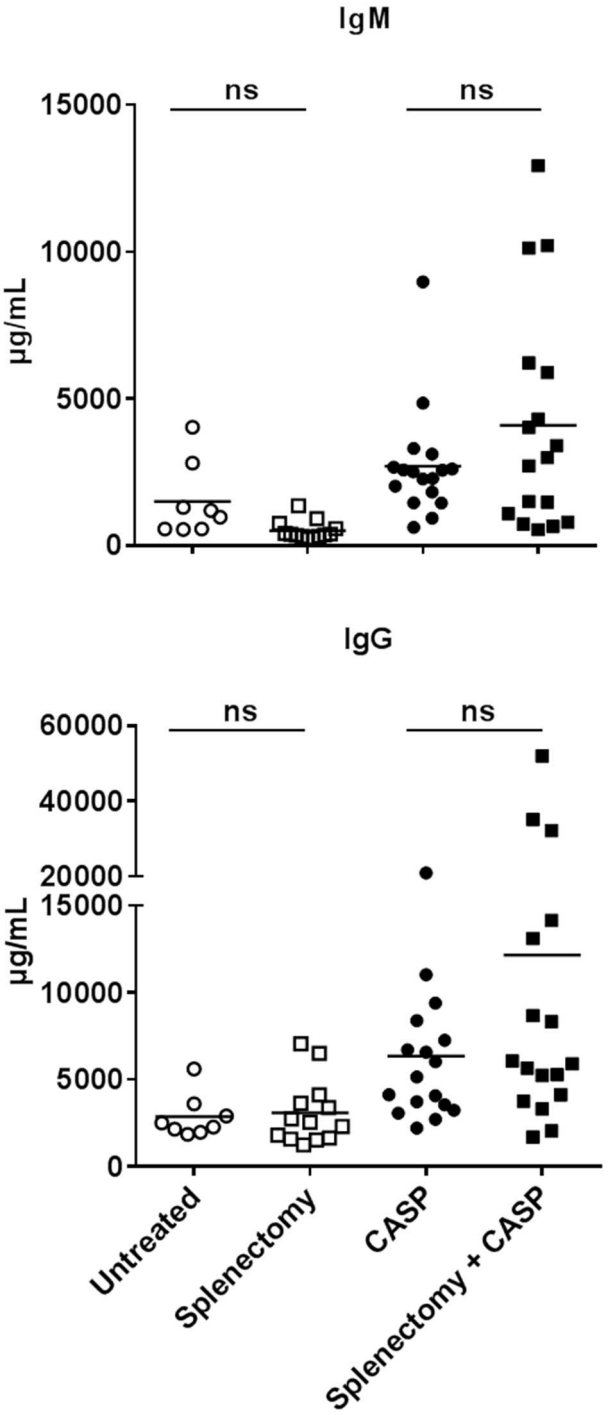

FIGURE 3 | Serum IgM and IgG concentration 14 days after sepsis and splenectomy. Female C57BL/6 mice were CASP-operated and their spleen was explanted in parallel. Untreated, splenectomized-only and CASP-only animals served as controls. 14 days later animals were anesthetized and blood was collected. IgM and IgG serum concentrations were measured by Luminex®-technology. Shown is the mean of the collective data from two independent experiments with a similar tendency. We used the One Way ANOVA and Bonferroni *post-hoc* test for selected pairs for statistical evaluation. * $p < 0.05$; $N = 8$–17 per group.

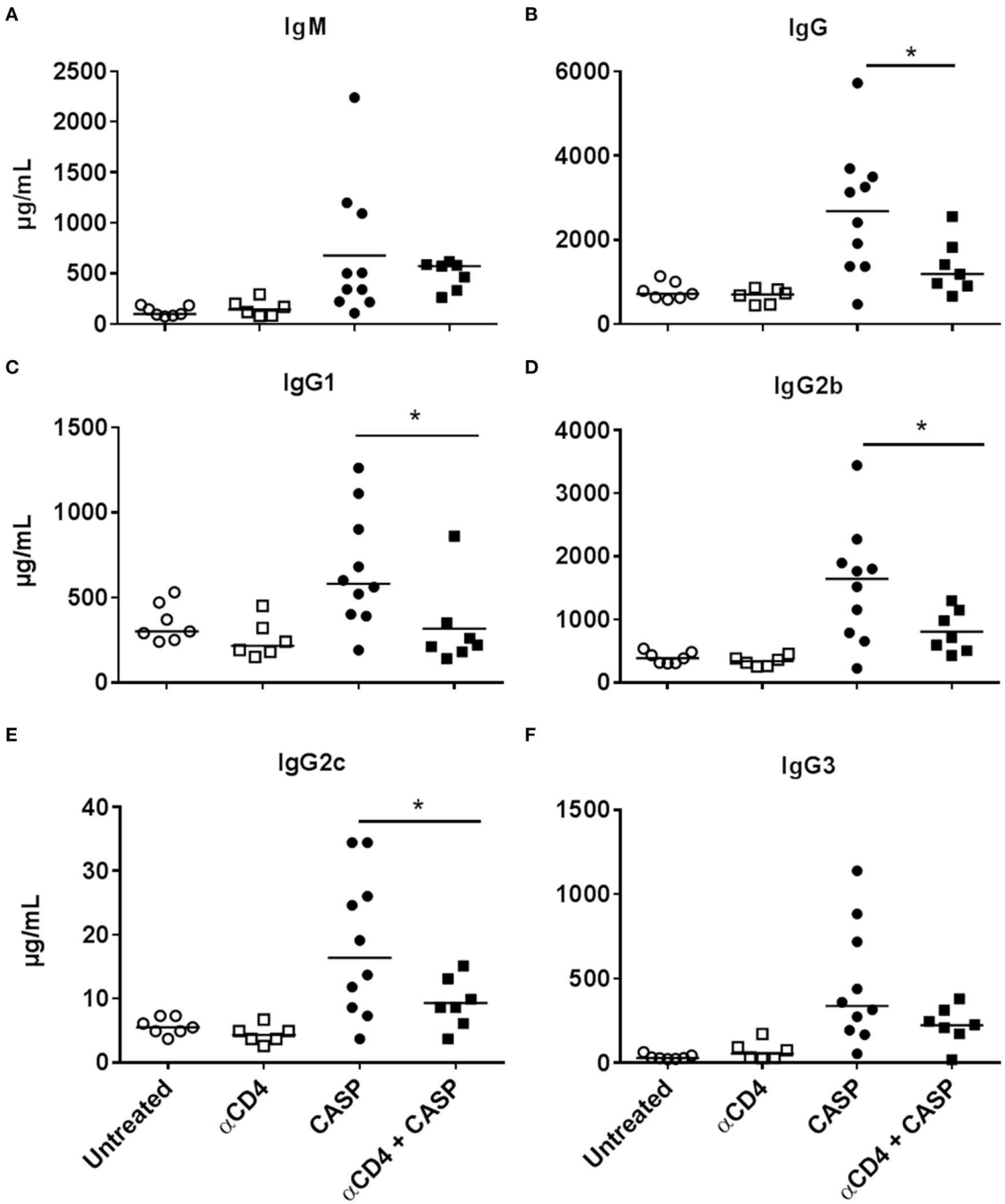

FIGURE 4 | Serum Ig concentration 14 days after CASP and CD4+ cell depletion. Female C57BL/6 mice received 150 µg of a depleting anti-CD4 antibody (αCD4; Gk1.5) *i.p.* three and one day before sepsis induction via CASP. Control animals remained untreated or received the depleting antibody only. Fourteen days after CASP, animals were anesthetized and blood was collected. IgM **(A)** and IgG **(B)** serum concentrations, as well as IgG subclass concentrations **(C–F)**, were measured by Luminex®-technology. Shown is the mean of the collective data from two independent experiments with a similar tendency. We used the One Way ANOVA and Bonferroni *post-hoc* test for selected pairs for statistical evaluation $^*p < 0.05$. $N = 6$–10 per group.

formed after 3 days. Four days later, high numbers of IgM and IgG-secreting cells were detected, especially in the spleen.

However, splenectomy did not impair the humoral immune response, as measured by the increase in serum antibody concentration. It seemed that splenic follicular as well as MZ B cells, despite being rapidly activated, were redundant. This was surprising in light of previous reports of a strongly reduced humoral response against bacterial antigens in splenectomized mice (78–81). In those studies, mice were infected 7–70 days following splenectomy. In yet another study, splenectomy led to a 75% reduction in B-1a cells after 6 days (60), which might explain the reduced humoral response in this setting. B-1a cells

are known to participate in anti-bacterial and anti-viral responses (38, 82–84). We splenectomized the mice in parallel to CASP induction; hence extra-splenic B cell populations could still react to the multitude of antigens. Furthermore, in studies with *Borrelia hermsii*, MZ B cells did not play an important role either, because B-1 cells were the main producers of protective serum IgM (85, 86).

The fact that splenectomy did not decrease the serum IgM and IgG concentrations, despite the fact that we have clearly disclosed the spleen as the main source of ASCs, strongly argues for the hypothesis that most ASCs found in the spleen developed from immigrating B cells. These were probably peritoneal B cells, which – upon activation – left the peritoneum and migrated to spleen and peripheral lymph nodes (49, 86, 87). Some of these are obviously able to class switch to IgG. Our data also suggest that soon after splenectomy other lymphoid organs, be it mesenterial lymph nodes, the milky spots in the omentum and/or the parathymic lymph nodes, can compensate for the spleen.

Several groups have shown that antigen-specific priming is impaired after sepsis (21, 22, 88). So the question remains, what drives the strong antibody-increase in murine serum after sepsis? Obviously, microbial structures, such as LPS or CpG, flood the host system during sepsis, and are able to polyclonally activate B cells via their appropriate receptors (TLR4 or TLR9) (32, 89). Especially MZ B cells and B-1 cells differentiate into plasma cells (34, 35). Interestingly, LPS *per se* can induce class switch to IgG2b and IgG3, but also activated NKT cells, activated DCs and thrombocytes, all of which are abundant in sepsis, can at least partially compensate a lack of T cell help and promote TI antibody class switch (90–93).

On the other hand, the disseminating bacteria as well as dying host cells also confront the adaptive immune system with a wealth of antigens in the setting of sepsis. The pronounced germinal center reaction, in conjunction with the increase in all IgG subclasses support the idea that, besides polyclonal B cell activation, there may also be a significant antigen-driven component in the Ig response to sepsis.

Indeed, depletion of CD4+ T cells before sepsis reduced IgG-production, leaving the IgM-response intact. Especially IgG1 did not increase over the basal level in the absence of T cells. Although IgG2b, IgG2c, and IgG3 production was also less than in T cell competent septic animals, there was still a measurable increase. That shows that the IgG response to sepsis comprises both TD and TI components. Nevertheless, the observed significant TD IgG response seems to contradict reports of impaired antigen priming following sepsis induction (19, 21, 22, 88, 94, 95). The contrasting findings can, however, be reconciled by the following observations made by our research group (88): at sepsis onset, the T cell response to a primary antigen stimulus was not only fully intact but even enhanced, presumably through the adjuvant effects of the abundant pathogen-associated molecular patterns (PAMPs) and danger-associated molecular patterns (DAMPs) (88, 96). However, later during the disease, the T cell response to antigen priming was reduced, with a nadir 7 days after sepsis onset, where T cells in severely affected animals did not react at all (19, 88).

Our data reveal a strong humoral immune response in animals who survived sepsis. It is composed of T cell-dependent as well as T cell-independent components, takes place mainly in the spleen and probably involves the activation of all B cell populations. The task would now be to determine the antigen specificity of this Ig response in sepsis. This is addressed in the companion paper by Nicolai and co-workers (Nicolai et al., under revision).

In summary, in the present study, the origin of the strong antibody increase in sepsis was investigated, which identified the spleen as the main source of ASCs. Explanting the spleen parallel to sepsis induction revealed that both splenic follicular and MZ B cells are redundant in the humoral response to sepsis. Moreover, depletion of CD4+ T cells prior to sepsis induction highlighted the fact that both T cell-dependent and T cell-independent components govern the IgG response to sepsis.

DATA AVAILABILITY STATEMENT

All datasets generated for this study are included in the article/**Supplementary Material**.

ETHICS STATEMENT

The animal study was reviewed and approved by Animal ethics committee of the local animal protection authority (LALLF, State Office for Agriculture, Food Safety and Fisheries Mecklenburg-Western Pomerania).

AUTHOR CONTRIBUTIONS

Conceptualization and project design: ON, CP, KS, and BB. Methodology and performance of experiments: ON, CP, and JL. Data evaluation: ON, CP and BB. Interpretation of data: ON, CP, KS, MD, JL, DR, and BB. Writing–original draft preparation: ON, MD, DR, and BB. Writing–review and editing. All authors critically reviewed the manuscript.

FUNDING

This research was funded by the German Research Foundation (DFG; RTG-840) to ON, CP, and KS.

ACKNOWLEDGMENTS

We are grateful to Maria Ozsvar Kozma for excellent technical support. We acknowledge support for the Article Processing Charge from the DFG (German Research Foundation, 393148499) and the Open Access Publication Fund of the University of Greifswald.

SUPPLEMENTARY MATERIAL

The Supplementary Material for this article can be found online at: https://www.frontiersin.org/articles/10.3389/fimmu.2020.00828/full#supplementary-material

REFERENCES

1. Slade E, Tamber PS, Vincent JL. The surviving sepsis campaign: raising awareness to reduce mortality. *Crit Care*. (2003) 7:1–2. doi: 10.1186/cc1876
2. Singer M, Deutschman CS, Seymour CW, Shankar-Hari M, Annane D, Bauer M, et al. The third international consensus definitions for sepsis and septic shock (sepsis-3). *JAMA*. (2016) 315:801–10. doi: 10.1001/jama.2016.0287
3. Rudd KE, Johnson SC, Agesa KM, Shackelford KA, Tsoi D, Kievlan DR, et al. Global, regional, and national sepsis incidence and mortality, 1990–2017: analysis for the global burden of disease study. *Lancet*. (2020) 395:200–11. doi: 10.1016/S0140-6736(19)32989-7
4. Angus DC, van der Poll T. Severe sepsis and septic shock. *N Engl J Med*. (2013) 369:840–51. doi: 10.1056/NEJMra1208623
5. La Suarez De Rica A, Gilsanz F, Maseda E. Epidemiologic trends of sepsis in western countries. *Ann Transl Med*. (2016) 4:325. doi: 10.21037/atm.2016.08.59
6. Hotchkiss RS, Monneret G, Payen D. Sepsis-induced immunosuppression: from cellular dysfunctions to immunotherapy. *Nat Rev Immunol*. (2013) 13:862–74. doi: 10.1038/nri3552
7. Yende S, Kellum JA, Talisa VB, Peck Palmer OM, Chang C-CH, Filbin MR, et al. Long-term host immune response trajectories among hospitalized patients with sepsis. *JAMA Netw Open*. (2019) 2:e198686. doi: 10.1001/jamanetworkopen.2019.8686
8. Francois B, Jeannet R, Daix T, Walton AH, Shotwell MS, Unsinger J, et al. Interleukin-7 restores lymphocytes in septic shock: the IRIS-7 randomized clinical trial. *JCI Insight*. (2018) 3:e98960. doi: 10.1172/jci.insight.98960
9. Grimminger F, Mayer K, Seeger W. [Is there a reliable immunotherapy in infection?]. *Internist*. (1997) 38:541–52. doi: 10.1007/PL00002644
10. Hotchkiss RS, Tinsley KW, Swanson PE, Schmieg RE Jr, Hui JJ, Chang KC, et al. Sepsis-induced apoptosis causes progressive profound depletion of B and CD4+ T lymphocytes in humans. *J Immunol*. (2001) 166:6952–63. doi: 10.4049/jimmunol.166.11.6952
11. Tinsley KW, Grayson MH, Swanson PE, Drewry AM, Chang KC, Karl IE, et al. Sepsis induces apoptosis and profound depletion of splenic interdigitating and follicular dendritic cells. *J Immunol*. (2003) 171:909–14. doi: 10.4049/jimmunol.171.2.909
12. Wesche DE, Lomas-Neira JL, Perl M, Chung CS, Ayala A. Leukocyte apoptosis and its significance in sepsis and shock. *J Leukoc Biol*. (2005) 78:325–37. doi: 10.1189/jlb.0105017
13. Flohe SB, Agrawal H, Schmitz D, Gertz M, Flohe S, Schade FU. Dendritic cells during polymicrobial sepsis rapidly mature but fail to initiate a protective Th1-type immune response. *J Leukoc Biol*. (2006) 79:473–81. doi: 10.1189/jlb.0705413
14. Hotchkiss RS, Coopersmith CM, McDunn JE, Ferguson TA. The sepsis seesaw: tilting toward immunosuppression. *Nat Med*. (2009) 15:496–7. doi: 10.1038/nm0509-496
15. Cavassani KA, Carson WF, Moreira AP, Wen H, Schaller MA, Ishii M, et al. The post sepsis-induced expansion and enhanced function of regulatory T cells create an environment to potentiate tumor growth. *Blood*. (2010) 115:4403–11. doi: 10.1182/blood-2009-09-241083
16. Muenzer JT, Davis CG, Chang K, Schmidt RE, Dunne WM, Coopersmith CM, et al. Characterization and modulation of the immunosuppressive phase of sepsis. *Infect Immun*. (2010) 78:1582–92. doi: 10.1128/IAI.01213-09
17. Osuchowski MF, Welch K, Siddiqui J, Remick DG. Circulating cytokine/inhibitor profiles reshape the understanding of the SIRS/CARS continuum in sepsis and predict mortality. *J Immunol*. (2006) 177:1967–74. doi: 10.4049/jimmunol.177.3.1967
18. Adib-Conquy M, Cavaillon J-M. Compensatory anti-inflammatory response syndrome. *Thromb Haemost*. (2009) 101:36–47. doi: 10.1160/TH08-07-0421
19. Schmoeckel K, Mrochen DM, Hühn J, Pötschke C, Bröker BM. Polymicrobial sepsis and non-specific immunization induce adaptive immunosuppression to a similar degree. *PLoS ONE*. (2018) 13:e0192197. doi: 10.1371/journal.pone.0192197
20. Pötschke C, Kessler W, Maier S, Heidecke C-D, Bröker BM. Experimental sepsis impairs humoral memory in mice. *PLoS ONE*. (2013) 8:e81752. doi: 10.1371/journal.pone.0081752
21. Sjaastad FV, Condotta SA, Kotov JA, Pape KA, Dail C, Danahy DB, et al. Polymicrobial sepsis chronic immunoparalysis is defined by diminished Ag-specific T cell-dependent B cell responses. *Front Immunol*. (2018) 9:2532. doi: 10.3389/fimmu.2018.02532
22. Mohr A, Polz J, Martin EM, Griessl S, Kammler A, Potschke C, et al. Sepsis leads to a reduced antigen-specific primary antibody response. *Eur J Immunol*. (2012) 42:341–52. doi: 10.1002/eji.201141692
23. Gustave C-A, Gossez M, Demaret J, Rimmelé T, Lepape A, Malcus C, et al. Septic shock shapes B cell response toward an exhausted-like/Immunoregulatory profile in patients. *J Immunol*. (2018) 200:2418–25. doi: 10.4049/jimmunol.1700929
24. Nutt SL, Hodgkin PD, Tarlinton DM, Corcoran LM. The generation of antibody-secreting plasma cells. *Nat Rev Immunol*. (2015) 15:160–71. doi: 10.1038/nri3795
25. Garcia De Vinuesa C, O'Leary P, Sze DM, Toellner KM, MacLennan IC. T-independent type 2 antigens induce B cell proliferation in multiple splenic sites, but exponential growth is confined to extrafollicular foci. *Eur J Immunol*. (1999) 29:1314–23. doi: 10.1002/(SICI)1521-4141(199904)29:04<1314::AID-IMMU1314>3.0.CO;2-4
26. Coutinho A, Gronowicz E, Bullock WW, Moller G. Mechanism of thymus-independent immunocyte triggering. Mitogenic activation of B cells results in specific immune responses. *J Exp Med*. (1974) 139:74–92. doi: 10.1084/jem.139.1.74
27. Krieg AM, Yi AK, Matson S, Waldschmidt TJ, Bishop GA, Teasdale R, et al. CpG motifs in bacterial DNA trigger direct B-cell activation. *Nature*. (1995) 374:546–9. doi: 10.1038/374546a0
28. Lutzker S, Rothman P, Pollock R, Coffman R, Alt FW. Mitogen- and IL-4-regulated expression of germ-line Ig gamma 2b transcripts: evidence for directed heavy chain class switching. *Cell*. (1988) 53:177–84. doi: 10.1016/0092-8674(88)90379-0
29. Severinson E, Fernandez C, Stavnezer J. Induction of germ-line immunoglobulin heavy chain transcripts by mitogens and interleukins prior to switch recombination. *Eur J Immunol*. (1990) 20:1079–84. doi: 10.1002/eji.1830200520
30. Mandler R, Finkelman FD, Levine AD, Snapper CM. IL-4 induction of IgE class switching by lipopolysaccharide-activated murine B cells occurs predominantly through sequential switching. *J Immunol*. (1993) 150:407–18.
31. Schnare M, Barton GM, Holt AC, Takeda K, Akira S, Medzhitov R. Toll-like receptors control activation of adaptive immune responses. *Nat Immunol*. (2001) 2:947–50. doi: 10.1038/ni712
32. Pasare C, Medzhitov R. Control of B-cell responses by toll-like receptors. *Nature*. (2005) 438:364–8. doi: 10.1038/nature04267
33. Barr TA, Brown S, Ryan G, Zhao J, Gray D. TLR-mediated stimulation of APC: distinct cytokine responses of B cells and dendritic cells. *Eur J Immunol*. (2007) 37:3040–53. doi: 10.1002/eji.200636483
34. Genestier L, Taillardet M, Mondiere P, Gheit H, Bella C, Defrance T. TLR agonists selectively promote terminal plasma cell differentiation of B cell subsets specialized in thymus-independent responses. *J Immunol*. (2007) 178:7779–86. doi: 10.4049/jimmunol.178.12.7779
35. Meyer-Bahlburg A, Rawlings DJ. Differential impact of toll-like receptor signaling on distinct B cell subpopulations. *Front Biosci*. (2012) 17:1499–516. doi: 10.2741/4000
36. Cerutti A, Cols M, Puga I. Marginal zone B cells: virtues of innate-like antibody-producing lymphocytes. *Nat Rev Immunol*. (2013) 13:118–32. doi: 10.1038/nri3383
37. Panda S, Ding JL. Natural antibodies bridge innate and adaptive immunity. *J Immunol*. (2015) 194:13–20. doi: 10.4049/jimmunol.1400844
38. Baumgarth N. The double life of a B-1 cell: self-reactivity selects for protective effector functions. *Nat Rev Immunol*. (2011) 11:34–46. doi: 10.1038/nri2901
39. Savage HP, Baumgarth N. Characteristics of natural antibody-secreting cells. *Ann N Y Acad Sci*. (2015) 1362:132-42. doi: 10.1111/nyas.12799
40. Mebius RE, Kraal G. Structure and function of the spleen. *Nat Rev Immunol*. (2005) 5:606–16. doi: 10.1038/nri1669
41. Weill JC, Weller S, Reynaud CA. Human marginal zone B cells. *Annu Rev Immunol*. (2009) 27:267–85. doi: 10.1146/annurev.immunol.021908.132607
42. Martin F, Kearney JF. B-cell subsets and the mature -preimmune repertoire. Marginal zone and B1 B cells as part of a natural immune memory. *Immunol Rev*. (2000) 175:70–9. doi: 10.1111/j.1600-065X.2000.imr017515.x

43. Martin F, Oliver AM, Kearney JF. Marginal zone and B1 B cells unite in the early response against T-independent blood-borne particulate antigens. *Immunity*. (2001) 14:617–29. doi: 10.1016/S1074-7613(01)00129-7
44. Sha WC, Liou HC, Tuomanen EI, Baltimore D. Targeted disruption of the p50 subunit of NF-kappa B leads to multifocal defects in immune responses. *Cell*. (1995) 80:321–30. doi: 10.1016/0092-8674(95)90415-8
45. Cariappa A, Liou HC, Horwitz BH, Pillai S. Nuclear factor kappa B is required for the development of marginal zone B lymphocytes. *J Exp Med*. (2000) 192:1175–82. doi: 10.1084/jem.192.8.1175
46. MacLennan IC, Toellner KM, Cunningham AF, Serre K, Sze DM, Zuniga E, et al. Extrafollicular antibody responses. *Immunol Rev*. (2003) 194:8–18. doi: 10.1034/j.1600-065X.2003.00058.x
47. Garcia De Vinuesa C, Gulbranson-Judge A, Khan M, O'Leary P, Cascalho M, Wabl M, et al. Dendritic cells associated with plasmablast survival. *Eur J Immunol*. (1999) 29:3712–21.
48. Fairfax KA, Corcoran LM, Pridans C, Huntington ND, Kallies A, Nutt SL, et al. Different kinetics of blimp-1 induction in B cell subsets revealed by reporter gene. *J Immunol*. (2007) 178:4104–11. doi: 10.4049/jimmunol.178.7.4104
49. Berberich S, Dahne S, Schippers A, Peters T, Muller W, Kremmer E, et al. Differential molecular and anatomical basis for B cell migration into the peritoneal cavity and omental milky spots. *J Immunol*. (2008) 180:2196–203. doi: 10.4049/jimmunol.180.4.2196
50. Berberich S, Förster R, Pabst O. The peritoneal micromilieu commits B cells to home to body cavities and the small intestine. *Blood*. (2007) 109:4627–34. doi: 10.1182/blood-2006-12-064345
51. Nguyen H-H, Tran B-T, Muller W, Jack RS. IL-10 acts as a developmental switch guiding monocyte differentiation to macrophages during a murine peritoneal infection. *J Immunol*. (2012) 189:3112–20. doi: 10.4049/jimmunol.1200360
52. Jacobs S, Sobki S, Morais C, Tariq M. Effect of pentaglobin and piperacillin on survival in a rat model of faecal peritonitis: importance of intervention timings. *Acta Anaesthesiol Scand*. (2000) 44:88–95. doi: 10.1034/j.1399-6576.2000.440116.x
53. Shrum B, Anantha RV, Xu SX, Donnelly M, Haeryfar SM, McCormick JK, et al. A robust scoring system to evaluate sepsis severity in an animal model. *BMC Res Notes*. (2014) 7:233. doi: 10.1186/1756-0500-7-233
54. Maier S, Traeger T, Entleutner M, Westerholt A, Kleist B, Hüser N, et al. Cecal ligation and puncture versus colon ascendens stent peritonitis: two distinct animal models for polymicrobial sepsis: two distinct animal models for polymicrobial sepsis. *Shock*. (2004) 21:505–11. doi: 10.1097/01.shk.0000126906.52367.dd
55. Traeger T, Koerner P, Kessler W, Cziupka K, Diedrich S, Busemann A, et al. Colon ascendens stent peritonitis (CASP)–a standardized model for polymicrobial abdominal sepsis. *J Vis Exp*. (2010) 18:2299. doi: 10.3791/2299
56. Zantl N, Uebe A, Neumann B, Wagner H, Siewert JR, Holzmann B, et al. Essential role of gamma interferon in survival of colon ascendens stent peritonitis, a novel murine model of abdominal sepsis. *Infect Immun*. (1998) 66:2300–9. doi: 10.1128/IAI.66.5.2300-2309.1998
57. Wang Z, Rui T, Yang M, Valiyeva F, Kvietys PR. Alveolar macrophages from septic mice promote polymorphonuclear leukocyte transendothelial migration via an endothelial cell Src kinase/NADPH oxidase pathway. *J Immunol*. (2008) 181:8735–44. doi: 10.4049/jimmunol.181.12.8735
58. Allman D, Pillai S. Peripheral B cell subsets. *Curr Opin Immunol*. (2008) 20:149–57. doi: 10.1016/j.coi.2008.03.014
59. Madan R, Demircik F, Surianarayanan S, Allen JL, Divanovic S, Trompette A, et al. Nonredundant roles for B cell-derived IL-10 in immune counter-regulation. *J Immunol*. (2009) 183:2312–20. doi: 10.4049/jimmunol.0900185
60. Wardemann H, Boehm T, Dear N, Carsetti R. B-1a B cells that link the innate and adaptive immune responses are lacking in the absence of the spleen. *J Exp Med*. (2002) 195:771–80. doi: 10.1084/jem.20011140
61. Dogan I, Bertocci B, Vilmont V, Delbos F, Megret J, Storck S, et al. Multiple layers of B cell memory with different effector functions. *Nat Immunol*. (2009) 10:1292–9. doi: 10.1038/ni.1814
62. Busse M, Traeger T, Potschke C, Billing A, Dummer A, Friebe E, et al. Detrimental role for CD4+ T lymphocytes in murine diffuse peritonitis due to inhibition of local bacterial elimination. *Gut*. (2008) 57:188–95. doi: 10.1136/gut.2007.121616
63. Terasawa M, Nagata K, Kobayashi Y. Neutrophils and monocytes transport tumor cell antigens from the peritoneal cavity to secondary lymphoid tissues. *Biochem Biophys Res Commun*. (2008) 377:589–94. doi: 10.1016/j.bbrc.2008.10.011
64. Rangel-Moreno J, Moyron-Quiroz JE, Carragher DM, Kusser K, Hartson L, Moquin A, et al. Omental milky spots develop in the absence of lymphoid tissue-inducer cells and support B and T cell responses to peritoneal antigens. *Immunity*. (2009) 30:731–43. doi: 10.1016/j.immuni.2009.03.014
65. Moon H, Lee JG, Shin SH, Kim TJ. LPS-induced migration of peritoneal B-1 cells is associated with upregulation of CXCR4 and increased migratory sensitivity to CXCL12. *J Korean Med Sci*. (2012) 27:27–35. doi: 10.3346/jkms.2012.27.1.27
66. Manz RA, Thiel A, Radbruch A. Lifetime of plasma cells in the bone marrow. *Nature*. (1997) 388:133–4. doi: 10.1038/40540
67. Chu VT, Beller A, Nguyen TT, Steinhauser G, Berek C. The long-term survival of plasma cells. *Scand J Immunol*. (2011) 73:508–11. doi: 10.1111/j.1365-3083.2011.02544.x
68. Weinstein JS, Delano MJ, Xu Y, Kelly-Scumpia KM, Nacionales DC, Li Y, et al. Maintenance of anti-Sm/RNP autoantibody production by plasma cells residing in ectopic lymphoid tissue and bone marrow memory B cells. *J Immunol*. (2013) 190:3916–27. doi: 10.4049/jimmunol.1201880
69. Cohen J. The immunopathogenesis of sepsis. *Nature*. (2002) 420:885–91. doi: 10.1038/nature01326
70. Hotchkiss RS, Karl IE. The pathophysiology and treatment of sepsis. *N Engl J Med*. (2003) 348:138–50. doi: 10.1056/NEJMra021333
71. Hotchkiss RS, Nicholson DW. Apoptosis and caspases regulate death and inflammation in sepsis. *Nat Rev Immunol*. (2006) 6:813–22. doi: 10.1038/nri1943
72. Brunner M, Krenn C, Roth G, Moser B, Dworschak M, Jensen-Jarolim E, et al. Increased levels of soluble ST2 protein and IgG1 production in patients with sepsis and trauma. *Intensive Care Med*. (2004) 30:1468–73. doi: 10.1007/s00134-004-2184-x
73. Amlot PL, Hayes AE. Impaired human antibody response to the thymus-independent antigen, DNP-Ficoll, after splenectomy. Implications for post-splenectomy infections. *Lancet*. (1985) 1:1008–11. doi: 10.1016/S0140-6736(85)91613-7
74. Ochsenbein AF, Pinschewer DD, Odermatt B, Ciurea A, Hengartner H, Zinkernagel RM. Correlation of T cell independence of antibody responses with antigen dose reaching secondary lymphoid organs: implications for splenectomized patients and vaccine design. *J Immunol*. (2000) 164:6296–302. doi: 10.4049/jimmunol.164.12.6296
75. Altamura M, Caradonna L, Amati L, Pellegrino NM, Urgesi G, Miniello S. Splenectomy and sepsis: the role of the spleen in the immune-mediated bacterial clearance. *Immunopharmacol Immunotoxicol*. (2001) 23:153–61. doi: 10.1081/IPH-100103856
76. Martin F, Kearney JF. Marginal-zone B cells. *Nat Rev Immunol*. (2002) 2:323–35. doi: 10.1038/nri799
77. Kelly-Scumpia KM, Scumpia PO, Weinstein JS, Delano MJ, Cuenca AG, Nacionales DC, et al. B cells enhance early innate immune responses during bacterial sepsis. *J Exp Med*. (2011) 208:1673–82. doi: 10.1084/jem.20101715
78. Jones JM, Amsbaugh DF, Prescott B. Kinetics of the antibody response to type III pneumococcal polysaccharide. II. Factors influencing the serum antibody levels after immunization with an optimally immunogenic dose of antigen. *J Immunol*. (1976) 116:52–64.
79. Amlot PL, Grennan D, Humphrey JH. Splenic dependence of the antibody response to thymus-independent (TI-2) antigens. *Eur J Immunol*. (1985) 15:508–12. doi: 10.1002/eji.1830150516
80. Teixeira FM, Fernandes BF, Rezende AB, Machado RR, Alves CC, Perobelli SM, et al. *Staphylococcus aureus* infection after splenectomy and splenic autotransplantation in BALB/c mice. *Clin Exp Immunol*. (2008) 154:255–63. doi: 10.1111/j.1365-2249.2008.03728.x
81. Fernandes BF, Rezende AB, Alves CC, Teixeira FM, Farias RE, Ferreira AP, et al. Splenic autotransplantation restores IL-17 production and antibody response to *Streptococcus pneumoniae* in splenectomized mice. *Transpl Immunol*. (2010) 22:195–7. doi: 10.1016/j.trim.2009.12.002
82. Ochsenbein AF, Fehr T, Lutz C, Suter M, Brombacher F, Hengartner H, et al. Control of early viral and bacterial distribution and disease by natural antibodies. *Science*. (1999) 286:2156–9. doi: 10.1126/science.286.5447.2156

83. Baumgarth N, Herman OC, Jager GC, Brown LE, Herzenberg LA, Chen J. B-1 and B-2 cell-derived immunoglobulin M antibodies are nonredundant components of the protective response to influenza virus infection. *J Exp Med*. (2000) 192:271–80. doi: 10.1084/jem.192.2.271
84. Hayakawa K, Hardy RR. Development and function of B-1 cells. *Curr Opin Immunol*. (2000) 12:346–53. doi: 10.1016/S0952-7915(00)00098-4
85. Alugupalli KR, Michelson AD, Joris I, Schwan TG, Hodivala-Dilke K, Hynes RO, et al. Spirochete-platelet attachment and thrombocytopenia in murine relapsing fever borreliosis. *Blood*. (2003) 102:2843–50. doi: 10.1182/blood-2003-02-0426
86. Ha SA, Tsuji M, Suzuki K, Meek B, Yasuda N, Kaisho T, et al. Regulation of B1 cell migration by signals through toll-like receptors. *J Exp Med*. (2006) 203:2541–50. doi: 10.1084/jem.20061041
87. Yang Y, Tung JW, Ghosn EE, Herzenberg LA. Division and differentiation of natural antibody-producing cells in mouse spleen. *Proc Natl Acad Sci USA*. (2007) 104:4542–6. doi: 10.1073/pnas.0700001104
88. Schmoeckel K, Traffehn S, Eger C, Potschke C, Broker BM. Full activation of CD4+ T cells early during sepsis requires specific antigen. *Shock*. (2015) 43:192–200. doi: 10.1097/SHK.0000000000000267
89. Lanzavecchia A, Bernasconi N, Traggiai E, Ruprecht CR, Corti D, Sallusto F. Understanding and making use of human memory B cells. *Immunol Rev*. (2006) 211:303–9. doi: 10.1111/j.0105-2896.2006.00403.x
90. Gao N, Dang T, Yuan D. IFN-gamma-dependent and -independent initiation of switch recombination by NK cells. *J Immunol*. (2001) 167:2011–8. doi: 10.4049/jimmunol.167.4.2011
91. Litinskiy MB, Nardelli B, Hilbert DM, He B, Schaffer A, Casali P, et al. DCs induce CD40-independent immunoglobulin class switching through BLyS and APRIL. *Nat Immunol*. (2002) 3:822–9. doi: 10.1038/ni829
92. Elzey BD, Tian J, Jensen RJ, Swanson AK, Lees JR, Lentz SR, et al. Platelet-mediated modulation of adaptive immunity. A communication link between innate and adaptive immune compartments. *Immunity*. (2003) 19:9–19. doi: 10.1016/S1074-7613(03)00177-8
93. Elzey BD, Sprague DL, Ratliff TL. The emerging role of platelets in adaptive immunity. *Cell Immunol*. (2005) 238:1–9. doi: 10.1016/j.cellimm.2005.12.005
94. Wang F, Wang YY, Li J, You X, Qiu XH, Wang YN, et al. Increased antigen presentation but impaired T cells priming after upregulation of interferon-beta induced by lipopolysaccharides is mediated by upregulation of B7H1 and GITRL. *PLoS ONE*. (2014) 9:e105636. doi: 10.1371/journal.pone.0105636
95. Gurung P, Rai D, Condotta SA, Babcock JC, Badovinac VP, Griffith TS. Immune unresponsiveness to secondary heterologous bacterial infection after sepsis induction is TRAIL dependent. *J Immunol*. (2011) 187:2148–54. doi: 10.4049/jimmunol.1101180
96. Cinel I, Opal SM. Molecular biology of inflammation and sepsis: a primer. *Crit Care Med*. (2009) 37:291–304. doi: 10.1097/CCM.0b013e31819267fb

Conflict of Interest: The authors declare that the research was conducted in the absence of any commercial or financial relationships that could be construed as a potential conflict of interest.

frontiers in Immunology

ORIGINAL RESEARCH
published: 30 April 2020
doi: 10.3389/fimmu.2020.00675

Sepsis Triggers a Late Expansion of Functionally Impaired Tissue-Vascular Inflammatory Monocytes During Clinical Recovery

*Camille Baudesson de Chanville[1], Benjamin Glenn Chousterman[2], Pauline Hamon[1], Marie Laviron[1], Noelline Guillou[1], Pierre Louis Loyher[1], Aida Meghraoui-Kheddar[1], Sandrine Barthelemy[1], Philippe Deterre[1], Alexandre Boissonnas[1] and Christophe Combadière[1]**

[1] Sorbonne Université, Inserm, CNRS, Centre d'Immunologie et des Maladies Infectieuses, Cimi-Paris, Paris, France, [2] Inserm UMRS 1160, Département d'Anesthésie-Réanimation, Hôpitaux Universitaires Lariboisière-Saint-Louis, Paris, France

OPEN ACCESS

Edited by:
Vladimir Badovinac, University of Iowa, United States

Reviewed by:
Philipp von Hundelshausen, Ludwig Maximilian University of Munich, Germany
Mathieu Paul Rodero, UMR8601 Laboratoire de Chimie et Biochimie Pharmacologiques et Toxicologiques, France

***Correspondence:**
Christophe Combadière
christophe.combadiere@upmc.fr

Specialty section:
This article was submitted to Inflammation, a section of the journal Frontiers in Immunology

Received: *09 December 2019*
Accepted: *25 March 2020*
Published: *30 April 2020*

Citation:
Baudesson de Chanville C, Chousterman BG, Hamon P, Laviron M, Guillou N, Loyher PL, Meghraoui-Kheddar A, Barthelemy S, Deterre P, Boissonnas A and Combadière C (2020) Sepsis Triggers a Late Expansion of Functionally Impaired Tissue-Vascular Inflammatory Monocytes During Clinical Recovery. Front. Immunol. 11:675. doi: 10.3389/fimmu.2020.00675

Sepsis is characterized by a systemic inflammation that can cause an immune dysfunction, for which the underlying mechanisms are unclear. We investigated the impact of cecal ligature and puncture (CLP)-mediated polymicrobial sepsis on monocyte (Mo) mobilization and functions. Our results show that CLP led to two consecutive phases of Mo deployment. The first one occurred within the first 3 days after the induction of the peritonitis, while the second phase was of a larger amplitude and extended up to a month after apparent clinical recovery. The latter was associated with the expansion of Mo in the tissue reservoirs (bone marrow and spleen), their release in the blood and their accumulation in the vasculature of peripheral non-lymphoid tissues. It occurred even after antibiotic treatment but relied on inflammatory-dependent pathways and inversely correlated with increased susceptibility and severity to a secondary infection. The intravascular lung Mo displayed limited activation capacity, impaired phagocytic functions and failed to transfer efficient protection against a secondary infection into monocytopenic CCR2-deficient mice. In conclusion, our work unveiled key dysfunctions of intravascular inflammatory Mo during the recovery phase of sepsis and provided new insights to improve patient protection against secondary infections.

Keywords: monocytes, sepsis, lung, secondary infection, phagocytosis

INTRODUCTION

Representing the major cause of admission and death in intensive care units (ICU) (1), sepsis is defined as a life-threatening organ dysfunction caused by a dysregulated host response to an infection (2). Despite adequate treatments, over 20% of septic patients die within 28 days after their admission to the ICU or within the first year after recovery, from secondary infections. Survivors suffer from long-term chronic critical illness often associated with prolonged inflammation, immune suppression, organ injury, and lean tissue wasting (3, 4). It is thought that dysfunctions in both the innate and the adaptive immune system account for the poor outcome in sepsis.

Recent works have focused on understanding how the immune system dysfunctions may contribute to long-term immunosuppression and prolonged sensitivity to secondary infections (4).

In the early phase of sepsis, the expansion of immature myeloid cells has attracted much attention (5). They display impaired functions and are reminiscent of myeloid-derived suppressor cells (MDSC) with potent immunosuppressive properties (6). Early sepsis-impaired myeloid functions have been shown to promote nosocomial infections (5, 7). The late phase of sepsis is characterized by T cell exhaustion and a relative increase in regulatory T cells (8, 9), a quantitative and qualitative defect of dendritic cells (10), the deactivation of Mo, demonstrated by the reduced expression of the activation marker HLA-DR (11, 12) as well as the impaired production of cytokines (13). However, not much is known about the kinetic of monocyte (Mo) mobilization throughout sepsis. Two subsets of blood Mo are commonly described in mice and humans: the classical or inflammatory Mo, which are rapidly mobilized upon inflammation in a CC-chemokine receptor 2 (CCR2)-dependent manner, and the non-classical or patrolling Mo that patrols the intraluminal side of the endothelium. In the mouse, inflammatory Mo are short lived, express high levels of Ly6C and CCR2. They are precursors of longer-lived patrolling Mo that lack Ly6C and CCR2 but express higher CX3C-chemokine receptor 1 (CX3CR1) (14). In a previous work, we showed that, soon after the induction of a highly-lethal peritonitis, inflammatory Mo ($Ly6C^{high}$ Mo) migrate from the bone marrow to the blood, adhere in a CX3CR1-dependent way to the endothelium of the renal cortex and protect the kidneys from inflammatory-triggered damages (15). However, the model used in this study does not sufficiently resemble the clinical setting of sepsis in humans, for which the mortality rate is not as elevated. We thus chose to study the distribution, the phenotype and the role of the Mo in a sublethal murine model of peritonitis induced by cecal ligation and puncture (CLP), during the sepsis and following a secondary bacterial infection.

MATERIALS AND METHODS

Mice

All experiments and protocols were approved by the local animal experimentation ethics committee validated by the "Service Protection et Santé Animales, Environnement" with the number APAFIS#4369-2016030218219240 v3. Specific pathogen-free C57BL/6 mice were purchased from Janvier Labs (Le Genest, Saint Isle, France). $Ccr2^{-/-}$(#004999, JAX), $Cx3cr1^{-/-}$ (16), $Cx3cr1^{gfp/gfp}$ (17), MacBlue or *Csf1r-Gal4VP16/UAS-ECFP* (18), MacBlue x $Cx3cr1^{gfp/+}$ mice were bred in our animal facility. Age-matched mice (8–12 weeks old) were used for this study.

Polymicrobial Sepsis Induction

We used a cecal ligation and puncture model as previously described (19). Mice were anesthetized and underwent laparotomy. For Sham-operated mice, the cecum was exteriorized and reinserted in the abdomen. For the CLP-operated mice, sepsis was triggered by the ligature of one third of the cecum and a double enterotomy with a 25-gauge needle. A small amount of fecal material was extruded after removing the needle and the cecum was reinserted in the abdomen. After surgery, the animals were injected with a saline solution and buprenorphine (Vetergesic, Oostkamp, Belgium) for postoperative analgesia. For some experiments, 2 mg/kg of Dexamethasone (Intervet, Beaucouze, France) or 10 mg/kg Enrofloxacine (Axience, Pantin, France) were injected intraperitoneally 24 h after CLP and every 2 for 10 days. Splenectomies were performed prior to CLP procedure. A small upper-quadrant incision was made to expose the spleen. The splenic vessels were tied up and the spleen was removed by transecting the vessels just distal to the ligature.

Escherichia coli Lung Infection

The fluorescent Escherichia coli strain MG1655 ykgH::pTet-dsRed (BGene Genetics, Grenoble, France) was grown overnight in Luria-Bertani (LB) broth (Sigma-aldrich, St Louis, USA) then transferred to fresh medium and grown for 4–5 h to mid-log phase. The OD_{600} was adjusted to give the appropriate desired inoculums, then centrifuged at 4,000 g for 15 min. Bacterial pellets were resuspended in 30 µl of sterile phosphate-buffered saline (PBS) for each sample. To induce secondary *E. coli* lung infection, 10 days after CLP, the trachea was exposed and 30 µl of a bacterial suspension (5×10^7 cfu/mouse for survival studies, 5×10^9 cfu/mouse for adoptive transfer experiments, or 1×10^7 cfu/mouse for all other studies) or sterile PBS were administered intratracheally to sham- or CLP-operated mice 24 and 48 h before sacrifice. This procedure was performed under Ketamine/Xylazine anesthesia.

Adoptive Transfer Experiments

Bone marrow cells were isolated 10 days after CLP or sham procedure in WT mice. Mo were isolated after negative selection removal of other cell types, with Ly6G, CD3, CD4, CD19, NK1.1, and SiglecF-PE labeled antibodies. Marked cells were then captured via a magnetic device for cell separation and anti-PE magnetic beads, according to the manufacturer's instructions (Miltenyi Biotec, Paris, France). Thirty million monocytes were injected intravenously in $Ccr2^{-/-}$ mice, and *E.coli* (5×10^9 cfu/mouse) were injected intratracheally 30 min later. The proportions of Mo adoptively transferred from each condition were controlled before transfer by flow cytometry and were identical. Mo represented between 12 and 16% of myeloid cells and were enriched by 70–80% after sorting. PMN population was <1%. Mice were monitored every 12 h for survival and surviving mice were used for quantification of protein in lung homogenates at day 4.

Bronchoalveolar Lavage (BAL) and Bacterial Load

BAL were performed on mice 48 h after the secondary lung injection. The BAL performed with 3 ml of sterile PBS was diluted and plated on LB agar plates to obtain viable bacterial counts (cfu/BAL).

Cell Isolation and Preparation

Heparinized blood samples were stained with antibodies and erythrocytes were lysed with buffer containing 0.15M NH4Cl, 0.01 mM KHCO3, and 0.1 mM EDTA. Bone marrow cells were harvested by flushing out the thighbone with PBS. Lung,

spleen, kidney, and liver were harvested and digested in RPMI medium (Gibco, Invitrogen, Cergy Pontoise, France) with 1 mg/ml collagenase IV (Sigma, St Quentin Fallavier, France), 0,1 mg/ml DNAse 1 (Roche, Boulogne Billancourt, France) for 30 min at 37°C and dissociated through a 40-μm-pore cell strainer (Becton Dickinson, Rungis, France). Diluted suspension cells were incubated with 1 μg/ml purified anti-CD16/32 (clone 2.4G2, BD Biosciences) for 10 min at 4°C then surface staining was performed with an additional 20 min incubation with appropriate dilution of the surface marker antibodies. Cell suspensions were washed once in FACS buffer (0.5% BSA, 2 mM EDTA and PBS) and analyzed directly by flow cytometry.

Blood/Tissue Partitioning

Intravascular CD45 labeling was performed as previously described (20, 21). Mice were injected intravenously with 2 μg of anti-CD45 (clone 30-F11, BD Biosciences). Two minutes after injection, blood was drawn and the mice were sacrificed. Harvested organs were bathed in a large volume of PBS. CD45 labeled cells in all tissues were considered to be intravascular (CD45vivo+) and unlabelled cells (CD45vivo-) were considered to be parenchymal.

Flow Cytometry

The panel of antibodies comprised: BUV395-CD11b (clone M1/70), APC-Cy7-Ly6C (clone AL21), V450-Ly6G (clone 1A8), BV711-NK1.1 (clone PK136), BV605-CD11c (clone HL3), BV510-I-A/I-E (clone M5/114.15.2), BV786-SiglecF (clone E50-2440), BUV737-CD80 (clone 16-10A1), APC-R700-CD86 (clone GL1), APC-PDL1 (clone MIH5), APC-IL6 (clone MP5-20F3), BV421-TNFα (clone MP6-XT22), which were from BD Biosciences, and FITC-CX3CR1 (clone SA011F11) and PE-Cy7-CD64 (clone X54-5/7.1), which were from Biolegend. Relative changes in cytosolic nitric oxide (NO) concentration were monitored using the fluorescent nitric oxide probe DAF-FM (Molecular Probes, Eugene, OR). The cells extracted from the lungs were incubated with DAF-FM diacetate (5 μM) for 30 min at 37°C. After an extensive wash, cells were stained with fluorescent surface antibodies and NO production was measured in monocytes by flow cytometry. For IL-6 and TNFα staining, cells were preincubated for 3 h at 37°C in RPMI medium supplemented with GlutaMAX with a cell activation cocktail containing Brefeldin A according to the manufacturer's instructions (BioLegend). After surface staining, the cells were fixed in 4% paraformaldehyde for 20 min, washed twice in Perm/Wash solution (BD Biosciences), incubated for 10 min with 1 μg/mL purified anti-CD16/32 in Perm/Wash at room temperature, and incubated for 30 min in Perm/Wash in the presence of APC-anti-IL-6 (BD Pharmingen) or BV421-anti-TNFα (BD Horizon). Flow cytometry acquisition was performed on the flow cytometer FACS LSRFortessa X-20® (BD, Franklin Lakes, NJ, USA) with DIVA® Flow Cytometry software, and the data was analyzed with FlowJo software (Tree Star, Inc, Ashland, Or, USA). Absolute numbers were calculated by adding to each vial a fixed number (10,000) of non-fluorescent 10-μm polybead® carbocylate microspheres (Polysciences, Niles, IL, USA) according to the formula: No. Cells = (No. acquired cells x 10,000)/(No. acquired beads) x dilution factor of cells.

In vitro Cell Stimulation

Lung cell suspensions (3×10^5 cells from Sham mice or 3×10^4 cells from CLP-operated mice) were plated in 96 well plates and stimulated with either Cell Activation Cocktail PMA/Ionomycin at 1X (Biolegend, San Diego, USA) or 2 ng/ml of LPS (Sigma-Aldrich, St Louis, USA) in RPMI containing 10% FBS for 3 h at 37°C with 5% CO_2. Cells were recovered and washed with fresh PBS 1X and then stained for flow cytometry analysis.

Phagocytosis Assay

For *in vivo* phagocytosis, a total of 1×10^7 cfu/mouse of DS-Red fluorescent *Escherichia coli* were intratracheally injected 10 days after CLP surgery (as described previously). Phagocytosis by lung cells was analyzed 24 and 48 h after infection by flow cytometry. The fluorescence of phagocytic cells was also observed in histological sections. Control mice were injected with sterile PBS under the same experimental conditions. *In vitro* phagocytosis was performed with lung cells suspension obtained 10 days after CLP mixed with 5×10^5 cfu of DS-Red fluorescent *Escherichia coli* at a 1:5 ratio (cells/bacteria) during 4 h at 37° or 4°C for the control experiment. Percentage of $Ly6C^{high}$ Mo phagocytosis was determined by flow cytometry. In the 4°C control condition, phagocytosis index was <3%.

RNA Extraction and Quantitative Real-Time PCR

Lungs were harvested 48 h after the E. coli lung infection 10 days post CLP. Cells were isolated as described above. Total RNA was extracted using the RNeasy Mini Kit (QIAGEN, Les ulis, France) according to the manufacturer's instructions. RNA concentration was determined by absorption at 260 nm. cDNA synthesis was performed with SuperScript VILO cDNA Synthesis Kit (Invitrogen). The polymerase chain reaction was performed on an ABI prizm 7300 using Power SYBR Green PCR Master Mix (Life technologies, California, USA) and GAPDH was used as the control gene. Primers for iNOS: F-CCAAGCCCTCACCTAC TTCC; R-CTCTGAGGGCTGACACAAGG, IL-4: F- CCATAT CCACGGATGCGACA; R- AAGCCCGAAAGAGTCTCTGC, IL-10: F- GCTCTTACTGACTGGCATGAG; R- CGCAGCT CTAGGAGCATGTG, IL-6: F- CGGCCTTCCTACTTCACAA; R- GGTACTCCAGAAGACCAGAGGA, TGFB: F- atgctaaagag gtcacccgc; R- GTATCAGTGGGGGTCAGCAG, CCL2: F- CCCC ACTCACCTGCTGGTA; R- TTACGGGTCAACTTCACAT TCAAA.

For transcript-level analysis, results were expressed as a fold increase relative to sham condition at day 10.

Multi-Photon Imaging

Freshly explanted lungs were immobilized in an imaging chamber perfused with oxygenated (95% O2 plus 5% CO_2) RPMI medium containing 10% FCS. The local temperature was monitored and maintained at 37°C. For some experiments, 10 μg of anti-CD31 (AF647; clone 390) were injected intravenously 2 min before euthanasia. The Two-Photon Laser Scanning

Microscopy (TPLSM) set-up used was a Zeiss 7MP (Carl Zeiss, Germany) coupled to a Ti:Sapphire Crystal multiphoton laser (Coherent ChameleonU, CA, USA) which provides 140fs pulses of NIR light, selectively tunable between 680 and 1,050 nm and an optical parametric oscillator (OPO-MPX, Coherent) selectively tunable between 1,050 and 1,600 nm. The system included a set of external non-descanned detectors in reflection with a combination of a LP-600 nm followed by LP-462 nm and LP-500 nm dichroic mirrors to split the light and collect the ECFP with a 480/40 nm emission filter, EGFP with a 525/50 nm emission filter. The excitation wavelength was 870 nm for the NLO beam and 1,100 nm for the OPO beam.

Lung Protein Quantification

The mouse lung vasculature was gently flushed with an intracardiac injection of PBS until complete blood clearance, then lungs were collected and crushed in 1 ml of PBS. The supernatant of pulmonary crushed tissue was used to quantify protein level by enzymatic assay, BCA protein assay (Pierce, Waltham, USA) according to the manufacturer's standard protocol.

Data Presentation and Statistical Analysis

The data are presented as mean ± standard error of the mean (s.e.m.) of the indicated number of experiments. Groups were compared with Prism software (Graphpad, San Diego, USA). Statistical analyses were performed using two-tailed Student's *t*-test for two-group comparisons, or one-way and two-way ANOVA tests with Bonferoni multiple comparison tests: * for $p < 0.05$; ** for $p < 0.01$; *** for $p < 0.001$; **** for $p < 0.0001$. Kaplan-Meier survival curves were compared with a log-rank test, where $p < 0.05$ was considered statistically.

RESULTS

Polymicrobial Sepsis Induces Two Distinct Phases of Monocyte and of Neutrophil Deployment in the Blood and Organs

We characterized the myeloid composition of the blood and organs in a mouse model of peritonitis induced by cecal ligation and puncture (CLP) which results in polymicrobial sepsis and inflammation (15, 19). In the chosen conditions, 100% of the mice suffered from severe weight loss (**Supplementary Figure 1A**) and about 10% of the mice succumbed in the first 4 days (**Supplementary Figure 1B**). For surviving mice, normal weight was almost recovered within 10 days following surgery (**Supplementary Figure 1A**). Mo subsets and PMN distributions were analyzed by flow cytometry using a conventional gating strategy (**Figure 1A**) to identify classical Mo named here Ly6C^{high} Mo (defined as CD11b$^+$/Ly6G$^-$/CX3CR1$^+$/Ly6C^{high}), non-classical Mo named here Ly6C^{low} Mo (defined as CD11b$^+$/Ly6G$^-$/CX3CR1$^+$/Ly6C^{low}) and PMN (defined as CD11b$^+$/Ly6G$^+$/CX3CR1$^-$). Eosinophils were excluded by SiglecF expression, Natural Killer cells by NK1.1 and alveolar macrophages by siglecF and CD64 (not shown). During the acute phase, a few hours after sepsis induction (**Figure 1B**, left panels), Ly6C^{high} Mo numbers decreased in the bone marrow (upper panels) and the spleen (upper middle panel) and remained low until day 5. During this period, Ly6C^{low} Mo numbers remained fairly constant in these tissues. The numbers of blood Ly6C^{high} and Ly6C^{low} Mo remained stable for the first few days after sepsis (lower middle panel) whereas both Mo subpopulations accumulated rapidly in the lungs (day 1–2; first wave) as previously observed in the kidney (15), and returned to baseline by day 5 (lower panel). Along with mice weight recovery (a week after CLP induction), the numbers of Ly6C^{high} Mo increased dramatically in all tissues; bone marrow (∼2-fold), blood (∼50-fold), spleen (∼3-fold) and lungs (∼20-fold) peaking between day 10 and 15 and returning back to sham values only by day 50. Again, variations in the number of Ly6C^{low} Mo were modest during this time period (7–50 days) compared to that of Ly6C^{high} Mo. PMN underwent a kinetic of mobilization similar to that of Ly6C^{high} Mo in all four studied tissues (**Figure 1B**, right panels). Between 4 and 10 days, the number of alveolar macrophages dropped massively and recovered thereafter (**Supplementary Figure 1C**). Strong accumulations of both Ly6C^{high} Mo and PMN were also observed during weight recovery in the kidneys (∼5 and 10-fold, respectively) and in the liver (∼40 and 30-fold, respectively) arguing for a systemic accumulation of Mo and PMN in non-lymphoid tissues (**Figure 1C**). Globally, polymicrobial sepsis induced two distinct phases. The "early acute phase" is characterized by extensive weight loss and death. This phase is associated with a massive Mo and PMN mobilization to the lungs correlating with a deep draining of the myeloid tissue reservoirs, the bone marrow and the spleen. The second phase is characterized by clinical improvements and weight recovery. This "recovery phase" is associated with Mo and PMN expansion in the tissue reservoirs, release in the blood and accumulation in peripheral non-lymphoid tissues including the lungs, liver and kidneys.

Ly6C^{high} Mo Deployment During the Recovery Phase Requires Inflammatory Pathways

We looked into characterizing what drives Mo and PMN redistributions during weight recovery. Expanded populations of both Mo and PMN in septic conditions are thought to originate from bone marrow precursors (22), but in inflammatory conditions the spleen can develop extra medullary myelopoiesis (23). The accumulation of Ly6C^{high} Mo in blood, lungs and bone marrow were similar in mice both splenectomized or not (**Figure 2A**). These data indicate that the spleen is dispensable in CLP-elicited Mo deployment and suggest that this phenomenon may rely solely on bone marrow. Because both infections and inflammation are known to elicit changes in myelopoiesis and mobilization, CLP-operated mice were treated with antibiotics or anti-inflammatory drugs. The broad-spectrum antibiotic treatment did not alter the late accumulation of either Ly6C^{high} Mo nor PMN in the different tissues (**Figure 2A** and **Supplementary Figure 2A**). Conversely, anti-inflammatory treatment with Dexamethasone abrogated the CLP-triggered accumulation of Ly6C^{high} Mo, Ly6C^{low} Mo (**Supplementary Figure 2B**) and PMN

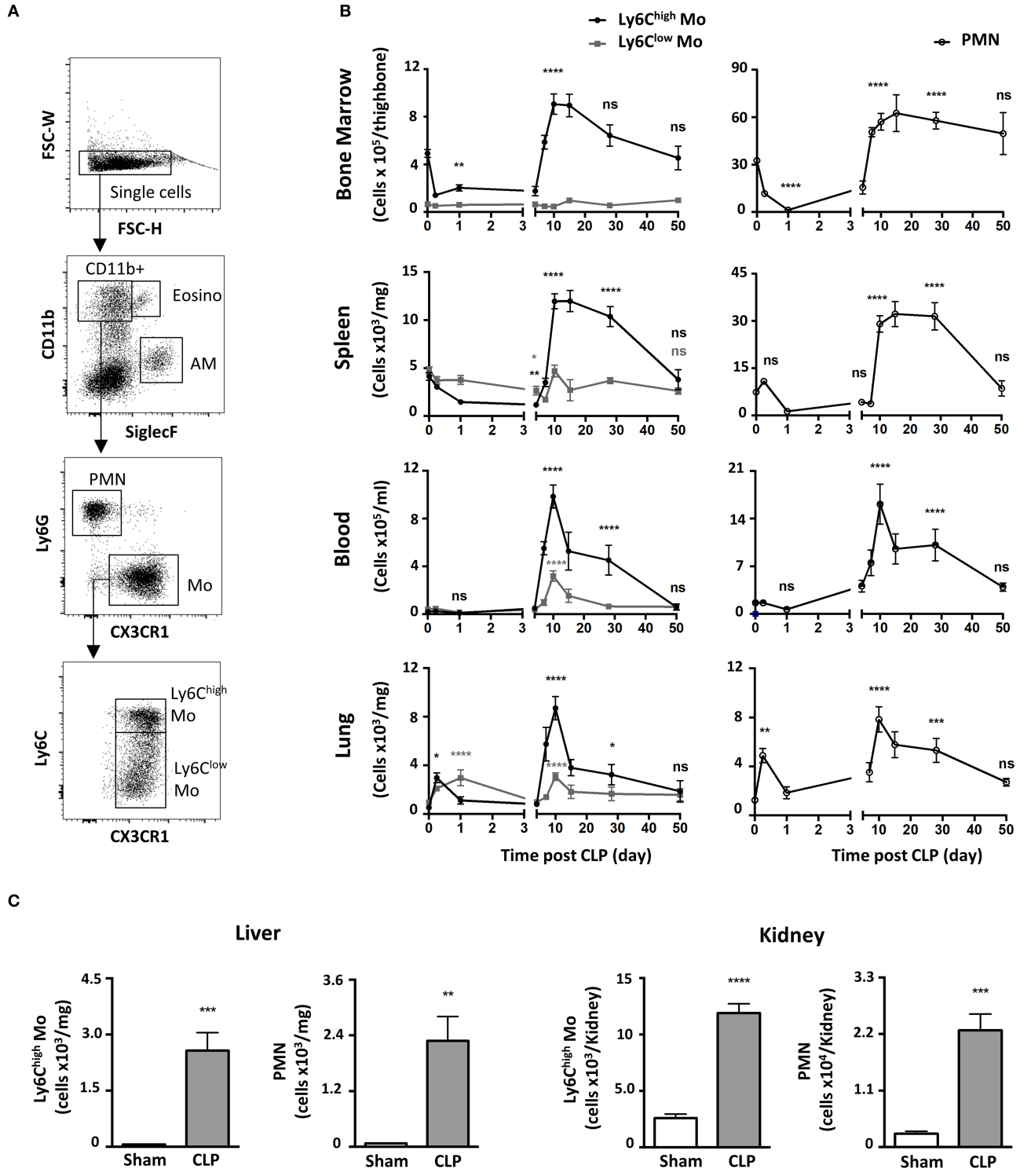

FIGURE 1 | Polymicrobial sepsis induces two distinct phases of Mo and of neutrophil deployment in the blood and organs. **(A)** Representative flow cytometry gating strategy for myeloid subsets in the lung: Eosinophils (Eosino), Alveolar Macrophages (AM), Polymorphonuclear Neutrophils (PMN), classical Mo (Ly6C^{high} Mo), non-classical Mo (Ly6C^{low} Mo). **(B)** Ly6C^{high}, Ly6C^{low} Mo, and PMN numbers in the bone marrow, spleen, blood, and lungs as determined by flow cytometry at different time points after CLP. Tissue-resident macrophages were excluded from analysis based on CD64 expression. The baseline was defined on the cell number obtained in sham-operated mice. Each time point represents at least three independent experiments run with 6 to 12 mice. Statistical analyses compare the different time points after CLP to baseline. **(C)** Numbers of Ly6C^{high} Mo and PMN in the liver (left panel) and the kidneys (right panel), 10 days after sham- (white) and CLP-operated (gray) mice. Values represent the mean and standard error of the mean (sem) of 6 mice per group from two independent experiments. Unpaired Student's *t* test was performed. $^{*}p < 0.05$; $^{**}p < 0.01$; $^{***}p < 0.001$; $^{****}p < 0.0001$.

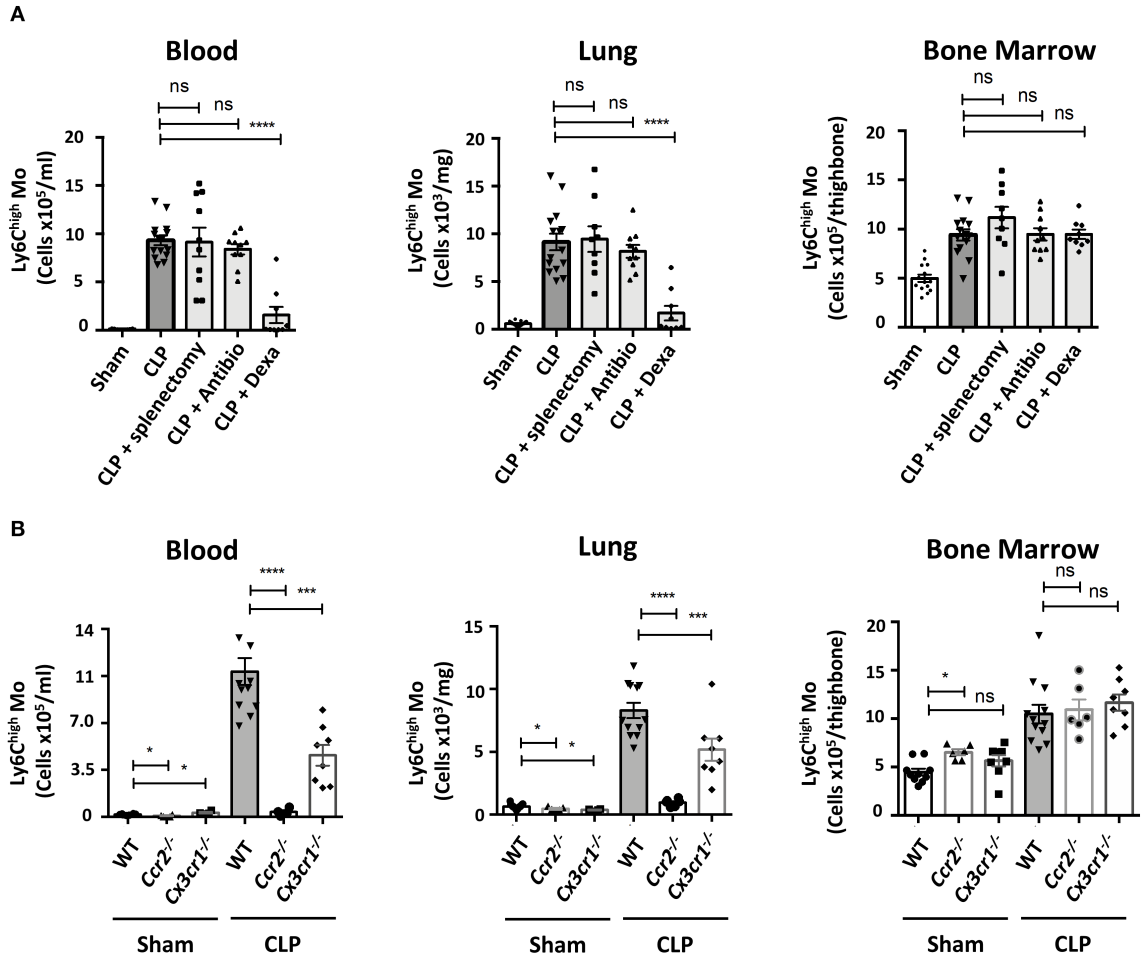

FIGURE 2 | Ly6C^{high} Mo deployment during the recovery phase requires inflammatory pathways. **(A)** Numbers of Ly6C^{high} Mo in the blood, lungs and bone marrow determined by flow cytometry in sham and septic mice, 10 days after CLP and treatments. Splenectomies were performed a few minutes before the CLP. Antibiotic or Dexamethasone treatments were injected 24 h after CLP. Values represent the mean and standard error of the mean of 9–14 mice per group from two independent experiments. Two-way ANOVA tests with Bonferoni multiple comparison tests compare each group (light gray) to the CLP controls (dark gray); **** for $p < 0.0001$. **(B)** Numbers of Ly6C^{high} Mo in the blood, lungs, and bone marrow determined by flow cytometry, 10 days after sham- and CLP-operated WT ($n = 12$), *Ccr2*$^{-/-}$ ($n = 6$), and *Cx3cr1*$^{-/-}$ ($n = 8$) mice from at least two independent experiments. Two-way ANOVA tests with Bonferoni multiple comparison tests compare chemokine receptor deficient mice to the WT mice, * for $p < 0.05$; *** for $p < 0.001$; **** for $p < 0.0001$.

(**Supplementary Figure 2A**) in the blood and the lungs but had no effect on bone marrow. We next thought to identify inflammatory chemokine receptors leading to Mo mobilization (**Figure 2B**). As previously observed, *Ccr2*$^{-/-}$ or *Cx3cr1*$^{-/-}$ sham operated mice displayed less classical Mo in the lungs (20, 24). In septic mice, monocytosis was totally or partially reduced in the blood and the lungs of *Ccr2*$^{-/-}$ or *Cx3cr1*$^{-/-}$ mice, respectively. The absolute number of the Ly6C^{high} Mo in the bone marrow remained unaffected by these chemokine receptor deficiencies (**Figure 2B**). CCR2 and CX3CR1 deficiency did not affect PMN or alveolar macrophage numbers compared to WT mice (**Supplementary Figures 2C,D**), confirming the selective role of these two chemokine axes in the regulation of Mo deployment to the lungs during the recovery phase.

Late-Expanded Mo Display an Altered Phenotype and Remain Intravascular in the Lungs of Septic Mice

We next characterized the phenotype of the Mo accumulating into the lungs during the recovery phase of sepsis. Ten days after CLP (**Figure 3A**), MHC class II expression on Ly6C^{high} Mo was reduced by more than 50%, as previously reported (11, 12). CX3CR1 expression was reduced by 20% compared to sham-operated mice, whereas expression of the EGFP reporter from *Cx3cr1*$^{egfp/+}$ mice was severely reduced, as previously reported (25, 26). Conversely, CD64 expression doubled on Ly6C^{high} Mo from CLP-operated mice and CD11b expression was modestly increased. CD62L expression remained unchanged. In order to further investigate the tissue localization of Mo in the lung, we performed blood/tissue partitioning using *in vivo* CD45 labeling

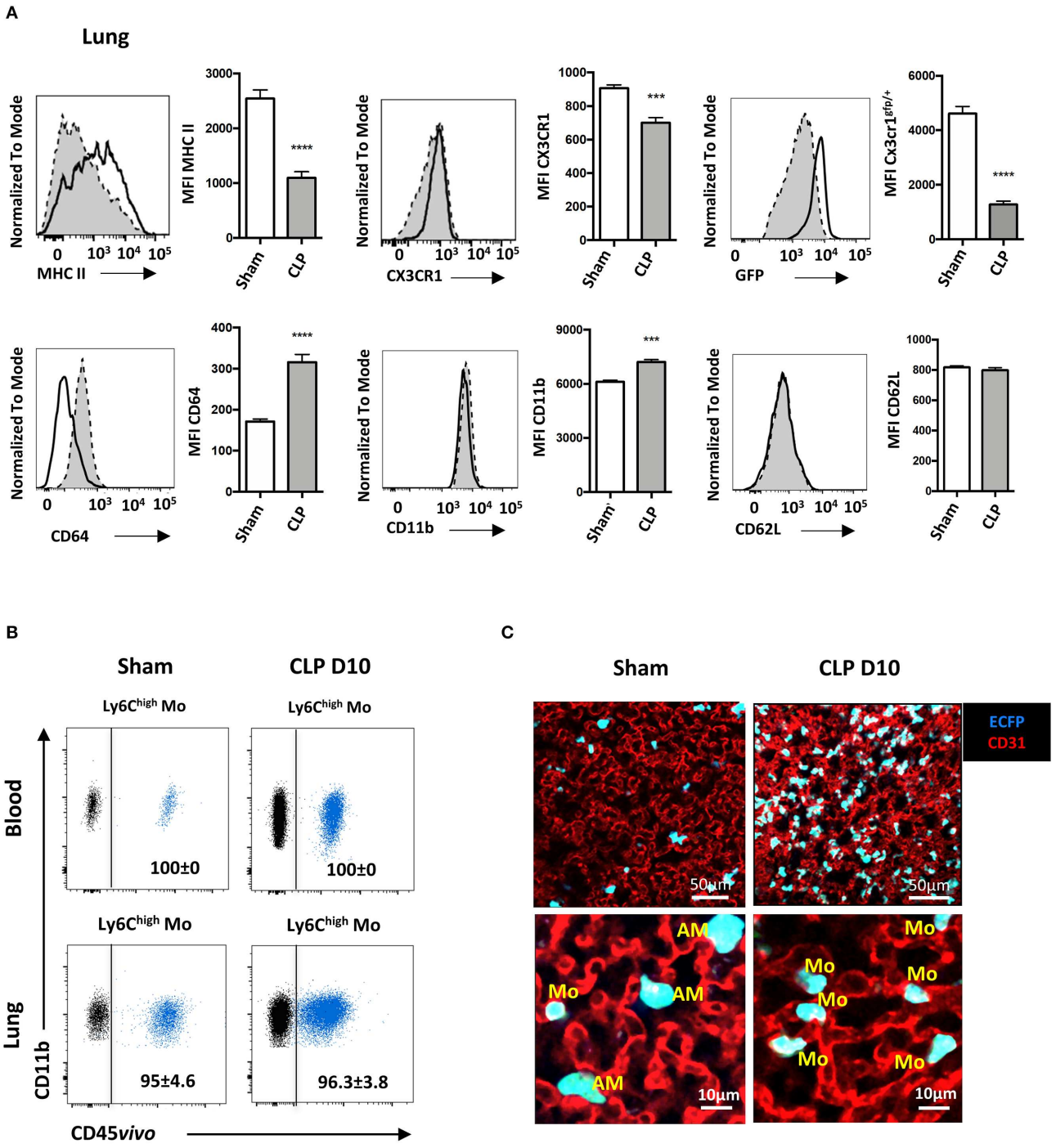

FIGURE 3 | Late-expanded Mo display an altered phenotype and remain intravascular in the lungs of septic mice. **(A)** Overlay of flow cytometric surface marker expression gated on Ly6C^{high} Mo in the lungs of sham- (black line) and CLP-operated (dotted line) mice, 10 days after CLP. Histograms represent mean fluorescence intensity (MFI) of surface marker expression: MHC-II, CX3CR1, GFP, CD64, CD11b, and CD62L. Values represent the mean and standard error of the mean of 15 sham- and 12 CLP-operated mice from three repeated experiments. The GFP fluorescent reporter of Cx3cr1 expression was performed on 9 sham- and 9 CLP-operated *Cx3cr1*$^{gfp/+}$ mice. Unpaired Student's *t* test was performed. **(B)** Representative overlayed dot plots of *in vivo* CD45 staining (blue) gated on blood (upper panels) and lung (lower panels) of Ly6C^{high} Mo. Background staining shown in black was measured in mice not injected with the anti-CD45. **(C)** Representative images of two-photon microscopy of explanted lungs from sham- or CLP-operated MacBlue x Cx3cr1$^{gfp/+}$ mice. Lung vasculature is visualized using anti-CD31 staining (red), and Mo were observed using ECFP reporter. Inserts represent a 5x zoom showing a few alveolar macrophages (AM) in the alveolar lumen (black space) in a sham-operated mouse and intravascular Mo in a CLP-operated mouse. ***$p < 0.001$; ****$p < 0.0001$.

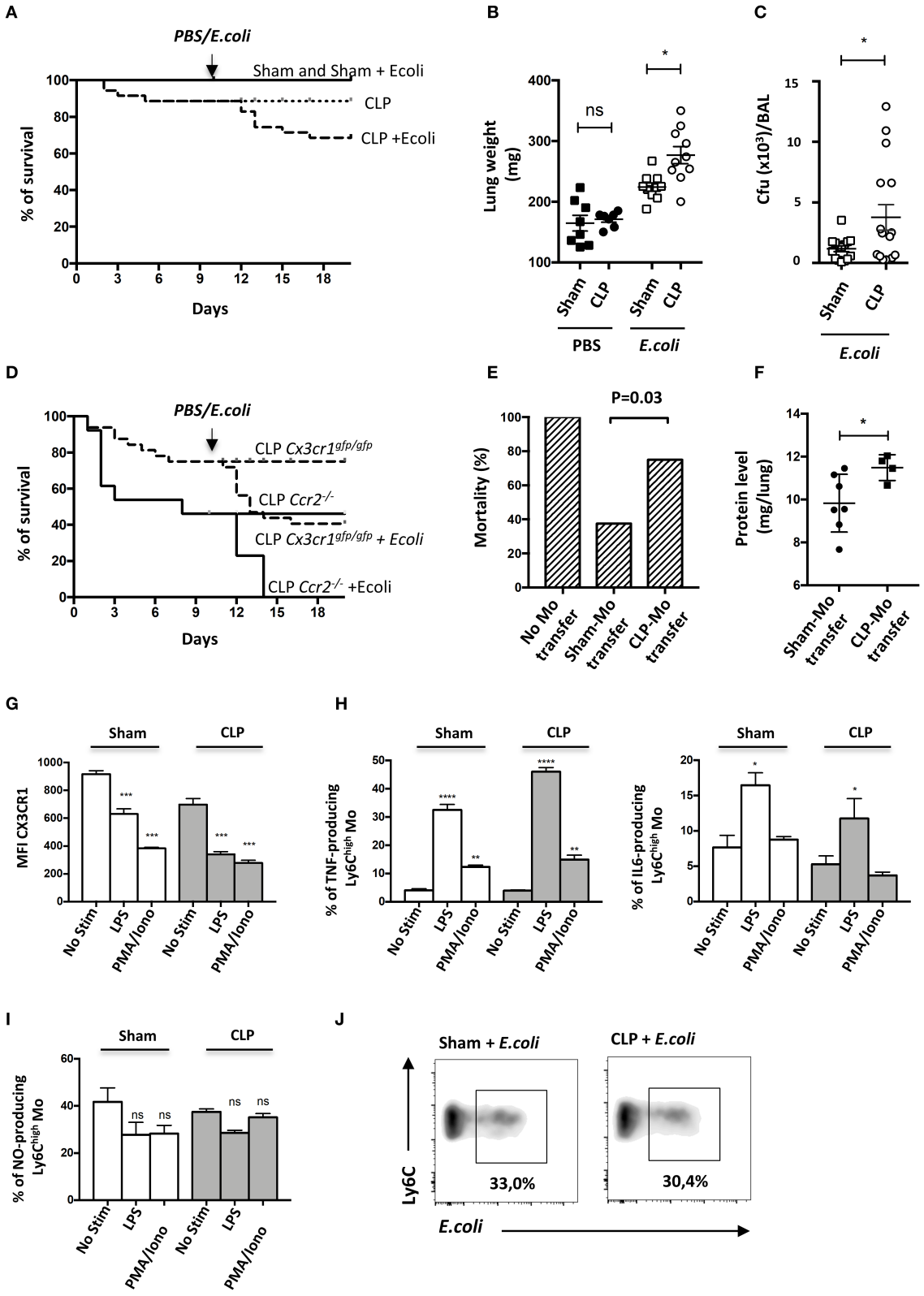

FIGURE 4 | Mo of the late recovery phase of sepsis display an altered phenotype and fail to protect from a secondary infection. **(A)** Survival of sham- or CLP-operated *Cx3cr1*$^{gfp/+}$ mice with intratracheal injection of *Escherichia coli* on day 10 after surgery (n = 8–12 per group). **(B)** Total lung weight of sham- and CLP-operated C57Bl6 mice at 48 h after *E. coli* secondary infection. Unpaired Student's t test was performed. **(C)** Bacterial colonization of bronchoalveolar lavages

(Continued)

FIGURE 4 | (BAL) from sham- and CLP-operated C57Bl6 mice at 48 h after *E. coli* secondary infection. Unpaired Student's *t* test was performed. **(D)** Survival of sham^{-} or CLP-operated *Cx3cr1*$^{gfp/gfp}$ ($n = 12$ per group) and *Ccr2*$^{-/-}$ ($n = 8$–10 per group) mice with intratracheal injection of *Escherichia coli* on day 10 after surgery. **(E)** Histogram represents the percentage of death in *Ccr2*$^{-/-}$ mice after transfer of purified Mo from Sham- or CLP-operated mice at 4 days after *E. coli* infection 5×10^9 cfu/mouse ($n = 16$ mice from three repeated experiments). *p* was determined using a chi-square test between the mice that received adoptive transfer. **(F)** Protein quantification in lung homogenates after adoptive transfer and E.coli pulmonary infection in *Ccr2*$^{-/-}$ surviving mice. Unpaired Student's *t* test was performed. **(G)** Mean fluorescence intensity (MFI) of CX3CR1 surface marker of lung Ly6C^{high} Mo from sham- and CLP-operated mice at day 10. Cells are stimulated or not with LPS or PMA-Ionomycin *in vitro*. Values represent the mean +/– Sem of 10 mice from two repeated experiments. **(H)** Percent of TNFα-(left panel) or IL-6-(right panel) producing lung Ly6C^{high} Mo (left panel) from sham- and CLP-operated mice at day 10. Values represent the mean +/– Sem of 4–6 mice. One-way ANOVA tests with Bonferoni multiple comparison tests compare Sham and CLP, respectively. **(I)** Percent of NO-producing lung Ly6C^{high} Mo from sham- and CLP-operated mice at day 10. Values represent the mean +/– Sem of 4–6 mice. One-way ANOVA tests with Bonferoni multiple comparison tests compare Sham and CLP, respectively. **(J)** Representative dot plot (out of 8 mice from two repeated experiments) of phagocytic Ly6C^{high} Mo percentage, 4 h after *in vitro* co-culture between lung cells suspension and fluorescent *E. coli*. *$p < 0.05$; **$p < 0.01$; ***$p < 0.001$; ****$p < 0.0001$.

(20). All blood Mo (**Figure 3B**, upper panels) and more than 95% of lung Mo (**Figure 3B**, lower panels) were strongly positive for CD45 staining either in sham- or CLP-operated mice, indicating that the Mo reside exclusively in the lung vasculature and did not infiltrate the tissue even in septic mice. Similar results were obtained with Ly6C^{low} Mo (**Supplementary Figure 3A**) and PMN (**Supplementary Figure 3B**). In the MacBlue transgenic mouse, the *Csf1r* promoter lacks the 150 bp trophoblast and osteoclast-specific transcription start sites, driving the expression of ECFP on classical and non-classical Mo, alveolar macrophages with a lower intensity and a fraction of granulocytes, but not in lung interstitial macrophages (18, 20). Imaging fresh explanted lungs of sham- and CLP-operated MacBlue mice using multiphoton microscope after *in vivo* labeling of the vasculature using fluorescent anti-CD31 (**Figure 3C**), confirmed their anatomical localization. In the lungs of sham-operated MacBlue mice, a few small cyan round-shaped Mo (ECFP^{+}) were detected in the vasculature (upper left picture and 5X magnification below) escorted by larger round-shaped ECFP+ alveolar macrophages that stayed exclusively in the alveolar lumen. In septic mice, ECFP+ Mo strongly accumulated within the lung capillaries (upper right picture and magnification below) whereas alveolar macrophages were barely detectable (**Figure 3C**), in accordance with the flow cytometry data (**Supplementary Figure 1**). Both flow cytometry and microscopy analyses revealed that during the recovery phase of sepsis, inflammatory Mo with altered expression of cell activation markers, such as MHC class II, CX3CR1 and CD64, invaded the lungs (and probably the kidneys and liver) but remained fully intravascular. They do not infiltrate the parenchymal and stromal tissues, nor the alveolar space.

Mo of the Late Recovery Phase of Sepsis Display an Altered Phenotype and Fail to Protect From Secondary Infection

Septic patients have a higher risk of developing secondary nosocomial infections (27). To determine whether mice are more susceptible to pneumonia after sublethal CLP, they were infected with E. coli by intratracheal injection (10 days post-CLP) and the survival rates of each group were evaluated (**Figure 4A**). Sham-operated mice were fully resistant to the second infection whereas about 20% of septic mice died during the first week following the bacteria inoculation. This excess of mortality was associated with an increased lung weight (**Figure 4B**) and bacterial lung load in bronchoalveolar lavage (BAL) (**Figure 4C**). These results confirm that sepsis triggers an increased susceptibility and severity to secondary infections. Because Mo recruitment is associated with disease severity in chronic inflammation (28), we used *Ccr2*$^{-/-}$ and *Cx3cr1*$^{egfp/egfp}$ to study the impact of Mo mobilization in response to the secondary infection. *Ccr2*$^{-/-}$ mice were more likely to die after CLP with about 46% mortality by day 10 and succumbed rapidly to secondary infection with 100% of death by day 4 post-secondary infection (**Figure 4D**). *Cx3cr1*$^{egfp/egfp}$ mice also displayed increased mortality in both primary (20%) and secondary infection (40%). Susceptibility to secondary infection was thus inversely proportional to the extent of Mo expansion observed in CCR2- and CX3CR1-deficient mice, suggesting a protective role of Mo in these infectious conditions. We postulated that Mo accumulated in the vasculature of septic mice may not be as efficient to protect from secondary infection as Mo from control mice. Adoptive transfer in *Ccr2*$^{-/-}$ mice is a model to evaluate the functional role of Mo (29, 30). We thus compared the survival of *Ccr2*$^{-/-}$ mice to lethal E.coli infection after Sham- and CLP- Mo adoptive transfer. In *Ccr2*$^{-/-}$, E.coli infection led to 100% of mortality after 4 days (**Figure 4E**). Adoptive transfer of Mo purified from sham-operated mice rescued about 62% of the mice, whereas only 25% were rescued after being transferred with Mo purified from CLP-operated mice. Coincidently, protein levels in lung homogenates of surviving mice were higher in mice transferred with Mo purified from CLP-operated mice compared to those of mice that received Mo purified from Sham-operated mice (**Figure 4F**), possibly indicating an increased vessel permeability due to increased microvascular lung lesions. In order to assess endotoxin tolerance (31) that may render cells unresponsive when re-challenged with lipopolysaccharide (LPS) produced by fecal microbiota induced by the CLP surgery, Mo purified from either sham- or CLP-operated mice were challenged *ex vivo* with LPS (**Figures 4G–I**). As predicted, it triggered a strong downmodulation of the CX3CR1 (**Figure 4G**) on Mo from sham-operated mice, as shown in **Figure 3A**. The chemical stimulation (PMA/ionomycine) used as an activation that is TLR-independent also triggered a strong downmodulation of CX3CR1. LPS triggered a strong production of TNFa and IL-6 (**Figure 4H**) in Mo from both sham- and CLP-operated mice in comparison to PMA/ionomycine stimulation. Nitric

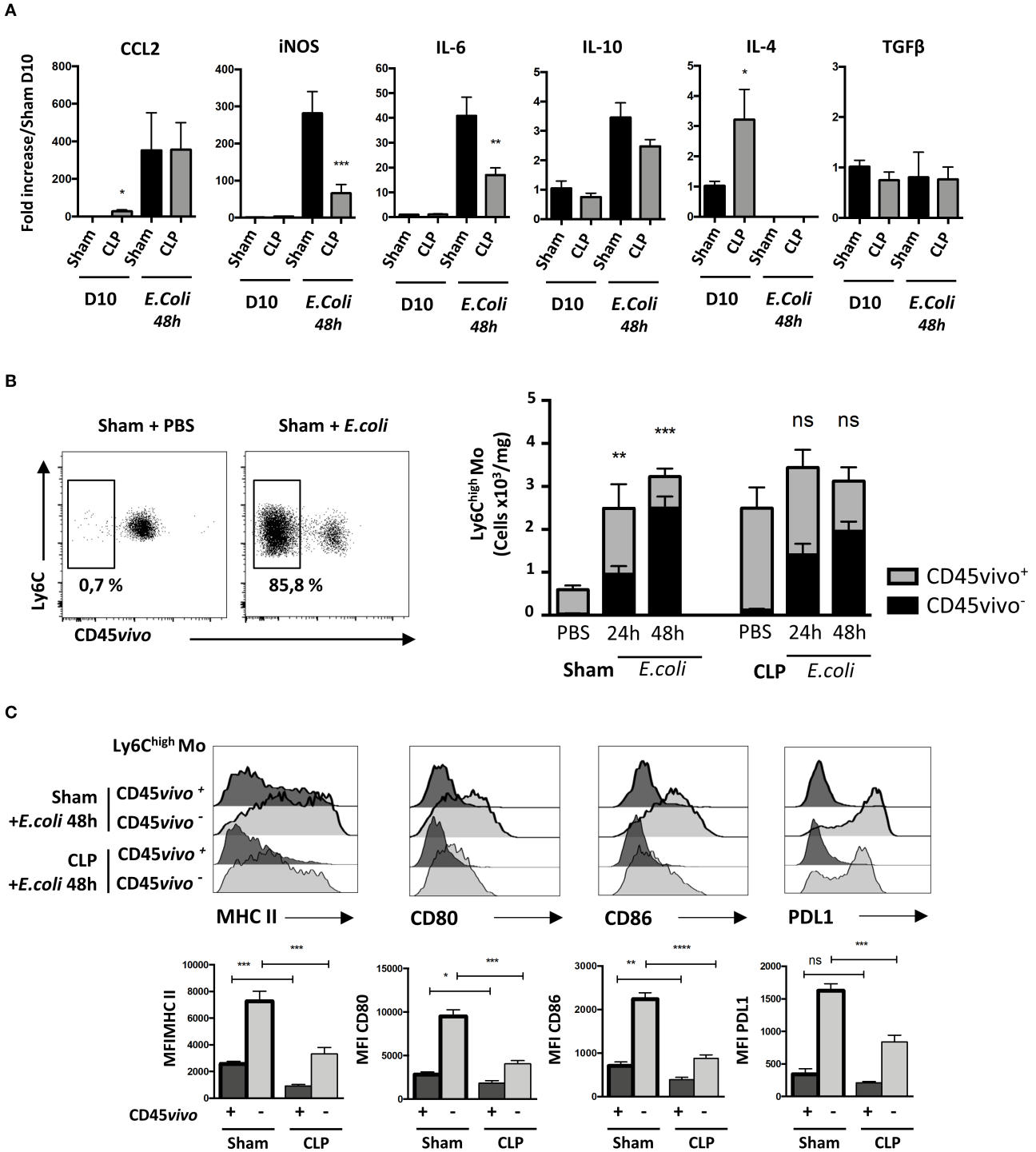

FIGURE 5 | Primary sepsis hampers Mo activation without altering Mo infiltration. **(A)** mRNA levels in lung cells measured by qPCR compared to sham-operated mice. Unpaired Student's *t* test was performed to compare Sham and CLP-operated mice in presence or absence of *E. coli*. **(B)** The left panels are representative dot plots of lung infiltrated Ly6C^{high} Mo from sham-operated mice injected with PBS or after *E. coli* infection. The histogram (right panels) represents the total numbers of Ly6C^{high} Mo per mg of lung from sham- or CLP-operated mice, 24 and 48 h after *E. coli* infection or PBS injection. Black bars represent the CD45vivo^{-} infiltrated cells and gray bars are CD45vivo^{+} vascular cells. Values represent the mean +/– sem of 10 mice per group. **(C)** Overlay of flow cytometric surface marker expression gated on lung vascular (CD45vivo $^{+}$) and infiltrated (CD45vivo $^{-}$) Ly6C^{high} monocytes in sham- (thick black lines) and CLP- (thin black line) operated mice, 48 h post E. coli infection. Mean fluorescence intensity (MFI) of CMH II, CD80, CD86, and PDL1 surface markers on infiltrated CD45vivo^{-} (light gray) or vascular CD45vivo^{+} (dark gray) Ly6C^{high} Mo in the lungs of sham- (thick black lines) and CLP- (thin black line) operated mice 48 h after second infection. *$p < 0.05$; **$p < 0.01$; ***$p < 0.001$; ****$p < 0.0001$.

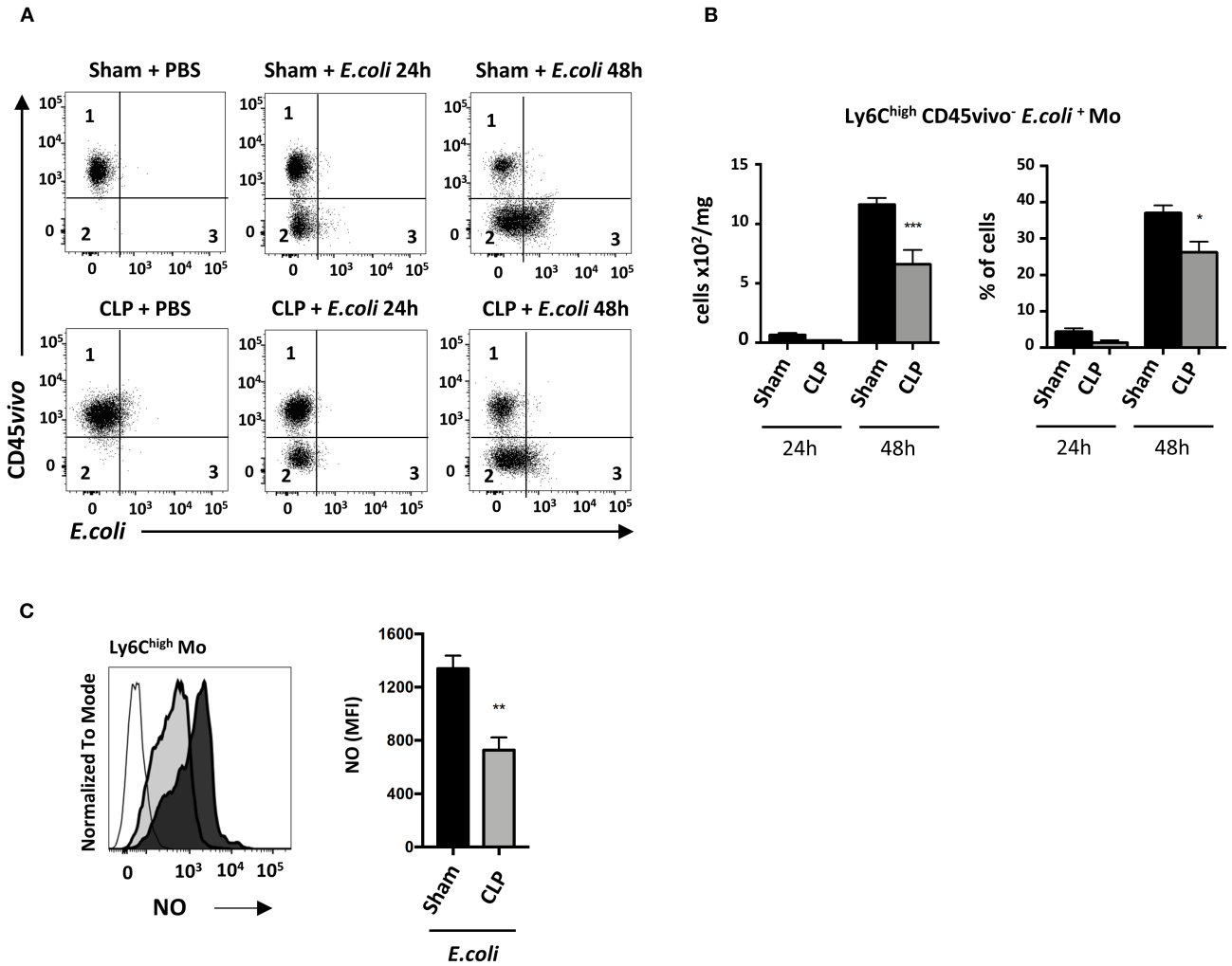

FIGURE 6 | In septic mice, infiltrated Ly6C^{high} Mo displays defective phagocytic activity. **(A)** Dot plot showing Ly6C^{high} Mo in lung from sham- (upper panels) and CLP- (lower panels) operated mice after PBS (left panels) or 24 h (middle panels) and 48 h (right panels) post *E. coli.* Quadrant 1 represents vascular non-phagocytic cells (CD45vivo^{+} *E. coli*$^{-}$), quadrant 2 identifies infiltrated non-phagocytic cells (CD45vivo^{-} *E. coli*$^{-}$) and quadrant 3 represents the infiltrated phagocytic monocytes (CD45vivo^{-} *E. coli*$^{+}$) in lungs. **(B)** Numbers and proportions of lung infiltrated phagocytic Ly6C^{high} Mo (quadrant 3) at 24 or 48 h post *E. coli* pulmonary infection in sham- and CLP-operated mice ($n = 8$ mice from three repeated experiments). Unpaired Student's *t* test was performed to compare Sham and CLP-operated mice in presence of *E. coli.* **(C)** Representative overlay (left panel) and mean fluorescence intensity of FITC (right panel) for NO production of Ly6C^{high} Mo 48 h post *E. coli* pulmonary infection in sham- (black section) and CLP-(gray section) operated mice by flow cytometry ($n = 6$–8 mice from two repeated experiments). FMO is represented in the overlay by a thick gray line. Unpaired Student's *t* test was performed to compare Sham and CLP-operated mice in presence of *E. coli*. $^{*}p < 0.05$; $^{**}p < 0.01$; $^{***}p < 0.001$.

oxide (NO) production by Ly6C^{high} Mo was measured using a photo-stable fluorescent probe named DAF-FM. No additional NO production was induced after LPS or PMA/ionomycine stimulation. Globally, LPS stimulation on Mo from CLP-operated mice was similar to that observed on Mo from sham-operated mice, indicating that Mo from CLP-operated mice were still responsive to LPS. In addition, Mo were challenged *ex vivo* with E. coli fluorescently labeled for phagocytic activity that was measured in a flow cytometry assay (**Figure 4J**). Again, lung Mo from CLP-operated mice (and thus exposed to fecal *E. coli*) were as efficient as Mo from sham-operated mice to phagocyte bacteria *in vitro*.

Primary Sepsis Hampers Mo Activation Without Altering Mo Infiltration

We then analyzed transcript levels of chemokines and cytokines in the whole lung to identify potential alterations leading to increased susceptibility and severity to secondary infections in septic mice (**Figure 5A**). Ten days after surgery, only *Ccl2* and *Il4* transcript levels were statistically more abundant in the lungs of CLP-operated mice compared to those of sham-operated mice. *E. coli* infection triggered a massive increase in transcript levels for Ccl2, i*Nos* or *Il6*, a modest increase in *Il10* transcripts but totally abrogated *IL4* transcript expression in both Sham- and CLP-operated mice. It had no effect on *Tgfß*

transcripts. *Ccl2* transcript levels in septic mice were unaffected by *E. coli* injection. Interestingly, the lungs of septic mice had less abundant transcripts for *iNos* and *Il6* than sham-operated mice. We thought that the altered cytokine environment observed 10 days after CLP may be associated with a defect in Mo deployment. We studied the distribution of Ly6C^{high} Mo between the lung vasculature and the parenchyma after *E. coli* infection using CD45 intravascular staining (**Figure 5B**, left panel). In sham-operated mice, *E. coli* injection triggered a strong accumulation of vascular (CD45vivo^{+}) Ly6C^{high} Mo and a strong tissue infiltration (CD45vivo^{-}) at 24 h post E. coli infection (**Figure 5B**, right panel). Although Mo did not accumulate further between 24 and 48 h, the relative proportion of Mo that infiltrated the lung increased. As previously described in **Figure 1**, septic mice at day 10 post-CLP already displayed increased numbers of Mo residing in the lung vasculature compared to Sham-operated mice before the second infection. Forty-eight hours after E. coli infection, no additional Mo accumulation was detected when compared to CLP-operated mice injected with PBS. Mo from septic mice extravasated in the lung parenchyma (CD45vivo^{-}) in similar proportion than Mo from sham-operated mice, suggesting that sepsis does not alter the capacity of Mo to infiltrate into the lung tissue.

We thus compared the phenotype of infiltrated and vascular Ly6C^{high} Mo in lungs 48 h after secondary infection in sham- and CLP-operated mice (**Figure 5C**). Representative overlays (upper panels) and mean fluorescence intensity analysis (lower panels) revealed that in sham- or CLP-operated mice, all activation markers tested were more intensively expressed on infiltrated (CD45vivo^{-}) compared to on vascular (CD45vivo^{+}) Mo. However, both vascular and infiltrated Mo from septic mice displayed severely reduced expression of MHC-II and of the co-stimulation markers CD80, CD86, and PDL-1. Globally, these data indicate that the increased susceptibility and severity of septic mice to secondary infections is associated to a defective cytokine environment and a limited Mo activation rather than to an altered Mo infiltration.

In Septic Mice, Infiltrated Ly6C^{high} Mo Display Defective Phagocytic Activity

We next investigated the functional defect of septic Mo. Phagocytic Ly6C^{high} Mo were quantified by flow cytometry (**Figure 6A**). Twenty-four hours after *E. coli* infection, very few infiltrated Ly6C^{high} Mo (CD45vivo^{-}) were associated with *E. coli* staining (CD45vivo^{-} *E. coli*$^{+}$) in sham and CLP-operated mice (middle upper and lower panels). At 48 h (right upper and lower panels), many more Ly6C^{high} Mo were infiltrated and positive for *E. coli* in both control and septic mice. Quantitative analysis (**Figure 6B**) revealed that E. coli phagocytosis by Ly6C^{high} Mo was reduced, in both absolute number and proportion, in septic mice compared to control mice. The NO production was reduced by about 50% in septic compared to control mice (**Figure 6C**). Altogether, these data indicate that both Mo phagocytic and antibacterial activities are reduced during late sepsis.

DISCUSSION

Although initially underestimated, the onset of severe immunosuppression in patients with sepsis is now a well-established phenomenon (1, 32). Most patients now survive the initial inflammatory phase thanks to the timely administration of antibiotics and efficient life-support systems but suffer from prolonged recurrent secondary infections (27). Indeed, their survival is impaired by the increased risk of recurrent infections, heart failure, and additional debilitating conditions (33). Reasons for such deteriorations are multifactorial but post-septic immune alterations are suspected to have a major impact on patient health. Understanding the kinetic of inflammatory events leading to immunosuppression and the development of secondary infections is important for the development of therapeutic strategies.

Here we used a sublethal polymicrobial sepsis murine model followed by bacterial Escherichia Coli-induced pneumonia to investigate the role of Ly6C^{high} Mo cells during the recovery phase following acute sepsis. Our study revealed a two-step Mo deployment after CLP; the first wave was associated with early acute clinical events (severe weight loss and death) and the second appeared much later during the clinical recovery of the mice, with no obvious signs of disease. Indeed, CLP triggered an early and transitory mobilization of Mo and PMN in the lungs. During the recovery phase, a secondary deployment of Mo and PMN was observed in all non-lymphoid organs studied. This secondary wave was of larger amplitude and lasted longer than the primary wave of the acute phase. Previous works had already demonstrated a strong mobilization of myeloid cells CD11b^{+}GR1^{+} in the blood and the bone marrow 1 week post CLP (34). Interestingly, we demonstrated that the deployed Mo remained exclusively localized to the vasculature of the lungs without accumulating in the lung parenchyma. Anti-inflammatory drugs, but not the antibiotic treatment, abrogated Mo mobilization to the lungs, showing that this accumulation was driven by persistent inflammatory signals independent of the infectious state of the mice. This phenomenon was observed in the blood and in several organs (if not all). These data and the myeloid redistribution indicate that even though the mice recovered from the acute infection and appeared healthy, they were still affected at the cellular level by the primary bacterial exposure. The reason for this recurrent chronic inflammation that leads to a secondary, stronger wave is unclear, but it may be associated with a systemic activation caused by organ failure occurring as a consequence of the first infection.

Studies have shown that Ly6C^{high} Mo are involved in controlling inflammation caused by gram-negative pneumonia and abdominal infections (35, 36). Accordingly, our previous work uncovered that Ly6C^{high} Mo in the kidney play a protective role during the early phase of sepsis, involving anti-inflammatory pathways such as IL1-RA (15). However, the role of Ly6C^{high} Mo in lungs during late sepsis had not been described until now. The role of Mo margination to the vasculature of non-lymphoid organs during the recovery phase remained unclear. However, the genetic deletion of CCR2 blocks Mo egress from the BM and the deletion of CX3CR1 impairs their retention

in the lung vasculature, hence both reducing the number of marginating Mo (37, 38) in the lungs. These deficiencies are associated with increased death rates, which would argue in favor of a protective role of Mo also during the later phase. Alternatively, Mo accumulation in the lung capillaries could reflect a bystander effect of the sepsis-induced monocytosis. Live imaging of explanted lungs suggested that ECFP monocytes trapped in the lung capillaries were relatively sessile either in Sham- and CLP-operated mice, indicating no change in their migratory behaviors during sepsis. Our results showed that the adoptive transfer of Ly6C^{high} Mo from septic mice to CCR2-deficient mice reduced organ failure and improved survival less efficiently than Mo from sham-operated mice, suggesting that the protective role is impaired in Mo from CLP-surviving mice. Several function markers on Mo are associated with their defect to efficiently control inflammation but also to contain potential secondary infection here caused by *E. coli* airway inhalation. The immunocompromised phase in sepsis is often associated with endotoxin tolerance (31), arguing that initial bacterial endotoxin activation (here the exposition to the fecal microbiota induced by the CLP surgery) renders cells unresponsive when rechallenged with LPS. Our data showed that Ly6C^{high} Mo from septic mice were fully responsive to LPS in terms of cytokine production and surface markers, suggesting a limited endotoxin tolerance effect. A decrease in the expression of MHC-II and CX3CR1 has been described and asscociated with defective Mo activation and sepsis severity (39, 40). The increased expression of integrin CD11b is also consistent with a margination of cells to the vascular endothelium (41). In our results, the cytokine profiles of the lung environment showed an increase of *Ccl2* and *Il4* transcripts, 10 days after sepsis. Unsurprisingly, CCL2 is involved in Mo mobilization and IL-4 participates in T cell polarization toward a Th2 phenotype (34). After secondary infection, transcript production for iNOS, IL-6, and IL-10 was increased while *Il4* was strongly reduced in sham and CLP-operated mice. Previous studies have shown a weakened lung bacterial clearance in two-hit models of sepsis (42, 43). We observed a smaller increase of *iNos* and *Il6* transcripts for septic mice compared to sham-operated mice after the secondary infection. Again, iNOS and IL-6 are involved in the phagocytic function of cells and in bacterial clearance (44, 45). Thus, these molecules may be linked to the impaired Mo function and the increased susceptibility to infection of the mice.

Wolk et al. showed that decreased expression of MHC-II and CD86 on Mo after LPS stimulation limited their ability to induce T-cell proliferation (46). In addition, immune tolerance during septic shock has been associated with abnormalities of the costimulatory pathway (47). Interestingly, we identified a decrease in PDL1 expression on infiltrated septic Ly6C^{high} Mo compared to sham Mo, whereas we did not observe any difference in PD1 expression on any of the cell types studied (data not shown). Nevertheless, blocking PD1 or PDL1 inhibitory signals are shown to be beneficial for survival in murine sepsis models (48, 49). This can also be observed in septic patients where the expression of PD1 and PDL1 by Mo is increased, but more modestly in those who do not survive (50). Recent work from Bianchini et al. shows that PDL-1 identifies non-classical Mo (here Ly6C^{low} Mo) and regulates T cell survival in tertiary lymphoid organs (51). Here we observed that PDL-1 expression was upregulated on Ly6C^{high} Mo while infiltrating the alveolar space upon *E. coli* infection. It is possible that a higher expression of PDL1 on Mo participate in an infectious context to the fine regulation of the immune response. Whether a beneficial effect of PDL-1 blockade is carried out by infiltrating classical or non-classical Mo remains to be explored. Our results indicate that an alteration of the balance between costimulatory and regulatory pathways could participate in the dysregulation of the innate immune response leading to the inefficient control of secondary infections, and could also reduce its efficacy in protecting against tissue dysfunction.

Overall, we conclude that during the recovery phase following acute sepsis, a recurrent systemic inflammation independent of the infectious status occurs. This inflammatory process leads to a long-term deployment of functionally impaired inflammatory Mo to the vasculature of non-lymphoid organs, which fail to favor lung recovery and protection against secondary infections.

DATA AVAILABILITY STATEMENT

All datasets generated for this study are included in the article/**Supplementary Material**.

ETHICS STATEMENT

All experiments and protocols were approved by the Comité d'éthique en expérimentation animale Charles Darwin N°5 under the agreement of the French Ministère de l'Education Nationale, de l'Enseignement Supérieur et de la Recherche with the number APAFIS#4369-2016030218219240 v3.

AUTHOR CONTRIBUTIONS

CB, BC, AB, and CC designed the study. CB, PH, ML, NG, PL, AM-K, PD, SB, and AB performed experimental work. CB, AB, and CC performed data analysis, developed figures, and wrote the manuscript. AB, BC, and CC provided financial support. All authors contributed in reviewing the manuscript.

FUNDING

This work was supported by grants from the Fondation pour la recherche Médicale Equipe labelisée and from the Agence Nationale de la Recherche, project CMOS (CX3CR1 expression on monocytes during sepsis) 2015 (ANR-EMMA-050) and project TETRAAA (Targeting TREM1Receptor in abdominal aortic aneurysm).

ACKNOWLEDGMENTS

The authors thank Mia Rozenbaum for manuscript editing, the Plateforme Imagerie Pitié-Salpêtrière (PICPS) for its assistance with the two-photon microscope and the animal facility NAC for mice breeding.

SUPPLEMENTARY MATERIAL

The Supplementary Material for this article can be found online at: https://www.frontiersin.org/articles/10.3389/fimmu.2020.00675/full#supplementary-material

Supplementary Figure 1 | Effect of polymicrobial sepsis on body weight, survival, and kinetics of alveolar macrophages. **(A)** Percentage of body weight loss in CLP (dotted line) and Sham-operated mice normalized to 100%. Animal weight was measured before surgery and on day 1, 2, 3, 7, and 10. **(B)** Survival of sham- or CLP- operated *Cx3cr1*$^{gfp/+}$ mice after surgery. The survival study was carried out on 25 mice for each group. **(C)** Numbers of Alveolar Macrophage (AM) determined by flow cytometry at different time points after CLP. The time zero was defined based on the cell number obtained in sham-operated mice. Each time point represents at least three independent experiments run with 6 to 12 mice.

Supplementary Figure 2 | Neutrophil (PMN) and alveolar macrophage (AM) numbers are not impacted by treatments and CX3CR1 or CCR2 deletion. **(A)** Numbers of PMN in the blood, lungs, and bone marrow determined by flow cytometry in sham and septic mice, 10 days after CLP and treatments. Splenectomies were performed a few minutes before the CLP. Antibiotic or Dexamethasone treatments were injected 24 h after CLP. Values represent the mean +/– sem of 10 mice per group from two independent experiments. **(B)** Numbers of Ly6C^{low} in the lungs determined by flow cytometry in sham and septic mice, 10 days after CLP and antibiotic treatments. **(C)** Numbers of PMN and d-AM in the blood, lung and bone marrow determined by flow cytometry, 10 days after sham- and CLP-operated WT ($n = 10$), *Ccr2*$^{-/-}$ ($n = 6$) and *Cx3cr1*$^{-/-}$ ($n = 8$) mice from at least two independent experiments.

Supplementary Figure 3 | Late-expanded myeloid cells remain intravascular in the lung of septic mice. **(A,B)** Proportion of Ly6C^{low} CD45vivo+ Mo and PMN CD45vivo+ in lungs 10 days after sham- or CLP-operated mice.

REFERENCES

1. Angus DC, Linde-Zwirble WT, Lidicker J, Clermont G, Carcillo J, Pinsky MR. Epidemiology of severe sepsis in the United States: analysis of incidence, outcome, and associated costs of care. *Crit Care Med.* (2001) 29:1303–10. doi: 10.1097/00003246-200107000-00002
2. Singer M, Deutschman CS, Seymour CW, Shankar-Hari M, Annane D, Bauer M, et al. The third international consensus definitions for sepsis and septic shock (Sepsis-3). *JAMA*. (2016) 315–801–10. doi: 10.1001/jama.2016.0287
3. Hotchkiss RS, Moldawer LL, Opal SM, Reinhart K, Turnbull IR, Vincent JL. Sepsis and septic shock. *Nat Rev Dis Primer*. (2016) 2:16045. doi: 10.1038/nrdp.2016.45
4. Hutchins NA, Unsinger J, Hotchkiss RS, Ayala A. The new normal: immunomodulatory agents against sepsis immune suppression. *Trends Mol Med.* (2014) 20:224–33. doi: 10.1016/j.molmed.2014.01.002
5. Uhel F, Azzaoui I, Grégoire M, Pangault C, Dulong J, Tadié JM, et al. Early expansion of circulating granulocytic myeloid-derived suppressor cells predicts development of nosocomial infections in patients with sepsis. *Am J Respir Crit Care Med.* (2017) 196:315–27. doi: 10.1164/rccm.201606-1143OC
6. Gabrilovich DI, Nagaraj S. Myeloid-derived suppressor cells as regulators of the immune system. *Nat. Rev. Immunol.* (2009) 9:162–74. doi: 10.1038/nri2506
7. Landelle C, Lepape A, Voirin N, Tognet E, Venet F, Bohé J, et al. Low monocyte human leukocyte antigen-DR is independently associated with nosocomial infections after septic shock. *Intensive Care Med.* (2010) 36:1859–66. doi: 10.1007/s00134-010-1962-x
8. Angus DC, Opal S. Immunosuppression and Secondary Infection in sepsis: part, not all, of the story. *JAMA*. (2016) 315:1457–9. doi: 10.1001/jama.2016.2762
9. Venet F, Chung CS, Monneret G, Huang X, Horner B, Garber M, et al. Regulatory T cell populations in sepsis and trauma. *J. Leukoc. Biol.* (2008) 83:523–35. doi: 10.1189/jlb.0607371
10. Pène F, Zuber B, Courtine E, Rousseau C, Ouaaz F, Toubiana J, et al. Dendritic cells modulate lung response to *Pseudomonas aeruginosa* in a murine model of sepsis-induced immune dysfunction. *J Immunol.* (2008) 181:8513–20. doi: 10.4049/jimmunol.181.12.8513
11. Livingston DH, Appel SH, Wellhausen SR, Sonnenfeld G, Polk HC. Depressed interferon gamma production and monocyte HLA-DR expression after severe injury. *Arch Surg Chic.* (1988) 123:1309–12. doi: 10.1001/archsurg.1988.01400350023002
12. Venet F, Tissot S, Debard AL, Faudot C, Crampé C, Pachot A, et al. Decreased monocyte human leukocyte antigen-DR expression after severe burn injury: correlation with severity and secondary septic shock. *Crit. Care Med.* (2007) 35:1910–7. doi: 10.1097/01.CCM.0000275271.77350.B6
13. Rigato O, Salomao R. Impaired production of interferon-gamma and tumor necrosis factor-alpha but not of interleukin 10 in whole blood of patients with sepsis. *Shock Augusta Ga.* (2003) 19:113–6. doi: 10.1097/00024382-200302000-00004
14. Serbina NV, Jia T, Hohl TM, Pamer EG. Monocyte-mediated defense against microbial pathogens. *Annu Rev Immunol.* (2008) 26:421–52. doi: 10.1146/annurev.immunol.26.021607.090326
15. Chousterman BG, Boissonnas A, Poupel L, Baudesson de Chanville C, Adam J, Tabibzadeh N, et al. Ly6Chigh monocytes protect against kidney damage during sepsis via a CX3CR1-dependent adhesion mechanism. *J Am Soc Nephrol.* (2016) 27:792–803. doi: 10.1681/ASN.2015010009
16. Combadière C, Potteaux S, Gao JL, Esposito B, Casanova S, Lee EJ, et al. Decreased atherosclerotic lesion formation in CX3CR1/apolipoprotein E double knockout mice. *Circulation.* (2003) 107:1009–16. doi: 10.1161/01.CIR.0000057548.68243.42
17. Jung S, Aliberti J, Graemmel P, Sunshine MJ, Kreutzberg GW, Sher A, et al. Analysis of fractalkine receptor CX(3)CR1 function by targeted deletion and green fluorescent protein reporter gene insertion. *Mol Cell Biol.* (2000) 20:4106–14. doi: 10.1128/MCB.20.11.4106-4114.2000
18. Ovchinnikov DA, van Zuylen WJ, DeBats CE, Alexander KA, Kellie S, Hume DA. Expression of Gal4-dependent transgenes in cells of the mononuclear phagocyte system labeled with enhanced cyan fluorescent protein using Csf1r-Gal4VP16/UAS-ECFP double-transgenic mice. *J Leukoc Biol.* (2008) 83:430–3. doi: 10.1189/jlb.0807585
19. Rittirsch D, Huber-Lang MS, Flierl MA, Ward PA. Immunodesign of experimental sepsis by cecal ligation and puncture. *Nat Protoc.* (2009) 4:31–6. doi: 10.1038/nprot.2008.214
20. Rodero MP, Poupel L, Loyher PL, Hamon P, Licata F, Pessel C, et al. Immune surveillance of the lung by migrating tissue monocytes. *Elife.* (2015) 4:e07847. doi: 10.7554/eLife.07847
21. Anderson KG, Mayer-Barber K, Sung H, Beura L, James BR, Taylor JJ, et al. Intravascular staining for discrimination of vascular and tissue leukocytes. *Nat Protoc.* (2014) 9:209–22. doi: 10.1038/nprot.2014.005
22. Scumpia PO, Kelly-Scumpia KM, Delano MJ, Weinstein JS, Cuenca AG, Al-Quran S, et al. Cutting edge: bacterial infection induces hematopoietic stem and progenitor cell expansion in the absence of TLR signaling. *J Immunol Baltim. Md 1950.* (2010) 184:2247–51. doi: 10.4049/jimmunol.0903652
23. Robbins CS, Chudnovskiy A, Rauch PJ, Figueiredo JL, Iwamoto Y, Gorbatov R, et al. Extramedullary hematopoiesis generates Ly-6C(high) monocytes that infiltrate atherosclerotic lesions. *Circulation.* (2012) 125:364–74. doi: 10.1161/CIRCULATIONAHA.111.061986
24. Hamon P, Loyher PL, Baudesson de Chanville C, Licata F, Combadière C, Boissonnas A. CX3CR1-dependent endothelial margination modulates Ly6Chigh monocyte systemic deployment upon inflammation in mice. *Blood.* (2017) 129:1296–307. doi: 10.1182/blood-2016-08-732164
25. Pachot A, Cazalis MA, Venet F, Turrel F, Faudot C, Voirin N, et al. Decreased expression of the fractalkine receptor CX3CR1 on circulating monocytes as new feature of sepsis-induced immunosuppression. *J. Immunol.* (2008) 180:6421–9. doi: 10.4049/jimmunol.180.9.6421
26. Friggeri A, Cazalis MA, Pachot A, Cour M, Argaud L, Allaouchiche B, et al. Decreased CX3CR1 messenger RNA expression is an independent molecular biomarker of early and late mortality in critically ill patients. *Crit. Care.* (2016) 20:204. doi: 10.1186/s13054-016-1362-x

27. Hotchkiss RS, Monneret G, Payen D. Immunosuppression in sepsis: a novel understanding of the disorder and a new therapeutic approach. *Lancet Infect. Dis.* (2013) 13:260–8. doi: 10.1016/S1473-3099(13)70001-X
28. Combadière C, Potteaux S, Rodero M, Simon T, Pezard A, Esposito B, et al. Combined inhibition of CCL2, CX3CR1, and CCR5 abrogates Ly6C(hi) and Ly6C(lo) monocytosis and almost abolishes atherosclerosis in hypercholesterolemic mice. *Circulation.* (2008) 117:1649–57. doi: 10.1161/CIRCULATIONAHA.107.745091
29. Tsou CL, Peters W, Si Y, Slaymaker S, Aslanian AM, Weisberg SP, et al. Critical roles for CCR2 and MCP-3 in monocyte mobilization from bone marrow and recruitment to inflammatory sites. *J Clin Invest.* (2007) 117:902–9. doi: 10.1172/JCI29919
30. Arnold L, Perrin H, de Chanville CB, Saclier M, Hermand P, Poupel L, et al. CX3CR1 deficiency promotes muscle repair and regeneration by enhancing macrophage ApoE production. *Nat Commun.* (2015) 6:8972. doi: 10.1038/ncomms9972
31. López-Collazo E, del Fresno C. Pathophysiology of endotoxin tolerance: mechanisms and clinical consequences. *Crit Care Lond Engl.* (2013) 17:242. doi: 10.1186/cc13110
32. Martin GS, Mannino DM, Eaton S, Moss M. The epidemiology of sepsis in the United States from 1979 through 2000. *N Engl J Med.* (2003) 348:1546–54. doi: 10.1056/NEJMoa022139
33. Prescott HC, Osterholzer JJ, Langa KM, Angus DC, Iwashyna TJ. Late mortality after sepsis: propensity matched cohort study. *BMJ.* (2016) 353:i2375. doi: 10.1136/bmj.i2375
34. Delano MJ, Scumpia PO, Weinstein JS, Coco D, Nagaraj S, Kelly-Scumpia KM, et al. MyD88-dependent expansion of an immature GR-1 $^{+}$ CD11b $^{+}$ population induces T cell suppression and Th2 polarization in sepsis. *J Exp Med.* (2007) 204:1463–74. doi: 10.1084/jem.20062602
35. Dunay IR, Damatta RA, Fux B, Presti R, Greco S, Colonna M, et al. Gr1(+) inflammatory monocytes are required for mucosal resistance to the pathogen *Toxoplasma gondii*. *Immunity.* (2008) 29:306–17. doi: 10.1016/j.immuni.2008.05.019
36. Winter C, Taut K, Srivastava M, Länger F, Mack M, Briles DE, et al. Lung-specific overexpression of CC chemokine ligand (CCL) 2 enhances the host defense to *Streptococcus pneumoniae* infection in mice: role of the CCL2-CCR2 axis. *J Immunol Baltim Md 1950.* (2007) 178:5828–38. doi: 10.4049/jimmunol.178.9.5828
37. Grainger JR, Wohlfert EA, Fuss IJ, Bouladoux N, Askenase MH, Legrand F, et al. Inflammatory monocytes regulate pathologic responses to commensals during acute gastrointestinal infection. *Nat Med.* (2013) 19:713–21. doi: 10.1038/nm.3189
38. Antonelli LR, Gigliotti Rothfuchs A, Gonçalves R, Roffê E, Cheever AW, Bafica A, et al. Intranasal Poly-IC treatment exacerbates tuberculosis in mice through the pulmonary recruitment of a pathogen-permissive monocyte/macrophage population. *J Clin Invest.* (2010) 120:1674–82. doi: 10.1172/JCI40817
39. Ge XY, Fang SP, Zhou M, Luo J, Wei J, Wen XP, et al. TLR4-dependent internalization of CX3CR1 aggravates sepsis-induced immunoparalysis. *Am J Transl Res.* (2016) 8:5696–5705.
40. Monneret G, Venet F, Pachot A, Lepape A. Monitoring immune dysfunctions in the septic patient: a new skin for the old ceremony. *Mol Med Camb Mass.* (2008) 14:64–78. doi: 10.2119/2007-00102.Monneret
41. Solovjov DA, Pluskota E, Plow EF. Distinct roles for the alpha and beta subunits in the functions of integrin alphaMbeta2. *J Biol Chem.* (2005) 280:1336–45. doi: 10.1074/jbc.M406968200
42. Chen W, Lian J, Ye JJ, Mo QF, Qin J, Hong GL, et al. Ethyl pyruvate reverses development of *Pseudomonas aeruginosa* pneumonia during sepsis-induced immunosuppression. *Int Immunopharmacol.* (2017) 52:61–9. doi: 10.1016/j.intimp.2017.08.024
43. Deng D, Li X, Liu C, Zhai Z, Li B, Kuang M, et al. Systematic investigation on the turning point of over-inflammation to immunosuppression in CLP mice model and their characteristics. *Int. Immunopharmacol.* (2017) 42:49–58. doi: 10.1016/j.intimp.2016.11.011
44. MacMicking J, Xie Q, Nathan C. Nitric oxide and Macrophage function. *Annu Rev Immunol.* (1997) 15:323–50. doi: 10.1146/annurev.immunol.15.1.323
45. Yang ML, Wang CT, Yang SJ, Leu CH, Chen SH, Wu CL, et al. IL-6 ameliorates acute lung injury in influenza virus infection. *Sci Rep.* (2017) 7:43829. doi: 10.1038/srep43829
46. Wolk K, Döcke WD, von Baehr V, Volk HD, Sabat R. Impaired antigen presentation by human monocytes during endotoxin tolerance. *Blood.* (2000) 96:218–23. doi: 10.1182/blood.V96.1.218.013k04_218_223
47. Roger PM, Hyvernat H, Breittmayer JP, Dunais B, Dellamonica J, Bernardin G, et al. Enhanced T-cell apoptosis in human septic shock is associated with alteration of the costimulatory pathway. *Eur J Clin Microbiol Infect Dis Off Publ Eur Soc Clin Microbiol.* (2009) 28:575–84. doi: 10.1007/s10096-008-0673-5
48. Huang X, Venet F, Wang YL, Lepape A, Yuan Z, Chen Y, et al. PD-1 expression by macrophages plays a pathologic role in altering microbial clearance and the innate inflammatory response to sepsis. *Proc Natl Acad Sci USA.* (2009) 106:6303–8. doi: 10.1073/pnas.0809422106
49. Zhang J, Patel JM. Role of the CX3CL1-CX3CR1 axis in chronic inflammatory lung diseases. *Int J Clin Exp Med.* (2010) 3:233–44.
50. Ferreira da Mota NV, Brunialti MKC, Santos SS, Machado FR, Assuncao M, Azevedo LCP, et al. Immunophenotyping of monocytes during human sepsis shows impairment in antigen presentation: a shift toward non-classical differentiation and upregulation of FcγRi-receptor. *Shock 1.* (2017) 50:293–300. doi: 10.1097/SHK.0000000000001078
51. Bianchini M, Duchêne J, Santovito D, Schloss MJ, Evrard M, Winkels H, et al. PD-L1 expression on nonclassical monocytes reveals their origin and immunoregulation function. *Sci Immunol.* (2019) 4:36. doi: 10.1126/sciimmunol.aar3054

Conflict of Interest: The authors declare that the research was conducted in the absence of any commercial or financial relationships that could be construed as a potential conflict of interest.

The reviewer MR declared a past co-authorship with several of the authors to the handling editor.

frontiers in Immunology

ORIGINAL RESEARCH
published: 05 May 2020
doi: 10.3389/fimmu.2020.00768

Increased Plasma Levels of Mitochondrial DNA and Normal Inflammasome Gene Expression in Monocytes Characterize Patients With Septic Shock Due to Multidrug Resistant Bacteria

*Stefano Busani[1], Sara De Biasi[2], Milena Nasi[3], Annamaria Paolini[3], Sophie Venturelli[1], Martina Tosi[1], Massimo Girardis[1] and Andrea Cossarizza[2,4]**

[1] Intensive Care Unit, Policlinico di Modena, University of Modena and Reggio Emilia, Modena, Italy, [2] Department of Medical and Surgical Sciences for Children and Adults, University of Modena and Reggio Emilia, Modena, Italy, [3] Department of Surgical, Medical and Dental Morphological Sciences Related to Transplant, Oncology and Regenerative Medicine, University of Modena and Reggio Emilia, Modena, Italy, [4] National Institute for Cardiovascular Research – INRC, Bologna, Italy

OPEN ACCESS

Edited by:
Florian Uhle,
Heidelberg University Hospital,
Germany

Reviewed by:
Valerio Chiurchiù,
Campus Bio-Medico University, Italy
Katherina Psarra,
Evaggelismos General Hospital,
Greece

***Correspondence:**
Andrea Cossarizza
andrea.cossarizza@unimore.it

Specialty section:
This article was submitted to Inflammation, a section of the journal Frontiers in Immunology

Received: 16 February 2020
Accepted: 06 April 2020
Published: 05 May 2020

Citation:
Busani S, De Biasi S, Nasi M, Paolini A, Venturelli S, Tosi M, Girardis M and Cossarizza A (2020) Increased Plasma Levels of Mitochondrial DNA and Normal Inflammasome Gene Expression in Monocytes Characterize Patients With Septic Shock Due to Multidrug Resistant Bacteria. Front. Immunol. 11:768. doi: 10.3389/fimmu.2020.00768

Introduction: The activity and regulation of inflammasome is receiving increasing attention in septic shock. Moreover, there is a growing body of evidence suggesting that mitochondrial DNA (mtDNA) can play a role as biomarker of disease severity and even mortality both in adults and children in critically ill setting. However, no data are available on the amount of circulating mtDNA and inflammasome gene expression in multi-drug resistant (MDR) bacteria septic shock. For this reason, the aim of this study was to determine whether plasma mtDNA levels and inflammasome gene expression in monocytes could be related to severity in patients admitted to intensive care unit (ICU) with septic shock due to MDR pathogens.

Materials and Methods: Peripheral blood mononuclear cells (PBMC) and plasma were isolated from up to 20 ml of venous blood by density gradient centrifugation in patients admitted to ICU with the diagnosis of septic shock due to MDR-bacteria. Then, CD14+ monocytes were sorted, and RNA and DNA were extracted. NLRP3, PYCARD, AIM2 and NAIP expression level was analyzed by RT-PCR. Plasma circulating mtDNA levels were quantified by digital droplet PCR. Basal and outcome characteristics of the patients were collected. Age-matched healthy subjects were chosen as controls.

Results: Nineteen patients with septic shock and 20 healthy subjects were enrolled in the study. A small trend toward an increased expression of inflammasome genes was observed in septic shock patients, who also displayed a marked tendency to an increased expression of IL-18 and IL-1β genes. Circulating mtDNA levels were significantly higher in septic shock patients if compared to healthy subjects, and patients who died in ICU were characterized by higher level of mtDNA if compared to those who were dismissed after 7 days. No correlations were found between mtDNA and inflammasome level and other clinical variables.

Conclusion: Despite many limitations, our data suggest that in patients with septic shock caused by MDR pathogens the expression of main inflammasome genes was comparable to that of healthy patients without infection. Furthermore, our data evidence a possible role of mtDNA as a prognostic marker of severity in septic shock from MDR.

Keywords: septic shock, circulating mtDNA, multidrug resistance bacteria, inflammasome, intensive care unit

INTRODUCTION

Septic shock still represents the pathology with the highest risk of mortality worldwide despite the knowledge and attention dedicated to this disease over the past 20 years. Recent investigations of the pathogenic host response to infection have highlighted a different behavior depending on whether there is a hyperinflammatory state or a hypo-reactivity of the immune system (1). These new perspectives have brought up the role of pathogen-associated molecular patterns (PAMPs) and danger-associated molecular patterns (DAMPs) in the initiation and propagation of the inflammatory cascade. This "Danger Model" stipulates that when cells are injured they release their components into the extracellular space, which in turn drives an immune or inflammatory response (2). Inflammasomes, such as NLRP3, PYCARD, AIM2, and NAIP are multimeric protein complexes that serve as important cytosolic pattern recognition receptors required for recognizing DAMPs and PAMPs. The activation of inflammasome signaling pathways is involved in mounting a proinflammatory immune response by regulating the maturation from precursors of IL-1β, IL-18, IL-33, cytokines that can induce pyroptosis. Recently, mitochondrial DAMPs have been identified as important mediators of the innate immune response and implicated in various conditions such as trauma, sepsis, and autoimmune disorders [reviewed in (3)]. Accordingly, the ability of mitochondrial (mt) DNA to act as DAMPs in the activation/inhibition of the inflammatory cascade has been recently investigated (4, 5). In critically ill setting, mainly in septic shock patients, there is a growing body of literature suggesting that mtDNA plasma levels can probably be used as biomarker of disease severity and even mortality both in adults and children (6–8).

The role of inflammasome and mtDNA is a research field that is receiving more and more attention in septic shock, but, to our knowledge, no data exist on these two parameters during multi drug resistant (MDR)-bacteria septic shock. For this reason, we investigated whether plasma mtDNA levels and inflammasome gene expression in monocytes, cells that are crucial for innate immune response, could be related to severity in patients admitted to intensive care unit (ICU) with septic shock due to MDR pathogens infection.

MATERIALS AND METHODS

Patients' Population and Selection

We performed a prospective observational study in the ICU of the University Hospital Policlinico of Modena (Italy) between April 2014 and December 2018. Evaluation of entry criteria and subsequent enrollment in the study occurred during planned routine patients visits. Inclusion criteria were: patients aged 18 years or older admitted to our ICU with septic shock sustained by documented MDR bacteria. Definitions of septic shock and MDR bacteria are detailed in a previous report (9). Patients with autoimmune or hematologic disease, pregnancy, metastatic cancer, end-stage liver disease, end-of-life decisions, illnesses or with medications known to be toxic to mitochondria were excluded. The type of admission, relevant pre-existing diseases, the primary site of infection, microbiology lab results, SOFA scores when sepsis was diagnosed were collected. Age-matched healthy subjects without infections were chosen as controls (CTR). Blood from patients with septic shock was sampled from the arterial catheter within 24 h from the diagnosis of septic shock. The study was carried out in accordance with recommendations of the Prot. n 2630/CE approved by the Province of Modena Ethical Committee. All subjects gave written informed consent in accordance with the Declaration of Helsinki.

Biological Sample Collection, Processing and Storage

Peripheral blood mononuclear cells (PBMC) and plasma were isolated from up to 20 ml of venous blood by density gradient centrifugation, using standardized protocols and Lymphoprep reagent from Stemcell (Cambridge, MA, United States). Plasma was then stored at −80°C until use (10). A minimum of 1.5 million CD14+ monocytes were sorted starting from 20 million PBMC through immunomagnetic separation technique (Miltenyi Biotec, Bergish Gladbach, Germany). Purity of monocyte population was always >95%.

RNA Extraction, Reverse Transcription

RNA was extracted from CD14+ cells through Quick-RNA Miniprep Kit (Zymo Research, Irvine, United States) and quantified using NanoPhotometer NP80 (Implen, Munich, Germany). Then, 20 ng/μl of RNA was reverse transcribed with the iScript cDNA Synthesis kit (Bio-Rad, Hercules, CA, United States).

Pre-amplification and Real-Time Polymerase Chain Reaction (PCR) for Gene Quantification

In order to obtain a more accurate RNA quantification, cDNA samples were pre-amplified using Sso Advanced PreAmp Supermix (Bio-Rad). Quantification of inflammasome genes was performed by Real-Time PCR as previously described (11).

Changes in genes expression between the two groups of patients were calculated through the $\Delta\Delta$ cycle method.

DNA Extraction and Digestion

DNA was extracted from plasma samples using QIAmp DNA Mini Kit (QIAGEN, Venlo, Netherlands) and then digested with *Bam*HI enzyme. The reaction mix was prepared as follows: 1 µl *Bam*HI enzyme, 1 µl Buffer Fast Digest, 6 µl DNA, in a total volume of 10 µl. Samples were then incubated in C1000 Touch Thermal Cycler (Bio-Rad) for 5 min at 37°C followed by 5 min at 80°C.

Total Quantification of mtDNA Circulating in Plasma Using Droplet Digital PCR

Quantitative real-time PCR (qPCR) is often used for the detection of nucleic acid in research and diagnostic, but the methodology has several limitations, first of all the need of preparing dedicated standard curves. Thus, we have used droplet digital PCR (ddPCR) to quantify circulating mtDNA because there is no need of a standard curve, and because the results are less dependent from the efficiency of the reaction. The sample is indeed partitioned in droplets and each of them represents an isolated end-point PCR reaction. The frequency of positive to negative droplets in the reaction mixture thus allows a precise quantification of the concentration of target nucleic acids (12).

Before performing ddPCR, samples were diluted 1:10 in order to obtain more accurate results. Two different assays were performed in this set of experiments: ddPCR assay EIF2C1 (UniqueAssayID: dHsaCP2500349, Bio-Rad) (HEX fluorescence) for genomic DNA and ddPCR assay MT-ND4 for mtDNA (UniqueAssayID:dHsaCPE5043566, Bio-Rad) (FAM, fluorescence). Droplet Digital PCR was performed as previously described (12). Manufacturer's thermal cycling protocol was optimized, changing the annealing/extension step temperature from 55 to 57°C.

Statistical Analysis

Categorical (sex) and quantitative (age) variables were compared between groups by $\chi 2$ and Mann–Whitney tests, respectively. Differences between controls and septic shock patients were explored with Mann–Whitney test. A P-value < 0.05 was considered statistically significant. Data shown in graphs are represented as the mean ± SEM. Statistical analyses were performed using Prism 8.0 (GraphPad Software Inc., San Diego, CA, United States).

RESULTS

Patients Characteristics

A total of 19 ICU patients with septic shock induced by MDR pathogens were enrolled. Twenty healthy subjects without infections (8 males/12 females, mean age ± SD, 60.8 ± 4.4 years), were chosen as CTR. ICU patients had septic shock caused mainly by peritonitis and blood stream infection. While multi-resistant Gram-negative bacteria were the most represented pathogens, of these four were *Escherichia Coli* and two each *Pseudomonas Aeruginosa* and *Enterobacter Cloacae* (**Table 1**). Median SOFA score at ICU admission was 11 with mainly respiratory cardiovascular and hematological dysfunctions. In patients with septic shock the 30-day, ICU and 1-year mortality were 42.1, 52.6, and 63.2%, respectively (**Table 1**).

TABLE 1 | Clinical characteristics of the 19 patients with septic shock.

Sex	**Male *n* = 12 (63.2%) Females *n* = 7 (36.8%)**
Age [years, median (range)]	67 (33–81)
SOFA score [median (range)]	11 (7–21)
ICU mortality *n* (%)	10 (52.6%)
30-day mortality *n* (%)	8 (42.1%)
1-year mortality *n* (%)	12 (63.2%)
Sepsis focus*	
Abdomen *n* (%)	9 (47.4%)
Lung *n* (%)	4 (21.1%)
Blood *n* (%)	9 (47.4%)
Urinary tract *n* (%)	1 (5.3%)
Other *n* (%)	2 (10.5%)
Pathogens	
Gram positive *n* (%)	5 (26.3%)
Gram negative *n* (%)	14 (73.7%)

*ICU, intensive care unit, SOFA, sequential organ failure assessment. *To notice that sepsis focus was in 6 cases a mixed focus.*

Inflammasome Gene Expression and mtDNA in Septic Shock Patients and CTR

The gene expression profile of the entire inflammasome pathway was evaluated in isolated monocytes from septic patients. Pattern recognition receptors involved in inflammasomes comprise nucleotide-binding oligomerization domain and leucine-rich repeat-containing receptors (NLR) such as NLRP3 and NAIP, as well as absent in melanoma-2 (AIM-2). Through their caspase activation and recruitment domain (CARD) or pyrin domain (PYD), the inflammasome receptors interact with the adaptor protein ASC, which then recruits pro-caspase-1 *via* its CARD domain and activates the effector caspase through proteolytic cleavage. The activated caspase-1 finally cleaves the immature pro-inflammatory cytokines pro-IL-1β and pro-IL-18.

The intracellular levels of main inflammasome mRNAs was not significantly different in monocytes from patients of controls, even if a trend toward an increased expression of PYCARD, AIM2 and NAIP was observed in septic shock patients (**Figures 1A–D**). IL-18 and IL-1β gene expression was higher in patients with septic shock, even if the high variability among patients did not allow to reach statistical significance (**Figures 1E,F**).

Concerning mtDNA, we found that circulating mtDNA levels were significantly higher in septic shock patients if compared to controls (**Figures 2A,B**), and that patients who died in ICU were

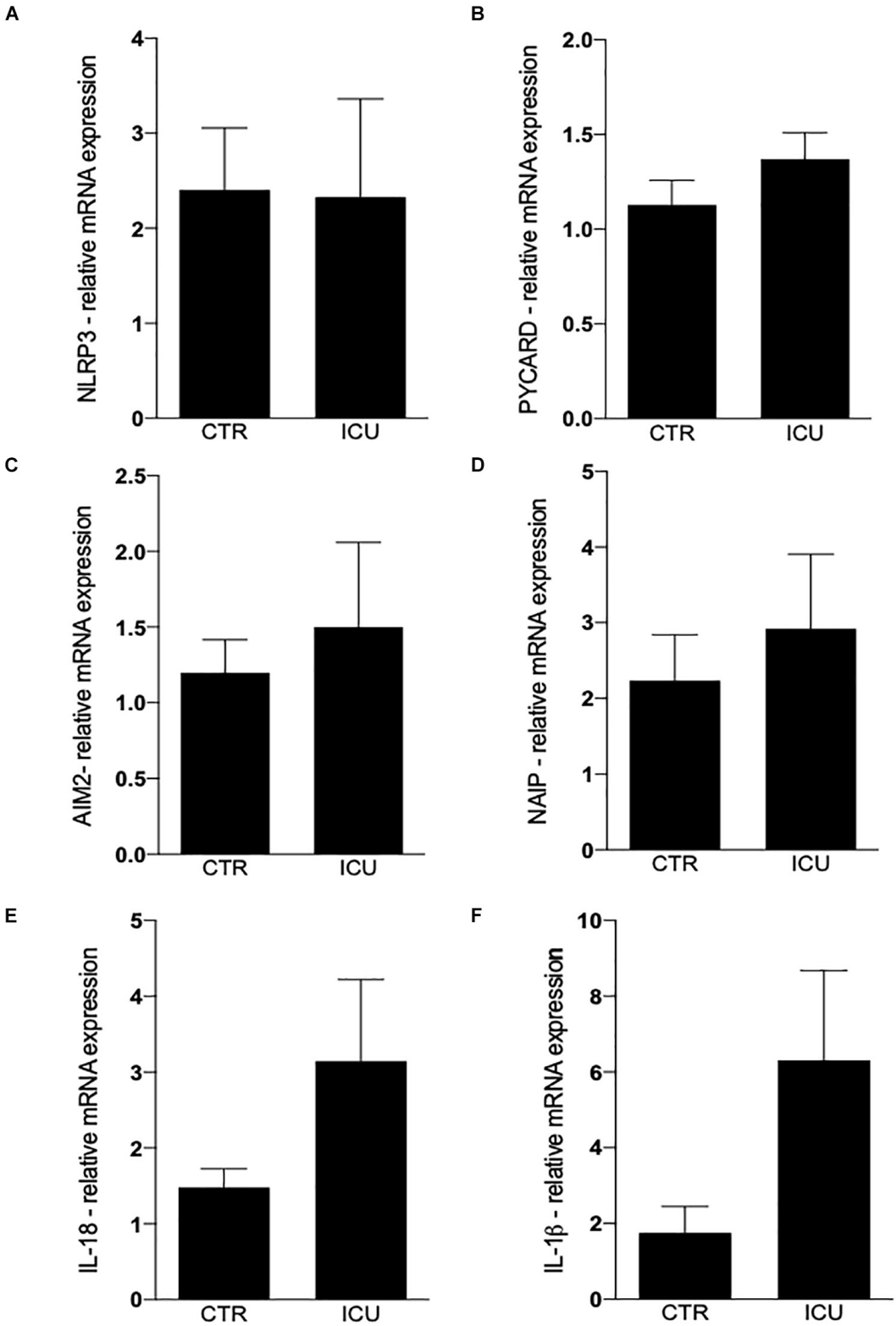

FIGURE 1 | Quantification of inflammasome genes by Real-Time PCR. **(A)** Quantification of NLRP3 in CD14+ cells on CTR and ICU septic shock patients. **(B)** PYCARD, **(C)** AIM2, **(D)** NAIP, **(E)** IL-18, **(F)** IL-1β. Data are represented as mean ± SEM. Analysis was performed using Mann–Whitney test.

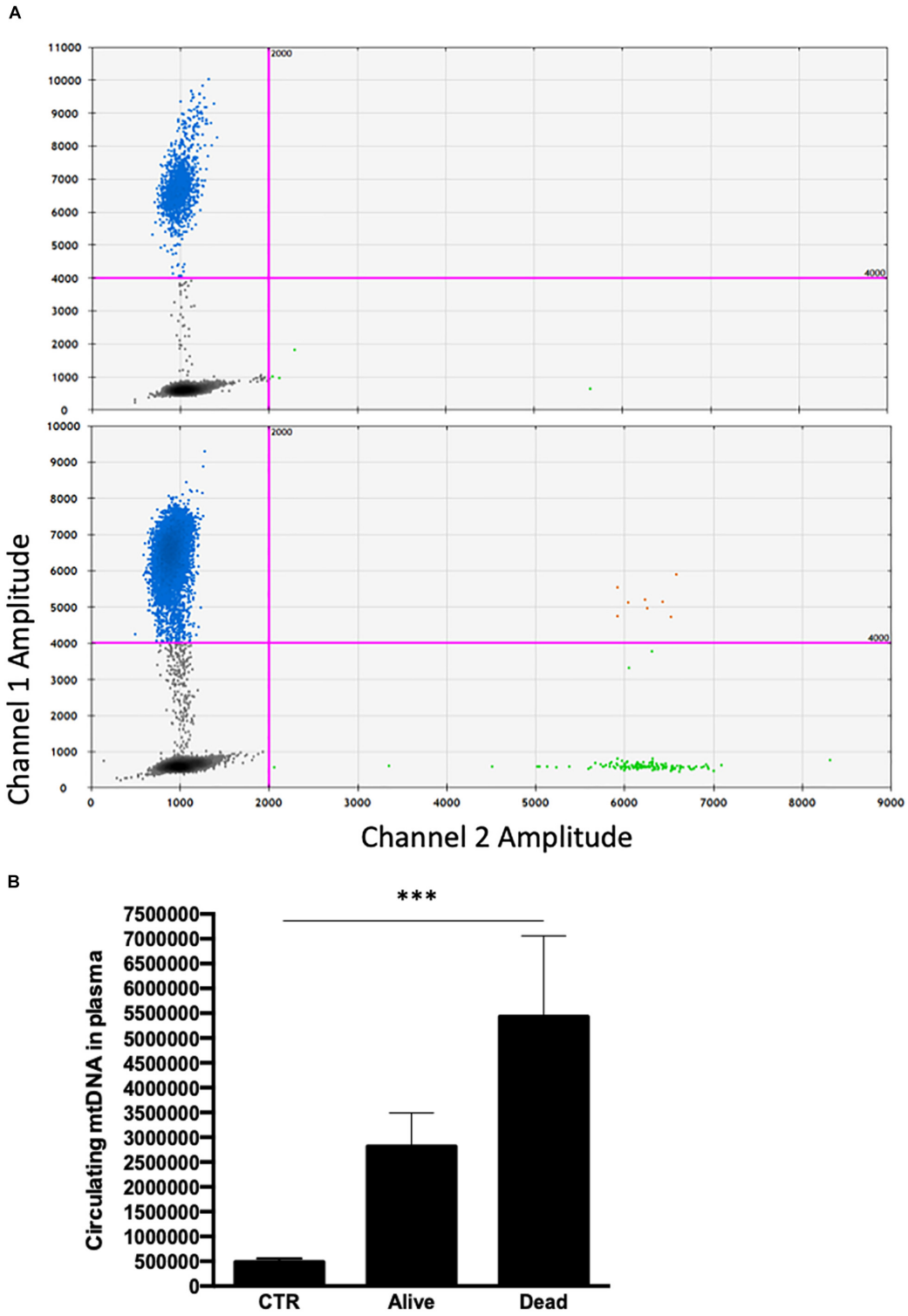

FIGURE 2 | (A) Representative 2D scatter plot of a ddPCR result, corresponding to mitochondrial (mt)-ND4 of healthy subject (upper panel) and septic patient (lower panel). The *y* axis shows FAM fluorescence amplitude of the mt-ND4 probe (channel 1) and the *x* axis shows the HEX fluorescence amplitude of the EIF2C1 probe (channel 2). The black cluster represents the negative droplets, the green cluster represents the droplets positive for EIF2C1, the blue cluster represents the droplets positive for mt-ND4 and the orange cluster represents the droplets that are positive for both targets. **(B)** Quantification of mtDNA circulating in plasma on CTR and ICU septic shock patients by ddPCR. Data are represented as mean ± SEM. Analysis was performed using Mann–Whitney test. ***$p < 0.05$. CTR, controls, ICU, intensive care unit.

characterized by higher level of mtDNA if compared to those patients with septic shock who were then discharged alive from the ICU (**Figures 2A,B**). No correlations were found between mtDNA and inflammasome gene expression level and other clinical variables reported in **Table 1**.

DISCUSSION

The spread of bacteria resistant to many classes of antibiotics is becoming one of the most worrying threats for the scientific community. The search for prognostic biomarkers during septic shock is currently the subject of great debate (13). However, few data exist on the role of inflammatory markers in the prognosis of septic shock caused by MDR bacteria (14) and, in particular, no studies investigate the role of inflammasome and mtDNA in this disease.

Sepsis clearly alters the innate and adaptive immune responses, causing immune suppression, chronic inflammation, and finally exhaustion of several cell defense mechanisms. Understanding how inflammatory processes are orchestrated, and in particular how their complex mechanisms work together could pave the way for the identification not only of suitable therapeutic targets, but also of predictive biomarkers. Here we observed that patients suffering from septic shock due to MDR bacteria, if compared to healthy subjects without infection, are characterized by similar level of inflammasome genes, but significantly higher level of circulating mtDNA.

Circulating cell-free mtDNA is a functional link between cell damage, mitochondrial damage and systemic inflammation and, indeed, mtDNA released after cell death can act as a DAMP, being able to induce an inflammatory response through hypomethylated CpG motifs resembling those of bacterial DNA (15). mtDNA is thus a potent DAMP capable of causing inflammation and propagating an immune response through its interaction with TLR9 and inflammasomes (16).

Plasma circulating mtDNA is elevated in critically ill patients, and increases with age, contributing to the maintenance of the low-grade, chronic inflammation observed in elderly people which has been defined "inflammaging" (17).

Results from clinical trials providing data on mtDNA during sepsis are not conclusive, so it cannot be established if mtDNA is associated with mortality or not (18). This phenomenon could be due to several reasons, that even regard technical aspects such as: (i) the lack of a standardized protocol for the measurements; (ii) the use of plasma or serum (freshly isolated or frozen); (iii) the preparation of plasma with or without the presence of platelets, that contain mitochondria (but not nuclear DNA) and thus can increase the number of molecules of mtDNA (17). To generate this data we took advantage of the sophisticated ddPCR approach, based on partitioning samples in 20,000 or more droplets, each of them representing an isolated end-point PCR reaction. Compared to Real-Time PCR, ddPCR provides absolute nucleic acids quantification and results are less dependent from reaction efficiency. Beyond technical issues, there is also the question of the appropriate patient population. Indeed, it is possible that the mechanism driving mtDNA release differs in patients with cellular injury from sepsis and those with a mechanical injury, as seen in phases like post-trauma or post-surgery. Anyway, in our patients mtDNA was definitely higher in septic shock population, especially in those who died in the ICU.

Concerning the levels of inflammasome gene expression in monocytes between septic shock patients and healthy controls, the hypothesis that MDR patients may have functionally exhausted the inflammatory response agrees with what stated by Hotchkiss et al. (19), who described this kind of patients as an expression of the state of hypo-reactivity of the immune system in the host's response to infection. Accordingly, our data would confirm that patients suffering from septic shock by MDR pathogens would be in that prevailing phase in which the inflammatory response has exhausted its thrust, returning to the levels of a healthy person not affected by an infectious disease. In other words, we could interpret this as an "abnormal normality," i.e., as the functional end of a normal inflammatory response that should have been much higher in a clinical situation such as sepsis.

We are aware that it would have been important to study the inflammasome in cells that are capable of triggering various inflammatory pathways, such as macrophages, which typically reside in the tissues. However, we were unable to obtain tissue samples and had to concentrate on circulating monocytes, which are simple enough to obtain, and study gene expression rather than protein levels due to the lack of biological material. In addition to the inability of studying macrophages we must also add that unfortunately, only anecdotical reports (20, 21) have dealt with the role of inflammasomes regarding strains of resistant bacteria, so our hypothesis of "abnormal normality" has to be verified with a more conspicuous number of patients.

The high level of mtDNA in patients with septic shock could also suggest that the exhaustion of inflammasome activity had favored the progression of the sepsis, and thus allowed the onset of further cellular damages.

Our study has two important limiting factors represented by the small size of the sample enrolled and the rather long period of time elapsed between the beginning and the end of the study itself. These limiting factors are related to the difficulty of enrolling patients with septic shock from MDR bacteria with a microbiological tests' confirmation obtained within 24 h from the onset of the shock (most of our patients had bloodstream infection or secondary or tertiary post-surgical peritonitis). So, our interest was aimed at testing the level of inflammasome gene expression and mtDNA at the early onset of the state of shock.

CONCLUSION

In conclusion, even considering the all limitations, our data suggest that patients with septic shock caused by MDR pathogens have a relatively low gene expression of inflammasomes, that is comparable to that of healthy patients without any infection. Furthermore, we show here that mtDNA could be considered an early prognostic marker of severity in septic shock from MDR. Further studies on other, more numerous cohorts are required to confirm our observations.

DATA AVAILABILITY STATEMENT

The raw data supporting the conclusions of this article will be made available by the authors, without undue reservation, to any qualified researcher.

ETHICS STATEMENT

The studies involving human participants were reviewed and approved by the Comitato Etico Provinciale di Modena e Reggio Emilia. The patients/participants provided their written informed consent to participate in this study.

AUTHOR CONTRIBUTIONS

SB and SD designed and carried out the study and drafted the manuscript. SD, MN, and AP performed the plasma tests. SV and MT were involved in clinical data acquisition. MG and AC supervised the study and revised the manuscript.

REFERENCES

1. Hotchkiss RS, Moldawer LL, Opal SM, Reinhart K, Turnbull IR, Vincent JL. Sepsis and septic shock. *Nat Rev Dis Primers*. (2016) 2:16045. doi: 10.1038/nrdp.2016.45
2. Nakahira K, Hisata S, Choi AM. The roles of mitochondrial damage-associated molecular patterns in diseases. *Antioxid Redox Signal*. (2015) 23:1329–50. doi: 10.1089/ars.2015.6407
3. Grazioli S, Pugin J. Mitochondrial damage-associated molecular patterns: from inflammatory signaling to human diseases. *Front Immunol*. (2018) 9:832. doi: 10.3389/fimmu.2018.00832
4. Kaczmarek A, Vandenabeele P, Krysko DV. Necroptosis: the release of damage-associated molecular patterns and its physiological relevance. *Immunity*. (2013) 38:209–23. doi: 10.1016/j.immuni.2013.02.003
5. West AP, Shadel GS. Mitochondrial DNA in innate immune responses and inflammatory pathology. *Nat Rev Immunol*. (2017) 17:363–75. doi: 10.1038/nri.2017.21
6. Yang Y, Yang J, Yu B, Li L, Luo L, Wu F, et al. Association between circulating mononuclear cell mitochondrial DNA copy number and in-hospital mortality in septic patients: a prospective observational study based on the Sepsis-3 definition. *PLoS One*. (2019) 14:e0212808. doi: 10.1371/journal.pone.0212808
7. Yan HP, Li M, Lu XL, Zhu YM, Ou-Yang WX, Xiao ZH, et al. Use of plasma mitochondrial DNA levels for determining disease severity and prognosis in pediatric sepsis: a case control study. *BMC Pediatr*. (2018) 18:267. doi: 10.1186/s12887-018-1239-z
8. Timmermans K, Kox M, Scheffer GJ, Pickkers P. Plasma nuclear and mitochondrial dna levels, and markers of inflammation, shock, and organ damage in patients with septic shock. *Shock*. (2016) 45:607–12. doi: 10.1097/SHK.0000000000000549
9. Busani S, Serafini G, Mantovani E, Venturelli C, Giannella M, Viale P, et al. Mortality in patients with septic shock by multidrug resistant bacteria: risk factors and impact of sepsis treatments. *J Intensive Care Med*. (2019) 34:48–54. doi: 10.1177/0885066616688165
10. Nasi M, Bianchini E, De Biasi S, Gibellini L, Neroni A, Mattioli M, et al. Increased plasma levels of mitochondrial DNA and pro-inflammatory cytokines in patients with progressive multiple sclerosis. *J Neuroimmunol*. (2020) 338:577107. doi: 10.1016/j.jneuroim.2019.577107
11. Nasi M, Pecorini S, De Biasi S, Bianchini E, Digaetano M, Neroni A, et al. Altered expression of PYCARD, interleukin 1beta, interleukin 18, and NAIP in successfully treated HIV-positive patients with a low ratio of CD4+ to CD8+ T cells. *J Infect Dis*. (2019) 219:1743–8. doi: 10.1093/infdis/jiy730
12. Gibellini L, Pecorini S, De Biasi S, Pinti M, Bianchini E, De Gaetano A, et al. Exploring viral reservoir: the combining approach of cell sorting and droplet digital PCR. *Methods*. (2018) 134–35:98–105. doi: 10.1016/j.ymeth.2017.11.014
13. Bermejo-Martin JF, Andaluz-Ojeda D, Martin-Fernandez M, Aldecoa C, Almansa R. Composed endotypes to guide antibiotic discontinuation in sepsis. *Crit Care*. (2019) 23:140. doi: 10.1186/s13054-019-2439-0
14. Gómez-Zorrilla S, Morandeira F, Castro MJ, Tubau F, Periche E, Cañizares R, et al. Acute inflammatory response of patients with pseudomonas aeruginosa infections: a prospective study. *Microb Drug Resist*. (2017) 23:523–30. doi: 10.1089/mdr.2016.0144
15. Collins LV, Hajizadeh S, Holme E, Jonsson IM, Tarkowski A. Endogenously oxidized mitochondrial DNA induces in vivo and in vitro inflammatory responses. *J Leukoc Biol*. (2004) 75:995–1000.
16. Harrington JS, Choi AMK, Nakahira K. Mitochondrial DNA in sepsis. *Curr Opin Crit Care*. (2017) 23:284–90. doi: 10.1097/MCC.0000000000000427
17. Pinti M, Cevenini E, Nasi M, De Biasi S, Salvioli S, Monti D, et al. Circulating mitochondrial DNA increases with age and is a familiar trait: implications for "inflamm-aging". *Eur J Immunol*. (2014) 44:1552–62. doi: 10.1002/eji.201343921
18. Schäfer ST, Franken L, Adamzik M, Schumak B, Scherag A, Engler A, et al. Mitochondrial DNA: an endogenous trigger for immune paralysis. *Anesthesiology*. (2016) 124:923–33. doi: 10.1097/ALN.0000000000001008
19. Hotchkiss RS, Monneret G, Payen D. Sepsis-induced immunosuppression: from cellular dysfunctions to immunotherapy. *Nat Rev Immunol*. (2013) 13:862–74. doi: 10.1038/nri3552
20. Codo AC, Saraiva AC, Dos Santos LL, Visconde MF, Gales AC, Zamboni DS, et al. Inhibition of inflammasome activation by a clinical strain of Klebsiella pneumoniae impairs efferocytosis and leads to bacterial dissemination. *Cell Death Dis*. (2018) 9:1182. doi: 10.1038/s41419-018-1214-5
21. Dikshit N, Kale SD, Khameneh HJ, Balamuralidhar V, Tang CY, Kumar P, et al. NLRP3 inflammasome pathway has a critical role in the host immunity against clinically relevant *Acinetobacter baumannii* pulmonary infection. *Mucosal Immunol*. (2018) 11:257–72. doi: 10.1038/mi.2017.50

Conflict of Interest: The authors declare that the research was conducted in the absence of any commercial or financial relationships that could be construed as a potential conflict of interest.

frontiers in Immunology

ORIGINAL RESEARCH
published: 15 May 2020
doi: 10.3389/fimmu.2020.00804

Distinct Neutrophil Populations in the Spleen During PICS

Satarupa Sengupta[1], *Charles C. Caldwell*[1,2] *and Vanessa Nomellini*[2,3]*

[1] Division of Research, Department of Surgery, University of Cincinnati College of Medicine, Cincinnati, OH, United States, [2] Division of Research, Shriners Hospital for Children, Cincinnati, OH, United States, [3] Section of General Surgery, Department of Surgery, University of Cincinnati College of Medicine, Cincinnati, OH, United States

While mortality after acute sepsis has decreased, the long-term recovery for survivors is still poor, particularly those developing persistent inflammation, immunosuppression, and catabolism syndrome (PICS). While previously thought that activated neutrophils responding to the acute phase of sepsis migrate to the spleen to undergo cell death and contribute to immunosuppression, our data show a significant accumulation of distinct, yet functional, neutrophil populations in the spleen in a murine model of PICS. The exact role and function of neutrophils in this response is still unclear. The objective of our study was to better define the immune function of splenic neutrophils to determine if this could give insight into the pathogenesis of PICS. Using a murine model of cecal ligation and puncture (CLP), which demonstrates all characteristics of PICS by 8 days, spleens were harvested, and neutrophils were identified by Ly6G and CD11b expression via flow cytometry. Nearly all splenic neutrophils expressed CD54, but there were distinct $CD54^{hi}$ and $CD54^{lo}$ cells, with the majority being $CD54^{lo}$ cells during PICS. The $CD54^{hi}$ population showed traditional, proinflammatory properties, but a relatively decreased chemotactic response, while $CD54^{lo}$ cells had significantly higher chemotaxis, yet significantly decreased proinflammatory functions. Using 5-ethynyl-2′-deoxyuridine (EdU) incorporation, we found that the $CD54^{hi}$ population on day 2 after CLP may be participating in emergency myelopoiesis. However, the vast majority of the $CD54^{lo}$ population were paused in the G_1 phase at this time point and not proliferating. By day 8 after CLP, most of the $CD54^{hi}$ cells in the spleen were no longer proliferating, while the $CD54^{lo}$ cells were, indicating that $CD54^{lo}$ dominate in extramedullary myelopoiesis at later time points. Almost none of the neutrophils produced arginase or inducible nitric oxide synthase (iNOS), indicating that these are not suppressor cells. Overall, our data demonstrate that neutrophil accumulation in the spleen during PICS is related to extramedullary myelopoiesis, leading to the production of immature neutrophils. While not suppressor cells, the majority have greater chemotactic function but less inflammatory responsiveness, which may contribute to the immunosuppression seen in PICS. Attention to these distinct neutrophil populations after septic or other systemic inflammatory responses is therefore critical to understanding the mechanisms of PICS.

Keywords: sepsis, PICS, neutrophils, CD54, immunosuppression

OPEN ACCESS

Edited by:
Thomas Griffith, University of Minnesota Twin Cities, United States

Reviewed by:
Peter A. Ward, University of Michigan, United States
Daniel Remick, Boston University School of Medicine, United States

***Correspondence:**
Vanessa Nomellini
nomellva@ucmail.uc.edu

Specialty section:
This article was submitted to Inflammation, a section of the journal Frontiers in Immunology

Received: *11 February 2020*
Accepted: *08 April 2020*
Published: *15 May 2020*

Citation:
Sengupta S, Caldwell CC and Nomellini V (2020) Distinct Neutrophil Populations in the Spleen During PICS. Front. Immunol. 11:804. doi: 10.3389/fimmu.2020.00804

INTRODUCTION

Recent advancements in the initial diagnosis and management of sepsis have resulted in improved overall survival. However, the long-term recovery among sepsis survivors is still poor, often leading to a state of chronic critical illness (1). This condition is frequently associated with a compromised immune system, also called persistent inflammation, immunosuppression, and catabolism syndrome (PICS) (2). As a result, these patients suffer from multiple complications, poor wound healing, increased disability, and susceptibility to secondary infections leading to prolonged hospitalizations (3). Despite extensive care and intervention, ∼50% of chronic critically ill patients die within 6 months of ICU discharge, and for those that are able to survive to 1 year after discharge, at least 20% show significant physical and cognitive disabilities, with almost 10% never returning home (3, 4). Failure of therapeutic interventions for sepsis-associated chronic critical illness is largely due to the insufficient information available about the immune dysfunction that occurs after sepsis.

Neutrophils are the key responders to infection in that activated neutrophils are recruited to the site of bacterial invasion to fulfill their antimicrobial function (5). Historically, it was thought that, following bacterial clearance, neutrophils mostly migrate to the spleen to undergo cell death, while the bone marrow undergoes emergency myelopoiesis to regenerate the neutrophil population (6). However, our data show a significant accumulation of distinct, yet functional, neutrophil populations in the spleen in a murine model of PICS, suggesting a possible role for these cells in secondary infections and/or the overall systemic response to sepsis.

Neutrophil rolling and migration involves the transmembrane glycoprotein and adhesion molecule, L-selectin (CD62L) in conjunction with β_2-integrin activation and adhesion to counter-receptors such as intracellular adhesion molecules (ICAM-1) (CD54) (7, 8). The ectodomain shedding of CD62L from neutrophil plasma membrane denotes neutrophil activation or partial activation (priming), concordant with upregulation of CD11b, a component of the macrophage-1 antigen (Mac-1) (CD11b/CD18) β_2-integrin subfamily (9). Appearance of the surface marker, CD54, on activated neutrophils correlates with reverse transendothelial migration, and its expression is known to be increased by inflammatory stimuli (10, 11). Neutrophils showing antitumorigenic phenotypes show increased CD54 expression (12), while CD54 expressing neutrophils are also associated with chronic systemic inflammation (13). However, the functional properties of these neutrophil subpopulations remain elusive (14). In our study utilizing a murine PICS model, we found that the myeloid-derived splenic neutrophils ($Ly6G^+CD11b^+$) distinctly comprised two populations based on the surface CD54 expression. We therefore decided to pursue this further to characterize the CD54 subpopulations (CD54 high and low) to help understand the immunosuppression in PICS. While it is known that the spleen can act as a site of extramedullary myelopoiesis, the exact role and functional properties of these splenic neutrophils is still not clear. Therefore, the objective of our study was to better characterize and define the immune function of these neutrophil subpopulations to gain insight into and better understand the pathogenesis of PICS.

MATERIALS AND METHODS

Cecal Ligation and Puncture Model

Cecal ligation and puncture was performed on 6 to 8-week-old male CD-1 mice from the Charles River Laboratories (Wilmington, MA, USA) as described previously (15). The animal protocol was approved under the Institutional Animal Care and Use Committee of the University of Cincinnati (Protocol No. 10-05-10-01). Briefly, the animals were provided with regular pellet diet and water *ab libitum* and were allowed to acclimatize for 1–2 weeks before experiments in standard environmental conditions. Acute polymicrobial sepsis was induced in the mice by 33% cecal ligation with a single, full-thickness 25-gauge needle puncture under 2.5% isoflurane followed by 3 and 24 h post-surgery primaxin administration. Time of surgery was kept consistent between experiments. The mortality rate remained 25–33% for 3 days after this cecal ligation and puncture (CLP) injury in mice, comparable to the 10–40% in human sepsis cases as defined previously (16, 17).

Persistent Inflammation, Immunosuppression, and Catabolism Syndrome Model

Mice that survived 8 days after CLP injury and displayed the syndromes including weight loss, lymphocyte depletion, increase in circulating myeloid cells, etc. were used in experiments as PICS mice as described previously (16). Untouched mice were used as control, as they have near-identical levels of systemic inflammation and coagulation parameters 8 days after sham surgery, which includes anesthetic administration and laparotomy without intervention.

Spleen Harvest and Cell Counts

Spleens were removed from untouched and PICS mice, weighed, and then homogenized in Roswell Park Memorial Institute (RPMI) medium followed by passing through a 70-μm cell strainer (Corning, MA, USA) to obtain a uniform single cell suspension. The total number of white blood cells (WBCs) was enumerated with a cell counter (Beckman Coulter, CA, USA). One to two million cells were used for further characterization of the splenic neutrophil compartment by flow cytometry.

Flow Cytometry

Flow cytometry was performed on the Attune NxT Flow Cytometer (Life Technologies, CA, USA). Cells were first gated for doublet exclusion [forward scatter height (FSC-H) vs. forward scatter area (FSC-A)] followed by side scatter height (SSC-H) vs. FSC-H gating. Cell viability was checked by negative gating of cells stained with "Live/Dead Fixable Aqua Dead Cell Staining Kit" (Life Technologies, CA, USA). Neutrophils were analyzed by detecting the surface antigens with the following antibodies: Ly6G (clone 1A-8, BD Biosciences, CA, USA), CD11b (clone M1/70, Biolegend, CA, USA), CD54 (clone 3E2), and CD62L (clone MEL-14) from BD Pharmingen, CA, USA; or

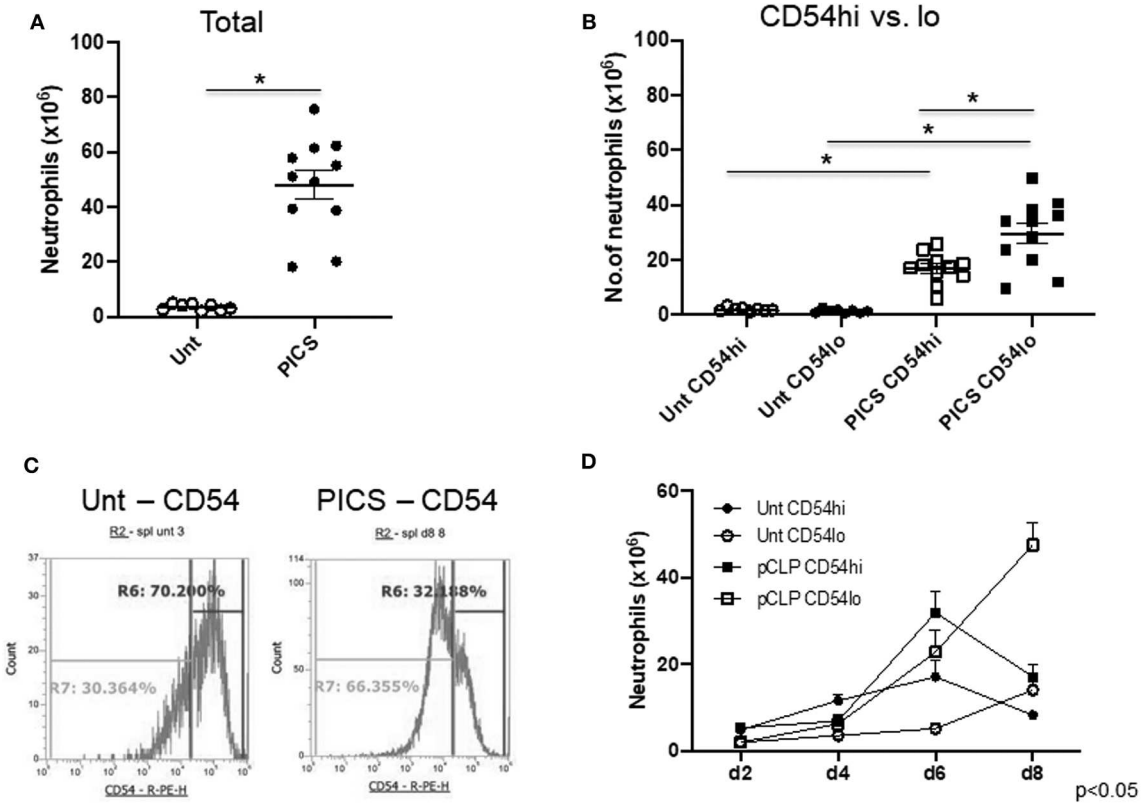

FIGURE 1 | The spleen harbors both CD54-high and CD54-low expressing neutrophils in persistent inflammation, immunosuppression, and catabolism syndrome (PICS) mice. Spleens were harvested from untouched (Unt) mice or mice post-CLP (pCLP) and single cell suspensions were colabeled with Ly6G, CD11b, and CD54 antibodies followed by flow cytometry analysis at different time points. Scatter plots depicting **(A)**, the total number of neutrophils (Ly6G+ CD11b+) in the spleen of Unt and pCLP day 8 (PICS) mice and **(B)** the number of neutrophils expressing high CD54 ($CD54^{hi}$) and low CD54 ($CD54^{lo}$) in Unt and PICS spleens. Black bars indicate the mean ± SEM values. *$p < 0.05$ was considered significant. **(C)** Histograms demonstrating CD54 expression pattern in splenic neutrophils with high (R6 gate) or low (R7 gate) expression in representative mice (Unt, left; PICS, right). Experiments were repeated at least three times. **(D)** Line graph showing the number of neutrophils with $CD54^{hi}$ or lo expression in the spleen of Unt and CLP mice at day 2 (d2), day 4 (d4), day 6 (d6), and day 8 (d8). A three-way ANOVA analysis of the Unt vs. pCLP, $CD54^{hi}$ vs. CD54lo, and time (days) rendered the data significant ($p < 0.05$).

total antigens (surface and intracellular) by antibodies: CXCR4 (clone L276F12) and CXCR2 (clone SA045E1) from Biolegend, CA, USA; or by intracellular labeling with antibodies: Arg-1 (clone A1exF5) and inducible nitric oxide synthase (iNOS) (clone CXNFT) from Invitrogen, MA, USA. Cells were fixed with 1% paraformaldehyde and permeabilized with Saponin buffer [0.1% Saponin (*w*/*v*), 0.1% bovine serum albumin (BSA), 0.01 M HEPES, and 0.1% sodium azide in phosphate-buffered saline (PBS)] prior to the intracellular labeling as described previously (18).

Functional Assays

DHR Assay

Dihydrorhodamine (DHR) 123 assay was performed to measure the formation of oxidized rhodamine 123 from the non-fluorescent DHR 123, thus to assess reactive oxygen species (ROS) production. Harvested spleen cells were resuspended in Hank's balanced salt solution (HBSS) ($Ca^{++}Mg^{++}$) and were incubated with DHR (Sigma, MO, USA) (final 1×) at 37°C for 10 min. The reaction was stopped in ice, and the cells were washed twice with ice-cold fluorescence-activated cell sorting (FACS) buffer (1×). Finally, the cells were labeled with fluorescence-conjugated antibodies against the surface markers of interest (Ly6G, CD11b, CD54), and flow cytometry analysis was performed to detect the green fluorescence of rhodamine 123 as a ROS indicator as described previously (16).

pHrodo Assay

pHrodo Green *Escherichia coli* BioParticles Conjugate for Phagocytosis (Invitrogen, MA, USA) were reconstituted in a glass tube and then sonicated in a water bath sonicator for 5 min. Opsonizing reagent was added (1:40) to the *E. coli* BioParticles and was incubated at 37°C for 1 h. The particles were washed twice with PBS, and 100 µl PBS resuspension was added to 1 million splenocytes followed by incubation in 37°C 5% CO_2 incubator for another hour. The reaction was stopped in ice, and the cells were fixed with 1% paraformaldehyde (PFA). After washing, the cells were labeled with antibodies against the surface markers of interest as described above, and finally, the phagocytosing cells were detected by measuring the

green fluorescence uptake of the *E. coli* BioParticles as described previously (19).

NETosis Assay

NETosis assay was performed as described previously (20). Briefly, cells were resuspended in RPMI and were stimulated with 100 nM phorbol-12-myristate-13-acetate (PMA) (Sigma, MO, USA) for 3 h at 37°C 5%CO_2 incubator. Cells were then washed and fixed with 1% PFA followed by further wash, blocking, and staining with primary H3 antibody (1:300, Abcam, MA, USA) for 30 min at room temperature. Then, the cells were incubated with the antibody cocktail of Alexa Fluor700-conjugated secondary antibody (1:300, Invitrogen, MA, USA) and fluorescein isothiocyanate (FITC)-conjugated antimyeloperoxidase (1:50, Abcam, MA, USA), along with the surface markers of interest as described above at room temperature for 30 min in the dark. Finally, the cells were washed and resuspended in FACS buffer for flow cytometry analysis as mentioned (20).

Chemotaxis Assay

After harvesting and cell counting, 2 million spleen WBCs were seeded on a Transwell insert (Thermo Fisher Scientific, MA, USA) of 3 μm pore size. One hundred nanograms of KC, as a main neutrophil chemoattractant, was added to each of the bottom wells, and the cells were incubated at 37°C CO_2 incubator for 3 h. Non-migrated cells from the upper Transwell insert and migrated cells from the bottom well were recovered to analyze further by flow cytometry. The percent of cells migrating to the bottom was then calculated as described previously (21).

Cell Cycle and Proliferation Assays

For cell cycle analysis, the splenocytes were labeled with fluorescence-conjugated antibody against Ki-67 (clone 16A8, Biolegend, CA, USA) and propidium iodide (PI) solution (25 μg/ml) followed by flow cytometry analysis as described previously (22). For the 5-ethynyl-2′-deoxyuridine (EdU) assay, mice were injected with EdU on day 7 after CLP, and the splenocytes were harvested on post-CLP day 8. EdU incorporation into newly synthesized DNA was measured by analyzing the cells using iClick EdU Andy Fluor 488 Flow Cytometry Assay Kit (ABP Biosciences, MD, USA).

Statistical Analyses

All analyses were performed using the software GraphPad Prism 8 (La Jolla, CA, USA). Student's *t*-test was performed to compare groups, and one-, two-, or a three-way ANOVA was performed for multiple comparisons as applicable. Data were reported as means ± SEM values. Any $p \leq 0.05$ was considered statistically significant.

RESULTS

The Spleen Harbors Both CD54-High and CD54-Low Expressing Neutrophils in PICS Mice

Single-cell suspensions of spleens from untouched (Unt) mice and mice post-CLP (cecal ligation and puncture) from different days were labeled with neutrophil and myeloid markers (Ly6G and CD11b, respectively) to detect mature neutrophils. Spleen-to-body mass ratio was also quantified to confirm the gradual increase in spleen mass in CLP mice compared to the healthy ones (**Figure S1**). The total number of neutrophils was significantly increased in PICS mice (post-CLP day 8) compared to the Unt mice (**Figure 1A**). Furthermore, the neutrophils in PICS spleens were analyzed based on CD54 surface marker expression. While most of the splenic neutrophils expressed CD54, there were distinct CD54-high ($CD54^{hi}$) and CD54-low ($CD54^{lo}$) expressing cells, with the majority being $CD54^{lo}$ cells during PICS (**Figure 1B**). In Unt spleens, however, the CD54-expressing cells were markedly less in number with no distinct separation or difference in the number of $CD54^{lo}$ cells compared to the $CD54^{hi}$ cells (**Figure 1B**). The percent population comprising $CD54^{lo}$ cells mostly formed a distinct peak from the $CD54^{hi}$ population in PICS spleen unlike the Unt cells as shown in the representative FACS image (**Figure 1C**). Interestingly, when we compared the neutrophil populations of $CD54^{hi}$ vs. $CD54^{lo}$ in PICS spleens from post-CLP day 2–8, we found that the $CD54^{hi}$ population was significantly higher in the acute phase after infection, but gradually over time, the $CD54^{lo}$ population became the dominant phenotype. By the time all mice develop PICS, the ratio was reversed, and the $CD54^{lo}$ neutrophils were significantly higher than the $CD54^{hi}$ population, unlike in the Unt mice (**Figure 1D**). The total WBC counts ranged from 86 to 174 million in the control Unt mice and 87 to a much increased number of 552 million in CLP mice starting from day 2 through day 8 post-CLP. Together, these results indicate the appearance of two distinct neutrophil populations in the PICS spleen.

$CD54^{hi}$ Neutrophils Show Proinflammatory Properties While $CD54^{lo}$ Neutrophils Show Chemotactic and Homing Properties

In order to explore the function of the $CD54^{hi}$ and $CD54^{lo}$ cells specifically during PICS, we then evaluated their ability to produce ROS, undergo phagocytosis, and form neutrophil extracellular traps (NETs). A DHR assay was performed to assess ROS production by measuring the oxidation of DHR. $CD54^{lo}$ cells showed significantly decreased ROS production compared to the $CD54^{hi}$ cells as depicted by the mean fluorescence intensity (MFI) in **Figure 2A**. Moreover, $CD54^{lo}$ cells had significantly decreased phagocytosis and NETosis, compared to $CD54^{hi}$ neutrophils (**Figures 2B**, **C**).

While these studies indicate that $CD54^{lo}$ cells may be less proinflammatory in nature, this population exhibited greater chemotactic ability compared to $CD54^{hi}$ cells (**Figure 3A**). To evaluate this further, the expressions of surface and total CXCR4 and CXCR2 were examined in both populations. The majority

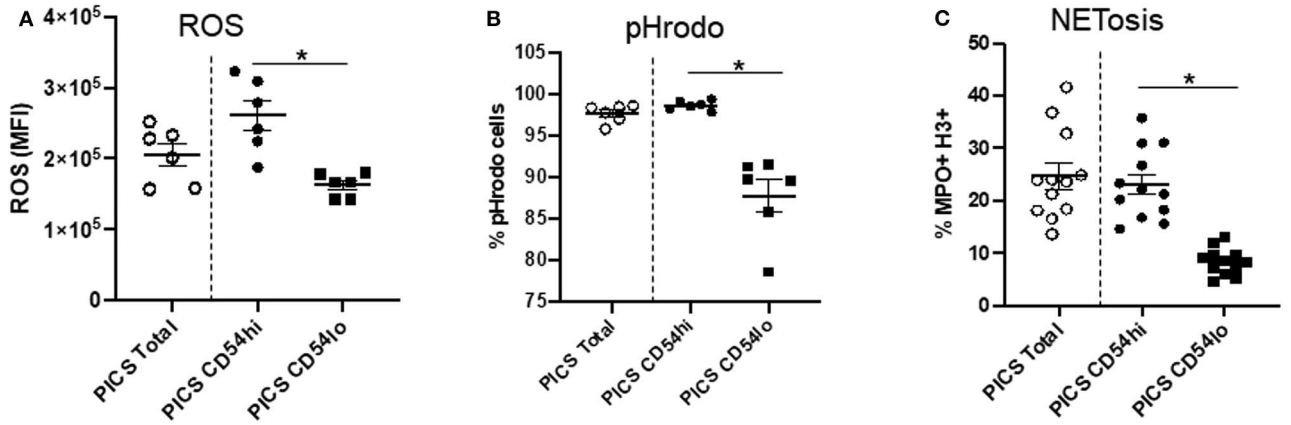

FIGURE 2 | CD54^{hi} neutrophils demonstrate proinflammatory properties. Spleen cells from persistent inflammation, immunosuppression, and catabolism syndrome (PICS) mice were labeled with Ly6G, CD11b, and CD54 and functional assays such as dihydrorhodamine (DHR) to measure reactive oxygen species (ROS), pHrodo (phagocytosis), and NETosis were separately performed using flow cytometry. Scatter plots showing **(A)** ROS mean fluorescence intensity (MFI) of DHR, **(B)** percent pHrodo+ cells, and **(C)** percent MPO+H3+ cells (NETosis) in total, and CD54^{hi} or CD54^{lo} expressing splenic neutrophils. Experiments were repeated at least three times. Black bars in scatter plots indicate the mean ± SEM values. *$p < 0.05$ was considered significant.

of CXCR4 expression on neutrophils in the spleen during PICS was intracellular, as evidenced by significantly more total CXCR4 relative to surface CXCR4 (mean total MFI value, 13,854 ± 4,849 vs. mean surface MFI, 3,034 ± 684). However, CD54^{lo} neutrophils had greatly reduced surface as well as total CXCR4 expression, compared with CD54^{hi} cells (**Figures 3B,D**). For CXCR2, the majority of expression was on the surface, as evidenced by almost similar total and surface levels of CXCR2 (mean total MFI value, 1,537 ± 444 vs. mean surface MFI, 1,321 ± 826). While both CD54^{hi} and lo cells had equivalent surface expression of CXCR2, the total levels were decreased in CD54^{lo} cells, indicating a lower availability of CXCR2 receptors to recycle back to the surface after stimulation (**Figures 3C**, **E**). Altogether, these results indicated a higher chemotactic and homing ability but less inflammatory function of CD54^{lo} cells, whereas CD54^{hi} cells have greater inflammatory function with decreased chemotactic responses during PICS.

CD54^{hi} Cells Are the First Proliferative Population While CD54^{lo} Cells Engage in Late Cycling

Next, we investigated the proliferation and cell cycle distribution of the CD54 high and low populations to assess whether they could differentially contribute to emergency myelopoiesis. To examine the cell cycle status of proliferating neutrophils, we analyzed the cells for the proliferation-specific marker, Ki-67, as well as for DNA content by propidium iodide (PI) staining using flow cytometry (22). The Ki-67^{+} population included the active cell cycle phases (G_1, S, and G_2/M), while the quiescent or resting (G_0) cells were negative in Ki-67. PI vs. Ki-67 gating was used to identify the distribution of CD54^{hi} and CD54^{lo} cells in sub-G_1 (apoptotic cells with fragmented DNA), G_1, S, G_2/M, and G_0 phases from mouse spleens post-CLP days 2–8 (**Figure S2**). No G_0 event was detected in either of the cell populations, indicating that all neutrophils had entered the active cell cycle phases following infection (**Figure S2**). CD54^{hi} cells were found cycling until post-CLP day 6, when the majority of the cells were found in G_2/M, with some in S phase, but the least in G_1 phase. By day 8, both S and G_1 events were further decreased, the lowest being in G_1, while the maximum (>80%) were in G_2/M (**Figure 4A**). This suggests that all the cycling cells gradually reached G_2/M with no further recycling or entry of new cells into G_1 by day 8 after CLP. On the other hand, CD54^{lo} neutrophils showed an almost opposite pattern of cell cycle kinetics from post-CLP days 2–8. The majority of events (>80%) was paused in the G_1 phase during post-CLP days 2–4 until around post-CLP day 6, when the CD54^{lo} population started progressing from G_1 to S phase (**Figure 4B**). The transition of CD54^{lo} cells further continued through G_1-S–G_2/M phases post-CLP day 8 (**Figure 4B**).

We also used the EdU incorporation method to detect and quantify the proliferating cells in CD54^{hi} and CD54^{lo} populations during PICS. Mice were injected with EdU on day 7 after CLP, and cells were harvested for analysis after 24 h on post-CLP day 8. Both populations had cells that finished maximum incorporation of EdU (EdU high) after a full S phase (**Figure 4C**), CD54^{hi} being slightly higher (∼4%) than CD54^{lo} cells but not statistically significant. Interestingly, cells that did not finish the S phase yet (ongoing S) and incorporated comparatively lesser EdU (EdU low) by post-CLP day 8 were significantly higher (∼10%) in CD54^{lo} compared to the CD54^{hi} population (**Figure 4D**). This result also supported our previous cell cycle data showing that the CD54^{hi} population gradually completed the S phase and progressed to the next phase (G_2/M) of the cycle, while the CD54^{lo} population started actively cycling post-CLP days 6–8 (**Figures 4A**, **B**). Taken together, these data suggest that immediately after CLP, CD54^{hi} cells may be participating in emergency myelopoiesis, as they were proliferating more in the acute phase of infection (post-CLP days 2–4). On the other hand, CD54^{lo} cells, which started cycling at day 6 post-CLP, may

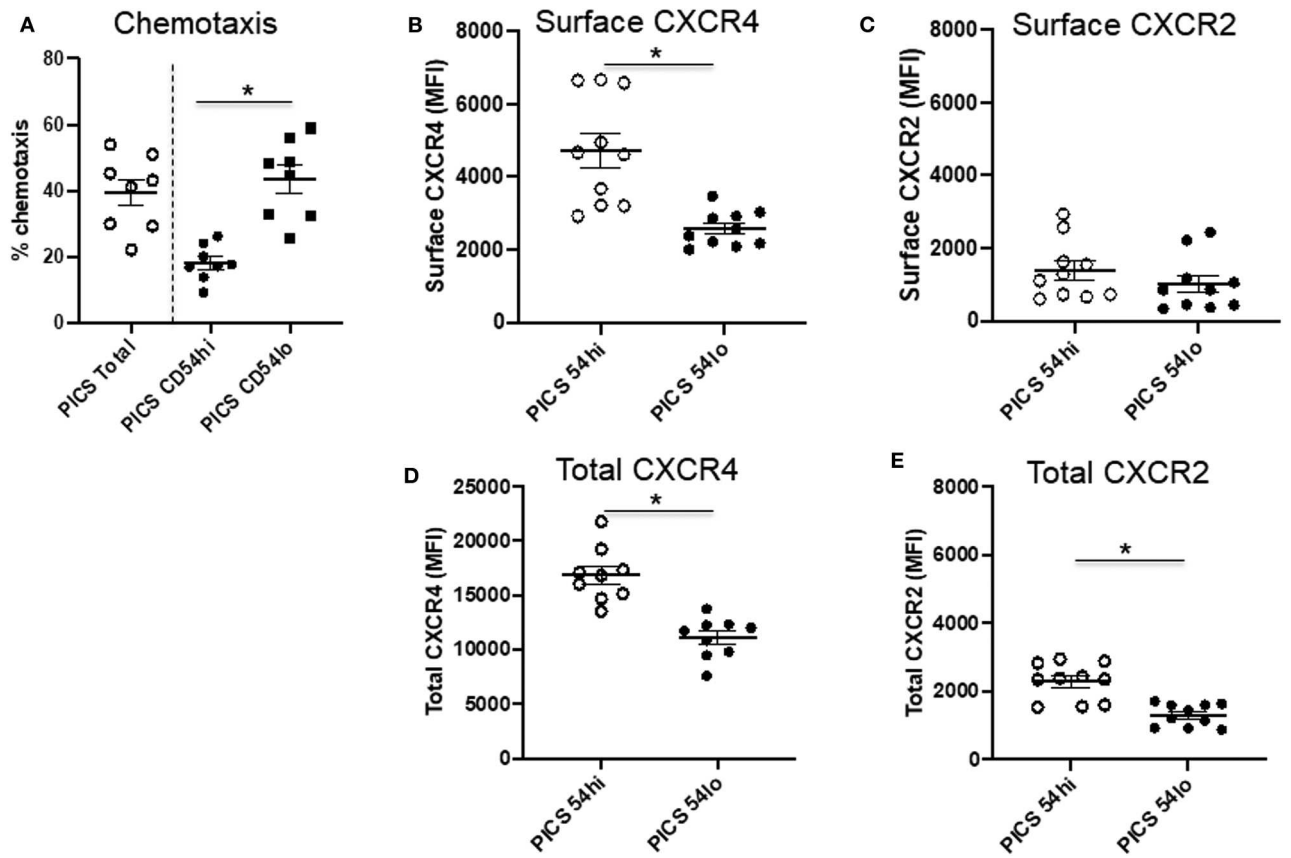

FIGURE 3 | CD54^{lo} neutrophils demonstrate increased chemotactic properties. Spleen cells isolated from persistent inflammation, immunosuppression, and catabolism syndrome (PICS) mice were subjected to either chemotaxis assays and then collected for labeling with Ly6G, CD11b, CD54, or were directly colabeled with CXCR4 and CXCR2 along with Ly6G, CD11b, and CD54 followed by flow cytometry analysis. **(A)** Percent chemotaxis of neutrophils from the spleen of PICS mice were plotted to quantify the chemotaxis in total, as well as in CD54^{hi}, and CD54^{lo} cells. Scatter plots showing **(B)** surface expression (MFI) of CXCR4 and **(C)** CXCR2, and **(D)** total expression (MFI) of CXCR4 and **(E)** CXCR2 on CD54^{hi} and CD54^{lo} splenic neutrophils from PICS mice. Experiments were repeated at least twice. Black bars in scatter plots indicate the mean ± SEM values. *$p < 0.05$ was considered significant.

be involved in extramedullary myelopoiesis at later time points (post-CLP days 6–8). This again supported our finding that CD54^{lo} cells comprised the majority of neutrophils by day 8 post-CLP (**Figure 1D**) compared to the CD54^{hi} cells that gradually decreased over time.

CD54^{lo} Neutrophils Are Not Suppressor Cells in PICS

As indicated above, CD62L expression may help determine the level of maturity of neutrophils. In addition, it has been reported that a subset of CD62L^{dim} neutrophils can serve as myeloid-derived suppressor cells (MDSCs) of granulocytic origin and can lead to immunosuppression via a Mac-1 (CD11b/CD18) or ROS-dependent manner (23). When we evaluated the CD54^{hi} and CD54^{lo} neutrophil subsets based on their CD62L expression in PICS mice, we found that CD54^{lo}CD62L^{lo} subset was significantly highest among all other subsets (**Figure 5A**). On the other hand, CD54^{hi}CD62L^{lo} neutrophils were significantly less and possibly comprised the minor population of CD54^{hi}-activated neutrophils that already shed the ectodomain of CD62L. In concordance, this population also showed the greatest CD11b expression (data not shown), indicating that these are more mature neutrophils. However, the other CD62L^{lo}CD54^{lo} cells showed significantly less CD11b expression compared to the CD54^{hi}CD62L^{lo} cells. As expected, all CD62L^{hi} subsets showed comparatively less CD11b expression than the CD62L^{lo} cells, again signifying that CD62L can help identify the maturation phase of neutrophils.

As some studies have indicated, emergency myelopoiesis may lead to the excessive release of MDSCs from the bone marrow, which may contribute to the immunosuppression seen in later phases after sepsis (24, 25). Therefore, we further examined other MDSC markers, such as intracellular arginase-1 (Arg-1) and iNOS (26, 27). However, our data indicated that <1% of neutrophils in the spleen of PICS mice express Arg-1 or iNOS (**Figures 5B,C**). While both subsets of CD54^{lo} neutrophils had significantly decreased Arg-1 and iNOS expression, the total

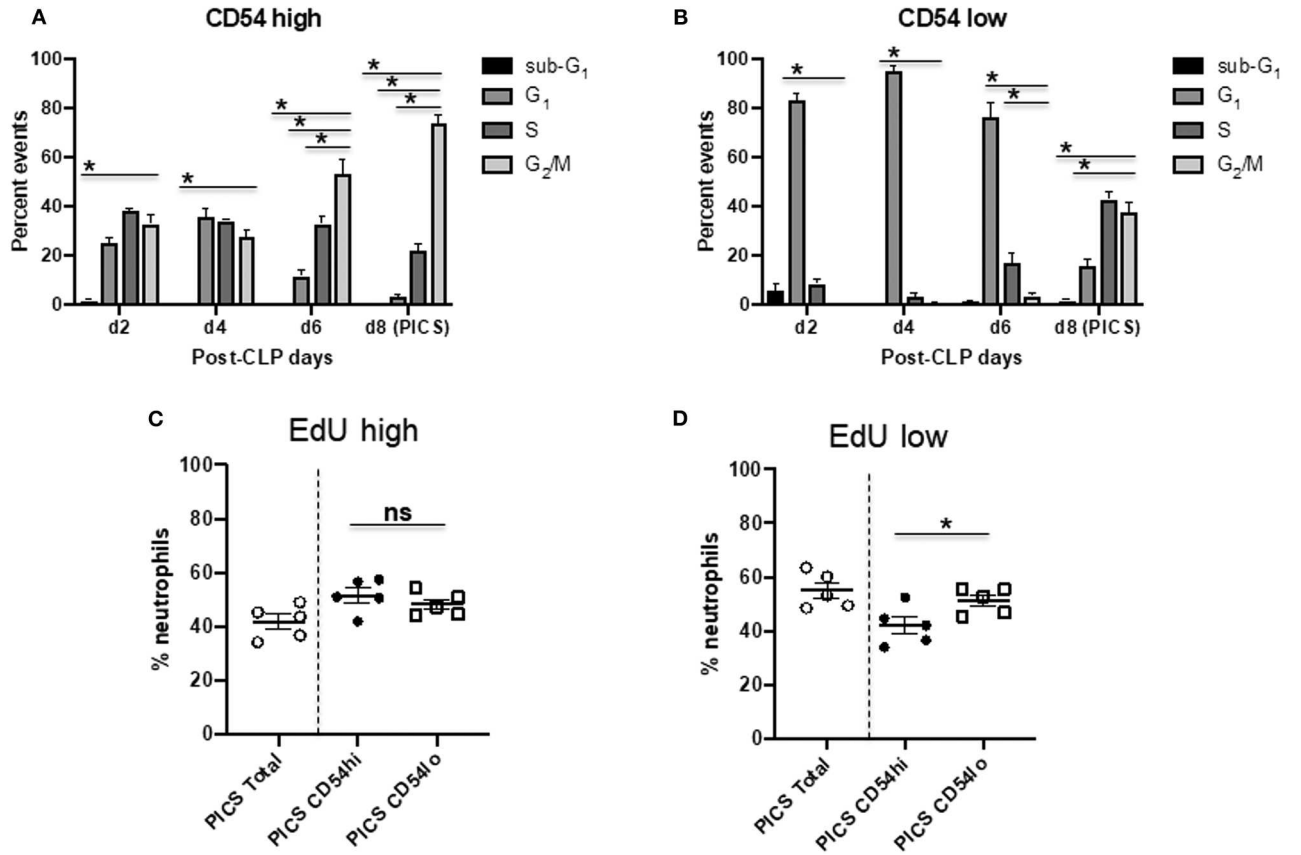

FIGURE 4 | CD54^{hi} cells are the first proliferative population while CD54^{lo} cells engage in late cycling. Spleen cells from mice at days 2, 4, 6, and 8 (d2, d4, d6, and d8, respectively) after CLP were colabeled with Ki-67 and PI along with Ly6G, CD11b, and CD54 to quantify the cell cycle phases by Ki-67 vs. PI gating using flow cytometry. Bar diagrams depicting percent events of sub-G_1 G_1, S, and G_2/M phases in **(A)** CD54^{hi} and **(B)** CD54^{lo} neutrophils from post-CLP mice. Each bar represents the mean ± SEM of percent events of each cell cycle phase at respective post-CLP day from mouse spleen after CLP (n = 5–8). 5-Ethynyl-2′-deoxyuridine (EdU) assays on neutrophils from the spleens of persistent inflammation, immunosuppression, and catabolism syndrome (PICS) mice were then performed as described earlier. Scatter plots showing **(C)** percent neutrophils with high EdU incorporation (EdU high) after completion of S phase, and **(D)** low EdU incorporation (EdU low) with an ongoing S phase in total vs. CD54^{hi} and CD54^{lo} splenic cells in PICS mice. Experiments were repeated at least twice. Black bars in scatter plots indicate the mean ± SEM values. *$p < 0.05$ was considered significant. ns, non-significant.

numbers of each of these cell types are negligible and likely not clinically significant (**Figures 5B,C**). Taken together, our results indicated that the comparatively immature CD54^{lo} neutrophils are not MDSCs but do have decreased overall immune functions.

DISCUSSION

This study intended to better characterize the immune function of the splenic neutrophil populations temporally after CLP to enhance the knowledge and understanding of the pathogenesis of PICS. Using our PICS murine model, we found two discrete neutrophil populations in the spleen. One population being the mature CD54^{hi} cells with traditional proinflammatory features that decreased significantly after CLP, and the other being CD54^{lo} cells that were less mature, had decreased inflammatory properties and dominated during the PICS phase. CD54^{lo} neutrophils were also more chemotactic and were actively proliferating, whereas the CD54^{hi} cells stopped reentering the cell cycle for further proliferation during PICS. None of these neutrophils showed any suppressor activity but were less functional with reduced inflammatory responsiveness. Our current study has identified a unique extramedullary CD54^{lo} neutrophil population in spleen characterized by reduced immune function during PICS that may explain the pathophysiology in sepsis-induced chronic critical illness.

Neutrophil heterogeneity can be phenotypic or functional and is pronounced at different levels of their life cycle, either in homeostatic or disease conditions (13, 28). Infectious inflammation can induce rapid changes in neutrophil variants as a function of maturity or activation state (11, 28). While the innate immune response is the initial responders to infection, the other cellular response are also important. It turns out that neutrophils, being the primary defenders of innate response, also interact with other cell types (particularly T cells) and can really shape the ensuing responses, both acutely and

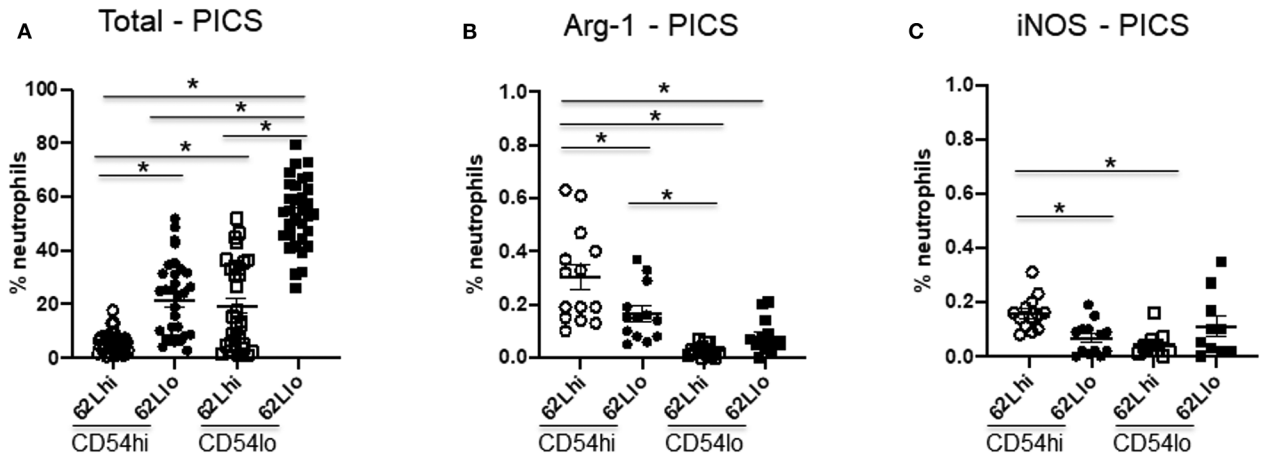

FIGURE 5 | CD54^{lo} neutrophils are not suppressor cells. Neutrophils with high or low CD54 expression (CD54^{hi} and CD54^{lo}) from the spleen of persistent inflammation, immunosuppression, and catabolism syndrome (PICS) mice were further characterized based on the adhesion marker, CD62L, and the intracellular expression levels of arginase 1 (Arg-1) and inducible nitric oxide synthase (iNOS) as markers for myeloid-derived suppressor cells using flow cytometry analysis. Scatter plots showing **(A)** percent neutrophils of each subtype, **(B)** percent neutrophils with arginase-1, and **(C)** iNOS expression in CD62L vs. CD54 subpopulations in PICS. Experiments were repeated three times. Black bars in scatter plots indicate the mean ± SEM values. *$p < 0.05$ was considered significant.

over time. In addition, it is known that the myeloid-derived suppressor cells (MDSCs), which are typically considered immature, may also comprise the neutrophil population (11, 29). In our PICS murine model, the early proliferation of CD54^{hi} cells immediately after acute infection suggested an emergency myelopoiesis, while the late onset of cell cycle in the gradually dominating CD54^{lo} phenotype in the spleen suggested an ongoing extramedullary myelopoiesis. However, the contribution of these differential neutrophil populations to the immunosuppression seen in the later stages of sepsis is not known. Earlier studies have indicated that the immunosuppression in septic patients might result from the expansion of persistent MDSCs immediately after the emergency myelopoiesis, which may result in chronic critical illness [reviewed in (30)]. However, in our study, we found a newly emerging population in PICS spleen—the population of CD54^{lo} neutrophils with decreased immune function. It has been shown that, in CLP mice 7 days post-sepsis, up to 95% BM cells are myeloid cells mostly immature and function like MDSCs, which gradually evolve with time to become more immunosuppressive and infiltrate the spleen, lymph nodes, lung, liver, skeletal muscle, and brain (2). MDSCs are generally granulocytic (CD11b+ Ly6G+) and monocytic (CD11b+ Ly6G− Ly6C+) cells. We chose to evaluate the granulocytes in spleen to gain a better sense of the changes in immune cells peripherally, than just simply measuring peripheral blood neutrophils and monocytes, which would not necessarily describe the happenings within remote tissues systemically. MDSCs have been so far mostly implicated in immunosuppression in sepsis while they can also be proinflammatory potentially damaging to parenchymal cells. Interestingly, in our study, we found that the proinflammatory granulocytic cells (CD11b+ Ly6G+ CD54^{hi}) were immunoresponsive but more mature and less in number, while the dominant population comprised the newly proliferating chemotactic granulocytes (CD11b+ Ly6G+ CD54^{lo}) lacking immune responsiveness. These CD54^{lo} cells also included the major subpopulation CD54^{lo}CD62L^{lo}, which had comparatively lower CD11b expression than the functional CD54^{hi}CD62L^{lo} cells and did not express intracellular Arg-1 or iNOS, indicating that these cells were not part of the MDSC community. Previously, other reports suggested a distinct human neutrophil phenotype in the blood during acute inflammation, characterized by CD54^{bright} cells (CD62L^{dim}/CD16^{bright}/CD11b^{bright}/CD54^{bright}) showing immune suppression capacity via T cell suppression (23). The effect of CD54^{hi} and CD54^{lo} cells on T cell function in our study, however, is not yet known.

Neutrophils capable of migration from the bone marrow after granulopoiesis or of reverse transmigration to the bone marrow for further homing are known to have down-regulated CXCR4 expression through decreased CXCR4/CXCL12 signaling (5). While decreased CXCR2 is associated with neutrophil adhesion (31), neutrophils lacking both CXCR4 and CXCR2 are known to display constitutive mobilization, with CXCR4 playing the dominating role in neutrophil trafficking (32). In our study, the CD54 populations showed overall decreased CXCR2 expression. It is well-known that the recruitment of mature and immature neutrophils from the bone marrow occurs to establish a niche in the spleen (33). However, the CD54^{lo} cells significantly lacked CXCR4 expression, which may indicate a greater transmigration or homing ability of this population.

This current study is only limited to a mouse model of PICS. Therefore, it is necessary to expand this study to patients with chronic critical illness. In addition, we do not yet know the role of these differential populations of splenic neutrophils in the setting of a secondary infection. Therefore, although the CD54^{lo} cells have decreased inflammatory functions, further studies are required to determine if they contribute to the

immunosuppression that occurs in PICS. Ongoing studies in our lab will reveal more information about the status and function of circulating neutrophils in both the early and later stages of sepsis and help determine the exact role of splenic neutrophils in the development of chronic critical illness after sepsis. Furthermore, focused studies will be interesting to investigate the role of any similar or other population of neutrophils and/or other innate immune cells in tissues other than spleen in PICS.

In conclusion, the comparatively immature, actively proliferating neutrophils arising in spleen have significantly less proinflammatory function, yet preserved chemotactic ability during PICS, which may act as a contributing factor of immunosuppression as seen after sepsis. Therapeutic strategies to target these neutrophils might benefit critically ill sepsis survivors and improve overall outcomes for this patient population.

DATA AVAILABILITY STATEMENT

All datasets generated for this study are included in the article/**Supplementary Material**.

ETHICS STATEMENT

This animal study was reviewed and approved by Institutional Animal Care and Use Committee of the University of Cincinnati (Protocol # 10-05-10-01).

AUTHOR CONTRIBUTIONS

SS: design of the work, data collection, data analysis and interpretation, drafting the article, critical revision of the article, and final approval of the version to be published. CC and VN: conception of the work, data analysis and interpretation, drafting the article, critical revision of the article, and final approval of the version to be published.

FUNDING

This work was supported by NIH K08 GM131284 (VN) from the National Institute of General Medical Sciences. This content was solely the responsibility of the authors and does not necessarily represent the official views of the National Institute of General Medical Sciences or the National Institutes of Health.

ACKNOWLEDGMENTS

The authors would like to acknowledge Lisa England and Holly Goetzman for their excellent veterinarian and flow cytometric support.

SUPPLEMENTARY MATERIAL

The Supplementary Material for this article can be found online at: https://www.frontiersin.org/articles/10.3389/fimmu.2020.00804/full#supplementary-material

REFERENCES

1. Shankar-Hari M, Rubenfeld GD. Understanding long-term outcomes following sepsis: implications and challenges. *Curr Infect Dis Rep.* (2016) 18:37. doi: 10.1007/s11908-016-0544-7
2. Hawkins RB, Raymond SL, Stortz JA, Horiguchi H, Brakenridge SC, Gardner A, et al. Chronic critical illness and the persistent inflammation, immunosuppression, and catabolism syndrome. *Front Immunol.* (2018) 9:1511. doi: 10.3389/fimmu.2018.01511
3. Mira JC, Gentile LF, Mathias BJ, Efron PA, Brakenridge SC, Mohr AM, et al. Sepsis pathophysiology, chronic critical illness, and persistent inflammation-immunosuppression and catabolism syndrome. *Crit Care Med.* (2017) 45:253–62. doi: 10.1097/CCM.0000000000002074
4. Gardner AK, Ghita GL, Wang Z, Ozrazgat-Baslanti T, Raymond SL, Mankowski RT, et al. The development of chronic critical illness determines physical function, quality of life, and long-term survival among early survivors of sepsis in surgical ICUs. *Crit Care Med.* (2019) 47:566–73. doi: 10.1097/CCM.0000000000003655
5. Christoffersson G, Phillipson M. The neutrophil: one cell on many missions or many cells with different agendas? *Cell Tissue Res.* (2018) 371:415–23. doi: 10.1007/s00441-017-2780-z
6. Hidalgo A, Chilvers ER, Summers C, Koenderman L. The neutrophil life cycle. *Trends Immunol.* (2019) 40:584–97. doi: 10.1016/j.it.2019.04.013
7. Simon SI, Burns AR, Taylor AD, Gopalan PK, Lynam EB, Sklar LA, et al. L-selectin (CD62L) cross-linking signals neutrophil adhesive functions via the Mac-1 (CD11b/CD18) beta 2-integrin. *J Immunol.* (1995) 155:1502–14.
8. Mastej K, Adamiec A. Neutrophil surface expression of CD11b and CD62L in diabetic microangiopathy. *Acta Diabetol.* (2008) 45:183–90. doi: 10.1007/s00592-008-0040-0
9. Ivetic A, Hoskins Green HL, Hart SJ. L-selectin: a major regulator of leukocyte adhesion, migration and signaling. *Front Immunol.* (2019) 10:1068. doi: 10.3389/fimmu.2019.01068
10. Yang L, Froio RM, Sciuto TE, Dvorak AM, Alon R, Luscinskas FW. ICAM-1 regulates neutrophil adhesion and transcellular migration of TNF-alpha-activated vascular endothelium under flow. *Blood.* (2005) 106:584–92. doi: 10.1182/blood-2004-12-4942
11. Grieshaber-Bouyer R, Nigrovic PA. Neutrophil heterogeneity as therapeutic opportunity in immune-mediated disease. *Front Immunol.* (2019) 10:346. doi: 10.3389/fimmu.2019.00346
12. Fridlender ZG, Sun J, Kim S, Kapoor V, Cheng G, Ling L, et al. Polarization of tumor-associated neutrophil phenotype by TGF-beta: "N1" versus "N2" TA. *Cancer Cell.* (2009) 16:183–94. doi: 10.1016/j.ccr.2009.06.017
13. Kruger P, Saffarzadeh M, Weber AN, Rieber N, Radsak M, von Bernuth H, et al. Neutrophils: between host defence, immune modulation, and tissue injury. *PLoS Pathog.* (2015) 11:e1004651. doi: 10.1371/journal.ppat.1004651
14. Mortaz E, Alipoor SD, Adcock IM, Mumby S, Koenderman L. Update on neutrophil function in severe inflammation. *Front Immunol.* (2018) 9:2171. doi: 10.3389/fimmu.2018.02171
15. Winer LK, Beckmann N, Veile RA, Goodman MD, Caldwell CC, Nomellini V. Consumptive coagulopathy is associated with organ dysfunction during PICS. *Am J Physiol Lung Cell Mol Physiol.* (2019) 316:L946–52. doi: 10.1152/ajplung.00521.2018
16. Pugh AM, Auteri NJ, Goetzman HS, Caldwell CC, Nomellini V. A Murine model of persistent inflammation, immune suppression, and catabolism syndrome. *Int J Mol Sci.* (2017) 18:1741. doi: 10.3390/ijms18081741
17. Wang X, Huang W, Yang Y, Wang Y, Peng T, Chang J, et al. Fan: Loss of duplexmiR-223 (5p and 3p) aggravates myocardial depression and mortality in polymicrobial sepsis. *Biochim Biophys Acta.* (2014) 1842:701–11. doi: 10.1016/j.bbadis.2014.01.012

18. Tschop J, Kasten KR, Nogueiras R, Goetzman HS, Cave CM, England LG, et al. Caldwell: the cannabinoid receptor 2 is critical for the host response to sepsis. *J Immunol.* (2009) 183:499–505. doi: 10.4049/jimmunol.0900203
19. Schuster RM, Konishi T, Goetzman HS, Caldwell CC, Lentsch AB. Fibrotic liver has prompt recovery after ischemia-reperfusion injury. *Am J Physiol Gastrointest Liver Physiol.* (2020) 318:G390–400. doi: 10.1152/ajpgi.00137.2019
20. Gavillet M, Martinod K, Renella R, Harris C, Shapiro NI, Wagner DD, Williams DA. Flow cytometric assay for direct quantification of neutrophil extracellular traps in blood samples. *Am J Hematol.* (2015) 90:1155–8. doi: 10.1002/ajh.24185
21. Xia BT, Beckmann N, Winer LK, Pugh AM, Pritts TA, Nomellini V, et al. Amitriptyline reduces inflammation and mortality in a murine model of sepsis. *Cell Physiol Biochem.* (2019) 52:565–79. doi: 10.33594/000000040
22. Kim KH, Sederstrom JM. Assaying cell cycle status using flow cytometry. *Curr Protoc Mol Biol.* (2015) 111:28. doi: 10.1002/0471142727.mb2806s111
23. Pillay J, Kamp VM, van Hoffen E, Visser T, Tak T, Lammers JW, et al. A subset of neutrophils in human systemic inflammation inhibits T cell responses through Mac-1. *J Clin Invest.* (2012) 122:327–36. doi: 10.1172/JCI57990
24. Cuenca AG, Delano MJ, Kelly-Scumpia KM, Moreno C, Scumpia PO, Laface DM, et al. A paradoxical role for myeloid-derived suppressor cells in sepsis and trauma. *Mol Med.* (2011) 17:281–92. doi: 10.2119/molmed.2010.00178
25. Schrijver IT, Theroude C, Roger T. Myeloid-derived suppressor cells in sepsis. *Front Immunol.* (2019) 10:327. doi: 10.3389/fimmu.2019.00327
26. Sippel TR, Shimizu T, Strnad F, Traystman RJ, Herson P, Waziri SA. Arginase I release from activated neutrophils induces peripheral immunosuppression in a murine model of stroke. *J Cereb Blood Flow Metab.* (2015) 35:1657–63. doi: 10.1038/jcbfm.2015.103
27. Ekmekcioglu S, Grimm EA, Roszik J. Targeting iNOS to increase efficacy of immunotherapies. *Hum Vaccin Immunother.* (2017) 13:1105–8. doi: 10.1080/21645515.2016.1276682
28. Ng LG, Ostuni R, Hidalgo A. Heterogeneity of neutrophils. *Nat Rev Immunol.* (2019) 19:255–65. doi: 10.1038/s41577-019-0141-8
29. Cassetta L, Baekkevold ES, Brandau S, Bujko A, Cassatella MA, Dorhoi A, et al. Deciphering myeloid-derived suppressor cells: isolation and markers in humans, mice and non-human primates. *Cancer Immunol Immunother.* (2019) 68:687–97. doi: 10.1007/s00262-019-02302-2
30. Loftus TJ, Mohr AM, Moldawer LL. Dysregulated myelopoiesis and hematopoietic function following acute physiologic insult. *Curr Opin Hematol.* (2018) 25:37–43. doi: 10.1097/MOH.0000000000000395
31. Hu N, Westra J, Rutgers A, Doornbos-Van der Meer B, Huitema MG, Stegeman CA. Decreased CXCR1 and CXCR2 expression on neutrophils in anti-neutrophil cytoplasmic autoantibody-associated vasculitides potentially increases neutrophil adhesion and impairs migration. *Arthritis Res Ther.* (2011) 13:R201. doi: 10.1186/ar3534
32. Eash KJ, Greenbaum AM, Gopalan PK, Link DC. CXCR2 and CXCR4 antagonistically regulate neutrophil trafficking from murine bone marrow. *J Clin Invest.* (2010) 120:2423–31. doi: 10.1172/JCI41649
33. Deniset JF, Surewaard BG, Lee WY, Kubes P. Splenic Ly6G(high) mature and Ly6G(int) immature neutrophils contribute to eradication of *S. pneumoniae*. *J Exp Med.* (2017) 214:1333-50 doi: 10.1084/jem.20161621

Conflict of Interest: The authors declare that the research was conducted in the absence of any commercial or financial relationships that could be construed as a potential conflict of interest.

frontiers in Immunology

REVIEW
published: 29 May 2020
doi: 10.3389/fimmu.2020.01043

The Metabolic Basis of Immune Dysfunction Following Sepsis and Trauma

*Margaret A. McBride[1], Allison M. Owen[2], Cody L. Stothers[1], Antonio Hernandez[2], Liming Luan[2], Katherine R. Burelbach[2], Tazeen K. Patil[2], Julia K. Bohannon[1,2], Edward R. Sherwood[1,2] and Naeem K. Patil[2]**

[1] Department of Pathology, Microbiology and Immunology, Vanderbilt University Medical Center, Nashville, TN, United States, [2] Department of Anesthesiology, Vanderbilt University Medical Center, Nashville, TN, United States

Critically ill, severely injured and high-risk surgical patients are vulnerable to secondary infections during hospitalization and after hospital discharge. Studies show that the mitochondrial function and oxidative metabolism of monocytes and macrophages are impaired during sepsis. Alternatively, treatment with microbe-derived ligands, such as monophosphoryl lipid A (MPLA), peptidoglycan, or β-glucan, that interact with toll-like receptors and other pattern recognition receptors on leukocytes induces a state of innate immune memory that confers broad-spectrum resistance to infection with common hospital-acquired pathogens. Priming of macrophages with MPLA, CPG oligodeoxynucleotides (CpG ODN), or β-glucan induces a macrophage metabolic phenotype characterized by mitochondrial biogenesis and increased oxidative metabolism in parallel with increased glycolysis, cell size and granularity, augmented phagocytosis, heightened respiratory burst functions, and more effective killing of microbes. The mitochondrion is a bioenergetic organelle that not only contributes to energy supply, biosynthesis, and cellular redox functions but serves as a platform for regulating innate immunological functions such as production of reactive oxygen species (ROS) and regulatory intermediates. This review will define current knowledge of leukocyte metabolic dysfunction during and after sepsis and trauma. We will further discuss therapeutic strategies that target leukocyte mitochondrial function and might have value in preventing or reversing sepsis- and trauma-induced immune dysfunction.

Keywords: sepsis, infection, trauma, trained immunity, mitochondria, metabolic reprogramming

OPEN ACCESS

Edited by:
Thomas Griffith, University of Minnesota Twin Cities, United States

Reviewed by:
Charles C. Caldwell, University of Cincinnati, United States
Bruce Walcheck, University of Minnesota Twin Cities, United States

***Correspondence:**
Naeem K. Patil
naeem.patil@vumc.org

Specialty section:
This article was submitted to Inflammation, a section of the journal Frontiers in Immunology

Received: *17 March 2020*
Accepted: *30 April 2020*
Published: *29 May 2020*

Citation:
McBride MA, Owen AM, Stothers CL, Hernandez A, Luan L, Burelbach KR, Patil TK, Bohannon JK, Sherwood ER and Patil NK (2020) The Metabolic Basis of Immune Dysfunction Following Sepsis and Trauma. Front. Immunol. 11:1043. doi: 10.3389/fimmu.2020.01043

INTRODUCTION

Serious infection is a major threat to critically ill patients and frequently precipitates sepsis, a complex disease spectrum that includes systemic inflammation and organ dysfunction. As such, sepsis is the leading cause of death in non-cardiac intensive care units (ICU) and accounts for 40% of ICU expenditures (1). Early investigators postulated that systemic inflammation was the underlying factor driving the pathogenesis of sepsis and septic shock (2–4). High concentrations of pro-inflammatory mediators such as tumor necrosis factor, IL-1, and platelet activating factor were present in plasma and fluids of septic animals and humans (3, 5). Blockade of pro-inflammatory mediators in experimental animals attenuated or prevented the development of septic shock (6, 7). Those observations prompted clinical trials aimed at blocking cytokine and

non-cytokine mediators of inflammation, which were not successful at improving survival in patients with severe sepsis or septic shock (8). Specifically, a trial of anakinra, a recombinant IL-1 receptor antagonist, was not found to be effective in improving mortality in sepsis (9). However, a subgroup analysis found that the use of anakinra improved survival in patients with concurrent hepatobiliary dysfunction and disseminated intravascular coagulation, which are specific features of macrophage activation syndrome (10). Therefore, subgroup analysis of diverse sepsis patients for underlying conditions needs to be considered in studies evaluating different sepsis treatments to better understand the therapeutic benefit in different sub-populations of sepsis patients. Later investigations showed that septic patients had impaired innate and adaptive antimicrobial immunity, which resulted in their inability to control primary and secondary infections. Likewise, patients that survive sepsis and severe trauma have long-term physical and cognitive disabilities and frequently require readmission to the hospital due to recurrent infections (11). Research indicates that the septic or severely injured host responds to severe inflammation by activating anti-inflammatory pathways to mitigate further inflammatory injury. Among those pathways are increased production of anti-inflammatory cytokines such as IL-10 and transforming growth factor-β (TGFβ) and upregulation of checkpoint inhibitors such as PD-1, CTLA-4, BTLA, and PDL1 by leukocytes (12, 13). Other investigators have shown large-scale apoptosis and dysfunction of lymphocytes and the proliferation of myeloid-derived suppressor cells, which act to suppress innate and adaptive antimicrobial responses (14, 15). Most recently, the concept of metabolic dysfunction has emerged as a factor underlying impaired function of the innate and adaptive immune systems of septic and severely injured patients. This paper will review current knowledge of leukocyte metabolic dysfunction in the setting of sepsis and severe injury and discuss interventions to improve leukocyte metabolism and function.

OVERVIEW OF SEPSIS-INDUCED MITOCHONDRIAL DYSFUNCTION

Glycolysis and mitochondrial oxidative phosphorylation form the backbone of cellular metabolism. Glucose is primarily metabolized to pyruvate through glycolysis, along with a net generation of two ATP molecules. Cells transport pyruvate into mitochondria where it is metabolized to acetyl-CoA via the enzymatic action of the pyruvate dehydrogenase complex (PDH). Acetyl- CoA is metabolized through a series of enzymatic reactions in the mitochondrial tricarboxylic acid (TCA) cycle to produce reducing intermediates including NADH and FADH2, which feed electrons into the TCA cycle-linked electron transport chain (ETC). Optimal flow of electrons through ETC complexes (I-IV) is required for maintenance of mitochondrial membrane potential and proton gradient, which ultimately facilitate ATP generation (16). Recent studies show that mitochondria not only generate adenosine triphosphate (ATP), but also are intricately involved in cellular signaling pathways that regulate calcium homeostasis, reactive oxygen species (ROS) generation, redox signaling, and maintenance of immune cell competence, all of which are critical for our survival (17–19).

The 3rd International Consensus Conference defined sepsis as organ dysfunction caused by a dysregulated host response to infection (20). Evidence indicates that mitochondrial dysfunction is a key player in induction and propagation of sepsis-induced organ injury, which is demonstrated in both animal and human studies (21, 22). Brealey et al., were among the first to demonstrate that sepsis leads to significant impairment of skeletal muscle mitochondrial ETC activity (specifically complex I), which correlates with the severity of septic shock in humans (23). Furthermore, decreased skeletal muscle ATP concentrations were predictive of increased mortality among sepsis patients. A clinical study by Matkovich et al., showed a striking 43% decline in levels of mRNA that encode proteins involved in mitochondrial TCA cycle and ETC complexes in the hearts of septic patients (24). Numerous animal studies also demonstrate a role for mitochondrial dysfunction in sepsis pathology. Using animal models, sepsis has been shown to cause a significant impairment of mitochondrial function in multiple organs including heart, kidney, liver, and skeletal muscle (25–28). Although these studies demonstrate a role for mitochondrial dysfunction in sepsis pathology, discrepancies in various studies also show a highly variable mitochondrial function in multiple organs depending on the sepsis model used, severity of sepsis induced, time course studied, and methodology used for measurement of mitochondrial function (29). Therefore, there remains some controversy in the field as to whether mitochondria are the actual initiators or concurrent amplifiers of organ dysfunction during sepsis (29).

SEPSIS-INDUCED MITOCHONDRIAL DYSFUNCTION IN LEUKOCYTES

Recent studies demonstrate that sepsis-induced impairment of leukocyte mitochondrial function contributes to impaired antimicrobial immune responses and increased susceptibility to secondary infections (30, 31). The majority of the studies implicating a role for sepsis-induced leukocyte mitochondrial dysfunction used Peripheral Blood Mononuclear Cells (PBMCs) isolated from septic patients (summarized in **Table 1**). Adrie et al., demonstrated significant sepsis-induced depolarization of mitochondrial membrane potential and increased expression of cell death markers in peripheral blood monocytes. Eventual non-survivors demonstrated higher depolarization of the mitochondrial membrane as compared to survivors (32). Other studies showed a reduction in mitochondrial respiration in the presence of high ADP and P_i (also known as state 3 respiration), ATP synthase complex activity and mitochondrial spare respiratory capacity in PBMCs from sepsis patients (33, 34, 39). Reduced mitochondrial respiration in leukocytes was associated with increased incidence of organ failure (34). Garrabou et al., demonstrated a significant impairment of mitochondrial ETC complexes I, III, and IV in PBMCs of patients with confirmed systemic infection but without septic shock (35).

TABLE 1 | Summary of clinical studies showing sepsis-induced alterations in leukocyte mitochondrial function.

References	Sepsis definition and patient age	Sample analyzed	Time of sample collection after sepsis diagnosis	Major alterations in mitochondrial function (as compared to controls)
Adrie et al. (32)	Severe sepsis and septic shock (>18 years)	PBMC	- Within 72 h - Between 7th and 10th day	- Increased membrane depolarization - Increased cell death markers
Belikova et al. (33)	Severe sepsis and septic shock (>18 years)	PBMC	- Within 48 h of ICU admission	- Reduced ADP-stimulated state 3 respiration and increased basal oxygen consumption
Japiassu et al. (34)	Septic shock (>18 years)	PBMC	- Within 48 h	- Reduced ADP-stimulated state 3 respiration and ATP synthase activity
Garrabou et al. (35)	SIRS with infection (no septic shock)	PBMC	- Exact time point not mentioned	- Decreased activities of ETC complexes I, III, and IV - Unaltered mitochondrial mass
Sjovall et al. (36)	Severe sepsis and septic shock (>18 years)	PBMC	- Within 48 h - Days 3–4 - Days 6–7	- Basal respiration and ETC complex I, II, and IV activities increased over time up to day 7
Weiss et al. (37) **(pediatric study)**	Septic shock with organ failure (<18 years)	PBMC	- Within 48 h - Days 5–7	- Unaltered basal and ATP linked respiration on days 1–2 - Spare respiratory capacity (SRC) decreased on days 1–2 - SRC recovered over days 5–7
Cheng et al. (31)	LPS infusion in healthy volunteers Bacterial and fungal sepsis patients (>18 years)	PBMC and monocytes	- LPS infusion for 4 h - Within 24 h for septic patients	- Decreased oxygen consumption in all models - Both glycolytic capacity and mitochondrial function impaired in septic PBMCs - Impaired ability to respond to a second stimulus
Merz et al. (38)	Septic shock (> 18 years)	Monocytes	- 24 and 48 h - At shock resolution	- ETC complex I, IV, and ATP synthase activities elevated - No difference in ATP content
Jang et al. (39)	Sepsis and septic shock (>18 years)	PBMC	- Within 24 h	- Decreased ATP-linked respiration and reduced uncoupled complex I activity, and no differences in ETC complex II and IV activities. - Decreased spare respiratory capacity
Kraft et al. (40)	Sepsis with evidence of organ injury (>18 years)	PBMC	- Days 1, 3, and 5	- Reduced mitochondrial DNA and mitochondrial biogenesis - Increased plasma D-loop indicating mitochondrial damage - Alterations normalized over a week with patients' recovery
Weiss et al. (41) **(pediatric study)**	Sepsis and septic shock (<18 years)	PBMC	- Days 1–2, 3–5 and 8–14	- Decreased spare respiratory capacity (SRC) and increased mitochondrial content on days 1–2 - SRC recovered over time as patients improved over 14 days. - Low SRC associated with residual organ injury at day 14.
Weiss et al. (42) **(pediatric study)**	Severe sepsis and septic shock (<18 years)	PBMC	- Within hours - Days 3–5 and 8–14	- Decreased mitochondrial respiration observed in those septic PBMCs which showed reduced LPS-induced TNF-α and HLA-DR expression.
Clere-Jehl et al. (43)	Septic shock (<18 years)	PBMC	- Within 12 hours of noradrenaline start	- Increased basal and maximal respiratory capacity - Lower ATP synthase activity

In a major study, Cheng et al., showed that both bacterial and fungal sepsis leads to a shift in cellular metabolism toward glycolysis (Warburg effect), and leukocytes isolated from septic patients, as well as those treated with lipopolysaccharide (LPS), demonstrated a reduced oxygen consumption capacity signifying mitochondrial defects (31, 44). Furthermore, these metabolic defects were associated with impaired ability of leukocytes to produce pro-inflammatory cytokines in response to a secondary stimulus, which the authors refer to as a state of immunoparalysis (31). A study by Kraft et al., brings to light an important observation that effective reversal of the initial sepsis-induced leukocyte mitochondrial damage via early activation of mitochondrial biogenesis improved clinical outcomes among septic patients (40). They showed that mRNA levels of genes related to mitochondrial biogenesis, including PGC-1α, NRF1, and TFAM, were significantly reduced 1 day after the initiation of sepsis along with a decrease in mitochondrial DNA copy number. Recovery of these parameters was paralleled by improved

clinical outcome and discharge from the ICU over a 1 week period (40). In multiple pediatric studies using PBMCs, Weiss et al., demonstrated that sepsis leads to a significant decrease in mitochondrial respiration and spare respiratory capacity implying a decreased bioenergetic reserve and mitochondrial dysfunction (37, 41, 42).

In contrast to these studies demonstrating sepsis-induced impairment of mitochondrial respiration, some studies show unaffected or increased mitochondrial respiration. Using PBMCs and monocytes from patients with severe sepsis and septic shock, Sjovall et al., and Merz et al., showed a significant increase in activities of mitochondrial ETC complexes I, II, and IV and did not observe a difference in these parameters among survivors vs. non-survivors (36, 38). In line with these studies, Clere-Jehl et al., showed that sepsis leads to a significant increase in mitochondrial respiratory capacity of PBMCs (43). However, mitochondrial respiration was impaired upon suspending the PBMCs in septic plasma, implying a role for a soluble plasma factor, which the authors attributed to a high level of HMGB1 (43). The contrasting findings might be attributed to the vast heterogeneity in sepsis patient populations, differing time points selected for measurements and underlying co-morbidities. Leukocyte-specific mitochondrial function in freshly isolated systemic immune cells has not been assessed in animal models.

In summary, the majority of studies implicate mitochondrial dysfunction as an important contributor toward sepsis-induced leukocyte and organ dysfunction. Importantly, early recovery of mitochondrial function correlates positively with improved clinical outcomes in septic patients (40, 45). Therefore, therapies targeting recovery of mitochondrial function hold potential for reversing leukocyte dysfunction during sepsis. Agents that target the AMP kinase pathway, such as AICAR (5-aminoimidazole-4-carboxamide ribonucleotide), or the mTOR signaling pathway, such as metformin, could provide benefit. Recent studies demonstrate that activation of pattern recognition receptors of innate leukocytes, especially monocytes and macrophages, augments mitochondrial function and rewires mitochondrial metabolism leading to accumulation of specific TCA cycle intermediates such as citrate, itaconate, succinate, fumarate, and others. Prophylactic treatment with TLR4 agonists can protect against severe infections for up to 14 days (46–48). That benefit is due, in part, to heightened mitochondrial and antimicrobial functions in macrophages Therefore, TLR agonist-induced mitochondrial metabolic reprogramming in innate leukocytes is associated with the generation of distinct innate immune memory. Mitochondrial reprogramming and innate immune memory are now being widely investigated as novel strategies for developing mitochondria-targeted therapies for protection against infections and sepsis in critically ill patients.

THE IMPACT OF TRAUMA ON LEUKOCYTE METABOLISM

Although similar to sepsis, trauma provides a different set of signals to the immune system. While infection and sepsis can be a complication of trauma, the direct impact of trauma on immune system function is generated through tissue injury, inflammation, and tissue ischemia and reperfusion (49, 50). The effect of trauma on immune function is variable and largely dependent on the severity of injury (51, 52). The release of endogenous cell products, such as mitochondrial DNA, oxidized phospholipids, and ATP can activate toll-like receptors and inflammasomes to precipitate immune system activation (53, 54). Excessive or inappropriate immune system activation following major trauma could lead to immune dysfunction. Impairment of neutrophil and monocyte chemotaxis and antimicrobial functions have been described (55–57) as have alterations in lymphocyte function (58). However, little is known about the impact of major trauma on the metabolic state of leukocytes, which raises an area for research.

POTENTIAL THERAPEUTIC STRATEGIES TARGETING LEUKOCYTE MITOCHONDRIAL FUNCTION DURING SEPSIS AND TRAUMA

Effective mitochondrial biogenesis requires a coordinated action of complex intracellular pathways including both nuclear and mitochondrial genome encoded proteins (59, 60). PGC-1α is recognized as one of the most important and inducible transcription factor that drives mitochondrial biogenesis in response to external stimuli for maintaining mitochondrial homeostasis (61). The activity of PGC-1α is regulated by post-translational modifications. Sirtuin 1 (SIRT1)-induced deacetylation and adenosine monophosphate-activated protein kinase (AMPK)-induced phosphorylation are known to activate PGC-1α (62). Along with PGC-1α, other cellular transcription factors and mediators, including NRF1 and NRF2, PGC-1β, TFAM, ERRα, CREB, also play an important role in regulating mitochondrial biogenesis (63). The following section will discuss some of the promising therapeutic strategies targeting augmentation of mitochondrial biogenesis, which could be applicable for protecting or restoring leukocyte mitochondrial function during sepsis and trauma.

Pharmacological Agents Targeting Mitochondrial Biogenesis and Function

Studies included in this section are summarized in **Table 2**.

Modulators of AMPK Activity

AMPK is one of the key cellular mediators required for maintaining cellular energy homeostasis. AMPK exists in multiple isoforms and it is a heterotrimeric complex composed of one alpha subunit (either α1 or α2), beta subunit (either β1 or β2), and gamma subunit (either γ1, γ2, or γ3) (113). Previous studies show that AMPK induced transcriptional upregulation of genes involved in mitochondrial metabolism require PGC-1α (114) and overexpression of AMPK increases PGC-1α expression (115). AMPK regulates PGC-1α activity via direct phosphorylation at threonine-177 and serine-538, and the effect of AMPK on increased expression on mitochondrial proteins and function is regulated via PGC-1α

TABLE 2 | Pharmacologic agents targeting mitochondrial biogenesis and function.

Agent class	Specific agent	References	Model	Effect
AMPK activity enhancer	AICAR	Canto et al. (64)	Mouse	- Reduced acetylation of PGC1α - Induced expression of PGC1α-target genes in skeletal muscle
		Inata et al. (65)	Mouse CLP	- Protected against cardiac architecture derangement and dysfunction
		Hall et al. (66)	Mouse endotoxemia	- Protected against loss in muscle mass
		Escobar et al. (67)	Mouse CLP	- Reduced pro-inflammatory cytokines - Reduced kidney and liver injury markers
	Metformin	Wang et al. (68)	Mice fed high fat diet	- Improved hepatic mitochondrial complex activity and mitochondrial density in AMPK-dependent manner
		Detaille et al. (69)	HMEC-1 (human immortalized endothelial cell line)	- Inhibited of mitochondrial complex I leading to modulation of the cellular AMP/ATP ratio to activate AMPK
		Meng et al. (70)	Hepa1–6 (mouse hepatoma cell line)	- Activated AMPK via increased phosphorylation of AMPKα at Thr-172
		Suwa et al. (71)	Rats	- Increased PGC-1α expression and mitochondrial biogenesis in skeletal muscle
		Tzanavari et al. (72)	Mouse endotoxemia	- Rescued cardiac dysfunction - Increased ATP synthesis - Reduced inflammatory markers
		Vaez et al. (73)	Isolated rat hearts exposed to LPS	- Activated AMPK - Decreased TLR4 activity - Improved cardiac function
		Vaez et al. (74)	Rat endotoxemia	- Activated AMPK in lung tissue - Reduced inflammatory cell infiltrate in alveolar walls
		Vaez et al. (75)	Rat endotoxemia	- Activated AMPK in cardiac tissue - Decreased myocardial TLR4 - Improved cardiac function
		Tang et al. (76)	Mouse CLP	- Decreased brain edema, preserved BBB, improved cognitive function, improved survival
		Liang et al. (77)	Metanalysis of cohort studies	- Preadmission metformin use was associated with decrease mortality in patients with sepsis and DM
	5HT	Freire-Garabal et al. (78)	Isolated mouse peritoneal macrophages	- Augmented phagocytic capacity of peritoneal macrophages
		Mikulski et al. (79)	Isolated mouse alveolar macrophages	- Increased expression of MCP-1(CCL2)
PPAR activators	Rosiglitazone	Drosatos et al. (80)	Mouse endotoxemia	- Protected mitochondria, reduced cardiac dysfunction, and improved survival
	Pioglitazone	Tsujimura et al. (81)	Mouse CLP	- Reduced inflammation and improved survival
		Majer et al. (82)	Mouse *Candida albicans* sepsis	- Reduced renal pathology and improved survival
	15d-PGJ(2) and	Zingarelli et al. (83)	Rat CLP	- Reduced inflammation, neutrophil infiltration in lung, colon, and liver, hypotension, and improved survival
	Ciglitazone 15d-PGJ(2) and Troglitazone	Maggi et al. (84)	RAW 264.7 cells and CD-1 mouse peritoneal macrophages	- Reduced iNOS, COX-2, IL-1 in cells treated with LPS and IFNγ
	15-PGJ(2)	Guyton et al. (85)	Isolated rat peritoneal macrophages	- Inhibited LPS-induced peritoneal macrophage inflammatory mediators
	15-PGJ(2) Troglitazone	Guyton et al. (86)	Isolated rat peritoneal macrophages	- 15-PGJ(2) inhibited LPS, E. coli, and S. aureus-induced NO and TXA - Troglitazone inhibited TXA synthesis in each condition
	Fenofibrate	Tancevski et al. (87)	Murine *Salmonella typhimurium* sepsis	- Reduced pro-inflammatory cytokines, increased neutrophil recruitment, augmented bacterial clearance, improved survival - These effects were independent of PPARα
		Cree et al. (88)	Clinical trial of pediatric burn patients	- Increased hepatic mitochondrial ATP, maintenance of cytochrome C oxidase and citrate synthase activity - Improved insulin sensitivity
	Clofribrate	Crisafulli and Cuzzocrea (89)	Isolated mouse peritoneal macrophages	- Reduced LPS/IFN-γ induced pro-inflammatory cytokine production

(Continued)

TABLE 2 | Continued

Agent class	Specific agent	References	Model	Effect
PDE inhibitors	Milrinone	Barton et al. (90)	Pediatric sepsis clinical trial	- Increased cardiac index, stroke volume index, and oxygen delivery - Decreased systemic vascular resistance
	Ro 20-1724	Carcillo et al. (91)	Rat endotoxemia	- Improved renal function and survival
		Thomas et al. (92)	Rat endotoxemia	- Protected cardiac contractility and function
	Rolipram	Holthoff et al. (93)	Mouse CLP	- Improved renal blood flow, protected renal microcirculation, improved GFR and renal function
		Sims et al. (94)	Rat pup CLP	- Improved renal, cardiac function, and survival
		Sanz et al. (95)	Rat endotoxemia	- Reduced leukocyte-endothelial interactions
	Rolipram and Roflumilast	Schick et al. (96)	Rat endotoxemia	- Reduced capillary leakage - Stabilized endothelial barrier
	Rolipram	Wollborn et al. (97)	Rat endotoxemia	- Improved hepatic microcirculation and protects liver architecture
	Cilostazol	Zuo et al. (98)	HUVEC	- Induced mitochondrial biogenesis (increased ATP mitochondrial DNA, cytochrome B, and mitochondrial mass) through PGC1α
	Rolipram	Ding et al. (99)	Mouse renal fibrosis by unilateral ureteral obstruction	- Increased mitochondrial biogenesis and PGC1α expression
Natural products	Resveratrol	Biala et al. (100)	Transgenic rat model of heart failure	- Increased PGC-1α, NRF1, NRF2 and Tfam, and mitochondrial biogenesis
		Wang et al. (101)	Rat CLP	- Inhibited of NFκB - Decreased kidney injury - Increased survival
		Luo et al. (102)	Rat CLP	- Decreased renal tubular pathology and proinflammatory cytokines
		Wang et al. (103)	Young rat CLP	- Activated NRF2 - Protects from kidney injury
		Shang et al. (104)	Rat LPS peritonitis	- Protected myocardium and decreased inflammatory markers
		Martin et al. (105)	*Ex-vivo* equine leukocytes	- Did not increase antimicrobial functions - Did not alter cytokine profiles
	ECGC	Valenti et al. (106)	Human Lymphoblasts and fibroblasts	- Increased SIRT1 and PGC1α - Increased mitochondrial complex activities and oxidative phosphorylation efficiently
		Chiou et al. (107)	Mouse endotoxemia	- Activated NRF2 via direct interaction with KEAP1 - Reduced LPS-induced TLR4 activation
		Wang et al. (108)	Mouse endotoxemia	- Protected against acute lung injury - Decreased proinflammatory cytokines
		Wheeler et al. (109)	Mouse and rat CLP	- Decreased hypotension - Improved survival
	Daidzein and Genistein (Phytoestrogens)	Cederroth et al. (110)	Mouse	- Diet containing both compounds increased PGC-1α expression
	Daidzein	Parida et al. (111)	Mouse CLP	- Suppressed lung injury, decreased bacterial load
	Genistein	Yi et al. (112)	Mouse endotoxemia	- Suppressed proinflammatory cytokines from endothelial cells

(62, 114). AMPK has also been shown to activate SIRT1, an enzyme which catalyzes deacetylation and activation of PGC-1α leading to mitochondrial biogenesis (116). Therefore, activation of the AMPK pathway is a promising approach to stimulate mitochondrial biogenesis in various disease conditions, such as sepsis, that negatively affect mitochondrial function.

Treatment with AICAR will induce mitochondrial biogenesis and function in skeletal muscle cells, an effect mediated through activation of SIRT1, which leads to deacetylation and activation of PGC-1α (64). In a murine cecal ligation and puncture (CLP) model, AICAR protected against the sepsis-induced derangements in cardiac architecture and dysfunction (65). AICAR treatment also protected against LPS-induced loss in muscle mass (66) and reduced pro-inflammatory cytokine production and sepsis-induced increases in markers of kidney and liver injury during CLP-induced sepsis. Inhibition of AMPK by compound C exacerbated sepsis-associated tissue injury (67).

Metformin, a clinically used biguanide anti-diabetic drug, improves mitochondrial function via activation of AMPK (68). The mechanisms leading to metformin-induced activation of

AMPK include increased phosphorylation of AMPKα at Thr-172 and via inhibition of mitochondrial complex I leading to modulation of the cellular AMP/ATP ratio (69, 70). Studies by Suwa et al. recognized that metformin, a first line oral drug for the treatment of type 2 diabetes, increases PGC1-α and mitochondrial protein content in muscle through AMPK activation (71). Metformin has been shown to be protective in studies employing animal models of sepsis (117). During LPS- and CLP-induced sepsis, metformin protected against sepsis-induced injury in brain, heart, liver, and lung. These benefits were mediated through inhibition of oxidative stress and inflammation, reduced infiltration of neutrophils, maintenance of mitochondrial membrane potential, and preservation of mitochondrial function (72–76, 118). In humans, a metanalysis including five observational cohort studies found that pre-admission use of metformin was associated with decreased mortality among patients with sepsis and diabetes mellitus (77). This association warrants further study of causality and the mechanism behind this association to assess the therapeutic benefit of metformin during sepsis.

Despite the described benefits of AICAR and metformin in reducing inflammation and providing organ protection in experimental models of sepsis, little is known about the impact of these drugs on immune function in the septic or severely injured host, which provides fertile ground for future research.

5-Hydroxytryptamine Receptor (5HT) Agonists

Specific agonists of the 5HT receptor family have been shown to induce mitochondrial biogenesis (119). 5HT is the chemical name for endogenous neurotransmitter serotonin. 5HT receptors are G-protein coupled receptors with serotonin functioning as its endogenous ligand. It remains to be determined if 5HT receptor agonists could provide therapeutic benefit to protect against sepsis-induced organ injury. Immune cells including macrophages, monocytes and T cells express 5HT receptors (120). Serotonin has been shown to augment the phagocytic capacity of murine peritoneal macrophages via $5HT_{1A}$ receptor subtype (78). Serotonin has also been shown to activate alveolar macrophages via $5HT_{2c}$ receptor leading to increased expression of the monocyte chemoattractant MCP-1 (79). Various studies have shown the stimulatory effect of serotonin on other immune cells including Natural Killer cells, dendritic cells, and T cells (120, 121). Studies evaluating the effect of serotonin and synthetic 5HT receptor agonists on mitochondrial biogenesis in leukocytes is currently lacking.

Peroxisome Proliferator-Activated Receptor (PPAR) Activators

PPARs are a class of nuclear receptors/transcription factors that are comprised of three isotypes including PPARα, PPARβ/δ, and PPARγ (122). PPARs are known to regulate various metabolic functions including triglyceride and lipoprotein metabolism, fatty acid synthesis, and oxidation and energy homeostasis to name a few (123). PGC1-α, the aforementioned transcription factor known for its role in mitochondrial biogenesis, also functions as a coactivator PPARγ (124). Thiazolidinediones are clinically used anti-diabetic drugs, which increase insulin sensitivity through activation of PPARγ (125). Rosiglitazone, a thiazolidinedione class drug, was shown to attenuate LPS-induced cardiac dysfunction and protect mitochondria leading to improved survival (80). Pioglitazone, another PPARγ agonist, has been shown to reduce inflammation and improve survival in a murine CLP and *Candida albicans*-induced sepsis (81, 82). Zingarelli et al. showed that treatment with PPARγ ligands, 15-deoxy-Delta(12,14)-PGJ(2) (15d-PGJ(2)), and ciglitazone attenuated inflammation, reduced excess neutrophil influx into various organs, decreased hypotension and improved survival through regulation of NF-κB and AP-1 signaling pathways using murine CLP model of sepsis (83). Other studies have also shown similar anti-inflammatory effects of synthetic PPARγ ligands including 15d-PGJ(2) and troglitazone on macrophages (84–86, 126). Fenofibrate, a known PPARα agonist used clinically for the management of dyslipidemia, reduced pro-inflammatory cytokines levels, promoted neutrophil recruitment to the site of infection and augmented bacterial clearance leading to improved survival in a murine model of *Salmonella typhimurium*-induced sepsis (87). The beneficial effect of fenofibrate was shown to be independent of PPARα but dependent on the preservation of neutrophil CXCR2 expression (87). Using another PPARα agonist, Crisafulli et al. demonstrated that clofibrate reduces LPS/IFNγ induced pro-inflammatory cytokine production in murine peritoneal macrophages (89). Treatment of pediatric burn patients with fenofibrate within the first week after burn injury has been shown to increase hepatic mitochondrial ATP production, maintain cytochrome c oxidase levels and citrate synthase activity along with improving insulin sensitivity, thereby indicating the therapeutic utility of fenofibrate-induced augmentation of mitochondrial function after burn injury (88). A study by Standage et al. showed that PPARα expression is decreased in the whole blood of pediatric sepsis patients and this correlated with the severity of sepsis outcomes and PPARα is required for maintaining optimal immune function during sepsis (127). In summary, PPAR agonists might have therapeutic potential in attenuation of sepsis induced inflammation and organ injury. However, the specific effect of various PPAR agonists on mitochondrial biogenesis and function in various organs and leukocytes in context of sepsis and trauma has not been investigated in detail and needs to be evaluated in future studies.

Phosphodiesterase (PDE) Inhibitors

Phosphodiesterases serve to hydrolyze cAMP and cGMP, increase levels of which reduces vascular tone, tightens endothelial junctions, and increases cardiac contractility. The cAMP-response-element-binding protein (CREB) is involved in transcriptional activation of PGC1α (128). In pediatric sepsis patients, treatment with PDE3 inhibitors increase both cAMP and cGMP levels and not only improve cardiac function (90, 129, 130) but also increase survival (131, 132). PDE4 inhibitors such as rolipram and Ro 20-1724 are selective for cAMP (133). Inhibition of PDE4 using Ro 20-1724 reduced systemic vascular resistance and improved cardiac and renal function in LPS model of sepsis in rats (91, 92). Treatment with rolipram improves renal blood flow, protects renal microcirculation and improves

glomerular filtrate rate and renal function in a murine model of CLP-induced sepsis, even when administered 6 h after CLP (93). Rolipram treatment also improved renal and cardiac function leading to improved survival in septic rat pups (94). PDE4 inhibitors, rolipram and roflumilast, have been shown to reduce leukocyte-endothelial interactions which inhibits inflammatory cell influx, and reduce capillary leakage during LPS-induced inflammation (95, 96). Wollborn et al. showed that treatment with rolipram improves hepatic microcirculation and protects liver architecture in a rat model of LPS induced inflammation (97). Pharmacological agents such as rolipram and cilastozol which are specifically inhibit PDE4 and PDE3, respectively, and have been shown to increase CREB phosphorylation, upregulate PGC-1α expression and contribute to the induction of mitochondrial biogenesis (98, 99, 134). Future studies addressing the impact of PDE inhibitors on mitochondrial function in organs and leukocytes in context of sepsis and trauma are warranted.

Natural Products That Induce Mitochondrial Biogenesis

Resveratrol, a polyphenol compound found in grapes and red wine, has been shown to activate PGC1α and mitochondrial biogenesis through SIRT1 or AMPK signaling (135). Resveratrol upregulates PGC-1α, NRF1, NRF2 and Tfam leading to potentiation of mitochondrial biogenesis (100). In multiple studies using a CLP model of polymicrobial sepsis in rats, resveratrol treatment results in increased survival as well as decreased kidney injury associated with inhibition of NFκB (101, 102). In a similar model of pediatric sepsis-induced kidney injury in young rats, resveratrol was shown to activate NRF2 and protect from injury (103). Shang et al. report that resveratrol is protective in LPS-induced cardiomyopathy in rats also through inhibition of NFκB (104). In horses, however, Martin et al. showed that a 3 week course of resveratrol did not increase antimicrobial function or alter cytokine release profiles of *ex vivo* stimulated leukocytes (105).

Epigallocatechin gallate (ECGC), a natural compound found in tea, promotes cAMP dependent signaling and increases SIRT1 and consequently PGC1α (106). In murine LPS-induced endotoxemia, ECGC protected against acute lung injury and decreased proinflammatory cytokine production (108). ECGC has been shown to induce the NRF2 antioxidant response element through direct interaction with its inhibitor KEAP1 thereby leading NRF2 activation (107). NRF2, like PGC1α, is known to be involved in mitochondrial biogenesis. In the CLP model, ECGC attenuated hypotension and improved survival (109).

Estrogen receptors are known to regulate mitochondrial biogenesis, so it follows that phytoestrogens may also induce mitochondrial biogenesis and have protective affects in sepsis. A diet high in two phytoestrogens daidzein and genistein has been shown to increase PGC-1α expression, and these two compounds were separately shown to decreases proinflammatory cytokines in LPS-induced endotoxemia, and increase survival and bacterial clearance in CLP-induced sepsis respectively (110–112).

METABOLIC REPROGRAMMING OF INNATE LEUKOCYTES BY MICROBIAL LIGANDS

Stimulation of innate immune cells with microbial ligands such as LPS, peptidoglycan, or β-glucan reprograms their metabolism, which supports the increased physiological demands needed to augment antimicrobial capacity to combat invading infections (47, 136, 137). The reprogrammed phenotype of innate leukocytes manifests as distinct augmentation of glycolysis and mitochondrial tricarboxylic acid cycle flux and oxidative phosphorylation, as detailed below (**Figure 1**).

Reprogramming of Glycolysis

Hard et al. discovered that immune macrophages, defined as those from peritoneal cavities of mice injected with bacteria, produced more lactate and consumed less oxygen than controls (138). Further investigations showed that macrophages stimulated with LPS manifest increased glucose uptake, an elevated glycolytic rate and augmentation of the pentose phosphate pathway (139, 140). These findings were reminiscent of the aerobic glycolysis noted by Warburg et al. in cancer cells, which preferentially utilize glycolysis, even in aerobic conditions that should favor oxidative phosphorylation as more energetically efficient (141). Aerobic glycolysis in macrophages in facilitated, in part, by stabilization of hypoxia-inducible factor (HIF)-1α. Early macrophage activation induces accumulation of succinate and itaconate, which are transported out of mitochondria in the cytosol where it acts to stabilize HIF-1α by impairing the activity of prolyl hydroxylases (142, 143). HIF-1α facilitates increased expression of numerous gene products that regulate inflammation including enzymes that promote glycolysis (140). Though this effect is notable in multiple types of murine macrophages, Vijayan et al. reported that LPS does not increase glycolysis in human PBMCs (144). Multiple purposes for this increase in glycolysis, over oxidative phosphorylation at the expense of energy efficiency, have been hypothesized. West et al. described that classically activated macrophages require mitochondrial reactive oxygen species for effective bacterial clearance (145). The contributions of mitochondrial complex I to ATP synthesis during oxidative phosphorylation may detract from mROS generation (145). As suggested in Viola et al., glycolysis may also be advantageous because it supplies biosynthetic intermediates important for rapid cellular adaptations, as well as NADPH through the pentose phosphate shunt, which is important for generation of ROS. The Warburg effect in macrophage activation is specific to the classical M1 phenotype, but not in alternatively activated M2 macrophages, which rely on oxidative phosphorylation (146). Interestingly, increases in oxidative phosphorylation and glycolysis occur in macrophages activated by the TLR4 agonist MPLA 72 h after exposure, resulting in a hybrid phenotype with metabolic characteristics common to both M1 and M2 macrophages (47).

LPS also induces the TCA cycle metabolite itaconate, in both murine and human macrophages (147) (**Figure 1**). It has been recently shown that itaconate inhibits glycolysis via

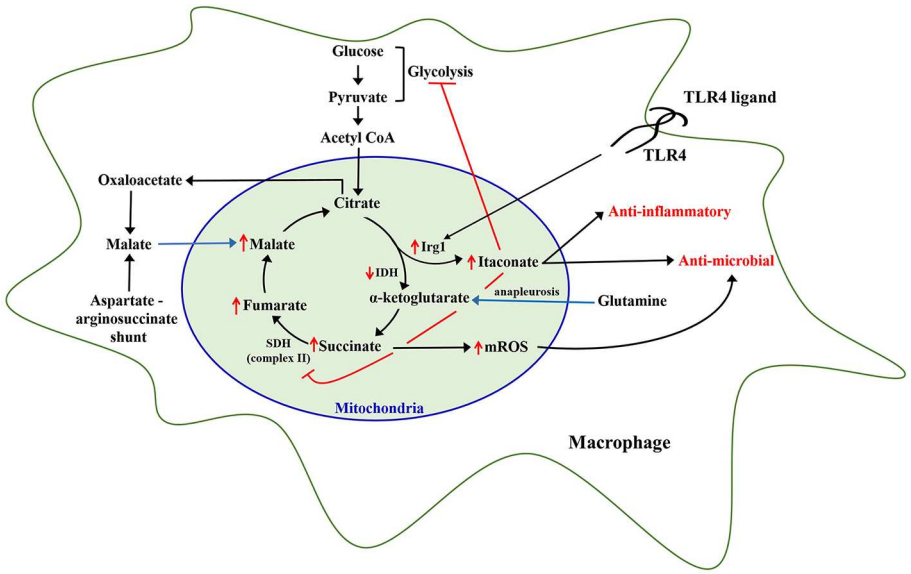

FIGURE 1 | Metabolic reprogramming of leukocytes. Inflammatory stimulation of leukocytes, specifically monocytes and macrophages, with Toll-like receptor 4 (TLR4) ligands like lipopolysaccharide, has been shown to rewire mitochondrial metabolic pathways including upregulation of immunoresponsive gene 1 (Irg1) leading to increased itaconate generation, and increased accumulation of other TCA cycle metabolites including succinate, fumarate, malate, and citrate which continue to be replenished via additional pathways including glutamine anapleurosis and aspartate-arginosuccinate shunt. Itaconate produced by Irg1 inhibits succinate dehydrogenase, which causes an increase in mitochondrial reactive oxygen species (mROS). Itaconate and mROS augment antimicrobial capacity of leukocytes.

inhibiting glycolytic enzymes aldolase A and glyceraldehyde-3-phosphate hydrogenase in RAW 264.7 macrophage cell lines (148, 149). Itaconate has also been shown to inhibit succinate dehydrogenase, which might reprogram citric acid cycle function and facilitate mROS generation due to reverse electron transport secondary to inhibition of SDH-dependent complex II (150).

Reprogramming of Mitochondrial Metabolism

The majority of recent studies demonstrate significant alterations in the generation of TCA cycle intermediates upon TLR agonist-induced inflammatory stimulation of monocytes and macrophages. Studies from our laboratory, and others, show that citrate, itaconate, and succinate accumulate during metabolic rewiring of macrophages and monocytes (47, 140, 151, 152). Recent studies have elucidated a unique role for each of these metabolites in the context of cellular metabolic and antimicrobial functions.

Citrate is converted to α-ketoglutarate by isocitrate dehydrogenase (IDH) through the intermediate cis-aconitate. Michelucci et al., demonstrated that stimulation of macrophages with LPS leads to significant upregulation of immunoresponsive gene 1 (Irg1) enzyme, which catalyzes the production of itaconate from cis-aconitate in the mitochondria, thus diverting pyruvate-derived citrate production away from energy generation and toward production of itaconate (153). Jha et al., also showed that LPS induces downregulation of IDH and succinate dehydrogenase (SDH) function in macrophages leading to a significant accumulation of citrate and succinate (151). In line with this, studies from our laboratory show that MPLA treatment reduces TCA cycle flux between citrate and α-ketoglutarate at 24 h after stimulation in association with induction of Irg1 expression and large scale itaconate production (47). Therefore, it is evident that inflammatory stimulation of macrophages drives citrate toward production of itaconate. Itaconate has now been shown to be a critical regulator of macrophage and monocytic function after LPS stimulation. Intracellular itaconate concentrations of up to 8 mM have been shown in macrophages at 6 h after LPS stimulation (153), which subsequently steadily decline over time (152). There are multiple known downstream cellular effects of this dramatic increase in itaconate. First, itaconate inhibits mitochondrial complex II or SDH function in a dose-dependent manner leading to succinate accumulation (154), which is supported by the observation that Irg1 knockout macrophages do not accumulate succinate following LPS stimulation (151). The implications of succinate accumulation are discussed later. Itaconate also plays a major role in potentiating cellular anti-inflammatory and anti-oxidant effects through activation and nuclear translocation of NRF2via alkylation of KEAP1, a known physiological inhibitor of NRF2 (147). Through activation of NRF2, 4-octyl-itacoante (a cell permeable analog of itaconate) increases expression of key anti-inflammatory genes including heme oxygenase 1 and potently inhibits proinflammatory cytokine release (147). Macrophages lacking the Irg1 enzyme produce increased proinflammatory cytokines, including IL-6, IL-18, and IL-1β, in response to LPS relative to wild type macrophages and treatment with a cell permeable itaconate derivative decreases proinflammatory cytokines in response to LPS (147, 155).

Itaconate is also known to be secreted by macrophages into the extracellular milieu and have direct antibacterial effects (156). Itaconate competitively inhibits the microbial enzyme isocitrate lyase, a required step in the glyoxylate shunt, thereby limiting bacterial growth under nutrient poor conditions as occur at the site of infection (157). The microbial glyoxylate shunt bypasses two decarboxylation steps in the tricarboxylic acid cycle, facilitating the assimilation of carbon when only two-carbon sources such as ethanol or acetate are available (151, 158–160). Pathogens that have shown sensitivity to itaconate-induced microbial growth inhibition include *Mycobacterium tuberculosis, Staphylococcus aureus, Legionella pneumonia, Acinetobacter baumanii*, and *Salmonella enterica* (153, 161, 162). Therefore, itaconate affects cellular metabolism and affords anti-inflammatory and anti-microbial protection upon inflammatory activation of immune cells. As such, our knowledge of the role of itaconate is currently limited to macrophages and monocytes, and future studies addressing its effects on other leukocytes such as neutrophils and dendritic cells will shed more light on the novel aspects of this critical metabolite. Nonetheless, based on studies, therapeutic utility of itaconate to protect against life-threatening infections and sepsis merits further investigation.

Succinate is another TCA cycle metabolite that significantly accumulates in LPS-stimulated macrophages and monocytes (150, 152, 163). Succinate is the principal substrate for succinate dehydrogenase, which not only participates in the TCA cycle but also in ETC complex II. Oxidation of succinate to fumarate results in reduction of FAD+ and ultimately Coenzyme Q, which continues in the ETC via complex III and IV, leading to ATP generation via ATP synthase (16). Itaconate-induced inhibition of SDH and facilitation of glutamine anapleurosis are the major sources of intracellular succinate accumulation upon LPS stimulation of macrophages (150, 151). High levels of succinate and succinate dehydrogenase activity are associated with inducing a pro-inflammatory phenotype in innate leukocytes as result of succinate-mediated hypoxia inducible factor α (HIF-1α) stabilization, increased mitochondrial ROS generation, and protein succinylation (137, 163). LPS-induced succinate accumulation is associated with stabilization of HIF-1α, leading to increased IL-1β production and inflammation (140, 164). Rapid oxidation of increased succinate to fumarate by SDH requires CoQ, which is consumed under LPS stimulation, thereby driving reverse electron transport leading to a substantial generation of mitochondrial ROS (165). Although uncontrolled generation of mitochondrial ROS can have deleterious effects on cellular functions, it has also been shown to play an important role in microbial clearance (145). However, further studies are needed to establish the antimicrobial role of SDH-generated ROS in *in vivo* models of infection.

Inflammation-induced increases in intracellular accumulation of citrate also affects cellular metabolism and functions. Activated macrophages accumulate citrate due to decreased isocitrate dehydrogenase activity (47, 151). De Souza and colleagues recently demonstrated that LPS-mediated increase in IFN-γ limits isocitrate dehydrogenase activity in an autocrine manner in macrophages, implying a role for IFN-γ in LPS-mediated increase in citrate levels (166). Accumulated citrate is not only converted to itaconate (153) in the mitochondria but also transported from the mitochondria into the cytosol via mitochondrial citrate carrier (CIC) (167). Increased CIC and cytosolic citrate has been shown to fuel the LPS-induced generation of pro-inflammatory mediators such as nitric oxide, ROS, and prostaglandins in macrophages (168). Our studies also show that MPLA-stimulated citrate transported into the cytosol is ultimately converted to malate and pyruvate, and the cytosolic malate replenishes mitochondrial oxaloacetate pools to further fuel a sustained increase in mitochondrial TCA cycle flux (47). Importantly, these alterations in citrate metabolism are associated with a sustained augmentation of mitochondrial density and oxygen consumption, along with increased macrophage phagocytic capacity (47). Therefore, citrate accumulation not only plays an important role in fueling acute inflammation but also potentiates a sustained increase in TCA cycle flux and antimicrobial functions, which need further evaluation.

Evidence for Metabolic Reprogramming in Murine and Human Sepsis Studies

The majority of studies demonstrating the effect of inflammatory activation on metabolic reprogramming of innate leukocytes such as macrophages and monocytes have been performed *in vitro*. Corroborating the changes described in the *in vitro* studies described above, metabolic reprogramming of innate immune cells in response to TLR activation has also been observed in some *in vivo* murine and human studies. Sterile endotoxemia (LPS administration) in mice causes peritoneal macrophages to more than double glucose uptake, suggesting an increase in glycolysis in this model (169). Functionally, monocytes from septic patients were found to have increased basal glycolysis compared to healthy controls (170). Shalova et al. performed a gene ontology analysis to compare monocytes from septic patients relative to healthy controls, and reported that the top 10 most significantly downregulated gene clusters were all related to cellular metabolism (171). Consistent with this, Cheng et al. found diminished glycolysis and oxidative phosphorylation in peripheral blood mononuclear cells (PBMCs) in septic patients with immunoparalysis as compared to control subjects (31). Genome-wide microarray analysis of PBMCs from patients with both bacterial and fungal sepsis in this study identified that genes for oxidative phosphorylation and glycolysis were both increased along with evidence of mitochondrial dysfunction pathways, suggesting that immune cell metabolism is significantly affected during sepsis. Further studies to separate the adaptive from the pathogenic changes in leukocyte metabolism could guide the development of therapies to augment or suppress these metabolic changes. For example, a study by Pan et al. demonstrated that a known anti-inflammatory compound, deoxyelephantophin, both blocks LPS-induced glycolytic increase and protects mice against endotoxemia (172).

There are limited *in vivo* studies analyzing the effect of sepsis on alterations of specific mitochondrial TCA cycle intermediates during sepsis. A murine study by Chao et al. employing scrub typhus infection demonstrated a 60-fold increase in plasma itaconate levels at 10 days after infection (173). A clinical study by Meiser et al. reported absence of any detectable

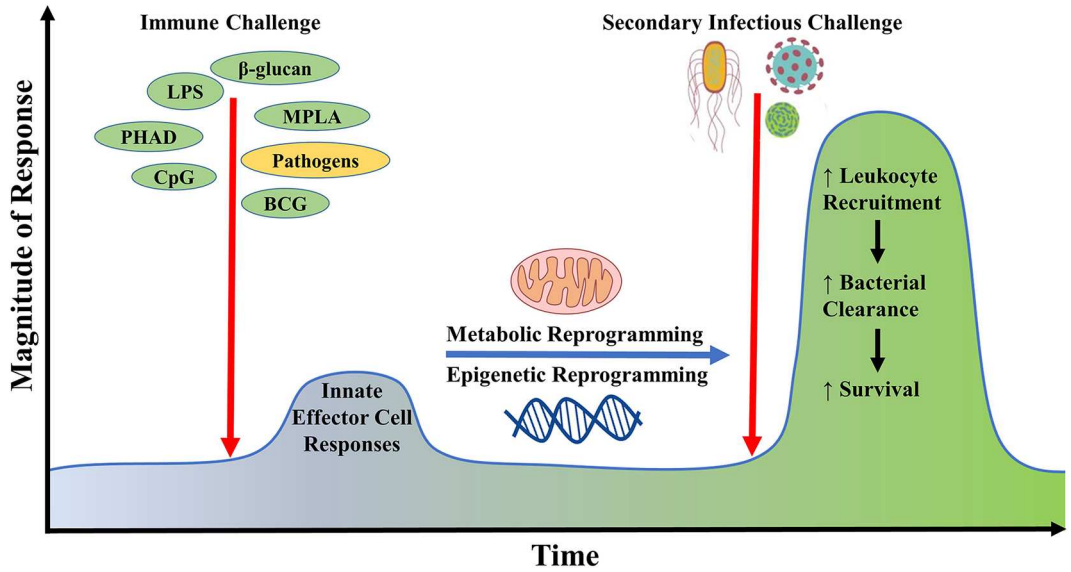

FIGURE 2 | Generation of innate immune memory using microbial ligands. Initial challenge with microbial ligands such as lipopolysaccharide, monophosphoryl lipid A, CpG, β-glucan potently stimulates host innate effector immune responses in cells such as neutrophils, monocytes, and macrophages, leading to the reprogramming of their metabolic and epigenetic status. Upon re-exposure of the initially primed host with a secondary inflammatory stimulus or infectious challenge, there occurs a heightened innate immune response against invading microbes via increased immune cell recruitment leading to improved microbial clearance and survival. This phenomenon is termed as innate immune memory.

itaconate in the plasma and urine of septic patients, in which the authors concluded that itaconate may not be a suitable systemic biomarker for predicting sepsis outcomes (174). That study evaluated the levels of itaconate at a single time point among sepsis patients and failed to elaborate on the clinical condition of patients during sample collection and the exact time point for collection. A recent study by Beloborodova et al. detected low concentrations of itaconic acid (0.5–2.3 μM) in the plasma of septic shock patients collected within 24 h and none was detected in patients at later stages of sepsis (175). The levels of succinate were higher in the late stage sepsis patients as compared to early stage, but lower than the control healthy group. It must, however, be noted that the early and late stage sepsis patients included in this study were entirely different patient cohorts and the authors do not report the changes in plasma itaconate levels as sepsis progressed in each septic patient subset. It is critical to follow septic patients and study the alterations in itaconate levels at various time points after sepsis induction to derive a definitive conclusion for the use of itaconate as a biomarker for sepsis outcomes or for supporting itaconate's use for therapeutic purpose to combat sepsis. Future studies evaluating sepsis-induced alterations in the levels of mitochondrial metabolites would be critical to further the field of metabolic reprogramming toward discovery of novel therapeutics to protect against infections and sepsis.

INNATE IMMUNE MEMORY AND TRAINED IMMUNITY

Classically, the role of the innate immune system is to recognize pathogens and mount a non-specific yet rapid response, whereas immunological memory has been traditionally considered a unique hallmark of the adaptive immune system. However, recent studies indicate that innate immune cells adapt upon exposure to a pathogen or pathogen-derived ligand, triggering augmentation of cell physiology and antimicrobial functions which allows for robust responses to a subsequent challenge either by the same or different pathogen (176). This phenomenon by which innate antimicrobial efficiency is increased due to the priming effect of prior exposure is termed "innate immune memory" or "trained immunity" (**Figure 2**). This immunoregulatory process confers host resistance to infection in plants and invertebrates that do not have adaptive immunity but also in mammals (177). The cell type (myeloid, natural killer, and innate lymphoid cells), stimuli (pattern recognition receptors and cytokines), genetic mechanism (epigenetic rewiring), and time scale (persisting weeks to months) are unique to innate immune memory, independent of those involved in classical immunological memory (178). An important player in health and disease, trained immunity may also serve as an innovative therapeutic strategy for protecting vulnerable patients from life-threatening infections in the future.

Metabolic Reprogramming and Innate Immune Memory

Recent findings strongly indicate that metabolic reprogramming is a key process underlying development of innate immune memory. Several studies have revealed that expression of key pro-inflammatory proteins and an effective immune response relies on intact mitochondrial respiration (179, 180), and the study of the metabolic demands of mounting an immune response has been a topic of increasing interest (181). It has

become widely appreciated that metabolism dynamics regulate innate immunity via production of metabolite intermediates which influence cellular phenotype and function (182). β-glucan immunomodulation has been associated with upregulated glycolysis in trained macrophages (183) and monocytes (184), likely to support pro-inflammatory macrophage antimicrobial functions (182, 185). This has been shown to be dependent on a shift from oxidative phosphorylation toward glycolysis through an Akt/mTOR/HIF-1α dependent pathway (183, 186). We recently reviewed regulation and function of HIF-1α in myeloid cells (187). On the other hand, TLR ligands (such as LPS, MPLA, and CPG) increase aerobic glycolysis in concert with increased antimicrobial functions (such as respiratory burst and phagocytosis) as well as induce mitochondrial biogenesis and increased oxidative metabolism (47). These metabolic alterations allow immediate leukocyte activation, cytokine secretion, and a more effective innate immune response to infection (46, 47, 188, 189). Our study using HIF-1α deficient macrophages demonstrated that HIF-1α is required for these metabolic alterations (46). Another study from our group showed that the inhibition of mTOR, which stabilizes HIF-1α, diminishes the protective response of TLR4 ligands (47).

Despite the apparent benefits of inducing innate immune memory, reprogramming of leukocyte oxidative metabolism could be a double-edged sword. As noted above, current research indicates that priming the immune system with microbial ligands at doses that do not cause damaging systemic inflammation induces protective immunity in association with an increase in leukocyte oxidative metabolism (47, 48). It appears that the heightened metabolic state induced under those conditions is utilized to facilitate augmented leukocyte antimicrobial functions such as phagocytosis, oxidative burst, and microbial killing. However, in cases of tissue injury, reprogrammed leukocytes could funnel energy to drive hyperinflammation. A recent paper by Di Gioia and colleagues showed that oxidized phospholipids derived from 1-palmitoyl-2-arachidonyl-sn-glycero-3-phosphorylcholine (oxPAPC) can induce increased leukocyte oxidative metabolism and hyperinflammation, especially in the presence of microbial ligands such as LPS (190). Oxidized phospholipids are damage associated molecular patterns (DAMPS) that are released following tissue injury. Di Gioia and colleagues reported that oxPAPC and LPS strongly drive production of pro-IL-1β in macrophages, which is cleaved and secreted as the mature protein upon activation of the inflammasome by DAMPS such as ATP (190). However, the ramifications of these alterations in models of acute inflammation remain to be fully elucidated since a study by Chu and colleagues showed that oxPAPC inhibits non-canonical inflammasome activation and is protective in an experimental model of septic shock (191).

INNATE IMMUNE MEMORY—A NOVEL THERAPEUTIC TARGET TO PROTECT AGAINST INFECTIONS AND SEPSIS

The non-specific protection conferred by trained immunity lends itself to an exciting novel therapeutic approach by which patients could be primed and protected from a wide array of infections thus preventing sepsis and subsequent mortality. Several microbial ligands have immunomodulatory potential, most notably, TLR and dectin-1 agonists. Rowley first reported in 1956 that priming mice with the TLR4 agonist lipopolysaccharide (LPS), a structural component of the cell wall of Gram-negative bacteria, conferred host protection to subsequent exposure to Gram-negative pathogens (192). Following this discovery, it has been found that LPS challenge protects against a wide array of pathogens, including fungal (193), Gram-positive *Staphylococcus aureus* (194), and several Gram-negative pathogens, including *Escherichia coli* (192), *Salmonella enterica serovar typhimurium* (195), and *Pseudomonas aeruginosa* (196, 197), as well as polymicrobial sepsis (198). Priming with LPS induces enhanced bacterial clearance (196, 199) and leukocyte recruitment (194, 200).

Leukocytes primed with LPS can also be described as not only trained, but also "endotoxin tolerant," which is defined by an attenuated pro-inflammatory response upon secondary challenge with the stimulus. A body of literature suggests that the phenomenon of endotoxin tolerance is a state of immunoparalysis during which the host is more susceptible to infection (201, 202), and results in poorer patient outcomes (203–206). However, the clear relationship between endotoxin tolerance and susceptibility to later infections has not been established. In fact, our group recently demonstrated that the cytokine response to LPS is not indicative of antimicrobial immunity (46), and a body of literature illustrates that altering proinflammatory cytokines during infection has had no protective benefit (207–210) thereby bringing into question whether proinflammatory cytokine levels are an essential element in determining immune competence.

TLR4 Agonist-Induced Innate Immune Memory and Protection Against Infection

As LPS is toxic to humans, experimental studies have progressed to investigate other agonists that confer this attractive phenotype of host resistance to infection after priming. Intriguingly, prophylactic administration of the vaccine adjuvant MPLA, which is derived by cleaving the C1 phosphate group from lipid A and is 100-fold less toxic than LPS (211–213) improves bacterial clearance, attenuates physiologic dysfunction, induces leukocyte expansion and recruitment to sites of infection, enhances antimicrobial functions, and profoundly improves survival during infection with a wide array of clinically relevant pathogens (47, 188, 214–217). TLR4 is unique among TLRs as it can generally signal through both the myeloid differentiation primary response gene 88 (MyD88)-dependent and the TIR-domain-containing adapter inducing interferon-β (TRIF)-dependent pathways. A study of human neutrophils, however, revealed that TLR4 activation by LPS does not activate the TRIF-dependent pathway in neutrophils, postulated to be due to neutrophil's more prominent role in bacterial responses compared to viral (218). Our group is investigating the relative contribution of these pathways in TLR-mediated trained innate immunity, and has shown that MyD88 deficient mice fail to augment leukocyte recruitment or G-CSF production in response to infection following priming with MPLA, both of which are

known to play a critical role in MPLA-mediated protection (188, 189). Further, the MyD88-selective TLR9 agonist CpG oligodeoxynucleotide (CpG) preserves physiologic function and improves bacterial clearance following infectious challenge with *Pseudomonas aeruginosa* (46). CpG similarly provided protection in a model of intracerebral *Escherichia coli* (219), which implies that TLR-mediated resistance to infection is dependent on MyD88 signaling.

TLR4 agonist-induced antimicrobial properties are independent of antibiotic therapy. This is of particular importance due to the current rise in global antibiotic resistance (220–222). The rate of antibiotic resistance has been far exceeding the rate of new antibiotic class development, and current market trends suggests pharmaceutical companies will not be able to support new antibiotic development programs (220, 223). Thus, there is an increasing need for novel antimicrobial therapeutic strategies, lending to the possibility of adopting agents that induce trained immunity as independent or adjunct antimicrobial therapeutic agents. Several synthetic ligands that target TLRs and dectin-1 are under development. Novel synthetic phosphorylated hexaacyl disaccharides (PHADs), which target TLR4, are equipotent with MPLA as agents to augment antimicrobial immunity and have strong potential to be developed into drug candidates (48). PHADs are synthesized *de novo* and are currently under investigation as immunopotentiating agents (48, 213). The antimicrobial functions of PHADs are linked to the increased recruitment of innate leukocytes to the sites of infection and augmentation of their antimicrobial activity.

Therapeutic Utility of Other Microbial Ligands

The class of TLR agonists that have strong potential for clinical translation extend beyond TLR4 ligands. The TLR9-selective agonist CpG oligodeoxynucleotide (CpG-ODN) is a short single-stranded synthetic bacterial DNA molecule that has been shown to confer host resistance to an array of pathogens including the parasite *Leishmania major* (224), the Gram-negative pathogens *Francisella tularensis* (225), *Pseudomonas aeruginosa* (226), and *Burkholderia pseudomallei* (227–229), Gram-positive *Listeria monocytogenes* (230), and viral HSV infections (231). Further, CpG-ODN also has promise as a vaccine adjuvant (232) and antitumor therapeutic (233, 234). There are several classes of CpG-ODN based on their variety of sequence and structure which elicit specific immunomodulatory profiles (232). Unlike TLR4, which signals through both MyD88- and TRIF-dependent pathways, activation of TLR9 triggers MyD88-dependent signaling alone. CpG-mediated host protection to infection seems to be dependent on downstream induction of Th1-type immune response, specifically the production of Interferon-β (224, 235). Further work is necessary to define the cellular and molecular underlying mechanisms by which CpG boosts antimicrobial responses and protects against infection.

Other microbial ligands and infections themselves can induce innate immune memory and enhance antimicrobial functions through different signaling mechanisms. β-glucans are structurally diverse polysaccharide components found mainly in fungal cell walls that are key pathogen-associated molecular patterns that trigger an immune response and are the quintessential inducers of trained immunity (236). Glucans are potent immunomodulators that augment host resistance against Gram-negative [*Escherichia coli*; (237, 238)], Gram-positive (*Staphylococcus aureus)* (239, 240), fungal [*Candida albicans*; (241)], and parasitic (*Leishmania braziliensis)* (242) infections. Glucan binds Dectin-1, which triggers downstream Raf-1/Akt-dependent signaling to augment phagocytosis, ROS production, microbial killing, and cytokine production (243–245). Further, glucan has been shown to decrease infectious complications in high risk surgical patients (246). The biological mechanisms underlying the immunomodulatory effects of glucan remain to be fully understood but glucan strongly induces metabolic reprogramming and epigenetic changes that alter gene expression and augment leukocyte function (236). Interestingly, trained immunity can also be induced by Bacillus Calmette-Guerin (BCG), which has conferred resistance to *Schistosoma mansoni* (247) and *Candida albicans* (248) infections in mice. These studies found that BCG-primed macrophages show increased phagocytosis and ROS production and improved clearance of pathogens. Epidemiological studies show that BCG, among other vaccines such as measles and oral polio vaccine, confer beneficial protective effects to unrelated pathogens in humans (249–251). Furthermore, evidence suggests that certain viral infections, such as malaria (252) and murine cytomegalovirus (253, 254), and parasitic infections [*Nippostrongylus brasiliensis*; (255)] induce a state of cross-protection to different pathogens through increased innate antimicrobial efficiency.

CONCLUSIONS

Here, we have reviewed the impact of sepsis on the mitochondrial function of innate leukocytes, and potential therapeutic strategies for reprogramming leukocyte metabolism to induce innate immune memory and restore host immune competency. Studies in both animal sepsis models and human septic patients reveal significant mitochondrial dysfunction in various organ systems, which correlates with sepsis severity and outcomes. In particular, sepsis-induced mitochondrial dysfunction in leukocytes is a key driver of impaired immune responses leading to increased susceptibility to secondary infections in septic patients. Studies show that early recovery of mitochondrial function in leukocytes correlates with improved septic patient outcomes.

TLR agonists are a class of microbial ligands with attractive immunomodulatory properties. Recent studies demonstrate that TLR agonists can mediate non-specific protection against infection with protective effects lasting up to 2 weeks, independent of the adaptive immune system. This induction of apparent innate immune memory is mediated by TLR agonist-induced metabolic reprogramming of leukocytes. The altered metabolic phenotype is characterized by increased glycolysis, oxidative phosphorylation, and intra-cellular concentrations of key metabolic intermediates such as itaconate and succinate, which influence cellular antimicrobial and anti-inflammatory

functions. Current studies show that administration of drugs such as TLR ligands which boost leukocyte oxidative metabolism days prior to infectious challenge improve survival. Therefore, pre-treatment of critically, who are at risk for acquiring life-threatening infections, with immunomodulators that induce metabolic reprogramming and innate immunity might augment host resistance to infection and improve survival. *In vitro* data demonstrates that oxidative metabolism is boosted ∼3 days after treatment. Though it is impossible to predict exactly which patients will face an infectious challenge when, patients at risk for hospital acquired infections could be dosed at admission or prior to an event that may lead to infection, such as abdominal surgery. A recent study by Casilag et al. shows that combination therapy with MPLA significantly augmented the efficacy of antibiotics leading to reduced bacterial burden and improved survival in a murine model of bacterial pneumonia, even when administered after induction of pneumonia (256). Therefore, treatment with immunomodulators such as TLR agonists and others may also be beneficial later in the course of sepsis to augment host innate immunity and improve outcomes.

With the increasing development of antimicrobial resistance, host-directed immunotherapies offer a promising approach to combat the risk of deadly infections in critically ill and injured patients. Immunomodulatory strategies aimed at augmenting host immunity provide a means of mediating sustained broad protection against a variety of common nosocomial pathogens. This review highlights the prospect of developing microbial ligands as novel therapeutics with the aim of augmenting leukocyte mitochondrial function and inducing innate immune memory for protection against life-threatening infections in critically ill patients.

AUTHOR CONTRIBUTIONS

All authors contributed toward writing of the manuscript sections and conceptualization of figures. NP and ES critically revised the manuscript for important intellectual concepts. All authors have read and approved the submitted version.

FUNDING

This work was supported by National Institutes of Health (NIH) grants R01 GM104306, R01 GM119197 and R01 AI151210 to ES, R01 GM121711 to JB, T32 GM108554-05 and Shock Society Faculty Research Award to NP, K08 GM123345 to AH, AHA grant 19PRE34430054 to CS, and T32 GM007347-41 to MM and CS. The content is solely the responsibility of the authors and does not necessarily represent the official views of the National Institutes of Health.

REFERENCES

1. Kahn JM, Le T, Angus DC, Cox CE, Hough CL, White DB, et al. The epidemiology of chronic critical illness in the United States*. *Crit Care Med.* (2015) 43:282–7. doi: 10.1097/CCM.0000000000000710
2. Filkins JP. Monokines and the metabolic pathophysiology of septic shock. *Fed Proc.* (1985) 44:300–4.
3. Beutler B, Cerami A. Cachectin/tumor necrosis factor: an endogenous mediator of shock and inflammation. *Immunol Res.* (1986) 5:281–93. doi: 10.1007/bf02935501
4. Tracey KJ, Lowry SF, Fahey TJ III, Albert JD, Fong Y, Hesse D, et al. Cachectin/tumor necrosis factor induces lethal shock and stress hormone responses in the dog. *Surg Gynecol Obstet.* (1987) 164:415–22.
5. Hesse DG, Tracey KJ, Fong Y, Manogue KR, Palladino MAJr, Cerami A, et al. Cytokine appearance in human endotoxemia and primate bacteremia. *Surg Gynecol Obstet.* (1988) 166:147–53.
6. Tracey KJ, Fong Y, Hesse DG, Manogue KR, Lee AT, Kuo GC, et al. Anti-cachectin/TNF monoclonal antibodies prevent septic shock during lethal bacteraemia. *Nature.* (1987) 330:662–4. doi: 10.1038/330662a0
7. Dinarello CA. Interleukin-1 and interleukin-1 antagonism. *Blood.* (1991) 77:1627–52.
8. Baumgartner JD, Calandra T. Treatment of sepsis: past and future avenues. *Drugs.* (1999) 57:127–32.
9. Opal SM, Fisher CJ Jr, Dhainaut JF, Vincent JL, Brase R, Lowry SF, et al. Confirmatory interleukin-1 receptor antagonist trial in severe sepsis: a phase III, randomized, double-blind, placebo-controlled, multicenter trial. The Interleukin-1 Receptor Antagonist Sepsis Investigator Group. *Crit Care Med.* (1997) 25:1115–24. doi: 10.1097/00003246-199707000-00010
10. Shakoory B, Carcillo JA, Chatham WW, Amdur RL, Zhao H, Dinarello CA, et al. Interleukin-1 receptor blockade is associated with reduced mortality in sepsis patients with features of macrophage activation syndrome: reanalysis of a prior phase III trial. *Crit Care Med.* (2016) 44:275–81. doi: 10.1097/CCM.0000000000001402
11. Mira JC, Gentile LF, Mathias BJ, Efron PA, Brakenridge SC, Mohr AM, et al. Sepsis pathophysiology, chronic critical illness, and persistent inflammation-immunosuppression and catabolism syndrome. *Crit Care Med.* (2017) 45:253–62. doi: 10.1097/CCM.0000000000002074
12. Patera AC, Drewry AM, Chang K, Beiter ER, Osborne D, Hotchkiss RS. Frontline Science: defects in immune function in patients with sepsis are associated with PD-1 or PD-L1 expression and can be restored by antibodies targeting PD-1 or PD-L1. *J Leukoc Biol.* (2016) 100:1239–54. doi: 10.1189/jlb.4HI0616-255R
13. Patil NK, Guo Y, Luan L, Sherwood ER. Targeting immune cell checkpoints during sepsis. *Int J Mol Sci.* (2017) 18:2413. doi: 10.3390/ijms18112413
14. Hotchkiss RS, Sherwood ER. Immunology. Getting sepsis therapy right. *Science.* (2015) 347:1201–2. doi: 10.1126/science.aaa8334
15. Alkhateeb T, Kumbhare A, Bah I, Youssef D, Yao ZQ, McCall CE, et al. S100A9 maintains myeloid-derived suppressor cells in chronic sepsis by inducing miR-21 and miR-181b. *Mol Immunol.* (2019) 112:72–81. doi: 10.1016/j.molimm.2019.04.019
16. Zhao RZ, Jiang S, Zhang L, Yu ZB. Mitochondrial electron transport chain, ROS generation and uncoupling (Review). *Int J Mol Med.* (2019) 44:3–15. doi: 10.3892/ijmm.2019.4188
17. McBride HM, Neuspiel M, Wasiak S. Mitochondria: more than just a powerhouse. *Curr Biol.* (2006) 16:R551–60. doi: 10.1016/j.cub.2006.06.054
18. Galluzzi L, Kepp O, Kroemer G. Mitochondria: master regulators of danger signalling. *Nat Rev Mol Cell Biol.* (2012) 13:780–8. doi: 10.1038/nrm3479
19. Mills EL, Kelly B, O'Neill LAJ. Mitochondria are the powerhouses of immunity. *Nat Immunol.* (2017) 18:488–98. doi: 10.1038/ni.3704
20. Singer M, Deutschman CS, Seymour CW, Shankar-Hari M, Annane D, Bauer M, et al. The third international consensus definitions for sepsis and septic shock (sepsis-3). *JAMA.* (2016) 315:801–10. doi: 10.1001/jama.2016.0287
21. Lee I, Huttemann M. Energy crisis: the role of oxidative phosphorylation in acute inflammation and sepsis. *Biochim Biophys Acta.* (2014) 1842:1579–86. doi: 10.1016/j.bbadis.2014.05.031
22. Singer M. The role of mitochondrial dysfunction in sepsis-induced multi-organ failure. *Virulence.* (2014) 5:66–72. doi: 10.4161/viru.26907

23. Brealey D, Brand M, Hargreaves I, Heales S, Land J, Smolenski R, et al. Association between mitochondrial dysfunction and severity and outcome of septic shock. *Lancet.* (2002) 360:219–23. doi: 10.1016/S0140-6736(02)09459-X
24. Matkovich SJ, Al Khiami B, Efimov IR, Evans S, Vader J, Jain A, et al. Widespread down-regulation of cardiac mitochondrial and sarcomeric genes in patients with sepsis. *Crit Care Med.* (2017) 45:407–14. doi: 10.1097/CCM.0000000000002207
25. Brealey D, Karyampudi S, Jacques TS, Novelli M, Stidwill R, Taylor V, et al. Mitochondrial dysfunction in a long-term rodent model of sepsis and organ failure. *Am J Physiol Regul Integr Comp Physiol.* (2004) 286:R491–7. doi: 10.1152/ajpregu.00432.2003
26. Vanasco V, Magnani ND, Cimolai MC, Valdez LB, Evelson P, Boveris A, et al. Endotoxemia impairs heart mitochondrial function by decreasing electron transfer, ATP synthesis and ATP content without affecting membrane potential. *J Bioenerg Biomembr.* (2012) 44:243–52. doi: 10.1007/s10863-012-9426-3
27. Patil NK, Parajuli N, MacMillan-Crow LA, Mayeux PR. Inactivation of renal mitochondrial respiratory complexes and manganese superoxide dismutase during sepsis: mitochondria-targeted antioxidant mitigates injury. *Am J Physiol Renal Physiol.* (2014) 306:F734–43. doi: 10.1152/ajprenal.00643.2013
28. Eyenga P, Roussel D, Morel J, Rey B, Romestaing C, Gueguen-Chaignon V, et al. Time course of liver mitochondrial function and intrinsic changes in oxidative phosphorylation in a rat model of sepsis. *Intensive Care Med Exp.* (2018) 6:31. doi: 10.1186/s40635-018-0197-y
29. Arulkumaran N, Deutschman CS, Pinsky MR, Zuckerbraun B, Schumacker PT, Gomez H, et al. Mitochondrial function in sepsis. *Shock.* (2016) 45:271–81. doi: 10.1097/SHK.0000000000000463
30. Vachharajani V, Liu T, McCall CE. Epigenetic coordination of acute systemic inflammation: potential therapeutic targets. *Expert Rev Clin Immunol.* (2014) 10:1141–50. doi: 10.1586/1744666X.2014.943192
31. Cheng SC, Scicluna BP, Arts RJ, Gresnigt MS, Lachmandas E, Giamarellos-Bourboulis EJ, et al. Broad defects in the energy metabolism of leukocytes underlie immunoparalysis in sepsis. *Nat Immunol.* (2016) 17:406–13. doi: 10.1038/ni.3398
32. Adrie C, Bachelet M, Vayssier-Taussat M, Russo-Marie F, Bouchaert I, Adib-Conquy M, et al. Mitochondrial membrane potential and apoptosis peripheral blood monocytes in severe human sepsis. *Am J Respir Crit Care Med.* (2001) 164:389–95. doi: 10.1164/ajrccm.164.3.2009088
33. Belikova I, Lukaszewicz AC, Faivre V, Damoisel C, Singer M, Payen D. Oxygen consumption of human peripheral blood mononuclear cells in severe human sepsis. *Crit Care Med.* (2007) 35:2702–8. doi: 10.1097/01.ccm.0000295593.25106.c4
34. Japiassu AM, Santiago AP, d'Avila JC, Garcia-Souza LF, Galina A, Castro Faria-Neto HC, et al. Bioenergetic failure of human peripheral blood monocytes in patients with septic shock is mediated by reduced F1Fo adenosine-5'-triphosphate synthase activity. *Crit Care Med.* (2011) 39:1056–63. doi: 10.1097/CCM.0b013e31820eda5c
35. Garrabou G, Moren C, Lopez S, Tobias E, Cardellach F, Miro O, et al. The effects of sepsis on mitochondria. *J Infect Dis.* (2012) 205:392–400. doi: 10.1093/infdis/jir764
36. Sjovall F, Morota S, Persson J, Hansson MJ, Elmer E. Patients with sepsis exhibit increased mitochondrial respiratory capacity in peripheral blood immune cells. *Crit Care.* (2013) 17:R152. doi: 10.1186/cc12831
37. Weiss SL, Selak MA, Tuluc F, Perales Villarroel J, Nadkarni VM, Deutschman CS, et al. Mitochondrial dysfunction in peripheral blood mononuclear cells in pediatric septic shock. *Pediatr Crit Care Med.* (2015) 16:e4–12. doi: 10.1097/PCC.0000000000000277
38. Merz TM, Pereira AJ, Schurch R, Schefold JC, Jakob SM, Takala J, et al. Mitochondrial function of immune cells in septic shock: a prospective observational cohort study. *PLoS ONE.* (2017) 12:e0178946. doi: 10.1371/journal.pone.0178946
39. Jang DH, Orloski CJ, Owiredu S, Shofer FS, Greenwood JC, Eckmann DM. Alterations in mitochondrial function in blood cells obtained from patients with sepsis presenting to an emergency department. *Shock.* (2019) 51:580–4. doi: 10.1097/SHK.0000000000001208
40. Kraft BD, Chen L, Suliman HB, Piantadosi CA, Welty-Wolf KE. Peripheral blood mononuclear cells demonstrate mitochondrial damage clearance during sepsis. *Crit Care Med.* (2019) 47:651–8. doi: 10.1097/CCM.0000000000003681
41. Weiss SL, Zhang D, Bush J, Graham K, Starr J, Murray J, et al. Mitochondrial dysfunction is associated with an immune paralysis phenotype in pediatric sepsis. *Shock.* (2019). doi: 10.1097/SHK.0000000000001486. [Epub ahead of print].
42. Weiss SL, Zhang D, Bush J, Graham K, Starr J, Tuluc F, et al. Persistent mitochondrial dysfunction linked to prolonged organ dysfunction in pediatric sepsis. *Crit Care Med.* (2019) 47:1433–41. doi: 10.1097/CCM.0000000000003931
43. Clere-Jehl R, Helms J, Kassem M, Le Borgne P, Delabranche X, Charles AL, et al. Septic shock alters mitochondrial respiration of lymphoid cell-lines and human peripheral blood mononuclear cells: the role of plasma. *Shock.* (2019) 51:97–104. doi: 10.1097/SHK.0000000000001125
44. Palsson-McDermott EM, O'Neill LA. The Warburg effect then and now: from cancer to inflammatory diseases. *Bioessays.* (2013) 35:965–73. doi: 10.1002/bies.201300084
45. Carre JE, Orban JC, Re L, Felsmann K, Iffert W, Bauer M, et al. Survival in critical illness is associated with early activation of mitochondrial biogenesis. *Am J Respir Crit Care Med.* (2010) 182:745–51. doi: 10.1164/rccm.201003-0326OC
46. Fensterheim BA, Guo Y, Sherwood ER, Bohannon JK. The cytokine response to lipopolysaccharide does not predict the host response to infection. *J Immunol.* (2017) 198:3264–73. doi: 10.4049/jimmunol.1602106
47. Fensterheim BA, Young JD, Luan L, Kleinbard RR, Stothers CL, Patil NK, et al. The TLR4 agonist monophosphoryl lipid a drives broad resistance to infection via dynamic reprogramming of macrophage metabolism. *J Immunol.* (2018) 200:3777–89. doi: 10.4049/jimmunol.1800085
48. Hernandez A, Luan L, Stothers CL, Patil NK, Fults JB, Fensterheim BA, et al. Phosphorylated hexa-acyl disaccharides augment host resistance against common nosocomial pathogens. *Crit Care Med.* (2019) 47:e930–8. doi: 10.1097/CCM.0000000000003967
49. Ioannou A, Dalle Lucca J, Tsokos GC. Immunopathogenesis of ischemia/reperfusion-associated tissue damage. *Clin Immunol.* (2011) 141:3–14. doi: 10.1016/j.clim.2011.07.001
50. Leung CH, Caldarone CA, Wang F, Venkateswaran S, Ailenberg M, Vadasz B, et al. Remote ischemic conditioning prevents lung and liver injury after hemorrhagic shock/resuscitation: potential role of a humoral plasma factor. *Ann Surg.* (2014) 261:1215–25. doi: 10.1097/SLA.0000000000000877
51. Chow CC, Clermont G, Kumar R, Lagoa C, Tawadrous Z, Gallo D, et al. The acute inflammatory response in diverse shock states. *Shock.* (2005) 24:74–84. doi: 10.1097/01.shk.0000168526.97716.f3
52. McGhan LJ, Jaroszewski DE. The role of toll-like receptor-4 in the development of multi-organ failure following traumatic haemorrhagic shock and resuscitation. *Injury.* (2012) 43:129–36. doi: 10.1016/j.injury.2011.05.032
53. Yao X, Carlson D, Sun Y, Ma L, Wolf SE, Minei JP, et al. Mitochondrial ROS induces cardiac inflammation via a pathway through mtDNA damage in a pneumonia-related sepsis model. *PLoS ONE.* (2015) 10:e0139416. doi: 10.1371/journal.pone.0139416
54. Chen R, Zhu S, Zeng L, Wang Q, Sheng Y, Zhou B, et al. AGER-mediated lipid peroxidation drives caspase-11 inflammasome activation in sepsis. *Front Immunol.* (2019) 10:1904. doi: 10.3389/fimmu.2019.01904
55. Hazeldine J, Dinsdale RJ, Harrison P, Lord JM. Traumatic injury and exposure to mitochondrial-derived damage associated molecular patterns suppresses neutrophil extracellular trap formation. *Front Immunol.* (2019) 10:685. doi: 10.3389/fimmu.2019.00685
56. Kartchner LB, Gode CJ, Dunn JLM, Glenn LI, Duncan DN, Wolfgang MC, et al. One-hit wonder: Late after burn injury, granulocytes can clear one bacterial infection but cannot control a subsequent infection. *Burns.* (2019) 45:627–40. doi: 10.1016/j.burns.2018.08.019
57. Sakuma M, Khan MAS, Yasuhara S, Martyn JA, Palaniyar N. Mechanism of pulmonary immunosuppression: extrapulmonary burn injury suppresses bacterial endotoxin-induced pulmonary neutrophil recruitment and neutrophil extracellular trap (NET) formation. *FASEB J.* (2019) 33:13602–16. doi: 10.1096/fj.201901098R

58. Patil NK, Luan L, Bohannon JK, Hernandez A, Guo Y, Sherwood ER. Frontline Science: anti-PD-L1 protects against infection with common bacterial pathogens after burn injury. *J Leukoc Biol.* (2018) 103:23–33. doi: 10.1002/JLB.5HI0917-360R
59. Scarpulla RC. Transcriptional paradigms in mammalian mitochondrial biogenesis and function. *Physiol Rev.* (2008) 88:611–38. doi: 10.1152/physrev.00025.2007
60. Dominy JE, Puigserver P. Mitochondrial biogenesis through activation of nuclear signaling proteins. *Cold Spring Harb Perspect Biol.* (2013) 5:a015008. doi: 10.1101/cshperspect.a015008
61. Scarpulla RC. Metabolic control of mitochondrial biogenesis through the PGC-1 family regulatory network. *Biochim Biophys Acta.* (2011) 1813:1269–78. doi: 10.1016/j.bbamcr.2010.09.019
62. Gureev AP, Shaforostova EA, Popov VN. Regulation of mitochondrial biogenesis as a way for active longevity: interaction between the Nrf2 and PGC-1alpha signaling pathways. *Front Genet.* (2019) 10:435. doi: 10.3389/fgene.2019.00435
63. Hock MB, Kralli A. Transcriptional control of mitochondrial biogenesis and function. *Annu Rev Physiol.* (2009) 71:177–203. doi: 10.1146/annurev.physiol.010908.163119
64. Canto C, Gerhart-Hines Z, Feige JN, Lagouge M, Noriega L, Milne JC, et al. AMPK regulates energy expenditure by modulating NAD+ metabolism and SIRT1 activity. *Nature.* (2009) 458:1056–60. doi: 10.1038/nature07813
65. Inata Y, Piraino G, Hake PW, O'Connor M, Lahni P, Wolfe V, et al. Age-dependent cardiac function during experimental sepsis: effect of pharmacological activation of AMP-activated protein kinase by AICAR. *Am J Physiol Heart Circ Physiol.* (2018) 315:H826–37. doi: 10.1152/ajpheart.00052.2018
66. Hall DT, Griss T, Ma JF, Sanchez BJ, Sadek J, Tremblay AMK, et al. The AMPK agonist 5-aminoimidazole-4-carboxamide ribonucleotide (AICAR), but not metformin, prevents inflammation-associated cachectic muscle wasting. *EMBO Mol Med.* (2018) 10:e8307. doi: 10.15252/emmm.201708307
67. Escobar DA, Botero-Quintero AM, Kautza BC, Luciano J, Loughran P, Darwiche S, et al. Adenosine monophosphate-activated protein kinase activation protects against sepsis-induced organ injury and inflammation. *J Surg Res.* (2015) 194:262–72. doi: 10.1016/j.jss.2014.10.009
68. Wang Y, An H, Liu T, Qin C, Sesaki H, Guo S, et al. Metformin improves mitochondrial respiratory activity through activation of AMPK. *Cell Rep.* (2019) 29:1511–23 e1515. doi: 10.1016/j.celrep.2019.09.070
69. Detaille D, Guigas B, Chauvin C, Batandier C, Fontaine E, Wiernsperger N, et al. Metformin prevents high-glucose-induced endothelial cell death through a mitochondrial permeability transition-dependent process. *Diabetes.* (2005) 54:2179–87. doi: 10.2337/diabetes.54.7.2179
70. Meng S, Cao J, He Q, Xiong L, Chang E, Radovick S, et al. Metformin activates AMP-activated protein kinase by promoting formation of the alphabetagamma heterotrimeric complex. *J Biol Chem.* (2015) 290:3793–802. doi: 10.1074/jbc.M114.604421
71. Suwa M, Egashira T, Nakano H, Sasaki H, Kumagai S. Metformin increases the PGC-1alpha protein and oxidative enzyme activities possibly via AMPK phosphorylation in skeletal muscle *in vivo*. *J Appl Physiol.* (2006) 101:1685–92. doi: 10.1152/japplphysiol.00255.2006
72. Tzanavari T, Varela A, Theocharis S, Ninou E, Kapelouzou A, Cokkinos DV, et al. Metformin protects against infection-induced myocardial dysfunction. *Metabolism.* (2016) 65:1447–58. doi: 10.1016/j.metabol.2016.06.012
73. Vaez H, Najafi M, Rameshrad M, Toutounchi NS, Garjani M, Barar J, et al. AMPK activation by metformin inhibits local innate immune responses in the isolated rat heart by suppression of TLR 4-related pathway. *Int Immunopharmacol.* (2016) 40:501–7. doi: 10.1016/j.intimp.2016.10.002
74. Vaez H, Najafi M, Toutounchi NS, Barar J, Barzegari A, Garjani A. Metformin Alleviates lipopolysaccharide-induced acute lung injury through suppressing toll-like receptor 4 signaling. *Iran J Allergy Asthma Immunol.* (2016) 15:498–507.
75. Vaez H, Rameshrad M, Najafi M, Barar J, Barzegari A, Garjani A. Cardioprotective effect of metformin in lipopolysaccharide-induced sepsis via suppression of toll-like receptor 4 (TLR4) in heart. *Eur J Pharmacol.* (2016) 772:115–23. doi: 10.1016/j.ejphar.2015.12.030
76. Tang G, Yang H, Chen J, Shi M, Ge L, Ge X, et al. Metformin ameliorates sepsis-induced brain injury by inhibiting apoptosis, oxidative stress and neuroinflammation via the PI3K/Akt signaling pathway. *Oncotarget.* (2017) 8:97977–89. doi: 10.18632/oncotarget.20105
77. Liang H, Ding X, Li L, Wang T, Kan Q, Wang L, et al. Association of preadmission metformin use and mortality in patients with sepsis and diabetes mellitus: a systematic review and meta-analysis of cohort studies. *Crit Care.* (2019) 23:50. doi: 10.1186/s13054-019-2346-4
78. Freire-Garabal M, Nunez MJ, Balboa J, Lopez-Delgado P, Gallego R, Garcia-Caballero T, et al. Serotonin upregulates the activity of phagocytosis through 5-HT1A receptors. *Br J Pharmacol.* (2003) 139:457–63. doi: 10.1038/sj.bjp.0705188
79. Mikulski Z, Zaslona Z, Cakarova L, Hartmann P, Wilhelm J, Tecott LH, et al. Serotonin activates murine alveolar macrophages through 5-HT2C receptors. *Am J Physiol Lung Cell Mol Physiol.* (2010) 299:L272–80. doi: 10.1152/ajplung.00032.2010
80. Drosatos K, Khan RS, Trent CM, Jiang H, Son NH, Blaner WS, et al. Peroxisome proliferator-activated receptor-γ activation prevents sepsis-related cardiac dysfunction and mortality in mice. *Circ Heart Fail.* (2013) 6:550–62. doi: 10.1161/CIRCHEARTFAILURE.112.000177
81. Tsujimura Y, Matsutani T, Matsuda A, Kutsukake M, Uchida E, Sasajima K, et al. Effects of pioglitazone on survival and omental adipocyte function in mice with sepsis induced by cecal ligation and puncture. *J Surg Res.* (2011) 171:e215–221. doi: 10.1016/j.jss.2011.08.012
82. Majer O, Bourgeois C, Zwolanek F, Lassnig C, Kerjaschki D, Mack M, et al. Type I interferons promote fatal immunopathology by regulating inflammatory monocytes and neutrophils during Candida infections. *PLoS Pathog.* (2012) 8:e1002811. doi: 10.1371/journal.ppat.1002811
83. Zingarelli B, Sheehan M, Hake PW, O'Connor M, Denenberg A, Cook JA. Peroxisome proliferator activator receptor-gamma ligands, 15-deoxy-Delta(12,14)-prostaglandin J2 and ciglitazone, reduce systemic inflammation in polymicrobial sepsis by modulation of signal transduction pathways. *J Immunol.* (2003) 171:6827–37. doi: 10.4049/jimmunol.171.12.6827
84. Maggi LB Jr, Sadeghi H, Weigand C, Scarim AL, Heitmeier MR, Corbett JA. Anti-inflammatory actions of 15-deoxy-delta 12,14-prostaglandin J2 and troglitazone: evidence for heat shock-dependent and -independent inhibition of cytokine-induced inducible nitric oxide synthase expression. *Diabetes.* (2000) 49:346–55. doi: 10.2337/diabetes.49.3.346
85. Guyton K, Bond R, Reilly C, Gilkeson G, Halushka P, Cook J. Differential effects of 15-deoxy-delta(12,14)-prostaglandin J2 and a peroxisome proliferator-activated receptor gamma agonist on macrophage activation. *J Leukoc Biol.* (2001) 69:631–8. doi: 10.1189/jlb.69.4.631
86. Guyton K, Zingarelli B, Ashton S, Teti G, Tempel G, Reilly C, et al. Peroxisome proliferator-activated receptor-gamma agonists modulate macrophage activation by gram-negative and gram-positive bacterial stimuli. *Shock.* (2003) 20:56–62. doi: 10.1097/01.shk.0000070903.21762.f8
87. Tancevski I, Nairz M, Duwensee K, Auer K, Schroll A, Heim C, et al. Fibrates ameliorate the course of bacterial sepsis by promoting neutrophil recruitment via CXCR2. *EMBO Mol Med.* (2014) 6:810–20. doi: 10.1002/emmm.201303415
88. Cree MG, Zwetsloot JJ, Herndon DN, Qian T, Morio B, Fram R, et al. Insulin sensitivity and mitochondrial function are improved in children with burn injury during a randomized controlled trial of fenofibrate. *Ann Surg.* (2007) 245:214–21. doi: 10.1097/01.sla.0000250409.51289.ca
89. Crisafulli C, Cuzzocrea S. The role of endogenous and exogenous ligands for the peroxisome proliferator-activated receptor alpha (PPAR-alpha) in the regulation of inflammation in macrophages. *Shock.* (2009) 32:62–73. doi: 10.1097/shk.0b013e31818bbad6
90. Barton P, Garcia J, Kouatli A, Kitchen L, Zorka A, Lindsay C, et al. Hemodynamic effects of i.v. milrinone lactate in pediatric patients with septic shock. A prospective, double-blinded, randomized, placebo-controlled, interventional study. *Chest.* (1996) 109:1302–12. doi: 10.1378/chest.109.5.1302
91. Carcillo JA, Herzer WA, Mi Z, Thomas NJ, Jackson EK. Treatment with the type IV phosphodiesterase inhibitor Ro 20-1724 protects renal and mesenteric blood flow in endotoxemic rats treated with norepinephrine. *J Pharmacol Exp Ther.* (1996) 279:1197–204.
92. Thomas NJ, Carcillo JA, Herzer WA, Mi Z, Tofovic SP, Jackson EK. Type IV phosphodiesterase inhibition improves cardiac

contractility in endotoxemic rats. *Eur J Pharmacol.* (2003) 465:133–9. doi: 10.1016/s0014-2999(03)01456-0
93. Holthoff JH, Wang Z, Patil NK, Gokden N, Mayeux PR. Rolipram improves renal perfusion and function during sepsis in the mouse. *J Pharmacol Exp Ther.* (2013) 347:357–64. doi: 10.1124/jpet.113.208520
94. Sims CR, Singh SP, Mu S, Gokden N, Zakaria D, Nguyen TC, et al. Rolipram improves outcome in a rat model of infant sepsis-induced cardiorenal syndrome. *Front Pharmacol.* (2017) 8:237. doi: 10.3389/fphar.2017.00237
95. Sanz MJ, Cortijo J, Taha MA, Cerda-Nicolas M, Schatton E, Burgbacher B, et al. Roflumilast inhibits leukocyte-endothelial cell interactions, expression of adhesion molecules and microvascular permeability. *Br J Pharmacol.* (2007) 152:481–92. doi: 10.1038/sj.bjp.0707428
96. Schick MA, Wunder C, Wollborn J, Roewer N, Waschke J, Germer CT, et al. Phosphodiesterase-4 inhibition as a therapeutic approach to treat capillary leakage in systemic inflammation. *J Physiol.* (2012) 590:2693–708. doi: 10.1113/jphysiol.2012.232116
97. Wollborn J, Wunder C, Stix J, Neuhaus W, Bruno RR, Baar W, et al. Phosphodiesterase-4 inhibition with rolipram attenuates hepatocellular injury in hyperinflammation *in vivo* and *in vitro* without influencing inflammation and HO-1 expression. *J Pharmacol Pharmacother.* (2015) 6:13–23. doi: 10.4103/0976-500X.149138
98. Zuo L, Li Q, Sun B, Xu Z, Ge Z. Cilostazol promotes mitochondrial biogenesis in human umbilical vein endothelial cells through activating the expression of PGC-1alpha. *Biochem Biophys Res Commun.* (2013) 433:52–7. doi: 10.1016/j.bbrc.2013.02.068
99. Ding H, Bai F, Cao H, Xu J, Fang L, Wu J, et al. PDE/cAMP/Epac/C/EBP-beta signaling cascade regulates mitochondria biogenesis of tubular epithelial cells in renal fibrosis. *Antioxid Redox Signal.* (2018) 29:637–52. doi: 10.1089/ars.2017.7041
100. Biala A, Tauriainen E, Siltanen A, Shi J, Merasto S, Louhelainen M, et al. Resveratrol induces mitochondrial biogenesis and ameliorates Ang II-induced cardiac remodeling in transgenic rats harboring human renin and angiotensinogen genes. *Blood Press.* (2010) 19:196–205. doi: 10.3109/08037051.2010.481808
101. Wang N, Mao L, Yang L, Zou J, Liu K, Liu M, et al. Resveratrol protects against early polymicrobial sepsis-induced acute kidney injury through inhibiting endoplasmic reticulum stress-activated NF-κB pathway. *Oncotarget.* (2017) 8:36449–61. doi: 10.18632/oncotarget.16860
102. Luo CJ, Luo F, Bu QD, Jiang W, Zhang W, Liu XM, et al. Protective effects of resveratrol on acute kidney injury in rats with sepsis. *Biomed Pap Med Fac Univ Palacky Olomouc Czech Repub.* (2019) 164:49–56. doi: 10.5507/bp.2019.006
103. Wang Y, Feng F, Liu M, Xue J, Huang H. Resveratrol ameliorates sepsis-induced acute kidney injury in a pediatric rat model via Nrf2 signaling pathway. *Exp Ther Med.* (2018) 16:3233–40. doi: 10.3892/etm.2018.6533
104. Shang X, Lin K, Yu R, Zhu P, Zhang Y, Wang L, et al. Resveratrol protects the myocardium in sepsis by activating the phosphatidylinositol 3-kinases (PI3K)/AKT/Mammalian target of rapamycin (mTOR) pathway and inhibiting the nuclear factor-κB (NF-κB) signaling pathway. *Med Sci Monit.* (2019) 25:9290–8. doi: 10.12659/MSM.918369
105. Martin LM, Johnson PJ, Amorim JR, DeClue AE. Effects of orally administered resveratrol on TNF, IL-1β, leukocyte phagocytic activity and oxidative burst function in horses: a prospective, randomized, double-blinded, placebo-controlled study. *Int J Mol Sci.* (2020) 21:1453. doi: 10.3390/ijms21041453
106. Valenti D, De Rasmo D, Signorile A, Rossi L, de Bari L, Scala I, et al. Epigallocatechin-3-gallate prevents oxidative phosphorylation deficit and promotes mitochondrial biogenesis in human cells from subjects with Down's syndrome. *Biochim Biophys Acta.* (2013) 1832:542–52. doi: 10.1016/j.bbadis.2012.12.011
107. Chiou YS, Huang Q, Ho CT, Wang YJ, Pan MH. Directly interact with Keap1 and LPS is involved in the anti-inflammatory mechanisms of (-)-epicatechin-3-gallate in LPS-induced macrophages and endotoxemia. *Free Radic Biol Med.* (2016) 94:1–16. doi: 10.1016/j.freeradbiomed.2016.02.010
108. Wang J, Fan SM, Zhang J. Epigallocatechin-3-gallate ameliorates lipopolysaccharide-induced acute lung injury by suppression of TLR4/NF-κB signaling activation. *Braz J Med Biol Res.* (2019) 52:e8092. doi: 10.1590/1414-431X20198092
109. Wheeler DS, Lahni PM, Hake PW, Denenberg AG, Wong HR, Snead C, et al. The green tea polyphenol epigallocatechin-3-gallate improves systemic hemodynamics and survival in rodent models of polymicrobial sepsis. *Shock.* (2007) 28:353–9. doi: 10.1097/shk.0b013e3180485823
110. Cederroth CR, Vinciguerra M, Gjinovci A, Kühne F, Klein M, Cederroth M, et al. Dietary phytoestrogens activate AMP-activated protein kinase with improvement in lipid and glucose metabolism. *Diabetes.* (2008) 57:1176–85. doi: 10.2337/db07-0630
111. Parida S, Singh TU, Thangamalai R, Narasimha Reddy CE, Panigrahi M, Kandasamy K, et al. Daidzein pretreatment improves survival in mouse model of sepsis. *J Surg Res.* (2015) 197:363–73. doi: 10.1016/j.jss.2015.03.059
112. Yi L, Zhou Z, Zheng Y, Chang M, Huang X, Guo F, et al. Suppressive effects of GSS on lipopolysaccharide-induced endothelial cell injury and ALI via TNF-α and IL-6. *Mediators Inflamm.* (2019) 2019:4251394. doi: 10.1155/2019/4251394
113. Herzig S, Shaw RJ. AMPK: guardian of metabolism and mitochondrial homeostasis. *Nat Rev Mol Cell Biol.* (2018) 19:121–35. doi: 10.1038/nrm.2017.95
114. Jager S, Handschin C, St-Pierre J, Spiegelman BM. AMP-activated protein kinase (AMPK) action in skeletal muscle via direct phosphorylation of PGC-1alpha. *Proc Natl Acad Sci USA.* (2007) 104:12017–22. doi: 10.1073/pnas.0705070104
115. Garcia-Roves PM, Osler ME, Holmstrom MH, Zierath JR. Gain-of-function R225Q mutation in AMP-activated protein kinase gamma3 subunit increases mitochondrial biogenesis in glycolytic skeletal muscle. *J Biol Chem.* (2008) 283:35724–34. doi: 10.1074/jbc.M805078200
116. Ruderman NB, Xu XJ, Nelson L, Cacicedo JM, Saha AK, Lan F, et al. AMPK and SIRT1: a long-standing partnership? *Am J Physiol Endocrinol Metab.* (2010) 298:E751–60. doi: 10.1152/ajpendo.00745.2009
117. Ismail Hassan F, Didari T, Khan F, Niaz K, Mojtahedzadeh M, Abdollahi M. A review on the protective effects of metformin in sepsis-induced organ failure. *Cell J.* (2020) 21:363–70. doi: 10.22074/cellj.2020.6286
118. Liu G, Wu K, Zhang L, Dai J, Huang W, Lin L, et al. Metformin attenuated endotoxin-induced acute myocarditis via activating AMPK. *Int Immunopharmacol.* (2017) 47:166–72. doi: 10.1016/j.intimp.2017.04.002
119. Cameron RB, Beeson CC, Schnellmann RG. Development of therapeutics that induce mitochondrial biogenesis for the treatment of acute and chronic degenerative diseases. *J Med Chem.* (2016) 59:10411–34. doi: 10.1021/acs.jmedchem.6b00669
120. Wu H, Denna TH, Storkersen JN, Gerriets VA. Beyond a neurotransmitter: the role of serotonin in inflammation and immunity. *Pharmacol Res.* (2019) 140:100–14. doi: 10.1016/j.phrs.2018.06.015
121. Ahern GP. 5-HT and the immune system. *Curr Opin Pharmacol.* (2011) 11:29–33. doi: 10.1016/j.coph.2011.02.004
122. Berger J, Moller DE. The mechanisms of action of PPARs. *Annu Rev Med.* (2002) 53:409–35. doi: 10.1146/annurev.med.53.082901.104018
123. Han L, Shen WJ, Bittner S, Kraemer FB, Azhar S. PPARs: regulators of metabolism and as therapeutic targets in cardiovascular disease. Part I: PPAR-alpha. *Future Cardiol.* (2017) 13:259–78. doi: 10.2217/fca-2016-0059
124. Liang H, Ward WF. PGC-1alpha: a key regulator of energy metabolism. *Adv Physiol Educ.* (2006) 30:145–51. doi: 10.1152/advan.00052.2006
125. Lebovitz HE. Thiazolidinediones: the forgotten diabetes medications. *Curr Diab Rep.* (2019) 19:151. doi: 10.1007/s11892-019-1270-y
126. Ruiz PA, Kim SC, Sartor RB, Haller D. 15-deoxy-delta12,14-prostaglandin J2-mediated ERK signaling inhibits gram-negative bacteria-induced RelA phosphorylation and interleukin-6 gene expression in intestinal epithelial cells through modulation of protein phosphatase 2A activity. *J Biol Chem.* (2004) 279:36103–11. doi: 10.1074/jbc.M405032200
127. Standage SW, Caldwell CC, Zingarelli B, Wong HR. Reduced peroxisome proliferator-activated receptor alpha expression is associated with decreased survival and increased tissue bacterial load in sepsis. *Shock.* (2012) 37:164–9. doi: 10.1097/SHK.0b013e31823f1a00
128. Fernandez-Marcos PJ, Auwerx J. Regulation of PGC-1α, a nodal regulator of mitochondrial biogenesis. *Am J Clin Nutr.* (2011) 93:884S–90. doi: 10.3945/ajcn.110.001917

129. Irazuzta J, Sullivan KJ, Garcia PC, Piva JP. Pharmacologic support of infants and children in septic shock. *J Pediatr.* (2007) 83:S36–45. doi: 10.2223/JPED.1623
130. Meyer S, Gortner L, Brown K, Abdul-Khaliq H. The role of milrinone in children with cardiovascular compromise: review of the literature. *Wien Med Wochenschr.* (2011) 161:184–91. doi: 10.1007/s10354-011-0869-7
131. de Oliveira CF, de Oliveira DS, Gottschald AF, Moura JD, Costa GA, Ventura AC, et al. ACCM/PALS haemodynamic support guidelines for paediatric septic shock: an outcomes comparison with and without monitoring central venous oxygen saturation. *Intensive Care Med.* (2008) 34:1065–75. doi: 10.1007/s00134-008-1085-9
132. Brierley J, Carcillo JA, Choong K, Cornell T, Decaen A, Deymann A, et al. Clinical practice parameters for hemodynamic support of pediatric and neonatal septic shock: 2007 update from the American College of Critical Care Medicine. *Crit Care Med.* (2009) 37:666–88. doi: 10.1097/CCM.0b013e31819323c6
133. Maurice DH, Ke H, Ahmad F, Wang Y, Chung J, Manganiello VC. Advances in targeting cyclic nucleotide phosphodiesterases. *Nat Rev Drug Discov.* (2014) 13:290–314. doi: 10.1038/nrd4228
134. MacKenzie SJ, Houslay MD. Action of rolipram on specific PDE4 cAMP phosphodiesterase isoforms and on the phosphorylation of cAMP-response-element-binding protein (CREB) and p38 mitogen-activated protein (MAP) kinase in U937 monocytic cells. *Biochem J.* (2000) 347(Pt 2):571–8. doi: 10.1042/0264-6021:3470571
135. Lagouge M, Argmann C, Gerhart-Hines Z, Meziane H, Lerin C, Daussin F, et al. Resveratrol improves mitochondrial function and protects against metabolic disease by activating SIRT1 and PGC-1alpha. *Cell.* (2006) 127:1109–22. doi: 10.1016/j.cell.2006.11.013
136. Van Wyngene L, Vandewalle J, Libert C. Reprogramming of basic metabolic pathways in microbial sepsis: therapeutic targets at last? *EMBO Mol Med.* (2018) 10:e8712. doi: 10.15252/emmm.201708712
137. Patil NK, Bohannon JK, Hernandez A, Patil TK, Sherwood ER. Regulation of leukocyte function by citric acid cycle intermediates. *J Leukoc Biol.* (2019) 106:105–17. doi: 10.1002/JLB.3MIR1118-415R
138. Hard GC. Some biochemical aspects of the immune macrophage. *Br J Exp Pathol.* (1970) 51:97–105.
139. Haschemi A, Kosma P, Gille L, Evans CR, Burant CF, Starkl P, et al. The sedoheptulose kinase CARKL directs macrophage polarization through control of glucose metabolism. *Cell Metab.* (2012) 15:813–26. doi: 10.1016/j.cmet.2012.04.023
140. Tannahill GM, Curtis AM, Adamik J, Palsson-McDermott EM, McGettrick AF, Goel G, et al. Succinate is an inflammatory signal that induces IL-1beta through HIF-1alpha. *Nature.* (2013) 496:238–42. doi: 10.1038/nature11986
141. Warburg O. On respiratory impairment in cancer cells. *Science.* (1956) 124:269–70.
142. Selak MA, Armour SM, MacKenzie ED, Boulahbel H, Watson DG, Mansfield KD, et al. Succinate links TCA cycle dysfunction to oncogenesis by inhibiting HIF-alpha prolyl hydroxylase. *Cancer Cell.* (2005) 7:77–85. doi: 10.1016/j.ccr.2004.11.022
143. Seim GL, Britt EC, John SV, Yeo FJ, Johnson AR, Eisenstein RS, et al. Two-stage metabolic remodelling in macrophages in response to lipopolysaccharide and interferon-gamma stimulation. *Nat Metab.* (2019) 1:731–42. doi: 10.1038/s42255-019-0083-2
144. Vijayan V, Pradhan P, Braud L, Fuchs HR, Gueler F, Motterlini R, et al. Human and murine macrophages exhibit differential metabolic responses to lipopolysaccharide - A divergent role for glycolysis. *Redox Biol.* (2019) 22:101147. doi: 10.1016/j.redox.2019.101147
145. West AP, Brodsky IE, Rahner C, Woo DK, Erdjument-Bromage H, Tempst P, et al. TLR signalling augments macrophage bactericidal activity through mitochondrial ROS. *Nature.* (2011) 472:476–80. doi: 10.1038/nature09973
146. Wang F, Zhang S, Vuckovic I, Jeon R, Lerman A, Folmes CD, et al. Glycolytic stimulation is not a requirement for M2 macrophage differentiation. *Cell Metab.* (2018) 28:463–75.e464. doi: 10.1016/j.cmet.2018.08.012
147. Mills EL, Ryan DG, Prag HA, Dikovskaya D, Menon D, Zaslona Z, et al. Itaconate is an anti-inflammatory metabolite that activates Nrf2 via alkylation of KEAP1. *Nature.* (2018) 556:113–7. doi: 10.1038/nature25986
148. Liao ST, Han C, Xu DQ, Fu XW, Wang JS, Kong LY. 4-Octyl itaconate inhibits aerobic glycolysis by targeting GAPDH to exert anti-inflammatory effects. *Nat Commun.* (2019) 10:5091. doi: 10.1038/s41467-019-13078-5
149. Qin W, Qin K, Zhang Y, Jia W, Chen Y, Cheng B, et al. S-glycosylation-based cysteine profiling reveals regulation of glycolysis by itaconate. *Nat Chem Biol.* (2019) 15:983–91. doi: 10.1038/s41589-019-0323-5
150. Mills EL, Kelly B, Logan A., Costa ASH, Varma M, Bryant CE, et al. Succinate dehydrogenase supports metabolic repurposing of mitochondria to drive inflammatory macrophages. *Cell.* (2016) 167:457–−70 e413. doi: 10.1016/j.cell.2016.08.064
151. Jha AK, Huang SC, Sergushichev A, Lampropoulou V, Ivanova Y, Loginicheva E, et al. Network integration of parallel metabolic and transcriptional data reveals metabolic modules that regulate macrophage polarization. *Immunity.* (2015) 42:419–30. doi: 10.1016/j.immuni.2015.02.005
152. Zhu X, Meyers A, Long D, Ingram B, Liu T, Yoza BK, et al. Frontline Science: monocytes sequentially rewire metabolism and bioenergetics during an acute inflammatory response. *J Leukoc Biol.* (2019) 105:215–28. doi: 10.1002/JLB.3HI0918-373R
153. Michelucci A, Cordes T, Ghelfi J, Pailot A, Reiling N, Goldmann O, et al. Immune-responsive gene 1 protein links metabolism to immunity by catalyzing itaconic acid production. *Proc Natl Acad Sci USA.* (2013) 110:7820–5. doi: 10.1073/pnas.1218599110
154. Cordes T, Wallace M, Michelucci A, Divakaruni AS, Sapcariu SC, Sousa C, et al. Immunoresponsive gene 1 and itaconate inhibit succinate dehydrogenase to modulate intracellular succinate levels. *J Biol Chem.* (2016) 291:14274–84. doi: 10.1074/jbc.M115.685792
155. Lampropoulou V, Sergushichev A, Bambouskova M, Nair S, Vincent EE, Loginicheva E, et al. Itaconate links inhibition of succinate dehydrogenase with macrophage metabolic remodeling and regulation of inflammation. *Cell Metab.* (2016) 24:158–66. doi: 10.1016/j.cmet.2016.06.004
156. Sugimoto M, Sakagami H, Yokote Y, Onuma H, Kaneko M, Mori M, et al. Non-targeted metabolite profiling in activated macrophage secretion. *Metabolomics.* (2012) 8:624–33. doi: 10.1007/s11306-011-0353-9
157. Cordes T, Michelucci A, Hiller K. Itaconic acid: the surprising role of an industrial compound as a mammalian antimicrobial metabolite. *Annu Rev Nutr.* (2015) 35:451–73. doi: 10.1146/annurev-nutr-071714-034243
158. McFadden BA, Purohit S. Itaconate, an isocitrate lyase-directed inhibitor in *Pseudomonas indigofera*. *J Bacteriol.* (1977) 131:136–44.
159. Dolan SK, Welch M. The glyoxylate shunt, 60 years on. *Annu Rev Microbiol.* (2018) 72:309–30. doi: 10.1146/annurev-micro-090817-062257
160. Williams NC, O'Neill LAJ. A role for the krebs cycle intermediate citrate in metabolic reprogramming in innate immunity and inflammation. *Front Immunol.* (2018) 9:141. doi: 10.3389/fimmu.2018.00141
161. Sasikaran J, Ziemski M, Zadora PK, Fleig A, Berg IA. Bacterial itaconate degradation promotes pathogenicity. *Nat Chem Biol.* (2014) 10:371–7. doi: 10.1038/nchembio.1482
162. Naujoks J, Tabeling C, Dill BD, Hoffmann C, Brown AS, Kunze M, et al. IFNs modify the proteome of legionella-containing vacuoles and restrict infection via IRG1-derived itaconic acid. *PLoS Pathog.* (2016) 12:e1005408. doi: 10.1371/journal.ppat.1005408
163. Mills E, O'Neill LA. Succinate: a metabolic signal in inflammation. *Trends Cell Biol.* (2014) 24:313–20. doi: 10.1016/j.tcb.2013.11.008
164. Palsson-McDermott EM, Curtis AM, Goel G, Lauterbach MAR, Sheedy FJ, Gleeson LE, et al. Pyruvate kinase M2 regulates Hif-1alpha activity and IL-1beta induction and is a critical determinant of the warburg effect in LPS-activated macrophages. *Cell Metab.* (2015) 21:347. doi: 10.1016/j.cmet.2015.01.017
165. Chouchani ET, Pell VR, Gaude E, Aksentijevic D, Sundier SY, Robb EL, et al. Ischaemic accumulation of succinate controls reperfusion injury through mitochondrial ROS. *Nature.* (2014) 515:431–5. doi: 10.1038/nature13909
166. De Souza DP, Achuthan A, Lee MK, Binger KJ, Lee MC, Davidson S, et al. Autocrine IFN-I inhibits isocitrate dehydrogenase in the TCA cycle of LPS-stimulated macrophages. *J Clin Invest.* (2019) 129:4239–44. doi: 10.1172/jci127597
167. Palmieri F. The mitochondrial transporter family (SLC25): physiological and pathological implications. *Pflugers Arch.* (2004) 447:689–709. doi: 10.1007/s00424-003-1099-7

168. Infantino V, Convertini P, Cucci L, Panaro MA, Di Noia MA, Calvello R, et al. The mitochondrial citrate carrier: a new player in inflammation. *Biochem J.* (2011) 438:433–6. doi: 10.1042/BJ20111275
169. Fukuzumi M, Shinomiya H, Shimizu Y, Ohishi K, Utsumi S. Endotoxin-induced enhancement of glucose influx into murine peritoneal macrophages via GLUT1. *Infect Immun.* (1996) 64:108–12.
170. Schenz J, Tamulyte S, Nusshag C, Brenner T, Poschet G, Weigand MA, et al. Population-specific metabolic alterations in professional antigen-presenting cells contribute to sepsis-associated immunosuppression. *Shock.* (2020) 53:5–15. doi: 10.1097/shk.0000000000001337
171. Shalova IN, Lim JY, Chittezhath M, Zinkernagel AS, Beasley F, Hernandez-Jimenez E, et al. Human monocytes undergo functional re-programming during sepsis mediated by hypoxia-inducible factor-1alpha. *Immunity.* (2015) 42:484–98. doi: 10.1016/j.immuni.2015.02.001
172. Pan L, Hu L, Zhang L, Xu H, Chen Y, Bian Q, et al. Deoxyelephantopin decreases the release of inflammatory cytokines in macrophage associated with attenuation of aerobic glycolysis via modulation of PKM2. *Int Immunopharmacol.* (2020) 79:106048. doi: 10.1016/j.intimp.2019.106048
173. Chao CC, Ingram BO, Lurchachaiwong W, Ching WM. Metabolic characterization of serum from mice challenged with Orientia tsutsugamushi-infected mites. *New Microbes New Infect.* (2018) 23:70–6. doi: 10.1016/j.nmni.2018.01.005
174. Meiser J, Kraemer L, Jaeger C, Madry H, Link A, Lepper PM, et al. Itaconic acid indicates cellular but not systemic immune system activation. *Oncotarget.* (2018) 9:32098–107. doi: 10.18632/oncotarget.25956
175. Beloborodova N, Pautova A, Sergeev A, Fedotcheva N. Serum levels of mitochondrial and microbial metabolites reflect mitochondrial dysfunction in different stages of sepsis. *Metabolites.* (2019) 9:196. doi: 10.3390/metabo9100196
176. Netea MG. Training innate immunity: the changing concept of immunological memory in innate host defence. *Eur J Clin Invest.* (2013) 43:881–4. doi: 10.1111/eci.12132
177. Kurtz J. Specific memory within innate immune systems. *Trends Immunol.* (2005) 26:186–92. doi: 10.1016/j.it.2005.02.001
178. Netea MG, Joosten LA, Latz E, Mills KH, Natoli G, Stunnenberg HG, et al. Trained immunity: a program of innate immune memory in health and disease. *Science.* (2016) 352:aaf1098. doi: 10.1126/science.aaf1098
179. Karlsson H, Nassberger L. *In vitro* metabolic inhibition of the human lymphocyte: influence on the expression of interleukin-2 receptors. *Immunol Cell Biol.* (1992) 70 (Pt 5):309–13. doi: 10.1038/icb.1992.39
180. Sanchez-Alcazar JA, Hernandez I, De la Torre MP, Garcia I, Santiago E, Munoz-Yague MT, et al. Down-regulation of tumor necrosis factor receptors by blockade of mitochondrial respiration. *J Biol Chem.* (1995) 270:23944–50. doi: 10.1074/jbc.270.41.23944
181. Buttgereit F, Burmester GR, Brand MD. Bioenergetics of immune functions: fundamental and therapeutic aspects. *Immunol Today.* (2000) 21:192–9. doi: 10.1016/s0167-5699(00)01593-0
182. O'Neill LA, Kishton RJ, Rathmell J. A guide to immunometabolism for immunologists. *Nat Rev Immunol.* (2016) 16:553–65. doi: 10.1038/nri.2016.70
183. Cheng SC, Quintin J, Cramer RA, Shepardson KM, Saeed S, Kumar V, et al. mTOR- and HIF-1alpha-mediated aerobic glycolysis as metabolic basis for trained immunity. *Science.* (2014) 345:1250684. doi: 10.1126/science.1250684
184. Arts RJ, Novakovic B, Ter Horst R, Carvalho A, Bekkering S, Lachmandas E, et al. Glutaminolysis and fumarate accumulation integrate immunometabolic and epigenetic programs in trained immunity. *Cell Metab.* (2016) 24:807–19. doi: 10.1016/j.cmet.2016.10.008
185. Dominguez-Andres J, Netea MG. Long-term reprogramming of the innate immune system. *J Leukoc Biol.* (2019) 105:329–38. doi: 10.1002/JLB.MR0318-104R
186. Saeed S, Quintin J, Kerstens HH, Rao NA, Aghajanirefah A, Matarese F, et al. Epigenetic programming of monocyte-to-macrophage differentiation and trained innate immunity. *Science.* (2014) 345:1251086. doi: 10.1126/science.1251086
187. Stothers CL, Luan L, Fensterheim BA, Bohannon JK. Hypoxia-inducible factor-1alpha regulation of myeloid cells. *J Mol Med.* (2018) 96:1293–306. doi: 10.1007/s00109-018-1710-1
188. Bohannon JK, Luan L, Hernandez A, Afzal A, Guo Y, Patil NK, et al. Role of G-CSF in monophosphoryl lipid A-mediated augmentation of neutrophil functions after burn injury. *J Leukoc Biol.* (2016) 99:629–40. doi: 10.1189/jlb.4A0815-362R
189. Hernandez A, Bohannon JK, Luan L, Fensterheim BA, Guo Y, Patil NK, et al. The role of MyD88- and TRIF-dependent signaling in monophosphoryl lipid A-induced expansion and recruitment of innate immunocytes. *J Leukoc Biol.* (2016) 100:1311–22. doi: 10.1189/jlb.1A0216-072R
190. Di Gioia M, Spreafico R, Springstead JR, Mendelson MM, Joehanes R, Levy D, et al. Endogenous oxidized phospholipids reprogram cellular metabolism and boost hyperinflammation. *Nat Immunol.* (2020) 21:42–53. doi: 10.1038/s41590-019-0539-2
191. Chu LH, Indramohan M, Ratsimandresey RA, Gangopadhyay A, Morris EP, Monack DM, et al. The oxidized phospholipid oxPAPC protects from septic shock by targeting the non-canonical inflammasome in macrophages. *Nat Commun.* (2018) 9:996. doi: 10.1038/s41467-018-03409-3
192. Landy M, Pillemer L. Increased resistance to infection and accompanying alteration in properidin levels following administration of bacterial lipopolysaccharides. *J Exp Med.* (1956) 104:383–409. doi: 10.1084/jem.104.3.383
193. Rayhane N, Fitting C, Lortholary O, Dromer F, Cavaillon JM. Administration of endotoxin associated with lipopolysaccharide tolerance protects mice against fungal infection. *Infect Immun.* (2000) 68:3748–53. doi: 10.1128/iai.68.6.3748-3753.2000
194. Murphey ED, Fang G, Sherwood ER. Endotoxin pretreatment improves bacterial clearance and decreases mortality in mice challenged with *Staphylococcus aureus*. *Shock.* (2008) 29:512–8. doi: 10.1097/shk.0b013e318150776f
195. Lehner MD, Ittner J, Bundschuh DS, van Rooijen N, Wendel A, Hartung T. Improved innate immunity of endotoxin-tolerant mice increases resistance to *Salmonella enterica* serovar typhimurium infection despite attenuated cytokine response. *Infect Immun.* (2001) 69:463–71. doi: 10.1128/IAI.69.1.463-471.2001
196. Varma TK, Durham M, Murphey ED, Cui W, Huang Z, Lin CY, et al. Endotoxin priming improves clearance of Pseudomonas aeruginosa in wild-type and interleukin-10 knockout mice. *Infect Immun.* (2005) 73:7340–7. doi: 10.1128/IAI.73.11.7340-7347.2005
197. Murphey ED, Fang G, Varma TK, Sherwood ER. Improved bacterial clearance and decreased mortality can be induced by LPS tolerance and is not dependent upon IFN-gamma. *Shock.* (2007) 27:289–95. doi: 10.1097/01.shk.0000245024.93740.28
198. Wheeler DS, Lahni PM, Denenberg AG, Poynter SE, Wong HR, Cook JA, et al. Induction of endotoxin tolerance enhances bacterial clearance and survival in murine polymicrobial sepsis. *Shock.* (2008) 30:267–73. doi: 10.1097/shk.0b013e318162c190
199. Deng M, Scott MJ, Loughran P, Gibson G, Sodhi C, Watkins S, et al. Lipopolysaccharide clearance, bacterial clearance, and systemic inflammatory responses are regulated by cell type-specific functions of TLR4 during sepsis. *J Immunol.* (2013) 190:5152–60. doi: 10.4049/jimmunol.1300496
200. Shahin RD, Engberg I, Hagberg L, Svanborg Eden C. Neutrophil recruitment and bacterial clearance correlated with LPS responsiveness in local gram-negative infection. *J Immunol.* (1987) 138:3475–80
201. Wolk K, Docke WD, von Baehr V, Volk HD, Sabat R. Impaired antigen presentation by human monocytes during endotoxin tolerance. *Blood.* (2000) 96:218–23. doi: 10.1182/blood.V96.1.218
202. Biswas SK, Lopez-Collazo E. Endotoxin tolerance: new mechanisms, molecules and clinical significance. *Trends Immunol.* (2009) 30:475–87. doi: 10.1016/j.it.2009.07.009
203. Ward NS, Casserly B, Ayala A. The compensatory anti-inflammatory response syndrome (CARS) in critically ill patients. *Clin Chest Med.* (2008) 29:617–25, viii. doi: 10.1016/j.ccm.2008.06.010
204. Hotchkiss RS, Monneret G, Payen D. Sepsis-induced immunosuppression: from cellular dysfunctions to immunotherapy. *Nat Rev Immunol.* (2013) 13:862–74. doi: 10.1038/nri3552
205. Pena OM, Hancock DG, Lyle NH, Linder A, Russell JA, Xia J, et al. An endotoxin tolerance signature predicts sepsis and organ

dysfunction at initial clinical presentation. *EBiomedicine.* (2014) 1:64–71. doi: 10.1016/j.ebiom.2014.10.003
206. Davenport EE, Burnham KL, Radhakrishnan J, Humburg P, Hutton P, Mills TC, et al. Genomic landscape of the individual host response and outcomes in sepsis: a prospective cohort study. *Lancet Respir Med.* (2016) 4:259–71. doi: 10.1016/S2213-2600(16)00046-1
207. Fisher CJ Jr, Dhainaut JF, Opal SM, Pribble JP, Balk RA, Slotman GJ, et al. Recombinant human interleukin 1 receptor antagonist in the treatment of patients with sepsis syndrome. Results from a randomized, double-blind, placebo-controlled trial. Phase III rhIL-1ra Sepsis Syndrome Study Group. *JAMA.* (1994) 271:1836–43.
208. Fisher CJJr, Agosti JM, Opal SM, Lowry SF, Balk RA, Sadoff JC, et al. Treatment of septic shock with the tumor necrosis factor receptor:Fc fusion protein. The Soluble TNF Receptor Sepsis Study Group. *N Engl J Med.* (1996) 334:1697–702. doi: 10.1056/NEJM199606273342603
209. Reinhart K, Karzai W. Anti-tumor necrosis factor therapy in sepsis: update on clinical trials and lessons learned. *Crit Care Med.* (2001) 29:S121–5. doi: 10.1097/00003246-200107001-00037
210. Deans KJ, Haley M, Natanson C, Eichacker PQ, Minneci PC. Novel therapies for sepsis: a review. *J Trauma.* (2005) 58:867–74. doi: 10.1097/01.ta.0000158244.69179.94
211. Park BS, Song DH, Kim HM, Choi BS, Lee H, Lee JO. The structural basis of lipopolysaccharide recognition by the TLR4-MD-2 complex. *Nature.* (2009) 458:1191–5. doi: 10.1038/nature07830
212. Bohannon JK, Hernandez A, Enkhbaatar P, Adams WL, Sherwood ER. The immunobiology of toll-like receptor 4 agonists: from endotoxin tolerance to immunoadjuvants. *Shock.* (2013) 40:451–62. doi: 10.1097/SHK.0000000000000042
213. Hernandez A, Patil NK, Stothers CL, Luan L, McBride MA, Owen AM, et al. Immunobiology and application of toll-like receptor 4 agonists to augment host resistance to infection. *Pharmacol Res.* (2019) 150:104502. doi: 10.1016/j.phrs.2019.104502
214. Chase JJ, Kubey W, Dulek MH, Holmes CJ, Salit MG, Pearson FC III, et al. Effect of monophosphoryl lipid A on host resistance to bacterial infection. *Infect Immun.* (1986) 53:711–2.
215. Hirano T, Kodama S, Kawano T, Maeda K, Suzuki M. Monophosphoryl lipid A induced innate immune responses via TLR4 to enhance clearance of nontypeable *Haemophilus influenzae* and *Moraxella catarrhalis* from the nasopharynx in mice. *FEMS Immunol Med Microbiol.* (2011) 63:407–17. doi: 10.1111/j.1574-695X.2011.00866.x
216. Romero CD, Varma TK, Hobbs JB, Reyes A, Driver B, Sherwood ER. The Toll-like receptor 4 agonist monophosphoryl lipid a augments innate host resistance to systemic bacterial infection. *Infect Immun.* (2011) 79:3576–87. doi: 10.1128/IAI.00022-11
217. Roquilly A, Broquet A, Jacqueline C, Gautreau L, Segain JP, de Coppet P, et al. Toll-like receptor-4 agonist in post-haemorrhage pneumonia: role of dendritic and natural killer cells. *Eur Respir J.* (2013) 42:1365–78. doi: 10.1183/09031936.00152612
218. Tamassia N, Le Moigne V, Calzetti F, Donini M, Gasperini S, Ear T, et al. The MyD88-independent pathway is not mobilized in human neutrophils stimulated via TLR4. *J Immunol.* (2007) 178:7344–56. doi: 10.4049/jimmunol.178.11.7344
219. Ribes S, Meister T, Ott M, Redlich S, Janova H, Hanisch UK, et al. Intraperitoneal prophylaxis with CpG oligodeoxynucleotides protects neutropenic mice against intracerebral *Escherichia coli* K1 infection. *J Neuroinflammation.* (2014) 11:14. doi: 10.1186/1742-2094-11-14
220. Hampton T. Report reveals scope of US antibiotic resistance threat. *JAMA.* (2013) 310:1661–3. doi: 10.1001/jama.2013.280695
221. Hampton T. Novel programs and discoveries aim to combat antibiotic resistance. *JAMA.* (2015) 313:2411–3. doi: 10.1001/jama.2015.4738
222. Marston HD, Dixon DM, Knisely JM, Palmore TN, Fauci AS. Antimicrobial resistance. *JAMA.* (2016) 316:1193–204. doi: 10.1001/jama.2016.11764
223. Jacobs A. *Crisis Looms in Antibiotics as Drug Makers Go Bankrupt*. (2019) Available online at: https://www.nytimes.com/2019/12/25/health/antibiotics-new-resistance.html (accessed May 5, 2020).
224. Zimmermann S, Egeter O, Hausmann S, Lipford GB, Rocken M, Wagner H, et al. CpG oligodeoxynucleotides trigger protective and curative Th1 responses in lethal murine leishmaniasis. *J Immunol.* (1998) 160:3627–30.
225. Elkins KL, Rhinehart-Jones TR, Stibitz S, Conover JS, Klinman DM. Bacterial DNA containing CpG motifs stimulates lymphocyte-dependent protection of mice against lethal infection with intracellular bacteria. *J Immunol.* (1999) 162:2291–8.
226. Jiang M, Yao J, Feng G. Protective effect of DNA vaccine encoding pseudomonas exotoxin A and PcrV against acute pulmonary *P. aeruginosa* infection. *PLoS ONE.* (2014) 9:e96609. doi: 10.1371/journal.pone.0096609
227. Wongratanacheewin S, Kespichayawattana W, Intachote P, Pichyangkul S, Sermswan RW, Krieg AM, et al. Immunostimulatory CpG oligodeoxynucleotide confers protection in a murine model of infection with *Burkholderia pseudomallei*. *Infect Immun.* (2004) 72:4494–502. doi: 10.1128/IAI.72.8.4494-4502.2004
228. Rozak DA, Gelhaus HC, Smith M, Zadeh M, Huzella L, Waag D, et al. CpG oligodeoxyribonucleotides protect mice from *Burkholderia pseudomallei* but not *Francisella tularensis* Schu S4 aerosols. *J Immune Based Ther Vaccines.* (2010) 8:2. doi: 10.1186/1476-8518-8-2
229. Judy BM, Taylor K, Deeraksa A, Johnston RK, Endsley JJ, Vijayakumar S, et al. Prophylactic application of CpG oligonucleotides augments the early host response and confers protection in acute melioidosis. *PLoS ONE.* (2012) 7:e34176. doi: 10.1371/journal.pone.0034176
230. Krieg AM, Love-Homan L, Yi AK, Harty JT. CpG DNA induces sustained IL-12 expression *in vivo* and resistance to *Listeria monocytogenes* challenge. *J Immunol.* (1998) 161:2428–34.
231. Harandi AM, Eriksson K, Holmgren J. A protective role of locally administered immunostimulatory CpG oligodeoxynucleotide in a mouse model of genital herpes infection. *J Virol.* (2003) 77:953–62. doi: 10.1128/jvi.77.2.953-962.2003
232. Vollmer J, Krieg AM. Immunotherapeutic applications of CpG oligodeoxynucleotide TLR9 agonists. *Adv Drug Deliv Rev.* (2009) 61:195–204. doi: 10.1016/j.addr.2008.12.008
233. Krieg AM. Antitumor applications of stimulating toll-like receptor 9 with CpG oligodeoxynucleotides. *Curr Oncol Rep.* (2004) 6:88–95. doi: 10.1007/s11912-004-0019-0
234. Wang XS, Sheng Z, Ruan YB, Guang Y, Yang ML. CpG oligodeoxynucleotides inhibit tumor growth and reverse the immunosuppression caused by the therapy with 5-fluorouracil in murine hepatoma. *World J Gastroenterol.* (2005) 11:1220–4. doi: 10.3748/wjg.v11.i8.1220
235. Herbst MM, Pyles RB. Immunostimulatory CpG treatment for genital HSV-2 infections. *J Antimicrob Chemother.* (2003) 52:887–9. doi: 10.1093/jac/dkg481
236. Camilli G, Tabouret G, Quintin J. The complexity of fungal beta-glucan in health and disease: effects on the mononuclear phagocyte system. *Front Immunol.* (2018) 9:673. doi: 10.3389/fimmu.2018.00673
237. Williams DL, Browder W, McNamee R, Di Luzio NR. Glucan immunomodulation in experimental *E. coli* sepsis. *Adv Exp Med Biol.* (1982) 155:701–6. doi: 10.1007/978-1-4684-4394-3_77
238. Williams DL, Sherwood ER, Browder IW, McNamee RB, Jones EL, Di Luzio NR. Pre-clinical safety evaluation of soluble glucan. *Int J Immunopharmacol.* (1988) 10:405–14. doi: 10.1016/0192-0561(88)90127-0
239. Di Luzio NR, Williams DL. Protective effect of glucan against systemic *Staphylococcus aureus* septicemia in normal and leukemic mice. *Infect Immun.* (1978) 20:804–10.
240. Marakalala MJ, Williams DL, Hoving JC, Engstad R, Netea MG, Brown GD. Dectin-1 plays a redundant role in the immunomodulatory activities of beta-glucan-rich ligands *in vivo*. *Microbes Infect.* (2013) 15:511–5. doi: 10.1016/j.micinf.2013.03.002
241. Lagrange PH, Fourgeaud M, Neway T, Pilet C. Mycobacterial polar glycopeptidolipids enhance resistance to experimental murine candidiasis. *C R Acad Sci III.* (1995) 318:359–65.
242. Dos Santos JC, Barroso de Figueiredo AM, Teodoro Silva MV, Cirovic B, de Bree LCJ, Damen M, et al. Beta-glucan-induced trained immunity protects against *Leishmania braziliensis* infection: a crucial role for IL-32. *Cell Rep.* (2019) 28:2659–72 e2656. doi: 10.1016/j.celrep.2019.08.004
243. Di Luzio NR, Williams DL, Sherwood ER, Browder IW. Modification of diverse experimental immunosuppressive states by glucan. *Surv Immunol Res.* (1985) 4:160–7. doi: 10.1007/bf02918811
244. Williams DL, Sherwood ER, Browder IW, McNamee RB, Jones EL, Rakinic J, et al. Effect of glucan on neutrophil dynamics and immune

function in *Escherichia coli* peritonitis. *J Surg Res.* (1988) 44:54–61. doi: 10.1016/0022-4804(88)90122-9
245. Sherwood ER, Varma TK, Fram RY, Lin CY, Koutrouvelis AP, Toliver-Kinsky TE. Glucan phosphate potentiates endotoxin-induced interferon-gamma expression in immunocompetent mice, but attenuates induction of endotoxin tolerance. *Clin Sci.* (2001) 101:541–50.
246. Babineau TJ, Marcello P, Swails W, Kenler A, Bistrian B, Forse RA. Randomized phase I/II trial of a macrophage-specific immunomodulator (PGG-glucan) in high-risk surgical patients. *Ann Surg.* (1994) 220:601–9. doi: 10.1097/00000658-199411000-00002
247. Tribouley J, Tribouley-Duret J, Appriou M. [Effect of Bacillus Callmette Guerin (BCG) on the receptivity of nude mice to *Schistosoma mansoni*]. *C R Seances Soc Biol Fil.* (1978) 172:902–4.
248. van 't Wout JW, Poell R, van Furth R. The role of BCG/PPD-activated macrophages in resistance against systemic candidiasis in mice. *Scand J Immunol.* (1992) 36:713–9. doi: 10.1111/j.1365-3083.1992.tb03132.x
249. Kleinnijenhuis J, Quintin J, Preijers F, Joosten LA, Ifrim DC, Saeed S, et al. Bacille Calmette-Guerin induces NOD2-dependent nonspecific protection from reinfection via epigenetic reprogramming of monocytes. *Proc Natl Acad Sci USA.* (2012) 109:17537–42. doi: 10.1073/pnas.1202870109
250. Benn CS, Netea MG, Selin LK, Aaby P. A small jab - a big effect: nonspecific immunomodulation by vaccines. *Trends Immunol.* (2013) 34:431–9. doi: 10.1016/j.it.2013.04.004
251. Jensen KJ, Larsen N, Biering-Sorensen S, Andersen A, Eriksen HB, Monteiro I, et al. Heterologous immunological effects of early BCG vaccination in low-birth-weight infants in Guinea-Bissau: a randomized-controlled trial. *J Infect Dis.* (2015) 211:956–67. doi: 10.1093/infdis/jiu508
252. Ataide MA, Andrade WA, Zamboni DS, Wang D, Souza Mdo C, Franklin BS, et al. Malaria-induced NLRP12/NLRP3-dependent caspase-1 activation mediates inflammation and hypersensitivity to bacterial superinfection. *PLoS Pathog.* (2014) 10:e1003885. doi: 10.1371/journal.ppat.1003885
253. Nabekura T, Girard JP, Lanier LL. IL-33 receptor ST2 amplifies the expansion of NK cells and enhances host defense during mouse cytomegalovirus infection. *J Immunol.* (2015) 194:5948–52. doi: 10.4049/jimmunol.1500424
254. Schlums H, Cichocki F, Tesi B, Theorell J, Beziat V, Holmes TD, et al. Cytomegalovirus infection drives adaptive epigenetic diversification of NK cells with altered signaling and effector function. *Immunity.* (2015) 42:443–56. doi: 10.1016/j.immuni.2015.02.008
255. Chen F, Wu W, Millman A, Craft JF, Chen E, Patel N, et al. Neutrophils prime a long-lived effector macrophage phenotype that mediates accelerated helminth expulsion. *Nat Immunol.* (2014) 15:938–46. doi: 10.1038/ni.2984
256. Casilag F, Frank S, Matarazzo L, Figeac M, Michelet R, Kloft C, et al. Boosting Toll-like receptor 4 signaling enhances the therapeutic outcome of antibiotic therapy in pneumococcal pneumonia. *bioRXiv.* (2020). doi: 10.1101/2020.02.18.955500

Conflict of Interest: The authors declare that the research was conducted in the absence of any commercial or financial relationships that could be construed as a potential conflict of interest.

frontiers in Immunology

ORIGINAL RESEARCH
published: 24 June 2020
doi: 10.3389/fimmu.2020.01289

Identification of Unique mRNA and miRNA Expression Patterns in Bone Marrow Hematopoietic Stem and Progenitor Cells After Trauma in Older Adults

*Dijoia B. Darden[1], Julie A. Stortz[1], McKenzie K. Hollen[1], Michael C. Cox[1], Camille G. Apple[1], Russell B. Hawkins[1], Jaimar C. Rincon[1], Maria-Cecilia Lopez[2], Zhongkai Wang[3], Eduardo Navarro[1], Jennifer E. Hagen[4], Hari K. Parvataneni[4], Maigan A. Brusko[5], Michael Kladde[6], Rhonda Bacher[3], Babette A. Brumback[3], Scott C. Brakenridge[1], Henry V. Baker[2], Christopher R. Cogle[7], Alicia M. Mohr[1] and Philip A. Efron[1]**

[1] Department of Surgery, University of Florida College of Medicine, Gainesville, FL, United States, [2] Department of Molecular Genetics and Microbiology, University of Florida College of Medicine, Gainesville, FL, United States, [3] Department of Biostatistics, University of Florida, Gainesville, FL, United States, [4] Department of Orthopaedics, University of Florida College of Medicine, Gainesville, FL, United States, [5] Department of Biomedical Engineering, University of Florida College of Medicine, Gainesville, FL, United States, [6] Department of Pathology, Immunology and Laboratory Medicine, University of Florida College of Medicine, Gainesville, FL, United States, [7] Department of Hematology and Oncology, University of Florida College of Medicine, Gainesville, FL, United States

OPEN ACCESS

Edited by:
Thomas Griffith,
University of Minnesota Twin Cities,
United States

Reviewed by:
Jason M. Butler,
Hackensack Meridian Health,
United States
Tomasz Skirecki,
Medical Centre for Postgraduate Education, Poland

***Correspondence:**
Philip A. Efron
philip.efron@surgery.ufl.edu

Specialty section:
This article was submitted to Inflammation, a section of the journal Frontiers in Immunology

Received: 15 February 2020
Accepted: 21 May 2020
Published: 24 June 2020

Citation:
Darden DB, Stortz JA, Hollen MK, Cox MC, Apple CG, Hawkins RB, Rincon JC, Lopez M-C, Wang Z, Navarro E, Hagen JE, Parvataneni HK, Brusko MA, Kladde M, Bacher R, Brumback BA, Brakenridge SC, Baker HV, Cogle CR, Mohr AM and Efron PA (2020) Identification of Unique mRNA and miRNA Expression Patterns in Bone Marrow Hematopoietic Stem and Progenitor Cells After Trauma in Older Adults. Front. Immunol. 11:1289. doi: 10.3389/fimmu.2020.01289

Older adults have significantly worse morbidity and mortality after severe trauma than younger cohorts. The competency of the innate immune response decreases with advancing age, especially after an inflammatory insult. Subsequent poor outcomes after trauma are caused in part by dysfunctional leukocytes derived from the host's hematopoietic stem and progenitor cells (HSPCs). Our objective was to analyze the bone marrow (BM) HSPC transcriptomic [mRNA and microRNA (miR)] responses to trauma in older and younger adults. BM was collected intraoperatively <9 days after initial injury from trauma patients with non-mild injury [ISS ≥ 9] *or* with shock (lactate ≥ 2, base deficit ≥ 5, MAP ≤ 65) who underwent operative fixation of a pelvic or long bone fracture. Samples were also analyzed based on age (<55 years and ≥55 years), ISS score and transfusion in the first 24 h, and compared to age/sex-matched controls from non-cancer elective hip replacement or purchased healthy younger adult human BM aspirates. mRNA and miR expression patterns were calculated from lineage-negative enriched HSPCs. 924 genes were differentially expressed in older trauma subjects vs. age/sex-matched controls, while 654 genes were differentially expressed in younger subjects vs. age/sex-matched control. Only 68 transcriptomic changes were shared between the two groups. Subsequent analysis revealed upregulation of transcriptomic pathways related to quantity, function, differentiation, and proliferation of HSPCs in only the younger cohort. miR expression differences were also identified, many of which were associated with cell cycle regulation. In summary, differences in the BM HSPC mRNA and miR expression

were identified between older and younger adult trauma subjects. These differences in gene and miR expression were related to pathways involved in HSPC production and differentiation. These differences could potentially explain why older adult patients have a suboptimal hematopoietic response to trauma. Although immunomodulation of HSPCs may be a necessary consideration to promote host protective immunity after host injury, the age related differences further highlight that patients may require an age-defined medical approach with interventions that are specific to their transcriptomic and biologic response. Also, targeting the older adult miRs may be possible for interventions in this patient population.

Keywords: hematopoietic stem and progenitor cell, bone marrow, trauma, age, transcriptome, RNA, microRNA

INTRODUCTION

Traumatic injury remains one of the leading causes of morbidity and mortality in the United States and the world, despite advances in the management of these patients (1, 2). The majority of trauma patients are known to recover rapidly; however, 3-year mortality remains ∼16%, and about 20% of trauma patients develop chronic critical illness (CCI) (3–6), defined as > 14 days in ICU with continued organ dysfunction (7–9). Importantly, studies have revealed that risk factors for poor post-traumatic outcomes include age and injury severity score (ISS) at admission as well as total blood transfusion in the first 12 h after injury (3, 10–13).

A dysfunctional host immune system is responsible in part for post-traumatic morbidity and mortality (8). This includes innate immune cells originating from the host's hematopoietic stem and progenitor cells (HSPC) in the setting of unresolving organ failure—leukocytes derived from these HSPCs are not able to adequately resolve secondary, post-traumatic infectious insults (8, 13–15).

Importantly, advanced age is associated with an attenuated acute peripheral leukocyte response and age is known to be one of the strongest risk factors for poor outcome after severe trauma with hemorrhagic shock (6, 11, 16). Older adults have a baseline dysfunction in their immune system (immunosenescence) and low grade systemic inflammation (inflammaging) that in part can contribute to their suboptimal immune response to inflammation, increasing poor outcomes after severe injury (17). Our laboratory, as well as others, have demonstrated that elderly mice after severe injury are unable to mount an effective immune response as compared to juvenile mice. This is secondary, in part, to a failure of bone marrow progenitors to effectively respond to trauma (18). In a murine trauma model, this resulted in increased mortality with delivery of post-trauma *Pseudomonas pneumonia* (18–21).

Numerous attempts at pharmacological and therapeutic interventions to prevent or attenuate post-traumatic insults in this high risk group of older adults have not sufficiently taken into account their unique response to severe injury (22–25). This includes the HSPC response to trauma, as well as the epigenome that in part controls the transcription of these host cells. Specifically, microRNAs (miRs), a class small, non-coding RNAs that regulate gene expression, are important to cellular transcriptional/epigenetic modification of multiple processes such as cell development and differentiation (26). miRs can functions in several ways, including RNA silencing and post-transcriptional regulation of gene expression, and are known to modulate immune responses (27). Modulating miRs has emerged as powerful therapeutic target for cell specific therapy in personalized medicine (28).

We hypothesized that the bone marrow (BM) HSPC transcriptomic and miR response to trauma would be dependent upon the age of the subject and could in part explain the post-trauma dysfunctional myelopoiesis in these individuals, and reveal potential therapeutic targets.

METHODS

Study Approval

Approval was obtained from the University of Florida (UF) Institutional Review Board and was performed from 2014 to 2019 at UF Health Shands Hospital, a 996-bed academic quaternary-care referral center. The study was registered with *clinicaltrials.gov* (*NCT02577731*) and conducted by the Sepsis and Critical Illness Research Center at UF. In every case, signed, informed consent was obtained from the individual patient or their designated legal representative. If informed consent was obtained from the legal representative, the patient was re-consented after they had achieved a clinical state where they could provide informed consent. If written informed consent could not be obtained from the patient or their legal representative within 96 h of study enrollment, the patient was removed from the study and all collected biologic samples and clinical data were destroyed.

Cohort Selection

We enrolled adult trauma patients (age ≥18) that were admitted to UF Health Shands Hospital according to the UF Institutional Review Board protocol #201601386. Patients with blunt and/or penetrating trauma resulting in long bone or pelvic fractures requiring open reduction and internal fixation or closed reduction, percutaneous pinning) were selected if they demonstrated an injury severity score (ISS) ≥ 9 *or* hemorrhagic shock (HS; defined by systolic blood pressure ≤ 90 mmHg or

mean arterial pressure $\leq$ 65 mmHg or base deficit (BD) $\geq$ 5 meq or lactate $\geq$ 2) within the first 24 h of admission. Patients were excluded if pregnant, prisoners, expected survival was $<$ 48 h, receiving chronic corticosteroids or immunosuppression therapies, previous bone marrow transplantation, previous diagnosis of End Stage Renal Disease, or any pre-existing hematological disease.

Age/sex-matched controls were either purchased whole human bone marrow (Lonza, Biosciences, Berkshire, U.K.) or bone marrow collected from non-cancer, non-infectious elective hip repair patients. Control patients were enrolled according to the same IRB protocol above and were excluded if pregnant, prisoners, receiving chronic corticosteroids or immunosuppression therapies, previous chemotherapy or radiation therapy, previous bone marrow transplantation, previous diagnosis of end stage renal disease, or any pre-existing hematological disease, pathological fractures, cancer, HIV or connective tissue disease.

TABLE 1 | Patient characteristics.

	Older $\geq$ 55 (n = 8)	Younger $<$ 55 (n = 25)
Age, median (Q1, Q3)	62.5 (59, 65.75)	37 (28.5, 50)
Percent Male (%)	50	64
Race		
White (%)	87.5	76
African American (%)	12.5	24
Mechanism of injury		
Motor Vehicle Crash (%)	32.5	72
Motor Cycle Crash (%)	12.5	16
Pedestrian vs. Car (%)	12.5	12
Fall (%)	12.5	0
ISS, median (Q1, Q3)	24 (19, 31.5)	18 (15.5, 31.5)
Lactate, median (Q1, Q3)	3.05 (2.23, 3.71)	2.68 (1.96, 3.46)
MAP, median (Q1, Q3)	80.5 (68.75, 91.5)	81 (74, 91.5)
Days to Surgery, median (Q1, Q3)	4.5 (2, 7.5)	2 (1.5, 4.5)

Bone Marrow Collection

A 10 ml aspirate sample of whole bone marrow was collected intraoperatively. Of note, this aspirate contained tissue and not just cellular material. This tissue was considered a waste sample as it would have to be removed to make room for the hardware being placed by the orthopedic surgeons. Bone marrow was collected into a heparinized tube, placed on ice and transferred to the laboratory and processed $<$ 12 h after collection (29).

HSPC Transcriptomic Profile Analysis

Bone marrow collection and bone marrow cell isolation were conducted as previously published by our laboratory (29). HSPCs from either trauma, control or purchased whole human bone marrow were negatively isolated from bone marrow via magnetic separation using a lineage-positive, cell depletion kit according to protocol (Miltenyi Biotec). Total RNA was isolated using QIAGEN RNeasy™ Mini Kit (Qiagen) and labeled and hybridized onto GeneChip® Human Transcriptome Array 2.0 (Affymetrix, Santa Clara, CA) and processed following manufacturer's instructions. BRBArray Tools® was used to identify significant microarray gene expression differences. Fold expression changes of the significant genes were calculated vs. age/sex-matched controls. Three separate analyses were performed based on: (1) Patient age: younger $<$ 55 years or old $\geq$ 55 years; (2) ISS score; and (3) blood transfusion.

The significant, differentially expressed genes were further analyzed with Ingenuity Pathway Analysis (IPA) software™ and Gene Ontology™ (GO) enrichment analysis. IPA software was employed to make downstream functional predictions from these groups of genes with a Z-score greater than two indicating significance. GO enrichment analysis identifies significant representative pathways/biogroups that are over-represented, indicating that their expression is influenced by the intervention. We selected pathways with $p \leq 0.005$, determined by the LS/KS permutation test and Efron-Tibshirani's GSA maxmean test utilized in GO software to find significant gene sets.

miRNA Expression and miRNA Target Gene Prediction

miRNA (miR) profiling was performed using GeneChip™ miRNA 4.0 Array (ThermoFisher Scientific), covering 2,578 human microRNAs annotated in miRBase V2.0. miR expression patterns were calculated with a $\log_2$-transformed expression matrix with significant expression differences (fold expression changes over age/sex-matched control) identified using BRBArrayTools® ($p < 0.05$). Predicted target genes of the differentially expressed miR were identified with TargetScan Human 7.2, which predicts biological targets of miRs, by searching for conserved 8-mer, 7-mer and 6-mer sites matching the seed region of each miR (30).

Statistics

Results for continuous variables are reported as mean $\pm$ SD for normally distributed variables or median $\pm$ interquartile range for non-normally distributed variables. Normality was checked via the Shapiro-Wilk test. Student's t-test or nonparametric Mann-Whitney test was used to compare normal or non-normal variables respectively between different groups or time points. Tukey's multiple comparison procedure was used to adjust p-values for multiple comparisons. Data were analyzed using Prism 7 (GraphPad Software, CA) and SAS 9.4 (SAS Institute Inc., Cary NC).

RESULTS

Patient Characteristics

The overall and age-defined characteristics of the younger and older adult trauma patient cohorts of this study are displayed in **Table 1**. Previous studies have demonstrated that age $\geq$55 years is associated with worse outcomes after severe trauma (11, 31, 32). Younger and older adult groups were relatively similar with the exception of a higher percentage of trauma-related falls in the older group, as opposed to zero in the younger adult group. ISS,

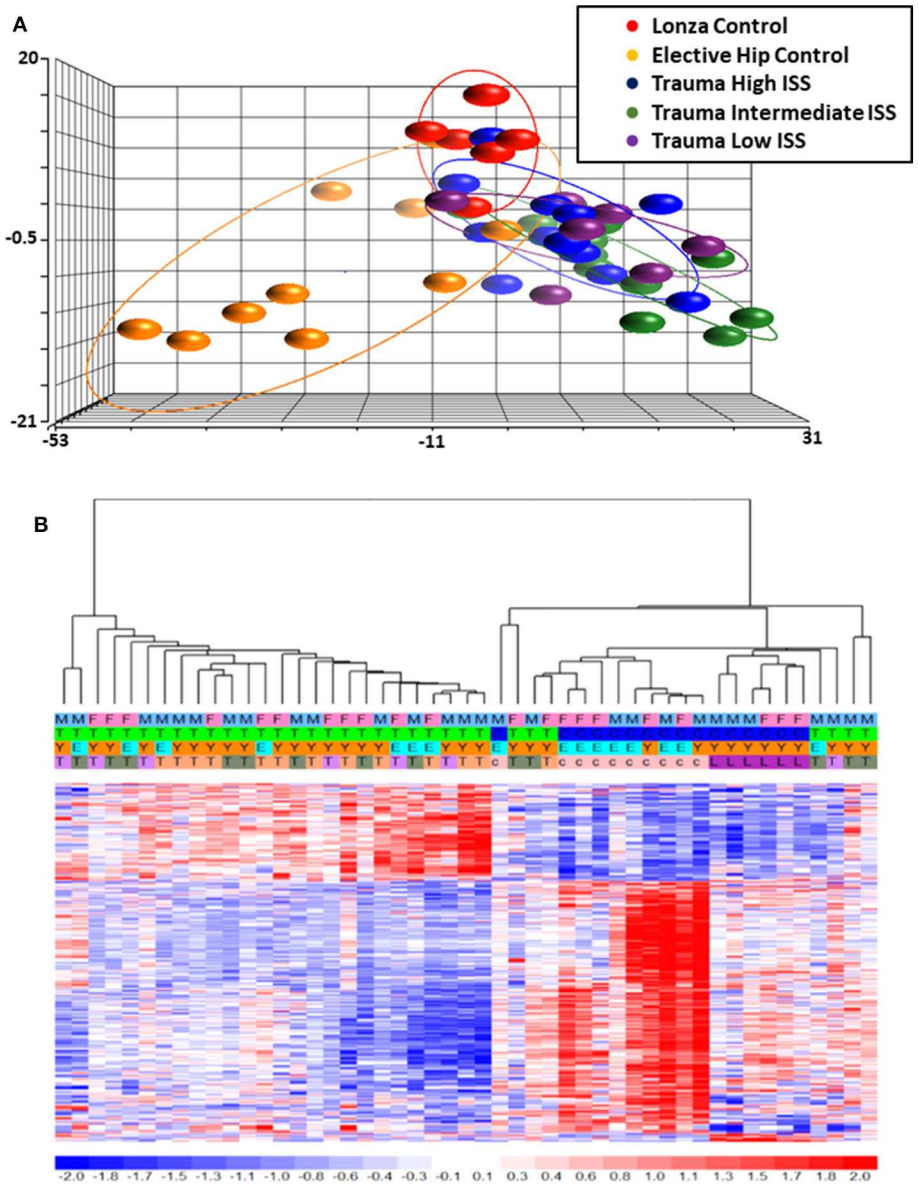

FIGURE 1 | Microarray Transcriptomic Analysis of Leukocytes from Trauma Patients with Low, Intermediate and High ISS and Healthy Control Subjects. The genomic response of isolated leukocyte RNA in healthy controls and trauma patients and healthy controls. **(A)** Conditional principal component analysis of ISS and healthy control leukocyte gene expression patterns. **(B)** Heat map (log_2) of the hierarchical clustering of leukocyte gene expression patterns and variation between trauma patients with differing ISS healthy control subjects. M, Male; F, Female; Y, Younger group; E, Older group; T, Trauma subject (three colors on row four represent three different ISS groups); c, Elective hip control subject; L, Lonza control subject.

lactate, blood transfusion, and Apache II score from the first 24 h from admission did not significantly differ between the two groups ($p = 0.48$, $p = 0.64$, $p = 0.85$, and $p = 0.58$, respectively) (33–36).

Trauma bone marrow samples were obtained during long bone or pelvic fracture repair < 9 days following blunt trauma (3.5 ± 2.4 days), and control samples (mean age 60.0 ± 9.1 years) were obtained at the time of elective surgery or from a commercial vendor (mean age 28.3 ± 4.4 years).

Hematopoietic Stem and Progenitor Cells Genomic Analysis

Total RNA was isolated from negatively-isolated bone marrow HSPCs for transcriptomic analysis. In an analysis of all trauma patients ($n = 33$) vs. healthy controls ($n = 16$), 1,845 genes were differentially expressed by enriched HSPC populations ($p < 0.001$). Sub-group analysis revealed that the severity of injury (ISS categories) did not significantly influence HSPC genome-wide expression ($p = 0.083$) (**Figure 1**). Transcriptomic differences were also not detectable between

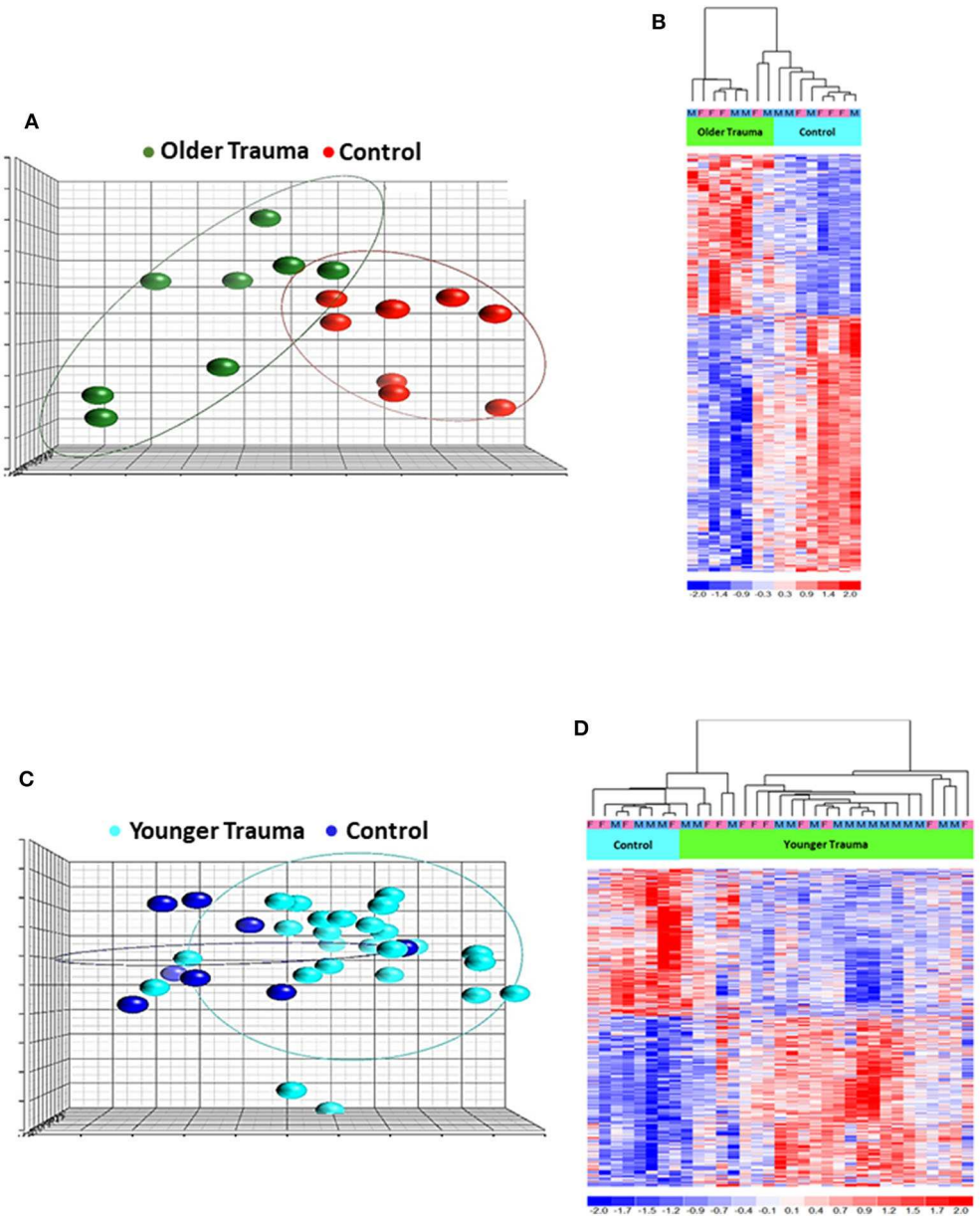

FIGURE 2 | Microarray Transcriptomic Analysis of Leukocytes from Older Trauma Patients and Younger Trauma Patients vs. Healthy Control Subjects. The genomic response of isolated leukocyte RNA in healthy controls and trauma patients and healthy controls. **(A)** Conditional principal component analysis of older adult trauma patients and healthy control leukocyte gene expression patterns. **(B)** Heat map (log_2) of the hierarchical clustering of leukocyte gene expression patterns and variation between older adult trauma patients and healthy control subjects. **(C)** Conditional principal component analysis of younger adult trauma patients and healthy control leukocyte gene expression patterns. **(D)** Heat map (log_2) of the hierarchical clustering of leukocyte gene expression patterns and variation between younger adult trauma patients and healthy control subjects. M, Male; F, Female.

patients with or without blood transfusion ($n = 7$ and 26, respectively) within 24 h after injury. However, HSPC genome-wide expression did vary after trauma in older vs. younger adult patients. Older adult trauma patients (vs. age-matched controls) had a total of 924 probe sets representing 749 unique genes that were differentially expressed ($p < 0.005$; **Figures 2A,B**). Analysis of HSPCs in younger trauma vs. age-matched controls, however, revealed differential expression of 709 probe sets representing 654 unique genes ($p < 0.0005$; **Figures 2C,D**).

Interestingly, we determined that the majority of genes with significant up or down regulation after trauma (vs. control) were dissimilar between the older and younger adult trauma patients (**Table 2**). Of the 749 and 654 genes identified after trauma in older and younger adult trauma patients, respectively, only 68 genes were observed to be in common (∼10%). In

TABLE 2 | Top 10 genes with the greatest significant expression changes in only older or younger adult trauma patients (relative to/vs. age-matched controls) in bone marrow HSPCs.

Expression	Genes
Upregulated in older trauma patients	*TREM1, RGS2, AQP9, PI3, LY96, GZMA, FCGR3B, TNFAIP6, IGSF6, IL1R2*
Downregulated in older trauma patients	*LMAN1, EEF2, CD34, LRBA, HSP90AB1, CSNK2A2, RSL1D1, MIR4737, SPTBN1, NORAD*
Upregulated in younger trauma patients	*JUNB, PRAM1, NFAM1, CEBPE, CSF3R, ADGRG3, MYO1F, CORO2A, PRKCD, MYH9*
Downregulated in younger trauma patients	*SNORD61, SNORD11, HLA-DRB5, MIR973, SAP30, CRHBP, CAMLG HEMGN, HLF, NBDY*

TABLE 3 | Genes with common transcriptomic up or down regulation in HSPCs from older trauma and younger trauma patients (as compared to their age/sex matched healthy controls).

Expression	Genes
Upregulated	*ABCA7, SLC45A4, ZNF276, CEMP1, TNFAIP2, HCG27, APOBR, METTL7B, BTG2*
Downregulated	*MYCT1, KIT, NRIP1, SPINK2, NPR3, PRKG2, ACSM3, DSG2, MMRN1, FLT3, NOG, EPB41L4A-AS1, ANGPT1, C11orf1, CCDC152, CFH, MEIS1, C3orf80, DPPA4, HNRNPA0, RPS23, NFE2L3, PRKCQ-AS1, PRKCQ, TFPI, AKT3, C1orf21, PAWR, CCDC171, MPP5, PPFIBP1, SFT2D3, ST8SIA6, LOC100130992, ZNF667-AS1, BCL2, CLGN, PLEKHA5, PARP11, ARHGAP5, SLC39A10, SPIN1, WDR35, ZNF711, BBS9, CRISPLD1, DZIP3, FAM135A, FAM213A, HCG4B, LANCL1, ZBTB20, NREP, PDGFC, SCAI*

TABLE 4 | Prominent genes and miRs found to be significantly altered in old, but not young, bone marrow HSPCs following severe trauma vs. age/sex-matched healthy controls.

Genes/ mi-RNAs	Up/down-regulated	Function
CCR10	⬆	Regulates chemokine expression (*JVI* 2017)
CCR3	⬆	Eosinophil differentiation (*JI* 2003)
CD34	⬇	Hematopoietic differentiation (*International Immunology* 1991)
CXCL12	⬇	Regulates migration of hematopoietic stem (HSPC) and progenitor cells (*Cytokine* 2015)
miR-125a/b	⬇	Hematopoietic differentiation and activation of NF-κB (*PNAS* 2012)
SATB1	⬇	Self-renewal & lymphopoiesis of adult HSPCs (*Cell Reports* 2018)
TLR5	⬆	Activation of innate immune response (*Nature* 2001)
VNN2	⬆	Encodes proteins in hematopoietic cell trafficking (*NCBI* 2019)

this set of common genes between older and younger adult trauma, the directionality of the change was identical, implying their importance to the common mammalian response to severe injury. Fifty-six genes were found to be downregulated, while the remaining 12 genes were upregulated (**Table 3**). Many of these genes are known to be important in inflammation and innate immunity, such as *MYCT1, NRIP1, FLT3, TNFAIP2, and BCL2* (37–40).

The older adult trauma cohort was noted to have significant downregulation in the expression of genes involved in hematopoiesis, not seen in younger trauma patients, when compared to age/sex-matched controls ($p < 0.001$). This included, but was not limited to, *CD34*, *CASP2, CDK6, CXCL12, SMARCA2,* and *SATB1* (**Table 4**) (37, 41–44). Analysis of genes that were only significant in younger trauma HSPCs (vs. age/sex-matched controls) revealed significant upregulation of genes for receptors important to HSPC proliferation, migration and differentiation, e.g., IL-8Rα, GM-CSFRα, and G-CSFR.

We utilized IPA and GO for further overall and pathway analysis of our genomic data. The use of these software allows greater biological insight into the functional processes activated or inhibited in each trauma group. IPA functional pathways revealed that bone marrow HSPCs from older adult trauma patients had an attenuated transcriptomic/epigenetic response to severe trauma, as displayed in **Figure 3**. In addition, only HSPCs from younger trauma patients demonstrated significant (z-score $> |2|$) upregulation of hematopoiesis pathways of function, quantity, and differentiation (**Figure 4**; **Supplemental Tables 1, 2**; **Supplemental Figure 1**).

GO analysis of the differentially expressed genes illustrated involvement of the older adult HSPC transcriptome mainly in biological processes related to energy and protein metabolism (**Supplementary Table 3**). Regulation of IL-10 production was only statistically represented in older adult trauma patients, supporting the concept that the inflammatory response of each age group is dissimilar and potentially dysregulated in older vs. younger adults (**Figure 5A**). The younger trauma patients were predicted to have over-representation of several biological process categories important for immune response, such as myeloid and neutrophil mediated immunity (**Figures 5B,C**), which was not seen in the older patients (**Supplementary Table 4**). This post-analysis provided further insights into the important pathways potentially involved in younger and older trauma HSPCs.

HSPC miR Expression Patterns

A comparison of bone marrow HSPC miR expression from all trauma ($n = 27$) and control ($n = 16$) subjects revealed 60 miRs that were differentially expressed ($p < 0.005$). The expression of 27 miRs were significantly downregulated and 33 were significantly upregulated. Fifteen of these miRs from trauma patients demonstrated at least a 2-fold positive or negative change in expression when compared with control subjects (**Table 5**).

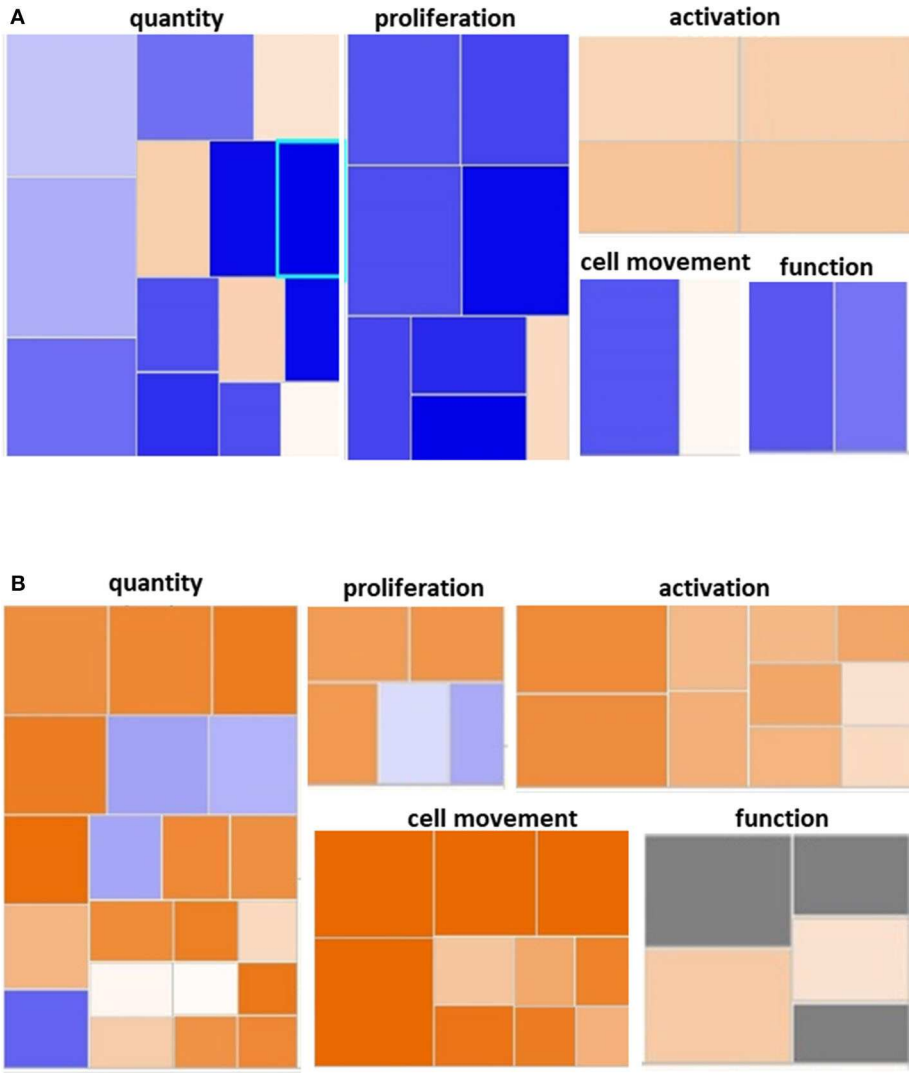

FIGURE 3 | Hematological System Development and Function Pathway from Younger and Older Trauma Patients vs. Age-Matched Controls. Ingenuity Pathway Analysis engendered figure illustrating significant **(A)** down regulation of many genes in the hematological system development and function pathways in older trauma patients as opposed to **(B)** upregulation in younger trauma patients. Orange to red = upregulation, green to blue = downregulation.

Among these were miRs 125a/b and 146a of which are known to influence HSPC function persistence (45, 46).

Interestingly, miR-125a/b and −146a were amongst the 8 miRs with the highest fold-change difference between expressions of bone marrow HSPC miR from older trauma vs. younger trauma patients. The elderly trauma patients had markedly greater down-regulation of these miRs. Additionally among the miR with the highest fold-change differences, miR-7515 and miR-3128 (47, 48), both implicated in tumor suppression, were upregulated in older trauma patients and down-regulated in younger trauma patients (**Table 6**).

Analysis using TargetScan revealed that the predicted gene targets of the expressed miR with the largest fold changes from HSPCs isolated from older trauma patients overlap with the genes found significantly expressed in the same subjects (**Table 7**). The predicted gene targets for the up-regulated miRs had a higher overlap with the genes down-regulated in HSPCs of older trauma patients. These included genes associated with HSPC proliferation and function like *AREG, CXCR1, KIT,* and *MGAM*.

DISCUSSION

Advanced age is a known risk factor for poor outcomes in trauma patients (11). Increased mortality in the elderly is largely attributed to their diminished physiologic and immunologic reserves, resulting in higher rates of nosocomial infections and sepsis post-trauma (11, 12). Previous murine studies by our laboratory demonstrate that the increased incidence of infection in the elderly is also related to HSPC failure in the aged host

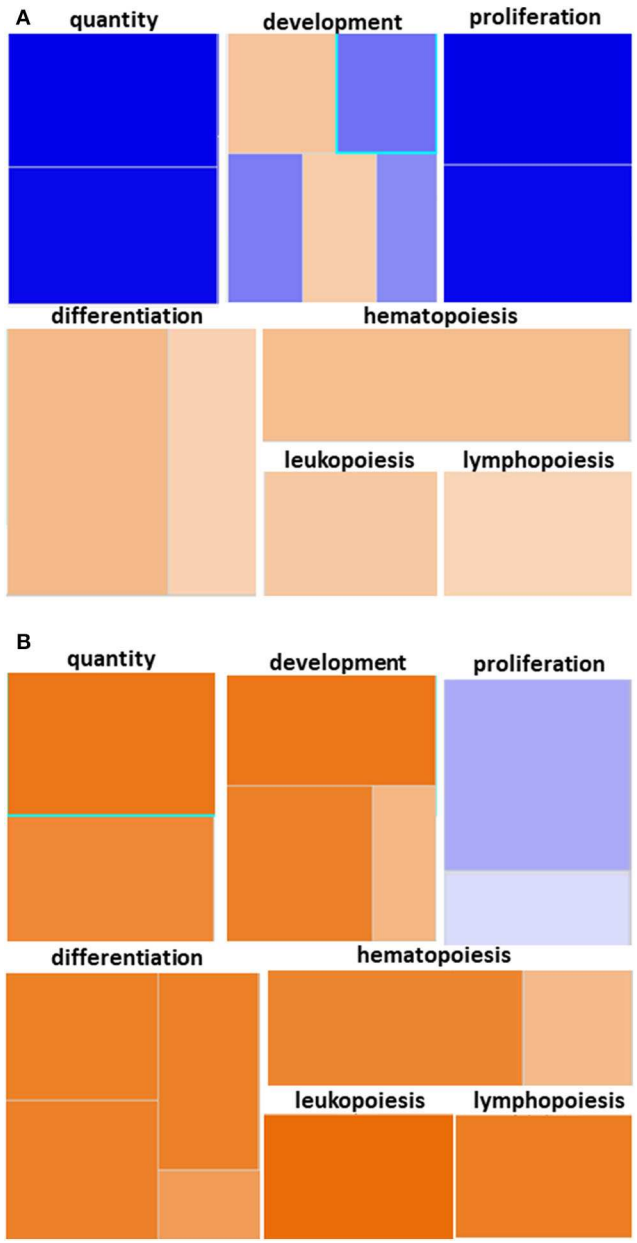

FIGURE 4 | Hematopoiesis Diseases and Functions Pathway from Younger and Older Trauma Patients vs. Age-Matched Controls. Ingenuity Pathway Analysis engendered figure illustrating significant **(A)** down regulation of genes in the hematopoiesis diseases and function pathways in old trauma patients as opposed to **(B)** upregulation in younger trauma patients. Orange to red = upregulation, green to blue = downregulation.

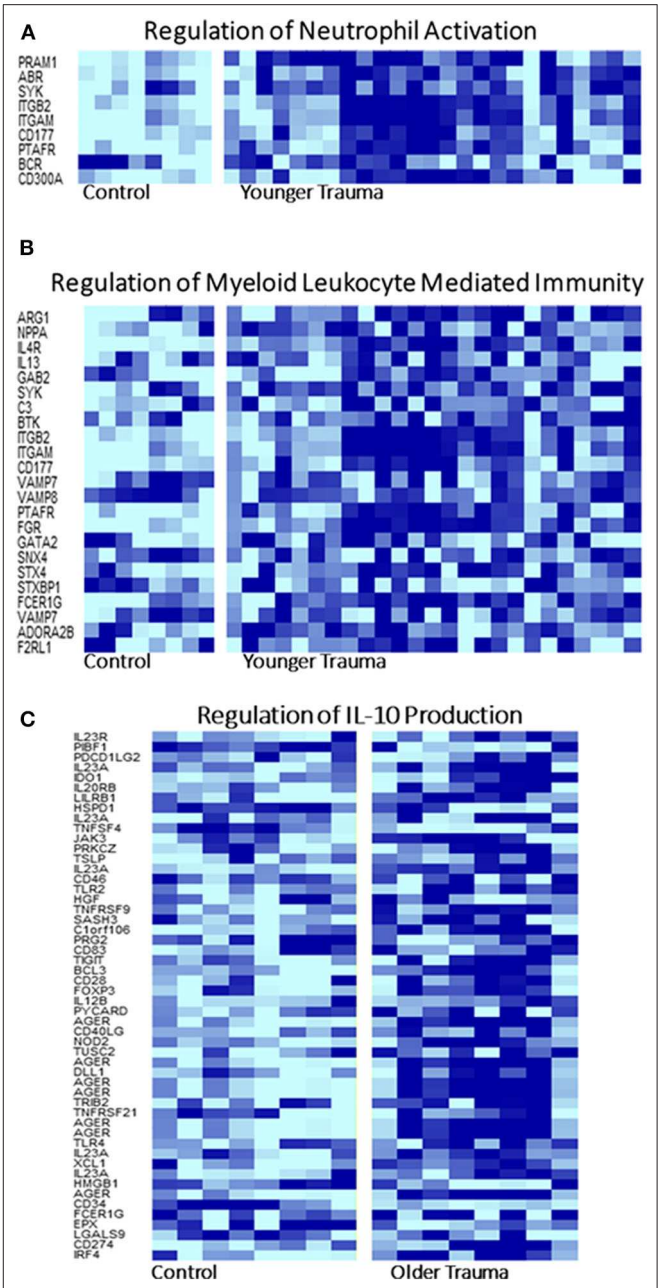

FIGURE 5 | Selected Gene Ontology Pathway Heat Maps in Younger and Older Trauma Patients. Gene ontology pathway analysis demonstrated that several pathways involved in innate and adaptive immunity, **(A)** neutrophil activation and **(B)** myeloid leukocyte mediated immunity, only in the younger trauma patients were significantly different from controls. **(C)** Only older trauma patients had over-representation of the regulation of IL-10 production. Dark blue = upregulation, light blue = down regulation.

after severe injury (18). Therefore, we sought to determine if similar hematopoietic defects are present in humans. While there was no difference in genomic expression patterns based on the magnitude of the traumatic injury (ISS) nor based on blood transfusion in the first 24 h, age was associated with significantly different genomic expression patterns when compared to younger trauma patients of equivalent severity.

Transcriptomic evaluation of bone marrow HSPC from older adult trauma patients illustrates a diminished functional status as well as a blunted capacity for the terminal differentiation of myeloid cells (49). Many genes important in HSPC proliferation, differentiation and mobilization, such as *CD34, CXCL12,*

TABLE 5 | HSPC miRNA from trauma patients with fold-change (FC) > |2|.

MicroRNA	Trauma vs. control FC
hsa-miR-4454	4.3
hsa-miR-4656	2.2
hsa-miR-193a-5p	4.5
hsa-mir-711	2.1
hsa-miR-185-5p	3.2
hsa-miR-338-5p	2.3
hsa-miR-4284	2.9
snoRNA U62	2.3
hsa-miR-125a-5p	−4.7
hsa-miR-99a-5p	−3.1
hsa-miR-146a-5p	−5.4
hsa-miR-10a-5p	−3
hsa-miR-125b-5p	−5.7
hsa-miR-126-3p	−8
hsa-let-7e-5p	−7.2

TABLE 6 | miRNA in Human HSPCs from older vs. younger adult trauma patients with largest absolute fold-change (FC) difference.

miRNA	Older adult trauma FC	Younger adult trauma FC	FC difference
hsa-miR-3201	−1.8	−10.2	8.4
hsa-miR-150-5p	9.4	1.4	8
hsa-mir-7515	1.8	−5.1	6.9
hsa-miR-3128	1.6	−3.6	5.2
hsa-miR-146a-5p	−9	−2.8	−6.2
hsa-miR-126-3p	−12.7	−6	−6.7
hsa-miR-125a-5p	−9.4	−2.4	−7
hsa-miR-125b-5p	−16.4	−2.4	−14

TABLE 7 | List of select significant upregulated HSPC miRNAs from old trauma patients and their predicted targets of significant genes of the same cells as analyzed by Target Scan software.

miRNA	Associated genes
hsa-miR-150-5p	*ACVR1B*
hsa-miR-22-3p	*ACVR1B, PRR14L*
hsa-miR-145-5p	*NR4A2, ACVR1B, ANKFY1, CRK, PRR14L, TSPAN14, ZNF436*
hsa-miR-148a-3p	*KIT*
hsa-mir-7515	*AQP9, CXCR2, GYPE, SART3, SNCA, ANKFY1, MFAP3, MON1B, PRR14L, PTK2B, TRIM27, TSPAN14, ZNF436, ZNF672*
hsa-miR-3128	*MGAM, SNCA, ACVR1B, ANKFY1, C12orf65, MON1B, MYCT1, PAGR1, PRR14L, TNFAIP8L2, TSPAN14, ZKSCAN4, ZNF436*

Genes in red were significantly down-regulated, while genes in black were significantly upregulated.

miR-125a/b, SATB1, APEX1, and PRDX1, were all found to be downregulated and only differentially expressed in older trauma HSPCs (50, 51). Interestingly, the genes found differentially expressed only in younger trauma patients were predicted by IPA to have increased activation of hematopoietic function pathways not seen in older trauma patients (**Supplemental Tables 1, 2**). Pathway analysis also revealed significantly down regulated IL-4 and IL-8 signaling in HSPCs from older trauma patients compared to the younger patients (**Supplemental Figure 2**).

The older trauma patients show a more blunted and down regulation of many genes in the CXCR4 pathway leading presumably to decreased capacity for cell migration in comparison to the younger trauma patient with significant upregulation in this signaling pathway (**Supplemental Figure 3**). A few studies have demonstrated that *CXCL12* expressed by surrounding cells in the bone marrow niche promotes HSPC quiescence and retention in the bone marrow via the CXCR4 signaling pathway (52–54). Although, our data demonstrates a downregulation of *CXCL12* in HSPCs of trauma patients in this study, Ding et al. showed that deletion of *CXCL12* in HSPCs had no effect on HSPC mobilization (55). Downregulation of *CXCR4* has been noted in the literature to increase mobilization of HSPCs (56–58). However, we did not find a significant change in CXCR4 gene expression in our study. Additionally, many studies have noted modulation of CXCL12 expression via epigenetics (59–62). Specifically, miR-23a, noted to be upregulated in old trauma patient HSPCs in our study, down-regulates *CXCL12* mRNA and protein expression (59). The role of endogenous CXCL12 is not completely understood, but these points highlight the complexity of the bone marrow niche in the regulation of the HSPC response to certain stressors. More research to study the effect of trauma on specific pathways in the bone marrow niche, its crosstalk with HSPCs, and HSPC migration from the bone marrow is warranted.

Our laboratory previously determined that elderly patients with complicated outcomes have significantly decreased plasma cytokine and chemokine concentrations 0–4 days after severe injury and hemorrhage (11). Interestingly, HSPC genomic analysis in this study revealed many pro-inflammatory related genes differentially expressed and upregulated only in older trauma patients such as TLR5, TLR8, TNFAIP6, TGFA, IL1R2, IL23A, IL7R, CCR3, and IL10RA. However, GO analysis of the differentially expressed genes in the older trauma patients revealed over-representation of biological process categories related to only one inflammatory molecule—IL-10. Additionally, GO revealed over-representation of many processes involved in immune activation in the younger trauma HPSC mRNAs not seen in the older adult patients (**Supplementary Tables 3, 4**). Taken together, this data suggests that older patients fail to activate the appropriate immune response early after severe injury and show a dysregulated inflammatory response.

miR analysis also revealed differential HSPC regulation after trauma dependent upon age, with significant differences in expression patterns of miRs known to be important for HSPC function. This included increased expression of miR-143/145

in the young, as well as decreased expression of miR-125a/b in the old, all of which are vital to HSPC function (45, 46). Under-expression of miR-143 and−145 have been noted in many malignancies, and overexpression in these malignant cell lines impair cell growth, differentiation, and cause apoptosis of $CD34^+$ HSPCs (63, 64). Expression of miR-125a has been noted to increase the number of HSPCs (65), while overexpression of miR-125b in hematopoietic stem cells has been noted to promote self-renewal, differentiation and expansion (66). Additionally, expression of miR-125a/b inhibits TNFAIP3, leading to activation of the NF-κB pathway (45). Evidence indicates that NF-κB signaling leads to a loss of HSPC quiescence and increased differentiation (67). The markedly lowered expression of miR-125a/b seen in HSPCs from the older trauma patients may translate to a markedly decreased NF-κB activity, which in turn contributes to the continued quiescence of HSPCs after traumatic injury.

Our study was limited in several ways. First, HSPCs were negatively isolated by depletion of lineage-committed cells. This is due to the limited amount of bone marrow that can be safely be obtained from these patients, and with hematopoietic stem cells being an extremely rare population. Therefore, the transcriptomics in this study represent all lineage-negative cells including hematopoietic stem and early progenitor cells. HSPCs are known to expand after trauma and also with advanced age, so the expression patterns likely reflect this phenomena as well (18, 49, 68). However, multi-potent progenitor cells (MPPs) and some other progenitor cells, like HSCs, do represent early cell populations present that are host-capable of engendering differentiated hematopoietic cells (69). However, the number of lineage negative cells that we could isolate was limited due to being a rare population, constricting our ability to perform detailed fluorescence-activated cell sorting/flow cytometry. Future studies using novel technology such as single cell RNAseq, Cellular Indexing of Transcriptomes and Epitopes by Sequencing (CITE-Seq), and Assay for Transposase Accessible Chromatin using sequencing (ATAC-Seq) are currently underway in our laboratory and will be required to better comprehend how each cell type may contribute to the suboptimal aged response to injury (70). In addition, sample size and the number of lineage negative cells that we could isolate limited our ability to perform several sub-analyses such as methylcellulose colony assays and functional assays to evaluate mobilization of HSPCs into peripheral blood. Additionally, age-specific data analysis of miR arrays was unable to be performed due to the small sample size of the older adult patient cohort. This may have led to a bias toward the younger adult arrays in the analysis of miR in all trauma patients.

However, trends can still be seen that suggest age-specific differences in epigenetic expression in response to trauma. In addition, we were unable to perform multi-variant logistic regression analysis on all risk factors between older and younger adults (e.g., co-morbidities on arrival) so that age could be determined to be independently associated with the HSPC differences. However, there are limitations to how many bone marrow samples can be obtained in these patients. In addition, in a somewhat practical analysis of older subjects, this is the HSPC response present after trauma for patients $\geq$55 years old, regardless of other factors (11).

CONCLUSIONS

Bone marrow HSPCs from older human trauma patients have a unique, and in some ways, subdued mRNA/miR response to trauma compared to younger patients. Independent of injury severity and blood transfusion requirement, advanced age may be the key driver of post-traumatic bone marrow HSPC transcriptomic and some epigenetic changes. The regulation of vital miRs and genes involved in HSPC production and differentiation may suggest why older patients have a blunted hematopoietic response to trauma, contributing to their subsequent immune dyscrasia. Although immunomodulation of HSPCs is possible, elderly patients may not respond well to standard cytokines or growth factors. Precision medicine may require epigenetic manipulation to modify HSPC protective immunity to improve long-term outcomes in the elderly.

DATA AVAILABILITY STATEMENT

The raw data supporting the conclusions of this article will be made available by the authors, without undue reservation, to any qualified researcher.

ETHICS STATEMENT

The studies involving human participants were reviewed and approved by University of Florida Institutional Review Board. The patients/participants provided their written informed consent to participate in this study.

AUTHOR CONTRIBUTIONS

Project conception and design: DD, JS, MH, MC, CA, RH, JR, JH, MB, MK, RB, BB, SB, HB, CC, AM, and PE. Data collection: DD, JS, MH, MC, CA, EN, JH, and HP. Data analysis and interpretation: DD, JS, MH, M-CL, ZW, BB, and HB. Original manuscript drafting: DD, MH, and PE. Manuscript review and editing: DD, JS, MH, MC, CA, RH, JR, M-CL, MB, MK, RB, SB, HB, CC, AM, and PE. Manuscript final approval: DD, SB, HB, CC, AM, and PE. All authors contributed to the article and approved the submitted version.

FUNDING

This work was supported in part by the following National Institutes of Health grants: NIGMS: R01 GM-040586, R01 GM-104481, R01 GM-113945, P50 GM-111152, T32 GM-008721, and NIA: 1P30AG028740.

ACKNOWLEDGMENTS

The authors would like to acknowledge Ricardo Ungaro, Marvin L. Dirain, and Dina C. Nacionales for their assistance in technical support. Thank you to Drs. Frederick A. Moore, Lyle L. Moldawer, Azra Bihorac, and Todd Brusko for advice with the project concept and design. We would also like to thank Drs. Frederick A. Moore and Lyle L. Moldawer for assistance in editing the manuscript in its final form.

SUPPLEMENTARY MATERIAL

The Supplementary Material for this article can be found online at: https://www.frontiersin.org/articles/10.3389/fimmu.2020.01289/full#supplementary-material

REFERENCES

1. DiMaggio C, Ayoung-Chee P, Shinseki M, Wilson C, Marshall G, Lee DC, et al. Traumatic injury in the United States: in-patient epidemiology 2000-2011. *Injury*. (2016) 47:1393–403. doi: 10.1016/j.injury.2016.04.002
2. Murphy SL, Xu J, Kochanek KD, Arias E. Mortality in the United States, 2017. *NCHS Data Brief*. (2018) 1–8.
3. Gardner AK, Ghita GL, Wang Z, Ozrazgat-Baslanti T, Raymond SL, Mankowski RT, et al. The development of chronic critical illness determines physical function, quality of life, and long-term survival among early survivors of sepsis in surgical ICUs. *Crit Care Med*. (2019) 47:566–73. doi: 10.1097/CCM.0000000000003655
4. Brakenridge SC, Efron PA, Stortz JA, Ozrazgat-Baslanti T, Ghita G, Wang Z, et al. The impact of age on the innate immune response and outcomes after severe sepsis/septic shock in trauma and surgical intensive care unit patients. *J Trauma Acute Care Surg*. (2018) 85:247–55. doi: 10.1097/TA.0000000000001921
5. Efron PA, Mohr AM, Bihorac A, Horiguchi H, Hollen MK, Segal MS, et al. Persistent inflammation, immunosuppression, and catabolism and the development of chronic critical illness after surgery. *Surgery*. (2018) 164:178–84. doi: 10.1016/j.surg.2018.04.011
6. Mira JC, Cuschieri J, Ozrazgat-Baslanti T, Wang Z, Ghita GL, Loftus TJ, et al. The epidemiology of chronic critical illness after severe traumatic injury at two level-one trauma centers. *Crit Care Med*. (2017) 45:1989–96. doi: 10.1097/CCM.0000000000002697
7. Kahn JM, Le T, Angus DC, Cox CE, Hough CL, White DB, et al. The epidemiology of chronic critical illness in the United States. *Crit Care Med*. (2015) 43:282–7. doi: 10.1097/CCM.0000000000000710
8. Vanzant EL, Lopez CM, Ozrazgat-Baslanti T, Ungaro R, Davis R, Cuenca AG, et al. Persistent inflammation, immunosuppression, and catabolism syndrome after severe blunt trauma. *J Trauma Acute Care Surg*. (2014) 76:21–30. doi: 10.1097/TA.0b013e3182ab1ab5
9. Davidson GH, Hamlat CA, Rivara FP, Koepsell TD, Jurkovich GJ, Arbabi S. Long-term survival of adult trauma patients. *JAMA*. (2011) 305:1001–7. doi: 10.1001/jama.2011.259
10. Moore FA, Sauaia A, Moore EE, Haenel JB, Burch JM, Lezotte DC. Postinjury multiple organ failure: a bimodal phenomenon. *J Trauma*. (1996) 40:501–10. doi: 10.1097/00005373-199604000-00001
11. Vanzant EL, Hilton RE, Lopez CM, Zhang J, Ungaro RF, Gentile LF, et al. Host response to injury, advanced age is associated with worsened outcomes and a unique genomic response in severely injured patients with hemorrhagic shock. *Crit Care*. (2015) 19:77. doi: 10.1186/s13054-015-0788-x
12. Taylor MD, Tracy JK, Meyer W, Pasquale M, Napolitano LM. Trauma in the elderly: intensive care unit resource use and outcome. *J Trauma*. (2002) 53:407–14. doi: 10.1097/00005373-200209000-00001
13. Rosenthal MD, Kamel AY, Rosenthal CM, Brakenridge S, Croft CA, Moore FA. Chronic critical illness: application of what we know. *Nutr Clin Pract*. (2018) 33:39–45. doi: 10.1002/ncp.10024
14. Warren HS, Elson CM, Hayden DL, Schoenfeld DA, Cobb JP, Maier RV, et al. Inflammation, and P. Host response to injury large scale collaborative research, a genomic score prognostic of outcome in trauma patients. *Mol Med*. (2009) 15:220–7. doi: 10.2119/molmed.2009.00027
15. de Kruijf EFM, Fibbe WE, van Pel M. Cytokine-induced hematopoietic stem and progenitor cell mobilization: unraveling interactions between stem cells and their niche. *Ann N Y Acad Sci*. (2019) 1466:24–38. doi: 10.1111/nyas.14059
16. Hashmi A, Ibrahim-Zada I, Rhee P, Aziz H, Fain MJ, Friese RS, et al. Predictors of mortality in geriatric trauma patients: a systematic review and meta-analysis. *J Trauma Acute Care Surg*. (2014) 76:894–901. doi: 10.1097/TA.0b013e3182ab0763
17. Horiguchi H, Loftus TJ, Hawkins RB, Raymond SL, Stortz JA, Hollen MK, et al. Critical illness research center, innate immunity in the persistent inflammation, immunosuppression, and catabolism syndrome and its implications for therapy. *Front Immunol*. (2018) 9:595. doi: 10.3389/fimmu.2018.00595
18. Nacionales DC, Szpila B, Ungaro R, Lopez MC, Zhang J, Gentile LF, et al. A detailed characterization of the dysfunctional immunity and abnormal myelopoiesis induced by severe shock and trauma in the aged. *J Immunol*. (2015) 195:2396–407. doi: 10.4049/jimmunol.1500984
19. Chen MM, Palmer JL, Plackett TP, Deburghgraeve CR, Kovacs EJ. Age-related differences in the neutrophil response to pulmonary pseudomonas infection. *Exp Gerontol*. (2014) 54:42–6. doi: 10.1016/j.exger.2013.12.010
20. Nacionales DC, Gentile LF, Vanzant E, Lopez MC, Cuenca A, Cuenca AG, et al. Aged mice are unable to mount an effective myeloid response to sepsis. *J Immunol*. (2014) 192:612–22. doi: 10.4049/jimmunol.1302109
21. Dykstra B, Olthof S, Schreuder J, Ritsema M, de Haan G. Clonal analysis reveals multiple functional defects of aged murine hematopoietic stem cells. *J Exp Med*. (2011) 208:2691–703. doi: 10.1084/jem.20111490
22. Flierl MA, Perl M, Rittirsch D, Bartl C, Schreiber H, Fleig V, et al. The role of C5a in the innate immune response after experimental blunt chest trauma. *Shock*. (2008) 29:25–31. doi: 10.1097/shk.0b013e3180556a0b
23. Mock CN, Dries DJ, Jurkovich GJ, Maier RV. Assessment of two clinical trials: interferon-gamma therapy in severe injury. *Shock*. (1996) 5:235–40. doi: 10.1097/00024382-199604000-00001
24. Rosenthal MD, Patel J, Staton K, Martindale RG, Moore FA, Upchurch GR Jr. Can specialized pro-resolving mediators deliver benefit originally expected from fish oil? *Curr Gastroenterol Rep*. (2018) 20:40. doi: 10.1007/s11894-018-0647-4
25. Huber-Lang M, Gebhard F, Schmidt CQ, Palmer A, Denk S, Wiegner R. Complement therapeutic strategies in trauma, hemorrhagic shock and systemic inflammation - closing Pandora's box? *Semin Immunol*. (2016) 28:278–84. doi: 10.1016/j.smim.2016.04.005
26. Rupaimoole R, Slack FJ. MicroRNA therapeutics: towards a new era for the management of cancer and other diseases. *Nat Rev Drug Discov*. (2017) 16:203–22. doi: 10.1038/nrd.2016.246
27. Fleshner M, Crane CR. Exosomes, DAMPs and miRNA: features of stress physiology and immune homeostasis. *Trends Immunol*. (2017) 38:768–76. doi: 10.1016/j.it.2017.08.002
28. Baue AE. Sepsis, systemic inflammatory response syndrome, multiple organ dysfunction syndrome, and multiple organ failure: are trauma surgeons lumpers or splitters? *J Trauma*. (2003) 55:997–8. doi: 10.1097/01.TA.0000094631.54198.07

29. Loftus TJ, Mira JC, Miller ES, Kannan KB, Plazas JM, Delitto D, et al. The postinjury inflammatory state and the bone marrow response to anemia. *Am J Respir Crit Care Med*. (2018) 198:629–38. doi: 10.1164/rccm.201712-2536OC
30. Agarwal V, Bell GW, Nam JW, Bartel DP. Predicting effective microRNA target sites in mammalian mRNAs. *Elife*. (2015) 4:e05005. doi: 10.7554/eLife.05005
31. Sauaia A, Moore FA, Moore EE, Haenel JB, Read RA, Lezotte DC. Early predictors of postinjury multiple organ failure. *Arch Surg*. (1994) 129:39–45. doi: 10.1001/archsurg.1994.01420250051006
32. Demetriades D, Chan LS, Velmahos G, Berne TV, Cornwell EE 3rd, Belzberg H, et al. TRISS methodology in trauma: the need for alternatives. *Br J Surg*. (1998) 85:379–84. doi: 10.1046/j.1365-2168.1998.00610.x
33. Gale SC, Kocik JF, Creath R, Crystal JS, Dombrovskiy VY. A comparison of initial lactate and initial base deficit as predictors of mortality after severe blunt trauma. *J Surg Res*. (2016) 205:446–55. doi: 10.1016/j.jss.2016.06.103
34. Odom SR, Howell MD, Silva GS, Nielsen VM, Gupta A, Shapiro NI, et al. Lactate clearance as a predictor of mortality in trauma patients. *J Trauma Acute Care Surg*. (2013) 74:999–1004. doi: 10.1097/TA.0b013e3182858a3e
35. Callaway DW, Shapiro NI, Donnino MW, Baker C, Rosen CL. Serum lactate and base deficit as predictors of mortality in normotensive elderly blunt trauma patients. *J Trauma*. (2009) 66:1040–4. doi: 10.1097/TA.0b013e3181895e9e
36. Vandromme MJ, Griffin RL, Weinberg JA, Rue LW 3rd, Kerby JD. Lactate is a better predictor than systolic blood pressure for determining blood requirement and mortality: could prehospital measures improve trauma triage? *J Am Coll Surg*. (2010) 210:861–7:867–9. doi: 10.1016/j.jamcollsurg.2010.01.012
37. Holmfeldt P, Ganuza M, Marathe H, He B, Hall T, Kang G, et al. Functional screen identifies regulators of murine hematopoietic stem cell repopulation. *J Exp Med*. (2016) 213:433–49. doi: 10.1084/jem.20150806
38. Jia L, Shi Y, Wen Y, Li W, Feng J, Chen C. The roles of TNFAIP2 in cancers and infectious diseases. *J Cell Mol Med*. (2018) 22:5188–95. doi: 10.1111/jcmm.13822
39. Chung HT. RIP140, a Janus metabolic switch involved in defense functions. *Cell Mol Immunol*. (2013) 10:7–9. doi: 10.1038/cmi.2012.53
40. Parigi SM, Czarnewski P, Das S, Steeg C, Brockmann L, Fernandez-Gaitero S, et al. Flt3 ligand expands bona fide innate lymphoid cell precursors *in vivo*. *Sci Rep*. (2018) 8:154. doi: 10.1038/s41598-017-18283-0
41. Brown J, Greaves MF, Molgaard HV. The gene encoding the stem cell antigen, CD34, is conserved in mouse and expressed in haemopoietic progenitor cell lines, brain, and embryonic fibroblasts. *Int Immunol*. (1991) 3:175–84. doi: 10.1093/intimm/3.2.175
42. Mendt M, Cardier JE. Role of SDF-1 (CXCL12) in regulating hematopoietic stem and progenitor cells traffic into the liver during extramedullary hematopoiesis induced by G-CSF, AMD3100 and PHZ. *Cytokine*. (2015) 76:214–21. doi: 10.1016/j.cyto.2015.05.004
43. Doi Y, Yokota T, Satoh Y, Okuzaki D, Tokunaga M, Ishibashi T, et al. Variable SATB1 levels regulate hematopoietic stem cell heterogeneity with distinct lineage fate. *Cell Rep*. (2018) 23:3223–35. doi: 10.1016/j.celrep.2018.05.042
44. Laurenti E, Frelin C, Xie S, Ferrari R, Dunant CF, Zandi S, et al. CDK6 levels regulate quiescence exit in human hematopoietic stem cells. *Cell Stem Cell*. (2015) 16:302–13. doi: 10.1016/j.stem.2015.01.017
45. Kim SW, Ramasamy K, Bouamar H, Lin AP, Jiang D, Aguiar RC. MicroRNAs miR-125a and miR-125b constitutively activate the NF-kappaB pathway by targeting the tumor necrosis factor alpha-induced protein 3 (TNFAIP3, A20). *Proc Natl Acad Sci USA*. (2012) 109:7865–70. doi: 10.1073/pnas.1200081109
46. Zhao JL, Starczynowski DT. Role of microRNA-146a in normal and malignant hematopoietic stem cell function. *Front Genet*. (2014) 5:219. doi: 10.3389/fgene.2014.00219
47. Lee JM, Yoo JK, Yoo HY, Jung H, Lee DR, Jeong HC, et al. The novel miR-7515 decreases the proliferation and migration of human lung cancer cells by targeting c-Met. *Mol Cancer Res*. (2013) 11:43–53. doi: 10.1158/1541-7786.MCR-12-0355
48. Luo J, Guo Y, Liu X, Yang X, Xiao F, Zhou M. Long non-coding RNA LINC01410 promotes colon cancer cell proliferation and invasion by inhibiting miR-3128. *Exp Ther Med*. (2018) 16:4824–30. doi: 10.3892/etm.2018.6806
49. Pang WW, Price EA, Sahoo D, Beerman I, Maloney WJ, Rossi DJ, et al. Human bone marrow hematopoietic stem cells are increased in frequency and myeloid-biased with age. *Proc Natl Acad Sci U S A*. (2011) 108:20012–7. doi: 10.1073/pnas.1116110108
50. Xie JY, Li MX, Xiang DB, Mou JH, Qing Y, Zeng LL, et al. Elevated expression of APE1/Ref-1 and its regulation on IL-6 and IL-8 in bone marrow stromal cells of multiple myeloma. *Clin Lymphoma Myeloma Leuk*. (2010) 10:385–93. doi: 10.3816/CLML.2010.n.072
51. Venezia TA, Merchant AA, Ramos CA, Whitehouse NL, Young AS, Shaw CA, et al. Molecular signatures of proliferation and quiescence in hematopoietic stem cells. *PLoS Biol*. (2004) 2:e301. doi: 10.1371/journal.pbio.0020301
52. Wright DE, Bowman EP, Wagers AJ, Butcher EC, Weissman IL. Hematopoietic stem cells are uniquely selective in their migratory response to chemokines. *J Exp Med*. (2002) 195:1145–54. doi: 10.1084/jem.20011284
53. Sugiyama T, Kohara H, Noda M, Nagasawa T. Maintenance of the hematopoietic stem cell pool by CXCL12-CXCR4 chemokine signaling in bone marrow stromal cell niches. *Immunity*. (2006) 25:977–88. doi: 10.1016/j.immuni.2006.10.016
54. Nie Y, Han YC, Zou YR. CXCR4 is required for the quiescence of primitive hematopoietic cells. *J Exp Med*. (2008) 205:777–83. doi: 10.1084/jem.20072513
55. Ding L, Morrison SJ. Haematopoietic stem cells and early lymphoid progenitors occupy distinct bone marrow niches. *Nature*. (2013) 495:231–5. doi: 10.1038/nature11885
56. Ratajczak MZ, Adamiak M, Plonka M, Abdel-Latif A, Ratajczak J. Mobilization of hematopoietic stem cells as a result of innate immunity-mediated sterile inflammation in the bone marrow microenvironment-the involvement of extracellular nucleotides and purinergic signaling. *Leukemia*. (2018) 32:1116–23. doi: 10.1038/s41375-018-0087-z
57. Adamiak M, Ratajczak MZ. Innate immunity and mobilization of hematopoietic stem cells. *Curr Stem Cell Rep*. (2017) 3:172–80. doi: 10.1007/s40778-017-0087-3
58. Nagasawa T. CXCL12/SDF-1 and CXCR4. *Front Immunol*. (2015) 6:301. doi: 10.3389/fimmu.2015.00301
59. Arabanian LS, Fierro FA, Stolzel F, Heder C, Poitz DM, Strasser RH, et al. MicroRNA-23a mediates post-transcriptional regulation of CXCL12 in bone marrow stromal cells. *Haematologica*. (2014) 99:997–1005. doi: 10.3324/haematol.2013.097675
60. Qu R, Sun Y, Li Y, Hu C, Shi G, Tang Y, et al. MicroRNA-130a-3p suppresses cell viability, proliferation and invasion in nasopharyngeal carcinoma by inhibiting CXCL12. *Am J Transl Res*. (2017) 9:3586–98.
61. Cioffi M, Trabulo SM, Vallespinos M, Raj D, Kheir TB, Lin ML, et al. The miR-25-93-106b cluster regulates tumor metastasis and immune evasion via modulation of CXCL12 and PD-L1. *Oncotarget*. (2017) 8:21609–25. doi: 10.18632/oncotarget.15450
62. Yu PF, Huang Y, Xu CL, Lin LY, Han YY, Sun WH, et al. Downregulation of CXCL12 in mesenchymal stromal cells by TGFbeta promotes breast cancer metastasis. *Oncogene*. (2017) 36:840–9. doi: 10.1038/onc.2016.252
63. Iio A, Nakagawa Y, Hirata I, Naoe T, Akao Y. Identification of non-coding RNAs embracing microRNA-143/145 cluster. *Mol Cancer*. (2010) 9:136. doi: 10.1186/1476-4598-9-136
64. Hartmann JU, Brauer-Hartmann D, Kardosova M, Wurm AA, Wilke F, Schodel C, et al. MicroRNA-143 targets ERK5 in granulopoiesis and predicts outcome of patients with acute myeloid leukemia. *Cell Death Dis*. (2018) 9:814. doi: 10.1038/s41419-018-0837-x
65. Guo S, Lu J, Schlanger R, Zhang H, Wang JY, Fox MC, et al. MicroRNA miR-125a controls hematopoietic stem cell number. *Proc Natl Acad Sci USA*. (2010) 107:14229–34. doi: 10.1073/pnas.0913574107
66. Shaham L, Binder V, Gefen N, Borkhardt A, Izraeli S. MiR-125 in normal and malignant hematopoiesis. *Leukemia*. (2012) 26:2011–8. doi: 10.1038/leu.2012.90

67. Nakagawa MM, Rathinam CV. Constitutive activation of the canonical NF-kappaB pathway leads to bone marrow failure and induction of erythroid signature in hematopoietic stem cells. *Cell Rep*. (2018) 25:2094–109.e4. doi: 10.1016/j.celrep.2018.10.071
68. Beerman I, Maloney WJ, Weissmann IL, Rossi DJ. Stem cells and the aging hematopoietic system. *Curr Opin Immunol*. (2010) 22:500–6. doi: 10.1016/j.coi.2010.06.007
69. Seita J, Weissman IL. Hematopoietic stem cell: self-renewal versus differentiation. *Wiley Interdiscip Rev Syst Biol Med*. (2010) 2:640–53. doi: 10.1002/wsbm.86
70. La Manno G. From single-cell RNA-seq to transcriptional regulation. *Nat Biotechnol*. (2019) 37:1421–22. doi: 10.1038/s41587-019-0327-4

Conflict of Interest: The authors declare that the research was conducted in the absence of any commercial or financial relationships that could be construed as a potential conflict of interest.

frontiers in Immunology

ORIGINAL RESEARCH
published: 25 June 2020
doi: 10.3389/fimmu.2020.01200

An Inverse Relationship Between c-Kit/CD117 and mTOR Confers NK Cell Dysregulation Late After Severe Injury

*Björn Bösken, Monika Hepner-Schefczyk, Sonja Vonderhagen, Marcel Dudda and Stefanie B. Flohé**

Department of Trauma, Hand, and Reconstructive Surgery, University Hospital Essen, University Duisburg-Essen, Essen, Germany

Major trauma-induced tissue injury causes a dysregulation of the immune system. Severe systemic inflammation occurs early after the insult. Later on, an enhanced risk for life-threatening opportunistic infections develops that culminates at the end of the first week after trauma. CD56^{bright} Natural killer (NK) cells play a key role in the defense against infection due to their rapid release of Interferon (IFN) γ in response to Interleukin (IL) 12. NK cells are impaired in IFN-γ synthesis after severe injury due to a disturbed IL-12/IFN-γ axis. Thereby, a circulating factor mediates extrinsic suppression of NK cells. Yet unknown cell-intrinsic mechanisms manifest by day 8 after trauma and render NK cells unresponsive to stimulatory cytokines. In the present study, we investigated the origin of such late NK cell-intrinsic suppression after major trauma. Peripheral blood mononuclear cells (PBMC) were isolated from patients 8 day after severe injury and from healthy control subjects and were stimulated with inactivated *Staphylococcus aureus*. The expression of diverse cytokine receptors, intracellular signaling molecules, and the secretion of IFN-γ by CD56^{bright} NK cells were examined. After stimulation with *S. aureus*, NK cells from patients expressed enhanced levels of c-kit/CD117 that inversely correlated with IFN-γ synthesis and IL-12 receptor (IL-12R) β2 expression. Supplementation with IL-15 and inhibition of the transforming growth factor receptor (TGF-βR) I reduced CD117 expression and increased the level of IL-12Rβ2 and IFN-γ. NK cells from patients showed reduced phosphorylation of mammalian target of rapamycin (mTOR). Addition of IL-15 at least partly restored mTOR phosphorylation and increased IL-12Rβ2 expression. The reduced mTOR phosphorylation after severe injury was cell-intrinsic as it was not induced by serum factors. Inhibition of mTOR in purified NK cells from healthy donors by rapamycin decreased the synthesis of IFN-γ. Thus, impaired mTOR phosphorylation in response to a microbial challenge contributes to the cell-intrinsic mechanisms that underlie NK cell dysregulation after trauma. Restoration of the mTOR phosphorylation capacity along with inhibition of the TGF-βRI signaling in NK cells after severe injury might improve the immune defense against opportunistic infections.

Keywords: trauma, inflammation, IL-12 receptor, mTOR, functional reprogramming, natural killer cells, c-kit

OPEN ACCESS

Edited by:
Florian Uhle, Heidelberg University Hospital, Germany

Reviewed by:
Wenxing Chen, Nanjing University of Chinese Medicine, China
Karim Brohi, Queen Mary University of London, United Kingdom

****Correspondence:***
Stefanie B. Flohé
stefanie.flohe@uk-essen.de

Specialty section:
This article was submitted to Inflammation, a section of the journal Frontiers in Immunology

Received: *17 March 2020*
Accepted: *14 May 2020*
Published: *25 June 2020*

Citation:
Bösken B, Hepner-Schefczyk M, Vonderhagen S, Dudda M and Flohé SB (2020) An Inverse Relationship Between c-Kit/CD117 and mTOR Confers NK Cell Dysregulation Late After Severe Injury. Front. Immunol. 11:1200. doi: 10.3389/fimmu.2020.01200

INTRODUCTION

Severe traumatic injury induces systemic inflammation that may cause early multi-organ damage. In parallel, an enhanced susceptibility to opportunistic infections develops that culminates at the end of the first week after injury and may persist even after discharge (1). The origin of the long-lasting suppression of the immune defense mechanisms after major trauma is only poorly understood (2, 3). Accordingly, effective therapeutic strategies that aim to restore immune homeostasis are lacking. Appropriate therapy of the immune dysregulation of injured patients is further complicated as the unbalance between inflammation and immunosuppression may shift to either side and at its best requires a personalized treatment (4).

Natural killer (NK) cells are cells of the innate immune system and play a central role in the defense against diverse infectious diseases and cancer (5). In human blood, two main populations of NK cells are distinguished: $CD56^{dim}$ NK cells are highly cytotoxic and may kill cells infected with viruses or tumor cells. $CD56^{bright}$ NK cells are potent in the secretion of cytokines such as Interferon (IFN) γ that is required for the activation of macrophages and dendritic cells (DCs) during the elimination of bacterial infection (6, 7). Interleukin (IL) 12 is released by monocytes/macrophages and DCs upon contact with microbial components and stimulates NK cells for IFN-γ synthesis (8, 9). The IL-12 receptor (IL12R) consists of a constitutively expressed β1 and an induced β2 chain. Binding of IL-12 to its receptor induces the phosphorylation of Signal Transducer and Activator of Transcription (STAT) 4 that translocates into the nucleus where it enables the transcription of the *IFNG* gene (10, 11). The T-box transcription factor T-bet cooperates with STAT4 in *IFNG* gene transcription and additionally promotes *IL12RB2* gene transcription (12). The cytokines IL-2 and IL-15 increase the IL-12-induced IFN-γ synthesis by NK cells in a synergistic manner (13, 14).

NK cells express both T-box transcription factors T-bet and Eomesodermin (EOMES) and thereby may be distinguished from innate lymphoid cells (15). A part of circulating $CD56^{bright}$ NK cells expresses the tyrosine kinase CD117 (also known as c-kit) that was originally associated with the phenotype of NK cell progenitors (16, 17).

Considering the relevance of NK cells in immune defense it is apparent that NK cells might be involved in the immune dysregulation after major injury. A recent study followed total NK cells for 5 d after trauma and observed a transient decrease in the expression of T-bet and IFN-γ (18). We have previously shown that $CD56^{bright}$ NK cells are rapidly and long-lasting suppressed after major trauma in terms of IFN-γ synthesis in response to *Staphylococcus aureus*, a frequent cause of opportunistic infections after injury (19). We identified an impaired IL-12Rβ2 expression that was associated with decreased STAT4 activation and IFN-γ synthesis. Although NK cells were similarly suppressed in IFN-γ synthesis from 24 h to at least 4 weeks after injury there were qualitative differences in the underlying mechanisms: extrinsic suppression of NK cells occurs early after injury and is mediated by a soluble factor that signals through the transforming growth factor (TGF) β receptor (TGF-βR) I. In addition, so far unknown endogenous changes establish in NK cells between 6 and 8 day after trauma that impair the IL-12/IFN-γ axis independent of the suppressive factor in the serum (19). Thus, the endogenous changes in NK cells overlap with the reported time window of cumulating infectious complications after trauma. In the present study, we aimed to shed light on the endogenous mechanisms in NK cells that arise late after traumatic injury and contribute to the impaired IFN-γ synthesis in the context of *S. aureus* infection.

MATERIALS AND METHODS

Study Design and Patients

Severely injured patients (Injury Severity Score ≥16; age ≥18 years) who were admitted to the emergency room of the Department of Trauma, Hand and Reconstructive Surgery of the University Hospital Essen between August 2017 and September 2018 were included after approval by an independent physician. Exclusion criteria were isolated head injury, immunosuppressive therapies, cancer, and autoimmune diseases. Serum and heparinized blood samples were obtained from $n = 14$ patients 8 day after trauma. Blood from sex and age matched healthy donors was drawn as controls. The patient characteristics are shown in **Supplementary Table 1**.

The study was approved by the local ethic committee of the University Hospital Essen and written informed consent was obtained from patients or their legal representatives and from healthy donors. The study was conducted according to the Declaration of Helsinki.

Isolation of Mononuclear Cells and Preparation of Serum

Peripheral blood mononuclear cells (PBMC) were isolated from heparinized blood by Ficoll density gradient centrifugation and subsequent red blood cell lysis (Sigma-Aldrich, Taufkirchen, Germany). PBMCs were used for cell culture or immediately stained for FACS analysis. Serum was obtained from clotted whole blood after centrifugation at 2,000 g for 10 min and immediately used or stored at −20°C for further analysis.

Cell Culture

PBMC were cultured in VLE RPMI 1640 Medium (containing stable glutamine; Biochrom, Berlin, Germany) supplemented with 100 U/ml Penicillin and 100 µg/ml Streptomycin (Sigma-Aldrich Chemie, Taufkirchen, Germany) and 10% autologous serum.

4×10^5 cells/well were cultured in 96-well flat bottom plates (BD Biosciences, Heidelberg, Germany) in a total volume of 200 µl/well and incubated at 37 °C and 5% CO_2 in a humidified atmosphere.

After 1 h rest, PBMC were stimulated with heat-killed *S. aureus* (10^6 bacteria /ml; Invivogen, San Diego, CA). Eighteen hour later, the cells were harvested for FACS analysis. Where indicated, 4 µM SB431542 (inhibitor of ALK4, ALK5, and ALK7; Tocris Bioscience, Bristol, UK), 5 ng/ml recombinant human IL-15 (PeproTech, Hamburg, Germany), or a combination of both was added to the cells before stimulation with the bacteria.

For the preparation of "conditioned medium," PBMC were cultured in 2% FCS and stimulated with heat-killed *S. aureus* (0.5 $\times$ 10^6 bacteria /ml). Supernatants were harvested after 18 h.

NK Cell Assay

NK cells were isolated from PBMC of healthy donors using the "Human NK cell isolation kit" (Miltenyi Biotec, Bergisch Gladbach, Germany) according to the manufacturer's protocol. NK cells were seeded in 96-well plates (2×10^4/well) in medium supplemented with 5% serum from healthy donors. Conditioned medium from PBMC was added at 25% v/v. The mTOR inhibitor rapamycin (2 nM; PeproTech, Hamburg, Germany) or its solvent (DMSO) was added. Eighteen hour later, the cells were harvested for FACS analyses.

Flow Cytometry

Three color staining of cell surface molecules was performed as described previously (19) using antibodies against CD3 (clone MEM-57, FITC-labeled, ImmunoTools, Friesoythe, Germany) and CD56 (clone CMSSB, APC-labeled, Thermo Fisher Scientific, Waltham, MA) in combination with one of the following PE-labeled antibodies: anti-IL-12Rβ2 (clone REA333, Miltenyi Biotec), anti-CD94 (clone DX22, BioLegend, San Diego, CA), anti-CD122 (clone TU27, BioLegend), anti-CD132 (clone TUGh4, BioLegend). Where indicated PE-Cy7-labeled antibodies against CD117 (clone 104D2, BioLegend) was used as a fourth color.

Intracellular staining of IFN-γ was performed as described previously (19) using antibodies against IFN-γ (clone 4S.B3, PE-labeled, BioLegend) in combination with anti-CD3 and anti-CD56. Intracellular staining of mTOR, EOMES, and T-bet was performed using the "FoxP3/Transcription Factor Staining Buffer Set" (Thermo Fisher Scientific) according to the manufacturer's instructions. After surface staining with anti-CD3 and anti-CD56 as described above, the cells were fixed and permeabilized before staining with PE-labeled antibodies (all from eBioscience, Thermo Fisher Scientific) against T-bet (clone 4B10), EOMES (clone WD1928), or mTOR (clone MRRBY). For all stainings appropriate isotype control antibodies were used to determine the threshold of positive staining.

Data were acquired using a FACSCalibur (BD Biosciences; Franklin Lakes, NJ) and analyzed using NovoExpress software (ACEA Biosciences, San Diego, CA). The expression of respective molecules was determined on gated $CD3^-CD56^{bright}$ NK cells.

Due to technical failure or an insufficient number of PBMC after isolation from whole blood it was unfeasible to generate all data from all patients.

Statistical Analyses

Statistical analysis and graphical presentation were performed using GraphPad Prism Version 5 software (GraphPad Software, La Jolla, CA). The non-parametric Mann-Whitney *U*-test and Wilcoxon signed rank test were used for statistical analysis as depicted in the figure legends. Spearman *r* analysis was used to test the correlation between two parameters.

RESULTS

$CD3^-CD56^{bright}$ Cells Express Characteristic Markers of Differentiated NK Cells Late After Trauma

We included $n = 14$ severely injured patients and $n = 14$ age- and sex-matched healthy controls in our study (patient characteristics are listed in **Supplementary Table 1**). On day 8 after trauma, the patients displayed elevated levels of C-reactive protein but normal levels of procalcitonin. Twenty-one percent of the patients developed sepsis that was diagnosed beyond day 8.

In order to evaluate the activity of $CD56^{bright}$ NK cells, PBMC obtained from patients 8 day after trauma and from healthy control subjects were stimulated with inactivated *S. aureus* bacteria and the expression of IFN-γ and of the IL-12Rβ2 chain by $CD3^-CD56^{bright}$ NK cells was determined by flow cytometry (for gating see **Figure 1A**). For our study, we used flow cytometry because it allows the analysis of surface and intracellular protein expression on and in selected cell subpopulations. As expected, NK cells from trauma patients displayed diminished levels of IFN-γ and IL-12Rβ2 (**Figures 1B,C**). The expression of IFN-γ correlated with the expression of the IL-12Rβ2 chain (**Figure 1D**).

$CD3^-CD56^{bright}$ cells from patients expressed the transcription factors T-bet and EOMES as well as CD94 *ex vivo* that are all characteristic markers for NK cells [(20); **Figures 2A–D**]. $CD56^{bright}$ NK cells moreover expressed the β and γ chains of the IL-15 receptor comparable to NK cells from controls (**Supplementary Figure 1**). The percentage of NK cells that expressed CD117, a marker that has been linked with NK cell progenitors, was decreased after trauma (**Figure 2E**). Thus, despite their reduced capacity to secrete IFN-γ late after trauma $CD3^-CD56^{bright}$ cells display a phenotype of mature NK cells similar to NK cells from controls.

Expression of CD117 Is Linked With the Suppressed Cytokine Release of NK Cells After Trauma

The expression of the IL-12Rβ2 chain is a check point in IFN-γ synthesis by NK cells after major trauma (19). In search of a potential mechanism that controls the expression of the IL-12Rβ2 chain we investigated how NK cells that do not express the IL-12Rβ2 (and therefore do not secrete IFN-γ) differ from $IL\text{-}12R\beta2^+$cells. In order to induce IL-12Rβ2 expression PBMC from patients and controls were stimulated with *S. aureus*. There was a striking difference in terms of CD117 expression between $IL\text{-}12R\beta2^+$ and $IL\text{-}12R\beta2^-$ NK cells: the IL-12Rβ2 chain was almost exclusively expressed on $CD117^-$ NK cells (**Figure 3A**). Further analysis of $IL\text{-}12R\beta2^-$ NK cells revealed a two-fold increased percentage of $CD117^+$ NK cells after major injury (**Figure 3B**). The expression of CD117 inversely correlated with the expression of the IL-12Rβ2 chain (**Figure 3C**) and with the production of IFN-γ (**Figure 3D**).

Next, the potential relationship between the expression of CD117 and NK cell function was examined. The expression of CD117 on NK cells is regulated by IL-15 in the environment (21).

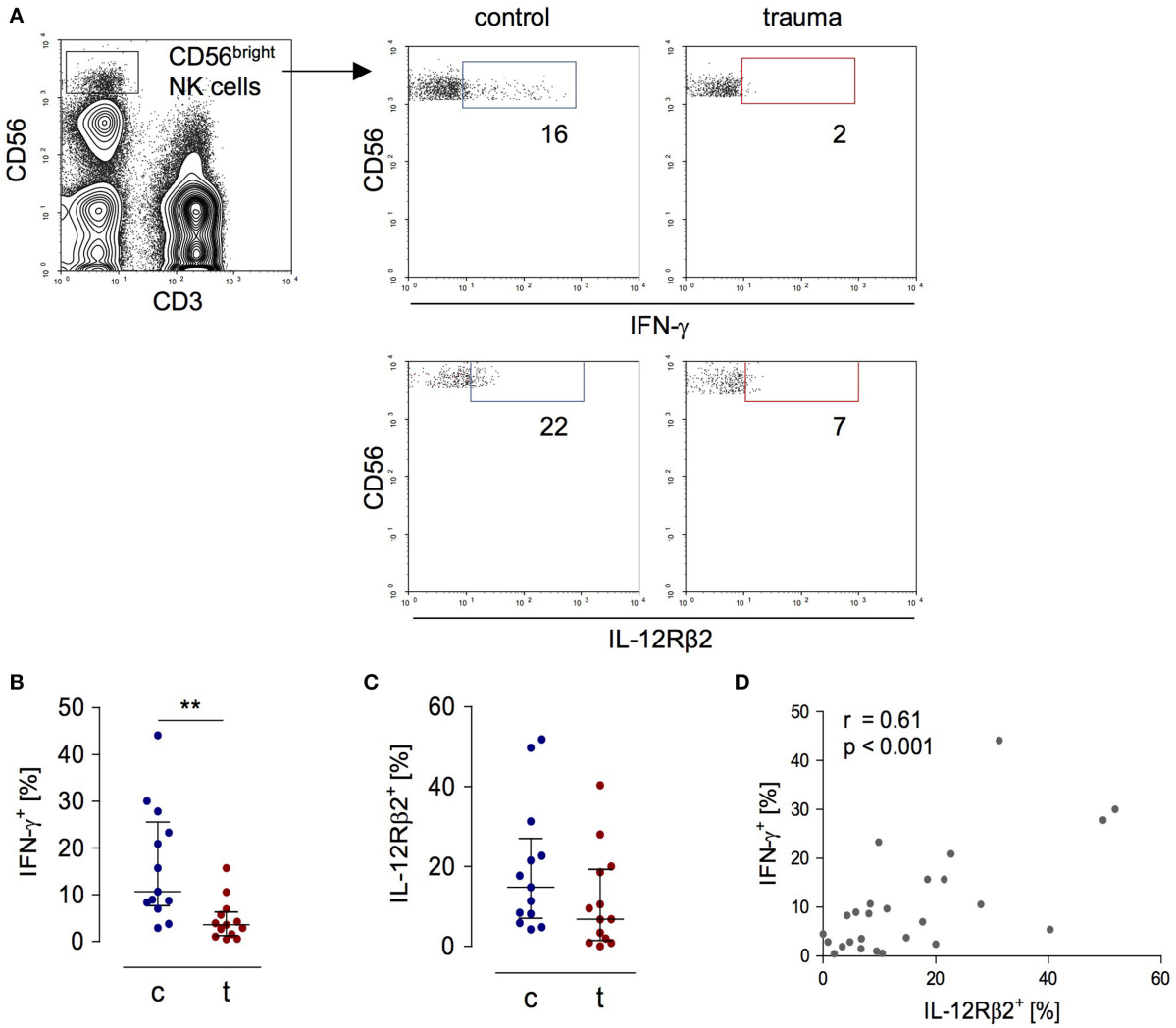

FIGURE 1 | Impaired IFN-γ synthesis of CD56^{bright} NK cells after severe trauma correlates with reduced expression of the IL-12Rβ2 chain. PBMCs were isolated from healthy donors (c) and trauma patients (t) 8 day after trauma. Cells were exposed to heat-killed *S. aureus*. After 18 h, the IFN-γ synthesis and IL-12Rβ2 expression were determined by flow cytometry. **(A)** Gating strategy of CD3$^-$CD56^{bright} NK cells. Representative dot plots are shown. Numbers indicate the percentage of positive cells. **(B,C)** Cumulative results of the percentage of IFN-γ$^+$ cells (**B**; $n = 13$) and IL-12Rβ2$^+$ cells (**C**; $n = 13$) among CD56^{bright} NK cells. Horizontal lines indicate the median/interquartile range. Statistical differences between control and trauma were tested using the Mann-Whitney *U*-test. **(D)** Spearman correlation between the percentage of IL-12Rβ2$^+$ and IFN-γ$^+$ CD56^{bright} NK cells. $^{**}p < 0.01$.

NK cell function after trauma is regulated by TGF-βRI signaling (19). Therefore, PBMC from injured patients were stimulated with *S. aureus* in the presence of recombinant IL-15, with an inhibitor of the TGF-βRI, or with the combination of both. Each component alone decreased the expression of CD117 on NK cells from injured patients. Even more effective was the combination of IL-15 with the TGF-βRI inhibitor (**Figure 3E**). Likewise, but in the inverse direction, the expression of the IL-12Rβ2 changed and increased by up to six-fold in the presence of IL-15 and the TGF-βRI inhibitor (**Figure 3F**). In contrast, only the combination of IL-15 with the TGF-βRI inhibitor enhanced the synthesis of IFN-γ (**Figure 3G**). Thus, IL-15 and inhibition of TGF-βRI signaling decrease the expression of CD117 that is associated with impaired NK cell function after trauma.

T-bet Expression Is Reduced in NK Cells After Trauma

T-bet is a relevant transcription factor that promotes *IL12RB2* and *IFNG* gene transcription in T lymphocytes and NK cells (12, 22). We examined the expression of T-bet in NK cells after severe injury and asked whether the expression of T-bet was altered in the presence of IL-15 or upon inhibition of the TGF-βRI. T-bet expression did not differ between NK cells from injured patients and healthy controls when analyzed *ex vivo* (**Figure 1B**). In contrast, after stimulation with *S. aureus*, NK cells from injured patients expressed less T-bet than NK cells from healthy subjects (**Figures 4A,B**). The expression of T-bet slightly increased in the presence of IL-15 (**Figure 4C**) or of the TGF-βRI inhibitor (**Figure 4D**). Thus, the changes of IL-12Rβ2 expression

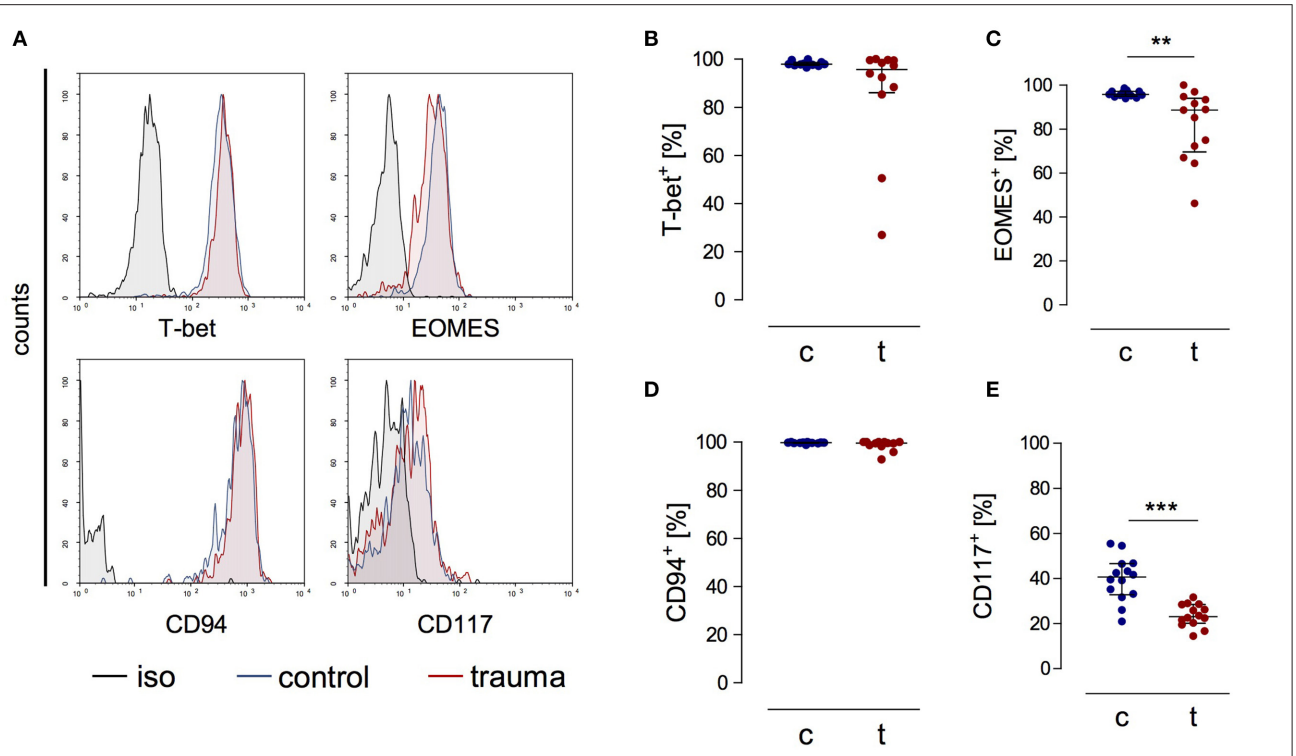

FIGURE 2 | CD56^{bright} NK cells from trauma patients express characteristic markers of mature NK cells. PBMCs from control subjects (c) and trauma patients (t) were stained *ex vivo* for the expression of T-bet, EOMES, CD94, and CD117. CD3$^-$CD56^{bright} NK cells were gated. **(A)** Representative histograms. **(B–E)** Cumulative data on the expression of T-bet (**B**; $n = 12$), EOMES (**C**; $n = 13$), CD94 (**D**; $n = 12$), and CD117 (**E**; $n = 14$). Horizontal lines indicate the median/interquartile range. Statistical differences between control and trauma were tested using the Mann-Whitney *U*-test. $^{**}p < 0.01$ and $^{***}p < 0.001$. iso, isotype control.

that are mediated by IL-15 and inhibition of the TGF-βRI in NK cells from injured patients are in part reflected by altered T-bet expression.

Decreased Phosphorylation of mTOR Correlates With CD117 Expression

A central molecule in the IL-15 signaling pathway during NK cell activation is "mammalian target of rapamycin" (mTOR) (23). We determined the expression of phosphorylated mTOR in NK cells after trauma and evaluated its potential regulation by IL-15 and inhibition of the TGF-βRI. There was no difference in mTOR phosphorylation in NK cells from injured patients and from healthy controls when analyzed *ex vivo* (**Figures 5A,B**). Stimulation with *S. aureus* strongly induced the phosphorylation of mTOR in NK cells from healthy controls but not in NK cells from trauma patients (**Figures 5C,D**). The presence of IL-15 during stimulation with *S. aureus* increased the phosphorylation of mTOR in NK cells from trauma patients while the inhibition of the TGF-βRI remained without consequences (**Figure 5E**). The pattern of mTOR phosphorylation resembled the changes in CD117 expression on NK cells (**Figure 3E**) though in the opposite direction. Indeed, there is a negative correlation between mTOR and CD117 (**Figure 5F**). Thus, mTOR phosphorylation in NK cells after severe injury is reduced and inversely correlates with CD117 expression.

mTOR Phosphorylation in NK Cells Promotes the Synthesis of IFN-γ

Considering the suppressive activity of serum from injured patients on the function of NK cells (19) the question arose whether any factors in the serum interfere with mTOR phosphorylation in NK cells. To address this issue, PBMC from healthy subjects were stimulated with *S. aureus* in the presence of serum from trauma patients or from healthy controls. The basal level of mTOR phosphorylation in NK cells was not affected by serum from injured patients but tended to decrease upon stimulation with *S. aureus* (**Figure 6A**).

In order to examine the relevance of mTOR in NK cell function we established a cell culture system with purified NK cells. Purified NK cells do not respond to *S. aureus* since they require the interaction with monocytes or DCs as source of IL-12 (24). Therefore, isolated NK cells from healthy donors were cultured in conditioned cell-free medium obtained from PBMC after stimulation with *S. aureus*. Rapamycin was used to inhibit mTOR activity. The presence of rapamycin diminished the production of IFN-γ (**Figure 6B**) by NK cells but did not affect the expression of the IL-12Rβ2 chain (**Figure 6C**). Furthermore, inhibition of mTOR did not change the expression of CD117 on

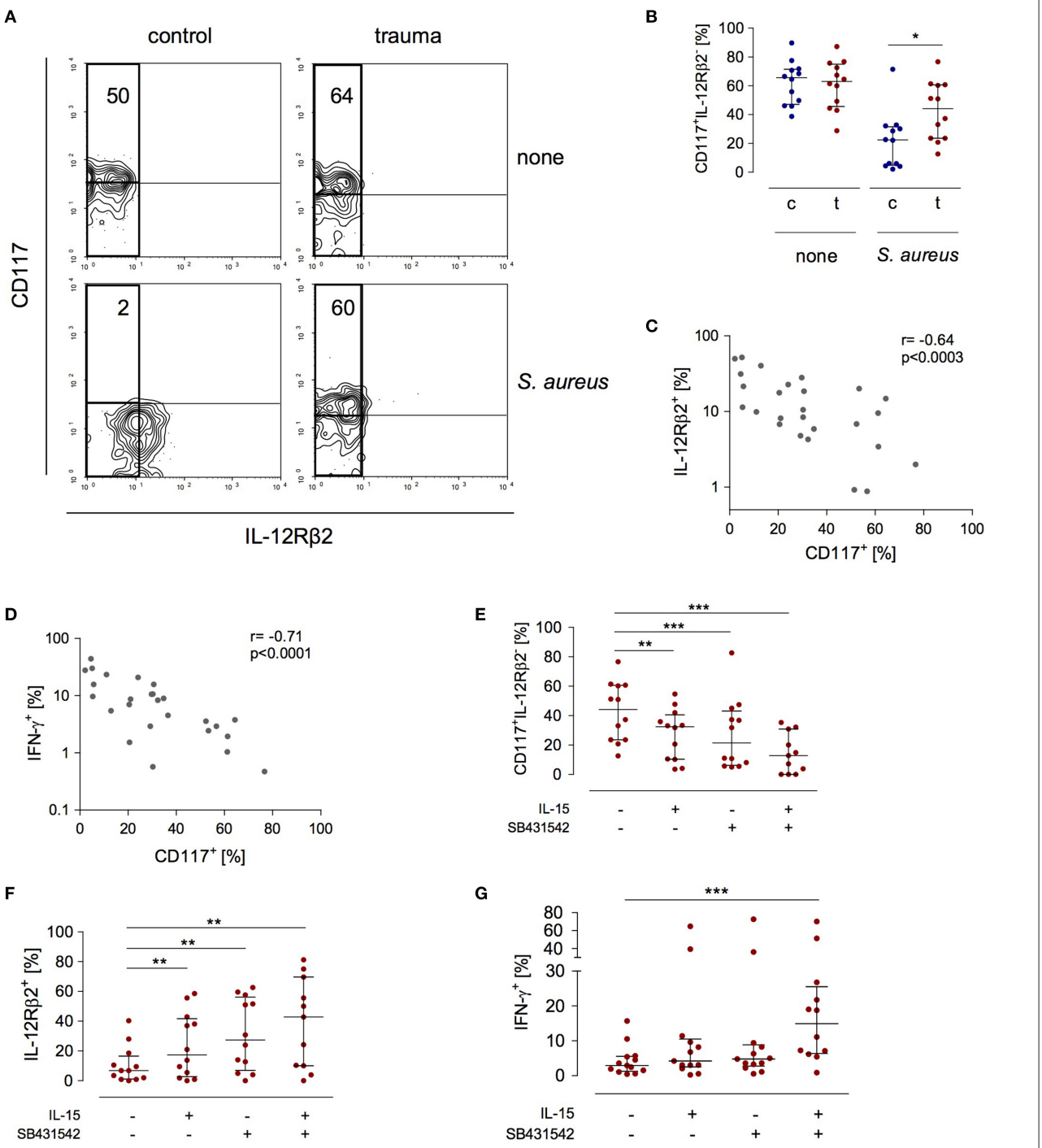

FIGURE 3 | Stimulated CD56^{bright} NK cells express increased levels of CD117 after trauma that inversely correlates with IFN-γ synthesis and IL-12Rβ2 expression. PBMC from control subjects (c) or patients (t) were stimulated with *S. aureus* and the expression of CD117, IFN-γ, and the IL-12Rβ2 chain was examined. Unstimulated cells (none) served as control. **(A)** Representative contour plots of the expression of CD117 and IL-12Rβ2 on gated CD3$^-$CD56^{bright} NK cells. Numbers indicate the percentage of CD117$^+$ among IL-12Rβ2$^-$ cells (rectangle). **(B)** Cumulative data of the percentage of CD117$^+$ cells among IL-12Rβ2$^-$ cells ($n = 12$). **(C,D)** Spearman correlation of CD117 expression with IFN-γ synthesis **(C)** and IL-12Rβ2 expression **(D)** on CD3$^-$CD56^{bright} NK cells. **(E–G)** Recombinant IL-15 or SB431542 (inhibitor of the TGF-βRI) was added during stimulation of PBMC from trauma patients with *S. aureus* [the values for cells stimulated with *S. aureus* alone are also shown in **Figures 1B,C** and **(B)**]. **(E)** Percentage of CD117$^+$ cells among IL-12Rβ2$^-$CD3$^-$CD56^{bright} NK cells ($n = 11$–12). **(F)** Expression of the IL-12Rβ2 chain on CD3$^-$CD56^{bright} NK cells ($n = 11$–12). **(G)** Expression of IFN-γ in CD3$^-$CD56^{bright} NK cells ($n = 12$–13). Horizontal lines indicate the median/interquartile range. Statistical differences between control and trauma **(B)** were tested using the Mann-Whitney U-test, differences between different culture conditions **(E–G)** were tested using the Wilcoxon signed rank test. *$p < 0.05$; **$p < 0.01$; and ***$p < 0.001$.

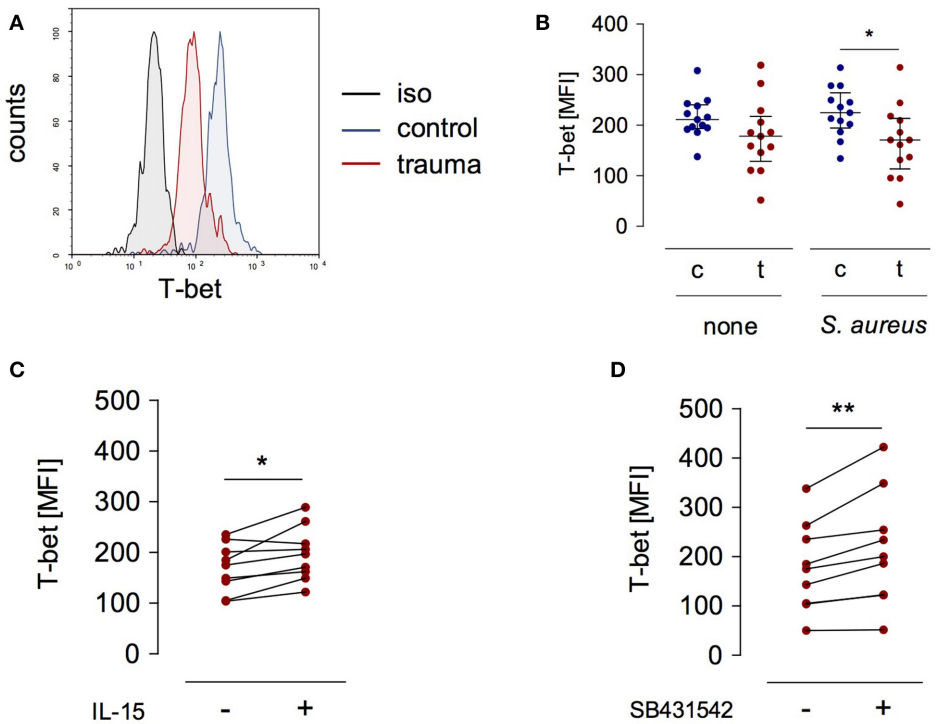

FIGURE 4 | T-bet expression in stimulated CD56^{bright} NK cells is reduced after trauma. PBMC from control subjects (c) or patients (t) were stimulated with *S. aureus* and the expression of intracellular T-bet was examined. **(A)** Representative histogram of T-bet expression in gated CD3$^-$CD56^{bright} NK cells. **(B)** Cumulative data of T-bet expression in CD56^{bright} NK cells ($n = 13$). **(C,D)** Recombinant IL-15 (**C**; $n = 9$) or SB431542 (**D**; $n = 9$) was added during stimulation of PBMC from trauma patients with *S. aureus* [the values for cells stimulated with *S. aureus* alone are also shown in **(B)**]. Horizontal lines indicate the median/interquartile range. Statistical differences between control and trauma **(B)** were tested using the Mann-Whitney *U*-test, differences between different culture conditions **(C,D)** were tested using the Wilcoxon signed rank test. $^*p < 0.05$ and $^{**}p < 0.01$. iso, isotype control.

NK cells (**Figure 6D**). Thus, mTOR is an intrinsic regulator of IFN-γ synthesis in NK cells in the context of *S. aureus* infection.

DISCUSSION

Immediately after major injury, circulating NK cells display a long-lasting impaired capacity to produce IFN-γ in response to microbial stimuli (19). While soluble factors in the serum mediate NK cell suppression early after injury, cell-intrinsic changes in NK cells are responsible for the anergic state late after trauma that renders NK cell unresponsive to otherwise stimulatory cytokines such as IL-12 and IL-2 (19). NK cells do not show signs of activation such as CD25 and CD69 after injury (19) nor differed in the expression of various characteristic markers of mature NK cells from cells of control subjects (except a reduced expression of CD117). Thus, the impaired function of NK cells after severe injury is not reflected by an altered phenotype at least according to the markers that we have examined so far. According to a recent study, CD39 is differentially expressed on NK cells after trauma (25) and might be a candidate for phenotyping NK cells from trauma patients.

The striking modulation of NK cells after major injury was only visible when the cells were exposed to *S. aureus* that mimicked an infectious challenge. This finding indicates that severe injury "primes" NK cells for an altered responsiveness to infectious agents. We propose that major injury induces a functional reprogramming of NK cells that is responsible for the impaired capacity of the cells to secrete IFN-γ while their cytotoxic function remains unaffected (19).

Our previous work has shown that the cell-intrinsic inhibition of NK cells requires 8 day to be fully established (19). Here, we provide first evidence that CD117 and mTOR are potential key molecules in the development of NK cell dysregulation after trauma. The expression of CD117 inversely correlated with the expression of IL-12Rβ2 and IFN-γ. This finding points to a potential inhibitory effect of the CD117-induced signaling pathway on the IL-12Rβ2/IFN-γ axis. Cell type-specific differences in the biological effect of CD117 signaling have been reported: in mast cells the activation of the CD117 tyrosine kinase triggers PI3K, MAPK, and JAK/STAT pathways and thereby induces the release of pro-inflammatory cytokines and histamine (26). In DCs, signaling through CD117 induces the secretion of IL-6 through PI3K activation (27). Some of these CD117-induced pathways overlap with IL-12Rβ2 signaling (28). Since CD117-induced signaling in NK cells has not been addressed so far it remains speculative whether and how CD117 interferes with IL-12-induced IFN-γ synthesis in NK cells.

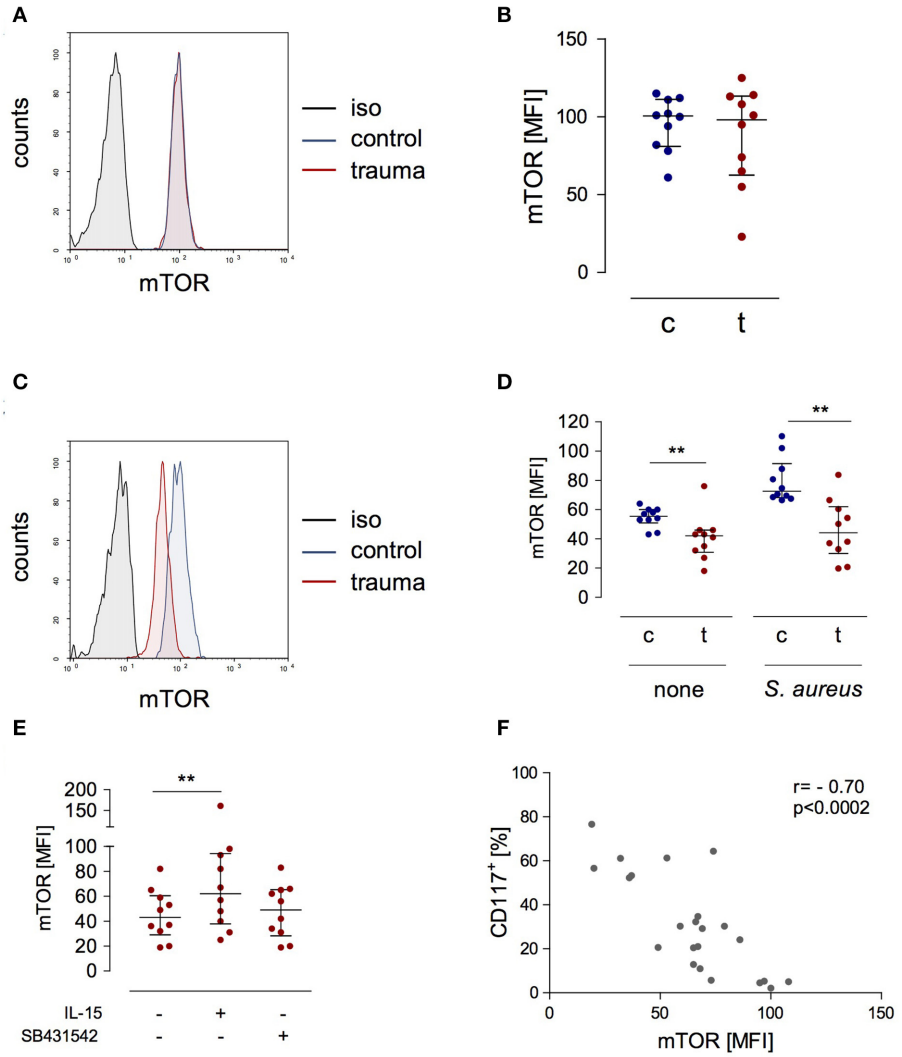

FIGURE 5 | The expression of phosphorylated mTOR is reduced in stimulated CD56^{bright} NK cells after trauma and inversely correlates with the expression of CD117. **(A)** Representative histograms of phosphorylated mTOR expression in CD56^{bright} NK cells from control subjects (c) and trauma patients (t) *ex vivo*. **(B)** Cumulative data of phosphorylated mTOR expression *ex vivo* ($n = 10$). **(C,D)** PBMC were stimulated with *S. aureus* and intracellular expression of phosphorylated mTOR was determined after 18 h. Representative histograms after stimulation with *S. aureus* **(C)** and cumulative data ($n = 10$) of phosphorylated mTOR **(D)** are shown. **(E)** Recombinant IL-15 or SB431542 was added during stimulation of PBMC from trauma patients ($n = 10$) with *S. aureus* [the values for cells stimulated with *S. aureus* alone are also shown in **(D)**]. Horizontal lines indicate the median/interquartile range. Statistical differences between control and trauma **(B,D)** were tested using the Mann-Whitney *U*-test, differences between different culture conditions **(E)** were tested using the Wilcoxon signed rank test. **(F)** Spearman correlation between expression of CD117 and phosphorylated mTOR after stimulation with *S. aureus*. $^{**}p < 0.01$. iso, isotype control.

We observed a striking inverse correlation of CD117 expression with the phosphorylation of mTOR in NK cells late after trauma. mTOR is an intracellular serine/threonine kinase and plays a central role in cytokine secretion, survival, and proliferation through its role as master switch in cell metabolism. CD117 signaling has been described to regulate mTOR phosphorylation in mesenchymal stem cells (29). A similar regulatory function of CD117 on mTOR might take place in NK cells and explain the inverse correlation of CD117 and mTOR. Detailed analyses of signaling pathways in NK cells are required in future to prove this assumption of such a functional relationship between CD117 and mTOR.

Previous studies have shown that mTOR is critical for the maintenance of the cytotoxic activity and for metabolic control of NK cells but not for their IFN-γ secretion in response to recombinant cytokines (23, 30, 31). We established a novel *in vitro* model that mimicked the activation of NK cells as it takes place during stimulation of PBMC with *S. aureus* but that was independent from recombinant cytokines and from accessory cells such as monocytes. We provide evidence that under certain circumstances mTOR indeed promotes the synthesis of IFN-γ by NK cells. However, so far we could not identify the mediators that are responsible for mTOR activation in NK cells in our *in vitro* model. Based on these findings we assume that reduced

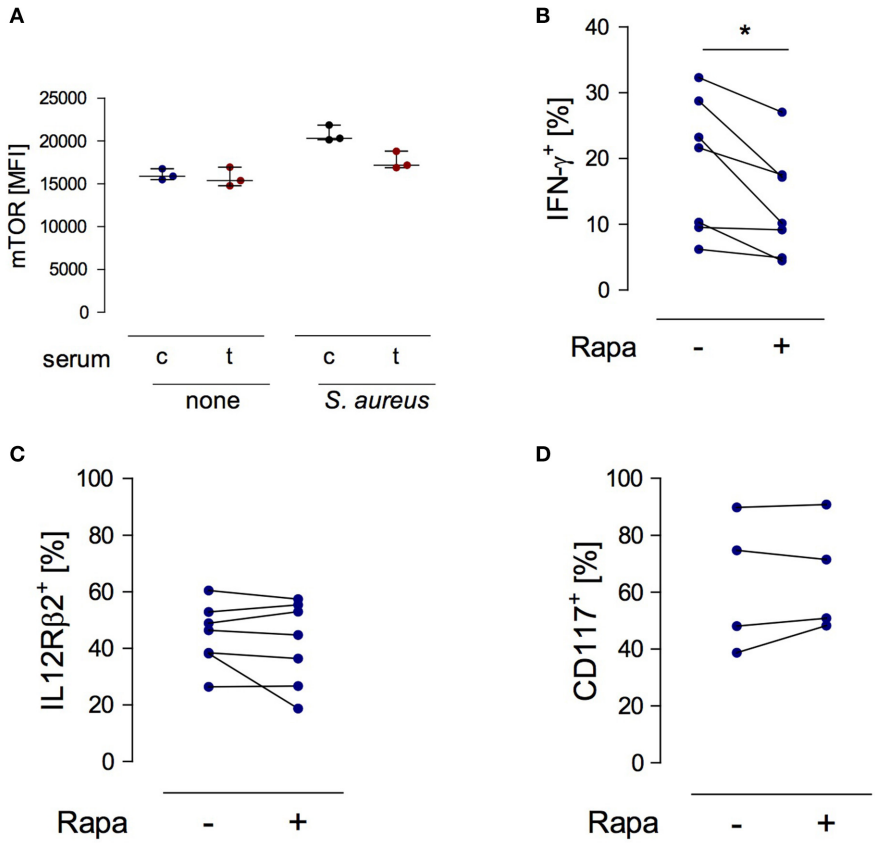

FIGURE 6 | mTOR is a cell-intrinsic regulator of IFN-γ synthesis in NK cells exposed to *S. aureus*. **(A)** Cultures of PBMC from healthy donors ($n = 3$) were set up in serum from control subjects (c) or from trauma patients (t) and were stimulated with *S. aureus*. Unstimulated cells served as control (none). The mean fluorescence intensity (MFI) of phosphorylated mTOR was determined in gated $CD3^{-}CD56^{bright}$ NK cells after 18 h. Horizontal lines indicate the median/interquartile range. **(B–D)** Purified NK cells from healthy donors ($n = 2$–4) were exposed to conditioned medium of PBMC from healthy donors that had been obtained after stimulation with *S. aureus* (2–3 different batches). Rapamycin (rapa) was added or not (–). The percentage of $CD56^{bright}$ NK cells positive for IFN-γ **(B)**, IL-12Rβ2 **(C)**, and CD117 **(D)** was quantified. Statistical differences were tested using the Wilcoxon signed rank test. $^{*}p < 0.05$.

phosphorylation of mTOR in NK cells late after trauma and signaling through the TGF-βRI both contribute to their impaired capacity to produce IFN-γ in response to *S. aureus*.

In contrast to IFN-γ synthesis, the inhibition of mTOR in NK cells did not affect the expression of CD117. Thus, it is unlikely that the expression of CD117 is directly regulated by mTOR in NK cells.

It has been described that Smad1/5/8, components of the signaling pathway downstream of the TGF-β receptor, promote the expression of CD117 in primordial follicles (32). In line, we detected decreased CD117 expression on NK cells from injured patients upon inhibition of the TGF-βRI. We have previously shown that growth/differentiation factor (GDF) 15 is present in the serum at high levels after major trauma, signals through the TGF-βRI and activates Smad1/5/8 (19). Accordingly, the increased expression of CD117 on NK cells after major injury might be mediated by circulating GDF-15. In contrast, the inhibition of TGF-βRI signaling did not affect the phosphorylation of mTOR in NK cells of the patients. This finding further supports our assumption that CD117 is not under control of mTOR.

In line with a previous study (21), we observed that the expression of CD117 on NK cells decreased when recombinant IL-15 was added during stimulation with *S. aureus*. Maximal reduction of CD117 expression was achieved with a combination of IL-15 and inhibition of the TGF-βRI that was at the same time the most effective in upregulation of the IL-12Rβ2 chain. Interestingly, IL-12Rβ2 was only expressed on $CD117^{-}$ NK cells. This finding implies that the signaling pathways induced by CD117 and TGF-βRI cooperate and prevent the expression of the IL-12Rβ2 chain. Certainly, additional studies are required to confirm the existence of this novel cross-talk between CD117 and TGF-βRI in NK cells.

The synthesis of IFN-γ by NK cells correlated with the expression of the IL-12Rβ2 chain. Unexpectedly, addition of IL-15 or inhibition of the TGF-βRI did not result in increased IFN-γ synthesis by NK cells after major trauma despite augmented expression of the IL-12Rβ2 chain. This is in contrast to the well-known capacity of IL-15 to enhance IFN-γ secretion by NK

cells from healthy subjects (33). NK cells from trauma patients expressed the IL-15 receptor subunits at levels comparable to NK cells from controls. This finding argues against a reduced sensing of IL-15 as the origin of the unchanged IFN-γ synthesis. But IL-15 was efficient in amplifying the production of IFN-γ when it was combined with the inhibitor of the TGF-βRI inhibitor. We suggest that yet unknown mechanisms exist in NK cells of severely injured patients that interfere with the signaling pathway downstream of the IL-12Rβ2 chain and that are regulated by IL-15- and TGF-βRI-induced signaling. In this regard, the transcription factor T-bet might be of relevance as it was reduced after trauma and increased in response to IL-15 and inhibition of the TGF-βRI.

Increased mTOR activity is a central component in the development of so called "trained immunity" that describes the long-term increased response to a secondary stimulus after an acute, often infectious insult (34). Trained immunity of NK cells is a consequence of cytomegalo virus infection and is associated with enhanced cytotoxicity in response to repeated infection (35). Defective trained immunity of monocytes occurs during sepsis and is considered to enhance the risk for secondary infections (36). Considering the reduced mTOR phosphorylation and the relevance of IFN-γ in immune defense we hypothesize that NK cells undergo an impaired trained immunity after major traumatic injury that, in case of a subsequent infectious insult, may result in a disturbed NK cell function. Due to the small sample size of our pilot study we could not differentiate NK cell function between patients who later developed infectious complications and those who remained free of an infection to prove this hypothesis.

In conclusion, there exists an inverse relationship between CD117 and phosphorylated mTOR in $CD56^{bright}$ NK cells after exposure to *S. aureus*. After trauma, this relationship is shifted toward CD117 and is associated with a disturbed IL-12/IFN-γ axis. Restoration of the capacity for mTOR phosphorylation by application of IL-15 in combination with inhibition of the TGF-βRI signaling pathway might represent a potential therapeutic option to improve the function of NK cells after major trauma.

DATA AVAILABILITY STATEMENT

All datasets generated for this study are included in the article/**Supplementary Material**.

ETHICS STATEMENT

The studies involving human participants were reviewed and approved by the ethics committee of the University Hospital Essen. The patients/participants provided their written informed consent to participate in this study.

AUTHOR CONTRIBUTIONS

BB and MH-S designed and performed the experiments, analyzed and interpreted the data, and wrote the manuscript. SV and MD provided material of the patients and contributed to the study design. SF supervised the study, designed the experiments, analyzed and interpreted the data, and wrote the manuscript. All authors contributed to the article and approved the submitted version.

FUNDING

This work was supported by the German Research Foundation (Deutsche Forschungsgemeinschaft, RTG1949 to SF).

SUPPLEMENTARY MATERIAL

The Supplementary Material for this article can be found online at: https://www.frontiersin.org/articles/10.3389/fimmu.2020.01200/full#supplementary-material

REFERENCES

1. Mira JC, Cuschieri J, Ozrazgat-Baslanti T, Wang Z, Ghita GL, Loftus TJ, et al. The epidemiology of chronic critical illness after severe traumatic injury at two level-one trauma centers. *Crit Care Med.* (2017) 45:1989–96. doi: 10.1097/CCM.0000000000002697
2. Lord JM, Midwinter MJ, Chen YF, Belli A, Brohi K, Kovacs EJ, et al. The systemic immune response to trauma: an overview of pathophysiology and treatment. *Lancet.* (2014) 384:1455–65. doi: 10.1016/S0140-6736(14)60687-5
3. Kimura F, Shimizu H, Yoshidome H, Ohtsuka M, Miyazaki M. Immunosuppression following surgical and traumatic injury. *Surg Today.* (2010) 40:793–808. doi: 10.1007/s00595-010-4323-z
4. Horiguchi H, Loftus TJ, Hawkins RB, Raymond SL, Stortz JA, Hollen MK, et al. Innate immunity in the persistent inflammation, immunosuppression, and catabolism syndrome and its implications for therapy. *Front Immunol.* (2018) 9:595. doi: 10.3389/fimmu.2018.00595
5. Lodoen MB, Lanier LL. Natural killer cells as an initial defense against pathogens. *Curr Opin Immunol.* (2006) 18:391–398. doi: 10.1016/j.coi.2006.05.002
6. Caligiuri MA. Human natural killer cells. *Blood.* (2008) 112:461–9. doi: 10.1182/blood-2007-09-077438
7. Poli A, Michel T, Theresine M, Andres E, Hentges F, Zimmer J. CD56bright natural killer (NK) cells: an important NK cell subset. *Immunology.* (2009) 126:458–65. doi: 10.1111/j.1365-2567.2008.03027.x
8. Michel T, Hentges F, Zimmer J. Consequences of the crosstalk between monocytes/macrophages and natural killer cells. *Front Immunol.* (2013) 3:403. doi: 10.3389/fimmu.2012.00403
9. Thomas R, Yang X. NK-DC crosstalk in immunity to microbial infection. *J Immunol Res.* (2016) 2016:6374379. doi: 10.1155/2016/6374379
10. Thierfelder WE, van Deursen JM, Yamamoto K, Tripp RA, Sarawar SR, Carson RT, et al. Requirement for Stat4 in interleukin-12-mediated responses of natural killer and T cells. *Nature.* (1996) 382:171–4. doi: 10.1038/382171a0
11. Jacobson NG, Szabo SJ, Weber-Nordt RM, Zhong Z, Schreiber RD, Darnell JE, et al., Interleukin 12 signaling in T helper type 1 (Th1) cells involves tyrosine phosphorylation of signal transducer and activator of transcription (Stat)3 and Stat4. *J Exp Med.* (1995) 181:1755–62. doi: 10.1084/jem.181.5.1755
12. Afkarian M, Sedy JR, Yang J, Jacobson NG, Cereb N, Yang SY, et al. T-bet is a STAT1-induced regulator of IL-12R expression in naive CD4+ T cells. *Nat Immunol.* (2002) 3:549–57. doi: 10.1038/ni794

13. Wang KS, Frank DA, Ritz J. Interleukin-2 enhances the response of natural killer cells to interleukin-12 through up-regulation of the interleukin-12 receptor and STAT4. *Blood.* (2000) 95:3183–90. doi: 10.1182/blood.V95.10.3183.010k36_3183_3190
14. Lucas M, Schachterle W, Oberle K, Aichele P, Diefenbach A. Dendritic cells prime natural killer cells by trans-presenting interleukin 15. *Immunity.* (2007) 26:503–17. doi: 10.1016/j.immuni.2007.03.006
15. Zhang J, Marotel M, Fauteux-Daniel S, Mathieu AL, Viel S, Marcais A, et al. T-bet and eomes govern differentiation and function of mouse and human NK cells and ILC1. *Eur J Immunol.* (2018) 48:738–50. doi: 10.1002/eji.201747299
16. Freud AG, Yokohama A, Becknell B, Lee MT, Mao HC, Ferketich AK, et al. Evidence for discrete stages of human natural killer cell differentiation *in vivo*. *J Exp Med.* (2006) 203:1033–43. doi: 10.1084/jem.20052507
17. Matos ME, Schnier GS, Beecher MS, Ashman LK, William DE, Caligiuri MA. Expression of a functional c-kit receptor on a subset of natural killer cells. *J Exp Med.* (1993) 178:1079–84. doi: 10.1084/jem.178.3.1079
18. Seshadri A, Brat GA, Yorkgitis BK, Keegan J, Dolan J, Salim A, et al. Phenotyping the immune response to trauma: a multiparametric systems immunology approach. *Crit Care Med.* (2017) 45:1523–30. doi: 10.1097/CCM.0000000000002577
19. Kleinertz H, Hepner-Schefczyk M, Ehnert S, Claus M, Halbgebauer R, Boller L, et al. Circulating growth/differentiation factor 15 is associated with human CD56(bright) natural killer cell dysfunction and nosocomial infection in severe systemic inflammation. *EBioMedicine.* (2019) 43:380–91. doi: 10.1016/j.ebiom.2019.04.018
20. Abel AM, Yang C, Thakar MS, Malarkannan S. Natural killer cells: development, maturation, and clinical utilization. *Front Immunol.* (2018) 9:1869. doi: 10.3389/fimmu.2018.01869
21. Pradier A, Tabone-Eglinger S, Huber V, Bosshard C, Rigal E, Wehrle-Haller B, et al. Peripheral blood CD56(bright) NK cells respond to stem cell factor and adhere to its membrane-bound form after upregulation of c-kit. *Eur J Immunol.* (2014) 44:511–520. doi: 10.1002/eji.201343868
22. Szabo SJ, Sullivan BM, Stemmann C, Satoskar AR, Sleckman BP, Glimcher LH. Distinct effects of T-bet in TH1 lineage commitment and IFN-gamma production in CD4 and CD8 T cells. *Science.* (2002) 295:338–42. doi: 10.1126/science.1065543
23. Marcais A, Cherfils-Vicini J, Viant C, Degouve S, Viel S, Fenis A, et al. The metabolic checkpoint kinase mTOR is essential for IL-15 signaling during the development and activation of NK cells. *Nat Immunol.* (2014) 15:749–57. doi: 10.1038/ni.2936
24. Haller D, Serrant P, Granato D, Schiffrin EJ, Blum S. Activation of human NK cells by staphylococci and lactobacilli requires cell contact-dependent costimulation by autologous monocytes. *Clin Diagn Lab Immunol.* (2002) 9:649–57. doi: 10.1128/CDLI.9.3.649-657.2002
25. Seshadri A, Brat GA, Yorkgitis BK, Giangola M, Keegan J, Nguyen JP, et al. Altered monocyte and NK cell phenotypes correlate with posttrauma infection. *J Trauma Acute Care Surg.* (2019) 87:337–41. doi: 10.1097/TA.0000000000002264
26. Reber L, Da Silva CA, Frossard N. Stem cell factor and its receptor c-Kit as targets for inflammatory diseases. *Eur J Pharmacol.* (2006) 533:327–40. doi: 10.1016/j.ejphar.2005.12.067
27. Krishnamoorthy N, Oriss TB, Paglia M, Fei M, Yarlagadda M, Vanhaesebroeck B, et al. Activation of c-Kit in dendritic cells regulates T helper cell differentiation and allergic asthma. *Nat Med.* (2008) 14:565–73. doi: 10.1038/nm1766
28. Watford WT, Hissong BD, Bream JH, Kanno Y, Muul L, O'Shea JJ. Signaling by IL-12 and IL-23 and the immunoregulatory roles of STAT4. *Immunol Rev.* (2004) 202:139–56. doi: 10.1111/j.0105-2896.2004.00211.x
29. Lee Y, Jung J, Cho KJ, Lee SK, Park JW, Oh IH, et al. Increased SCF/c-kit by hypoxia promotes autophagy of human placental chorionic plate-derived mesenchymal stem cells via regulating the phosphorylation of mTOR. *J Cell Biochem.* (2013) 114:79–88. doi: 10.1002/jcb.24303
30. Morgan DJ, Davis DM. Distinct effects of dexamethasone on human natural killer cell responses dependent on cytokines. *Front Immunol.* (2017) 8:432. doi: 10.3389/fimmu.2017.00432
31. Keating SE, Zaiatz-Bittencourt V, Loftus RM, Keane C, Brennan K, Finlay DK, et al. Metabolic reprogramming supports IFN-gamma production by CD56bright NK cells. *J Immunol.* (2016) 196:2552–60. doi: 10.4049/jimmunol.1501783
32. Ding X, Zhang X, Mu Y, Li Y, Hao J. Effects of BMP4/SMAD signaling pathway on mouse primordial follicle growth and survival via up-regulation of Sohlh2 and c-kit. *Mol Reproduct Dev.* (2013) 80:70–8. doi: 10.1002/mrd.22138
33. Ali AK, Nandagopal N, Lee SH. IL-15-PI3K-AKT-mTOR: a critical pathway in the life journey of natural killer cells. *Front Immunol.* (2015) 6:355. doi: 10.3389/fimmu.2015.00355
34. Netea MG, Joosten LA, Latz E, Mills KH, Natoli G, Stunnenberg HG, et al. Trained immunity: a program of innate immune memory in health and disease. *Science.* (2016) 352: aaf1098. doi: 10.1126/science.aaf1098
35. Sun JC, Madera S, Bezman NA, Beilke JN, Kaplan MH, Lanier LL. Proinflammatory cytokine signaling required for the generation of natural killer cell memory. *J Exp Med.* (2012) 209:947–954. doi: 10.1084/jem.20111760
36. Cheng SC, Scicluna BP, Arts RJ, Gresnigt MS, Lachmandas E, Giamarellos-Bourboulis EJ, et al.s Broad defects in the energy metabolism of leukocytes underlie immunoparalysis in sepsis. *Nat Immunol.* (2016) 17:406–13. doi: 10.1038/ni.3398

Conflict of Interest: The authors declare that the research was conducted in the absence of any commercial or financial relationships that could be construed as a potential conflict of interest.

frontiers in Immunology

ORIGINAL RESEARCH
published: 01 July 2020
doi: 10.3389/fimmu.2020.01238

Agaricus brasiliensis Mushroom Protects Against Sepsis by Alleviating Oxidative and Inflammatory Response

*Kely Campos Navegantes-Lima[1], Valter Vinicius Silva Monteiro[2,3], Silvia Leticia de França Gaspar[4], Ana Ligia de Brito Oliveira[1], Juliana Pinheiro de Oliveira[4], Jordano Ferreira Reis[4], Rafaelli de Souza Gomes[5], Caroline Azulay Rodrigues[5], Herta Stutz[6], Vanessa Sovrani[7], Alessandra Peres[8], Pedro Roosevelt Torres Romão[8] and Marta Chagas Monteiro[1,4,5]**

[1] Neuroscience and Cellular Biology Post Graduation Program, Institute of Biological Sciences, Federal University of Pará, Pará, Brazil, [2] Center for Research in Inflammatory Diseases (CRID), Department of Pharmacology, Ribeirão Preto Medical School, University of São Paulo, São Paulo, Brazil, [3] Graduate Program in Basic and Applied Immunology, Ribeirao Preto Medical School, University of São Paulo, São Paulo, Brazil, [4] School of Pharmacy, Health Science Institute, Federal University of Pará, Pará, Brazil, [5] Pharmaceutical Science Post-Graduation Program, Faculty of Pharmacy, Federal University of Pará, Pará, Brazil, [6] Department of Food Engineering, Midwest State University-UNICENTRO, Guarapuava, Brazil, [7] Department of Biochemistry, Federal University of Rio Grande de Sul, Porto Alegre, Brazil, [8] Laboratory of Cellular and Molecular Immunology, Department of Basic Health Sciences, Federal University of Health Sciences of Porto Alegre, Porto Alegre, Brazil

Sepsis is characterized by the host's dysregulated immune response to an infection followed by a potentially fatal organ dysfunction. Although there have been some advances in the treatment of sepsis, mainly focused on broad-spectrum antibiotics, mortality rates remain high, urging for the search of new therapies. Oxidative stress is one of the main features of septic patients, so antioxidants can be a good alternative treatment. *Agaricus brasiliensis* is a nutraceutical rich in bioactive compounds such as polyphenols and polysaccharides, exhibiting antioxidant, antitumor, and immunomodulatory activities. Here, we investigated the immunomodulatory and antioxidant effects of *A. brasilensis* aqueous extract in the cecal ligation and puncture (CLP) sepsis model. Our data showed that aqueous extract of *A. brasiliensis* reduced systemic inflammatory response and improved bacteria clearance and mice survival. In addition, *A brasiliensis* decreased the oxidative stress markers in serum, peritoneal cavity, heart and liver of septic animals, as well as ROS production (*in vitro* and *in vivo*) and *tert*-Butyl hydroperoxide-induced DNA damage in peripheral blood mononuclear cells from healthy donors *in vitro*. In conclusion, the aqueous extract of *A. brasiliensis* was able to increase the survival of septic animals by a mechanism involving immunomodulatory and antioxidant protective effects.

Keywords: polymicrobial sepsis, CLP, *Agaricus brasiliensis*, sun mushroom, antioxidant, immunomodulator, protection

OPEN ACCESS

Edited by:
Thomas Griffith, University of Minnesota Twin Cities, United States

Reviewed by:
Lucinéia Gainski Danielski, Universidade de Sul de Santa Catarina, Brazil
Thais Martins De Lima, University of São Paulo, Brazil

***Correspondence:**
Marta Chagas Monteiro
martachagas2@yahoo.com.br

Specialty section:
This article was submitted to Inflammation, a section of the journal Frontiers in Immunology

Received: *09 March 2020*
Accepted: *18 May 2020*
Published: *01 July 2020*

Citation:
Navegantes-Lima KC, Monteiro VVS, de França Gaspar SL, de Brito Oliveira AL, de Oliveira JP, Reis JF, de Souza Gomes R, Rodrigues CA, Stutz H, Sovrani V, Peres A, Romão PRT and Monteiro MC (2020) Agaricus brasiliensis Mushroom Protects Against Sepsis by Alleviating Oxidative and Inflammatory Response. Front. Immunol. 11:1238. doi: 10.3389/fimmu.2020.01238

INTRODUCTION

According to the World Health Organization (WHO), sepsis leads to about 6 million deaths per year worldwide (1) and is considered the main cause of death in intensive care units, especially in patients with comorbidities (2, 3). Sepsis is currently defined as a syndrome caused by a dysregulated immune response to infection (4) accompanied by an imbalance between pro-oxidant and antioxidant defenses in response to pro-inflammatory cytokines, nitric oxide (NO) and reactive oxygen species (ROS), which can cause lipid peroxidation, DNA damage, mitochondrial dysfunction, and multiple organ failure (5–7). Thus, new therapies based on compounds with antioxidant and/or immunomodulatory action may be effective as alternative therapy.

To study the pathogenesis and therapeutic targets in sepsis, several animal models have been widely used, but cecal ligation puncture (CLP) procedure is considered one that most closely resembles human sepsis (8). Recently, our group showed that in a murine model of moderate CLP-induced sepsis, animal mortality (up to six days after sepsis) was correlated with increased leukocyte migration to the peritoneal cavity and oxidative stress in several organs (spleen, heart, liver and lung) within 24 h of infection (9) and that the pretreatment of animals with salivary gland extract from *Aedes aegypti* improved mice survival through immunomodulatory and antimicrobial effects associated with lower oxidative status (decreased lipid peroxidation and increased antioxidant defense) (9). In this regard, it is of great interest to research new therapies with antioxidant and immunomodulatory properties through nutraceuticals such as *Agaricus brasiliensis* (Ab) (10).

Ab is a mushroom rich in bioactive compounds such as organic acids, amino acids, phenolic compounds and polysaccharides such as β-glucans (11, 12). The β-glucans found in mushrooms like Ab have a β-(1–3) structure associated with β-(16), which is able to stimulate cellular and humoral immune response, increase NO production, phagocytosis and lymphocyte proliferation (13–15). According to Carvajal et al., Ab present compounds such as lactic and fumaric acid, as well as secondary metabolites such as sesquiterpenes, steroids, anthraquinones, quinolines and derivatives of benzoic acid, inhibitors of bacterial growth (10). In addition, Ab has a high antioxidant potential mainly due to the presence of phenolic compounds such as gallic acid, serum acid and pyrogallol, karmic acid and other compounds such as ascorbic acid and α-tocopherol (11, 12, 16).

Therefore, considering sepsis as one of the major global public health challenges, the urgency for new therapeutic alternatives and the immunomodulatory properties of Ab, the aim of this study was to evaluate for the first time the effects of prophylactic administration of aqueous extract of Ab on survival, immunological and oxidative parameters in a murine sepsis model.

Abbreviations: Ab, *Agaricus brasiliensis*; ABTS, 2,2′-Azino-bis (3-ethylbenzothiazoline-6-sulfonic acid); ANOVA, Analysis of Variance; Bcl10, B-Cell Lymphoma/Leukemia 10; CARD9, Caspase Recruitment Domain-Containing Protein 9; CEF, Ceftriaxone; CFU, Colony-Forming Units; CLP, Cecal Ligation and Puncture; DCF, Dichloro-Fluorescein; DMSO – Dimethylsulfoxide; DTNB, 5,5′-Dithiobis (2-nitrobenzoic acid); EDTA, Ethylenediamine Tetraacetic Acid; ELISA, Enzime-Linked Immunosorbent Assay; FBS, Fetal Bovine Serum; GCS, Glutamylcysteine Synthase; *G-CSF*, Granulocyte Colony-Stimulating Factor; GSH, Glutathione; H_2DCF-DA, Dichlorodihydrofluorescein Diacetate; HEPES, 4-(2-Hydroxyethyl)-1-Piperazineethanesulfonic Acid; ICF, Informed Consent Form; IL, Interleukin; LPS – Lipopolysaccharide; MALT1, Mucosa-Associated Lymphoid Tissue Lymphoma Translocation Protein 1; MDA, Malondialdehyde; MIP-1β – Macrophage Inflammatory Protein 1β; NF-κB, Nuclear Factor Kappa B; NO, Nitric Oxide; NO_2, Nitrite; OM, Olive Moment; PBMC, Peripheral Blood Mononuclear Cells; PBS, Phosphate-Buffered Saline; PPARα, Peroxisome *Proliferator-Activated Receptor* alpha; RNS, Reactive Nitrogen Species; ROS, Reactive Oxygen Species; RPMI, Roswell Park Memorial Institute; TAS, Total Antioxidant Status; TBA, Thiobarbituric Acid; TBARS, Thiobarbituric Acid-Reactive Substances; tBHP, *tert*-Butyl Hydroperoxide; TCA, Trichloroacetic Acid; TEAC, Trolox Equivalent Antioxidant Capacity; TL, Tail Length; TLR, Toll-Like Receptor; TM, Tail Moment; TNF-α, Tumor Necrosis Factor Alpha.

MATERIALS AND METHODS

Ethics Statement

This study was carried out in strict accordance with the recommendations of the Guide for the Care and Use of Laboratory Animals of the Brazilian National Council of Animal Experimentation (http://www.sbcal.org.br/) and the NIH Guidelines for the Care and Use of Laboratory Animals. The institutional Committee for Animal Ethics of Federal University of Pará/UFPA (CEUA, Protocol: 02/15) approved all the procedures used in this study.

To *in vitro* tests, human venous blood was collected from healthy volunteers that signed the Informed Consent Form (ICF). This study was approved by the Institutional Committee of Ethics in Research involving human beings from the health sciences sector of UFPA (CEP-ICS/UFPA), under n° 3544380 and CAAE 12776619.0.0000.0018.

Mice

Male Swiss mice (7–8 weeks old) were used in this study and were obtained from the Animal Facility of the Federal University of Pará. Mice were kept in cages under controlled conditions of temperature (22 ± 3°C), light (12 h light/dark cycle) with food and water *ad libitum*, and acclimatized conditions for 3 days before use.

Preparation of *Agaricus brasiliensis* (Ab) Aqueous Extract

Ab was kindly donated by Dr. Herta Stutz Dalla Santa from the fungi collection of bioprocesses of the Bioprocesses Laboratory, Food Engineering Department, Universidade Estadual do Centro Oeste (UNICENTRO), Paraná, Brazil. To obtain an Ab aqueous extract rich in bioactive substances such as carbohydrates, in special β-glucans, proteins and phenolic compounds (17–19), we used a methodology described before (20), where 20 g of dried and pulverized mycelium of Ab were boiled in 20 mL of distilled water for 10 min and then the solution was filtered and lyophilized. A stock solution at 100 mg/mL was prepared in sterile distilled water and used for *in vivo* (135 mg/Kg) and *in vitro* experiments (2.81 and 22.5 mg/mL). These doses were chosen based on *in vitro* tests of cytotoxicity using macrophages and peripheral blood mononuclear cells. Before initiate the

experimental sets, the antioxidant activity of Ab aqueous extract was confirmed by the *in vitro* assay for total antioxidant activity (TAC) (data not shown).

Design of *in vivo* Experiments

The animals were separated into 4 groups according to the treatment schedule, as follows: saline (saline 0.9% + cecal ligation and puncture –CLP/ $n = 18$ animals), Ceftriaxone (Cef −20 mg/kg + CLP/ $n = 6$ animals), aqueous extract of *Ab* (Ab −135 mg/kg + CLP, $n = 18$ animals) and sham (surgery control, $n = 18$ animals). All treatments were administered in a volume of 100 μL orally by gavage, 24 h before and immediately before CLP induction (time 0). In the first set of experiments, 24 animals were used to monitor the survival rate during 12 days. In the next set of experiments 36 animals were used, septic mice were euthanized at specific time points to evaluate the therapeutic potential and immunomodulatory/antioxidant activities of Ab. In this study, 18 mice (6/group) were euthanized 12 h after CLP to analyze oxidative stress parameters and 18 mice (6/group) were euthanized 24 h after CLP to analyze pro-inflammatory cytokines based on previous studies (9, 21) (**Figure 1**).

CLP Model

The polymicrobial sepsis was induced using the cecal ligation and puncture (CLP) model according to D'Acampora and Locks, with some adaptations (9, 22). To summarize, animals were anesthetized with intraperitoneal injection of ketamine (100 mg/kg) and xylazine (10 mg/kg), a small one-centimeter laparotomy performed, and the cecum exposed and then ligated using a 3–0 silk suture. Then, the cecum was punctured one single time with 22G needle to induce a moderate severity CLP. The cecum was gently squeezed to extrude a small amount of fecal content and was left to its original position in the abdominal cavity. Sham-operated mice underwent the same procedure, except for ligation and perforation of the cecum. The abdominal wall was closed, and fluid resuscitation was conducted with subcutaneous injection of 1 mL of saline 0.9%.

Survival and Weight Analysis of Septic Mice

After induction of sepsis, mice of each group ($n = 6$) were weighted twice a day for twelve consecutive days. To reduce suffering, mice presenting signs of imminent death (i.e., ataxia, inability to maintain upright position, tremor, and/or agonal breathing) were euthanized by ketamine/xylazine (>100/10 mg/kg, sc) overdose. The animals that survived for longer than 12 days were euthanized. The survival rate and weight were calculated followed by delineation of survival and weight curve.

Blood Samples and Leukocyte Counts

Peripheral blood was obtained by cardiac puncture of mice anesthetized with ketamine (100 mg/kg) and xylazine (10 mg/Kg) at 12 and 24 h after CLP induction. Aliquots (500 μL) of blood collected with ethylenediamine tetraacetic acid (EDTA) 5% were analyzed using an automatic hematologic analyzer (Hematoclin 2.8 VET, Starlab, Salvador, BA, BRA) and blood samples (1000 μL) collected without anticoagulant were used to obtain serum for analyses of oxidative stress (12 and 24 h post CLP) and cytokines (24 h post CLP).

Cytokines Measurement

The levels of TNF-α and IL-1β in serum and peritoneal lavage fluid collected at 24 h post CLP induction were quantified by Enzime-Linked Immunosorbent Assay (ELISA) using an appropriate commercial kit (R&D Systems, Minneapolis, Canada) according to the manufacturer's instructions. The detection limits of each cytokine were IL-1β, 12.5–800 pg/mL with sensitivity of 4.8 pg/mL; TNF-α, 10.9–700 pg/mL with sensitivity of 7.21 pg/mL.

Determination of Nitric Oxide (NO) Production

The nitrite (NO_2) was estimated colorimetrically at 12 and 24 h post CLP on the basis of reduction of nitrate to nitrite using Griess method (23). Nitrite level was determined in 100 μL of samples (serum and lavage peritoneal) incubated with an equal volume of Griess reagent for 10 min at room temperature. The absorbance was measured at 550 nm and calculated from a standard curve with sodium nitrite expressed per μMol/mL (24).

Bacterial Load Determination

For determination of colony-forming units (CFU) in blood and peritoneal fluid of mice ($n = 6$ per/group), 10 μL of samples were diluted with sterile Phosphate-Buffered Saline (PBS) 1:10, and then 10 μL of each dilution was cultured in Müller Hinton Agar and incubated at 37 °C for 24 h. The colonies were counted and expressed in CFU/mL.

Peritoneal Leukocyte Counts

Twenty-four h after sepsis induction, peritoneal cells of animals were harvested with 3 mL of PBS containing 1 mM EDTA and the number of total leukocytes was determined using a hemocytometer. The number of differential cell counts was carried out counting a total of 200 cells on cytocentrifuge slides stained with panoptic dye. The results are presented as the number of neutrophils and mononuclear cells per cavity.

Phagocytic Capacity of Peritoneal Macrophages

The phagocytic capacity of peritoneal macrophages of septic and sham mice was evaluated as previously described (25). Peritoneal macrophages from sham, CLP-saline and CLP-Ab groups were collected 24 h post sepsis induction and incubated in 96-well microplates (2×10^5 cells/well) for 40 min at 37°C and 5% CO_2. Then, 10 μL of neutral-red stained zymosan (1×10^8 particles/mL) were added to each well and after 30 min the supernatants were removed and cells fixed with Baker's formol-calcium (4% formaldehyde, 2% sodium chloride, 1% calcium acetate) for 30 min. Following, the cells were washed two times by centrifugation in PBS (450g for 5 min). After solubilization of neutral-red stain with 0.1 mL of acidified alcohol (10% acetic acid, 40% ethanol in distilled water) the absorbance was measured in a microplate reader at 550 nm.

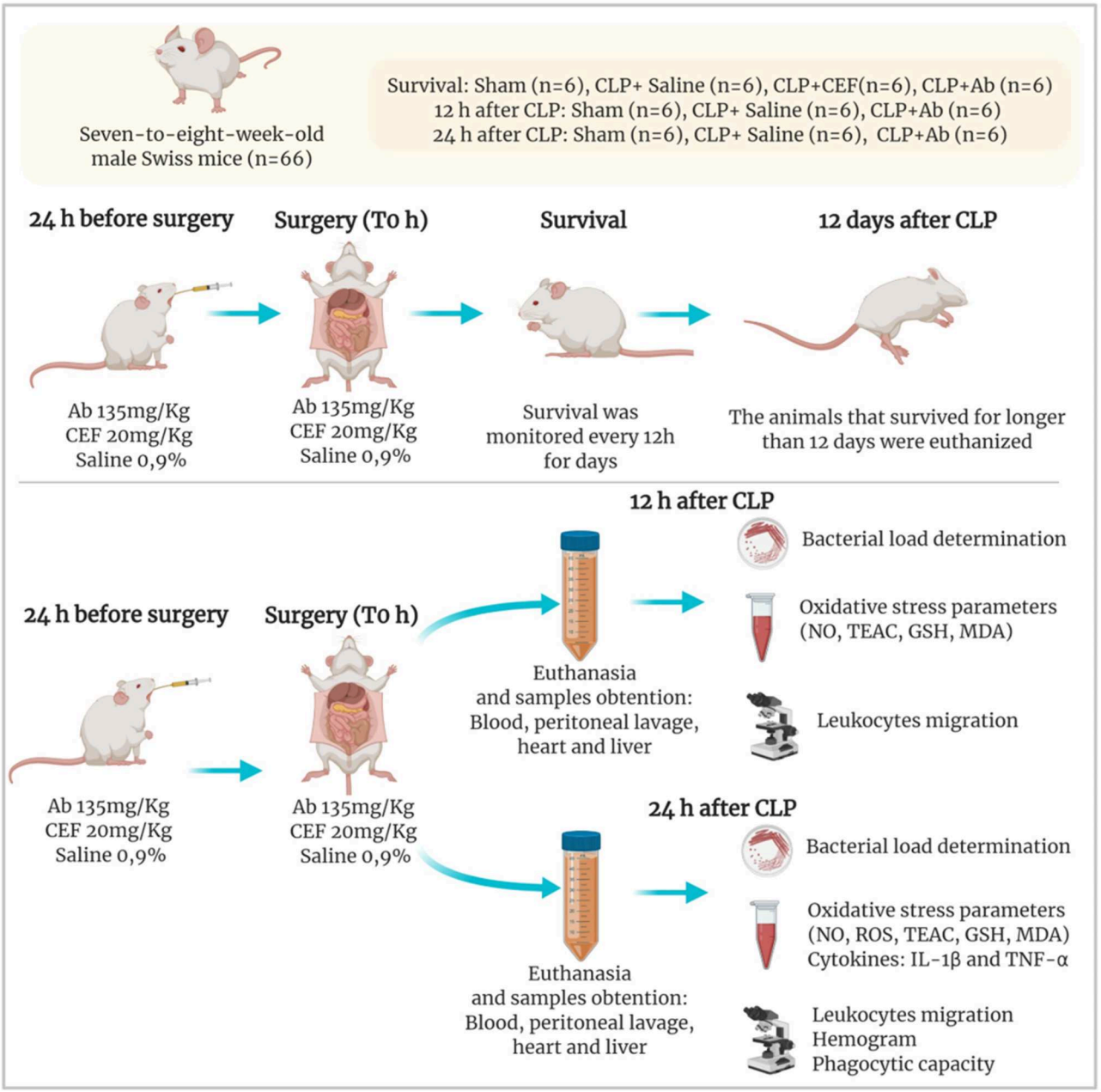

FIGURE 1 | Experimental protocol of CLP model and pre-treatments. Ab, aqueous extract of *Agaricus brasiliensis;* CLP, cecal ligation and puncture; CEF, ceftriaxone; CFU, colony-forming unit; GSH, Glutathione; MDA, malondialdeihyde; ROS, reactive oxygen species; TEAC, Trolox equivalent antioxidant capacity.

Measurement of Reactive Oxygen Species (ROS) Production

Reactive oxygen species (ROS) production in peritoneal macrophages of septic animals was quantified using 2′,7′-Dichlorodihydrofluorescein diacetate (H_2DCF-DA) (26). Briefly, peritoneal cells obtained 24 h post CLP induction were incubated at 37° C during 15 min with 30 mM N-(2-Hydroxyethyl)piperazine-N′-(2-ethanesulfonic acid) (HEPES) (pH 7.2), 200 mM KCl, 1 mM $MgCl_2$, and 16 μM of H_2DCF-DA. The conversion of DCFH-DA to the fluorescent product DCF was measured using a fluorescence microplate reader (Victor 2, Perkin Elmer) every 5 min during 30 min with excitation/emission at 488/530 nm. Background fluorescence was determined before the addition of H2DCF-DA and data were expressed as fluorescence intensity.

Determination of Lipid Peroxidation

Lipid peroxidation was measured in serum, peritoneal cavity, heart and liver samples collected from septic animals at 12 and 24 h post CLP induction as an indicator of oxidative stress, using the thiobarbituric acid-reactive substances (TBARS) assay (27, 28). Briefly, samples were mixed with 0.05 M trichloroacetic acid (TCA) and 0.67% thiobarbituric acid (TBA; Sigma-Aldrich, St. Louis, MO) in 2 M sodium sulfate, and heated in a water bath at 94°C for 90 min. The chromogen formed was extracted in n-butanol and measured at 535 nm. An MDA standard solution was used to construct a standard curve against which unknown samples were plotted. Results are expressed as malondialdehyde equivalents in nmol/L.

Total Evaluation of Trolox Equivalent Antioxidant Capacity (TEAC)

The total antioxidant capacity (TAC) of serum, peritoneal fluid, heart and liver samples of septic mice (collected 24 h post CLP induction) was evaluated by Trolox ((±)-6-Hydroxy-2,5,7,8-tetramethylchromane-2-carboxylic acid; Sigma-Aldrich) equivalent antioxidant capacity assay (TEAC), which provides relevant information that may effectively describe the dynamic equilibrium between pro-oxidant and antioxidant compounds. In this assay, 2,2′-Azino-bis (3-ethylbenzothiazoline-6-sulfonic acid) diammonium salt (ABTS) (Sigma Aldrich) was incubated with potassium persulphate (Sigma Aldrich) to produces $ABTS^{\bullet+}$, a green/blue chromophore. The inhibition of $ABTS^{\bullet+}$ formation by antioxidants in the samples were expressed as Trolox equivalents, determined at 740 mm using a calibration curve plotted with different amounts of Trolox (Sigma Aldrich) (29, 30).

Glutathione (GSH) Levels

The level of GSH was determined in samples of serum and peritoneal lavage fluid of septic mice at 12 and 24 h post CLP induction using Ellman's reagent (31). This assay was based on the production of yellow color when 5,5′-Dithiobis(2-nitrobenzoic acid) (DTNB) is added to compounds containing sulfhydryl groups. The GSH concentration was determined using a standard curve constructed with different concentrations of GSH in the reduced form. The absorbance was recorded at 412 nm in a microplate reader (SpectraMax 250, Molecular Devices, Union City, CA, USA) and results were expressed in μmol/mL.

In vitro Studies

Peripheral Blood Mononuclear Cells (PBMC) Isolation and *in vitro* Stimulation

PBMC of healthy volunteers who were abstainers of alcohol and tobacco (both sexes, ages 20 to 45 years) were isolated from blood using Ficoll (Sigma-Aldrich). PBMC viability was determined by trypan blue exclusion and the viability was always >95%. Then, the cells were washed and suspended in Roswell Park Memorial Institute-1640 medium (RPMI-1640, Sigma-Aldrich) supplemented with 2 g/L sodium bicarbonate, 10% fetal bovine serum (FBS, Sigma-Aldrich), 2% glutamine, and 100 U/mL penicillin-0.1 mg/mL streptomycin (Sigma-Aldrich) and incubated *in vitro* with RPMI medium (control), *tert*-Butyl hydroperoxide (tBHP: 200 μM) or tBHP plus *Ab* (22.5 mg/mL) for 30 min at 37°C.

Measurement of Reactive Oxygen Species (ROS) Production

In this assay, mice were injected intraperitoneally with 2.5 mL of 3% thioglycollate (Sigma-Aldrich) and 48 h latter, peritoneal macrophages were harvested as previously described in 2.10. Macrophages (2×10^5) were incubated *in vitro* with tBHP (40 μM) or tBHP plus *A. brasilienses* (22.5 mg/mL) for 30 min at 37°C. ROS production was detected as described in item 2.11 (32).

DNA Damage Using Comet Assay

PBMC were treated *in vitro* with tBHP (200 μM) or tBHP plus *A. brasilienses* (2.81 or 22.50 mg/mL) for 3 h. To perform the Comet assay, each sample was mixed with low melting-point agarose at 37°C to a final concentration of 0.5%. The mixture (100 μL) was added to the slides precoated with 1.5% normal-melting-point agarose to retain the agarose cell suspension. The drop containing cells was covered with a glass cover slip and left at 4°C for 5 min. The slides were treated with a lysis solution (2.5 M NaCl, 100 mM EDTA, 100 mM TRIS, 1% Triton X-100, 10% DMSO, pH ∼ 10.2) for 24 h at 4°C. After, the slides were placed horizontally on an electrophoresis tray and the resultant nucleoids were immersed in electrophoresis buffer (300 mM NaOH, 100 mM EDTA, pH > 13) for 20 min at 4°C to cleave the alkali-labile sites. Then the electrophoresis was started using an electric field of 23 V/cm for 20 min. At the end of the process, the slides were gently removed from the tray and washed with distilled water for 5 min for neutralization. The slides were dehydrated for 3 min in absolute ethanol and were then air dried. Finally, the slides were stained with ethidium bromide (20 μg/mL) and viewed using fluorescence microscopy ZEISS AxioCam HRc with green barrier filter 510–560 nm and 400x coupled to a video camera. The cell images were analyzed using Tritek Comet Score Freeware 1.6 software. Registered parameters included the percent of DNA in the tail (Tail DNA %), Tail Length (TL), Tail Moment (TM), and Olive Moment (OM) as marker of DNA damage. One hundred comets were scored randomly for each concentration employed. All steps described previously were carried out in a darkroom to prevent the interference of additional DNA damage.

Statistical Analysis

Statistical analyses were performed using Graphpad Prism 6 software (GraphPad Software Inc., La Jolla, USA). We assessed differences in the survival groups after CLP using Kaplan-Meier analysis followed by a log-rank test. Other data were analyzed using Analysis of Variance (ANOVA) followed by Tukey multiple comparison test. Data are presented as mean ± SD values. In all cases the significance level adopted was 5% ($p < 0.05$).

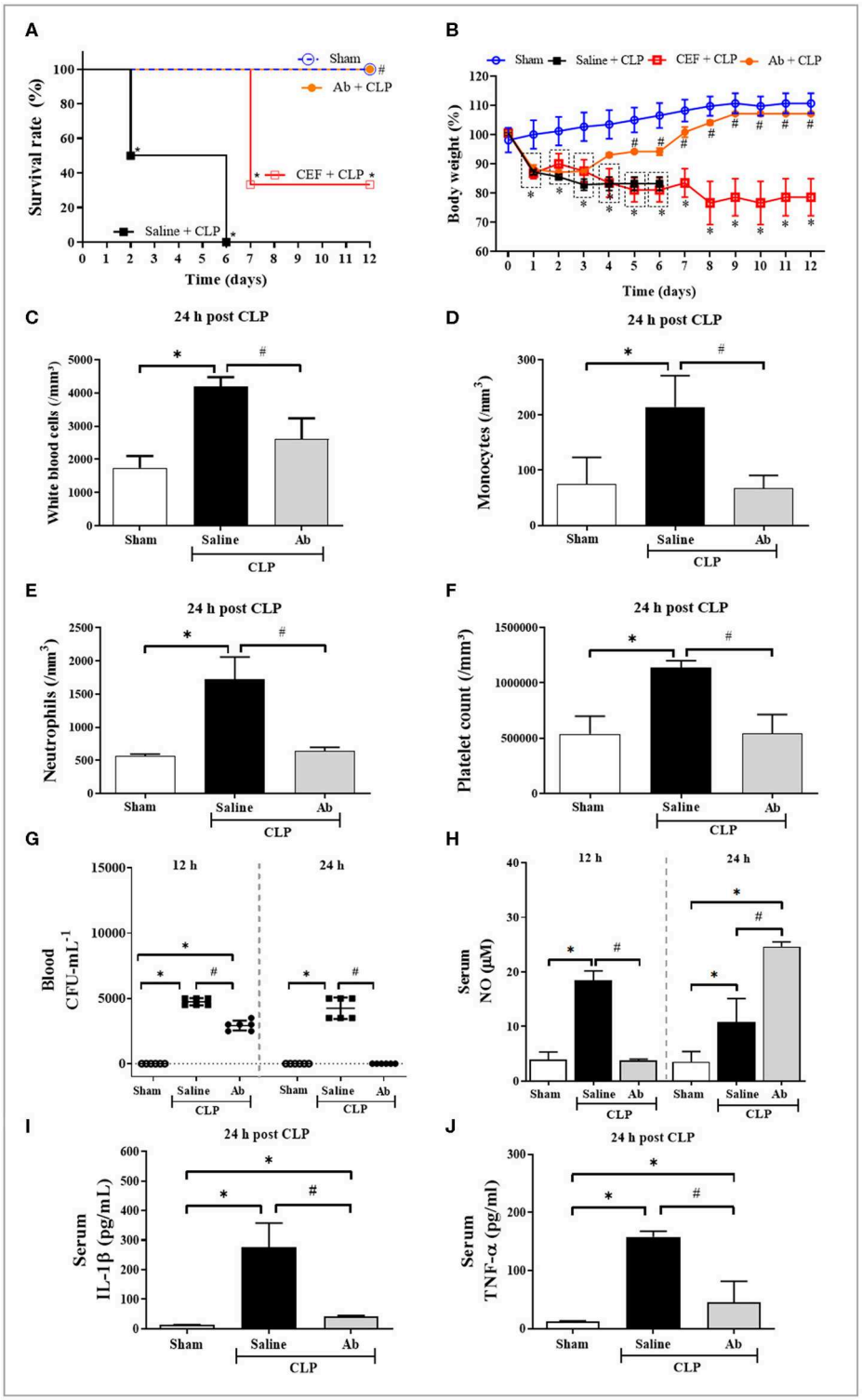

FIGURE 2 | Effects of *A. brasiliensis* aqueous extract on survival rate (%), body weight, hematological[[Inline Image]] parameters, bacterial burden, and systemic inflammatory response in septic mice. **(A)** Survival of septic animals pretreated with Ab (135 mg/kg), CEF (20 mg/Kg), or saline (0.9%). **(B)** Body weight during 12 days. **(C)** Total leukocyte counts 24 h post CLP. **(D)** Monocyte counts 24 h post CLP. **(E)** Neutrophil counts 24 h post CLP. **(F)** Platelet counts 24 h post CLP. **(G)** Bacterial load in the blood 12 and 24 h post CLP. **(H)** NO levels 12 h and 24 h after CLP. **(I)** IL-1β and **(J)** TNF-α levels in serum of septic animals 24 h post CLP. Data presented as mean ± SD. (*$p < 0.05$ Saline-CLP or Ab-CLP vs. Sham; #$p < 0.05$ Ab-CLP vs. Saline-CLP).

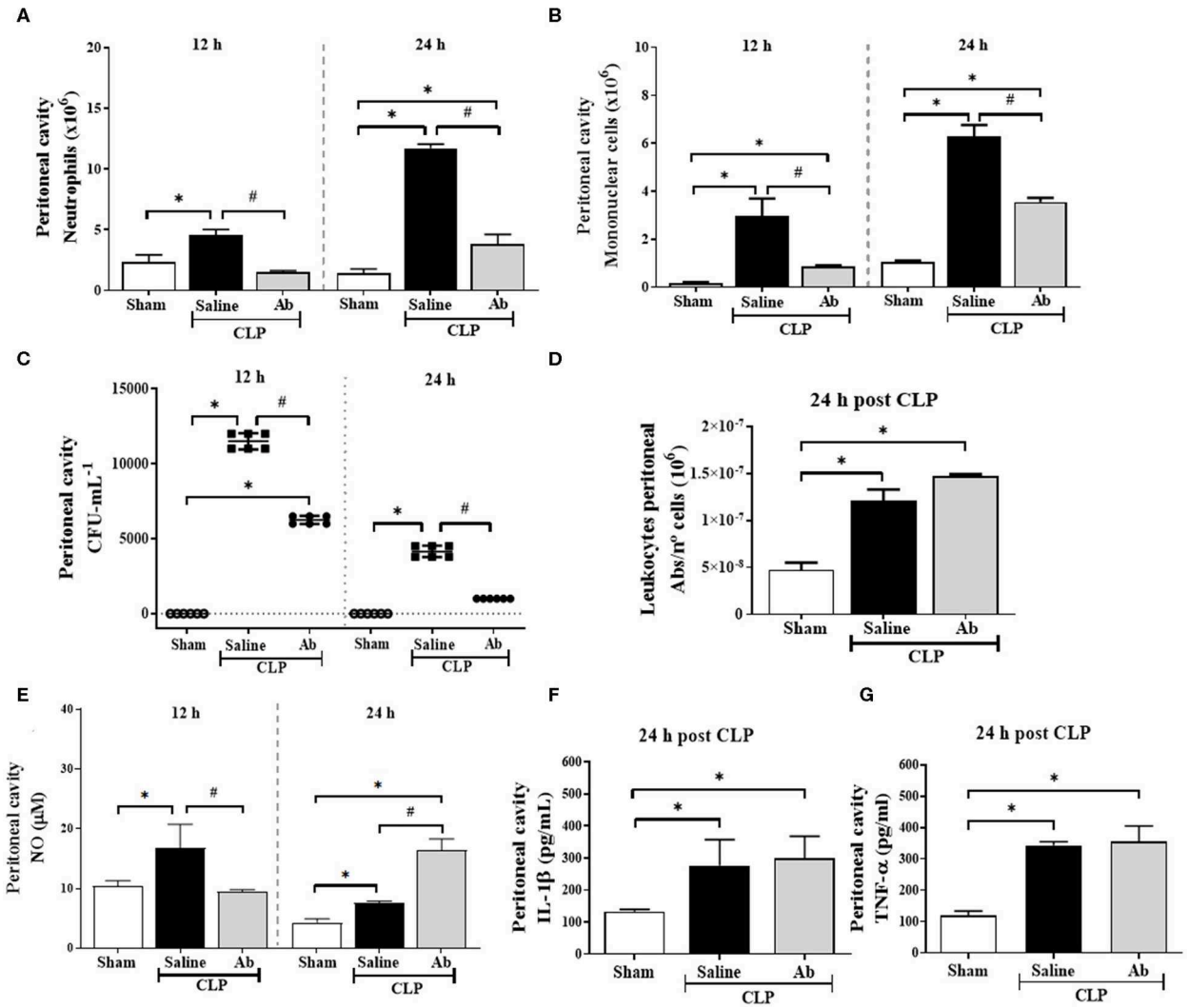

FIGURE 3 | Effects of *A. brasiliensis* aqueous extract on microbicidal activity, cell migration, bacterial burden, and inflammatory mediators in the peritoneal cavity of septic mice. **(A)** Neutrophils, **(B)** mononuclear cells count and **(C)** CFU quantification in the peritoneal cavity of septic mice at 12 and 24 h post CLP. **(D)** *In vitro* phagocytic activity of zymosan particles by phagocytic peritoneal cells from septic animals after 24 h of CLP induction. **(E)** Nitric oxide, **(F)** IL-1β and **(G)** TNF-α levels in the peritoneal lavage fluid of septic mice. Data presented as mean ± SD. (*$p < 0.05$ Saline-CLP or Ab-CLP vs. Sham; #$p < 0.05$ Ab-CLP vs. saline-CLP).

RESULTS

Aqueous Extract of *A. brasiliensis* Improve Survival and Inflammatory Systemic Markers in Septic Mice

As showed in **Figure 2A**, saline-pretreated septic mice (saline-CLP) died within six days, while 100% of Ab-pretreated septic animals (Ab-CLP) survived up to 12 days after CLP induction. Moreover, ceftriaxone-pretreated CLP group showed only 40% survival until 12th day. Regarding hematological parameters and inflammatory mediators, mice from saline-CLP group showed a significant augment in the number of circulating total leukocytes (**Figure 2C**), monocytes (**Figure 2D**), neutrophils (**Figure 2E**), and platelets (**Figure 2F**). Moreover, CLP increased the systemic levels of NO (**Figure 2H**), IL-1β (**Figure 2I**), and TNF-α (**Figure 2J**). On the other hand, Ab-CLP group maintained normal hematological parameters compared to sham group (**Figures 2C–F**). These animals produced low systemic levels of NO at 12 h of infection compared to saline-CLP group, increasing this production at 24 h post infection (**Figure 2H**). In addition, the pretreatment with Ab extract leads to a complete control of bacteremia 24 h post infection (**Figure 2G**), associated with an augment in NO (**Figure 2H**), and a significant decrease in IL-1β (**Figure 2I**) and TNF-α (**Figure 2J**) levels in septic animals.

Aqueous Extract of *A. brasiliensis* Modulate Inflammatory Response and Increase Bacterial Killing

Septic mice showed a significant increase in neutrophil and mononuclear cell recruitment to the peritoneal cavity at 12 h after sepsis induction (**Figures 3A,B**), as well as high bacterial load (**Figure 3C**) and increased NO levels (**Figure 3E**). In addition,

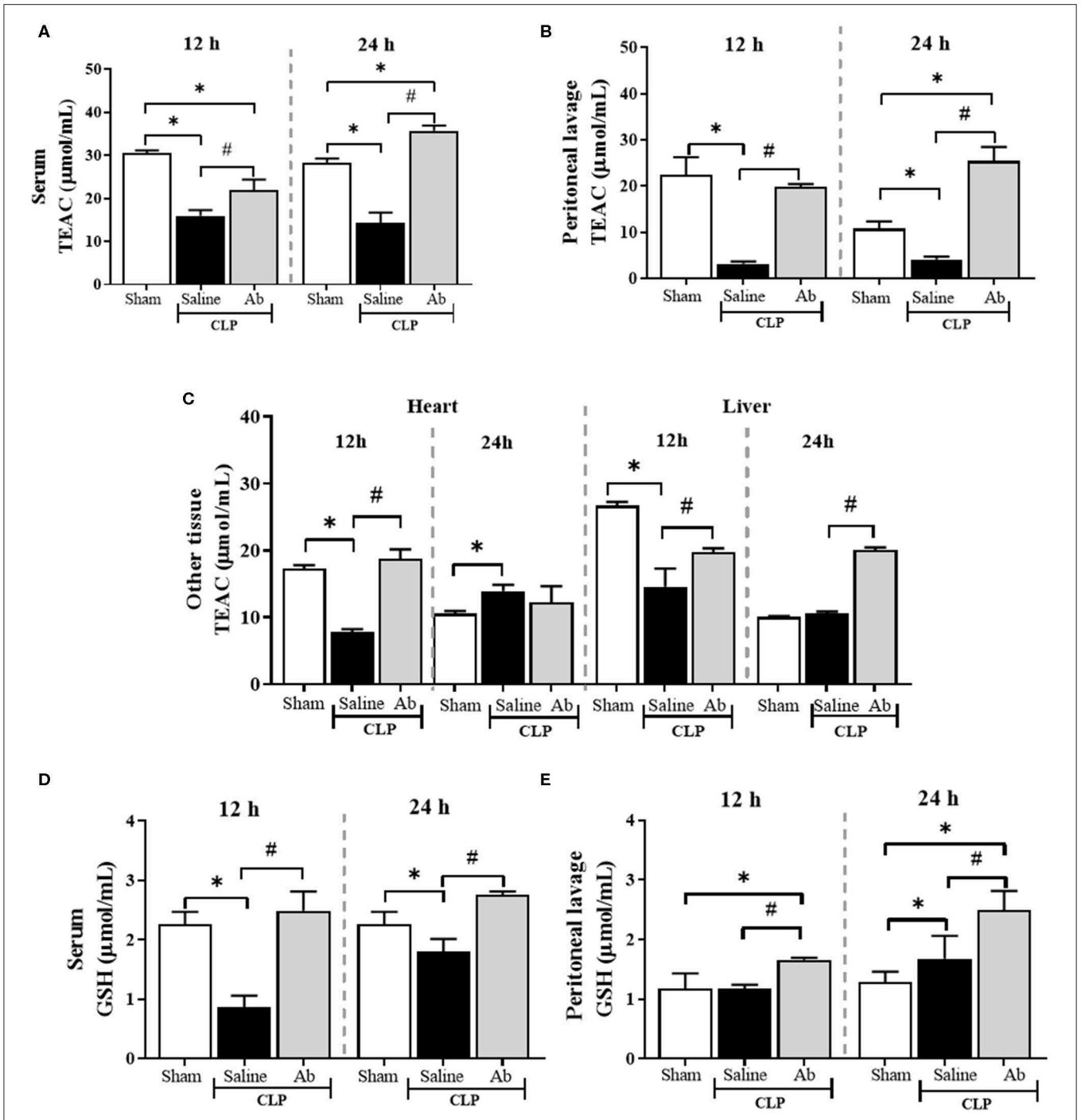

FIGURE 4 | Effects of aqueous extract of *A. brasiliensis* on antioxidant parameters of septic mice 12 and 24 h after CLP. **(A)** TEAC in serum. **(B)** TEAC in the peritoneal lavage fluid. **(C)** TEAC levels in heart and liver. **(D)** GSH levels in serum. **(E)** GSH levels in peritoneal lavage fluid. The results were expressed as the mean ± SD. (*$p < 0.05$ Saline-CLP or Ab-CLP vs. Sham; #$p < 0.05$ Ab-CLP vs. saline-CLP).

at 24 h, these animals presented significant amount of NO (**Figure 3E**), IL-1β (**Figure 3F**), and TNF-α (**Figure 3G**) into peritoneal fluid and recruited cells showed increased phagocytic ability compared to that from sham group (**Figure 3D**). However, Ab-CLP group, at 12 h, showed a significant reduction in the influx of neutrophils and mononuclear cells (**Figures 3A,B**) and in NO production (**Figure 3E**) compared to saline-CLP animals. On the other hand, at 24 h post CLP, the Ab-CLP group showed an increase in NO production in the peritoneal fluid (**Figure 3E**), without alteration in phagocytosis (**Figure 3D**),

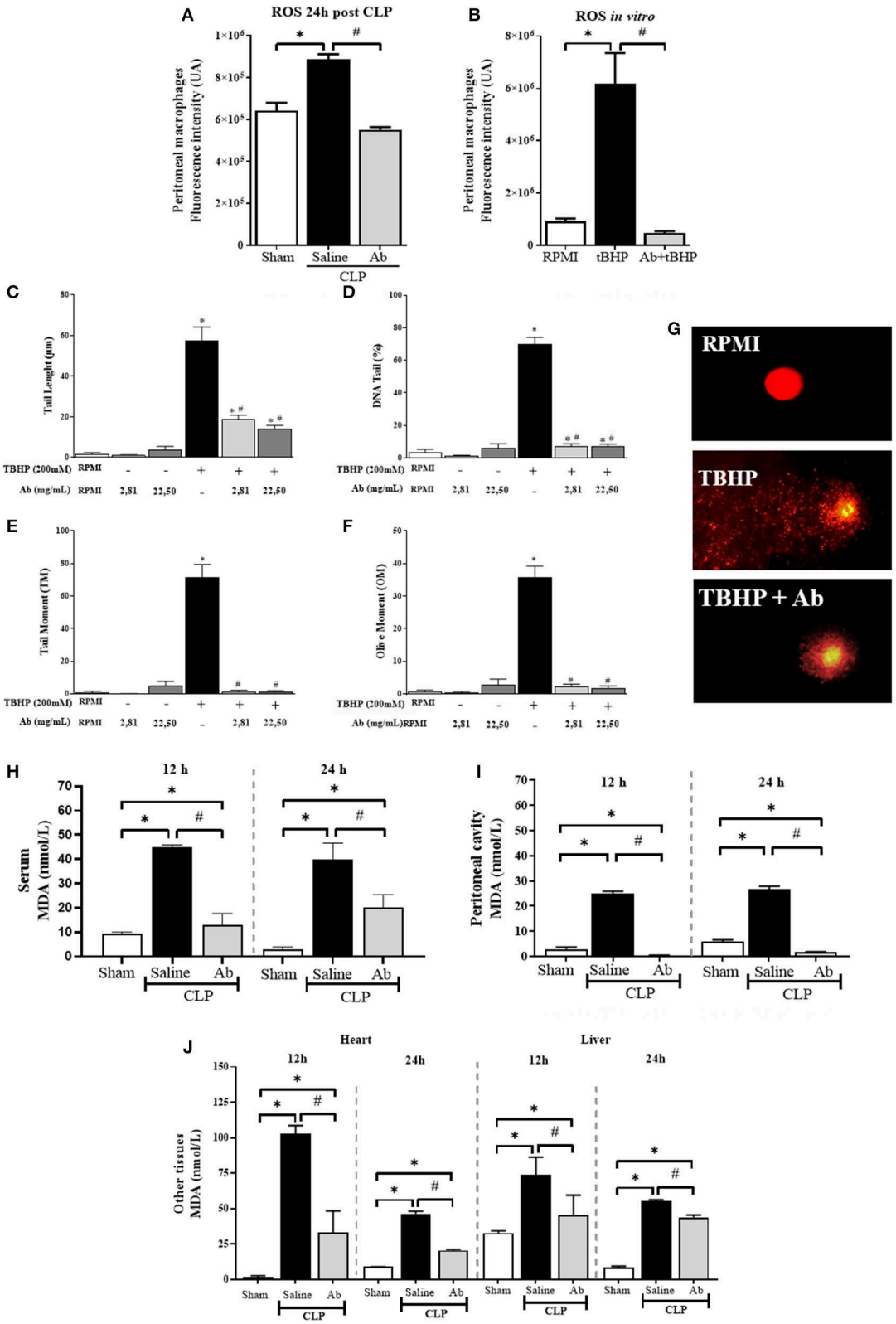

FIGURE 5 | Effects of aqueous extract of *A. brasiliensis* on oxidative and genotoxic parameters of septic mice. **(A)** ROS production by peritoneal cells collected from septic animals 24 h after CLP induction. **(B)** ROS production by thioglycollate-elicited peritoneal macrophages after *in vitro* incubation with tBHP or tBHP plus Ab

(Continued)

FIGURE 5 | (22.5 mg/mL) **(C)** Tail length (μm), **(D)** DNA tail (%), **(E)** Tail Moment (TM), **(F)** Olive Moment (OM) in peripheral blood mononuclear cells from healthy volunteers incubated *in vitro* with tBHP or tBHP plus *A. brasiliensis*. **(G)** Representative images of comet assay of human cells incubated in RPMI medium, RPMI plus tBHP and tBHP plus Ab, **(H)** MDA levels in serum, **(I)** MDA levels in peritoneal cavity, and **(J)** MDA levels in heart and liver at 12 and 24 h after CLP. The results were expressed as the mean ± SD. (*$p < 0.05$ Saline-CLP or Ab-CLP vs. Sham; #$p < 0.05$ Ab-CLP vs. saline-CLP).

TABLE 1 | MDA/TEAC ratios in samples from CLP-induced septic mice treated or not with *A. brasiliensis*.

MDA/TEAC (mean ± SD)					
Time	**Group**	**Serum**	**Peritoneal cavity**	**Heart**	**Liver**
12 h	Sham	0.30 ± 0.017	0.11 ± 0.001	0.07 ± 0.008	1.19 ± 0.026
	Saline-CLP	2.83 ± 0.18[a]	8.04 ± 1.135[a]	13.53 ± 0.178[a]	5.52 ± 0.416[a]
	Ab-CLP	0.51 ± 0.051[b]	0.02 ± 0.002[b]	2.15 ± 0.412[a,b]	1.94 ± 0.561[a,b]
24 h	Sham	0.08 ± 0.024	0.55 ± 0.017	0.83 ± 0.300	0.89 ± 0.013
	Saline-CLP	2.78 ± 0.004[a]	6.49 ± 0.833[a]	3.45 ± 0.120[a]	5.33 ± 0.076[a]
	Ab-CLP	0.50 ± 0.050[b]	0.05 ± 0.009[b]	1.66 ± 0.462[a,b]	2.20 ± 0.074[b]

[a]$p < 0.05$ *Saline-CLP or Ab-CLP vs. Sham.*
[b]$p < 0.05$ *Ab-CLP vs. Saline-CLP.*

IL-1β (**Figure 3F**), and TNF-α (**Figure 3G**), accompanied by inhibition of bacterial load (**Figure 3C**).

A. brasiliensis Increases the Antioxidant Status of Septic Mice

In general, the antioxidant defense state was lower in septic animals compared to control animals (**Figures 4A–D**). Twelve hours post CLP, TEAC levels were reduced in serum, peritoneal cavity, heart and liver of septic mice treated with saline. Regarding antioxidant capacity based on GSH, saline-CLP animals showed a decrease in serum GSH levels at 12 and 24 h (**Figure 4D**). On the other hand, the pretreatment with Ab extract was able to improve the antioxidant defense state of septic animals in all tissues at 12 and 24 h post CLP (**Figures 4A–E**), with exception of heart at 24 h.

Aqueous Extract of *A. brasiliensis* Reduce Oxidative Stress Markers and DNA Damage in Septic Animals

The *in vivo* treatment of septic mice with Ab caused significant inhibition in ROS production in response to infection (**Figure 5A**). In addition, Ab extract was also able to inhibit tBHP-induced ROS production *in vitro* by macrophages (**Figure 5B**), as well as tBHP-induced DNA damage in PBMC of health donors (**Figures 5C–G**). Regarding the most used lipid marker of oxidative stress, MDA levels were significantly increased in serum, peritoneal cavity, heart and liver of septic mice (**Figures 5H–J**). The pretreatment of animals with Ab caused strong decrease in MDA levels in all tissues evaluated, being completely inhibited in the peritoneal cavity, the main focus of bacteria (**Figures 5H–J**). These protective findings of *A. brasiliensis* were also demonstrated by the MDA/TEAC ratio (**Table 1**).

DISCUSSION

In the present study, we showed for the first time the immunomodulatory and antioxidant protective effect of prophylactic *A. brasiliensis* aqueous extract treatment in the CLP-induced sepsis. Ab protected mice against sepsis by increasing bacterial clearance and survival, maintaining normal hematological parameters. The pretreatment with Ab reduced the systemic levels of inflammatory cytokines (TNF-α, IL-1β), increased the antioxidant response in several organs and tissues (GSH and TEAC) with concomitant inhibition of oxidative damage (lipid peroxidation in serum, peritoneal cavity, heart and liver) of septic mice.

Ab is a basidiomycete mushroom considered nutraceutical. Our group have reported that Ab has bioactive compounds such as phytosterols, aromatic amino acids, flavonoids and phenolic compounds (33). Phenolic compounds have a high antioxidant capacity according to their structure, depending on the number and position of the hydroxyl and act through enzymatic inhibition or in the trace elements sequestration, reducing reactive species formation (34). In addition, the aqueous extract of Ab is rich in polysaccharides such as β-glucans (11), which can activate leukocytes and increase phagocytosis and antimicrobial activity (35, 36).

In this study, Ab improved the survival of septic mice by an immunomodulatory mechanism. Our data are in agreement with previous reports showing that oral supplementation of Ab improved Crohn's disease through the reduction of systemic pro-inflammatory cytokines such as IL-1β, IL-6 and G-CSF. In addition, patients with ulcerative colitis presented decreased levels of IL-2, IL-5 and MIP-1β after 21 days of consumption compared placebo group (37). Moreover, the antitumor effect in multiple myeloma and cervical cancer mediated by an immunomodulatory activity have been reported (38, 39). These antimicrobial, antioxidant and immunomodulation properties described in preclinical and

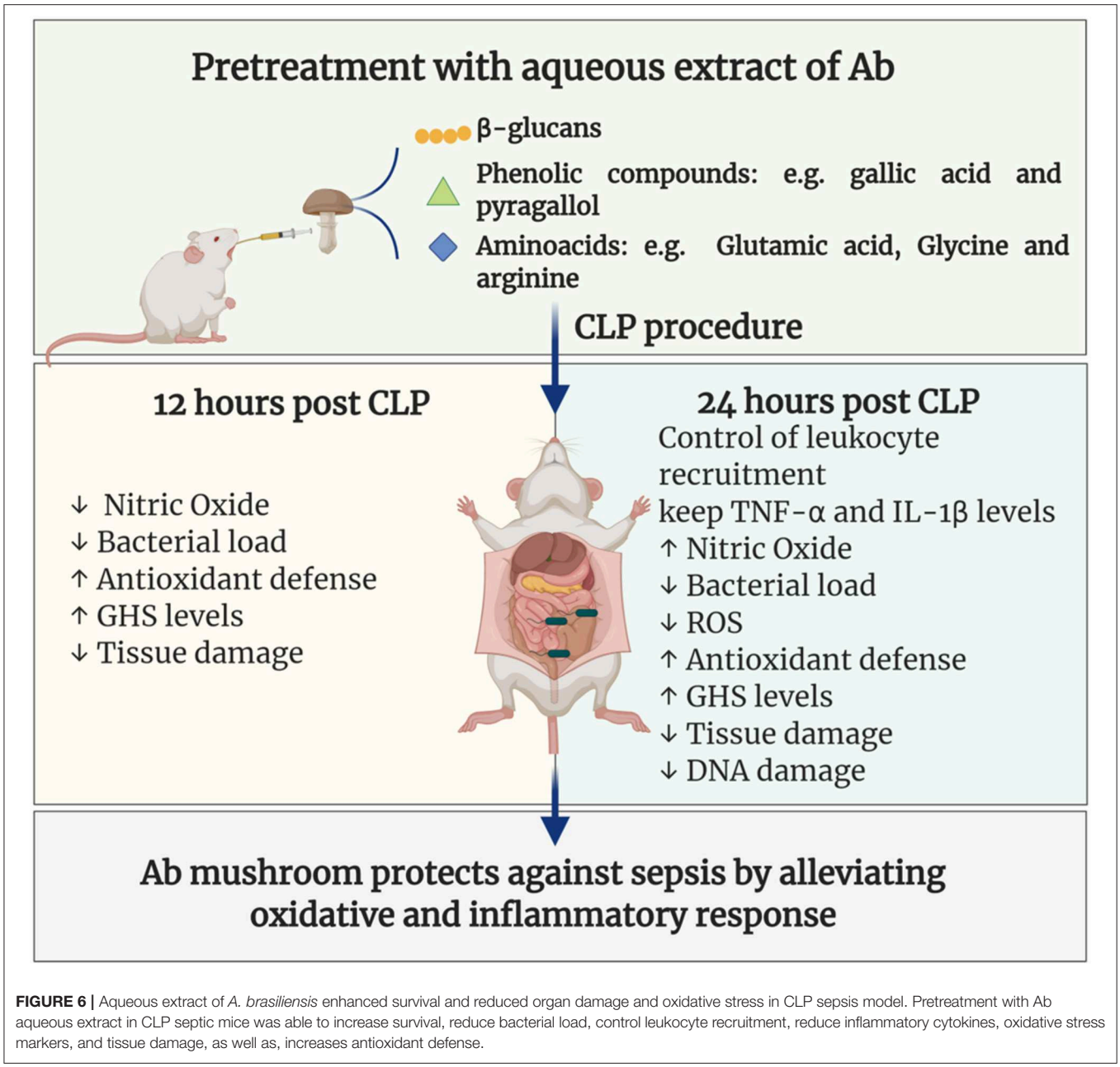

FIGURE 6 | Aqueous extract of *A. brasiliensis* enhanced survival and reduced organ damage and oxidative stress in CLP sepsis model. Pretreatment with Ab aqueous extract in CLP septic mice was able to increase survival, reduce bacterial load, control leukocyte recruitment, reduce inflammatory cytokines, oxidative stress markers, and tissue damage, as well as, increases antioxidant defense.

clinical studies with Ab supplementation may be associated with bioactive compounds found in mushroom, such as phenolic compounds, organic acids, amino acids and β-glucans (11, 12).

In sepsis, the pretreatment with antibiotics have a role to prevent complications such as systemic infections, reducing the mortality of patients (40). Here, the pretreatment with aqueous extract of Ab modulated the systemic and local release of proinflammatory cytokines, inhibited the leukocyte infiltration into peritoneal cavity, increased phagocytosis and NO production in infectious focus, leading to complete inhibition of bacterial burden in blood and peritoneal cavity. Smiderle et al. showed that the expression of proinflammatory cytokines (TNF-α and IL-1β) in LPS-stimulated THP-1 macrophages were inhibited by *in vitro* incubation with Ab-isolated β-glucans in presence of LPS (35). In addition, it was showed that the β-glucans negatively downregulated TLR-2 and TLR-4 receptors, decreasing exacerbated systemic immune system activation (41). It is important to point out that until now, there are no studies with *A. braziliensis* aqueous extract or any isolated compound in sepsis model.

In relation to the primary site of infection, Ab treatment modulated the inflammatory response into peritoneal cavity of septic mice, inducing almost complete bacterial burden elimination 24 h post CLP and a significant augment in NO

levels, without alterations in IL-1β and TNF-α levels in relation to CLP-saline treated mice. In agreement, it was demonstrated that (16)-β-D-glucans activates dectin-1 receptors in monocytes, neutrophils and dendritic cells leading to phosphorylation of Syk and activation of CARD9/Bcl10/MALT-1 4 with consequent augment in phagocytic capacity and increased generation of ROS and RNS (42). Furthermore, according to Vitak et al., Ab is rich in arginine, a precursor to nitric oxide production by NO synthases responsible for the conversion of L-arginine to NO and L-citrulline (43).

Studies have shown that NO has dual effect during sepsis. NO contributes to elimination of pathogens through DNA nitrosation and desamination and inhibiting the action of bacterial DNA repair enzymes at the site of infection (44). On the other hand, studies have shown that NO modulates the expression of adhesion molecules and reduces leukocyte recruitment which can lead to microvascular dysfunction (45). However, although pretreatment with Ab reduced migration of leukocytes we observed an increase in NO levels and decreased bacterial burden. This may be due to the immunomodulatory property of Ab which might be correlated with increased phagocytic capacity and mechanisms reported above (44).

In addition, in sepsis the uncontrolled inflammatory response can cause oxidative stress, that plays a critical role in the pathogenesis and dysfunctions in multiple organs (46). In this respect our data showed that macrophages from septic animals produce higher levels of ROS compared to cells from sham or *Ab* treated animals. Moreover, *Ab* was able to inhibit the production of ROS by macrophages stimulated *in vitro* with tBHP, and also tBHP-induced DNA damage in human PBMC. In this context, Angeli et al. reported that the pretreatment with β-glucans extracted from Ab presented protective effect in human hepatic cells against the genotoxic and mutagenic effects of carcinogenic compound (Benzo[a]Pyrene) (47).

In septic patients, MDA levels are elevated and may be correlated with clinical worsening (48, 49). In our study, the levels of lipid peroxidation were significantly decreased in serum, peritoneal cavity, heart and liver of septic animals treated with Ab. These results are in agreement with evidences showing that the association of oxidative stress with systemic abnormalities in microcirculatory blood flow lead to cardiovascular and hepatic changes, that contributes to the high mortality of patients (50). In fact, Yan et al. reported that in CLP model, liver tissue damage starts ∼1 h after sepsis, while cardiac dysfunction starts at 6 h (50).

In relation to the antioxidant defense, decreased levels of GSH and the inhibition of total antioxidant capacity are associated with organ failure and high mortality in sepsis (51). In contrast to septic animals, *Ab*-treated animals showed increased TEAC and GSH levels in serum and peritoneal cavity, and also enhanced antioxidant capacity in heart in liver tissues, as well as increased MDA/TEAC ratios in serum, peritoneal cavity, heart and liver, suggesting that the protective effect of *Ab* in CLP model is at least in part due to its antioxidant property.

Recently, De Souza et al. showed that the treatment of adjuvant-induced arthritic rats with Ab aqueous extract, at dose of 400 mg/kg, cause significant decrease in lipid damage in liver, brain, and plasma of treated rats. Moreover, the extract maintained the antioxidant defense, preserving the levels of reduced glutathione and protein thiol (52). In this line, it was demonstrated that in diabetic rats, the administration of Ab restored superoxide dismutase, catalase, and gluthatione peroxidase activity (43). This ability may be, at least in part, due to the presence of glutamic acid and glycine in Ab, since these amino acids are precursors of GSH synthesis, where glutamic acid reacts with cysteine to produce γ-glutamylcysteine (GCS) and subsequently reacts with glycine to form GSH (11, 53).

CONCLUSION

In conclusion, it was showed for the first time that the pretreatment with *Ab* aqueous extract was able to increase the survival of septic animals by a mechanism involving immunomodulatory and antioxidant protective effects as summarized in **Figure 6**. Further studies are needed to better elucidate the immunomodulatory mechanisms and ensure the safety of their clinical use.

DATA AVAILABILITY STATEMENT

The datasets generated for this study are available on request to the corresponding author.

ETHICS STATEMENT

This study was carried out in strict accordance with the recommendations of the Guide for the Care and Use of Laboratory Animals of the Brazilian National Council of Animal Experimentation (http://www.sbcal.org.br/) and the NIH Guidelines for the Care and Use of Laboratory Animals. The institutional Committee for Animal Ethics of Federal University of Pará/UFPA (CEUA, Protocol: 02/15) approved all the procedures used in this study. The *in vitro* tests, human venous blood was collected from healthy volunteers signing the Informed Consent Form (ICF). This study was approved by the Institutional Committee of Ethics in Research involving human beings from the health sciences sector of UFPA (CEP-ICS/UFPA), under n° 3544380 and CAAE 12776619.0.0000.0018.

AUTHOR CONTRIBUTIONS

KN-L and MM designed the study. KN-L, VM, AO, SF, and JO conducted most of the experiments and wrote the main manuscript. HS and VS donated *Agaricus brasiliensis*. CR and JR conducted oxidative stress assay. RS conducted most of the experiments. AP and PR performed quantification of cytokines corrected the manuscript. All authors read and approved the final manuscript.

FUNDING

This research was funded by Conselho Nacional de Desenvolvimento Científico e Tecnológico (CNPq),

Coordenação de Aperfeiçoamento de Pessoal de Nível Superior (CAPES), Fundação Amazônia Paraense de Amparo à Pesquisa (FAPESPA), and Federal University of Pará (UFPA). MM, AP, and PR are grateful to CNPq for the PQ productivity scholarship.

REFERENCES

1. World Health Organization. *Sepsis.* (2018). Available online at: https://www.who.int/news-room/fact-sheets/detail/sepsis (Accessed March 01, 2020).
2. Barros LLS, Maia CSF, Monteiro MC. Fatores de risco associados ao agravamento de sepse em pacientes em unidade de terapia intensiva. *Cad saúde colet.* (2016) 24:388–96. doi: 10.1590/1414-462x201600040091
3. Vincent JL, Jones G, David S, Olariu E, Cadwell KK. Frequency and mortality of septic shock in europe and north america: a systematic review and meta-analysis. *Crit Care.* (2019) 23:196. doi: 10.1186/s13054-019-2478-6
4. Gül F, Arslantaş MK, Cinel I, Kumar A. Changing definitions of sepsis. *Turk J Anaesthesiol Reanim.* (2017) 45:129–38. doi: 10.5152/TJAR.2017.93753
5. Nagar H, Piao S, Kim CS. Role of mitochondrial oxidative stress in sepsis. *Acute Crit Care.* (2018) 33:65–72. doi: 10.4266/acc.2018.00157
6. Kumar S, Gupta E, Srivastava VK, Kaushik S, Saxena J, Goyal LK, et al. Nitrosative stress and cytokines are linked with the severity of sepsis and organ dysfunction. *Br J Biomed Sci.* (2019) 76:29–34. doi: 10.1080/09674845.2018.1543160
7. Prauchner CA. Oxidative stress in sepsis: pathophysiological implications justifying antioxidant co-therapy. *Burns.* (2017) 43:471–85. doi: 10.1016/j.burns.2016.09.023
8. Ruiz S, Vardon-Bounes F, Merlet-Dupuy V, Conil JM, Buléon M, Fourcade O, et al. Sepsis modeling in mice: ligation length is a major severity factor in cecal ligation and puncture. *Intensive Care Med Exp.* (2016) 4:22. doi: 10.1186/s40635-016-0096-z
9. de Souza Gomes R, Navegantes-Lima KC, Monteiro VVS, de Brito Oliveira AL, Rodrigues DVS, Reis JF, et al. Salivary gland extract from *aedes aegypti* improves survival in murine polymicrobial sepsis through oxidative mechanisms. *Cells.* (2018) 7:182. doi: 10.3390/cells7110182
10. Carvajal AESS, Koehnlein EA, Soares AA, Eler GJ, Nakashima ATA, Bracht A, et al. Bioactives of fruiting bodies and submerged culture mycelia of *Agaricus brasiliensis* (*A. blazei*) and their antioxidant properties. *Food Sci Technol.* (2012) 46:493–9. doi: 10.1016/j.lwt.2011.11.018
11. Cho SM, Jang KY, Park HJ, Park JS. Analysis of the chemical constituents of *Agaricus brasiliensis*. *Mycobiology.* (2008) 36:50-54. doi: 10.4489/MYCO.2008.36.1.050
12. da Silva de Souza AC, Correa VG, Goncalves GA, Soares AA, Bracht A, Peralta RM. Agaricus blazei bioactive compounds and their effects on human health: benefits and controversies. *Curr Pharm Des.* (2017) 23:2807–34. doi: 10.2174/1381612823666170119093719
13. Navegantes KC, Albuquerque, RFV, Dalla-Santa HS, Soccol CR, Monteiro MC. *Agaricus brasiliensis* mycelium and its polysaccharide modulate the parameters of innate and adaptive immunity. *Food Agricult Immunol.* (2013) 24:393–408. doi: 10.1080/09540105.2012.691089
14. Rubel R, Santa HSD, Dos Santos LF, Fernandes LC, Figueiredo BC, Soccol CR. Immunomodulatory and antitumoral properties of *ganoderma lucidum* and *Agaricus brasiliensis* (Agaricomycetes) medicinal mushrooms. *Int J Med Mushrooms.* (2018) 20:393–403. doi: 10.1615/IntJMedMushrooms.2018025979
15. Akramiene D, Kondrotas A, Didziapetriene J, Kevelaitis E. Effects of beta-glucans on the immune system. *Medicina (Kaunas).* (2007) 43:597–606. doi: 10.3390/medicina43080076
16. Firenzuoli F, Gori L, Lombardo G. The medicinal mushroom *Agaricus blazei* murrill: review of literature and pharmaco-Toxicological problems. *Evid Based Complement Alternat Med.* (2008) 5:3–15. doi: 10.1093/ecam/nem007
17. Yim HS, Chye FY, Tan CT, Ng YC, Ho CW. Antioxidant activities and total phenolic content of aqueous extract of *pleurotus ostreatu*s (cultivated oyster mushroom). *Malays J Nutr.* (2010) 16:281–91.
18. Val CH, Brant F, Miranda AS, Rodrigues FG, Oliveira BCL, Santos EA, et al. Effect of mushroom *Agaricus blazei* on immune response and development of experimental cerebral malaria. *Malar J.* (2015) 14:1–13. doi: 10.1186/s12936-015-0832-y
19. González-Palma I, Escalona-Buendía HB, Ponce-Alquicira E, Téllez-Téllez M, Gupta VK, Díaz-Godínez G, et al. Evaluation of the antioxidant activity of aqueous and methanol extracts of *pleurotus ostreatus* in different growth stages. *Front Microbiol.* (2016) 7:1099. doi: 10.3389/fmicb.2016.01099
20. Dalla Santa HS, Rubel R, Vitola FMD, Leifa F, Tararthuch AL, Lima Filho Cavalcante JH, et al. Kidney function indices in mice after long intake of *Agaricus brasiliensis* mycelia (*Agaricus blazei*, *Agaricus subrufescens*) produced by solid state cultivation. *J Biol Sci.* (2009) 9:21–8. doi: 10.3844/ojbsci.2009.21.28
21. Song T, Yang M, Chen J, Huang L, Yin H, He T, et al. Prognosis of sepsis induced by cecal ligation and puncture in mice improved by anti-Clonorchis *sinensis cyclopholin* a antibodies. *Parasites Vec.* (2015) 8:1–10. doi: 10.1186/s13071-015-1111-z
22. D'Acampora AJ, Locks G de F. Median lethal needle caliber in two models of experimental sepsis. *Acta Cir Bras.* (2014) 29:1–6. doi: 10.1590/S0102-86502014000100001
23. Granger DL, Taintor RR, Boockvar KS, Hibbs JB. Measurement of nitrate and nitrite in biological samples using nitrate reductase and griess reaction. *Methods Enzymol.* (1996) 268:142–51. doi: 10.1016/s0076-6879(96)68016-1
24. Stuehr DJ, Marletta M A. Mammalian nitrate biosynthesis: mouse macrophages produce nitrite and nitrate in response to *escherichia coli* lipopolysaccharide. *Proc Natl Acad Sci USA.* (1985) 82:7738–42. doi: 10.1073/pnas.82.22.7738
25. Yamazaki RK, Bonatto SJR, Folador A, Pizatto N, Oliveira HHP, Vecchi R, et al. Lifelong exposure to dietary fish oil alters macrophage responses in walker 256 tumor-bearing rats. *Cell Immunol.* (2004) 231:56–62. doi: 10.1016/j.cellimm.2004.12.001
26. Albuquerque R V, Malcher NS, Amado LL, Coleman MD, Dos Santos DC, Borges RS, et al. *In vitro* protective effect and antioxidant mechanism of resveratrol induced by dapsone hydroxylamine in human cells. *PLoS ONE.* (2015) 10:e134768. doi: 10.1371/journal.pone.0134768
27. Kohn H, Liversedge M. On a new aerobic metabolite whose production by brain is inhibited by apomorphine, emetine, ergotamine, epinephrine, and menadione. *J Pharmacol Experimen Ther Nov.* (1944) 82:292–300.
28. Percario S, Vital A, Jablonka F. Dosagem do malondialdeido. *Newslab.* (1944) 2:46–50.
29. Miller NJ, Rice-evans C, Davies M, Gopinathan V, Milner A. A novel method for measuring antioxidant capacity and its application to monitoring the antioxidant status in premature neonates. *Clin Sci.* (1993) 84:407–12. doi: 10.1042/cs0840407
30. Re R, Pellegrini N, Proteggente A, Pannala A, Yang M, Rice-Evans C. Antioxidant activity applying an improved aBTS radical cation decolorization assay. *Free Radic Biol Med.* (1999) 26:1231–7. doi: 10.1016/s0891-5849(98)00315-3.36
31. Ellman GL. Tissue sulfhydryl groups. *Arch Biochem Biophys.* (1959) 82:70–7. doi: 10.1016/0003-9861(59)90090-6
32. Ferreira-Cravo M, Piedras FR, Moraes TB, Ferreira JLR, de Freitas DPS, Machado MD, et al. Antioxidant responses and reactive oxygen species generation in different body regions of the estuarine polychaeta *Laeonereis acuta* (Nereididae). *Chemosphere.* (2008) 66:1367–74. doi: 10.1016/j.chemosphere.2006.06.050
33. de Oliveira FM, Mokochinski JB, Reyes Torres Y, Dalla Santa HS, González-Borrero PP. Photoacoustic spectroscopy applied to the direct detection of bioactive compounds in *Agaricus brasiliensis* mycelium. *J Biol Phys.* (2018) 44:93-100. doi: 10.1007/s10867-017-9478-z
34. Minatel IO, Borges CV, Ferreira MI, Gomez HAG, Chen C-YO, Lima GPP. Phenolic compounds: functional properties, impact of processing and bioavailability. *Phenolic Compd - Biol Act.* (2017) 1:1–24 doi: 10.5772/66368
35. Smiderle FR, Alquini G, Tadra-Sfeir MZ, Iacomini M, Wichers HJ, Van Griensven LJLD. *Agaricus bisporus* and *Agaricus brasiliensis* (1 → 6)-β-d-glucans show immunostimulatory activity on

human THP-1 derived macrophages. *Carbohydr Polym.* (2013) 94:91–9. doi: 10.1016/j.carbpol.2012.12.073
36. Yamanaka D, Tada R, Adachi Y, Ishibashi K, Motoi M. *Agaricus brasiliensis*-derived β-glucans exert immunoenhancing effects via a dectin-1-dependent pathway. *Int Immunopharmacol. Elsevier B.V.* (2012) 14:311–9. doi: 10.1016/j.intimp.2012.07.017
37. Therkelsen SP, Hetland G, Lyberg T, Lygren I, Johnson E. Effect of the medicinal *Agaricus blazei* murill-Based mushroom extract, andoSanTM, on symptoms, fatigue and quality of life in patients with crohn's disease in a randomized single-Blinded placebo controlled study. *PLoS ONE.* (2016) 11:e159288. doi: 10.1371/journal.pone.0159288
38. Tangen JM, Tierens A, Caers J, Binsfeld M, Olstad OK, Trøseid A-MS, et al. Immunomodulatory effects of the *Agaricus blazei* murrill-based mushroom extract andoSan in patients with multiple myeloma undergoing high dose chemotherapy and autologous stem cell transplantation: a randomized, double blinded clinical study. *Biomed Res Int.* (2015) 2015:1–11. doi: 10.1155/2015/718539
39. Ahn W-S, Kim D-J, Chae G-T, Lee J-M, Bae S-M, Sin J-I, et al. Natural killer cell activity and quality of life were improved by consumption of a mushroom extract, *Agaricus blazei* murill kyowa, in gynecological cancer patients undergoing chemotherapy. *Int J Gynecol Cancer.* (2004) 14:589–94. doi: 10.1111/j.1048-891X.2004.14403.x
40. Mourad MM, Evans R, Kalidindi V, Navaratnam R, Dvorkin L, Bramhall SR. Prophylactic antibiotics in acute pancreatitis: endless debate. *Ann R Coll Surg Engl.* (2017) 99:107–12. doi: 10.1308/rcsann.2016.0355
41. Shah VB, Williams DL, Keshvara L. beta-Glucan attenuates tLR-2 and tLR4-mediated cytokine production by microglia. *Neurosci Lett.* (2009) 458:111–5. doi: 10.1016/j.neulet.2009.04.039
42. Camilli G, Tabouret G, Quintin J. The complexity of fungal β-Glucan in health and disease: effects on the mononuclear phagocyte system. *Front Immunol.* (2018) 9:673. doi: 10.3389/fimmu.2018.00673
43. Vitak TY, Wasser SP, Nevo E, Sybirna NO. Effect of medicinal mushrooms on l-arginine / nO system in red blood cells of streptozotocin-induced diabetic rats. *Adv Diab Metab.* (2016) 4:25–31. doi: 10.13189/adm.2016.040201
44. Kutty SK, Ho KKK, Kumars N. Nitric oxide donors as antimicrobial agents. In: Seabra AB, editor. *Nitric Oxide Donors*. Cambridge: Elsevier (2017). p. 169–89. doi: 10.1016/B978-0-12-809275-0.00007-7
45. Benjamim CF, Silva JS, Fortes ZB, Oliveira MA, Ferreira SH, Cunha FQ. Inhibition of leukocyte rolling by nitric oxide during sepsis leads to reduced migration of active microbicidal neutrophils. *Infect Immun.* (2002) 70:3602–10. doi: 10.1128/IAI.70.7.3602-3610.2002
46. Luan YY, Dong N, Xie M, Xiao XZ, Yao YM. The significance and regulatory mechanisms of innate immune cells in the development of sepsis. *J Interf Cytokine Res.* (2014) 34:2–15. doi: 10.1089/jir.2013.0042
47. Angeli JPF, Ribeiro LR, Bellini MF, Mantovani MS. Beta-Glucan extracted from the medicinal mushroom *Agaricus blazei* prevents the genotoxic effects of benzo[a]pyrene in the human hepatoma cell line hepG2. *Arch Toxicol.* (2009) 83:81–6. doi: 10.1007/s00204-008-0319-5
48. Weiss SL, Deutschman CS. Elevated malondialdehyde levels in sepsis - something to "stress" about? *Crit Care.* (2014) 18:125. doi: 10.1186/cc13786
49. Lorente L, Martín MM, Abreu-González P, Domínguez-Rodríguez A, Labarta L, Díaz C, et al. Prognostic value of malondialdehyde serum levels in severe sepsis: a multicenter study. *PLoS ONE.* (2013) 8:e53741. doi: 10.1371/journal.pone.0053741
50. Yan J, Li S, Li S. The role of the liver in sepsis. *Int Rev Immunol.* (2014) 33:498–510. doi: 10.3109/08830185.2014.889129
51. Kim JS, Kwon WY, Suh GJ, Kim KS, Jung YS, Kim SH, et al. Plasma glutathione reductase activity and prognosis of septic shock. *J Surg Res.* (2016) 200:298–307. doi: 10.1016/j.jss.2015.07.044
52. de Souza ACDS, Gonalves GA, Soares AA, de Sá-Nakanishi AB, de Santi-Rampazzo AP, Natali MRM, et al. Antioxidant action of an aqueous extract of royal sun medicinal mushroom, *Agaricus brasiliensis* (Agaricomycetes), in rats with adjuvant-Induced arthritis. *Int J Med Mushrooms.* (2018) 20:101–17. doi: 10.1615/IntJMedMushrooms.2018025309
53. Salyha NO. Effects of l-glutamic acid and pyridoxine on glutathione depletion and lipid peroxidation generated by epinephrine-induced stress in rats. *Ukr.Biochem.J.* (2018) 90:102–10. doi: 10.15407/ubj90.04.102

Conflict of Interest: The authors declare that the research was conducted in the absence of any commercial or financial relationships that could be construed as a potential conflict of interest.

frontiers in Immunology

REVIEW
published: 07 July 2020
doi: 10.3389/fimmu.2020.01364

CD4 T Cell Responses and the Sepsis-Induced Immunoparalysis State

Matthew D. Martin[1], *Vladimir P. Badovinac*[2,3,4] *and Thomas S. Griffith*[1,5,6,7,8]*

[1] Department of Urology, University of Minnesota, Minneapolis, MN, United States, [2] Department of Pathology, University of Iowa, Iowa City, IA, United States, [3] Interdisciplinary Graduate Program in Immunology, University of Iowa, Iowa City, IA, United States, [4] Department of Microbiology and Immunology, University of Iowa, Iowa City, IA, United States, [5] Microbiology, Immunology, and Cancer Biology PhD Program, University of Minnesota, Minneapolis, MN, United States, [6] Center for Immunology, University of Minnesota, Minneapolis, MN, United States, [7] Masonic Cancer Center, University of Minnesota, Minneapolis, MN, United States, [8] Minneapolis VA Healthcare System, Minneapolis, MN, United States

Sepsis remains a major cause of death in the United States and worldwide, and costs associated with treating septic patients place a large burden on the healthcare industry. Patients who survive the acute phase of sepsis display long-term impairments in immune function due to reductions in numbers and function of many immune cell populations. This state of chronic immunoparalysis renders sepsis survivors increasingly susceptible to infection with newly or previously encountered infections. CD4 T cells play important roles in the development of cellular and humoral immune responses following infection. Understanding how sepsis impacts the CD4 T cell compartment is critical for informing efforts to develop treatments intended to restore immune system homeostasis following sepsis. This review will focus on the current understanding of how sepsis impacts the CD4 T cell responses, including numerical representation, repertoire diversity, phenotype and effector functionality, subset representation (e.g., Th1 and Treg frequency), and therapeutic efforts to restore CD4 T cell numbers and function following sepsis. Additionally, we will discuss recent efforts to model the acute sepsis phase and resulting immune dysfunction using mice that have previously encountered infection, which more accurately reflects the immune system of humans with a history of repeated infection throughout life. A thorough understanding of how sepsis impacts CD4 T cells based on previous studies and new models that accurately reflect the human immune system may improve translational value of research aimed at restoring CD4 T cell-mediated immunity, and overall immune fitness following sepsis.

Keywords: CD4 T cell, sepsis, immunoparalysis, adaptive immunity, therapy

OPEN ACCESS

Edited by:
Peter Katsikis,
Erasmus University Rotterdam, Netherlands

Reviewed by:
Tara Marlene Strutt,
University of Central Florida, United States
Karl Kai McKinstry,
University of Central Florida, United States

***Correspondence:**
Thomas S. Griffith
tgriffit@umn.edu

Specialty section:
This article was submitted to Immunological Memory, a section of the journal Frontiers in Immunology

Received: *01 April 2020*
Accepted: *28 May 2020*
Published: *07 July 2020*

Citation:
Martin MD, Badovinac VP and Griffith TS (2020) CD4 T Cell Responses and the Sepsis-Induced Immunoparalysis State. Front. Immunol. 11:1364. doi: 10.3389/fimmu.2020.01364

INTRODUCTION

Sepsis is life-threatening organ dysfunction that results from an exaggerated host immune response to disseminated infection (1). It is characterized (in part) by increased production of both pro- and anti-inflammatory cytokines, resulting in transient severe lymphopenia and long-lasting immune dysfunction (2). Each year at least 1.7 million adult Americans develop sepsis and nearly 270,000 Americans die as a result of sepsis (3). Hospital costs associated with treating sepsis total >$23 billion each year, making it the most expensive condition treated in the U.S. (4). Due to advances

in medical care, the majority (∼75%) of today's septic patients survive the cytokine storm that results from the initial septic event (5). However, surviving patients suffer from a long-lasting state of immune dysfunction termed immunoparalysis and display increased susceptibility to secondary infection, increased viral reactivation, and decreased 5-year survival compared to individuals who did not develop sepsis (6–8).

The first signs of immunoparalysis can be seen during and shortly after resolution of the cytokine storm in the numerical loss of many cell types, but most notably lymphocytes (9). Lymphocyte numbers recover after resolution of the cytokine storm, but the functional capacity of lymphocytes that reconstitute the immune system is impaired for an extended period (10). Therefore, experimental therapies aimed at alleviating sepsis-induced immunoparalysis have focused on reducing cell loss, increasing numerical recovery, and restoring function of cells that repopulate the immune system (11). Experimental mouse models have been instrumental in informing our knowledge of the impact of sepsis on the immune system and the benefits of perspective therapies for promoting recovery of immune cell numbers and function. However, the translational value of mouse studies depends on how accurately they reflect the human condition (12, 13), and recent studies have highlighted how some aspects of the immune response in inbred, SPF mice do not accurately reflect the immune response in the outbred, non-SPF human population. For example, studies conducted in outbred Swiss Webster mice have shown how inbred mice fail to reflect variation in immune outcomes seen in a genetically diverse population more similar to the human population (14–16). Additionally, studies using microbially-experienced pet store mice or laboratory mice cohoused with pet store mice (a.k.a. "dirty mice") have shown that exposure to a diverse array of pathogens shapes the immune system. Notably, in contrast to SPF mice that possess an immune system more similar to infants, the immune system of dirty mice more closely resembles that of adult humans (17–21). These studies suggest that incorporating genetic diversity and/or a history of diverse pathogen exposures may improve the translational value of experimental models.

This review will focus on our understanding of how CD4 T cells are impacted by sepsis and how changes within the CD4 T cell compartment affect overall immune fitness. To provide context for this, we will begin with an overview of the effects of sepsis on immune cell subsets, and end with a discussion of therapeutic strategies to alleviate sepsis-induced immunoparalysis, and implications of recent mouse studies that more accurately model sepsis in humans.

EFFECTS OF SEPSIS ON IMMUNE CELL SUBSETS

Sepsis causes a seismic shift in representation and function of immune cell subsets (**Figure 1**), which contributes to both the pathophysiology of sepsis and resulting immunoparalysis. Sepsis is initially characterized by leukocytosis in the first 2–4 days, with marked increases in neutrophil and monocyte populations, which is followed quickly by a state of lymphopenia (22, 23). Lymphocyte populations are especially susceptible to apoptosis, and numbers of B cells and CD4 and CD8 T cells are markedly reduced following sepsis onset (9, 23–29). Failure to normalize cell numbers during either the stages of leukocytosis or lymphopenia is associated with increased mortality. In surviving patients, cell numbers return to normal within a month, but failure to prevent viral reactivation and reduced effectiveness at handling new infections suggests long-lasting functional impairments (6–8).

Due to the important roles they play in initial pathogen recognition and response and orchestration of adaptive immune responses, defects in innate immune cells including monocytes/macrophages, neutrophils, NK cells, and dendritic cells (DCs) greatly impact overall immune fitness. Unlike monocytes/macrophages and neutrophils, numbers and on-per-cell basis function of NK cells and DCs initially decline following sepsis (9, 23, 30, 31). RNA-sequencing has revealed that multiple immune-response pathways are down-regulated in monocytes of sepsis patients (32), and mass cytometry (CyTOF), which allows for simultaneous analysis of more parameters than conventional flow cytometry, has shown that monocytes of sepsis patients have increased expression of the inhibitory ligand PD-L1 and decreased expression of HLA-DR (33). Considering that increased expression of inhibitory molecules BTLA and PD-1 on monocytes/macrophages following sepsis has been shown to impact bacterial clearance (34, 35), these findings suggest that alterations in monocytes/macrophages contribute to defective host innate immunity resulting from sepsis. Additionally, decreased expression of HLA-DR could reduce the ability of monocytes/macrophages to present antigen (Ag) and prime B and T cell responses, so these data also suggest that alterations in monocytes/macrophages may also contribute defective host adaptive immunity resulting from sepsis. NK cells that remain following sepsis have a reduced ability to produce the effector cytokine IFN-γ in response to inflammatory cytokines IL-12 and IL-18 or following infection, as well as the reduced ability to degranulate and execute cytolytic activity following Ly49H receptor-mediated activation. Consequently, these numerical and functional defects resulting from sepsis lead to decreased NK cell-mediated control of viral infection (30). In addition, DCs present following sepsis have a decreased ability to produce "signal 3" cytokines (e.g., IFN-γ) in response to TLR stimulation or pathogen challenge, and to prime T cell responses (31, 36). Taken together, these studies suggest that defects in innate immune cell subsets following sepsis contribute to immunoparalysis through both reduced innate antimicrobial activity and decreased ability to stimulate adaptive immune responses (**Figure 1**).

In addition to quantitative and qualitative alterations in multiple innate immune cell populations, it has become clear that cell-intrinsic defects in B cells and T cells also persist following sepsis (**Figure 1**). Sepsis results in reduced representation of immature B cells and increased representation of mature B cells, with increased numbers of plasma cells and shifts in representation of B1 and B2 B cells (29, 36, 37). Despite increased plasma cell numbers, Ag-specific antibody production

is impaired following sepsis (36–38), suggesting sepsis decreases host ability to develop Ag-specific plasma cells. Following sepsis, CD8 T cells have a reduced ability to prevent infection (39), which is likely due to many factors. Recovery of naïve CD8 T cells following sepsis is incomplete, resulting in loss of some precursor specificities and inability to form responses to some newly encountered Ags (40). The memory CD8 T cells that remain following sepsis display defects in Ag-dependent and -independent functions including reduced Ag-sensitivity, proliferative capacity, and ability to produce cytokines in a bystander manner (41). Furthermore, memory CD8 T cells from hosts that have recovered from sepsis are more prone to undergo exhaustion when combating chronic infections, displaying increased expression of inhibitory receptors PD-1 and 2B4, reduced ability to produce effector cytokines IFN-γ and TNF-α, and reduced ability to clear the infection (42–44). Interestingly, numerical loss and functional defects are not as profound for infection-induced tissue resident memory (T_{RM}) CD8 T cells in hosts that survive sepsis. However, immune responses initiated by CD8 T_{RM} from septic hosts are still ineffective due to the inability of endothelial cells to transmit alarm signals, resulting in reduced recruitment of circulating effector cells to the site of infection (45). Decreased protective capacity of CD8 T cells following sepsis extends beyond pathogenic infection, as tumor-infiltrating CD8 T cells from septic hosts have reduced ability to proliferate, produce IFN-γ, and prevent tumor growth (46). However, CD8 T cells from tumor-bearing hosts that experienced sepsis, under certain conditions, could be even reinvigorated due to sepsis-induced release of tumor Ags, leading to the surprising reduction in tumor burden (47). Many defects in CD4 T cells have also been found, and due to their role in providing help to B cells and CD8 T cells, we will discuss the effects of sepsis on CD4 T cells in further detail in the following section.

EFFECTS OF SEPSIS ON CD4 T CELLS

CD4 T Cell Loss, Recovery, and Repertoire Changes Following Sepsis

Numbers of CD4 T cells are greatly reduced following sepsis onset (24–27, 48–50). Absolute CD4 T cell numbers return to pre-septic levels after a month for most patients, but failure to recover sufficient numbers of immunocompetent CD4 T cells is associated with poor prognosis, especially in the elderly (24, 27, 49, 50). However, questions remain as to how numerical recovery of CD4 T cells occurs and the roles that thymic output, homeostatic proliferation, and Ag-driven proliferation play in that recovery. Initial experiments examining numerical recovery of CD4 T cells showed increased percentages of CD4 T cells expressing markers associated with memory (e.g., $CD44^{hi}$, $CD62L^{low}$) following sepsis, suggesting recovery occurs through homeostatic proliferation of naïve cells, Ag-driven proliferation, and/or outgrowth of endogenous memory CD4 T cell populations (49). However, the authors

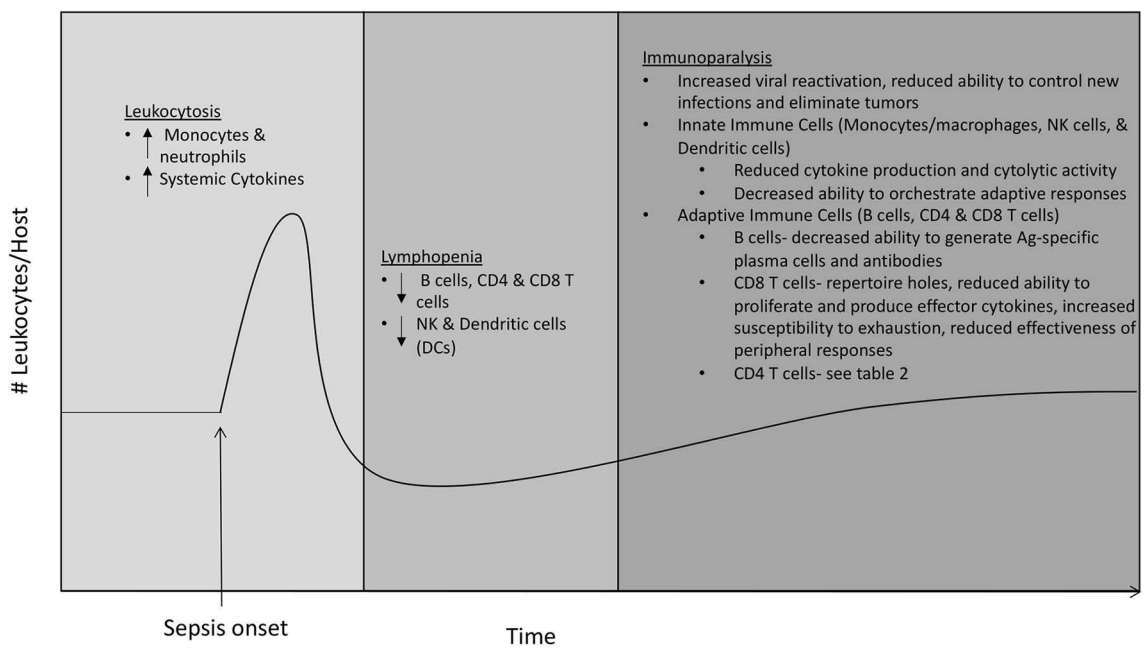

FIGURE 1 | Effects of sepsis on immune cell subsets. The immune system enters a state of leukocytosis during the first 2−4 days following sepsis onset, with marked increases in neutrophil and monocyte populations and increased levels of circulating pro- and anti-inflammatory cytokines. The state of leukocytosis is followed by a state of lymphopenia, characterized by a marked decrease in numbers of adaptive immune cells including B cells, CD4 and CD8 T cells, and innate immune cells including NK cells and dendritic cells (DCs). The state of lymphopenia resolves ∼1 month after sepsis onset, as numbers of leukocytes return to normal. Despite the numerical recovery of immune cells, hosts that have recovered from sepsis suffer from a long-lasting state of immune dysfunction termed immunoparalysis. The state of immunoparalysis is characterized by reduced functionality of both innate and adaptive immune cells, increased viral reactivation, and reduced ability to control new infections and to eliminate solid tumors.

found that adoptively transferred naïve TCR-transgenic OT-II CD4 T cells did not proliferate when transferred into septic hosts suggesting CD4 T cell recovery does not occur through homeostatic proliferation. Additionally, no skewing in TCR Vβ expression in memory CD4 T cells following sepsis was observed, suggesting numerical recovery was not due to Ag-driven proliferation of cells responding to infection during sepsis. By ruling out homeostatic proliferation and Ag-driven proliferation, the authors concluded that numerical recovery results from outgrowth of endogenous memory CD4 T cells—even though this conclusion was not formally proven in this study. In contrast, a later study found decreased TCR Vβ diversity in human sepsis patients, which was associated with increased risk of death (51). Data published from our group (50) found CD4 T cell numerical recovery occurred similarly in wild type and thymectomized mice, suggesting numerical recovery occurs independently of thymic output. As in previous studies, numerical recovery of CD4 T cells was accompanied by accumulation of cells with an Ag-experienced phenotype (i.e., upregulation of CD11a and CD49d). However, both adoptively transferred TCR-transgenic CD4 T cells and endogenous CD4 T cells of known epitope specificity that were present during the septic event (rather than transferred post-sepsis) proliferated in septic hosts, suggesting that numerical recovery of CD4 T cells is driven at least in part by homeostatic proliferation. Ag-driven proliferation also is likely to play a role for some Ag-specific CD4 T cell populations, as CD4 T cells recognizing epitopes derived from gut-derived segmented filamentous bacterium (SFB) were found to proliferate in an Ag-dependent manner following sepsis (52). Importantly, recovery of epitope-specific CD4 T cells occurred asymmetrically following homeostatic proliferation. When numerical representation of six different Ag-specific CD4 T cell populations was determined in sham and 1 month post-sepsis mice, half of Ag-specific populations recovered numerically, while one population was found in greater numbers and two were numerically reduced post-sepsis (50). Furthermore, Ag-specific populations that failed to recover numerically displayed functional defects including decreased ability to proliferate and to produce cytokines following infection or incubation with cognate Ag and to mount Th17 polarized responses. Thus, changes within the CD4 T cell compartment during numerical recovery (**Table 1**) impact their ability to respond to newly encountered Ags, which likely impacts their ability to provide protection against newly encountered infections.

TABLE 1 | Effects of sepsis on CD4 T cells.

Category	Effects	References
Repertoire changes	Decreased TCR Vβ diversity in humans	(51)
	Incomplete recovery of some epitope specificities	(50)
	Ag-dependent proliferation for some specificities	(52)
Functional defects	Impaired DTH responses and higher rates of viral reactivation	(53–55)
	Global anergy	
	• Reduced ability to produce cytokines	(2, 56–61)
	• Reduced ability to proliferate	(50, 56, 62)
	• Increased expression of inhibitory receptors	(34, 35, 63–68)
Changes in subset representation	Decreased transcript levels of T-bet, GATA3, and ROR-γT	(69)
	Repressive histone methylation at IFN-γ and GATA3 promoter regions	(62)
	Increased Treg cell representation	(26, 59, 70, 71)
	Decreased representation of Th1, Th2, Th17, and Tfh subsets	(28, 59, 71, 72)

CD4 T Cell Functional Defects Following Sepsis

Evidence for functional defects of CD4 T cells in septic patients was first inferred from studies showing impaired DTH skin reactions (53). Later studies pointed to the significantly higher rates of CMV and HSV reactivation in septic patients (54, 55)—infections for which effective CD4 T cell immunity is essential for limiting frequency and severity of recrudescence in humans (54, 73–75). Early studies that examined cytokine production by CD4 T cells from septic patients showed that cytokines produced under Th1 or Th2 conditions were altered (56–60), leading to the suggestion that sepsis caused a phenotypic switch of CD4 T cells from Th1 to Th2 (61). However, a later study examining cytokine production by freshly isolated, postmortem spleen and lung samples found almost no production of IFN-γ, TNF-α, IL-6, and IL-10 after anti-CD3/CD28 mAb stimulation (2), providing evidence for the suggestion that post-septic CD4 T cells display a global state of anergy (56). This argument was strengthened by studies showing reduced proliferative capacity; decreased mRNA transcript levels of T-bet, GATA3, and ROR-γt transcription factors that regulate differentiation into Th1, Th2, and Th17 CD4 T cell subsets, respectively; and repressive histone methylation marks at the IFN-γ and GATA-3 promoter regions of CD4 T cells taken from septic hosts (50, 62, 69). Decreased ability to proliferate and produce effector cytokines is reminiscent of functional defects arising during T cell exhaustion caused by prolonged antigen exposure and inflammation in the face of chronic viral infection and cancer (76–78). Exhaustion is accompanied by increased expression of inhibitory receptors that dampen immune responses, and CD4 T cells from septic hosts have greater expression of inhibitory receptors including PD-1, 2B4, BTLA, and TRAIL, which directly impacts their ability to effectively respond to infection (34, 35, 63–68). Furthermore, expression of inhibitory receptors has the potential to impact CD4 T cell-derived help to other cells, including B cells and T cells. In support of this, reduced effectiveness of CD8 T cell immune responses in septic hosts has been shown to be due in part to TRAIL-dependent mechanisms (67, 68, 79). Thus, sepsis causes global changes in expression of factors regulating CD4 T cell effector responses (**Table 1**), which limits help provided to other immune cells and effectiveness of *de novo* immune responses.

It should be noted, however, that triggering events and microorganisms capable of inducing sepsis are numerous. The most common triggering event in humans is pulmonary infection, with other common triggers including infections of the abdomen (e.g., those arising from a perforated or ischemic bowel), soft tissues (often as a result of burns), and the urinary tract (80, 81). Microorganisms that commonly cause sepsis include gram-positive (*Staphylococcus aureus* and *Streptococcus pneumoniae*) and gram-negative (*Escherichia coli* and *Klebsiella* species) bacteria, fungal organisms, and viruses including SARS-CoV-2 (82–85). Triggering events and causative microbes for studies that suggested CD4 T cells from recovered sepsis patients exist in a state of global anergy varied among patients (2). It is unclear if or how different triggering events or factors unique to the causative pathogens, such as their mitogenic capacity or quality and/or severity of the cytokine storm they elicit, influence the severity of CD4 T cell functional defects observed in patients who have recovered from sepsis.

Changes in CD4 T Cell Subsets Following Sepsis

One of the defining features of CD4 T cells is that they are able to differentiate into subsets capable of performing unique effector functions best suited to drive responses against perceived threats based upon polarizing inflammatory cytokine and co-stimulatory molecule signals present during Ag-presentation. Based on the literature, it is clear that sepsis disrupts both representation of and function of CD4 T cell subsets, including Th1, Th2, Th17, Tfh, and Treg subsets (**Table 1**). A number of studies have noted an increased frequency of Treg cells in the periphery of septic patients (26, 70, 71), which was later shown to be the result of preferential loss of other subsets (i.e., Th1, Th2, Th17, and Tfh) (28, 59, 71, 72, 86). It should be noted, however, that these observations in humans are based upon analysis of cells found in the blood. Considering that mouse studies have shown lymphocytes in tissues are less susceptible to sepsis-induced alterations (28, 45), similar shifts in CD4 T cell subset representation may not be observed in peripheral tissues of humans. Losses in CD4 T cell subsets impacts CD4 T cell-mediated help provided to other cell types, as was recently demonstrated for reduced antibody production resulting from CD4 T cell-dependent B cell responses, which was caused in part by reduced Tfh differentiation following immunization of septic hosts (38). In addition, the effects of sepsis on the ability to produce effector cytokines (IL-10 in the case of Treg) may be less severe for Treg than for other CD4 T cell subsets (87). The impact of increased Treg cell representation following sepsis has been debated, as some have correlated it with worse outcomes (88), while others have suggested it correlates with better outcomes and immunity (89–91). Studies using anti-GITR mAb to block Treg function (92) and siRNA to downregulate Foxp3 expression (93) showed that reducing Treg numbers and/or function in septic hosts improved overall immune function and pathogen control. However, later studies concluded that depletion of Tregs did not lead to improvements in survival (94), although interpretation of this study is compounded by the use of anti-CD25 mAb, which can deplete CD25-expressing cells (such as effector T cells) other than Tregs. In addition to the factors mentioned above, discrepancies for the role of Treg cells in sepsis pathology and immunoparalysis may be due to timing of analysis, as a recent study has suggested Treg cells contribute to positive outcomes during the early stages of sepsis, but do not significantly impact immunosuppression seen following recovery (95). Regardless, the continued debate concerning the role Treg cells play in sepsis pathology and immunoparalysis calls for a more detailed analysis.

If targeting changes in CD4 T cell subset representation could provide a therapeutic benefit to sepsis patients, understanding the factors leading to these imbalances becomes important. Altered functions and loss of other immune cell subsets likely plays a role in the remodeling of CD4 T cell subsets following sepsis. Adoptive transfer of bone marrow-derived DCs (BMDCs) to septic animals elevated levels of Th1 cytokines, reduced expression of the inhibitory receptor PD-1 on CD4 T cells, reduced proliferation and differentiation of Treg cells, and increased rates of survival (96). Additionally, IL-33—a cytokine that plays a role in promoting Treg expansion—is elevated in septic patients, and recent studies showed neutralization of IL-33 limited the immunosuppressive effects of sepsis and improved outcomes following secondary infection (97). These studies suggest therapies designed to restore numbers and function of immune cells other than CD4 T cells may be beneficial for reestablishing the balance of CD4 T cell subsets following sepsis and for reducing the effects of increased Treg representation. Furthermore, it is becoming appreciated that sepsis alters the metabolic capacity of T cells (98), and targeting the effects of sepsis on immunometabolism presents an intriguing opportunity to restore T cell dysfunction resulting from sepsis. Targeting metabolism may help to prevent undesirable shifts in CD4 T cell subsets following sepsis, based on recent data showing administration of glutamine led to decreased representation of Th2 and Treg cells in septic hosts (99). While there is much work to be done to fully understand how changes in CD4 T cell subsets observed following sepsis impact the state of immunoparalysis, these studies present the exciting possibility that therapies may be developed to limit CD4 T cell subset alterations following sepsis and promote restoration of protective T cell immunity.

EXPERIMENTAL THERAPIES TO ALLEVIATE SEPSIS-INDUCED IMMUNOPARALYSIS

Due to the contributions of numerical cell loss and functional defects, therapies designed to alleviate sepsis-induced immunoparalysis have focused on reducing cell death, expanding numbers of surviving cells, and restoring function of those cells. Initial experiments designed to block apoptosis through overexpression of the antiapoptotic molecule Bcl-2 or inhibition of caspases showed a clear survival benefit for septic hosts (100–103). However, the use of caspase inhibitors to treat sepsis

was not widely adopted due to the importance of caspases to other cellular processes and difficulties in establishing doses and timing of administration that provided clinical benefit. Because of this, the most promising strategies currently involve single or combination therapies with γc receptor-dependent cytokines and blockade of inhibitory molecules, which both have the potential to increase cell numbers and restore cell functions.

Common γc cytokines, including IL-2, IL-7, and IL-15, promote the survival of naïve, effector, and memory CD4 and CD8 T cells. While IL-2 and IL-15 have shown therapeutic benefits (104–106), indicating that further exploration of their use in treatment of sepsis is warranted, therapeutic administration of IL-7 is well-tolerated and shows promise to reverse immunoparalysis of sepsis patients. Studies conducted over the last several years have shown that IL-7 administration improves T cell survival; functionality of surviving T cells including ability to proliferate, traffic, and to produce effector cytokines including IFN-γ, TNF-α, and IL-17; and ability to stimulate DTH responses and clear secondary infections (107–110). IL-7 treatment may also help to restore metabolic defects of T cells present after sepsis recovery, as IL-7 was recently shown to promote activation of mTOR, an important regulator of oxidative phosphorylation, in T cells of sepsis patients (108). Importantly, recent results from clinical trials have shown IL-7 administration is well-tolerated in sepsis patients and results in improved numbers and functions of CD4 and CD8 T cells (110), pointing to the translational value of this treatment for sepsis patients. It will be important to follow septic patients treated with IL-7 in the future to see if improvements in immune cell numbers and functions translate to improved ability to prevent opportunistic secondary infections and better long-term outcomes.

Interactions between inhibitory receptors, such as PD-1, CTLA-4, BTLA, Tim-3, LAG-3, 2B4, and TRAIL expressed by T cells and their cognate ligands can be generally described to have inhibitory effects on T cell function. Immune checkpoint modulation therapy, which is used to block interactions of inhibitory receptors and their ligands, has shown great promise for reducing functional defects of exhausted T cells in settings of chronic infection and as a therapeutic treatment of certain cancers (111–113). Because T cells of sepsis patients share such similarities to exhausted T cells, including increased expression of inhibitory receptors and functional anergy (34, 35, 63–68), immune checkpoint modulation has been explored as a therapeutic strategy to reverse sepsis-induced immunosuppression. Therapeutic administration of agents blocking inhibitory receptor interactions of PD-1/PDL-1, 2B4, Tim-3, CTLA-4, LAG-3, and TRAIL have all shown some benefit for improving function of T cells and monocytes of septic hosts, including improving expression of the costimulatory molecule CD28, ability of T cells and macrophages to produce inflammatory cytokines, and ability of CD8 T cells to form memory populations (68, 107, 114–123). However, the immunomodulatory effects of treatments targeting immune checkpoint pathways in septic hosts are dependent upon dose and timing of administration (116, 117), which will require careful consideration for clinical use. Additionally, treatments based on administration of IL-7 and PD-1 blockade have differing effects on reversing sepsis-induced immunosuppression (107), suggesting that combined treatments may have synergistic effects. While their long-term effects on restoring fully protective immune responses of septic patients remain to be elucidated, improvements in immune cell numbers and function following administration of γc cytokines and checkpoint blockade inhibitors are promising signs for their use as therapies to reverse immunoparalysis resulting from sepsis.

ADVANCEMENT OF ANIMAL MODELS THAT MORE ACCURATELY REFLECT SEPSIS IN HUMANS

While mouse-based preclinical studies have resulted in development of therapies that have shown great efficacy in the clinic, such as the immune checkpoint blockade therapies for the treatment of some cancers, it has also been argued that differences between mice and humans are a major reason for the inability to translate therapies described in laboratories to successful clinical outcomes (124–128). Therefore, developing experimental mouse models that more closely resemble the human condition may improve the translational potential of preclinical sepsis studies. One of the major differences between mouse studies and humans is that the majority of preclinical mouse studies are conducted using inbred mice, which does not reflect the genetic diversity present in the human population. We know from human sepsis studies that outcomes, including survival and resulting parameters of immunoparalysis, vary greatly from person to person (129). While this may be due to a number of factors including patient age, severity of sepsis, and underlying health conditions, genetics may also play a role. Studies utilizing outbred mice have shown inbred mice fail to capture diversity of immune outcomes seen in genetically diverse populations (14–16). Only a limited number of sepsis studies have included outbred mice and/or mice of varied genetic background, but these experiments have provided insight into how models of sepsis in mice might compare to outcomes in humans. Studies using outbred Swiss mice have shown that immunoparalysis following sepsis, including reduced numbers and function of both DCs and CD8 T cells, can be observed in outbred as well as inbred mice (31, 41, 42, 45), suggesting some aspects of immunoparalysis are likely to be universal in a population of mixed genetics. However, other parameters of immunoparalysis might differ based in part on genetics, as the percentage of MHC II-expressing lymphocytes and representation of Treg cells post-sepsis was found to differ between BALB/c and outbred CD-1 mice (130). Thus, use of genetically diverse mice in sepsis studies should be encouraged, as they could help uncover aspects of sepsis that are influenced by genetics, as well as help to pinpoint genetic factors responsible for divergent sepsis outcomes in the human population.

Another big difference between mouse studies, which are primarily conducted using SPF mice, and humans is that humans are exposed to a diverse array of pathogens throughout life. Recent studies have shown that the immune system of

SPF mice is more similar to human infants, while "dirty" mice that have been exposed to a diverse array of pathogens through co-housing with pet store mice possess an immune system more similar to adult humans (17–21). Importantly, the training and shaping of the immune system that occurred as a result of pathogen exposure rendered mice less susceptible to newly encountered infections, suggesting the history of infection may also influence how organisms respond to a septic insult. Recent work from our laboratory, however, found that microbial exposure results in an enhanced cytokine storm following sepsis and increases risk of mortality (131). While changes in the microbiome due to cohousing were partially responsible for this outcome, changes in function of immune cells due to history of pathogen encounter also played a role, as leukocytes of cohoused mice displayed increased expression of TLR4 and produced greater amounts of inflammatory cytokines in response to LPS. Thus, changes in the immune system due to history of infection with diverse pathogens, which varies from person to person shape the response to septic insult. This also could impact the effectiveness of treatments for sepsis, as antibiotic treatment of septic hosts possessing pre-established memory populations was more effective when combined with memory cell reactivation (132). Mouse models that incorporate a history of pathogen exposure also may improve translatability of sepsis studies, as was recently demonstrated using laboratory mice born to wild mice, which possess similar microbiota and history of pathogen exposure to dams (21). Using this model, the authors were able to replicate clinical trial data showing TNF-α neutralization was ineffective in their dirty mice (just like in human sepsis patients), even though it was an effective therapy for SPF mice. Clearly, increased use of mouse models that incorporate history of pathogen exposure have the potential to increase our understanding of sepsis pathology and resulting immunoparalysis in humans, and to improve translatability of sepsis studies that utilize animals.

CONCLUSIONS

Advancing therapies to reverse sepsis-induced immunoparalysis will require a thorough understanding of defects in immune cell subsets resulting from sepsis, and how those defects contribute to decreased host immune fitness. CD4 T cells play an important role in orchestrating successful immune responses due to their ability to provide help to a range of immune cell types. Therefore, understanding how CD4 T cells are impacted by sepsis, including numerical and functional alterations and changes in subset representation, is an important goal in sepsis-based research. Mouse models that more closely represent the human condition through incorporation of host genetic differences and history of infection with diverse pathogens have the potential to increase our understanding of defects in immune cells of various types caused by sepsis and to improve the translational value of animal-based sepsis studies.

AUTHOR CONTRIBUTIONS

All authors listed have made a substantial, direct and intellectual contribution to the work, and approved it for publication.

FUNDING

Supported by National Institutes of Health Grants: GM115462 (TG), AI114543 (VB), GM113961 (VB), and GM134880 (VB); and a Veterans Administration Merit Review Award (I01BX001324; to TG).

REFERENCES

1. Singer M, Deutschman CS, Seymour CW, Shankar-Hari M, Annane D, Bauer M, et al. The third international consensus definitions for sepsis and septic shock (Sepsis-3). *JAMA*. (2016) 315:801–10. doi: 10.1001/jama.2016.0287
2. Boomer JS, To K, Chang KC, Takasu O, Osborne DF, Walton AH, et al. Immunosuppression in patients who die of sepsis and multiple organ failure. *JAMA*. (2011) 306:2594–605. doi: 10.1001/jama.2011.1829
3. Center for Disease Control and Prevention. *Sepsis: Data and Reports*. (2016). Available online at: https://www.cdc.gov/sepsis/datareports/index.html (accessed February 12, 2016).
4. Torio C (AHRQ), Moore B (Truven Health Analytics). *National Inpatient Hospital Costs: The Most Expensive Conditions by Payer, 2013. HCUP Statistical Brief #204*. Rockville, MD: Agency for Healthcare Research and Quality (2016). Available online at: http://www.hcup-us.ahrq.gov/reports/statbriefs/sb204-Most-Expensive-Hospital-Conditions.pdf (accessed February 12, 2020).
5. Gaieski DF, Edwards JM, Kallan MJ, Carr BG. Benchmarking the incidence and mortality of severe sepsis in the United States. *Crit Care Med*. (2013) 41:1916–27. doi: 10.1097/CCM.0b013e31827c09f8
6. Donnelly JP, Hohmann SF, Wang HE. Unplanned readmissions after hospitalization for severe sepsis at academic medical center-affiliated hospitals. *Crit Care Med*. (2015) 43:1916–27. doi: 10.1097/CCM.0000000000001147
7. Kutza AS, Muhl E, Hackstein H, Kirchner H, Bein G. High incidence of active cytomegalovirus infection among septic patients. *Clin Infect Dis*. (1998) 26:1076–82. doi: 10.1086/520307
8. Walton AH, Muenzer JT, Rasche D, Boomer JS, Sato B, Brownstein BH, et al. Reactivation of multiple viruses in patients with sepsis. *PLoS ONE*. (2014) 9:e98819. doi: 10.1371/journal.pone.0098819
9. Hohlstein P, Gussen H, Bartneck M, Warzecha KT, Roderburg C, Buendgens L, et al. Prognostic relevance of altered lymphocyte subpopulations in critical illness and sepsis. *J Clin Med*. (2019) 8:353. doi: 10.3390/jcm8030353
10. Jensen IJ, Sjaastad FV, Griffith TS, Badovinac VP. Sepsis-Induced T cell immunoparalysis: the ins and outs of impaired T cell immunity. *J Immunol*. (2018) 200:1543–53. doi: 10.4049/jimmunol.1701618
11. Ono S, Tsujimoto H, Hiraki S, Aosasa S. Mechanisms of sepsis-induced immunosuppression and immunological modification therapies for sepsis. *Ann Gastroenterol Surg*. (2018) 2:351–8. doi: 10.1002/ags3.12194
12. Masopust D, Sivula CP, Jameson SC. Of Mice, Dirty mice, and men: using mice to understand human immunology. *J Immunol*. (2017) 199:383–8. doi: 10.4049/jimmunol.1700453
13. Martin MD, Badovinac VP. Defining memory CD8 T Cell. *Front Immunol*. (2018) 9:2692. doi: 10.3389/fimmu.2018.02692
14. Rai D, Pham NL, Harty JT, Badovinac VP. Tracking the total CD8 T cell response to infection reveals substantial discordance in magnitude and

kinetics between inbred and outbred hosts. *J Immunol*. (2009) 183:7672–81. doi: 10.4049/jimmunol.0902874
15. Martin MD, Danahy DB, Hartwig SM, Harty JT, Badovinac VP. Revealing the complexity in CD8 T cell responses to infection in inbred C57B/6 versus outbred swiss mice. *Front Immunol*. (2017) 8:1527. doi: 10.3389/fimmu.2017.01527
16. Martin MD, Sompallae R, Winborn CS, Harty JT, Badovinac VP. Diverse CD8 T cell responses to viral infection revealed by the collaborative cross. *Cell Rep*. (2020) 31:107508. doi: 10.1016/j.celrep.2020.03.072
17. Beura LK, Hamilton SE, Bi K, Schenkel JM, Odumade OA, Casey KA, et al. Normalizing the environment recapitulates adult human immune traits in laboratory mice. *Nature*. (2016) 532:512–6. doi: 10.1038/nature17655
18. Reese TA, Bi K, Kambal A, Filali-Mouhim A, Beura LK, Burger MC, et al. Sequential infection with common pathogens promotes human-like immune gene expression and altered vaccine response. *Cell Host Microbe*. (2016) 19:713–9. doi: 10.1016/j.chom.2016.04.003
19. Japp AS, Hoffmann K, Schlickeiser S, Glauben R, Nikolaou C, Maecker HT, et al. Wild immunology assessed by multidimensional mass cytometry. *Cytometry A*. (2017) 91:85–95. doi: 10.1002/cyto.a.22906
20. Rosshart SP, Vassallo BG, Angeletti D, Hutchinson DS, Morgan AP, Takeda K, et al. Wild mouse gut microbiota promotes host fitness and improves disease resistance. *Cell*. (2017) 171:1015–28.e1013. doi: 10.1016/j.cell.2017.09.016
21. Rosshart SP, Herz J, Vassallo BG, Hunter A, Wall MK, Badger JH, et al. Laboratory mice born to wild mice have natural microbiota and model human immune responses. *Science*. (2019) 365:eaaw4361. doi: 10.1126/science.aaw4361
22. Heffernan DS, Monaghan SF, Thakkar RK, Machan JT, Cioffi WG, Ayala A, et al. Failure to normalize lymphopenia following trauma is associated with increased mortality, independent of the leukocytosis pattern. *Crit Care*. (2012) 16:R12. doi: 10.1186/cc11157
23. Hoser GA, Skirecki T, Zlotorowicz M, Zielinska-Borkowska U, Kawiak J. Absolute counts of peripheral blood leukocyte subpopulations in intraabdominal sepsis and pneumonia-derived sepsis: a pilot study. *Folia Histochem Cytobiol*. (2012) 50:420–6. doi: 10.5603/FHC.2012.0057
24. Inoue S, Suzuki-Utsunomiya K, Okada Y, Taira T, Iida Y, Miura N, et al. Reduction of immunocompetent T cells followed by prolonged lymphopenia in severe sepsis in the elderly. *Crit Care Med*. (2013) 41:810–9. doi: 10.1097/CCM.0b013e318274645f
25. Hotchkiss RS, Tinsley KW, Swanson PE, Schmieg RE Jr, Hui JJ, Chang KC, et al. Sepsis-induced apoptosis causes progressive profound depletion of B and CD4+ T lymphocytes in humans. *J Immunol*. (2001) 166:6952–63. doi: 10.4049/jimmunol.166.11.6952
26. Gouel-Cheron A, Venet F, Allaouchiche B, Monneret G. CD4+ T-lymphocyte alterations in trauma patients. *Crit Care*. (2012) 16:432. doi: 10.1186/cc11376
27. Chen X, Ye J, Ye J. Analysis of peripheral blood lymphocyte subsets and prognosis in patients with septic shock. *Microbiol Immunol*. (2011) 55:736–42. doi: 10.1111/j.1348-0421.2011.00373.x
28. Sharma A, Yang WL, Matsuo S, Wang, P. Differential alterations of tissue T-cell subsets after sepsis. *Immunol Lett*. (2015) 168:41–50. doi: 10.1016/j.imlet.2015.09.005
29. Monserrat J, De Pablo R, Diaz-Martin D, Rodriguez-Zapata M, De La Hera A, Prieto A, et al. Early alterations of B cells in patients with septic shock. *Crit Care*. (2013) 17:R105. doi: 10.1186/cc12750
30. Jensen IJ, Winborn CS, Fosdick MG, Shao P, Tremblay MM, Shan Q, et al. Polymicrobial sepsis influences NK-cell-mediated immunity by diminishing NK-cell-intrinsic receptor-mediated effector responses to viral ligands or infections. *PLoS Pathog*. (2018) 14:e1007405. doi: 10.1371/journal.ppat.1007405
31. Strother RK, Danahy DB, Kotov DI, Kucaba TA, Zacharias ZR, Griffith TS, et al. Polymicrobial sepsis diminishes dendritic cell numbers and function directly contributing to impaired primary CD8 T cell responses *In vivo*. *J Immunol*. (2016) 197:4301–11. doi: 10.4049/jimmunol.1601463
32. Washburn ML, Wang Z, Walton AH, Goedegebuure SP, Figueroa DJ, Van Horn S, et al. T cell- and monocyte-specific RNA-sequencing analysis in septic and nonseptic critically ill patients and in patients with cancer. *J Immunol*. (2019) 203:1897–908. doi: 10.4049/jimmunol.1900560
33. Gossez M, Rimmele T, Andrieu T, Debord S, Bayle F, Malcus C, et al. Proof of concept study of mass cytometry in septic shock patients reveals novel immune alterations. *Sci Rep*. (2018) 8:17296. doi: 10.1038/s41598-018-35932-0
34. Shubin NJ, Chung CS, Heffernan DS, Irwin LR, Monaghan SF, Ayala A. BTLA expression contributes to septic morbidity and mortality by inducing innate inflammatory cell dysfunction. *J Leukoc Biol*. (2012) 92:593–603. doi: 10.1189/jlb.1211641
35. Huang X, Venet F, Wang YL, Lepape A, Yuan Z, Chen Y, et al. PD-1 expression by macrophages plays a pathologic role in altering microbial clearance and the innate inflammatory response to sepsis. *Proc Natl Acad Sci USA*. (2009) 106:6303–8. doi: 10.1073/pnas.0809422106
36. Mohr A, Polz J, Martin EM, Griessl S, Kammler A, Potschke C, et al. Sepsis leads to a reduced antigen-specific primary antibody response. *Eur J Immunol*. (2012) 42:341–52. doi: 10.1002/eji.201141692
37. Potschke C, Kessler W, Maier S, Heidecke CD, Broker, BM. Experimental sepsis impairs humoral memory in mice. *PLoS ONE*. (2013) 8:e81752. doi: 10.1371/journal.pone.0081752
38. Sjaastad FV, Condotta SA, Kotov JA, Pape KA, Dail C, Danahy DB, et al. Polymicrobial sepsis chronic immunoparalysis is defined by diminished ag-specific T cell-dependent B cell responses. *Front Immunol*. (2018) 9:2532. doi: 10.3389/fimmu.2018.02532
39. Danahy DB, Strother RK, Badovinac VP, Griffith TS. Clinical and experimental sepsis impairs CD8 T-cell-mediated immunity. *Crit Rev Immunol*. (2016) 36:57–74. doi: 10.1615/CritRevImmunol.2016017098
40. Condotta SA, Rai D, James BR, Griffith TS, Badovinac VP. Sustained and incomplete recovery of naive CD8+ T cell precursors after sepsis contributes to impaired CD8+ T cell responses to infection. *J Immunol*. (2013) 190:1991–2000. doi: 10.4049/jimmunol.1202379
41. Duong S, Condotta SA, Rai D, Martin MD, Griffith TS, Badovinac VP, et al. Polymicrobial sepsis alters antigen-dependent and -independent memory CD8 T cell functions. *J Immunol*. (2014) 192:3618–25. doi: 10.4049/jimmunol.1303460
42. Condotta SA, Khan SH, Rai D, Griffith TS, Badovinac VP. Polymicrobial sepsis increases susceptibility to chronic viral infection and exacerbates CD8+ T cell exhaustion. *J Immunol*. (2015) 195:116–25. doi: 10.4049/jimmunol.1402473
43. Xie J, Crepeau RL, Chen CW, Zhang W, Otani S, Coopersmith CM, et al. Sepsis erodes CD8(+) memory T cell-protective immunity against an EBV homolog in a 2B4-dependent manner. *J Leukoc Biol*. (2019) 105:565–75. doi: 10.1002/JLB.4A0718-292R
44. Choi YJ, Kim SB, Kim JH, Park SH, Park MS, Kim JM, et al. Impaired polyfunctionality of CD8(+) T cells in severe sepsis patients with human cytomegalovirus reactivation. *Exp Mol Med*. (2017) 49:e382. doi: 10.1038/emm.2017.146
45. Danahy DB, Anthony SM, Jensen IJ, Hartwig SM, Shan Q, Xue HH, et al. Polymicrobial sepsis impairs bystander recruitment of effector cells to infected skin despite optimal sensing and alarming function of skin resident memory CD8 T cells. *PLoS Pathog*. (2017) 13:e1006569. doi: 10.1371/journal.ppat.1006569
46. Danahy DB, Kurup SP, Winborn CS, Jensen IJ, Harty JT, Griffith TS, et al. Sepsis-Induced state of immunoparalysis is defined by diminished CD8 T cell-mediated antitumor immunity. *J Immunol*. (2019) 203:725–35. doi: 10.4049/jimmunol.1900435
47. Danahy DB, Jensen IJ, Griffith TS, Badovinac VP. Cutting edge: polymicrobial sepsis has the capacity to reinvigorate tumor-infiltrating CD8 T cells and prolong host survival. *J Immunol*. (2019) 202:2843–8. doi: 10.4049/jimmunol.1900076
48. Roger PM, Hyvernat H, Ticchioni M, Kumar G, Dellamonica J, Bernardin G, et al. The early phase of human sepsis is characterized by a combination of apoptosis and proliferation of T cells. *J Crit Care*. (2012) 27:384–93. doi: 10.1016/j.jcrc.2012.04.010
49. Unsinger J, Kazama H, Mcdonough JS, Hotchkiss RS, Ferguson TA. Differential lymphopenia-induced homeostatic proliferation for CD4+ and CD8+ T cells following septic injury. *J Leukoc Biol*. (2009) 85:382–90. doi: 10.1189/jlb.0808491

50. Cabrera-Perez J, Condotta SA, James BR, Kashem SW, Brincks EL, Rai D, et al. Alterations in antigen-specific naive CD4 T cell precursors after sepsis impairs their responsiveness to pathogen challenge. *J Immunol*. (2015) 194:1609–20. doi: 10.4049/jimmunol.1401711
51. Venet F, Filipe-Santos O, Lepape A, Malcus C, Poitevin-Later F, Grives A, et al. Decreased T-cell repertoire diversity in sepsis: a preliminary study. *Crit Care Med*. (2013) 41:111–9. doi: 10.1097/CCM.0b013e3182657948
52. Cabrera-Perez J, Babcock JC, Dileepan T, Murphy KA, Kucaba TA, Badovinac VP, et al. Gut microbial membership modulates CD4 T cell reconstitution and function after sepsis. *J Immunol*. (2016) 197:1692–8. doi: 10.4049/jimmunol.1600940
53. Meakins JL, Pietsch JB, Bubenick O, Kelly R, Rode H, Gordon J, et al. Delayed hypersensitivity: indicator of acquired failure of host defenses in sepsis and trauma. *Ann Surg*. (1977) 186:241–50. doi: 10.1097/00000658-197709000-00002
54. Laing KJ, Dong L, Sidney J, Sette A, Koelle DM. Immunology in the clinic review series; focus on host responses: T cell responses to herpes simplex viruses. *Clin Exp Immunol*. (2012) 167:47–58. doi: 10.1111/j.1365-2249.2011.04502.x
55. Luyt CE, Combes A, Deback C, Aubriot-Lorton MH, Nieszkowska A, Trouillet JL, et al. Herpes simplex virus lung infection in patients undergoing prolonged mechanical ventilation. *Am J Respir Crit Care Med*. (2007) 175:935–42. doi: 10.1164/rccm.200609-1322OC
56. De AK, Kodys KM, Pellegrini J, Yeh B, Furse RK, Bankey P, et al. Induction of global anergy rather than inhibitory Th2 lymphokines mediates posttrauma T cell immunodepression. *Clin Immunol*. (2000) 96:52–66. doi: 10.1006/clim.2000.4879
57. Heidecke CD, Hensler T, Weighardt H, Zantl N, Wagner H, Siewert JR, et al. Selective defects of T lymphocyte function in patients with lethal intraabdominal infection. *Am J Surg*. (1999) 178:288–92. doi: 10.1016/S0002-9610(99)00183-X
58. Roth G, Moser B, Krenn C, Brunner M, Haisjackl M, Almer G, et al. Susceptibility to programmed cell death in T-lymphocytes from septic patients: a mechanism for lymphopenia and Th2 predominance. *Biochem Biophys Res Commun*. (2003) 308:840–6. doi: 10.1016/S0006-291X(03)01482-7
59. Venet F, Pachot A, Debard AL, Bohe J, Bienvenu J, Lepape A, et al. Increased percentage of CD4+CD25+ regulatory T cells during septic shock is due to the decrease of CD4+CD25- lymphocytes. *Crit Care Med*. (2004) 32:2329–31. doi: 10.1097/01.CCM.0000145999.42971.4B
60. Wick M, Kollig E, Muhr G, Koller M. The potential pattern of circulating lymphocytes TH1/TH2 is not altered after multiple injuries. *Arch Surg*. (2000) 135:1309–14. doi: 10.1001/archsurg.135.11.1309
61. O'Sullivan ST, Lederer JA, Horgan AF, Chin DH, Mannick JA, Rodrick ML, et al. Major injury leads to predominance of the T helper-2 lymphocyte phenotype and diminished interleukin-12 production associated with decreased resistance to infection. *Ann Surg*. (1995) 222:482–90. doi: 10.1097/00000658-199510000-00006
62. Carson WFT, Cavassani KA, Ito T, Schaller M, Ishii M, Dou Y, et al. Impaired CD4+ T-cell proliferation and effector function correlates with repressive histone methylation events in a mouse model of severe sepsis. *Eur J Immunol*. (2010) 40:998–1010. doi: 10.1002/eji.200939739
63. Guignant C, Lepape A, Huang X, Kherouf H, Denis L, Poitevin F, et al. Programmed death-1 levels correlate with increased mortality, nosocomial infection and immune dysfunctions in septic shock patients. *Crit Care*. (2011) 15:R99. doi: 10.1186/cc10112
64. Zhang Y, Li J, Lou J, Zhou Y, Bo L, Zhu J, et al. Upregulation of programmed death-1 on T cells and programmed death ligand-1 on monocytes in septic shock patients. *Crit Care*. (2011) 15:R70. doi: 10.1186/cc10059
65. Chen CW, Mittal R, Klingensmith NJ, Burd EM, Terhorst C, Martin GS, et al. Cutting edge: 2B4-mediated coinhibition of CD4(+) T cells underlies mortality in experimental sepsis. *J Immunol*. (2017) 199:1961–6. doi: 10.4049/jimmunol.1700375
66. Shubin NJ, Monaghan SF, Heffernan DS, Chung CS, Ayala A, B and T lymphocyte attenuator expression on CD4+ T-cells associates with sepsis and subsequent infections in ICU patients. (2013). *Crit Care* 17:R276. doi: 10.1186/cc13131
67. Unsinger J, Kazama H, Mcdonough JS, Griffith TS, Hotchkiss RS, Ferguson TA, et al. Sepsis-induced apoptosis leads to active suppression of delayed-type hypersensitivity by CD8+ regulatory T cells through a TRAIL-dependent mechanism. *J Immunol*. (2010) 184:6766–72. doi: 10.4049/jimmunol.0904054
68. Gurung P, Rai D, Condotta SA, Babcock JC, Badovinac VP, Griffith TS, et al. Immune unresponsiveness to secondary heterologous bacterial infection after sepsis induction is TRAIL dependent. *J Immunol*. (2011) 187:2148–54. doi: 10.4049/jimmunol.1101180
69. Pachot A, Monneret G, Voirin N, Leissner P, Venet F, Bohe J, et al. Longitudinal study of cytokine and immune transcription factor mRNA expression in septic shock. *Clin Immunol*. (2005) 114:61–69. doi: 10.1016/j.clim.2004.08.015
70. Leng FY, Liu JL, Liu ZJ, Yin JY, Qu HP. Increased proportion of CD4(+)CD25(+)Foxp3(+) regulatory T cells during early-stage sepsis in ICU patients. *J Microbiol Immunol Infect*. (2013) 46:338–44. doi: 10.1016/j.jmii.2012.06.012
71. Monneret G, Debard AL, Venet F, Bohe J, Hequet O, Bienvenu J, et al. Marked elevation of human circulating CD4+CD25+ regulatory T cells in sepsis-induced immunoparalysis. *Crit Care Med*. (2003) 31:2068–71. doi: 10.1097/01.CCM.0000069345.78884.0F
72. Cavassani KA, Carson WFT, Moreira AP, Wen H, Schaller MA, Ishii M, et al. The post sepsis-induced expansion and enhanced function of regulatory T cells create an environment to potentiate tumor growth. *Blood*. (2010) 115:4403–11. doi: 10.1182/blood-2009-09-241083
73. Ouwendijk WJ, Laing KJ, Verjans GM, Koelle DM. T-cell immunity to human alphaherpesviruses. *Curr Opin Virol*. (2013) 3:452–60. doi: 10.1016/j.coviro.2013.04.004
74. Limaye AP, Kirby KA, Rubenfeld GD, Leisenring WM, Bulger EM, Neff MJ, et al. Cytomegalovirus reactivation in critically ill immunocompetent patients. *JAMA*. (2008) 300:413–22. doi: 10.1001/jama.300.4.413
75. Rinaldo CR Jr, Torpey DJ III. Cell-mediated immunity and immunosuppression in herpes simplex virus infection. *Immunodeficiency*. (1993) 5:33–90.
76. Zajac AJ, Blattman JN, Murali-Krishna K, Sourdive DJ, Suresh M, Altman JD, et al. Viral immune evasion due to persistence of activated T cells without effector function. *J Exp Med*. (1998) 188:2205–13. doi: 10.1084/jem.188.12.2205
77. Pardoll DM. The blockade of immune checkpoints in cancer immunotherapy. *Nat Rev Cancer*. (2012) 12:252–64. doi: 10.1038/nrc3239
78. Wherry EJ. T cell exhaustion. *Nat Immunol*. (2011) 12:492–9. doi: 10.1038/ni.2035
79. Condotta SA, Cabrera-Perez J, Badovinac VP, Griffith TS. T-cell-mediated immunity and the role of TRAIL in sepsis-induced immunosuppression. *Crit Rev Immunol*. (2013) 33:23–40. doi: 10.1615/CritRevImmunol.2013006721
80. Leligdowicz A, Dodek PM, Norena M, Wong H, Kumar A, Kumar A, et al. Association between source of infection and hospital mortality in patients who have septic shock. *Am J Respir Crit Care Med*. (2014) 189:1204–13. doi: 10.1164/rccm.201310-1875OC
81. Ranieri VM, Thompson BT, Barie PS, Dhainaut JF, Douglas IS, Finfer S, et al. Drotrecogin alfa (activated) in adults with septic shock. *N Engl J Med*. (2012) 366:2055–64. doi: 10.1056/NEJMoa1202290
82. Opal SM, Garber GE, Larosa SP, Maki DG, Freebairn RC, Kinasewitz GT, et al. Systemic host responses in severe sepsis analyzed by causative microorganism and treatment effects of drotrecogin alfa (activated). *Clin Infect Dis*. (2003) 37:50–8. doi: 10.1086/375593
83. Martin GS, Mannino DM, Eaton S, Moss, M. The epidemiology of sepsis in the United States from 1979 through 2000. *N Engl J Med*. (2003) 348:1546–54. doi: 10.1056/NEJMoa022139
84. Bhatraju PK, Ghassemieh BJ, Nichols M, Kim R, Jerome KR, Nalla AK, et al. Covid-19 in critically ill patients in the seattle region - case series. *N Engl J Med*. (2020) 382:2012–22. doi: 10.1056/NEJMoa2004500
85. Arentz M, Yim E, Klaff L, Lokhandwala S, Riedo FX, Chong M, et al. Characteristics and outcomes of 21 critically ill patients with COVID-19 in washington state. *JAMA*. (2020) 323:1612–4. doi: 10.1001/jama.2020.4326
86. Scumpia PO, Delano MJ, Kelly KM, O'malley KA, Efron PA, Mcauliffe PF, et al. Increased natural CD4+CD25+ regulatory T cells and their suppressor

activity do not contribute to mortality in murine polymicrobial sepsis. *J Immunol*. (2006) 177:7943–9. doi: 10.4049/jimmunol.177.11.7943
87. Brinkhoff A, Siebericchs A, Engler H, Dolff S, Benson S, Korth J, et al. Pro-Inflammatory Th1 and Th17 cells are suppressed during human experimental endotoxemia whereas anti-inflammatory IL-10 producing T-cells are unaffected. *Front Immunol*. (2018) 9:1133. doi: 10.3389/fimmu.2018.01133
88. Ono S, Kimura A, Hiraki S, Takahata R, Tsujimoto H, Kinoshita M, et al. Removal of increased circulating CD4+CD25+Foxp3+ regulatory T cells in patients with septic shock using hemoperfusion with polymyxin B-immobilized fibers. *Surgery*. (2013) 153:262–71. doi: 10.1016/j.surg.2012.06.023
89. Okeke EB, Okwor I, Mou Z, Jia P, Uzonna JE. CD4+CD25+ regulatory T cells attenuate lipopolysaccharide-induced systemic inflammatory responses and promotes survival in murine escherichia coli infection. *Shock*. (2013) 40:65–73. doi: 10.1097/SHK.0b013e318296e65b
90. Zheng YS, Wu ZS, Ni HB, Ke L, Tong ZH, Li WQ, et al. Codonopsis pilosula polysaccharide attenuates cecal ligation and puncture sepsis via circuiting regulatory T cells in mice. *Shock*. (2014) 41:250–5. doi: 10.1097/SHK.0000000000000091
91. Kuhlhorn F, Rath M, Schmoeckel K, Cziupka K, Nguyen HH, Hildebrandt P, et al. Foxp3+ regulatory T cells are required for recovery from severe sepsis. *PLoS ONE*. (2013) 8:e65109. doi: 10.1371/journal.pone.0065109
92. Scumpia PO, Delano MJ, Kelly-Scumpia KM, Weinstein JS, Wynn JL, Winfield RD, et al. Treatment with GITR agonistic antibody corrects adaptive immune dysfunction in sepsis. *Blood*. (2007) 110:3673–81. doi: 10.1182/blood-2007-04-087171
93. Venet F, Chung CS, Kherouf H, Geeraert A, Malcus C, Poitevin F, et al. Increased circulating regulatory T cells (CD4(+)CD25 (+)CD127 (-)) contribute to lymphocyte anergy in septic shock patients. *Intensive Care Med*. (2009) 35:678–86. doi: 10.1007/s00134-008-1337-8
94. Carrigan SO, Yang YJ, Issekutz T, Forward N, Hoskin D, Johnston B, et al. Depletion of natural CD4+CD25+ T regulatory cells with anti-CD25 antibody does not change the course of Pseudomonas aeruginosa-induced acute lung infection in mice. *Immunobiology*. (2009) 214:211–22. doi: 10.1016/j.imbio.2008.07.027
95. Tatura R, Zeschnigk M, Hansen W, Steinmann J, Vidigal PG, Hutzler M, et al. Relevance of Foxp3(+) regulatory T cells for early and late phases of murine sepsis. *Immunology*. (2015) 146:144–56. doi: 10.1111/imm.12490
96. Wang HW, Yang W, Gao L, Kang JR, Qin JJ, Liu YP, et al. Adoptive transfer of bone marrow-derived dendritic cells decreases inhibitory and regulatory T-cell differentiation and improves survival in murine polymicrobial sepsis. *Immunology*. (2015) 145:50–9. doi: 10.1111/imm.12423
97. Nascimento DC, Melo PH, Pineros AR, Ferreira RG, Colon DF, Donate PB, et al. IL-33 contributes to sepsis-induced long-term immunosuppression by expanding the regulatory T cell population. *Nat Commun*. (2017) 8:14919. doi: 10.1038/ncomms14919
98. Kumar V. T cells and their immunometabolism: a novel way to understanding sepsis immunopathogenesis and future therapeutics. *Eur J Cell Biol*. (2018) 97:379–92. doi: 10.1016/j.ejcb.2018.05.001
99. Hou YC, Wu JM, Chen KY, Chen PD, Lei CS, Yeh SL, et al. Effects of prophylactic administration of glutamine on CD4(+) T cell polarisation and kidney injury in mice with polymicrobial sepsis. *Br J Nutr*. (2019) 122:657–65. doi: 10.1017/S0007114519000990
100. Hotchkiss RS, Swanson PE, Knudson CM, Chang KC, Cobb JP, Osborne DF, et al. Overexpression of Bcl-2 in transgenic mice decreases apoptosis and improves survival in sepsis. *J Immunol*. (1999) 162:4148–56. doi: 10.1097/00024382-199806001-00219
101. Hotchkiss RS, Tinsley KW, Swanson PE, Chang KC, Cobb JP, Buchman TG, et al. Prevention of lymphocyte cell death in sepsis improves survival in mice. *Proc Natl Acad Sci USA*. (1999) 96:14541–6. doi: 10.1073/pnas.96.25.14541
102. Hotchkiss RS, Chang KC, Swanson PE, Tinsley KW, Hui JJ, Klender P, et al. Caspase inhibitors improve survival in sepsis: a critical role of the lymphocyte. *Nat Immunol*. (2000) 1:496–501. doi: 10.1038/82741
103. Wesche-Soldato DE, Chung CS, Lomas-Neira J, Doughty LA, Gregory SH, Ayala A, et al. *In vivo* delivery of caspase-8 or Fas siRNA improves the survival of septic mice. *Blood*. (2005) 106:2295–301. doi: 10.1182/blood-2004-10-4086
104. Patil NK, Luan L, Bohannon JK, Guo Y, Hernandez A, Fensterheim B, et al. IL-15 superagonist expands mCD8+ T, NK and NKT cells after burn injury but fails to improve outcome during burn wound infection. *PLoS ONE*. (2016) 11:e0148452. doi: 10.1371/journal.pone.0148452
105. Inoue S, Unsinger J, Davis CG, Muenzer JT, Ferguson TA, Chang K, et al. IL-15 prevents apoptosis, reverses innate and adaptive immune dysfunction, and improves survival in sepsis. *J Immunol*. (2010) 184:1401–9. doi: 10.4049/jimmunol.0902307
106. West EE, Jin HT, Rasheed AU, Penaloza-Macmaster P, Ha SJ, Tan WG, et al. PD-L1 blockade synergizes with IL-2 therapy in reinvigorating exhausted T cells. *J Clin Invest*. (2013) 123:2604–15. doi: 10.1172/JCI67008
107. Shindo Y, Fuchs AG, Davis CG, Eitas T, Unsinger J, Burnham CD, et al. Interleukin 7 immunotherapy improves host immunity and survival in a two-hit model of Pseudomonas aeruginosa pneumonia. *J Leukoc Biol*. (2017) 101:543–54. doi: 10.1189/jlb.4A1215-581R
108. Venet F, Demaret J, Blaise BJ, Rouget C, Girardot T, Idealisoa E, et al. IL-7 restores T lymphocyte immunometabolic failure in septic shock patients through mTOR activation. *J Immunol*. (2017) 199:1606–15. doi: 10.4049/jimmunol.1700127
109. Unsinger J, Mcglynn M, Kasten KR, Hoekzema AS, Watanabe E, Muenzer JT, et al. IL-7 promotes T cell viability, trafficking, and functionality and improves survival in sepsis. *J Immunol*. (2010) 184:3768–79. doi: 10.4049/jimmunol.0903151
110. Francois B, Jeannet R, Daix T, Walton AH, Shotwell MS, Unsinger J, et al. Interleukin-7 restores lymphocytes in septic shock: the IRIS-7 randomized clinical trial. *JCI Insight*. (2018) 3:e98960. doi: 10.1172/jci.insight.98960
111. Dirks J, Egli A, Sester U, Sester M, Hirsch HH. Blockade of programmed death receptor-1 signaling restores expression of mostly proinflammatory cytokines in anergic cytomegalovirus-specific T cells. *Transpl Infect Dis*. (2013) 15:79–89. doi: 10.1111/tid.12025
112. Brahmer JR, Tykodi SS, Chow LQ, Hwu WJ, Topalian SL, Hwu P, et al. Safety and activity of anti-PD-L1 antibody in patients with advanced cancer. *N Engl J Med*. (2012) 366:2455–65. doi: 10.1056/NEJMoa1200694
113. Topalian SL, Hodi FS, Brahmer JR, Gettinger SN, Smith DC, Mcdermott DF, et al. Safety, activity, and immune correlates of anti-PD-1 antibody in cancer. *N Engl J Med*. (2012) 366:2443–54. doi: 10.1056/NEJMoa1200690
114. Chen CW, Xue M, Zhang W, Xie J, Coopersmith CM, Ford ML. 2B4 but not PD-1 blockade improves mortality in septic animals with preexisting malignancy. *JCI Insight*. (2019) 4:e127867. doi: 10.1172/jci.insight.127867
115. Xia Q, Wei L, Zhang Y, Sheng J, Wu W, Zhang Y, et al. Immune checkpoint receptors tim-3 and PD-1 regulate monocyte and T lymphocyte function in septic patients. *Mediators Inflamm*. (2018) 2018:1632902. doi: 10.1155/2018/1632902
116. Inoue S, Bo L, Bian J, Unsinger J, Chang K, Hotchkiss RS, et al. Dose-dependent effect of anti-CTLA-4 on survival in sepsis. *Shock*. (2011) 36:38–44. doi: 10.1097/SHK.0b013e3182168cce
117. Brahmamdam P, Inoue S, Unsinger J, Chang KC, Mcdunn JE, Hotchkiss RS, et al. Delayed administration of anti-PD-1 antibody reverses immune dysfunction and improves survival during sepsis. *J Leukoc Biol*. (2010) 88:233–40. doi: 10.1189/jlb.0110037
118. Chang KC, Burnham CA, Compton SM, Rasche DP, Mazuski RJ, Mcdonough JS, et al. Blockade of the negative co-stimulatory molecules PD-1 and CTLA-4 improves survival in primary and secondary fungal sepsis. *Crit Care*. (2013) 17:R85. doi: 10.1186/cc12711
119. Patera AC, Drewry AM, Chang K, Beiter ER, Osborne D, Hotchkiss RS, et al. Frontline science: defects in immune function in patients with sepsis are associated with PD-1 or PD-L1 expression and can be restored by antibodies targeting PD-1 or PD-L1. *J Leukoc Biol*. (2016) 100:1239–54. doi: 10.1189/jlb.4HI0616-255R
120. Zhang Y, Zhou Y, Lou J, Li J, Bo L, Zhu K, et al. PD-L1 blockade improves survival in experimental sepsis by inhibiting lymphocyte apoptosis and reversing monocyte dysfunction. *Crit Care*. (2010) 14:R220. doi: 10.1186/cc9354
121. Chang K, Svabek C, Vazquez-Guillamet C, Sato B, Rasche D, Wilson S, et al. Targeting the programmed cell death 1: programmed cell death ligand 1 pathway reverses T cell exhaustion in patients with sepsis. *Crit Care*. (2014) 18:R3. doi: 10.1186/cc13176

122. Thampy LK, Remy KE, Walton AH, Hong Z, Liu K, Liu R, et al. Restoration of T cell function in multi-drug resistant bacterial sepsis after interleukin-7, anti-PD-L1, OX-40 administration. *PLoS ONE*. (2018) 13:e0199497. doi: 10.1371/journal.pone.0199497
123. Patil NK, Guo Y, Luan L, Sherwood ER. Targeting immune cell checkpoints during sepsis. *Int J Mol Sci*. (2017) 18:2413. doi: 10.3390/ijms18112413
124. Von Herrath MG, Nepom GT. Lost in translation: barriers to implementing clinical immunotherapeutics for autoimmunity. *J Exp Med*. (2005) 202:1159–62. doi: 10.1084/jem.20051224
125. Rivera J, Tessarollo L. Genetic background and the dilemma of translating mouse studies to humans. *Immunity*. (2008) 28:1–4. doi: 10.1016/j.immuni.2007.12.008
126. Seok J, Warren HS, Cuenca AG, Mindrinos MN, Baker HV, Xu W, et al. Genomic responses in mouse models poorly mimic human inflammatory diseases. *Proc Natl Acad Sci USA*. (2013) 110:3507–12. doi: 10.1073/pnas.1222878110
127. Shay T, Jojic V, Zuk O, Rothamel K, Puyraimond-Zemmour D, Feng T, et al. Conservation and divergence in the transcriptional programs of the human and mouse immune systems. *Proc Natl Acad Sci USA*. (2013) 110:2946–51. doi: 10.1073/pnas.1222738110
128. Mak IW, Evaniew N, Ghert M. Lost in translation: animal models and clinical trials in cancer treatment. *Am J Transl Res*. (2014) 6:114–8.
129. Frattari A, Polilli E, Primiterra V, Savini V, Ursini T, Di Iorio G, et al. Analysis of peripheral blood lymphocyte subsets in critical patients at ICU admission: A preliminary investigation of their role in the prediction of sepsis during ICU stay. *Int J Immunopathol Pharmacol*. (2018) 32:2058738418792310. doi: 10.1177/2058738418792310
130. Spenlingwimmer T, Zipperle J, Jafarmadar M, Osuchowski MF, Drechsler S. Comparison of post-traumatic changes in circulating and bone marrow leukocytes between BALB/c and CD-1 mouse strains. *PLoS ONE*. (2019) 14:e0222594. doi: 10.1371/journal.pone.0222594
131. Huggins MA, Sjaastad FV, Pierson M, Kucaba TA, Swanson W, Staley C, et al. Microbial exposure enhances immunity to pathogens recognized by TLR2 but increases susceptibility to cytokine storm through TLR4 sensitization. *Cell Rep*. (2019) 28:1729–43. doi: 10.1016/j.celrep.2019.07.028
132. Nowill AE, Fornazin MC, Spago MC, Dorgan Neto V, Pinheiro VRP, Alexandre SSS, et al. Immune response resetting in ongoing sepsis. *J Immunol*. (2019) 203:1298–312. doi: 10.4049/jimmunol.1900104

Conflict of Interest: The authors declare that the research was conducted in the absence of any commercial or financial relationships that could be construed as a potential conflict of interest.

frontiers in Immunology

ORIGINAL RESEARCH
published: 21 July 2020
doi: 10.3389/fimmu.2020.01481

Pediatric Burn Survivors Have Long-Term Immune Dysfunction With Diminished Vaccine Response

Blair Z. Johnson[1], Sonia McAlister[2,3], Helen M. McGuire[4], Vetrichevvel Palanivelu[1], Andrew Stevenson[1], Peter Richmond[2,3], Debra J. Palmer[2,5], Jessica Metcalfe[2,5], Susan L. Prescott[2,5], Fiona M. Wood[2,6], Barbara Fazekas de St Groth[4], Matthew D. Linden[1], Mark W. Fear[1] and Vanessa S. Fear[7]*

[1] School of Biomedical Sciences, The University of Western Australia, Perth, WA, Australia, [2] School of Medicine, The University of Western Australia, Perth, WA, Australia, [3] Wesfarmers Centre of Vaccines and Infectious Diseases, Telethon Kids Institute, Perth, WA, Australia, [4] Ramaciotti Facility for Human Systems Biology and the Charles Perkins Centre, Discipline of Pathology, The University of Sydney, Sydney, NSW, Australia, [5] Centre for Allergy and Immunology Research, Telethon Kids Institute, Perth, WA, Australia, [6] Department of Health WA, Perth, WA, Australia, [7] Genetic and Rare Diseases, Telethon Kids Institute, Perth, WA, Australia

OPEN ACCESS

Edited by:
Florian Uhle,
Heidelberg University Hospital, Germany

Reviewed by:
Christian Koch,
University Hospital Giessen, Germany
Antonio Riva,
Foundation for Liver Research, United Kingdom

***Correspondence:**
Mark W. Fear
mark@fionawoodfoundation.com

Specialty section:
This article was submitted to Inflammation, a section of the journal Frontiers in Immunology

Received: 23 April 2020
Accepted: 08 June 2020
Published: 21 July 2020

Citation:
Johnson BZ, McAlister S, McGuire HM, Palanivelu V, Stevenson A, Richmond P, Palmer DJ, Metcalfe J, Prescott SL, Wood FM, Fazekas de St Groth B, Linden MD, Fear MW and Fear VS (2020) Pediatric Burn Survivors Have Long-Term Immune Dysfunction With Diminished Vaccine Response. Front. Immunol. 11:1481. doi: 10.3389/fimmu.2020.01481

Epidemiological studies have demonstrated that survivors of acute burn trauma are at long-term increased risk of developing a range of morbidities. The mechanisms underlying this increased risk remain unknown. This study aimed to determine whether burn injury leads to sustained immune dysfunction that may underpin long-term morbidity. Plasma and peripheral blood mononuclear cells were collected from 36 pediatric burn survivors >3 years after a non-severe burn injury (<10% total body surface area) and from age/sex-matched non-injured controls. Circulating cytokine and vaccine antibody levels were assessed using multiplex immunoassays and cell profiles compared using a panel of 40 metal-conjugated antibodies and mass cytometry. TNF-α (1.31-fold change from controls), IL-2 (1.18-fold), IL-7 (1.63-fold), and IFN-γ (1.18-fold) were all significantly elevated in the burn cohort. Additionally, burn survivors demonstrated diminished antibody responses to the diphtheria, tetanus, and pertussis vaccine antigens. Comparisons between groups using unsupervised clustering identified differences in proportions of clusters within T-cells, B-cells and myeloid cells. Manual gating confirmed increased memory T-regulatory and central memory CD4+ T-cells, with altered expression of T-cell, B-cell, and dendritic cell markers. Conclusions: This study demonstrates a lasting change to the immune profile of pediatric burn survivors, and highlights the need for further research into post-burn immune suppression and regulation.

Keywords: non-severe burn injury, immunity, vaccination, mass cytometry, acute trauma, systemic

INTRODUCTION

Burns continue to impact the lives of millions of people each year; from new injuries to ongoing recovery, the psychological, physical, and financial burden is persistent. In 2004 the World Health Organization (WHO) estimated that 11 million people globally required medical attention for a burn injury (1). A more recent annual report from the Burns Registry of Australia and New Zealand (BRANZ) recorded 3,295 cases treated at specialized burn clinics across the two countries

(2016–2017), with pediatric cases accounting for 30% of the cohort (2).

Patient outcomes are influenced by the severity of the burn injury (3, 4). Total body surface area (TBSA) involvement is used to classify burns as severe (≥20% TBSA) or non-severe (<20% TBSA). Due to their profound local and systemic effects (5, 6), severe burns remain the focus of the majority of burns research. However, the majority of burns (84%) involve a TBSA of <10% (2), and it is becoming increasingly apparent that even non-severe burns have a long-term impact on the health of survivors.

Epidemiological studies have found that burn survivors, regardless of severity, are at increased risk for a range of diseases even decades after injury, and typically have a longer length of stay when hospitalized for them. These include cardiovascular diseases (7, 8), nervous disorders (9), musculoskeletal diseases (notably infectious and inflammatory polyarthropathies) (10), cancers (11), diabetes mellitus (12), gastrointestinal diseases (13), and infections (14). Extensive data in the literature support a role for innate and adaptive immune cell dysfunction in the pathogenesis of the diseases that have an elevated incidence in burn survivors (15–19), suggesting immune dysfunction may contribute to post-burn morbidity.

In our laboratory pre-clinical studies in mice, modeling 8% TBSA involvement as a non-severe burn injury (NSBI), have demonstrated changes in innate and adaptive immunity up to 84 days post-injury (14, 20). In pediatric patients with severe burn injury, sustained elevation of circulating cytokines has been observed up to 3 years after the injury (21). In this study we have investigated whether there is an enduring change within the immune compartment of pediatric patients more than 3 years after a non-severe burn injury. We hypothesized that patients would manifest significant changes to the circulating immune profile compared to uninjured controls, reflecting a sustained impact of acute but non-severe burn trauma on the immune system.

MATERIALS AND METHODS

Specimen Collection

Children were recruited at least 3 years after presenting for a non-severe burn injury at Princess Margaret Hospital. They were aged 0–4 years of age at the time of original presentation. Age/sex-matched controls were selected from a pool of healthy donors. All samples were obtained with informed consent of a parent or guardian and the collection was conducted with ethical approval from the Child and Adolescent Health Service WA (approval numbers: 2015219EP; 1111EP; 768EP). All patients recruited had no history of pre-existing illness and were not currently on medication at time of sampling. No patients had visible signs or recent history of acute infection at the time of blood collection. Blood was collected into tubes containing preservative-free heparin, then centrifuged to collect the plasma. The remaining blood was resuspended in RPMI-1640 (Gibco, USA) and the peripheral blood mononuclear cells (PBMCs) were isolated using Lymphoprep (STEMCELL Technologies, Canada), and then cryopreserved in 10% DMSO upon slow freeze for storage.

Multiplex Cytokine Assay

Circulating cytokines were assessed using a customized Milliplex MAP human high sensitivity T cell panel multiplex bead assay (Merck). Cytokines tested were Tumor necrosis factor-alpha (TNF-α), Interleukin-8 (IL-8), Interleukin 7 (IL-7), Interleukin-6 (IL-6), Interleukin-5 (IL-5), Interleukin-2 (IL-2), Interleukin-1beta (IL-1β), Interleukin-17A (IL-17A), Interleukin-13 (IL-13), Interleukin-12 p70 (IL-12(p70)), Interleukin-10 (IL-10), Interferon-gamma (IFN-γ) and Granulocyte macrophage colony stimulating factor (GM-CSF). Briefly, plasma samples that had not been thawed since the original freeze were thawed, filtered using 0.45 μm syringe filters (Nalgene) and a 50 μl aliquot removed. Standards were prepared for each cytokine and plated in duplicate and assay conducted as per manufacturer's instructions. Each 96-well plate was read on a Luminex 200 instrument. Each sample was assayed in duplicate and the mean value for each cytokine/patient was used for statistical analysis.

Diphtheria-Tetanus-Acellular Pertussis Multiplex Immunoassay

Total IgG concentrations against vaccine antigens pertussis toxin (PT), pertactin (PRN), filamentous hemagglutinin (FHA), fimbriae 2/3 (FIM 2/3), tetanus toxin (TT), and diphtheria toxoid (DT) were measured using an in-house multiplex bead-based immunoassay. PT, PRN, and FHA were kindly provided by GlaxoSmithKline (Belgium). TT was purchased from Sigma-Aldrich while DT and FIM 2/3 was sourced from List biological laboratories (USA). A standard curve was generated using a 10-step 3-fold serial dilution of an in-house reference sera previously quantified against National Institute for Biological Standards and Control reference sera: PT (06/140), TT (TE-3), and DT (10/262). The concentration of FIM 2/3 IgG was previously assigned to 06/140 by an international collaborative study (22). Blanks and two QC samples were included on every plate to calculate% critical variance across all assays, which fell between 6 and 12.7%. Assay specificity was determined using inhibition and interference assays. No cross reactivity was detected (data not shown).

The multiplex immunoassay was carried out as per van Gageldonk et al. (23), with minor modifications. In brief, Bio-Plex® COOH-microspheres (6.25 × 106) were conjugated with optimized concentrations of antigen in 1 x PBS pH 7.2 (Life Technologies, AUS) as follows: PT 10 μg/ml, PRN 75 μg/mL, FHA 25 μg/ml, FIM 2/3 100 μg/ml, TT 100 μg/mL, and DT 100 μg/ml. Samples were diluted in PBS containing 3% bovine serum albumin (BSA) and 0.05% Tween 20 (Sigma-Aldrich). MultiScreen Filter Plates (Merck) were pre-wet with 50 μl PBS containing 0.05% Tween 20 (PBS.T) and the liquid removed by vacuum manifold (2–5 mmHg). Diluted plasma samples were mixed with bead-mix (25 μl; PBS containing 4000 beads/region) in individual wells and incubated on a plate shaker (500 rpm) protected from light for 30 min. Plates were washed twice with 100 μl of 0.05% PBS.T before the addition of 100 μl 1:200 RPE-conjugated goat-anti human IgG Fc secondary antibody (Jackson ImmunoResearch Laboratories Inc.) and incubated as above for a further 30-min. Following washing, the beads were resuspended in 125 μl 0.05% PBS.T and read using a bioplex-200 machine. Antigen-specific IgG concentrations (mIU/mL) were

determined using a 5-PL linear curve generated with Bioplex Manager software version 5.0.

Immunophenotyping by Mass Cytometry

All reagents used for mass cytometry were prepared in plastics that had not been exposed to detergents, to avoid barium contamination. Stain buffer was prepared as 0.1% bovine serum albumin (Sigma-Aldrich, Australia), 2 mM EDTA (Sigma-Aldrich), and 0.05% sodium azide (Sigma-Aldrich) dissolved in calcium/magnesium-free phosphate buffered saline (PBS; Gibco) and adjusted to pH 7.4. 4% paraformaldehyde (PFA) prepared fresh each day by dissolving PFA (Sigma-Aldrich) in PBS and adjusting pH to 7.4.

Metal-labeled antibodies (**Table 1**) were validated, pre-tittered, and supplied in per-test amounts by the Ramaciotti Facility for Human Systems Biology Reagent Bank. Reagent bank antibodies were either purchased from Fluidigm in pre-conjugated form or unlabeled antibodies were purchased in a carrier-protein-free format and conjugated at the Ramaciotti Facility with the indicated metal isotope using the MaxPAR conjugation kit (Fluidigm, South San Francisco, CA) according to the manufacturer's protocol. Four Element EQ Beads, Maxpar water, Cell-ID cisplatin, and Cell-ID DNA intercalator were purchased from Fluidigm.

Cryopreserved PBMCs were thawed rapidly then transferred into warm RPMI + 10% heat-inactivated fetal calf serum (FCS) (Bovogen, French origin) + Pierce universal nuclease (Thermofisher, Australia). Two million live PBMCs were stained as previously described (24), with amendments: 100 μL of the first surface antibody cocktail containing an individual barcoding reagent (either Pd104-CD45 for patients or Pd108-CD45 for controls, **Table 1**a) was added. Samples were incubated with stain at room temperature for 30 min. Cells were washed, then patient and control pairs were combined into a single tube and washed again. The remainder of the surface staining antibodies (**Table 1**b) were added, 100 μL per sample, and incubated on ice for 30 min. Cells were washed twice, then permeabilized with FoxP3 Fix/Perm buffer (Thermofisher) and incubated with the intracellular antibodies (**Table 1**c) on ice for 30 min. Cells were fixed overnight at 4°C in 4% PFA containing 0.125 μM DNA intercalator. After washing, cells were resuspended at 8.5×10^5 cells/mL in a 1:10 suspension of EQ beads and Maxpar water prior to data acquisition on a Fluidigm Helios mass cytometer.

Data were normalized using CyTOF Software (v6.7.1014, normalization passport EQ-P13H2303_ver2) (25, 26) and gated using Flowjo (v10.4.2). An overview of analysis is outlined in **Figure 1**. Files from each sample were cleaned by gating on Ir191_DNA, Ir193_DNA, event length, and bead-specific Ce140 to remove debris and non-cellular events. Patient and control events were debarcoded and the exported files further cleaned to remove dead cells based on high cisplatin staining (**Supplementary Figure 1**). T-cells (CD3+ CD19–), B-cells (CD19+ CD3–), and other cell lineages (CD3– CD19–) were gated and exported as individual files for use in downstream analysis. The CAPX data analysis pipeline (v2.5, Sydney Cytometry) (27) was then used to down-sample, transform (arcsine), cluster (FlowSOM) (28), and perform dimensionality reduction (tSNE) on the 3 gated populations for each subject. Events were clustered using all markers in each file except CD45, DNA-intercalator, cisplatin, and CD61. B-cells, T-cells, and "other cells" were analyzed with a range of cluster numbers between 10 and 90 to ensure cluster separation on meaningful markers. The intent was to identify the maximum number of clusters without artificially separating events that were biologically similar. A hierarchical

TABLE 1 | Antibody cocktails for immunophenotyping PBMCs by mass cytometry.

	Marker	mAb	Isotope label
a) Surface stain 1	CD45*	HI30	Pd_104
	CD45*	HI30	Pd_108
	CCR2	K036C2	Eu_151
	CD183 (CXCR3)	REA232	Dy_163
	CD184 (CXCR4)	12G5	Lu_175
	CCR7	G043H7	Tb_159
b) Surface stain 2	IgD	IA6-2	Y_89
	CD11c	Bu15	In_115
	CD19	HIB19	Nd_142
	CD56	NCAM16.2	Nd_143
	CD4	RPA-T4	Nd_145
	CD8a	RPA-T8	Nd_146
	CD20	2H7	Sm_147
	CD16	3G8	Nd_148
	CD25	M-A251	Sm_149
	CD275 (ICOSL)	MIH12	Nd_150
	CD45RO	UCHL1	Gd_152
	CD68	Y1/82A	Eu_153
	CD31	WM59	Gd_155
	CD86	IT2.2	Gd_156
	CD123	6H6	Dy_161
	CCR6	11A9	Pr_141
	CX3CR1	2A9-1	Er_164
	CD61	VI-PL2	Ho_165
	CD34	581	Er_166
	CD27	M-T271	Er_167
	CD45RA	HI100	Tm_169
	CD3	UCHT1	Er_170
	CD38	HIT2	Yb_172
	CD14	M5E2	Yb_173
	HLA-DR	G46-6	Yb_174
	CCR5	HEK/1/85a	Nd_144
	CD127	A019D5	Lu_176
	CD11b	ICRF44	Bi_209
	CCR4	L291H4	Gd_158
c) Intra-cellular stain	IDO-1	700838	Gd_154
	T-bet	4B10	Gd_160
	FoxP3	PCH101	Er_162
	Ki67	B56	Er_168
	Arginase I	14D2C43	Yb_171

**CD45 is on two isotopes in order to barcode patients (Pd_104) and controls (Pd_108). CD45 stains all leukocytes. mAb, monoclonal antibody.*

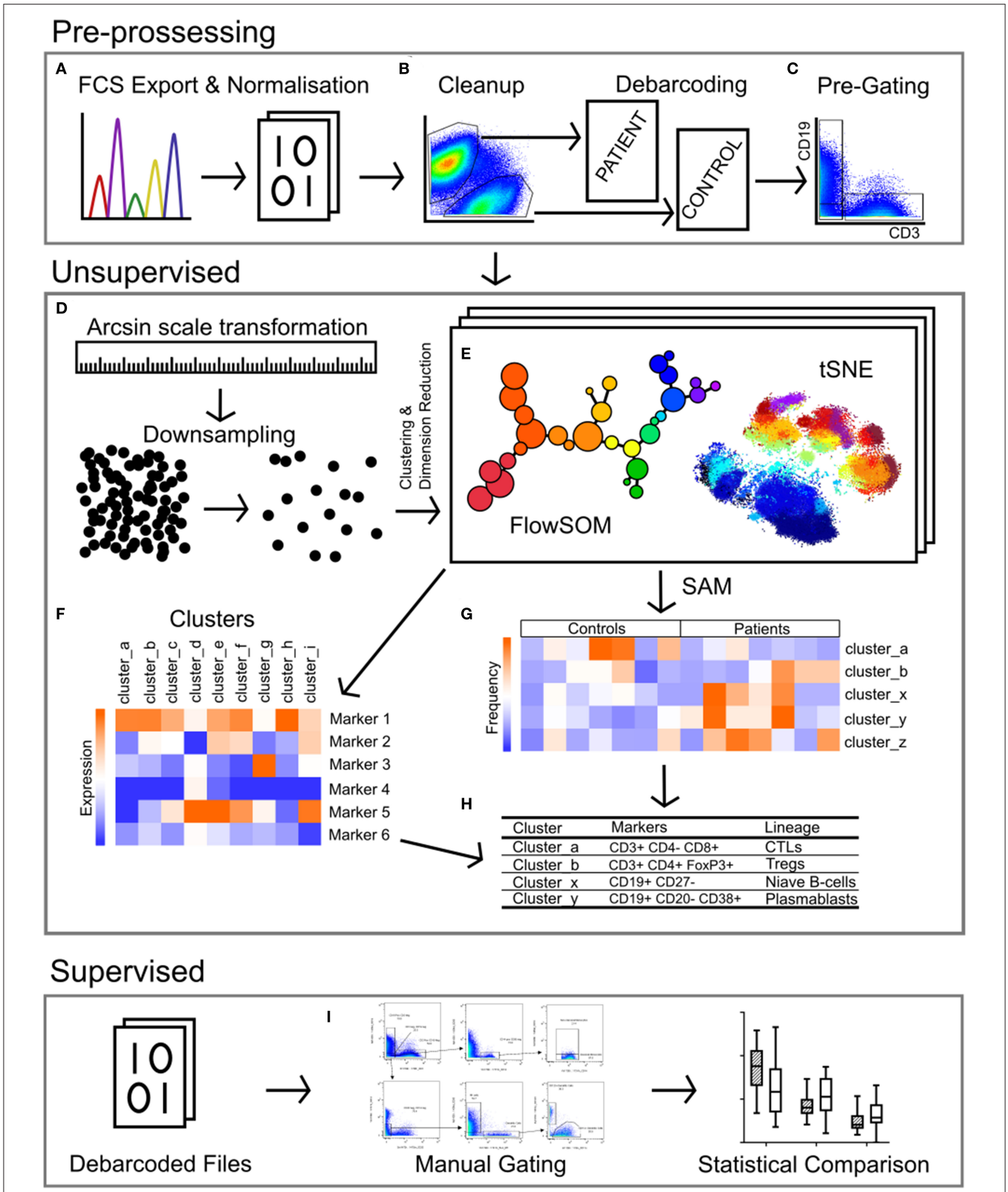

FIGURE 1 | Pipeline for the analysis of mass cytometry data. **(A)** Raw files acquired from the Helios mass cytometer were normalized based on the signal intensity of bead-specific isotopes, and exported as FCS files. **(B)** Files were manually cleaned to identify intact cells based on Ir_191 DNA staining, beads removed based on

(Continued)

FIGURE 1 | bead specific Ce_140, and doublets excluded using Ir_191 DNA staining vs. event length. Patient and control samples were debarcoded and exported into separate files based on staining with CD45-Pd_104 (patients) and CD45-Pd_108 (controls). Live cells were identified based on cisplatin stain intensity. **(C)** Events were pre-gated on CD3 vs. CD19 to export files containing T-cells (CD3+ CD19-), B-cells (CD19+ CD3-) and non-T-non-B cells (CD3- CD19-, i.e., monocytes, dendritic cells, NK cells). **(D)** The signal intensity of each marker was transformed by arcsin scaling and events from each individual were downsampled then concatenated for clustering analysis. **(E)** T-cells, B-cells, and non-T-non-B-cells were clustered separately by FlowSOM and visualized by t-stochastic neighbor embedding (tSNE). This was repeated multiple times with cluster numbers ranging from 40 to 90, in order to determine the most appropriate number of clusters **(F)** based on marker expression. **(G)** Significance analysis of microarrays (SAM) was used to identify clusters with different frequencies between patients and controls **(H),** and the lineage of these clusters was determined based on the expression of markers **(F)**. **(I)** Binary gating was employed to manually investigate previously characterized PBMC subpopulations, and to further investigate events corresponding to clusters identified in unsupervised analysis.

gating strategy (**Figure 2**) was also implemented to investigate previously described PBMC subpopulations (29) and populations identified during unsupervised clustering.

Statistics

For each sample, the mean of duplicate runs of the cytokine and vaccine antibody assays were used for Mann-Whitney comparisons of burn survivors vs. controls. Multiple Experiment Viewer (v4.9.0, TM4) (30) was used to visualize immune subset frequencies as heatmaps. Each cell in the heatmap represented the percentage of the cluster contributed by an individual subject. Significance analysis of microarrays (SAM), a technique used for large datasets (31), was implemented to identify clusters with a different frequency between paired patients and controls. Wilcoxon signed-rank test was performed on paired data from supervised gating and *p*-values adjusted for false-discovery rate. Graphs produced using GraphPad Prism (v8.0.1).

RESULTS

Sample Demographics

Blood was collected from 36 pediatric burn survivors aged 4–8 years old and compared to 36 age- and sex-matched uninjured controls. Mean burn size was 3.95 ± 3.1% TBSA, mean age at time of injury was 22 months ± 9 months and mean age at time of sample collection was 6.1 years ± 1.1 years. 17 female and 19 male burn survivors were recruited (47%:53% respectively). Age at time of injury, total body surface area, etiology of injury, and time between injury and sample collection are detailed in **Table 2**.

The Australian National Immunisation Program recommends all children receive primary diphtheria-tetanus-acellular pertussis (DTPa) vaccinations at 6–8 weeks, 4 months and 6 months of age, followed by booster doses at 18 months and 4 years. Vaccination status was verified using the Australian Immunisation Register. Records were available for 35 of the burn survivors and 27 of the controls, confirming they had completed all DTPa vaccinations according to the Australian schedule. This included receiving the vaccination at 4 years of age, which was after the burn injury for all the burn patients. Only individuals with vaccination status records were included in the vaccine-specific antibody analysis, and the others were excluded as we could not confirm vaccination status.

Cytokine Profiling

Plasma was isolated from each blood sample and tested for TNF-α, IL-8, IL-7, IL-6, IL-5, IL-2, IL-1 β, IL-17A, IL-13, IL-12(p70), IL-10, IFN-γ, and GM-CSF. Of the 13 cytokines analyzed, four were found to be significantly elevated in the burn survivors (**Figure 3A**). The inflammatory cytokine TNF-α was measured at a 1.31-fold concentration greater in patients compared to controls (mean ± SE controls, mean ± SE burn; $p < 0.01$). B cell and T cell modulating cytokines were also significantly increased in the burn group. Notably, IL-7 was 1.63-fold higher ($p < 0.01$), whilst IL-2 (mean ± SE con v burn) and IFN-γ (mean ± SE con v burn) both showed a 1.18-fold increase ($p < 0.05$). The elevation of these cytokines in the patient cohort suggests a sustained pro-inflammatory milieu may be present for many years after the initial acute trauma.

Vaccine Antibodies

Antibody responses to DTPa antigens, were compared between control and burn groups in individuals who had completed the DTPa vaccination protocol according to the Australian schedule. Burn survivors showed a diminished IgG response to pertussis toxin burn mean ± SE and control mean ± SE (0.48-fold reduction, $p < 0.05$). Similarly, pertactin IgG response was significantly decreased burn mean ± SE and control mean ± SE (0.46-fold reduction, $p < 0.01$) (**Figure 3B**). In addition, for pertussis (PT IgG ≥ 5 IU/mL) 31% of the patient cohort was below the seropositive cut-off, compared to 15% of the controls (**Figures 3C,D**). A significantly diminished response in the burn group was also observed for tetanus specific IgG, burn mean ± SE and control mean ± SE (0.48-fold, $p < 0.01$). While diphtheria toxoid IgG concentrations were comparable between groups, 11% of the burn cohort were below the threshold of long-term seroprotection against diphtheria (DT IgG ≥ 0.1 IU/mL) compared with none of the controls (**Figures 3C,D**). This decreased response to vaccine antigens in the patient cohort, observed despite the administration of a vaccine post-injury, suggests that the acute trauma may reduce the ability to respond to vaccination, mediated by a sustained systemic change, since the vaccine was administered in many cases over a year after the injury.

Immunophenotyping by Mass Cytometry

Of the 36 patients recruited, sufficient PBMCs were obtained from only 29 due to the small volume of blood collected. Of these 29, seven were excluded due to poor sample quality resulting from low cell viability, and two additional sample pairs were excluded as the barcoding step failed. Of the 20 remaining pairs,

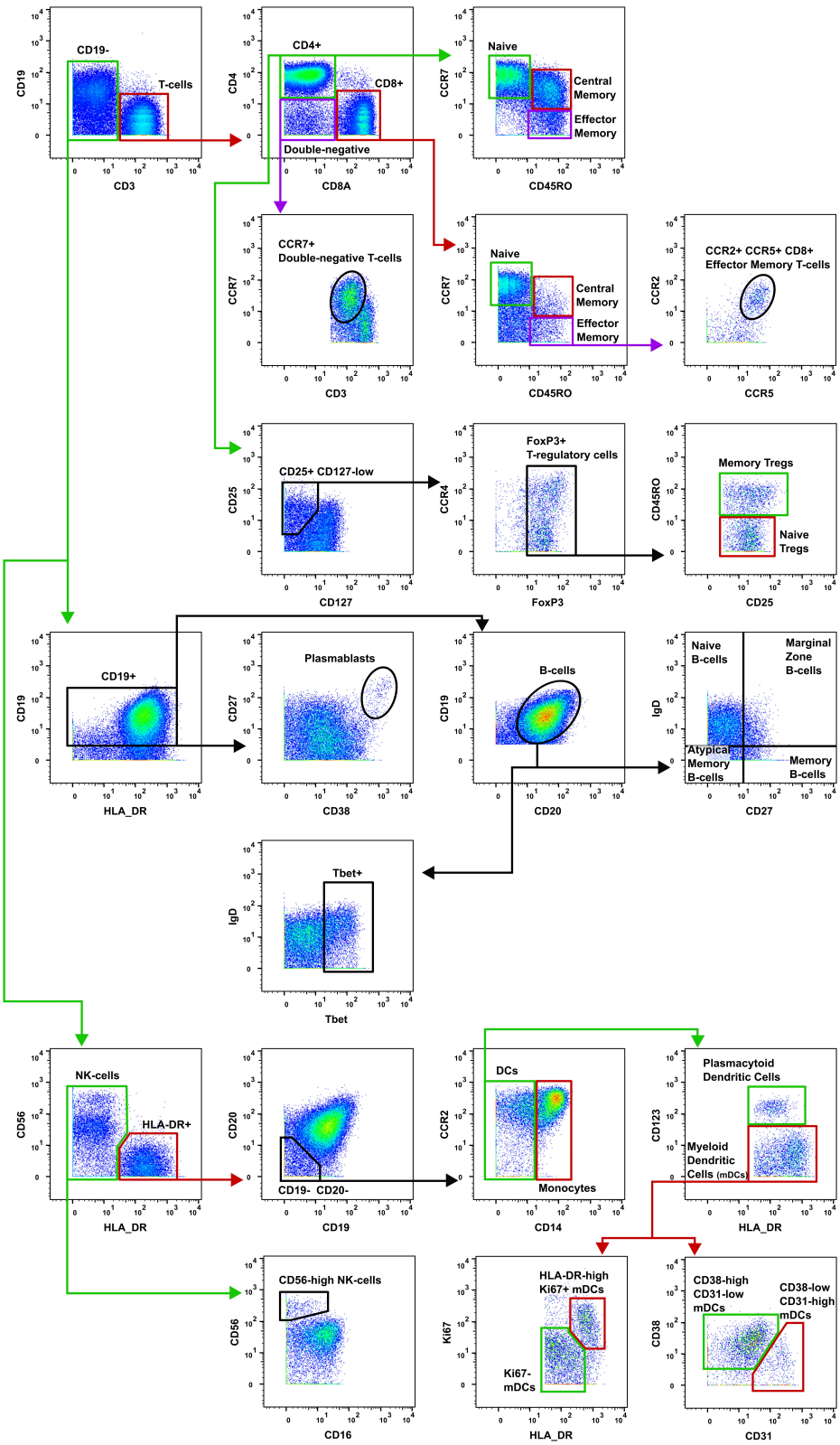

FIGURE 2 | Gating strategy for T-cell subsets. The gating strategy used to quantify the frequency of T-cell subsets in burn patients and controls. CD, cluster of differentiation; Tregs, T-regulatory cells; NK, natural killer; DCs, dendritic cells; mDCs, myeloid dendritic cells.

TABLE 2 | Details of burn injury population including age at time of injury, TBSA and etiology of the burn.

Age at burn/months	TBSA (%)	Cause of burn	Time since burn to sample collection/months
22	1	Frictional	65
13	7	Scald	59
15	3	Scald	54
18	3	Scald	51
24	<10	Scald	54
37	3	Scald	36
18	2	Frictional	44
25	2.50	Scald	52
25	8	Scald	49
18	1.5	Scald	50
16	<10	Scald	49
12	6	Scald	44
18	9	Scald	63
12	7	Scald	60
19	5	Scald	59
12	2	Chemical	65
7	1	Electrical	63
12	<2	Scald	66
18	1	Contact	62
6	<10	Sun burn	67
12	8	Scald	65
18	9	Scald	54
18	2	Thermal	55
12	1	Scald	51
18	<5	Chemical	57
12	5	Contact	53
10	<1	Contact	66
30	2	Contact	51
42	<2	Frictional	36
24	<1	Frictional	48
16	<2	Contact	55
14	3	Contact	67
41	<1	Frictional	50
38	10	Contact	59
38	1	Scald	61
36	2.50	Scald	62
36	9	Scald	54
30	<5	Frictional	63
22	1.50	Contact	60
36	1	Frictional	64
30	<1	Scald	67
36	2–3	Scald	64

13 were males and 7 were females, with a mean age of 6.3 years at time of sample collection.

Unsupervised analysis on pre-gated T-cells (CD3+), B-cells (CD19+), and all other cells (CD3-CD19-) using the CAPX pipeline (27) was used to identify 50 T-cell clusters (**Supplementary Figure 2**), 20 B-cell clusters (**Supplementary Figure 3**), and 10 non-T non-B clusters (**Supplementary Figure 4**). Analysis of the data using t-distributed stochastic neighbor embedding (t-SNE) did not demonstrate any apparent differences between patients and controls (**Supplementary Figures 2–4**). However, analysis using significance analysis of microarrays (SAM) indicated that four T-cell clusters (**Figure 4A**), four B-cell clusters (**Figure 4B**), and one non-T non-B cluster (**Figure 4C**) differed in frequency between burn survivors and controls (SAM test delta adjusted so that the type 1 error rate was 0%).

Supervised analysis using a curated gating strategy informed by the unsupervised analysis (whereby markers present on clustered populations were used to focus investigation) identified a difference in the frequencies of several T-cell subpopulations. However, there were no changes in frequency of B-cell, NK, or myeloid cell populations (**Figures 5A–C**). There was a significant increase in the frequency of central memory (CM) CD4+ T-cells (CD3+ CD4+ CD45RO+ CCR7+; 1.42-fold, $p < 0.05$) in the burn group compared to controls. There were also changes in the frequency of memory T-regulatory cells (32) (Tregs; CD3+ CD4+ CD25+ CD127-low FoxP3+ CD45RO+; 1.69-fold, $p < 0.05$) in the burn group compared to controls. In addition, there was a trend toward a higher frequency of CCR7+ double-negative (CD4- CD8-) T-cells in the burn group that failed to reach statistical significance (1.42-fold $p \approx 0.06$) (**Figure 5B**).

Several markers that were expressed by the clusters highlighted by SAM analysis of the FlowSOM data were investigated by geometric mean signal intensity on manually gated subpopulations corresponding with those identified by unsupervised analysis (**Figures 5D–G**). Interestingly, there was a significant increase in mean expression of the chemokine receptor CXCR4 on T-cells, B-cells, and mDCs in burn survivors compared to controls (1.67-fold, $p < 0.01$; 1.81-fold, $p < 0.01$; and 1.52-fold, $p < 0.05$, respectively). There was also a significant 0.73-fold decrease ($p < 0.05$) in the expression of CXCR3 on B-cells and CCR7+ DN T-cells (33, 34) in burn survivors, and a trend toward lower Tbet expression in B-cells and higher HLA-DR expression by mDCs.

DISCUSSION

Burns patients have a lifelong increase in the likelihood of developing a range of chronic inflammatory conditions (9–14, 35). The possibility of immune disruption in acute burn injuries, and more specifically severe burn trauma, has been extensively investigated. It has been established that burn injury shifts hematopoiesis to increased production of myeloid cells in the acute response to severe injury (36, 37), and there is a transient increase in circulating DC frequency after the sudden drop seen soon after severe burns (38). In cases involving sepsis, DCs fail to regain normal numbers in the circulation in the weeks following injury. Severe burn injury has also been found to abrogate proinflammatory DC responses and to disrupt DC-mediated T-cell priming, increasing the risk of infection for at least 5 days following injury (39). It is clear that

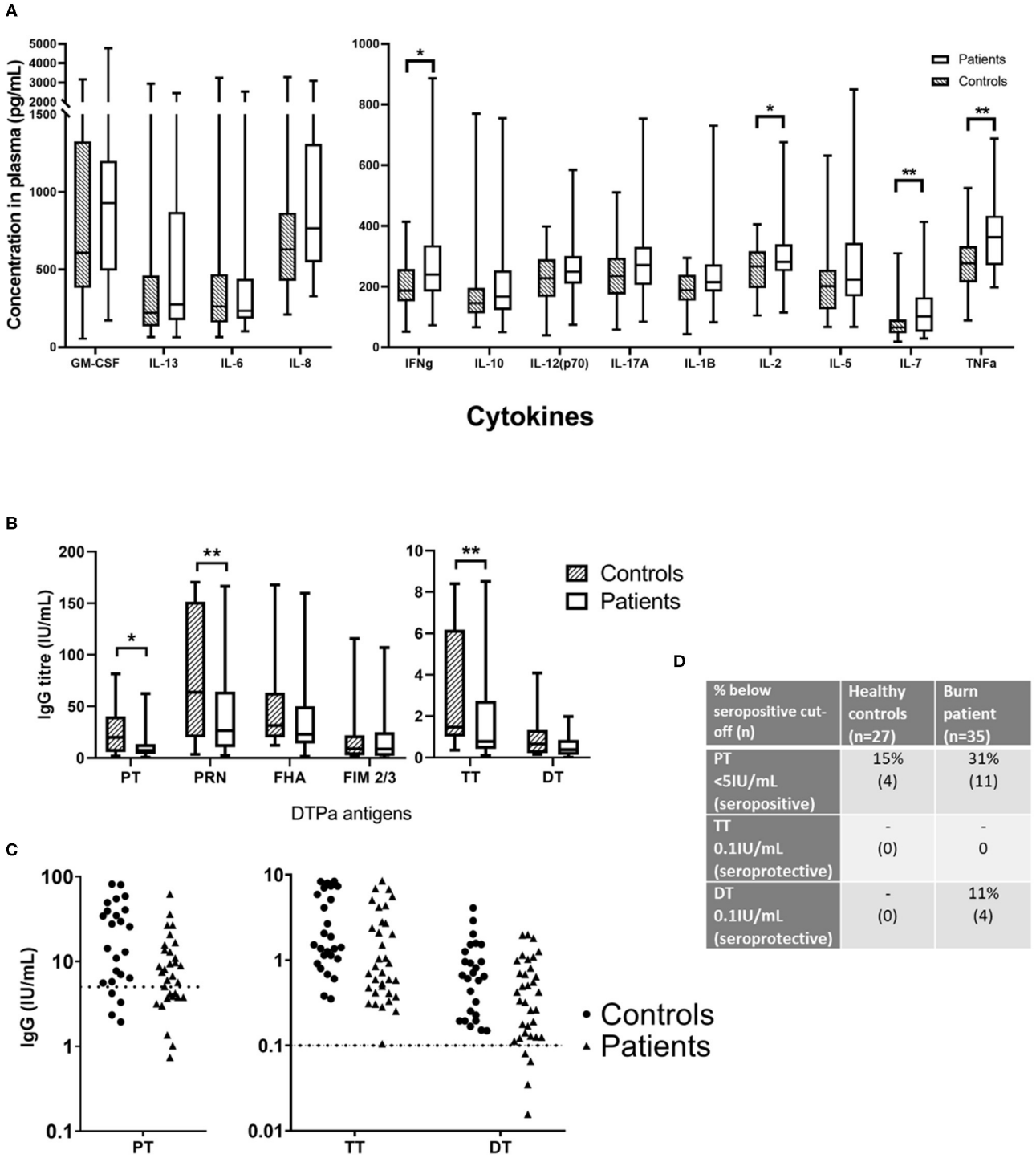

D

% below seropositive cut-off (n)	Healthy controls (n=27)	Burn patient (n=35)
PT <5IU/mL (seropositive)	15% (4)	31% (11)
TT 0.1IU/mL (seroprotective)	- (0)	- 0
DT 0.1IU/mL (seroprotective)	- (0)	11% (4)

FIGURE 3 | Concentrations of circulating cytokines and vaccine-specific IgG in plasma of burn survivors and controls. A multiplex cytokine assay was used to measure the concentration of 13 cytokines, and IgG targeting six antigens from the diphtheria, tetanus acellular pertussis (DTPa) vaccine. **(A)** Mann-Whitney tests used to compare burn survivors and controls ($n = 36$ age/sex-matched pairs) demonstrated four cytokines were elevated in burn survivors: interferon gamma, IL-2, IL-7, and tumor necrosis factor alpha. **(B)** IgG concentrations specific for pertussis toxin, pertactin, and tetanus toxin were lower in burn survivors; **(C)** dotted lines indicate thresholds of seropositivity (PT > 5 IU/mL, and long term seroprotection against tetanus and diphtheria (TT and DT IgG > 0.1IU/mL). **(D)** The rates of seropositivity/seroprotection in the burns cohort ($n = 35$) for pertussis toxin, tetanus toxin and diphtheria toxoid, compared to controls ($n = 27$). Experiments were performed in duplicate and the average used for analysis. $^{**}p < 0.01$, $^{*}p < 0.05$. GM-CSF, granulocyte-macrophage colony-stimulating factor; IL, interleukin; IFNg, interferon gamma; TNFa, tumor necrosis factor alpha; PT, pertussis toxin; PRN, pertactin; FHA, filamentous hemagglutinin; FIM 2/3, fimbriae types 2/3; TT, tetanus toxin; DT, diphtheria toxoid.

A

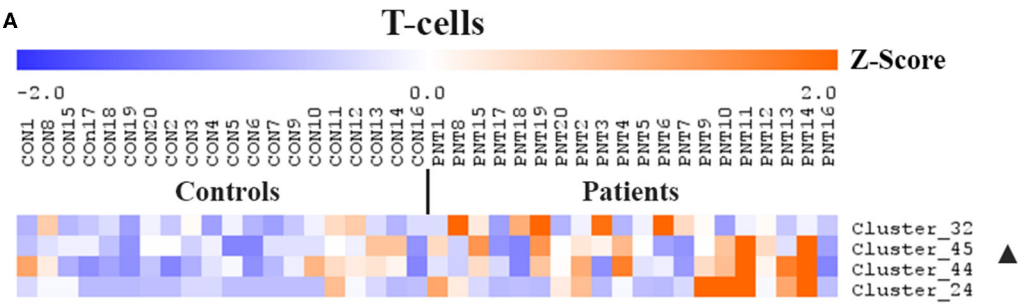

Cluster	Markers (Median expression)
T-Cluster 32	CD8a+, CD45RO-high, CCR7-low, T-bet-low, CCR5-high, CCR2-high
T-Cluster 45	CD4+, CD45RO-high, CCR7-low, CCR4-high
T-Cluster 44	CD4+, CD45RO-high, CCR7-high, CD38-low, CD127-high
T-Cluster 24	CD4–, CD8a–, CD45RA-high, CCR7-high, CXCR4-dim, CD38-dim, CXCR3-low, CD31-dim

B

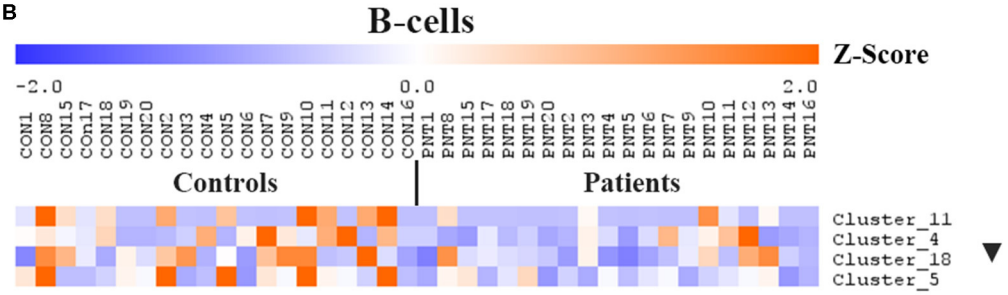

Cluster	Markers (Median expression)
B-Cluster 11	CD20+, CD27-low, IgD-low, CCR7-low, CXCR4-low, CD38-low, CXCR3-high, T-bet-high, CD11c-low
B-Cluster 4	CD20+, CD27-low, IgD-high, CCR7-low, CXCR4-low, CD38-dim
B-Cluster 18	CD20+, CD27-low, IgD-low, CCR7-low CXCR4-low, CD38-low
B-Cluster 5	CD20+, CD27-low, IgD-high, CCR7-low, CXCR4-low, T-bet-high, CD11c-low, CXCR3-low

C

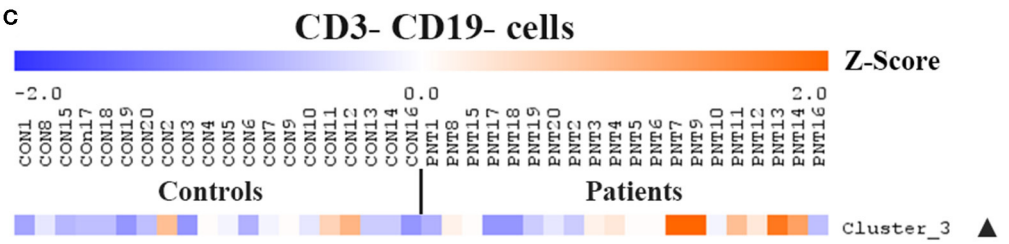

Cluster	Markers (Median expression)
Other-Cluster 3	HLA-DR-bright CD11c-high CD31-high CCR2–high CCR5-dim CD45RA-low CD38-high Ki67-high

FIGURE 4 | Clusters and cell lineages with disparate frequencies between burn survivors and controls determined by unsupervised clustering analysis. FlowSOM clustering was undertaken on paired data from patients and matched controls. Data was pre-gated on CD3+ and CD19+ to analyse **(A)** T-cell subpopulations, **(B)**

(Continued)

FIGURE 4 | B-cell subpopulations, and **(C)** CD3- CD19- subpopulations, respectively. Significance analysis of microarrays (SAM) was used to identify clusters with disproportionate frequencies between patients and controls, which are shown here. The frequency of events in a cluster from each individual has been normalized per-cluster (rows) and presented as a z-score. Positive and negative markers for identifying lineages were determined using median expression values of markers in each cluster. Ordered by age of pairing. n = 20 age/sex-matched pairs. CD, cluster of differentiation; ▲, increased frequency in patients compared to controls; ▼, decreased frequency in patients compared to controls.

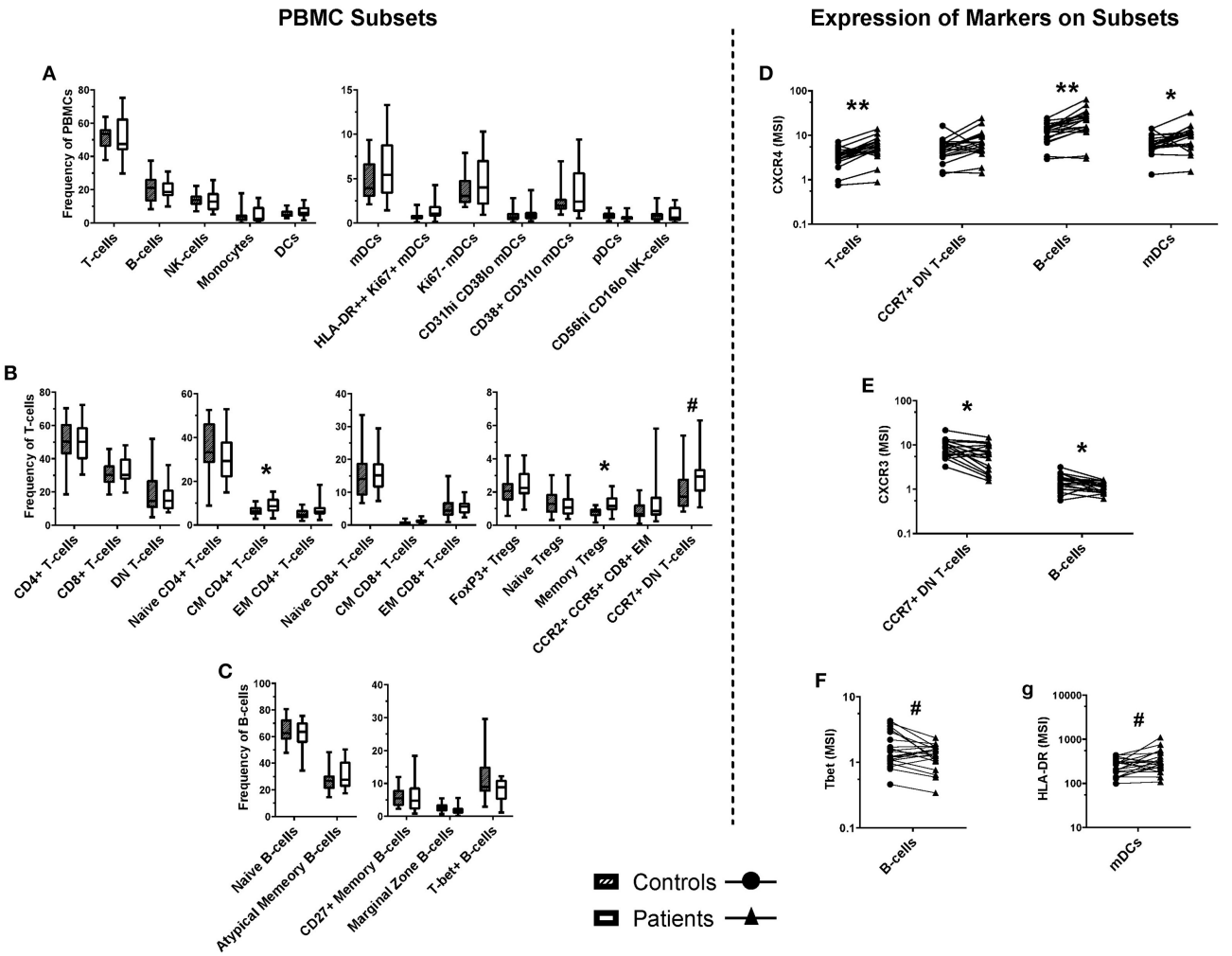

FIGURE 5 | Frequencies of cell populations in pediatric burn patients vs. matched controls, and the expression of markers on several subsets. A binary gating approach was used to manually identify leukocyte subpopulations in PBMCs stained for mass cytometry. Significant differences were identified using Wilcoxin signed-rank test. **(A)** Populations analyzed a frequency of total PBMCs, including overall CD3+ (T-cells) and CD19+ (B-cells), NK cells, monocytes, and dendritic cells. **(B)** T-cell subpopulations analyzed as a frequency of CD3+ cells. Significant increases were identified in the frequency of central memory CD4+ T-cells and memory Tregs, and a trending increase was identified in the frequency of CCR7+ double-negative (CD4- CD8-) T-cells. **(C)** B-cell subpopulations analyzed as a frequency of CD19+ CD20+ cells. Unsupervised analysis informed the investigation of signal intensity for **(D)** CXCR4 on T-cells, B-cells, and mDCs, **(E)** CXCR3 on DN T-cells and B-cells, **(F)** Tbet on B-cells, and **(G)** HLA-DR on mDC subpopulations. CXCR4 expression was found to be increased across T-cells, B-cells, and mDCs, while CXCR3 expression was decreased on CCR7+ DN T-cells and B-cells. A trending decrease in the expression of Tbet was identified in B-cells, and a trending increase in the expression of HLA-DR $^{**}p < 0.01$, $^{*}p < 0.05$, $^{\#}p < 0.1$. CD, cluster of differentiation; mDC, myeloid dendritic cells; pDC, plasmacytoid dendritic cells; CM, central memory; NK, natural killer; Th, T-helper; DN, double negative (CD4- CD8-), T-bet, T-box expressed in T-cells, CCR, C-C pattern chemokine receptor, CXCR, C-X-C pattern chemokine receptor, IgD, immunoglobulin D. MSI, mean signal intensity. $n = 20$ age/sex-matched controls.

burn injuries, specifically severe burn injuries, result in acute immune dysregulation. Current research has understandably focused on improving survival for those worst impacted by burn trauma. What remains unclear is whether these changes persist, and to what extent they manifest in survivors of non-severe burn injuries.

In this study we performed a comprehensive analysis of immune parameters in children who had suffered a burn

to <10% of total body surface area at least 3 years prior, compared to age- and sex-matched controls. We noted multiple abnormalities in the patient cohort, including increased plasma cytokines, decreased vaccine responses, and a number of changes in immune cell populations and the expression of immune molecules by those populations.

Circulating concentrations of TNF-α, IL-7, IL-2, and IFN-γ were all elevated in the patient cohort. DTPa-specific antibodies were lower resulting in diminished rates of seroprotection to diphtheria and pertussis seropositivity amongst the burn survivors. The frequency of memory T-cell subsets—central memory CD4+ T-cells and memory Tregs—was higher for burn survivors, and expression of CXCR4 across B-cells, T-cells, and myeloid dendritic cells was increased. CXCR3 expression on B-cells and a subset of double-negative T-cells was lower in patients than controls. The increase in central memory CD4+ T-cells and memory Tregs is consistent with the findings in a recent report that used mass cytometry to investigate blood immune subsets in complex regional pain syndrome, another condition in which inflammation persists long after the original injury (40).

Elevated plasma levels of TNF-α are associated with inflammation and are a risk factor for cardiovascular disease (41). TNF-α is also implicated in the development of diabetes mellitus and inflammatory polyarthropathies (42–44). A sustained elevation of TNF-α suggests that burn survivors have a chronic inflammatory condition. This would typically be driven by macrophages, which have been shown to persist in scar tissue many weeks after injury (45). However, TNF-α secreting M1 macrophages are generally replaced by M2 macrophages after several weeks of healing (46, 47). An alternative source of TNF-α (and IL-2 and IFN-γ) in the scar/skin microenvironment is tissue resident memory T-cells (Trm) (48). It is unknown whether a distinct population of Trm persists in burn scars or other parts of the dermis, but they have previously been associated with chronic inflammatory diseases and pose an interesting avenue for further research (48).

IL-7 is produced by stromal cells in the bone marrow, thymus, and lymph nodes, all hematopoietic tissues, and cells found in the skin, including keratinocytes and fibroblasts (49, 50). IL-7 is necessary for lymphoid proliferation and maturation, and acts to maintain peripheral homeostasis of T-cells (51). Exposure to IL-7 has been associated with increased expression of CXCR4 in mature T-cells, which may explain the significantly increased expression of CXCR4 on T-cell subsets in burn survivors. IL-7 is known to protect against apoptosis in T-cells via increased expression of Bcl2 (52), which contributes to T-cell survival. This may have an impact on the T-cell frequencies observed in burn survivors, particularly (central) memory T-cells, as IL-7 supports the transition from effector phenotypes to long-term memory (53).

CXCR4 is involved in the regulation of hematopoiesis, bone marrow homing, and sequestering progenitor cells in the bone marrow (54). We did not identify any differences in the frequency of circulating progenitor cells, and there was no significant decrease in the frequency of any PBMC subset despite an increase in CXCR4 expression across B-, T-, and myeloid cells. This study did not consider changes to the bone marrow niche, which may be disrupted by aberrant CXCR4 expression, or the expression of the CXCR4 ligand CXCL12, which is constitutively expressed by bone marrow stromal cells (55).

Dendritic cells have been shown to downregulate MHC-II expression in response to IL-7 (56). However, our data show a trend toward increased expression of HLA-DR in burn survivors at 3 years post-injury. Decreased expression of MHC-II on DCs has been reported in studies using mouse models of burn injury (20) at 3 months post-injury; the duration of this reduction is unknown, though the data presented here suggests it does not persist for 3 years. Elevated IL-7 concentrations could potentially be contributing to low seroprotection rates in burn survivors via DC MHC-II downregulation at the time of vaccination, although further studies will be required to confirm such a mechanism.

IFN-γ is secreted by CD4+ T-cells, CD8+ effector T-cells, macrophages, and NK cells. Although there were no significant differences in the frequencies of CD8+ T-cells or NK cells between burn survivors and controls (macrophages were not assessed in this study) there may have changes in cell phenotype. Potentially there is a skew in CD8+ T cells or NK cells toward cytokine secreting rather than cytotoxic cells that contributes to the elevated levels of IFN-γ in burn survivors. The expression of IFN-γ in response to stimulation was not assessed for this study, but should be considered for future work, along with cytotoxicity markers including Granzyme B and Perforin. The functional responses of these cells *ex vivo* or after stimulations with antigen may highlight changes in the burn survivor's immune system.

Of note, IFN-γ is a regulator of DC maturation (57), which is associated with the increased expression of CXCR4 on plasmacytoid DCs (58, 59), which are potent type I IFN producers. Interestingly in this burn patient cohort we found increased CXCR4 expression on the myeloid DC population. In keeping with recent findings of increased viral infection and cancer in burn patients (11, 14), studies indicate prolonged type I IFN production is linked with immune cell dysfunction in both viral infection and cancer (60). The implications for post-burn pathophysiology are unclear—however increased CXCR4 expression by circulating DCs may reflect an overall increase in DC maturation, particularly in secondary lymphoid tissues where DCs drive T-cell responses through antigen presentation and co-stimulatory activation.

IFN-γ has also been shown to directly upregulate the expression of the immune checkpoint molecule PD-L1 that contributes to immune tolerance (61, 62). It is likely that the long-term increase in IFN-γ titres in burn survivors is associated with an increase in expression of PD-1/PD-L1, similar to the increase in PD-1/PD-L1 across B- and T-cells in patients with sepsis or severe burn injury (63). Indeed, the multiorgan failure that is a major cause of morbidity in sepsis, and is associated with increased risk of infection and ineffective adaptive immunity, may be due to aberrant expression of checkpoint molecules leading to impaired immune responses, particularly in T-cells (64). Similar increases in PD-1/PD-L1 have been observed in patients undergoing surgery with systemic inflammatory response syndrome (65).

T-bet expression in B-cells is associated with antigen experience and IgG2a/c class-switching (66). Alternatively,

CXCR3 expression in B-cells is associated with IgG1 co-expression (67), and is involved in lymphoid follicular homing and this may contribute to reduced antibody isotype switching (33). We observed a decrease in CXCR3 expression on B-cells in burn survivors, with a trend for decreased T-bet expression, and this may contribute to the reduced DTPa IgG concentrations, and decreased seroprotection/seropositivity rates. Alternatively, an immunosuppressive environment may drive the difference between T- and B-cell phenotypes in patients and controls: the dominant function of IL-2 is to support the differentiation, survival and function of regulatory T-cells (68). The increased frequency of memory Tregs in burn survivors may reflect increased availability of IL-2. Additionally, IL-2 inhibits the development of T follicular helper cells which have a role in the regulation of B-cell proliferation and class-switching (69, 70). Immunosuppression and tolerance have an important role in the pathogenesis and progression of cancer and infection (15, 71), and this may further contribute to the severity of post-burn morbidities.

There are observed similarities with the changes observed in this study and those observed with severe burn injury and other severe pathologies such as sepsis. Multiorgan failure due to pronounced systemic inflammation is a major cause of morbidity in sepsis, however these patients are also observed to be at increased risk of infection and demonstrate ineffective adaptive immunity (64). Other studies of the impact of burn injury have shown sustained elevated cytokine levels, with IL-1α, Il-7 and IFN-γ all shown to be elevated for up to 1–2 months post-injury in pediatric patients (final follow-up (5, 72). In the long-term, widespread elevation of cytokines has been observed up to 3 years post-severe burn injury in children (21), with only IL-12p70 and MIP1β not showing sustained elevation. These studies also demonstrate long-term clinical impacts of the burn on metabolism and physical function, supporting a likely link of this hyperinflammation to pathology.

Our study did not include PD-1 or PD-L1 in our marker panel, so we cannot draw direct conclusions regarding long-term immune checkpoint dysfunction in survivors of NSBI. However, evidence exists that demonstrates a severe burn injury, in conjunction with bacterial infection, can lead to increased PD-L1 expression in a mouse model, with improved survival at 7 days following anti-PD-L1 therapy (73). Therefore, further studies to examine immune checkpoint in NSBI are warranted.

Our approach provides a broad snapshot of the immune system in pediatric burn survivors. Whilst many of the changes observed were subtle between the two groups, given the epidemiological, patient and animal study evidence for sustained impacts of burn injury (7–14, 20, 21), we believe it is likely these subtle immune changes, magnified over time, contribute to the increase in susceptibility to disease. However, there are limitations to these findings. The scope of the studywas restricted to the circulating components of the immune system and cannot provide any insight into the constituents of different tissues. Therefore, we cannot draw any conclusions regarding differences between patients and controls that may exist in the bone marrow, lymphoid organs, skin, and other tissues—e.g., it may be more informative to investigate immune memory in the bone marrow (74). The relatively small sample size is also a key limitation of this study and further patient recruitment will be important to validate findings from this cohort. Nevertheless, this study is comparable to those of others that have also identified changes in PBMC profiles associated with sustained pathology (40) and provides new insight into the possible consequences of acute burn injury and an important basis for further research. Most importantly, whilst these experiments provide observations of changes in these cell populations, functional assays will be critical to understand the potential clinical consequences of the observed disparity between groups.

In conclusion, this study provides evidence of an enduring change to the circulating components of the immune system in pediatric burn survivors at least 3 years after a non-severe burn injury. Burn survivors appeared to have a more limited response to the DTPa vaccine booster (administered at 4 years of age), and significant changes to T-cell lineages, coupled with disparate expression of surface proteins and transcription factors in T-, B- and dendritic cells. This suggests an ongoing impact of burn trauma on the immune system. These changes hint at a mechanism that may drive the rates of post-burn infections and other diseases controlled by the adaptive immune response. Further work to unravel the link between this disparity and the secondary morbidities observed in burn survivors will be important to understanding the systemic impacts of burn trauma, and the development of therapeutic pathways to reduce the incidence of morbidity in children who recover from a burn.

DATA AVAILABILITY STATEMENT

The raw data supporting the conclusions of this article will be made available by the authors, without undue reservation. Debarcoded files are uploaded to Flow Repository http://flowrepository.org/id/FR-FCM-Z2XE.

ETHICS STATEMENT

The studies involving human participants were reviewed and approved by Child and Adolescent Health Service Ethics committee. Written informed consent to participate in this study was provided by the participants' legal guardian/next of kin.

AUTHOR CONTRIBUTIONS

BJ, HM, AS, ML, FW, MF, and VF: study concept and design. FW, PR, VP, SP, DP, and JM: patient recruitment and clinical expertise. BJ, HM, SM, and VP: experimental work. BJ, HM, ML, MF, and BF: data analysis and interpretation. All authors: manuscript preparation and revision.

FUNDING

This work was funded through a grant provided by the Western Australian Department of Health Telethon-Perth Children's Hospital Research Fund and funding from the Fiona Wood Foundation. MF was supported by the Stan Perron Centre for Excellence for Childhood Burns and Perth Childrens' Hospital Foundation.

ACKNOWLEDGMENTS

We acknowledge the facilities and the Scientific and Technical Assistance of Microscopy Australia at the Centre for Microscopy, Characterization & Analysis, The University of Western Australia, a facility funded by the University, State and Commonwealth Governments, and furthermore the support of Andrea Holme and Irma Larma. Thanks to Felix Marsh-Wakefield and Thomas Ashhurst at the University of Sydney for their advice on analyzing mass cytometry datasets. We would also like to thank all the support staff at Sydney Cytometry and the Ramaciotti Facility for Human Systems Biology for their assistance with the mass cytometry studies. ML and HM are ISAC Marylou Ingram Scholars.

SUPPLEMENTARY MATERIAL

The Supplementary Material for this article can be found online at: https://www.frontiersin.org/articles/10.3389/fimmu.2020.01481/full#supplementary-material

REFERENCES

1. Mathers C, Fat DM, Boerma JT, World Health Organization. *The Global Burden of Disease: 2004 Update*. Geneva: World Health Organization (2008).
2. Tracy L, McInnes J, Gong J, Gabbe B, Thomas T. *BRANZ Annual Report July 2016.* Melbourne, VIC (2017). p. 61.
3. Duke J, Wood F, Semmens J, Spilsbury K, Edgar DW, Hendrie D, et al. A 26-Year Population-based study of burn injury hospital admissions in Western Australia. *J Burn Care Res.* (2011) 32:379–86. doi: 10.1097/BCR.0b013e318219d16c
4. Brusselaers N, Monstrey S, Vogelaers D, Hoste E, Blot S. Severe burn injury in europe: a systematic review of the incidence, etiology, morbidity, and mortality. *Crit Care.* (2010) 14:R188. doi: 10.1186/cc9300
5. Jeschke MG, Chinkes DL, Finnerty CC, Kulp G, Suman OE, Norbury WB, et al. The pathophysiologic response to severe burn injury. *Ann Surg.* (2008) 248:387–401. doi: 10.1097/SLA.0b013e3181856241
6. Gauglitz GG, Song J, Herndon DN, Finnerty CC, Boehning D, Barral JM, et al. Characterization of the inflammatory response during acute and post-acute phases after severe burn. *Shock.* (2008) 30:503–7. doi: 10.1097/SHK.0b013e31816e3373
7. Duke JM, Randall SM, Fear MW, O'Halloran E, Boyd JH, Rea S, et al. Long term cardiovascular impacts after burn and non-burn trauma: a comparative population-based study. *Burns.* (2017) 43:1662–72. doi: 10.1016/j.burns.2017.08.001
8. O'Halloran E, Shah A, Dembo L, Hool L, Viola H, Grey C, et al. The impact of non-severe burn injury on cardiac function and long-term cardiovascular pathology. *Sci Rep.* (2016) 6:34650. doi: 10.1038/srep34650
9. Vetrichevvel TP, Randall SM, Fear MW, Wood FM, Boyd JH, Duke JM. Burn injury and long-term nervous system morbidity: a population-based cohort study. *BMJ Open.* (2016) 6:e12668. doi: 10.1136/bmjopen-2016-012668
10. Randall SM, Fear MW, Wood FM, Rea S, Boyd JH, Duke JM. Long-term musculoskeletal morbidity after adult burn injury: a population-based cohort study. *BMJ Open.* (2015) 5:e009395. doi: 10.1136/bmjopen-2015-009395
11. Duke JM, Bauer J, Fear MW, Rea S, Wood FM, Boyd J. Burn injury, gender and cancer risk: population-based cohort study using data from Scotland and Western Australia. *BMJ Open.* (2014) 4:e003845. doi: 10.1136/bmjopen-2013-003845
12. Duke JM, Randall SM, Fear MW, Boyd JH, Rea S, Wood FM. Diabetes mellitus after injury in burn and non-burned patients: a population based retrospective cohort study. *Burns.* (2018) 44:566–72. doi: 10.1016/j.burns.2017.10.019
13. Stevenson AW, Randall SM, Boyd JH, Wood FM, Fear MW, Duke JM. Burn leads to long-term elevated admissions to hospital for gastrointestinal disease in a West Australian population based study. *Burns.* (2017) 43:665–73. doi: 10.1016/j.burns.2016.09.009
14. Fear VS., Boyd JH, Rea S, Wood FM, Duke JM, Fear MW. Burn injury leads to increased long-term susceptibility to respiratory infection in both mouse models and population studies. *PLoS ONE.* (2017) 12:e0169302. doi: 10.1371/journal.pone.0169302
15. Vinay DS, Ryan EP, Pawelec G, Talib WH, Stagg J, Elkord E, et al. Immune evasion in cancer: mechanistic basis and therapeutic strategies. *Semin Cancer Biol.* (2015) 35:S185–98. doi: 10.1016/j.semcancer.2015.03.004
16. Allan SM, Rothwell NJ. Inflammation in central nervous system injury. *Philos Trans R Soc Lond B Biol Sci.* (2003) 358:1669–77. doi: 10.1098/rstb.2003.1358
17. Hidalgo E, Essex SJ, Yeo L, Curnow SJ, Filer A, Cooper MS, et al. The response of T cells to interleukin-6 is differentially regulated by the microenvironment of the rheumatoid synovial fluid and tissue. *Arthritis Rheum.* (2011) 63:3284–93. doi: 10.1002/art.30570
18. Neuman MG. Immune dysfunction in inflammatory bowel disease. *Transl Res.* (2007) 149:173–86. doi: 10.1016/j.trsl.2006.11.009
19. Pickup JC. Inflammation and activated innate immunity in the pathogenesis of type 2 diabetes. *Diabetes Care.* (2004) 27:813–23. doi: 10.2337/diacare.27.3.813
20. Valvis SM, Waithman J, Wood FM, Fear MW, Fear VS. The immune response to skin trauma is dependent on the etiology of injury in a mouse model of burn and excision. *J Invest Dermatol.* (2015) 135:2119–28. doi: 10.1038/jid.2015.123
21. Jeschke MG, Gauglitz GG, Kulp GA, Finnerty CC, Williams FN, Kraft R, et al. Long-term persistence of the pathophysiologic response to severe burn injury. *PLoS ONE.* (2011) 6:e21245. doi: 10.1371/journal.pone.0021245
22. Xing D, Wirsing von König CH, Newland P, Riffelmann M, Meade BD, Corbel M, et al. Characterization of reference materials for human antiserum to pertussis antigens by an international collaborative study. *Clin Vaccine Immunol.* (2009) 16:303–11. doi: 10.1128/CVI.00372-08
23. van Gageldonk PGM, van Schaijk FG, van der Klis FR, Berbers GAM. Development and validation of a multiplex immunoassay for the simultaneous determination of serum antibodies to Bordetella pertussis, diphtheria and tetanus. *J Immunol Methods.* (2008) 335:79–89. doi: 10.1016/j.jim.2008.02.018
24. Kaur S, Sehgal R, Shastry SM, McCaughan G, McGuire HM, Fazekas de St Groth B, et al. Circulating endothelial progenitor cells present an inflammatory phenotype and function in patients with alcoholic liver cirrhosis. *Front Physiol.* (2018) 9:556. doi: 10.3389/fphys.2018.00556
25. Saeys Y, van Gassen S, Lambrecht BN. Computational flow cytometry: helping to make sense of high-dimensional immunology data. *Nat Rev Immunol.* (2016) 16:449–62. doi: 10.1038/nri.2016.56
26. Leipold MD, Obermoser G, Fenwick C, Kleinstuber K, Rashidi N, McNevin JP, et al. Comparison of CyTOF assays across sites: results of a six-center pilot study. *J Immunol Methods.* (2018) 453:37–43. doi: 10.1016/j.jim.2017.11.008
27. Ashhurst T. *Cytometry Analysis Pipeline for Large and CompleX Datasets v2.5.* (2018). Available online at: https://github.com/sydneycytometry/CAPX (accessed January 01, 2019).
28. van Gassen S, Callebaut B, van Helden MJ, Lambrecht BN, Demeester P, Dhaene T, et al. FlowSOM: using self-organizing maps for visualization

and interpretation of cytometry data. *Cytometry A.* (2015) 87:636–45. doi: 10.1002/cyto.a.22625
29. Maecker HT, McCoy JP, Nussenblatt R. Standardizing immunophenotyping for the human immunology project. *Nat Rev Immunol.* (2012) 12:191–200. doi: 10.1038/nri3158
30. Saeed A i., Sharov V, White J, Li J, Liang W, Bhagabati N, et al. TM4: a free, open-source system for microarray data management and analysis. *BioTechniques.* (2003) 34:374–8. doi: 10.2144/03342mt01
31. Tusher VG, Tibshirani R, Chu G. Significance analysis of microarrays applied to the ionizing radiation response. *PNAS.* (2001) 98:5116–21. doi: 10.1073/pnas.091062498
32. Rosenblum MD, Way SS, Abbas AK. Regulatory T cell memory. *Nat Rev Immunol.* (2016) 16:90–101. doi: 10.1038/nri.2015.1
33. D'Acquisto F, Crompton T. CD3+CD4-CD8- (double negative) T cells: saviours or villains of the immune response? *Biochem Pharmacol.* (2011) 82:333–40. doi: 10.1016/j.bcp.2011.05.019
34. Haug T, Aigner M, Peuser MM, Strobl CD, Hildner K, Mougiakakos D, et al. Human double-negative regulatory T-cells induce a metabolic and functional switch in effector T-cells by suppressing mTOR activity. *Front Immunol.* (2019) 10:883. doi: 10.3389/fimmu.2019.00883
35. Barrett LW, Fear VS., Waithman JC, Wood FM, Fear MW. Understanding acute burn injury as a chronic disease. *Burns Trauma.* (2019) 7:23. doi: 10.1186/s41038-019-0163-2
36. Posluszny JA, Muthumalaiappan K, Kini AR, Szilagyi A, He L-K, Li Y, et al. Burn injury dampens erythroid cell production through reprioritizing bone marrow hematopoietic response. *J Trauma*. (2011) 71:1288–96. doi: 10.1097/TA.0b013e31822e2803
37. Johnson NB, Posluszny JA, He LK, Szilagyi A, Gamelli RL, Shankar R, et al. Perturbed MafB/GATA1 axis after burn trauma bares the potential mechanism for immune suppression and anemia of critical illness. *J Leukoc Biol.* (2016) 100:725–36. doi: 10.1189/jlb.1A0815-377R
38. D'Arpa N, Accardo-Palumbo A, Amato G, D'Amelio L, Pileri D, Cataldo V, et al. Circulating dendritic cells following burn. *Burns.* (2009) 35:513–8. doi: 10.1016/j.burns.2008.05.027
39. Shen H, de Almeida PE, Kang KH, Yao P, Chan CW. Burn injury triggered dysfunction in dendritic cell response to TLR9 activation and resulted in skewed T cell functions. *PLoS One.* (2012) 7:e50238. doi: 10.1371/journal.pone.0050238
40. Russo MA, Fiore NT, van Vreden C, Bailey D, Santarelli DM, McGuire HM, et al. Expansion and activation of distinct central memory T lymphocyte subsets in complex regional pain syndrome. *J Neuroinflammation.* (2019) 16:63. doi: 10.1186/s12974-019-1449-9
41. Zhang H, Park Y, Wu J, Chen XP, Lee S, Yang J, et al. Role of TNF-α in vascular dysfunction. *Clin Sci.* (2009) 116:219–30. doi: 10.1042/CS20080196
42. Akash MSH, Rehman K, Liaqat A. Tumor necrosis factor-alpha: role in development of insulin resistance and pathogenesis of type 2 diabetes mellitus. *J Cell Biochem.* (2018) 119:105–10. doi: 10.1002/jcb.26174
43. Li P, Schwarz EM. The TNF-α transgenic mouse model of inflammatory arthritis. *Springer Semin Immunopathol.* (2003) 25:19–33. doi: 10.1007/s00281-003-0125-3
44. Vasanthi P, Nalini G, Rajasekhar G. Role of tumor necrosis factor-alpha in rheumatoid arthritis: a review: TNF-α in RA. *APLAR J Rheumatol.* (2007) 10:270–4. doi: 10.1111/j.1479-8077.2007.00305.x
45. Tarran S, Langlois NEI, Dziewulski P, Sztynda T. Using the inflammatory cell infiltrate to estimate the age of human burn wounds: a review and immunohistochemical study. *Med Sci Law.* (2006) 46:115–26. doi: 10.1258/rsmmsl.46.2.115
46. Parisi L, Gini E, Baci D, Tremolati M, Fanuli M, Bassani B, et al. Macrophage polarization in chronic inflammatory diseases: killers or builders? *J Immunol Res.* (2018) 2018:115–26. doi: 10.1155/2018/8917804
47. Chen L, Wang J, Li S, Yu Z, Liu B, Song B, et al. The clinical dynamic changes of macrophage phenotype and function in different stages of human wound healing and hypertrophic scar formation. *Int Wound J.* (2019) 16:360–9. doi: 10.1111/iwj.13041
48. Steinbach K, Vincenti I, Merkler D. Resident-memory T cells in tissue-restricted immune responses: for better or worse? *Front Immunol.* (2018) 9:2827. doi: 10.3389/fimmu.2018.02827
49. Yamanaka K–I, Clark R, Rich B, Dowgiert R, Hirahara K, Hurwitz D. Skin-derived interleukin-7 contributes to the proliferation of lymphocytes in cutaneous T-cell lymphoma. *Blood.* (2006) 107:2440–5. doi: 10.1182/blood-2005-03-1139
50. Hara T, Shitara S, Imai K, Miyachi H, Kitano S, Yao H, et al. Identification of IL-7-Producing cells in primary and secondary lymphoid organs using IL-7-GFP knock-in mice. *J Immunol.* (2012) 189:1577–84. doi: 10.4049/jimmunol.1200586
51. Gao J, Zhao L, Wan Y, Zhu B. Mechanism of action of IL-7 and its potential applications and limitations in cancer immunotherapy. *Int J Mol Sci.* (2015) 16:10267–80. doi: 10.3390/ijms160510267
52. Wykes M, Macpherson G. Dendritic cell-B-cell interaction: dendritic cells provide B cells with CD40-independent proliferation signals and CD40-dependent survival signals. *Immunology.* (2000) 100:1–3. doi: 10.1046/j.1365-2567.2000.00044.x
53. Li J, Huston G, Swain SL. IL-7 promotes the transition of CD4 effectors to persistent memory cells. *J Exp Med.* (2003) 198:1807–15. doi: 10.1084/jem.20030725
54. Burger JA, Bürkle A. The CXCR4 chemokine receptor in acute and chronic leukaemia: a marrow homing receptor and potential therapeutic target. *Br J Haematol.* (2007) 137:288–96. doi: 10.1111/j.1365-2141.2007.06590.x
55. Janssens R, Struyf S, Proost P. The unique structural and functional features of CXCL12. *Cell Mol Immunol.* (2018) 15:299–311. doi: 10.1038/cmi.2017.107
56. Guimond M, Veenstra RG, Grindler DJ, Zhang H, Cui Y, Murphy RD, et al. Interleukin 7 signaling in dendritic cells regulates the homeostatic proliferation and niche size of CD4+ T cells. *Nat Immunol.* (2009) 10:149–57. doi: 10.1038/ni.1695
57. Pan J, Zhang M, Wang J, Wang Q, Xia D, Sun W, et al. Interferon-γ is an autocrine mediator for dendritic cell maturation. *Immunol Lett.* (2004) 94:141–51. doi: 10.1016/j.imlet.2004.05.003
58. Lee B, Sharron M, Montaner LJ, Weissman D, Doms RW. Quantification of CD4, CCR5, and CXCR4 levels on lymphocyte subsets, dendritic cells, and differentially conditioned monocyte-derived macrophages. *Proc Natl Acad Sci USA.* (1999) 96:5215–20. doi: 10.1073/pnas.96.9.5215
59. McKenna K, Beignon A-S, Bhardwaj N. Plasmacytoid dendritic cells: linking innate and adaptive immunity. *J Virol.* (2005) 79:17–27. doi: 10.1128/JVI.79.1.17-27.2005
60. Snell LM, McGaha TL, Brooks DG. Type I interferon in chronic virus infection and cancer. *Trends Immunol.* (2017) 38:542–57. doi: 10.1016/j.it.2017.05.005
61. RoŽman P, Švajger U. The tolerogenic role of IFN-γ. *Cytokine Growth Factor Rev.* (2018) 41:40–53. doi: 10.1016/j.cytogfr.2018.04.001
62. Zhang X, Zeng Y, Qu Q, Zhu J, Liu Z, Ning W, et al. PD-L1 induced by IFN-γ from tumor-associated macrophages via the JAK/STAT3 and PI3K/AKT signaling pathways promoted progression of lung cancer. *Int J Clin Oncol.* (2017) 22:1026–33. doi: 10.1007/s10147-017-1161-7
63. Wilson JK, Zhao Y, Singer M, Spencer J, Shankar-Hari M. Lymphocyte subset expression and serum concentrations of PD-1/PD-L1 in sepsis - pilot study. *Crit Care.* (2018) 22:95. doi: 10.1186/s13054-018-2020-2
64. Patil NK, Guo Y, Luan L, Sherwood ER. Targeting immune cell checkpoints during sepsis. *Int J Mol Sci.* (2017) 18:2413. doi: 10.3390/ijms18112413
65. Monaghan SF, Thakkar RK, Tran ML, Huang X, Cioffi WG, Ayala A, et al. Programmed death 1 expression as a marker for immune and physiological dysfunction in the critically Ill surgical patient. *Shock.* (2012) 38:117–22. doi: 10.1097/SHK.0b013e31825de6a3
66. Myles A, Gearhart PJ, Cancro MP. Signals that drive T-bet expression in B cells. *Cell Immunol.* (2017) 321:3–7. doi: 10.1016/j.cellimm.2017.09.004
67. Muehlinghaus G, Cigliano L, Huehn S, Peddinghaus A, Leyendeckers H, Hauser AE, et al. Regulation of CXCR3 and CXCR4 expression during terminal differentiation of memory B cells into plasma cells. *Blood.* (2005) 105:3965–71. doi: 10.1182/blood-2004-08-2992
68. Malek TR. The main function of IL-2 is to promote the development of T regulatory cells. *J Leukoc Biol.* (2003) 74:961–5. doi: 10.1189/jlb.0603272
69. Liao W, Lin J-X, Leonard WJ. Interleukin-2 at the crossroads of effector responses, tolerance, and immunotherapy. *Immunity.* (2013) 38:13–25. doi: 10.1016/j.immuni.2013.01.004
70. Pallikkuth S, de Armas L, Rinaldi S, Pahwa S. T follicular helper cells and B cell dysfunction in aging and HIV-1 infection. *Front Immunol.* (2017) 8:1380. doi: 10.3389/fimmu.2017.01380

71. George MP, Masur H, Norris KA, Palmer SM, Clancy CJ, McDyer JF. Infections in the immunosuppressed host. *Ann Am Thorac Soc.* (2014) 11:S211–20. doi: 10.1513/AnnalsATS.201401-038PL
72. Finnerty CC, Jeschke MG, Herndon DN, Gamelli R, Gibran N, Klein M, et al. Temporal cytokine profiles in severely burned patients: a comparison of adults and children. *Mol Med.* (2008) 14:553–60. doi: 10.2119/2007-00132.Finnerty
73. Patil NK, Luan L, Bohannon JK, Hernandez A, Guo Y, Sherwood ER. Frontline science: anti-PD-L1 protects against infection with common bacterial pathogens after burn injury. *J Leukoc Biol.* (2018) 103:23–33. doi: 10.1002/JLB.5HI0917-360R
74. Chang H, Tokoyoda K, Radbruch A. Immunological memories of the bone marrow. *Immunol Rev.* (2018) 283:86–98. doi: 10.1111/imr.12656

Conflict of Interest: The authors declare that the research was conducted in the absence of any commercial or financial relationships that could be construed as a potential conflict of interest.

frontiers in Immunology

CORRECTION
published: 09 October 2020
doi: 10.3389/fimmu.2020.598646

Corrigendum: Pediatric Burn Survivors Have Long-Term Immune Dysfunction With Diminished Vaccine Response

Blair Z. Johnson[1], Sonia McAlister[2,3], Helen M. McGuire[4], Vetrichevvel Palanivelu[1], Andrew Stevenson[1], Peter Richmond[2,3], Debra J. Palmer[2,5], Jessica Metcalfe[2,5], Susan L. Prescott[2,5], Fiona M. Wood[2,6], Barbara Fazekas de St Groth[4], Matthew D. Linden[1], Mark W. Fear[1] and Vanessa S. Fear[7]*

[1] School of Biomedical Sciences, The University of Western Australia, Perth, WA, Australia, [2] School of Medicine, The University of Western Australia, Perth, WA, Australia, [3] Wesfarmers Centre of Vaccines and Infectious Diseases, Telethon Kids Institute, Perth, WA, Australia, [4] Ramaciotti Facility for Human Systems Biology and the Charles Perkins Centre, Discipline of Pathology, The University of Sydney, Sydney, NSW, Australia, [5] Centre for Allergy and Immunology Research, Telethon Kids Institute, Perth, WA, Australia, [6] Department of Health WA, Perth, WA, Australia, [7] Genetic and Rare Diseases, Telethon Kids Institute, Perth, WA, Australia

Keywords: non-severe burn injury, immunity, vaccination, mass cytometry, acute trauma, systemic

OPEN ACCESS

Approved by:
Frontiers Editorial Office, Frontiers Media SA, Switzerland

***Correspondence:**
Mark W. Fear
mark@fionawoodfoundation.com

Specialty section:
This article was submitted to Inflammation, a section of the journal Frontiers in Immunology

Received: *25 August 2020*
Accepted: *26 August 2020*
Published: *09 October 2020*

Citation:
Johnson BZ, McAlister S, McGuire HM, Palanivelu V, Stevenson A, Richmond P, Palmer DJ, Metcalfe J, Prescott SL, Wood FM, Fazekas de St Groth B, Linden MD, Fear MW and Fear VS (2020) Corrigendum: Pediatric Burn Survivors Have Long-Term Immune Dysfunction With Diminished Vaccine Response. Front. Immunol. 11:598646. doi: 10.3389/fimmu.2020.598646

A Corrigendum on

Pediatric Burn Survivors Have Long-Term Immune Dysfunction With Diminished Vaccine Response

by Johnson, B. Z., McAlister, S., McGuire, H. M., Palanivelu, V., Stevenson, A., Richmond, P., et al. (2020). Front. Immunol. 11:1481. doi: 10.3389/fimmu.2020.01481

In the original article, there was an error in the URL provided in Data Availability Statement. The updated statement appears below.

The authors apologize for this error and state that this does not change the scientific conclusions of the article in any way. The original article has been updated.

DATA AVAILABILITY STATEMENT

The raw data supporting the conclusions of this article will be made available by the authors, without undue reservation. Debarcoded files are uploaded to Flow Repository http://flowrepository.org/id/FR-FCM-Z2XE.

frontiers in Immunology

ORIGINAL RESEARCH
published: 31 July 2020
doi: 10.3389/fimmu.2020.01570

Oxidation-Specific Epitopes (OSEs) Dominate the B Cell Response in Murine Polymicrobial Sepsis

*Oliver Nicolai[1†], Christian Pötschke[1†], Dina Raafat[1,2], Julia van der Linde[3], Sandra Quosdorf[1], Anna Laqua[1†], Claus-Dieter Heidecke[3], Claudia Berek[4], Murthy N. Darisipudi[1], Christoph J. Binder[5] and Barbara M. Bröker[1]**

[1] Department of Immunology, Institute of Immunology and Transfusion Medicine, University Medicine Greifswald, Greifswald, Germany, [2] Department of Microbiology and Immunology, Faculty of Pharmacy, Alexandria University, Alexandria, Egypt, [3] Department of General Surgery, Visceral, Thoracic and Vascular Surgery, University Medicine Greifswald, Greifswald, Germany, [4] German Rheumatism Research Centre (DRFZ), Berlin, Germany, [5] Department of Laboratory Medicine, Medical University of Vienna, Center for Molecular Medicine of the Austrian Academy of Sciences, Vienna, Austria

In murine abdominal sepsis by colon ascendens stent peritonitis (CASP), a strong increase in serum IgM and IgG antibodies was observed, which reached maximum values 14 days following sepsis induction. The specificity of this antibody response was studied in serum and at the single cell level using a broad panel of bacterial, sepsis-unrelated as well as self-antigens. Whereas an antibacterial IgM/IgG response was rarely observed, studies at the single-cell level revealed that IgM antibodies, in particular, were largely polyreactive. Interestingly, at least 16% of the IgM mAbs and 20% of the IgG mAbs derived from post-septic mice showed specificity for oxidation-specific epitopes (OSEs), which are known targets of the innate/adaptive immune response. This identifies those self-antigens as the main target of B cell responses in sepsis.

Keywords: CASP, polymicrobial sepsis, B cell response, polyreactive antibodies, oxidation-specific epitopes

OPEN ACCESS

Edited by:
Florian Uhle, Heidelberg University Hospital, Germany

Reviewed by:
Huan Yang, Feinstein Institute for Medical Research, United States
Prasad Srikakulapu, University of Virginia, United States
Xuchu Que, University of California, San Diego, United States

***Correspondence:**
Barbara M. Bröker
broeker@uni-greifswald.de

†Present address:
Oliver Nicolai, Z.A.S. Zentral Archiv Service GmbH, Neubrandenburg, Germany
Christian Pötschke, Salutas Pharma GmbH, Barleben, Germany
Anna Laqua, Department of Hematology, University Hospital Schleswig-Holstein, Kiel, Germany

Specialty section:
This article was submitted to Inflammation, a section of the journal Frontiers in Immunology

Received: *14 February 2020*
Accepted: *15 June 2020*
Published: *31 July 2020*

Citation:
Nicolai O, Pötschke C, Raafat D, van der Linde J, Quosdorf S, Laqua A, Heidecke C-D, Berek C, Darisipudi MN, Binder CJ and Bröker BM (2020) Oxidation-Specific Epitopes (OSEs) Dominate the B Cell Response in Murine Polymicrobial Sepsis. Front. Immunol. 11:1570. doi: 10.3389/fimmu.2020.01570

INTRODUCTION

Sepsis, by definition, is a life-threatening organ dysfunction caused by a dysregulated host response to infection (1, 2), which is associated with high morbidity and mortality (3, 4). Due to an aging population, a steady increase in surgical interventions, and the occurrence of antibiotic resistance, sepsis is still of high clinical relevance (4–6).

B cells have been ascribed a protective function in sepsis which encompasses antibody-dependent as well as -independent mechanisms (7, 8). However, during sepsis, a large number of B cells and other immune cells are lost by apoptosis (9, 10) and it is assumed that B cell responses are severely impaired (11, 12). In fact, Mohr et al. have shown that B cell priming with defined antigens is defective in sepsis (13). By contrast, we and other research groups have shown that sepsis induces high concentrations of serum IgM and IgG antibodies of unknown specificities (13, 14). Since these may be responsible for the observed antibody-mediated protection, we set out to examine their antigen specificities in a mouse model of abdominal sepsis.

During sepsis, the organism is flooded with bacterial antigens as well as self-antigens, which are released by dying host cells. Moreover, there is an abundance of danger signals, both pathogen- and damage-associated molecular patterns (PAMPs and DAMPs, respectively) (15, 16). These may, on the one hand, act as adjuvants in an antigen-driven B cell response and, on the other, trigger a polyclonal B cell reaction (17–19). In addition to these danger signals, inflammation and cell death are accompanied by lipid peroxidation, resulting in the generation of oxidation-specific epitopes (OSEs), which are also recognized by pattern recognition receptors (PRR) of the innate immune system exerting an adjuvant effect (20–22). All of these factors could contribute to the B cell response in sepsis.

During sepsis, antibody production is induced by T cell-dependent (TD) as well as -independent (TI) mechanisms (14). In a TD immune reaction, follicular B cells are activated via the B cell receptor. With the help of activated T cells, they differentiate and form germinal centers, where class switch to all Ig (sub)classes and somatic hypermutation take place. At the end of this process, affinity-matured plasma cells have developed that continuously secrete antibodies (23). TI B cell responses may be triggered in two ways: TI-2 antigens like polysaccharides efficiently crosslink B cell receptors and initiate a strong and long-lasting antigen-specific primary response (24). In contrast, TI-1 antigens like lipopolysaccharide (LPS) and bacterial DNA (CpG) activate B cells polyclonally, i.e., independent of the B cell receptor, via TLR triggering (25–27). Predominantly B-1- and marginal zone (MZ) B cells can rapidly respond to TI-1 antigens (28).

The main reservoir of B-1 cells are the pleural and peritoneal cavities, but a small proportion can be found in all lymphoid organs. Not only are B-1 cells prone to TI responses, but they are also the main producers of natural antibodies (NAbs), defined as antibodies that circulate in normal individuals in the absence of exogenous antigenic stimulation (29). NAbs are considered polyreactive, usually lack somatic hypermutation and are said to use a restricted set of B cell receptor genes (30–32). NAbs are hence at the interface between innate and adaptive immune responses, and can bridge the time gap until the TD response has matured. In terms of their antigen specificity, B-1 cells are selected for a certain strength of self-antigen binding. Remarkably, ∼30% of B-1 cell-derived IgM binds to OSEs. B-1 cells are able to switch to all IgG subclasses *in vitro*, whereas *in vivo,* they are producers of NAbs, mainly of the IgM, IgG3, and IgA isotype [reviewed extensively in (32–34)].

MZ B cells are located close to the marginal sinus in the spleen, where they have direct access to blood-borne antigens (35). Although they have the capacity to generate TD and TI responses, their main function is the TI response against blood-borne pathogens (36, 37). Very early in the course of an infection, they differentiate to IgM- or IgG-secreting cells (38). Both TD as well as TI processes take place during sepsis, and all B cell populations become activated (8, 14). We have therefore tested sepsis-induced IgM- and IgG-binding to a broad panel of bacterial as well as autoantigens. OSE were identified as the dominant target of the B cell response.

MATERIALS AND METHODS

Animals and Ethics Statement

All experiments were performed on 8–12 weeks old female C57BL/6 wild type (WT) mice. All animals were housed in a conventional, temperature-controlled animal facility with a 12-h light and dark cycle, and provided with food and water *ad-libitum*. All experiments were approved by the animal ethics committee of the local animal protection authority (LALLF, State Office for Agriculture, Food Safety and Fisheries Mecklenburg-Western Pomerania; numbers LALLF M-V/TSD/7221.3-1.1-052/07 and LALLF M-V/TSD/7221.3-1.2-013/09). All efforts were made to minimize the suffering of mice.

CASP Surgery

CASP surgery was performed as described before (39, 40). Briefly, mice were anesthetized with Ketamin (Ketanest, Parke-Davis GmbH, Berlin) and xylazin (Rompun, Bayer Health Care, Leverkusen) intraperitoneally (100 mg/10 mg per kg bodyweight, respectively) and a 18G stent (Ohmeda AB, Helsingborg, Sweden) was implanted into their colon ascendens. Mice were monitored every 4 h until recovery.

Hybridoma Generation

Splenocytes from mice 10 or 14 days following CASP or sham surgeries were prepared and fused with X63 AG8.653 myeloma cells using polyethylene glycol (Sigma-Aldrich), following an extensive protocol for fusion and selection as described elsewhere (http://www.umass.edu/vetimm/docs/Wagner_Hybridoma.pdf). Briefly, 10 million X63-cells were fused with 1–3 $\times$ 10^7 splenocytes, and the fusion products were plated in several dilutions into 96-well cell culture plates. Ten days later, plates were screened under a light microscope for hybridoma growth. Only hybridomas from plates where <50% of the wells showed cell growth were taken into account, since this improves the probability of monoclonality to over 85% (41). In addition, wells were observed under a light microscope to select for single clone growth based on morphology.

Immunohistochemical Autoantibody Screening on HEp-2-Cells

Screening of autoantibodies was performed as described before (13). Briefly, serum samples, diluted 1:100 in PBS containing 20% FCS or undiluted hybridoma supernatants were incubated on HEp-2-ANA slides (INOVA Diagnostics, San Diego, CA, USA) overnight at 4°C. Slides were washed with PBS, and bound antibodies were detected either with polyclonal goat anti-mouse IgG or IgM conjugated to FITC (10 µg/mL, Southern Biotech, Atlanta, GA, USA). Slides were then equally exposed, and pictures were taken with a Zeiss Axio imager A.1 fluorescence microscope (Zeiss, Göttingen, Germany) equipped with Spotadvanced software (Diagnostic Instruments, Sterling Heights, MI, USA) using the same settings for all images.

ELISA

Antigens were prepared for ELISA as follows: (i) Bacterial antigens: Bacteria (*E. coli, E. faecalis, P. mirabilis, S. aureus*

8325-4 Δspa) were grown overnight in tryptic soy broth (TSB) medium as described previously (41). Cells were washed twice in cold PBS (3,340 *g* for 15 min at 4°C) and diluted to an optical density at 595 nm (OD_{595}) of 1.0 in PBS before being inactivated by irradiation with UV-light for 10 min; (ii) Self-antigens: Histone H2A (calf thymus, 2 μg/mL) and dsDNA (calf thymus, 10 μg/mL), both obtained from Sigma-Aldrich, were diluted in PBS, whereas murine IgG-Fc-fragments (Dianova, 1 μg/mL) were diluted in coating buffer (pH 9.6; Candor Bioscience GmbH, Wangen, Germany); (iii) LPS (*E. coli* O55:B5, Sigma Aldrich, 10 μg/mL) and sepsis unrelated antigens, including TNP (14)-bovine serum albumin (BSA, Biosearch Technologies, 10 μg/mL) and ovalbumin (OVA, Sigma-Aldrich, 10 μg/mL) were diluted in coating buffer to the indicated concentrations; (iv) OSEs: phosphocholine-conjugated BSA (PC-BSA) was obtained from Biosearch Technologies Inc. Malondialdehyde-acetaldehyde-modified BSA (MAA-BSA) was prepared as described elsewhere (42). Human native LDL was isolated, and Cu^{2+}-oxidized LDL (CuOx-LDL) and Malondialdehyde-modified LDL (MDA-LDL) were prepared as described previously (42).

96-well flat-bottom microplates (Nunc MaxiSorp™) were coated with the respective antigens overnight at 4°C (bacterial antigens, H2A: 100 μL per well), LPS, dsDNA, murine IgG-Fc-fragments and sepsis unrelated antigens: 50 μl per well). The plates were then washed three times with PBS containing 0.05% Tween20, and blocked with PBS containing 10% fetal calf serum (150 μL/°) for 1 h at room temperature (RT). Murine sera (dilution range 1:100–1:2,500) or hybridoma supernatants were added to the wells and incubated for 90 min at RT. After three washing steps, bound antibodies were detected using $F(ab)_2$-fragments of goat anti-mouse IgG or IgM conjugated to POD (Dianova) as previously described (43). Chemiluminescence was measured using a Tecan Sunrise photometer (Tecan Group Ltd., Maennedorf, Switzerland), and the data were expressed as relative light units (RLU) per 100 ms.

RNA Isolation From Hybridoma Cells and Complementary DNA Generation

Total RNA was isolated from about 1×10^5 hybridoma cells using the RNeasy Mini Kit (QIAGEN GmbH, Hilden, Germany) according to manufacturer's instructions. The isolation steps included a DNase-digestion step to eliminate genomic DNA. The quantity of RNA was determined by using the DS-11 Series Spectrophotometer (DeNovix Inc., DE, USA). One microgram of RNA was transcribed to cDNA using oligo DT Primers of the RevertAid™ First Strand cDNA Synthesis Kit (Fermentas) as per the manufacturer's instructions. For the amplification of V_H-domain sequences of the immunoglobulins, cDNA was amplified by multiplex PCR using msVHE as universal forward primer and a mixture of the Ig-specific reverse primers (**Table 1**). The reaction was performed in a total volume of 25 μL using 2 μL of cDNA, 0.2 μL of GoTaq-polymerase (Promega), 2.5 μL of dNTP (1 mM, Roche Diagnostics), 5 μL $MgCl_2$ (25 mM, Promega). Primers were used at a final concentration of 200 nM each, and the PCR was performed for 35 cycles at 95°C 30 s, 65°C 30 s, 72°C 45 s and a final elongation step at 72°C for 10 min. PCR products were analyzed on 1.5% agarose gels, and the DNA bands of around 400 bp size were cut under UV light for extraction of DNA using the Nucleo-Spin® Extract II kit (Machery-Nagel).

TABLE 1 | Primers used for V_H-gene sequence amplification.

Primer designation	Primer sequence	References
Forward Primer:		
msVHE	5′-GGGAATTCGAGGTGCAGCTGCAGGAGTCTGG-3′	(44)
Ig-Subclass-Specific Reverse Primers:		
IgG1	5′-GATCCAGGGGCCAGTGGATAG-3′	
IgG2b	5′-CACCCAGGGGCCAGTGGATAG-3′	
IgG2c inner	5′-GCTCAGGGAAATAACCCTTGAC-3′	(45)
IgG3 inner	5′-GCTCAGGGAAGTAGCCTTTGAC-3′	(46)
IgM	5′-GGCTCTCGCAGGAGACGAGG-3′	

Cloning and Transformation of Target DNA

The extracted DNA-fragments were cloned into the pCR® 2.1-TOPO® TA vector using the TOPO® TA Cloning® Kit (Life Technologies, Thermo Fisher Scientific, Carlsbad, CA, USA). All steps were done according to manufacturer's instructions. Products were transfected into chemically competent *E. coli* by the heat-shock method. Transformed *E. coli* were cultivated on LB agar plates containing 50 μg/mL of each IPTG, x-Gal and Ampicillin, and incubated at 37°C for 12 h. At least three single white colonies were picked and seeded further into single wells of a 96-well plate containing LB agar with 50 μg/mL Ampicillin.

V_H-N-D_H-N-J_H Fragment Sequencing and Analysis

Plasmid isolation and sequencing of the single colonies was performed by GATC Biotech AG, Konstanz, Germany, using the vector-specific M13 forward primer. The resulting sequences were further verified using IMGT/V-Quest database, (https://www.imgt.org/IMGT_vquest/vquest?livret=0&Option=mouseIg).

Statistical Analysis

Statistical analyses were performed using GraphPad Prism 6 (GraphPad software, San Diego, CA, USA). Data were assessed for significant differences using One-Way ANOVA with Bonferroni *post test* for selected pairs, or using the unpaired Student *t*-test, whenever appropriate. $P < 0.05$ were considered to be significant.

RESULTS

A Strong Induction of Total Serum IgG During Sepsis Was Not Due to an Antibacterial IgG Response

We and others have shown that sepsis induced a marked increase in serum IgM levels followed by an even stronger IgG response (11, 13). As we have previously shown, most ASCs reside in the spleen, and the class switch to IgG results from both TI and TD processes (14). Since the antigen-specific T cell response is still fully functional at the onset of sepsis (47), we assumed that the class switched IgG response was mainly directed at the invasive bacteria. To test this hypothesis, we induced sepsis in WT mice using the CASP sepsis model. First, systemically disseminated bacteria were identified by plating sera of septic mice onto agar plates followed by microbiological identification of growing colonies. *Enterococcus faecalis (E. faecalis)* and *Escherichia coli (E. coli)*, two microbial species of the intestinal flora, were regularly found in the blood of septic mice. Antibody binding to these bacteria as well as to *Staphylococcus aureus (S. aureus)*, which is often observed in the murine intestine, was then measured by ELISA. UV-inactivated washed bacterial cells served as antigens. To avoid non-specific IgG binding to *S. aureus*, the protein A-deficient mutant strain 8425-Δ*spa* was used. Additionally, LPS of *E. coli* was included. As shown in **Figure 1**, sepsis induced a significant increase in IgM-binding to whole bacteria as well as LPS. In contrast, there was no significant anti-bacterial or anti-LPS IgG response in the majority of animals. The absence of an anti-bacterial IgG response in sepsis was in striking contrast to immunization with inactivated bacteria (without adjuvant), where ímmunized animals did not develop disease symptoms, but elaborated high specific antibacterial IgG titres (**Supplementary Figure 1**). Thus, the very strong serum IgG increase in sepsis was not due to an anti-IgG response to the bacteria tested, namely *S. aureus*, *E. coli* and *E. faecalis*.

Sepsis-Induced Serum Antibodies Are Directed Against Self-Antigens

In sepsis, the strong general IgG response with only a modest reaction to bacterial antigens could be caused by polyclonal activation of B-cells due to the release of large amounts of PAMPs and DAMPs. We reasoned that autoreactive Ig should be increased in this case, because the normal B-cell pool contains numerous self-specificities (48–50). Moreover, the PAMPs and DAMPs could also act as adjuvants in a TD immune response to self-antigens that are released from damaged cells and tissues. Therefore, we tested the sera of septic and control mice for Ig-binding to eukaryotic cellular structures using HEp-2 cells as antigens and FITC-labeled anti-mouse-IgM or IgG antibodies for detection of binding. As shown in **Figure 2**, the sera of septic mice (data from two representative septic animals are depicted) showed an increase in autoreactive IgM and IgG response, as compared to untreated animals (left panel), 14 days after sepsis induction. The fluorescence patterns observed were mostly diverse, where often more than one cellular structure was stained (**Figure 2**, arrows). The binding patterns differed between individual septic mice from the same cage. Hence, sepsis, which was probably caused by very similar gut microbiota, induced autoantibodies of different specificities. Remarkably, a similar autoreactive response was observed in the sera of splenectomized animals upon sepsis induction (**Supplementary Figure 2**).

Sepsis Increased Serum Antibodies Directed Against Sepsis-Unrelated Antigens

An immune response which is largely polyclonal rather than antigen-driven would be expected to show increased antibody binding to antigens unrelated to sepsis. Hence, besides anti-bacterial and self-binding antibodies, we screened for the presence of antibodies binding to such sepsis-unrelated antigens. At first, we investigated the binding of serum antibodies to two antigens the animals had never been exposed to, namely the classical TD protein antigen ovalbumin (OVA) and the hapten 2,4,6-trinitrophenyl (TNP) conjugated to bovine serum albumin (TNP-(14)-BSA). Regarding OVA, only IgM binding increased significantly during sepsis (data not shown), whereas IgM- as well as IgG-binding to TNP-(14)-BSA were both very strongly enhanced (**Supplementary Figure 3**). Together, these results clearly support the concept of a polyclonal B cell response, which may be dominated by NAb specificities.

Sepsis Induced High Titer IgM and IgG Antibodies Directed Against Oxidation-Specific Epitopes (OSEs)

Since sepsis induced a robust autoreactive-antibody response, we questioned whether these antibodies would be able to bind to OSEs, which are present at high density on apoptotic cells, whose numbers are known to increase during sepsis. OSEs generated during sepsis act as an endogenous DAMPs, and initiate an innate immune response. It has been shown that a large proportion of NAbs, especially those produced by B-1 cells, bind to OSEs (20, 42). Therefore, we tested sera of septic and untreated animals at day 10 and 14 for OSE-specific antibodies by chemiluminescent ELISA. Sepsis elicited a very strong IgM and IgG response to known OSEs in all tested animals (**Figure 3** and **Supplementary Figure 4**), while there were very low levels of OSE-specific antibodies or none at all in untreated animals. Hence, at day 14 post sepsis, the IgM response to both modified LDL and BSA was significantly higher in septic mice than in the control group, where specific IgM was low or even under the limit of detection (**Figure 3**). On the same day, the IgG/IgM response to MAA-BSA was 4-fold higher than in the untreated group. The IgM response to CuOx-LDL showed a trend toward increased levels, while IgG levels were significantly higher compared to untreated animals (**Supplementary Figure 4**). Since under other conditions, such as hypercholesterolemia, IgM antibodies dominate the immune response to OSEs (51), the pronounced specific class-switched response in sepsis is remarkable.

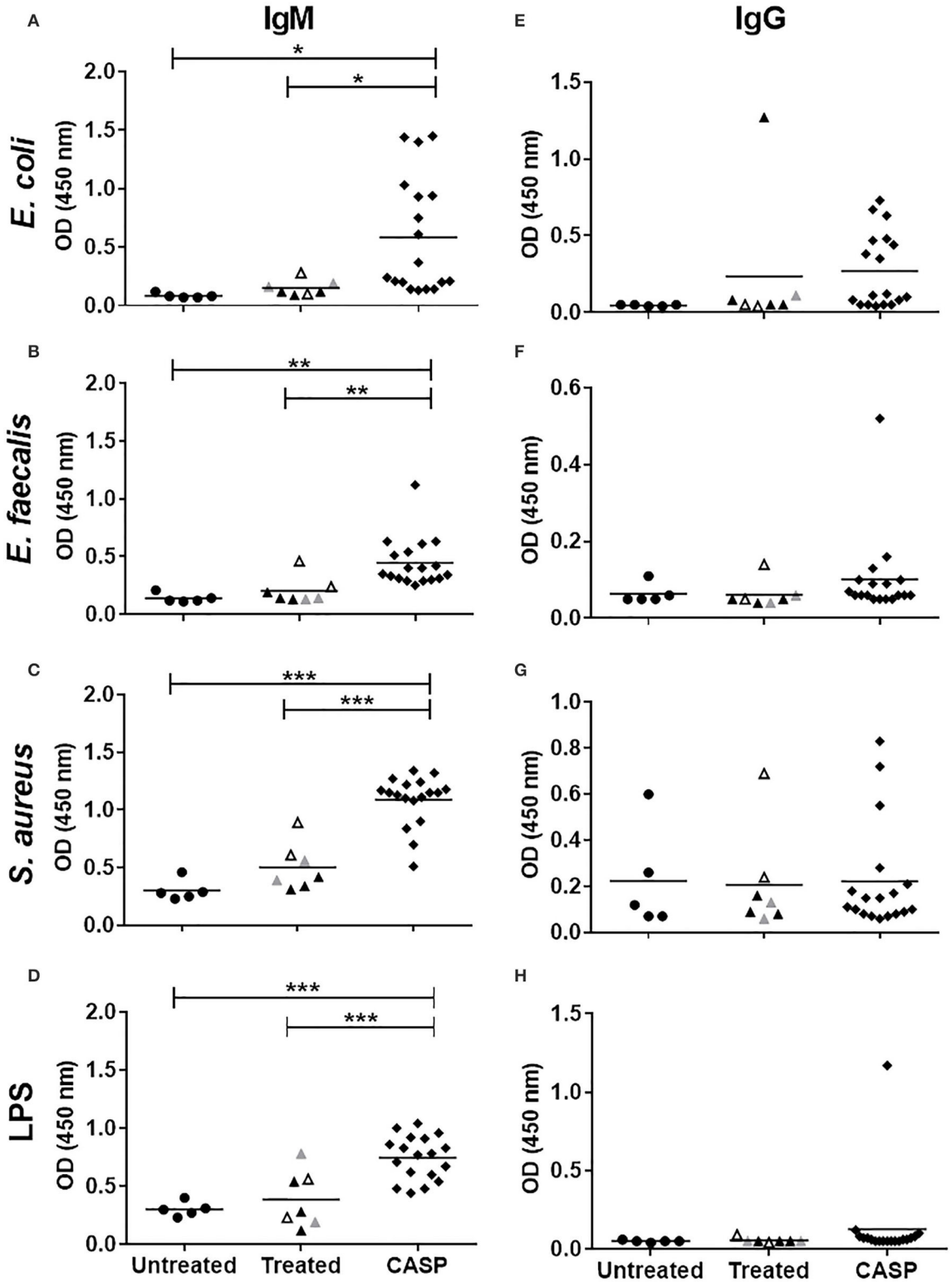

FIGURE 1 | Binding of sera IgM/IgG to bacteria and LPS. The binding of murine serum antibodies, IgM (A-D) or IgG (E-H), to indicated bacteria; *E. coli* **(A,C)**, *E. faecalis* **(B,F)**, *S. aureus* **(C,G)**, and LPS **(D,H)** was tested by ELISA. Fourteen days after sepsis induction, blood was collected, and sera were diluted 1:100 in blocking buffer. Sera from non-septic animals were used as controls. Control mice were untreated (•), whereas the treated mice were anesthetized only (▲), or additionally received a laparotomy (▲), or sham surgery (△). Mice that underwent CASP surgery are indicated by a black diamond (♦). Mean values of OD 450 nm are shown. Each symbol represents one animal ($N = 5–18$). Statistical analysis was done by One-way ANOVA with the Bonferroni *post test* for selected pairs. $^{*}p < 0.05$, $^{**}p < 0.01$, $^{***}p < 0.001$.

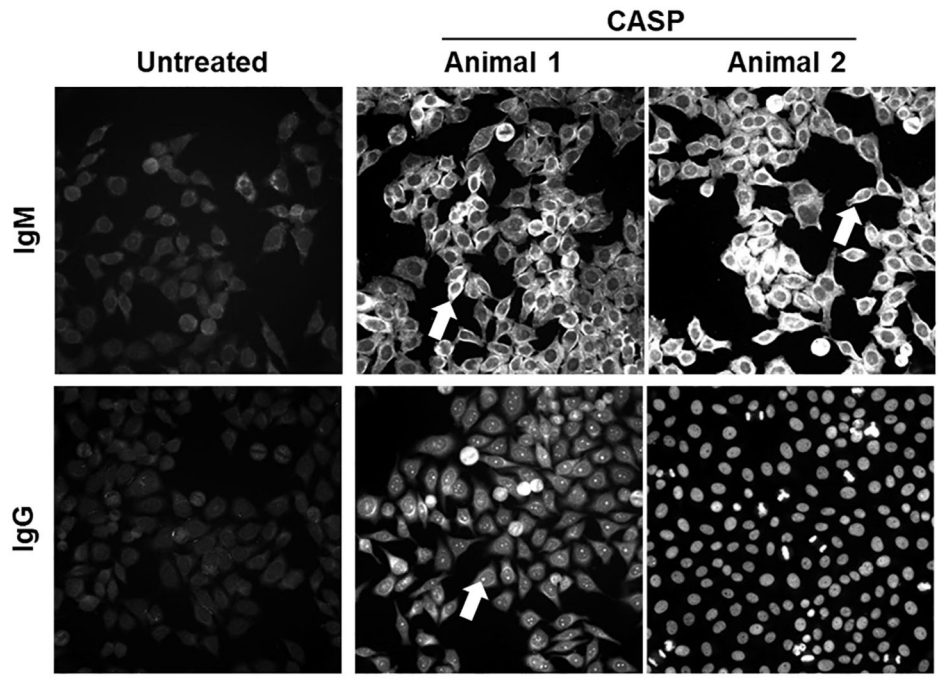

FIGURE 2 | Serum antibodies directed against self-antigens 14 days after sepsis induction. Sepsis was induced in C57BL/6 mice by 18G CASP. Control mice remained untreated. Fourteen days later blood was taken, and sera diluted 1:100 in 20% FCS/PBS were incubated on HEp-2-ANA slides. Bound antibodies were detected by FITC-labeled anti-mouse IgM or IgG antibodies. Out of the tested serum antibodies, 12/13 IgM and 12/13 IgG antibodies were autoreactive. Shown are representative pictures of septic and control mice. $N = 8$ per group. Serum IgM and IgG binding patterns varied greatly. In most cases more than one cellular structure is stained, albeit at variable intensities.

Studies at the Single Cell Level Revealed a High Proportion of Autoreactive IgM Antibodies

To study the sepsis-induced antibodies at a single-cell level, monoclonal antibodies (mAbs) were generated. Since we discovered the spleen as the main source of antibody secreting cells (ASCs) in sepsis (14), splenocytes from eight septic mice were obtained on day 10 after sepsis induction and fused. Three quarters (74.3%) of the hybridomas from septic mice produced IgM (**Table 2**). However, sepsis induced a much stronger increase in serum IgG than IgM, which peaked at day 14 (14). Assuming that the class switch to IgG may not have been completed on day 10 after sepsis induction, additional fusions were performed using splenocytes from six septic mice on day 14. However, choosing this later time point did not change the proportion of IgM- to IgG-producing cells, where 82% of the resulting hybridomas secreted IgM (**Table 2**). Several attempts to produce hybridomas from non-septic control mice failed, presumably due to the lack of activated B cells and plasmablasts in the spleen, which is a limitation of this study (data not shown). Determination of the mAb specificities confirmed and extended the observations made with serum antibodies, namely that sepsis induces autoreactive antibodies, predominantly IgM.

The total of 386 hybridoma supernatants derived from the 14 above mentioned septic mice and containing either IgM or IgG mAbs were screened for autoreactivity. A large proportion of IgM mAbs (31% to 40%) reacted with specific structures of the HEp-2 cells (**Table 2**). HEp-2-binding IgM mAbs were found in every animal, regardless of whether the spleen cells were obtained 10 or 14 days after sepsis. In contrast, only three out of 93 IgG mAbs showed detectable HEp-2-binding, when using undiluted hybridoma culture supernatants. These auto-reactive IgG hybridomas were obtained from three mice. **Figure 4** illustrates the variability of the binding patterns of the mAbs derived from splenic B cells of septic mice 10 or 14 days after CASP induction, which bind several cellular self-antigens. FITC-labeled anti-mouse IgG or IgM antibodies were used to determine the binding of those mAbs and clearly showed that, similar to our previous experiment at the serum level, the binding patterns of the individual antibodies were highly variable.

Most IgM Antibodies Are Polyreactive

Since we observed high titres of autoantibodies in sera of septic mice at day 10 or 14 (**Figure 2**), we wondered whether this also applies to the mAbs present in the hybridoma supernatants of six septic mice (generated from splenocytes at day 10 of sepsis).

We tested the hybridoma supernatants for mAb-binding to a broad panel of antigens, including bacterial and self-antigens, as well as two antigens that the animals had never been exposed to, namely TNP and OVA. Binding was observed with 27 out of 120 IgM-supernatants (22.5%) (**Table 3**) but with none of the 40 tested IgG supernatants (data not shown). The majority of the

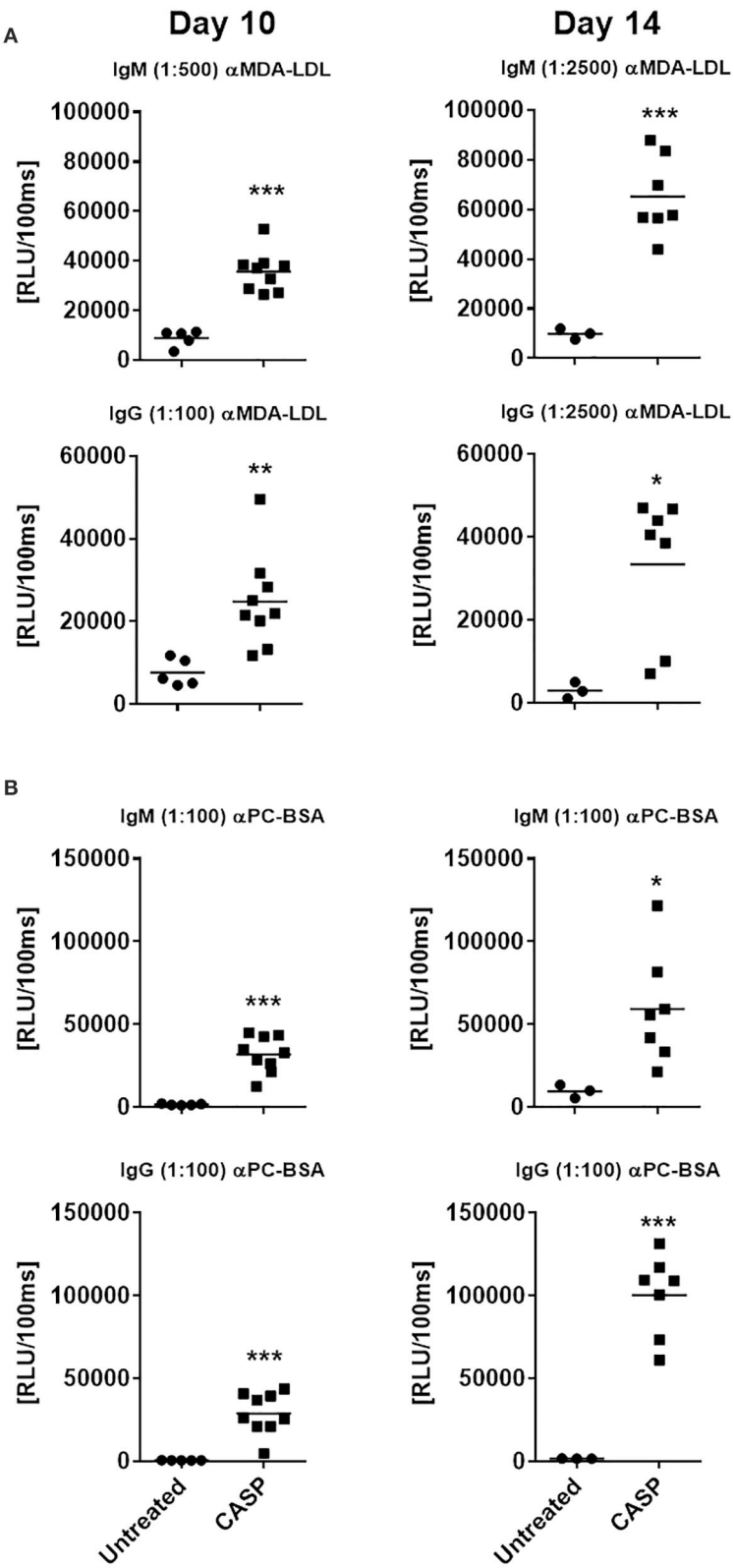

FIGURE 3 | Serum IgM and IgG binding to model oxidation-specific epitopes. C57BL/6 mice were subjected to CASP surgery, while control animals remained untreated. Ten and 14 days after sepsis induction, blood was drawn to determine serum IgM and IgG binding to malondialdehyde-modified LDL [MDA-LDL; **(A)**] and phosphocholine-conjugated BSA [PC-BSA; **(B)**], using chemiluminescent ELISA. Serum dilutions used are indicated in brackets. Statistical analysis was performed using the unpaired *t*-test. $N = 3–9$ per group. $^{*}p < 0.05$, $^{**}p < 0.01$, $^{***}p < 0.001$.

binding IgM mAbs (85%) were polyreactive, recognizing at least two antigens in the test panel used.

In Septic Mice, a Large Proportion of mAbs, Both IgM and IgG, Binds to Oxidation Specific Epitopes

Eighteen IgM mAbs that showed reactivity to the antigen panel in **Table 3**, as well as all available IgG mAbs ($N = 20$) of so far unknown specificity, were tested for binding to OSEs. Thirteen (72%) IgM and 5 (25%) IgG mAbs showed binding to one or several OSEs in ELISA (**Table 4**). Examples of IgG mAb titration curves are shown in the **Supplementary Figure 5**. The five OSE-specific IgG hybridomas were derived from four different mice. Remarkably, with the exception of IgG3, the OSE-specific mAbs encompassed all IgG subclasses. These findings underline that OSEs are prominent targets of the humoral immune response in sepsis.

TABLE 2 | HEp-2-positive IgM- or IgG-secreting hybridomas.

	HEp-2-positive hybridoma supernatants			
	IgM		IgG	
	N/total	%	*N*/total	%
CASP d10	91/225	**40**	3/78	**4**
CASP d14	21/68	**31**	0/15	**0**

The table shows the numbers of IgM or IgG hybridoma supernatants binding to cellular structures of HEp-2 cells, respective to the total numbers of tested hybridomas. Splenocytes were obtained on day 10 (eight animals, eight fusions) or 14 (six animals, seven fusions) after sepsis induction.

Most Sepsis-Induced IgG mAbs Carried Few Somatic Mutations

Many class switched antibody responses are TD and are characterized by somatic hypermutation. Therefore, the IgG mAbs were tested for somatic hypermutation by sequencing the variable domains of the IgG heavy chains. IgG mAbs at day 10 or 14 after sepsis mostly showed no significant differences in mutations (**Supplementary Figure 6A**). Most sequences were near germline, similar to 12 IgG monoclonal antibodies obtained from an untreated animal, which all had <4 mutations/100 nucleotides (**Supplementary Figure 6A**). However, four out of the 34 IgG mAbs derived from septic animals had five or more mutations per 100 nucleotides,

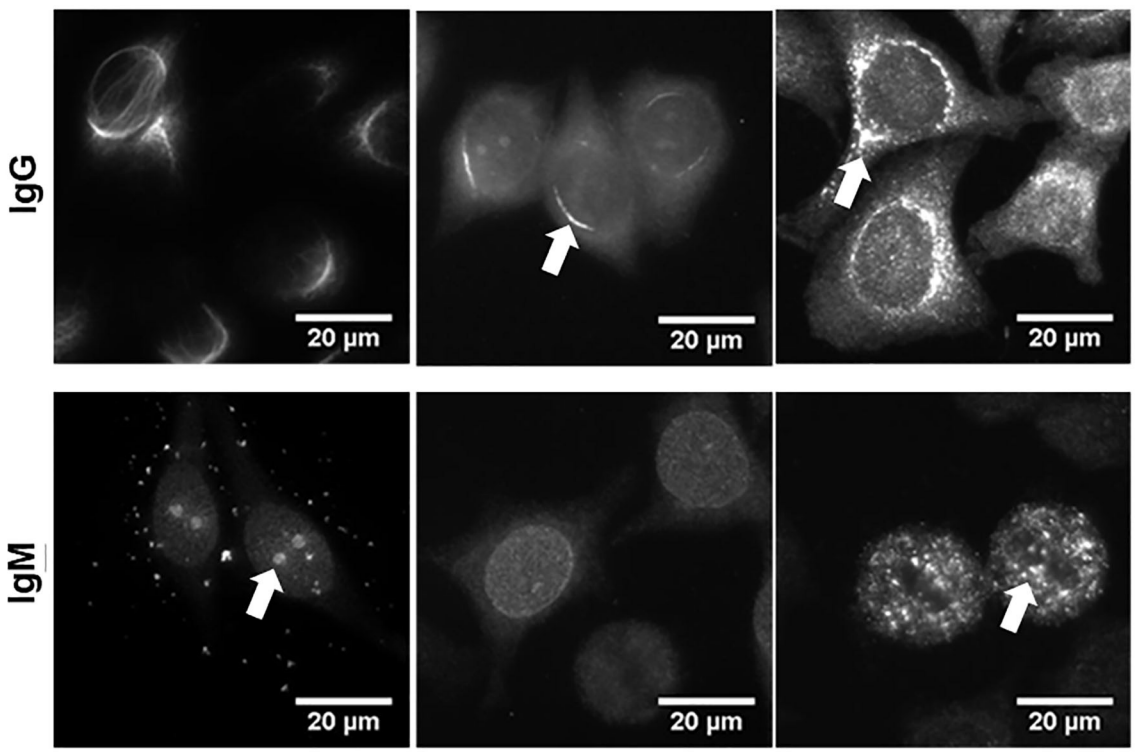

FIGURE 4 | Monoclonal antibodies derived from splenic B cells of septic mice bind several cellular self-antigens. Ten or 14 days after CASP induction, splenocytes were isolated and fused with myeloma cells to obtain hybridomas. Supernatants of monoclonal IgM- or IgG-producing hybridomas were incubated on HEp-2-ANA slides to detect auto-reactivity. Bound IgG or IgM was detected by FITC-labeled anti-mouse IgG or IgM antibodies. Three examples, respectively, of autoreactive monoclonal IgM- and IgG-antibodies are shown. The binding patterns of the various antibodies showed obvious differences, where in most cases more than one cellular structure was stained, albeit at varying intensities (indicated by arrows). For quantified data, regarding the numbers/percent of IgM or IgG hybridoma supernatants from septic mice directed against self-antigens, please refer to **Table 2**.

TABLE 3 | Antigen-binding patterns of positively-tested IgM hybridomas.

	Positive clones	Bacterial antigens				Foreign antigens		Self antigens			
		E. coli	*P. mirabilis*	*S. aureus*	LPS (*E. coli*)	TNP-BSA	OVA	ds DNA	histone HIIA	IgG-Fc	HEp-2-Test
1	F4_03		+							+	/
2	F4_04					+					+
3	F4_05			+		+		+	+	+	+
4	F4_09		+							+	+
5	F4_16	+	+			+				+	+
6	F4_23	+	+	+	+	+	+	+	+	+	+
7	F4_38			+				+	+		+
8	F4_46									+	+
9	F4_55					+					/
10	F5_10					+					+
11	F5_11	+		+						+	+
12	F5_17	+	+							+	
13	F6_20									+	
14	F7_07									+	+
15	F7_30					+					+
16	F7_32					+					+
17	F7_33					+					+
18	F7_36			+							+
19	F7_39					+					
20	F8_14					+				+	+
21	F9_09		+							+	+
22	F9_10		+			+				+	+
23	F9_12		+						+	+	/
24	F9_24			+		+				+	+
25	F9_29					+					+
26	F9_33					+					
27	F9_38			+		+		+		+	+

Overview of the antigen binding patterns of 27 binding (out of a total of 120 tested) IgM hybridoma-supernatants. The hybridomas were generated from splenocytes of septic mice at day 10 and tested for binding to a panel of bacterial, sepsis-unrelated (foreign) as well as self-antigens by ELISA. Binding to HEp-2 cells was tested by fluorescence microscopy. (+, binding; /, not tested). The corresponding OD (450 nm) values are shown in ***Supplementary Table 1****.*

indicative of somatic hypermutation. As such mAbs were present already at day 10, they were probably derived from memory B cells (52). OSE-specific and –non-specific IgG mAbs showed similar proportions of highly mutated IgG (**Figure 5**). Thus, most of the IgG antibodies generated during sepsis used near-germline gene sequences. Regarding the CDR3 length, the number of amino acid exchanges per V-region as well as the proportion of non-silent mutations, there were no significant differences between septic and non-septic animals (**Supplementary Figures 6, 7**).

DISCUSSION

Our data clearly show that OSEs are the main targets of the strong humoral immune response observed in sepsis. While Ig binding patterns to other self-epitopes were individual, OSE-specific binding was observed in all tested animals.

The sepsis-induced suppression of the adaptive immune system is well-documented (10, 13, 53). Nevertheless, we and others observed a strong increase in serum IgM and IgG concentrations following sepsis (13, 14). Interestingly, the peak of the IgG serum concentration exceeded that of IgM by a factor of four, and an Ig switching to all IgG subclasses was seen. However, at the single cell level, there were three times as many IgM hybridomas as those producing IgG. Although one could argue that fusion was performed too soon, we found essentially the same proportions on day 14 as on day 10, which rules out time as the causal factor. Although the numbers of hybridomas are in general too low to make a definitive conclusion, a plausible explanation for this observation may be found in the half-lives of IgM vs. IgG antibodies. IgM has a markedly shorter serum half-life than IgG, and the half-life of polyreactive IgM is further reduced by Ag-binding, leading to a relative accumulation of IgG (54, 55).

TABLE 4 | Binding pattern of CASP d10 monoclonal IgG and IgM to oxidation-specific epitopes.

Clone	Ig-class	Binding specificity			
		Oxidation-specific epitopes (OSE)			Human native LDL
		MAA-BSA	MDA-/CuOx-LDL	PC-BSA	
F4_32	IgG1	×	×	ND	-
F6_13	IgG2b	×	×	-	-
F8_07	IgG2c	×	×	×	×
F9_3_H7	IgG1	×	×	ND	-
F9_25	IgG2c	×	×	-	-
F4_38	IgM	×	×	-	-
F5_10	IgM	×	×	×	-
F7_07	IgM	×	×	-	-
F9_24	IgM	×	×	-	-
F9_38	IgM	×	×	×	-
F4_04	IgM	×	×	-	-
F4_16	IgM	×	×	-	-
F4_46	IgM	×	-	-	-
F7_32	IgM	×	×	-	-
F9_09	IgM	×	-	-	-
F9_29	IgM	×	×	-	-
F8_14	IgM	×	×	×	×
F9_10	IgM	×	×	×	×
F7_33	IgM	-	-	-	×
F4_09	IgM	-	-	-	-
F7_36	IgM	-	-	-	-
F7_39	IgM	-	-	-	-
F9_12	IgM	-	-	-	-

The hybridomas were generated from splenocytes of septic mice at day 10. Twenty IgG hybridoma-supernatants (diluted to 0.25 μg/mL) and 18 IgM hybridoma-supernatants (diluted to 0.125 μg/mL) were tested for binding to model oxidation-specific epitopes. Human native LDL served as control. Binding specificities of five positively-tested IgG, as well as all IgM clones, are shown. ×, binding; -, no binding; MAA-BSA, malondialdehyde-acetaldehyde-modified bovine serum albumin (BSA); MDA/CuOx-LDL, malondialdehyde-modifed (MDA)/Cu^{2+}-oxidized (CuOx)-LDL; PC-BSA, phosphorylcholine conjugated to BSA; ND, not determined.

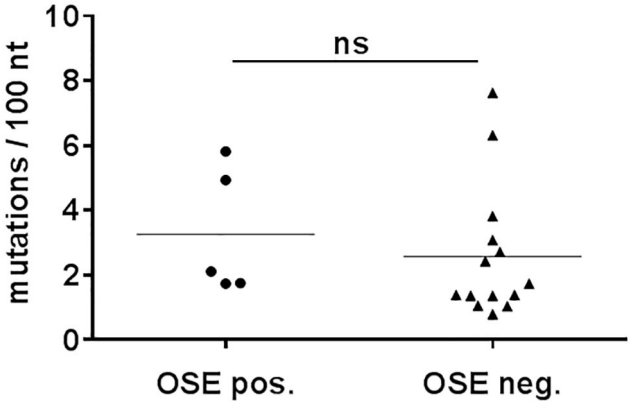

FIGURE 5 | Number of mutations in Vh-genes of monoclonal IgG. CASP surgery was performed on C57BL/6 mice. Hybridomas were generated by fusing splenocytes from 10- days-septic mice. The resultant monoclonal IgG hybridomas were sequenced for Vh-genes. Mutations of monoclonal IgG that showed binding to OSEs (OSE pos.) were compared to IgG that showed no binding (OSE neg.). Statistical analysis was performed using the unpaired *t*-test. $N = 5$–14 per group. nt, nucleotides; ns, not significant.

Since sepsis induces dissemination of endogenous bacteria into the bloodstream (11), a specific antibacterial IgG response would have been expected. However, there was very little serum IgG binding to bacteria in post-septic mice. Since we focussed our investigation on culturable bacteria in the sera of septic mice, it is possible that bacterial species other than the ones examined here were the culprits, since ELISA was performed only for *E. coli*, *S. aureus*, and *E. faecalis*. However, *E. coli* and *E. faecalis* originate from the serum of a septic animal. In fact, the bacterial strains used for testing are definitely present in large numbers in the intestine. When animals were injected *i.p.* with dead bacteria (*E. coli*, *S. aureus*, and *E. faecalis*) without sepsis, they were perfectly able to elaborate a specific IgG response. Depending on the bacterial species, we could show that 10^7-10^9 UV-inactivated bacteria trigger a robust specific IgG response (**Supplementary Figure 1**). Hence, we assume that sepsis interferes with an antibacterial antibody response. Interestingly enough, we rather observed Ig binding to autoantigens, as well as antigens, to which the animals had never been exposed. The production of natural autoantibodies against a spectrum of autoantigens has been described in sepsis patients (56–58). Using a relatively small panel of autoantigens, Burbelo et al. detected autoantibodies in 46% of severe sepsis patients, suggesting that this is a relatively common phenomenon (58). However, the production of autoantibodies is not confined to sepsis, but appears to be a general phenomenon observed with other types of bacterial, viral, and protozoan infections (18, 59–61), in addition to autoimmune disorders. In their recent study, Sakakibara et al. observed that the immune response to murine γ-herpesvirus 68 is accompanied by autoantibody production from polyreactive B cells in the germinal center, whose self-reactivity is generated through somatic hypermutation (61). More interestingly, several reports suggest a role of polyclonal activation in triggering anti-self responses, and hence leading to autoimmune disorders as a consequence of infections (18, 62). For instance, a direct link between infection and autoimmune encephalitis has been experimentally demonstrated in mice, and has been attributed to the production of autoantibodies (62).

It has been demonstrated that sepsis induces massive apoptosis of B and T lymphocytes, as well as DCs in mice and humans, and the release of danger molecules, known as PAMPs and DAMPs (8, 9, 63–67). We confirmed this in our model by TUNEL staining (terminal deoxynucleotidyl transferase dUTP nick end labeling) of the spleens for apoptotic nuclei (data not shown). The observed autoantigen response in sepsis could be explained by a polyclonal B cell activation through PAMPs and DAMPs, which activate B cells independent of the BCR, leading to the production of the so-called NAbs, which are polyreactive (68). To test whether polyreactive (natural) Abs or monoreactive Ig from a large variety of B cells dominate the humoral immune

response after sepsis, an analysis at the single cell level was conducted. It revealed that a large proportion of IgM-producing cells were polyreactive, as one would have expected based on the results obtained with serum.

Our results identify OSEs as the dominant target of the B cell response in murine polymicrobial sepsis: First, all post-septic animals had OSE-binding IgM and IgG, whereas antibody binding patterns to other tested autoantigens differed between individuals, even from the same cage. Second, anti-OSE titres were much higher than those of other tested bacterial or self-antigens. Finally, OSE-specific B cells were very frequent. Thirteen out of 18 tested IgM mAbs bound to OSEs even at low concentrations. Since 19% (23/120) of the IgM mAbs were polyreactive, at least 14% of IgM-producing B cells were OSE-specific. This frequency is somewhat similar to that of IgG mAbs, of which 25% were OSE-reactive.

Several points argue for a B-1 cell-driven immune response in the case of IgM. B-1 cells reside in the peritoneum and upon activation migrate to the spleen as well as other lymphatic organs, where they differentiate into ASCs (69, 70). These are the main producers of NAbs, which are polyreactive and utilize germline-near sequences (68). Chou et al. have shown that 20–30% of B-1 cell-derived IgM targets model-OSEs (42). This reflects the frequencies we find in monoclonal IgM and IgG. Moreover, Chang et al. have demonstrated that immunization of mice with apoptotic cells, which are abundant in sepsis, induces OSE-binding IgM (70).

In contrast, it is rather unlikely that the IgG response to OSEs is also dominated by B-1 cells. In B-1 cells, only a switch to IgG3 has been shown *in vivo* (31, 71). However, none of the five OSE-specific IgG mAbs were IgG3, whereas all other IgG subclasses were represented. Hence, a TD response of follicular B cells appears more likely. Chang et al. were able to induce OSE-binding IgG in mice by immunizing with model-OSE and apoptotic cells simultaneously (70). Moreover, Grasset et al. showed that some follicular B cells can bind fluorescently-labeled oxidized LDL. Repeated immunization with apoptotic cells induced OSE-binding IgG (72).

We suggest the following model: In sepsis, numerous immune cells undergo apoptosis. PAMPs and DAMPs polyclonally activate peritoneal B-1 cells to migrate to the spleen and differentiate into ASCs. These produce NAbs, explaining the increase in serum IgM targeting OSEs as well as other autoantigens. NAbs, including OSE-targeting IgM antibodies, may act as scavengers, promoting the clearance of apoptotic cells and debris, which would be relevant in sepsis (22, 42). In this study, however, we observed that OSE-specific antibodies had switched to IgG as well, presumably in a TD response. It may be speculated that the dominant response to OSEs restricts a specific antibody response to the sepsis-causing bacteria, which the organism would mount in the absence of apoptosis. Besides this, massive apoptosis has been shown to be tolerogenic, which explains the well-known fact that sepsis does not induce strong protective immune memory (11). The pathophysiological function of OSEs and OSE-specific IgM and IgG in sepsis should now be investigated, to determine whether OSE-specific antibodies could have therapeutic potential.

DATA AVAILABILITY STATEMENT

All datasets generated for this study are included in the article/**Supplementary Material**.

ETHICS STATEMENT

The animal study was reviewed and approved by The Animal Ethics Committee of the local animal protection authority (LALLF, State Office for Agriculture, Food Safety, and Fisheries Mecklenburg-Western Pomerania).

AUTHOR CONTRIBUTIONS

ON, CP, CB, and BB: conceptualization and project design. ON, CP, JL, SQ, and AL: methodology and performance of experiments. ON and CP: data evaluation. ON, CP, DR, C-DH, MD, and BB: interpretation of data. ON, DR, MD, CJB, and BB: writing—original draft preparation. All authors critically reviewed the manuscript and approved the submitted version.

FUNDING

This work was financially supported by the German Research Foundation (RTG 840; grants to ON, CP, and JL). We acknowledge support for the Article Processing Charge from the DFG (German Research Foundation, 393148499) and the Open Access Publication Fund of the University of Greifswald.

ACKNOWLEDGMENTS

We are grateful to Maria Ozsvar Kozma for excellent technical support. The authors would also like to thank Juliane Moritz for her contribution to this work.

SUPPLEMENTARY MATERIAL

The Supplementary Material for this article can be found online at: https://www.frontiersin.org/articles/10.3389/fimmu.2020.01570/full#supplementary-material

REFERENCES

1. Singer M, Deutschman CS, Seymour CW, Shankar-Hari M, Annane D, Bauer M, et al. The third international consensus definitions for sepsis and septic shock (sepsis-3). *JAMA*. (2016) 315:801–10. doi: 10.1001/jama.2016.0287
2. Angus DC, van der Poll T. Severe sepsis and septic shock. *N Engl J Med.* (2013) 369:840–51. doi: 10.1056/NEJMra1208623
3. Fleischmann C, Hartmann M, Hartog CS, Welte T, Heublein S, Thomas-Rueddel D, et al. Epidemiology of sepsis in Germany: incidence, mortality and associated costs of care 2007-2013. *Intensive Care Med Exp.* (2015) 3(Suppl. 1):A50. doi: 10.1186/2197-425X-3-S1-A50
4. La Suarez De Rica A, Gilsanz F, Maseda E. Epidemiologic trends of sepsis in western countries. *Ann Transl Med.* (2016) 4:325. doi: 10.21037/atm.2016.08.59

5. Fitzpatrick F, Tarrant C, Hamilton V, Kiernan FM, Jenkins D, Krockow EM. Sepsis and antimicrobial stewardship: two sides of the same coin. *BMJ Qual Saf.* (2019) 28:758–61. doi: 10.1136/bmjqs-2019-009445
6. Rudd KE, Johnson SC, Agesa KM, Shackelford KA, Tsoi D, Kievlan DR, et al. Global, regional, and national sepsis incidence and mortality, 1990–2017: analysis for the global burden of disease study. *Lancet.* (2020) 395:200–11. doi: 10.1016/S0140-6736(19)32989-7
7. Boes M, Prodeus AP, Schmidt T, Carroll MC, Chen J. A critical role of natural immunoglobulin M in immediate defense against systemic bacterial infection. *J Exp Med.* (1998) 188:2381–6. doi: 10.1084/jem.188.12.2381
8. Kelly-Scumpia KM, Scumpia PO, Weinstein JS, Delano MJ, Cuenca AG, Nacionales DC, et al. B cells enhance early innate immune responses during bacterial sepsis. *J Exp Med.* (2011) 208:1673–82. doi: 10.1084/jem.20101715
9. Hotchkiss RS, Tinsley KW, Swanson PE, Schmieg RE Jr, Hui JJ, Chang KC, et al. Sepsis-induced apoptosis causes progressive profound depletion of B and CD4+ T lymphocytes in humans. *J Immunol.* (2001) 166:6952–63. doi: 10.4049/jimmunol.166.11.6952
10. Inoue S, Unsinger J, Davis CG, Muenzer JT, Ferguson TA, Chang K, et al. IL-15 prevents apoptosis, reverses innate and adaptive immune dysfunction, and improves survival in sepsis. *J Immunol.* (2010) 184:1401–9. doi: 10.4049/jimmunol.0902307
11. Pötschke C, Kessler W, Maier S, Heidecke C-D, Bröker BM. Experimental sepsis impairs humoral memory in mice. *PLoS ONE.* (2013) 8:e81752. doi: 10.1371/journal.pone.0081752
12. Sjaastad FV, Condotta SA, Kotov JA, Pape KA, Dail C, Danahy DB, et al. Polymicrobial sepsis chronic immunoparalysis is defined by diminished Ag-specific T cell-dependent B cell responses. *Front Immunol.* (2018) 9:2532. doi: 10.3389/fimmu.2018.02532
13. Mohr A, Polz J, Martin EM, Griessl S, Kammler A, Potschke C, et al. Sepsis leads to a reduced antigen-specific primary antibody response. *Eur J Immunol.* (2012) 42:341–52. doi: 10.1002/eji.201141692
14. Nicolai O, Pötschke C, Schmoeckel K, Darisipudi MN, van der Linde J, Raafat D, et al. Antibody production in murine polymicrobial sepsis-kinetics and key players. *Front Immunol.* (2020) 11:828. doi: 10.3389/fimmu.2020.00828
15. Gentile LF, Moldawer LL. DAMPs, PAMPs, and the origins of SIRS in bacterial sepsis. *Shock.* (2013) 39:113–4. doi: 10.1097/SHK.0b013e318277109c
16. Sursal T, Stearns-Kurosawa DJ, Itagaki K, Oh S-Y, Sun S, Kurosawa S, et al. Plasma bacterial and mitochondrial DNA distinguish bacterial sepsis from sterile systemic inflammatory response syndrome and quantify inflammatory tissue injury in nonhuman primates. *Shock.* (2013) 39:55–62. doi: 10.1097/SHK.0b013e318276f4ca
17. Suthers AN, Sarantopoulos S. TLR7/TLR9- and B cell receptor-signaling crosstalk: promotion of potentially dangerous B cells. *Front Immunol.* (2017) 8:775. doi: 10.3389/fimmu.2017.00775
18. Montes CL, Acosta-Rodríguez EV, Merino MC, Bermejo DA, Gruppi A. Polyclonal B cell activation in infections: infectious agents' devilry or defense mechanism of the host? *J Leuk Biol.* (2007) 82:1027–32. doi: 10.1189/jlb.0407214
19. Lanzavecchia A, Bernasconi N, Traggiai E, Ruprecht CR, Corti D, Sallusto F. Understanding and making use of human memory B cells. *Immunol Rev.* (2006) 211:303–9. doi: 10.1111/j.0105-2896.2006.00403.x
20. Miller YI, Choi S-H, Wiesner P, Fang L, Harkewicz R, Hartvigsen K, et al. Oxidation-specific epitopes are danger-associated molecular patterns recognized by pattern recognition receptors of innate immunity. *Circ Res.* (2011) 108:235–48. doi: 10.1161/CIRCRESAHA.110.223875
21. Weismann D, Binder CJ. The innate immune response to products of phospholipid peroxidation. *Biochim Biophys Acta.* (2012) 1818:2465–75. doi: 10.1016/j.bbamem.2012.01.018
22. Binder CJ, Papac-Milicevic N, Witztum JL. Innate sensing of oxidation-specific epitopes in health and disease. *Nat Rev Immunol.* (2016) 16:485–97. doi: 10.1038/nri.2016.63
23. Shlomchik MJ, Weisel F. Germinal center selection and the development of memory B and plasma cells. *Immunol Rev.* (2012) 247:52–63. doi: 10.1111/j.1600-065X.2012.01124.x
24. Garcia De Vinuesa C, O'Leary P, Sze DM, Toellner KM, MacLennan IC. T-independent type 2 antigens induce B cell proliferation in multiple splenic sites, but exponential growth is confined to extrafollicular foci. *Eur J Immunol.* (1999) 29:1314–23. doi: 10.1002/(SICI)1521-4141(199904)29:04<1314::AID-IMMU1314>3.0.CO;2-4
25. Coutinho A, Gronowicz E, Bullock WW, Möller G. Mechanism of thymus-independent immunocyte triggering. Mitogenic activation of B cells results in specific immune responses. *J Exp Med.* (1974) 139:74–92. doi: 10.1084/jem.139.1.74
26. Krieg AM, Yi AK, Matson S, Waldschmidt TJ, Bishop GA, Teasdale R, et al. CpG motifs in bacterial DNA trigger direct B-cell activation. *Nature.* (1995) 374:546–9. doi: 10.1038/374546a0
27. Pasare C, Medzhitov R. Control of B-cell responses by Toll-like receptors. *Nature.* (2005) 438:364–8. doi: 10.1038/nature04267
28. Genestier L, Taillardet M, Mondiere P, Gheit H, Bella C, Defrance T. TLR agonists selectively promote terminal plasma cell differentiation of B cell subsets specialized in thymus-independent responses. *J Immunol.* (2007) 178:7779–86. doi: 10.4049/jimmunol.178.12.7779
29. Ehrenstein MR, Notley CA. The importance of natural IgM: scavenger, protector and regulator. *Nat Rev Immunol.* (2010) 10:778–86. doi: 10.1038/nri2849
30. Cerutti A, Cols M, Puga I. Marginal zone B cells: virtues of innate-like antibody-producing lymphocytes. *Nat Rev Immunol.* (2013) 13:118–32. doi: 10.1038/nri3383
31. Panda S, Ding JL. Natural antibodies bridge innate and adaptive immunity. *J Immunol.* (2015) 194:13–20. doi: 10.4049/jimmunol.1400844
32. Baumgarth N. The double life of a B-1 cell: self-reactivity selects for protective effector functions. *Nat Rev Immunol.* (2011) 11:34–46. doi: 10.1038/nri2901
33. Nutt SL, Hodgkin PD, Tarlinton DM, Corcoran LM. The generation of antibody-secreting plasma cells. *Nat Rev Immunol.* (2015) 15:160–71. doi: 10.1038/nri3795
34. Savage HP, Baumgarth N. Characteristics of natural antibody-secreting cells. *Ann N Y Acad Sci.* (2015) 23:12799. doi: 10.1111/nyas.12799
35. Martin F, Kearney JF. Marginal-zone B cells. *Nat Rev Immunol.* (2002) 2:323–35. doi: 10.1038/nri799
36. Zouali M, Richard Y. Marginal zone B-cells, a gatekeeper of innate immunity. *Front Immunol.* (2011) 2:63. doi: 10.3389/fimmu.2011.00063
37. MacLennan IC, Toellner KM, Cunningham AF, Serre K, Sze DM, Zuniga E, et al. Extrafollicular antibody responses. *Immunol Rev.* (2003) 194:8–18. doi: 10.1034/j.1600-065X.2003.00058.x
38. Martin F, Oliver AM, Kearney JF. Marginal zone and B1 B cells unite in the early response against T-independent blood-borne particulate antigens. *Immunity.* (2001) 14:617–29. doi: 10.1016/S1074-7613(01)00129-7
39. Maier S, Traeger T, Entleutner M, Westerholt A, Kleist B, Hüser N, et al. Cecal ligation and puncture versus colon ascendens stent peritonitis: two distinct animal models for polymicrobial sepsis: two distinct animal models for polymicrobial sepsis. *Shock.* (2004) 21:505–11. doi: 10.1097/01.shk.0000126906.52367.dd
40. Zantl N, Uebe A, Neumann B, Wagner H, Siewert JR, Holzmann B, et al. Essential role of gamma interferon in survival of colon ascendens stent peritonitis, a novel murine model of abdominal sepsis. *Infect Immun.* (1998) 66:2300–9. doi: 10.1128/IAI.66.5.2300-2309.1998
41. Holtfreter S, Nguyen TT, Wertheim H, Steil L, Kusch H, Truong QP, et al. Human immune proteome in experimental colonization with *Staphylococcus aureus*. *Clin Vaccine Immunol.* (2009) 16:1607–14. doi: 10.1128/CVI.00263-09
42. Chou M-Y, Fogelstrand L, Hartvigsen K, Hansen LF, Woelkers D, Shaw PX, et al. Oxidation-specific epitopes are dominant targets of innate natural antibodies in mice and humans. *J Clin Invest.* (2009) 119:1335–49. doi: 10.1172/JCI36800
43. Binder CJ, Hörkkö S, Dewan A, Chang M-K, Kieu EP, Goodyear CS, et al. Pneumococcal vaccination decreases atherosclerotic lesion formation: molecular mimicry between *Streptococcus pneumoniae* and oxidized LDL. *Nat Med.* (2003) 9:736–43. doi: 10.1038/nm876
44. Kantor AB, Merrill CE, Herzenberg LA, Hillson JL. An unbiased analysis of V(H)-D-J(H) sequences from B-1a, B-1b, and conventional B cells. *J Immunol.* (1997) 158:1175–86.
45. Tiller T, Busse CE, Wardemann H. Cloning and expression of murine Ig genes from single B cells. *J Immunol Methods.* (2009) 350:183–93. doi: 10.1016/j.jim.2009.08.009
46. Ehlers M, Fukuyama H, McGaha TL, Aderem A, Ravetch JV. TLR9/MyD88 signaling is required for class switching to

pathogenic IgG2a and 2b autoantibodies in SLE. *J Exp Med.* (2006) 203:553–61. doi: 10.1084/jem.20052438
47. Schmoeckel K, Traffehn S, Eger C, Potschke C, Broker BM. Full activation of CD4+ T cells early during sepsis requires specific antigen. *Shock.* (2015) 43:192–200. doi: 10.1097/SHK.0000000000000267
48. Wardemann H, Yurasov S, Schaefer A, Young JW, Meffre E, Nussenzweig MC. Predominant autoantibody production by early human B cell precursors. *Science.* (2003) 301:1374–7. doi: 10.1126/science.1086907
49. Tiller T, Tsuiji M, Yurasov S, Velinzon K, Nussenzweig MC, Wardemann H. Autoreactivity in human IgG+ memory B cells. *Immunity.* (2007) 26:205–13. doi: 10.1016/j.immuni.2007.01.009
50. Tiller T, Kofer J, Kreschel C, Busse CE, Riebel S, Wickert S, et al. Development of self-reactive germinal center B cells and plasma cells in autoimmune Fc gammaRIIB-deficient mice. *J Exp Med.* (2010) 207:2767–78. doi: 10.1084/jem.20100171
51. Palinski W, Hörkkö S, Miller E, Steinbrecher UP, Powell HC, Curtiss LK, et al. Cloning of monoclonal autoantibodies to epitopes of oxidized lipoproteins from apolipoprotein E-deficient mice. Demonstration of epitopes of oxidized low density lipoprotein in human plasma. *J Clin Invest.* (1996) 98:800–14. doi: 10.1172/JCI118853
52. Berek C, Milstein C. Mutation drift and repertoire shift in the maturation of the immune response. *Immunol Rev.* (1987) 96:23–41. doi: 10.1111/j.1600-065X.1987.tb00507.x
53. Cabrera-Perez J, Condotta SA, James BR, Kashem SW, Brincks EL, Rai D, et al. Alterations in antigen-specific naive CD4 T cell precursors after sepsis impairs their responsiveness to pathogen challenge. *J Immunol.* (2015) 194:1609–20. doi: 10.4049/jimmunol.1401711
54. Vieira P, Rajewsky K. The half-lives of serum immunoglobulins in adult mice. *Eur J Immunol.* (1988) 18:313–6. doi: 10.1002/eji.1830180221
55. Sigounas G, Harindranath N, Donadel G, Notkins AL. Half-life of polyreactive antibodies. *J Clin Immunol.* (1994) 14:134–40. doi: 10.1007/BF01541346
56. Barnay-Verdier S, Fattoum L, Borde C, Kaveri S, Gibot S, Maréchal V. Emergence of autoantibodies to HMGB1 is associated with survival in patients with septic shock. *Intensive care Med.* (2011) 37:957–62. doi: 10.1007/s00134-011-2192-6
57. Malfussi H, Santana IV, Gasparotto J, Righy C, Tomasi CD, Gelain DP, et al. Anti-NMDA receptor autoantibody is an independent predictor of hospital mortality but not brain dysfunction in septic patients. *Front Neurol.* (2019) 10:221. doi: 10.3389/fneur.2019.00221
58. Burbelo PD, Seam N, Groot S, Ching KH, Han BL, Meduri GU, et al. Rapid induction of autoantibodies during ARDS and septic shock. *J Transl Med.* (2010) 8:97. doi: 10.1186/1479-5876-8-97
59. Rivera-Correa J, Rodriguez A. Divergent roles of antiself antibodies during infection. *Trends Immunol.* (2018) 39:515–22. doi: 10.1016/j.it.2018.04.003
60. Portocala R, Spyrou N, Lambropoulou V, Pateraki E. The presence of both antivirus and antiself antibodies in sera from patients with adenovirus and influenza B. *Virologie.* (1988) 39:207–16.
61. Sakakibara S, Yasui T, Jinzai H, O'donnell K, Tsai C-Y, Minamitani T, et al. Self-reactive and polyreactive B cells are generated and selected in the germinal center during γ-herpesvirus infection. *Int Immunol.* (2020) 32:27–38. doi: 10.1093/intimm/dxz057
62. Joubert B, Dalmau J. The role of infections in autoimmune encephalitides. *Rev Neurol.* (2019) 175:420–6. doi: 10.1016/j.neurol.2019.07.004
63. Hotchkiss RS, Tinsley KW, Swanson PE, Grayson MH, Osborne DF, Wagner TH, et al. Depletion of dendritic cells, but not macrophages, in patients with sepsis. *J Immunol.* (2002) 168:2493–500. doi: 10.4049/jimmunol.168.5.2493
64. Peck-Palmer OM, Unsinger J, Chang KC, Davis CG, McDunn JE, Hotchkiss RS. Deletion of MyD88 markedly attenuates sepsis-induced T and B lymphocyte apoptosis but worsens survival. *J Leuk Biol.* (2008) 83:1009–18. doi: 10.1189/jlb.0807528
65. Tinsley KW, Grayson MH, Swanson PE, Drewry AM, Chang KC, Karl IE, et al. Sepsis induces apoptosis and profound depletion of splenic interdigitating and follicular dendritic cells. *J Immunol.* (2003) 171:909–14. doi: 10.4049/jimmunol.171.2.909
66. Wang SD, Huang KJ, Lin YS, Lei HY. Sepsis-induced apoptosis of the thymocytes in mice. *J Immunol.* (1994) 152:5014–21.
67. Busse M, Traeger T, Potschke C, Billing A, Dummer A, Friebe E, et al. Detrimental role for CD4+ T lymphocytes in murine diffuse peritonitis due to inhibition of local bacterial elimination. *Gut.* (2008) 57:188–95. doi: 10.1136/gut.2007.121616
68. Palma J, Tokarz-Deptuła B, Deptuła J, Deptuła W. Natural antibodies – facts known and unknown. *Cent Eur J Immunol.* (2018) 43:466–75. doi: 10.5114/ceji.2018.81354
69. Yang Y, Tung JW, Ghosn EE, Herzenberg LA. Division and differentiation of natural antibody-producing cells in mouse spleen. *Proc Natl Acad Sci USA.* (2007) 104:4542–6. doi: 10.1073/pnas.0700001104
70. Chang M-K, Binder CJ, Miller YI, Subbanagounder G, Silverman GJ, Berliner JA, et al. Apoptotic cells with oxidation-specific epitopes are immunogenic and proinflammatory. *J Exp Med.* (2004) 200:1359–70. doi: 10.1084/jem.20031763
71. Panda S, Zhang J, Tan NS, Ho B, Ding JL. Natural IgG antibodies provide innate protection against ficolin-opsonized bacteria. *EMBO J.* (2013) 32:2905–19. doi: 10.1038/emboj.2013.199
72. Grasset EK, Duhlin A, Agardh HE, Ovchinnikova O, Hägglöf T, Forsell MN, et al. Sterile inflammation in the spleen during atherosclerosis provides oxidation-specific epitopes that induce a protective B-cell response. *Proc Natl Acad Sci USA.* (2015) 112:E2030–8. doi: 10.1073/pnas.1421227112

Conflict of Interest: The authors declare that the research was conducted in the absence of any commercial or financial relationships that could be construed as a potential conflict of interest.

frontiers in Immunology

ORIGINAL RESEARCH
published: 07 August 2020
doi: 10.3389/fimmu.2020.01515

mTORC1 Is Not Principally Involved in the Induction of Human Endotoxin Tolerance

Kristin Ludwig[1], *Ralf A. Husain*[2] *and Ignacio Rubio*[1,3]*

[1] Institute of Molecular Cell Biology, Center for Molecular Biomedicine, University Hospital Jena, Jena, Germany, [2] Department of Neuropediatrics, University Hospital Jena, Jena, Germany, [3] Clinic of Anaesthesiology and Intensive Care and Center for Sepsis Control and Care (CSCC), University Hospital Jena, Jena, Germany

Endotoxin tolerance represents a safeguard mechanism for preventing detrimental prolonged inflammation and exaggerated immune/inflammatory responses from innate immune cells to recurrent harmless pathogens. On the other hand, excessive immune tolerance can contribute to pathological immunosuppression, e.g., as present in sepsis. Monocyte activation is accompanied by intracellular metabolic rearrangements that are reportedly orchestrated by the metabolic signaling node mTORC1. mTORC1-dependent metabolic re-wiring plays a major role in monocyte/macrophage polarization, but whether mTORC1 participates in the induction of endotoxin tolerance and other immune adaptive programs, such as immune training, is not clear. This connection has been difficult to test in the past due to the lack of appropriate models of human endotoxin tolerance allowing for the genetic manipulation of mTORC1. We have addressed this shortcoming by investigating monocytes from tuberous sclerosis (TSC) patients that feature a functional loss of the tumor suppressor TSC1/2 and a concomitant hyperactivation of mTORC1. Subjecting these cells to various protocols of immune priming and adaptation showed that the TSC monocytes are not compromised in the induction of tolerance. Analogously, we find that pharmacological mTORC1 inhibition does not prevent endotoxin tolerance induction in human monocytes. Interestingly, neither manipulation affected the capacity of activated monocytes to switch to increased lactic fermentation. In sum, our findings document that mTORC1 is unlikely to be involved in the induction of endotoxin tolerance in human monocytes and argue against a causal link between an mTORC1-dependent metabolic switch and the induction of immune tolerance.

Keywords: mTORC1, endotoxin tolerance, monocytes, macrophage, sepsis, immune suppression

OPEN ACCESS

Edited by:
Florian Uhle,
Heidelberg University Hospital, Germany

Reviewed by:
Liwu Li,
Virginia Tech, United States
Krzysztof Guzik,
Jagiellonian University, Poland

***Correspondence:**
Ignacio Rubio
ignacio.rubio@med.uni-jena.de

Specialty section:
This article was submitted to Inflammation, a section of the journal Frontiers in Immunology

Received: *14 February 2020*
Accepted: *09 June 2020*
Published: *07 August 2020*

Citation:
Ludwig K, Husain RA and Rubio I (2020) mTORC1 Is Not Principally Involved in the Induction of Human Endotoxin Tolerance. Front. Immunol. 11:1515. doi: 10.3389/fimmu.2020.01515

INTRODUCTION

Innate immune cells of the myeloblastic lineage constitute the first line of defense against infection and tissue breakdown in trauma. Upon identifying, spotting, tracking, or engulfing pathogens, pathogen-associated molecular patterns (PAMPs), or damage-associated molecular patterns, the myeloblastic cells elicit a cascade of inflammatory and immune responses mediated by the release of cytokine cocktails and eventually the direct presentation of antigen to lymphocytes. Due to their unique ability to recognize and rank infectious or traumatic triggers, the innate immune cells dictate the quality and the intensity of the host response and hence the course of an infection episode. Owing to this primordial role at the vanguard of the host response, the innate immune

cells possess intricate mechanisms for fine-tuning their immune responses according to the risk and the severity of any particular infection. One level of control is provided by the limited lifespan of monocytes or neutrophils (as new immunocytes continuously emerge from the bone marrow), which precludes the pernicious accumulation of hyper-reactive or aberrant immune cells. Additional fine-tuning proceeds at the molecular level as the innate immune cells are able to adapt dynamically to a particular infection and trauma scenarios and re-shape their response accordingly. For example, in a process known as immune training, the activated monocytes re-configure their response toward ensuing inflammatory cues in the long term *via* PAMP-induced changes in the epigenome (1, 2).

Another important process that can shape the amplitude and the quality of monocyte responses is endotoxin tolerance (ET) (3). ET represents a well-established state of hyporesponsiveness characterized by a skewed, largely anti-inflammatory response, which is intended to prevent exaggerated immune/inflammatory responses to recurrent and innocuous antigens. Several models have been put forward to explain tolerance induction in monocytes, but the precise molecular mechanisms remain elusive (3, 4). Besides the intellectual challenge of deciphering the molecular processes that mediate ET in the monocyte, understanding the tolerance mechanisms is relevant also from a clinical perspective because untimely or unleashed tolerance contributes to states of immunosuppression in lethal conditions such as sepsis (5, 6).

Most models of endotoxin tolerance invoke molecular rearrangements downstream of TLR4 or other pattern recognition receptors (PRR) in the tolerant immune cell (4, 7). Thus, up-regulation/activation of the downstream kinase IRAK-M has been shown to block TLR4 signaling at the level of Myd88-containing complex (Myddosome) formation, promoting a state of tolerance toward lipopolysaccharide (LPS) (8, 9). Another focus has been placed on the characterization of feedback mechanisms that attenuate signaling by PRRs in tolerized cells. Many of those feedback models invoke autocrine loops, including the secretion of anti-inflammatory cytokines such as IL-10 or TGFß that can, moreover, contribute to a generalized environment of immune suppression by impinging on other immune cells such as lymphocytes (10, 11). Indeed the endotoxin tolerance of circulating monocytes from sepsis patients correlates with high levels of IL-10 and other anti-inflammatory cytokines and is characterized by high intramonocytic levels of IRAK-M protein (8). Despite these advances in our understanding of endotoxin tolerance, however, a unifying model of tolerance induction is still lacking as several important features of ET in monocytes remain unaccounted for.

One such poorly understood aspect that has raised much interest is with regards the immunocyte's metabolism and the potential role of metabolic re-wiring processes in the course of ET induction. Recently, a metabolic switch toward anaerobic glycolysis, analogous to the Warburg effect originally described for cancer cells, has been put forward as a crucial step for immune training of monocytes (12, 13). Indeed as documented in multiple reports dating back to the 1960s, monocytes experience a pronounced Warburg-like metabolic switch upon immune activation, leading to more aerobic glucose fermentation and lactate production with a concomitant drop in cellular respiration (14, 15). It is generally assumed that these metabolic rearrangements serve the purpose of optimizing energy production and expenditure, arming and preparing the monocyte to combat the infectious threat in the inflamed tissue. However, whether or not Warburg-like metabolic rearrangements are an integral component of immune adaptive programs leading to ET or immune training is not clear.

The metabolic switch in immunocytes and other cell types is presumably orchestrated by a limited number of cellular master metabolic regulatory proteins, prominently the energy and nutrient sensors AMPK, HIF1α, and mTORC1. The metabolic signaling node mTOR containing complex 1 (mTORC1) is a multi-protein complex named after its core component, the Ser/Thr kinase mTOR. It acts as a master intracellular hub of metabolic control as it funnels and records hormonal, environmental, and intracellular cues reporting nutrient and energy availability [reviewed in (16)]. mTORC1 processes and converts this information into an appropriate signaling output that orchestrates catabolic and anabolic processes in the cell. Mechanistically, mTORC1 activity is controlled by the action of tuberous sclerosis 1 and 2 (TSC1/TSC2) tumor suppressor protein complex, an immediate upstream negative regulator acting as a GTPase-activating protein for the small G-protein Rheb (17, 18). mTORC1 activity is critical for immune cell function as the pharmacological inhibition of mTORC1 can substantially alter or, in some cases such as T-lymphocytes, completely ablate immune responses (19). Indeed the mTORC1 inhibitor rapamycin and its derivatives, like everolimus, are immunosuppressants commonly used in the clinic. Thus, while it is firmly established that mTORC1 activity is critical for immune cell function, it is not known whether it plays a direct role in adaptive processes such as ET. Such a connection has proved to be difficult to test experimentally, other than by using pharmacological inhibitors like rapamycin. However, pharmacological approaches suffer from a number of drawbacks and thus need to be complemented by genetic approaches, which are difficult to implement on primary immune cells.

To circumvent these methodological shortcuts, we have investigated monocytes from TSC patients that feature a functional loss of TSC1/2 and a concomitant hyperactivation of mTORC1. TSC is an autosomal dominant disorder caused by loss-of-function germ-line variants of either of the two TSC protein complex components TSC1 and TSC2 (20, 21). TSC1 and TSC2 together form the upstream negative regulator TSC complex for mTORC1. TSC patients manifest multiple benign neoplasias, designated as hamartomas, that can affect many organs and are often characterized by exorbitantly large, giant cells. Although TSC1 and/or TSC2 have been attributed additional functions beyond acting as a gatekeeper for mTORC1 (22), it is generally accepted that the clinical manifestations of TSC result principally from hyperactive mTORC1 signaling. Thus, TSC represents a "genetic model" for mTORC1 gain-of-function. Here we subjected monocytes

from TSC patients to various protocols of immune adaptation to test if they were compromised in the induction of tolerance or training. As presented and discussed below, our findings strongly argue against a role for mTORC1 in the induction of immune tolerance.

MATERIALS AND METHODS

TSC Patient Enrolment and Ethics

Patient enrolment and blood drawing were performed at the Department of Neuropediatrics, University Hospital Jena, Germany. The study was approved by the local ethics committee of the University Hospital Jena (study registry number: 4498-07/15). Written informed consent was obtained from all the study participants or their legal representatives before the blood drawing. All patients included were diagnosed with TSC on the basis of gene sequencing (16 out of 19 patients) and/or unambiguous clinical features of TSC (**Table 1**). The exclusion criteria included recent/acute episodes of inflammation or infection, a CrP value >10 mg/l, any type of chronic disease, and treatment with immunosuppressive other than everolimus at the time point of blood drawing. Further patient and healthy donor characteristics are listed in **Table 2**.

TABLE 1 | Spectrum of the genetic lesions mapped to TSC1/TSC2 and the clinical features of the patients enrolled in the study.

Internal subject #	Clinical features (tuberous sclerosis specific)	Genetic mutation
002	SEN, SEGA, EPI, ID, RAML, HM, FA	TSC2: c.5135C>T
003	SEN, CD, EPI, DD, RAML, RC	TSC2: c.2251C>T
005	SEN, CD, SEGA, EPI, ID, RAML, RC, CR, AR, HM, FA	TSC2: c.5110del
008	SEN, CD, SEGA, EPI, ID, RC, CR, HM, FA	TSC2: c.1287dup
009	SEN, CD, EPI, RAML, RC, CR, MMPH, HM, FA	TSC2: c.976-15G>A
010	EPI, FA	TSC1: c.211-1G>A
011	SEGA, EPI, ID, RC, CR, FA	TSC2: c.? (written report not available)
012	EPI, RC, CR, HM, FA	TSC2: deletion exons 30-41
013	EPI, RC, FA	Not available
016	SEN, CD, DD, RC, CR, AR, HM	TSC2: deletion exons 15-21
017	SEN, CD, EPI,DD, HM, FA	TSC2: c.1832G>A
018	SEN, CD, SEGA, EPI, ID, RAML, RC, CR, AR, HM, FA	TSC2: c.5110del
020	SEN, CD, SEGA, EPI, ID, RC, CR, HM	TSC2: c.4925G>A
021	SEN, CD, SEGA, EPI, ID, RAML, CR, HM, FA	TSC2: c.? (written report not available)
024	SEN, CD, SEGA, EPI, ID, RAML, RC, CR, HM, FA	TSC1: c.2029insC
026	SEN, CD, SEGA, EPI, ID, RAML, RC, HM, FA	TSC2: c.4646A>G
029	SEN, CD, EPI, DD, HM	TSC2: c.4712A>G
031	SEN, CD, EPI, ID, PI, RAML, RC, CR, HM, FA	TSC2: c.1832G>A
036	SEN, CD, RC, CR	TSC2: c.3284+1G>A

SEN, subependymal nodules; SEGA, subependymal giant cell astrocytomas; EPI, epilepsy; ID, intellectual disability; RAML, renal angiomyolipomas; HM, hypomelanotic macules; FA, facial angiofibromas; CD: cortical dysplasias; DD, developmental delay; RC, renal cysts; CR, cardiac rhabdomyomas; AR, arrhythmias; PI, psychiatric illness.

Materials

Rapamycine was from Calbiochem. Torin-1 was from TOCRIS. LPS (strain055:B5) was purchased from Sigma-Aldrich (#L2880). ß-Glucan was obtained from two sources: (1) a kind gift of Mihai Netea, Nijmegen, Netherlands and (2) a kind gift of David L. Williams, Johnson City, USA.

The proteome profiler Human Cytokine Array Kit was from R&D Systems; the cytometric-based bead array (CBA) flex sets for multiplexed cytokine determinations were acquired from BD Biosciences. Ficoll Histopaque®-1077 was from Sigma-Aldrich. The ELISA-standard TNFα was from Biolegend, Inc.

Antibodies

The antibodies for western blotting, S6-Protein (5G109), p-S6-Protein (Ser235/236), AKT, p-AKT (D9E) (Ser473), ERK1/2 (137F5), and p-ERK1/2 (E10) (Thr202/204), were all purchased from Cell Signaling. Anti-p38 and p-p38 (Thr108/Tyr182) were from BD Transduction. All antibodies were used at 1:1,000 dilution in TBS-Tween supplemented with 1% BSA. The antibody for flow cytometry was AntiCD14 (Immunotools).

Monocyte Isolation and Cultivation

Blood was drawn using Li/heparin monovettes by trained physicians. EDTA-blood from patients and control donors was blinded on-site at the neuropediatrics unit, transported at room temperature to the laboratory within <4 h of drawing, and processed immediately. Peripheral blood mononuclear cells (PBMCs) were isolated by standard density gradient centrifugation on Ficoll. Briefly, blood was diluted with isolation buffer [phosphate-buffered saline (PBS) without Ca^{2+}/Mg^{2+}, 1% BSA, 2 mM EDTA] to a final volume of 30 ml. The blood–buffer solution was carefully layered on 15 ml Ficoll Histopaque®-1077 solution and centrifuged at 800 g for 20 min (without break). The PBMC layer was harvested and washed twice with cold isolation buffer. The cells were resuspended in RPMI 1640 medium supplemented with 10 μg/ml gentamycine, 1% sodium pyruvate, 1% GlutaMax, and 10% heat-inactivated human serum (Sigma-Aldrich) and seeded at a density of 5–10 × 10^6 cells/ml. The monocytes were further purified on the basis of differential attachment to cell culture dish surfaces. The cells were left to settle and attach to the culture plate surface for 1 h at 37°C. The non-adherent cells representing non-monocytic fractions were washed off by three rounds of mild rinsing with warm PBS without Ca^{2+}/Mg^{2+}. The purity of the monocyte preparations was assessed by flow cytometry staining for surface CD14. Purity was routinely 90% or higher. The test runs of monocyte preparations using magnetic anti-CD14 beads yielded virtually identical purity and undistinguishable experimental results (not shown). The monocytes were cultured at 37°C and 5% CO_2 in a humidified atmosphere.

TABLE 2 | Patient and healthy donor characteristics.

Characteristics	Number
Tuberous sclerosis patients	
Total	19
Male	13
Female	6
Age (mean/median)	12/12
Age range (years)	0–38
Everolimus treatment	7
TSC1 mutation	2
TSC2 mutation	14
Mutation unknown	3
Healthy donors	
Total	25
Male	16
Female	9
Age (mean/median)	13/13
Age range	0–42

Monocyte Priming and Stimulation

Priming (either tolerance induction by LPS or training by ß-glucan) was performed by the treatment of monocyte cultures with 10–100 μg/ml LPS or with 3 μg/ml β-glucan for 24 h, respectively. At the end of the priming period, the cells were washed three times by rinsing with warm medium and subsequently stimulated with fresh medium containing 10 ng/ml LPS for additional 24 h. The cell culture supernatants were collected, cleared from cell debris by centrifugation (10,000 g for 10 min), and analyzed for cytokine production and metabolic parameters or stored at −20°C until analysis. The cells were collected by mild centrifugation (600 g for 10 min at 4°C) and analyzed by flow cytometry as appropriate. For inhibition of mTORC1, the cells were pre-incubated with a mixture of 20 ng/ml rapamycin and 10 ng/ml Torin-1 for 30 min prior to priming or stimulation with PAMPs. In the primed cells, both inhibitors were present during the 24-h period of priming.

Cytokine Profiling by Cytokine Strips/Proteome Profiler Human Cytokine Array

The cell culture supernatants were collected at the indicated time points, cleared from cell debris, and stored at −20°C until analysis. The cytokine profiles were determined using cytokine strips (R&D Systems) according to the manufacturer's instructions. The signals were detected by exposure to X-ray films and quantitated/imaged on a LAS system.

Cytokine Profiling by ELISA

TNFα production was measured in cleared cell culture supernatants by ELISA in accordance to the manufacturer's protocol. Colorimetric detection was performed with 3,3',5,5'-tetramethylbenzidine substrate solution (Biolegend, San Diego, CA, USA), and the reactions were quenched by the addition of 2N H_2SO_4. Absorbance was measured at 450 nm with a TECAN Microplate Reader (VersaMax) and analyzed using SOFTmax Pro software (Molecular Devices).

Cytokine Profiling by Multiplexed Bead Arrays/Cytometric Bead Array Flex Set

The production of nine defined inflammatory cytokines in cleared cell culture supernatants was measured by flow CBA on a FACSCanto™II, following the manufacturer's instructions. Data analysis was carried out using Flow Jo software (TreeStar Inc.). The calculated cytokine amounts were normalized to protein content (determined on the pelleted cells measured using Pierce® Micro BCA Protein Assay Kit) to account for different viability or growth patterns under the various treatment conditions (23). All cytokine concentrations are plotted as normalized cytokine amount per milliliter of supernatant.

Western Blotting

Human monocytes were seeded on six-well plates at a density of 10^7 cells/ml and left to attach for 1 h at 37°C, followed by three rounds of gentle washing to remove non-adherent cells. The cells were either primed with LPS or β-glucan in the presence or the absence of mTOR inhibitors or left untreated for 24 h. After priming, the cells were washed three times with medium, followed by stimulation with 10 ng/ml LPS for 30 or 60 min. The reactions were quenched with ice-cold RIPA lysis buffer (50 mM HEPES pH 7.5, 150 mM NaCl, 5 mM EDTA, 1% NP-40, 0.5% deoxycholate, and 0.1% SDS, supplemented with protease inhibitors) and the cell extracts were cleared by centrifugation. The protein concentration was determined with the BCA Protein Assay. The samples were treated with Laemmli buffer, boiled for 5 min, and equal amounts of total protein were resolved by SDS-PAGE. The proteins were transferred to polyvinylidene difluoride membranes using Trans-Blot Cell Tank system (Bio-Rad™) for wet blotting and probed with the indicated antibodies. The signals were quantified by densitometry on a ImageQuant™ LAS 4,000 instrument.

Stimulation With Conditioned Medium

Conditioned media were collected from human monocyte cultures as follows: the cells grown in full culture medium were challenged with 100 ng/ml LPS; at 1 h later, the cells were washed once and the medium was replaced with a fresh one without LPS. At 23 h later, the medium was collected, cleared from cell debris by centrifugation, and used immediately without intermediate storage as conditioned medium for the priming of naïve monocytes.

Lactate and Glucose Measurements

The lactate and glucose levels from monocyte culture supernatants were measured by the in-house clinical chemistry department of the Jena University Hospital.

Statistical Analysis

GraphPad Prism five and six were used for statistical analysis. All data are expressed as means ± SEM. A Wilcoxon matched-pairs

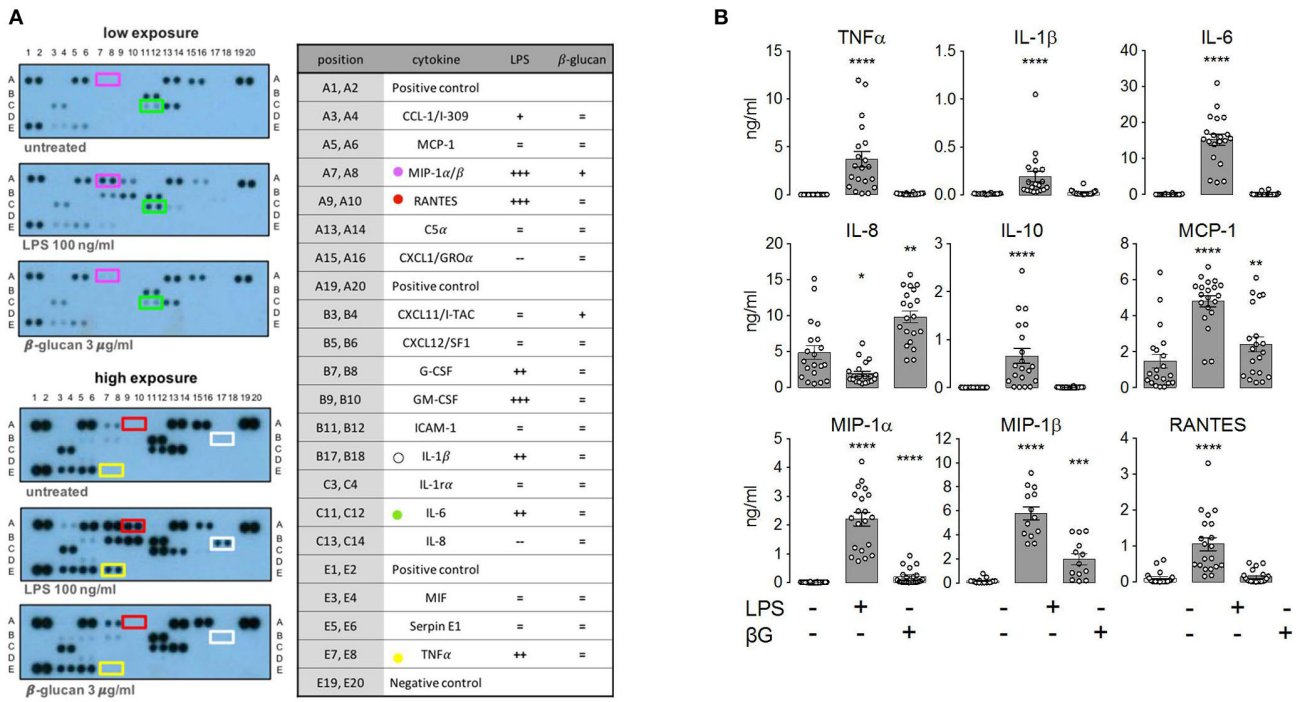

position	cytokine	LPS	β-glucan
A1, A2	Positive control		
A3, A4	CCL-1/I-309	+	=
A5, A6	MCP-1	=	=
A7, A8	MIP-1α/β	+++	+
A9, A10	RANTES	+++	=
A13, A14	C5α	=	=
A15, A16	CXCL1/GROα	--	=
A19, A20	Positive control		
B3, B4	CXCL11/I-TAC	=	+
B5, B6	CXCL12/SF1	=	=
B7, B8	G-CSF	++	=
B9, B10	GM-CSF	+++	=
B11, B12	ICAM-1	=	=
B17, B18	IL-1β	++	=
C3, C4	IL-1rα	=	=
C11, C12	IL-6	++	=
C13, C14	IL-8	--	=
E1, E2	Positive control		
E3, E4	MIF	=	=
E5, E6	Serpin E1	=	=
E7, E8	TNFα	++	=
E19, E20	Negative control		

FIGURE 1 | Lipopolysaccharide (LPS) and ß-glucan (ßG) exert distinct patterns of monocytic cytokine secretion. **(A)** Human peripheral monocytes from healthy volunteers were isolated, cultured, and stimulated with 10 ng/ml LPS or 3 μg/ml ß-glucan as described in the experimental section. At 24 h later, cytokine production was assessed with a human cytokine array encompassing 36 cytokines. The selected prototypical cytokines are highlighted with a color code. Changes in all 36 cytokines were scored and plotted in categories from strong down-regulation to strong up-regulation (−, –, -, =, +, ++, and + + +). **(B)** Human monocytes from healthy donors were isolated and treated as before. The cytokine levels were assessed by ELISA at 24 h post-stimulation. Different significance symbols were used to mark different inter-group comparisons.

signed rank test was performed to determine the significance between different treatments within one experimental group. Two-way ANOVA with Bonferroni post-test was used to determine the significance between two experimental groups ($^{*}p \leq 0.05$, $^{**}p \leq 0.01$, $^{***}p \leq 0.001$, $^{****}p \leq 0.0001$). Different significance symbols were used to mark different inter-group comparisons.

RESULTS

TSC Monocytes Feature Normal Response to LPS Challenge

In order to test the role of mTORC1 on the plasticity and the adaptation properties of human monocytes, we investigated, side by side, monocytes from TSC patients and healthy donors. To this end, we collected blood from mostly infant TSC patients that visited the neuropediatrics department for a routine medical check. Whenever possible, blood from age-matched healthy donors was collected and assayed on the same occasion. In order to avoid interference with the immunological parameters under investigation, the exclusion criteria for TSC patients included immunosuppressive therapies or recent infectious episodes, among others (see section Materials and Methods). Seven out of the 19 enrolled patients received everolimus therapy at the time point of blood withdrawal. Nine patients donated blood twice, with a gap of 6 months or more in between, but the obtained values were treated as individual data sets. Monocytes were isolated by differential plate attachment/washout protocols or magnetic isolation based on the surface expression of CD14. The cells isolated by either protocol showed undistinguishable results (data no shown). We did not observe any obvious phenotypic differences between control and TSC monocytes during routine cultivation. To assess general monocyte responsiveness, we challenged the cells with the PAMP LPS, a cell wall constituent of gram negatives and a strong inducer of ET (2). In parallel samples we stimulated also with ß-glucan from *Candida albicans* as a PAMP that reportedly induces immune training in these cells (24). In order to obtain a broad view of the cytokine spectrum induced by both PAMPs, we first challenged the control monocytes from healthy donors for 24 h and loaded the supernatant on cytokine strips (**Figure 1A**). As reported before (25), LPS induced the secretion of multiple cytokines, including TNFα, IL-1ß, IL-6, RANTES, and MIP1, while it reduced the secretion of others, prominently IL-8. By contrast, ß-glucan was a poor secretagogue, causing the mild upregulation of but a few cytokines, at least as measured under these conditions. To exclude a lack of activity of the employed ß-glucan, we tested two ß-glucan preparations of different origins (see the experimental

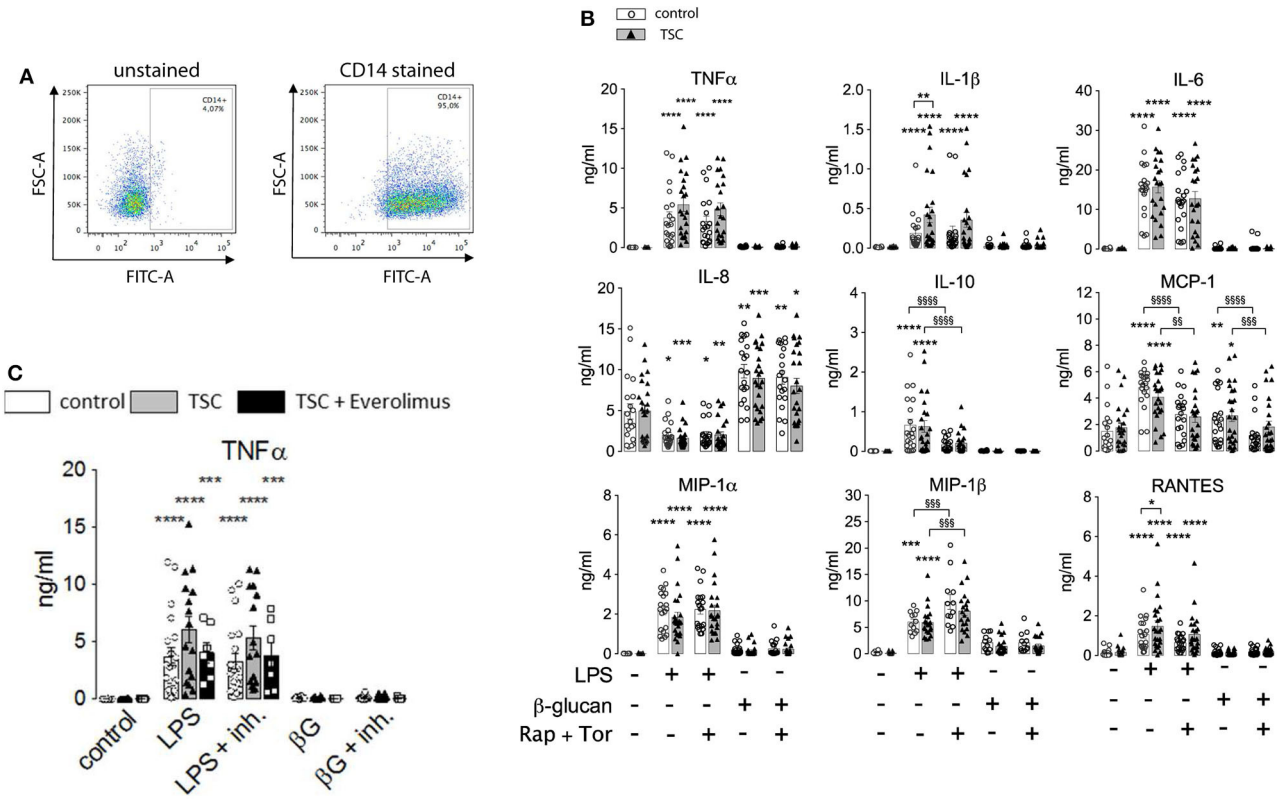

FIGURE 2 | Monocytes from tuberous sclerosis (TSC) patients feature a largely unperturbed cytokine response to lipopolysaccharide (LPS) and ß-glucan. **(A)** Purity of human monocyte preparations from TSC patients as assessed by CD14 surface staining. The identified peripheral blood mononuclear cells were pre-gated for cellularity and doublet exclusion, followed by surface staining with or without anti-CD14 Abs. **(B)** Human peripheral monocytes from TSC and control groups were treated as indicated with a mix of rapamycin (Rap) and Torin1 (Tor) at 30 min prior to stimulation with 10 ng/ml LPS or 3 μg/ml ß-glucan. The cytokine levels in the supernatant were determined by flow cytometry using a multiplex bead array. **(C)** The same data from TNFα panel in **(B)** stratified for +/– everolimus treatment. Different significance symbols were used to mark different inter-group comparisons.

section). Both batches yielded undistinguishable results. A flow cytometric bead array-based assay, which produced better quantifiable results, confirmed the marked difference in the cytokine release proficiency of LPS vs. that of ß-glucan, the latter inducing only a modest secretion of IL-8, MIP-1, and MCP-1 (**Figure 1B**).

To assess the role of mTORC1, we performed side-by-side measurements on control and TSC monocytes (**Figure 2**). The purity of the monocyte preparations routinely exceeded 90%, as assessed by flow cytometry (**Figure 2A**). These experiments evidenced that monocytes from TSC patients were not markedly affected in their cytokine response to LPS (**Figure 2B**). In line with previous findings in mouse monocytes (26), some pro-inflammatory mediators were released even more profusely by the stimulated TSC monocytes, perhaps reflecting a generalized higher protein translation rate as a consequence of hyperactive mTORC1 signaling. In our experiments, this was true for TNFα, IL-1ß, and RANTES, achieving statistical significance for the latter two mediators. Seven out of the 19 TSC patients included in our study received everolimus therapy at the time point of blood drawing. Stratification of the data with regard to everolimus therapy showed that the higher cytokine release resulted in its majority from patients that had not received therapy with the mTORC1 inhibitor, suggesting an association between chronic aberrantly high mTORC1 signaling and enhanced cytokine release (**Figure 2C**). To test if cytokine production was affected by acute mTORC1 inhibition, we administered a combination of two potent mTORC1 inhibitors acting by different mechanisms: the allosteric inhibitor rapamycin and the ATP-competitive drug Torin-1. We used this inhibitor mix because rapamycin reportedly shows a selective inhibition of distinct mTORC1 downstream targets under particular conditions (27). Both inhibitors were administered simultaneously at 30 min prior to the stimulation with PAMPs. As can be seen in **Figure 2B**, mTORC1 inhibition prevented the production of IL-10 and MCP1, whereas the production of MIP-1ß was mildly enhanced in mTORC1-inhibited cells. The levels of all other cytokines were largely unaffected. The elevated production of TNFα, IL-1, or RANTES in TSC monocytes was largely attributable to the patients who were not treated with everolimus (**Figure 2C**;

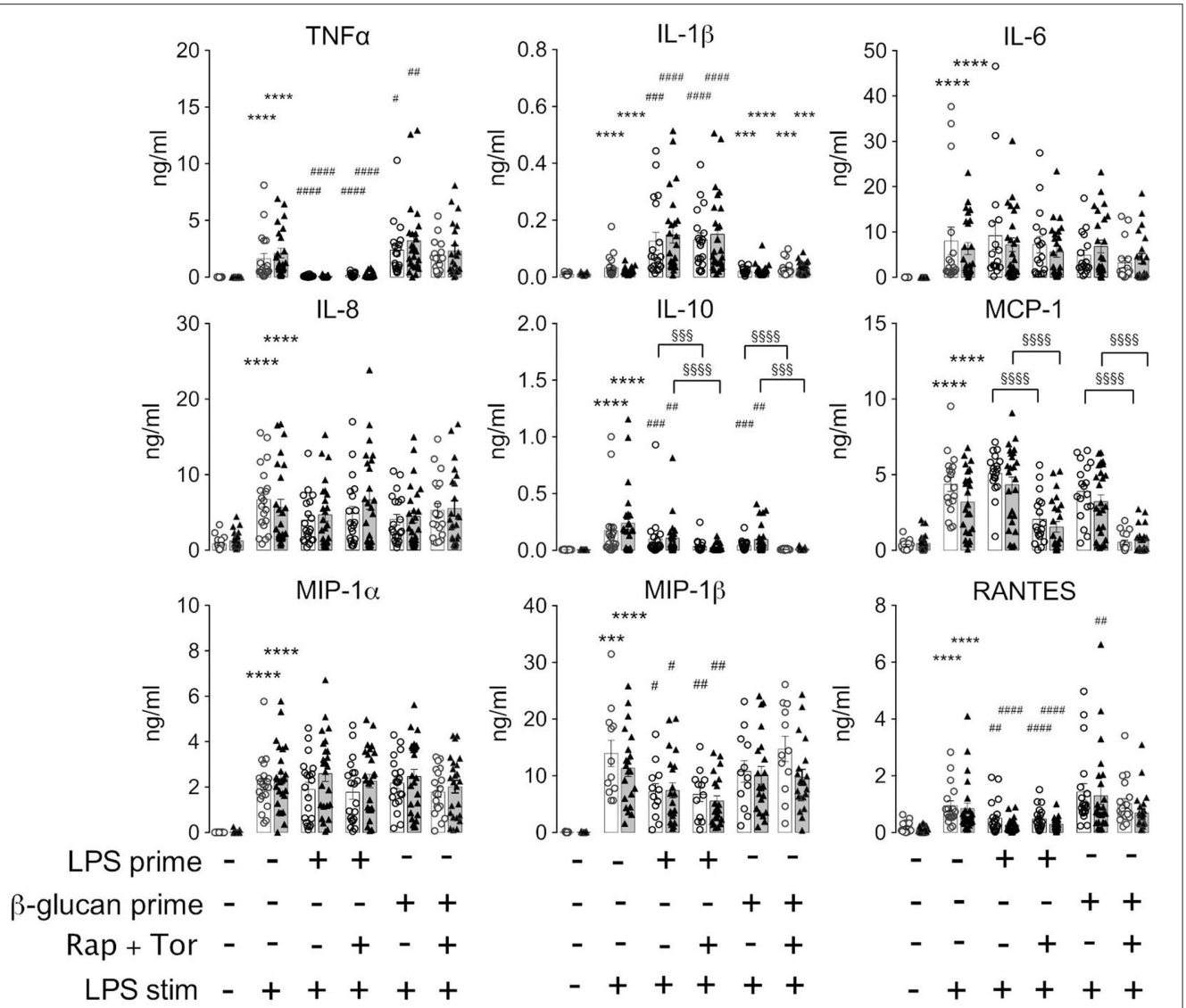

FIGURE 3 | Monocytes from tuberous sclerosis (TSC) patients can be rendered tolerant by endotoxin. Peripheral monocytes from TSC patients (black triangles) or control healthy donors (white circles) were isolated and subjected to a bi-phasic priming/stimulation protocol for induction of endotoxin tolerance. The cells were primed with LPS or ß-glucan for 24 h (prime), followed by stimulation with 10 ng/ml LPS (stim) for 24 h further. The cytokine levels were measured by flow cytometric multiplexed bead arrays as before. Different significance symbols were used to mark different inter-group comparisons.

data not shown). Intriguingly, this elevated cytokine response in TSC cells was not prevented by inhibitor treatment, suggesting that acute mTORC1 inhibition could not revert the effect of chronic mTORC1 upregulation. In summary, the generation of individual cytokines by human monocytes was differentially dependent on mTORC1 but was not significantly compromised by the presence of unleashed mTORC1 activity in TSC.

ET Proceeds Normally in TSC Monocytes

The above findings evidenced that the generation of cytokines was distinctively sensitive to chronic or acute changes in mTORC1 activity, as implemented by the TSC genotype and pharmacological mTORC1 inhibition. We went one step further and assessed whether mTORC1 played a role in the induction of ET. For this purpose, we altered the experimental protocol to include a priming step with LPS or ß-glucan. Whereas, priming with LPS for as short as 1 day is known to induce a state of tolerance in mouse macrophages and human monocytes, ß-glucan induces immune training in these cells (2, 24). At 24 h after the priming step, the cells were challenged with LPS and the cytokine levels were monitored 24 h later *via* flow cytometry on bead arrays. It is important to note that re-stimulation was accompanied by the replacement of the culture medium. This step largely removed all cytokines produced upon the initial LPS/ß-glucan priming step, as ascertained in control experiments

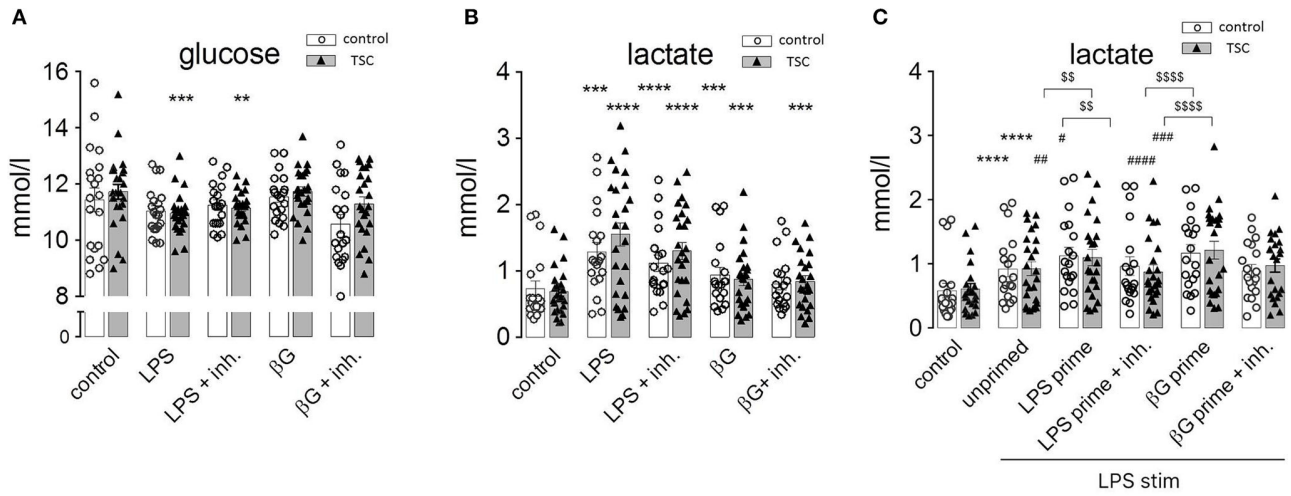

FIGURE 4 | Pathogen-associated molecular pattern stimulation upregulates lactic fermentation, but this metabolic switch does not correlate or associate with endotoxin tolerance (ET). **(A)** Lactate levels in the supernatant of monocyte cultures from control donors and tuberous sclerosis (TSC) patients. The cells were pretreated as indicated with a mix of rapamycin and Torin (Inh) and challenged with lipopolysaccharide or ß-glucan (ßG). **(B)** Glucose levels in the supernatant of the same monocyte samples as in **(A)**. **(C)** Lactic acid production by monocytes from control and TSC patients subjected to the two-step priming/stimulation protocol for analysis of ET. White columns: healthy controls. Gray columns: TSC patients. Different significance symbols were used to mark different inter-group comparisons.

(data not shown), excluding an adulteration of the measured cytokine levels. As shown in **Figure 3**, priming with LPS fully prevented the production of TNFα and partially suppressed that of RANTES, IL-10, and MIP-1ß. By contrast, LPS priming did not reduce the production of other cytokines, including IL-6, IL-8, or MCP-1, and even boosted the release of IL-1. Priming with ß-glucan for 24 h exerted only a little effect on the cytokine levels. Prolonging the priming step of ß-glucan to 5 days neither lead to training effects as those reported previously (24, 28). Importantly, the loss of TSC had no impact on ET induction as priming with LPS induced a largely undistinguishable re-wiring of cytokine production in control and TSC cells. These findings showed that mTORC1 hyperactivation, as present in TSC cells, did not prevent nor affect the molecular processes underlying the induction of ET in human monocytes. In line with a negligible role of mTORC1, the pharmacological inhibition of mTORC1 prior to and throughout the priming period did not also affect ET. Taken together, these data strongly suggested that mTORC1 activity or changes in its activity are not principally involved in the induction of ET in monocytes.

Metabolic Switch Is Not Affected in TSC Monocytes and Does Not Correlate With ET Induction or Cytokine Response

Monocytes exhibit dramatic metabolic rearrangements upon activation/stimulation with inflammatory agents (12, 14, 29). These changes supposedly represent a switch from aerobic mitochondrial respiration to anaerobic, glycolytic metabolism characterized by increased glucose consumption and lactic fermentation. Our own experiments were in line with this scenario as human monocytes exhibited a markedly and significantly enhanced release of lactate upon stimulation with LPS (**Figure 4A**). This was accompanied by higher glucose consumption, attaining a statistical significance for the TSC monocytes (**Figure 4B**). ß-Glucan exerted an analogous but somewhat weaker response than LPS. The TSC monocytes showed a trend toward higher lactate production than the control cells under LPS stimulation, whereas treatment with rapamycin/torin1 did not exert any marked effect on lactate levels. These data were consistent with the occurrence of a switch to lactic fermentation in LPS-stimulated monocytes. The inefficacy of rapamycin/Torin treatment in reverting the switch to aerobic glycolysis indicated that mTORC1 did not play a major role in this process.

In order to understand if this metabolic switch played a role in the induction of ET, we assessed lactate production by tolerant monocytes. As observed in **Figure 4C**, LPS-primed and re-stimulated (hence tolerant) monocytes exhibited an exacerbated lactate generation. Virtually the same effect was observed in ß-glucan-primed and restimulated (hence non-tolerant) monocytes. Thus, priming by LPS or ß-glucan induced an undistinguishable switch to lactic fermentation in tolerant and non-tolerant cells re-stimulated with LPS.

ET Does Not Correlate With mTORC1 Activity and Is Not Mediated by Paracrine Signaling Mediators

The absence of the effects of TSC genotype or pharmacological mTORC1 inhibition on ET parameters prompted the question whether mTORC1 was activated following exposure to PAMPs under these experimental conditions. We took monocytes from control, healthy donors, and measured the phosphorylation of the mTORC1 downstream target S6-protein (S6P) by western blotting as a readout of pathway activation. As shown

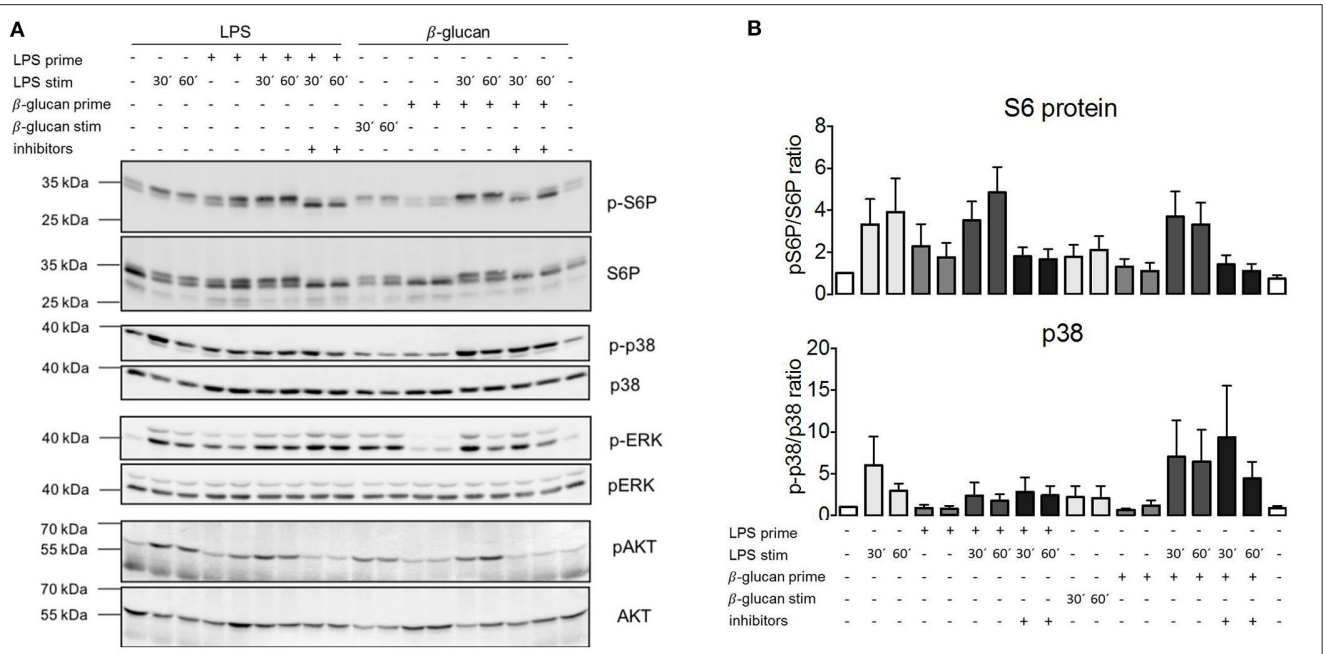

FIGURE 5 | MTORC1 activation is not affected by endotoxin tolerance but lipopolysaccharide (LPS) fails to activate p38α in tolerant monocytes. **(A)** Monocytes from healthy donors were isolated and subjected to the indicated two-step stimulation protocols with LPS and or ß-glucan, including pretreatment with mTORC1 inhibitor mix as indicated. The cell extracts were processed for western blot against the indicated phosphorylated and total protein levels. The molecular size markers are indicated on the left side of the panels. **(B)** Bands for phosphorylated and total p38α and pS6 were quantified by densitometry, and the extent of activation was determined by plotting the ratio of phosphorylated/total protein. The quantification includes all measured samples (S6P: $n = 6$, p38α: $n = 4$) depicted as fold activation of the unstimulated samples. Data are presented as mean ± SEM.

in **Figure 5A**, LPS activated mTORC1 as evidenced by the phosphorylation and concomitant mobility shift of S6P. This phosphorylation largely vanished after 24 h. Importantly, S6P was re-phosphorylated by a second LPS addition in tolerant cells (**Figure 5A**). The same pattern was observed for the phosphorylation/activation of Akt, an upstream activator of mTORC1. We concluded that the mTORC1 pathway was fully responsive to PAMP stimulation in the tolerant monocytes. Interestingly, activation of the parallel pro-inflammatory signaling pathway p38 was suppressed in the tolerized monocytes (**Figure 5A**), showing that ET had a distinct impact on the downstream transmission of the LPS signal to distinct pathways.

These data showed that LPS activates mTORC1 and that mTORC1 activation by endotoxin proceeded normally in the tolerized monocytes. At the same time, mTORC1 activity is necessary for the production of IL-10 (30) (**Figure 2A**), an anti-inflammatory cytokine that has been linked before to the induction of ET (3). Since mTORC1 inhibition did not prevent ET, we reasoned that IL-10 or other paracrine mediators released in a mTORC1-dependent manner were unlikely to mediate the induction of ET in human monocytes. To test this assumption, we collected conditioned supernatant from human monocytes stimulated with LPS and used this medium to prime naïve monocytes prior to stimulation with LPS. As shown in **Figure 6**, LPS-elicited TNFα production was not compromised by the previous administration of a conditioned medium from tolerant monocytes, indicating that the paracrine factors released during priming are not crucially involved in the induction of ET.

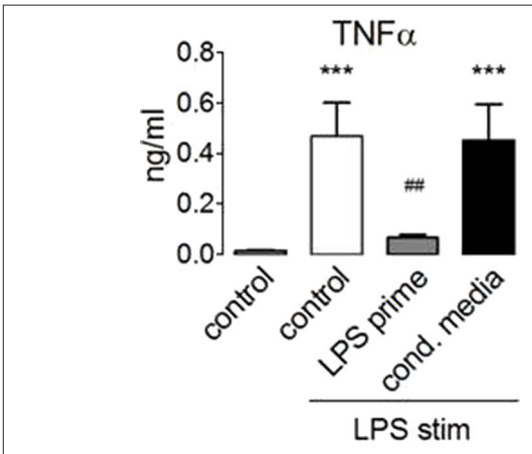

FIGURE 6 | Paracrine factors do not mediate endotoxin tolerance induction. Monocytes from healthy donors were primed for 24 h with 100 ng/ml LPS or with conditioned medium obtained from monocytes 24 h after stimulation with 100 ng/ml LPS. The cells were re-stimulated with lipopolysaccharide, and TNFα production was assessed by ELISA. Different significance symbols were used to mark different inter-group comparisons.

DISCUSSION

mTORC1 coordinates resource availability and hormonal status with intracellular energy and nutrient expenditure and, as such, is predicted to be involved in processes involving re-wiring of metabolic pathways. Our experiments document an increase in lactic fermentation in human monocytes challenged with LPS or ß-glucan, which is in line with previous studies that reported Warburg-like metabolic reprogramming in activated macrophages (31). However, our data argue against a dominant role of mTORC1 in this process as the increase in lactic acid production was indistinguishable in control and TSC monocytes or in the presence of mTORC1 inhibition. While we cannot exclude that mTORC1 activity may be relevant for metabolic changes in monocytes under particular circumstances, e.g., in a background of distinct energy or nutrient availability, our findings illustrate that the PAMP-induced metabolic switch proceeds in the absence of a functional mTORC1 module. Similarly, we did not observe prominent effects of the TSC genotype, which causes high mTORC1 activity, on the cytokine response of TSC patient monocytes to LPS or ß-glucan besides a trend to mild overproduction of certain cytokines such as TNFα. Indeed the higher cytokine production in cells from TSC patients was blunted in those that had received everolimus treatment, pointing to a causal link between mTORC1 and the secretory activity of human monocytes, which is consistent with previous reports (32). Inversely, mTORC1 activity was critically required for the production of selected cytokines (IL-10, MIP1ß), the secretion of which dropped in a background of mTORC1 inhibition. Together with similar previous findings (30), this observation suggested that mTORC1 is differentially involved in the generation/secretion of distinct inflammatory cytokines. The reasons for this differential repercussion (considering that mTORC1 acts as a gatekeeper of global protein translation) are intriguing and could reflect a mechanism for adaptation of inflammatory cytokine release to the reigning nutrient/energy status. In this regard, we observed that monocytes from TSC patients showed enhanced LPS-induced IL-1ß production (see **Figure 2**). Since the activation of the inflammasome requires an initial priming step to stimulate the synthesis of caspase 1 and IL-1ß precursor proteins, we speculate that the intrinsically high mTORC1 activity of TSC cells likely boosts this priming reaction that precedes IL-1ß production and secretion. Interestingly, while we observed an inhibitory effect of chronic everolimus therapy on the secretory activity of TSC monocytes, e.g., for IL-1ß or TNFα (**Figure 2B**), acute mTORC1 inhibition did not cause the same effect. This evidenced that not every consequence of aberrantly high mTORC1 activity in TSC cells could be reversed by the acute inhibition of mTORC1, an observation that is not unprecedented (33). In this context, it is interesting to consider mTOR-independent effects of TSC loss in human monocytes. In particular, TSC1 acts as a co-chaperone of HSP90 (22, 34), and HSP90, in turn, reportedly modulates PAMP/TLR signaling at multiple levels, including the stabilization of functional TLR receptor complexes at the plasma membrane of human monocytes/macrophages (35). Taking all these findings together, we concluded that the effects of mTORC1 on monocyte cytokine secretion are multifaceted and impact differentially on individual cytokines. Moreover, the effects are most likely not mediated by mTORC1-dependent changes in cellular metabolism as TSC loss or mTOR inhibition had little impact on metabolic reprogramming in our experiments.

The monocytes exhibit a dramatic readjustment of their secretory and functional status upon entering a state of immune tolerance (3). Our data highlight that the hyperactivation of mTORC1 in TSC or its pharmacological inhibition did not preclude the induction of endotoxin tolerance in human monocytes, monitored here by the reduced or the altered endotoxin-induced production of inflammatory cytokines. These findings indicate that changes in mTORC1 activity are not involved in the induction of ET and have far-reaching implications. For example, it would argue against a role for endocrine loops involving cytokines whose secretion depends on mTORC1, at least in settings of *in vitro* ET induction. This includes, e.g., the anti-inflammatory cytokine IL-10, whose secretion is strictly contingent on mTORC1 (**Figure 2**). Our experiments using conditioned medium from primed human monocytes argue in the same direction as they excluded a contribution of extracellular factors in the induction of ET. Taken together, these considerations suggest that the mechanisms responsible for ET involve intracellular re-wiring processes that are largely independent of mTORC1. Since all presented data argue also against a role of metabolic reprogramming, the straightforward conclusion is that changes in the signaling machinery and/or genetic re-programming of the primed monocyte underlie the induction for ET. In this regard, we document that tolerant monocytes become unresponsive at the level of the p38 pathway, while other pathways (mTOR, Erk, and Akt) remain sensitive to LPS challenge. These findings suggest that uncoupling of p38 from TLR signaling could be one important feature of ET. Irrespective of the mechanism, this finding is consistent with the notion that tolerance leads to a qualitative change in LPS signaling, e.g., perhaps to a rearrangement of the proximal TLR4 signaling network in the tolerant monocyte. It will be intriguing to evaluate the functional consequences of defective p38 signaling in the stimulated monocyte and whether this can explain some of the features of tolerized cells.

In our experiments, we did not observe a significant training effect of the PAMP ß-glucan despite testing various sources of ß-glucan and different protocols. This confirms previous findings (23, 36) but contrasts with reports documenting an enhanced cytokine production in ß-glucan-primed monocytes (2, 24). We suspect that differences in the experimental protocols and normalization procedures underlie these different outcomes. Irrespective of these considerations, the results of ß-glucan stimulation shown herein are nevertheless intriguing as ß-glucan induces a comparably strong switch to lactic fermentation as LPS, in line with previous reports (12, 29). Moreover, ß-glucan stimulates the mTORC1 pathway as monitored at the level of S6-protein phosphorylation (**Figure 5**), to the same extent as LPS, yet ß-glucan does not induce ET, proving that stimulation of mTORC1 and metabolic re-wiring are not sufficient for the induction of ET. Thus, our findings provide strong evidence that

mTORC1 activity and a metabolic switch to lactic fermentation are neither necessary nor sufficient for the induction of ET.

Taking this line of thinking one step further, it must be concluded that polarization of monocytes/macrophages [a strictly mTORC1-dependent process (26)] and tolerance induction (mTORC1-independent, as shown herein) are largely separate and independent processes. Indeed the relation between these two processes has been difficult to judge in the past because training or adaptation studies involved mostly experimental cytokine profiling, while polarization mostly relied on the assessment of marker signatures. Our data illustrate that ET does not depend on mTORC1 activity, which sets the adaptive process of ET clearly apart from the mTORC1-dependent program of monocyte/macrophage polarization.

ET represents a physiological adaptation process for shaping and adapting the inflammatory response to individual infection scenarios. However, unleashed or uncontrolled immune tolerance is thought to lie at the heart of critical conditions such as sepsis (5, 6). Sepsis is often accompanied and linked to metabolic comorbidities (insulin resistance, diabetes, obesity, and liver dysfunction) (5, 37), all of which do affect nutrient levels and nutrient/hormonal signaling in the critically ill patient. A better understanding of the role of mTORC1-dependent signaling in this context could help in devising new strategies of immune modulation in sepsis and other clinical settings. For another example, in solid organ transplantations, patients often receive mTORC1 inhibitors (everolimus and tacrolimus) as immunosuppressant. Our present findings, which show very limited consequences of TSC loss and/or mTORC1 inhibition on monocyte function and/or plasticity, suggest that immune suppression in these cases is most likely to result from a strong inhibition of adaptive immunity. Given the distinct contributions of innate vs. adaptive immune entities to the course of different syndromes and pathologies, it is tempting to consider mTORC1 inhibitors as a means to selectively modulate the immune response in different clinical settings in an individualized fashion.

In conclusion, while mTORC1 is a well-established player in the primary response of numerous immune cells [e.g., in T-cells (38) or monocytes, see **Figure 1**], our findings argue against a prominent contribution of mTORC1 to processes of immune cell adaptation, at least in monocytes. In line with this concept, TSC is not associated with a defective response to infection as judged by the absence of an increased incidence or severity of infectious episodes in TSC patients. Accordingly, we did not observe any conspicuous, unusually high incidence of infections or immune abnormalities in our TSC patient cohort, yet the clear impact of mTORC1 on monocyte polarization and the monocyte's secretory landscape [present data and (26)], along with its well-established function in T-cell activation and clonal expansion, underscore an important role of mTORC1 signaling in immune cell function and warrant further investigations to understand the role of metabolic mTORC1 signaling in the host response to infection.

DATA AVAILABILITY STATEMENT

The datasets generated for this study are available on request to the corresponding author.

ETHICS STATEMENT

The studies involving human participants were reviewed and approved by Local ethics committee at the University Hospital Jena (Ethik-Kommission der Friedrich-Schiller Universität Jena an der Medizinischen Fakultät). Written informed consent to participate in this study was provided by the participants' legal guardian/next of kin.

AUTHOR CONTRIBUTIONS

KL designed and performed most of the experiments. RH organized and performed patient and healthy control donor recruitment and blood draw. RH and IR wrote ethics application and study protocol. IR designed the study and experiments and wrote the manuscript. All authors corrected and approved the manuscript.

FUNDING

This work was supported by Grant No. DFG-RTG1715 from the Deutsche Forschungsgemeinschaft to KL and IR.

ACKNOWLEDGMENTS

We thank all the patients and their relatives and the healthy donors for participating in this study. We thank the Tuberöse Sklerose Deutschland e. V. (www.tsdev.org) for supporting the recruitment of patients. We thank David Williams and Mihai Netea for the generous provision of ß-glucan. We acknowledge the experimental and technical help by Anne Kresinsky, Fabienne Haas, Elisa Jentho, and Ronny Hänold, all from Jena, Germany. We are thankful to EGIS members (www.EGIS-online.eu) for the helpful discussions.

REFERENCES

1. Mulder WJM, Ochando J, Joosten LAB, Fayad ZA, Netea MG. Therapeutic targeting of trained immunity. *Nat Rev Drug Discov*. (2019) 18:553–66. doi: 10.1038/s41573-019-0025-4
2. Ifrim DC, Quintin J, Joosten LA, Jacobs C, Jansen T, Jacobs L, et al. Trained immunity or tolerance: opposing functional programs induced in human monocytes after engagement of various pattern recognition receptors. *Clin Vaccine Immunol.* (2014) 21:534–45. doi: 10.1128/CVI.00688-13
3. Biswas SK, Lopez-Collazo E. Endotoxin tolerance: new mechanisms, molecules and clinical significance. *Trends Immunol.* (2009) 30:475–87. doi: 10.1016/j.it.2009.07.009
4. Seeley JJ, Ghosh S. Molecular mechanisms of innate memory and tolerance to LPS. *J Leukoc Biol.* (2017) 101:107–19. doi: 10.1189/jlb.3MR0316-118RR

5. Rubio I, Osuchowski MF, Shankar-Hari M, Skirecki T, Winkler MS, Lachmann G, et al. Current gaps in sepsis immunology: new opportunities for translational research. *Lancet Infect Dis.* (2019) 19:e422–36. doi: 10.1016/S1473-3099(19)30567-5
6. Seeley JJ, Baker RG, Mohamed G, Bruns T, Hayden MS, Deshmukh SD, et al. Induction of innate immune memory via microRNA targeting of chromatin remodelling factors. *Nature.* (2018) 559:114–9. doi: 10.1038/s41586-018-0253-5
7. Liu D, Cao S, Zhou Y, Xiong Y. Recent advances in endotoxin tolerance. *J Cell Biochem.* (2019) 120:56–70. doi: 10.1002/jcb.27547
8. Escoll P, del Fresno C, Garcia L, Valles G, Lendinez MJ, Arnalich F, et al. Rapid up-regulation of IRAK-M expression following a second endotoxin challenge in human monocytes and in monocytes isolated from septic patients. *Biochem Biophys Res Commun.* (2003) 311:465–72. doi: 10.1016/j.bbrc.2003.10.019
9. Lyroni K, Patsalos A, Daskalaki MG, Doxaki C, Soennichsen B, Helms M, et al. Epigenetic and transcriptional regulation of IRAK-M expression in macrophages. *J Immunol.* (2017) 198:1297–307. doi: 10.4049/jimmunol.1600009
10. Freise N, Burghard A, Ortkras T, Daber N, Imam Chasan A, Jauch SL, et al. Signaling mechanisms inducing hyporesponsiveness of phagocytes during systemic inflammation. *Blood.* (2019) 134:134–46. doi: 10.1182/blood.2019000320
11. Dolch A, Kunz S, Dorn B, Alessandrini F, Muller W, Jack RS, et al. IL-10 signaling in dendritic cells is required for tolerance induction in a murine model of allergic airway inflammation. *Eur J Immunol.* (2019) 49:302–12. doi: 10.1002/eji.201847883
12. Cheng SC, Quintin J, Cramer RA, Shepardson KM, Saeed S, Kumar V, et al. mTOR- and HIF-1alpha-mediated aerobic glycolysis as metabolic basis for trained immunity. *Science.* (2014) 345:1250684. doi: 10.1126/science.1250684
13. Arts RJ, Joosten LA, Netea MG. Immunometabolic circuits in trained immunity. *Semin Immunol.* (2016) 28:425–30. doi: 10.1016/j.smim.2016.09.002
14. Oren R, Farnham AE, Saito K, Milofsky E, Karnovsky ML. Metabolic patterns in three types of phagocytizing cells. *J Cell Biol.* (1963) 17:487–501. doi: 10.1083/jcb.17.3.487
15. Rodriguez-Prados JC, Traves PG, Cuenca J, Rico D, Aragones J, Martin-Sanz P, et al. Substrate fate in activated macrophages: a comparison between innate, classic, and alternative activation. *J Immunol.* (2010) 185:605–14. doi: 10.4049/jimmunol.0901698
16. Saxton RA, Sabatini DM. mTOR signaling in growth, metabolism, and disease. *Cell.* (2017) 168:960–76. doi: 10.1016/j.cell.2017.02.004
17. Huang J, Manning BD. The TSC1-TSC2 complex: a molecular switchboard controlling cell growth. *Biochem J.* (2008) 412:179–90. doi: 10.1042/BJ20080281
18. Garami A, Zwartkruis FJ, Nobukuni T, Joaquin M, Roccio M, Stocker H, et al. Insulin activation of Rheb, a mediator of mTOR/S6K/4E-BP signaling, is inhibited by TSC1 and 2. *Mol Cell.* (2003) 11:1457–66. doi: 10.1016/S1097-2765(03)00220-X
19. Abraham RT, Wiederrecht GJ. Immunopharmacology of rapamycin. *Annu Rev Immunol.* (1996) 14:483–510. doi: 10.1146/annurev.immunol.14.1.483
20. Short MP, Richardson EP Jr, Haines JL, Kwiatkowski DJ. Clinical, neuropathological and genetic aspects of the tuberous sclerosis complex. *Brain Pathol.* (1995) 5:173–9. doi: 10.1111/j.1750-3639.1995.tb00591.x
21. van Eeghen AM, Black ME, Pulsifer MB, Kwiatkowski DJ, Thiele EA. Genotype and cognitive phenotype of patients with tuberous sclerosis complex. *Eur J Hum Genet.* (2012) 20:510–5. doi: 10.1038/ejhg.2011.241
22. Woodford MR, Sager RA, Marris E, Dunn DM, Blanden AR, Murphy RL, et al. Tumor suppressor Tsc1 is a new Hsp90 co-chaperone that facilitates folding of kinase and non-kinase clients. *EMBO J.* (2017) 36:3650–65. doi: 10.15252/embj.201796700
23. Leonhardt J, GroSse S, Marx C, Siwczak F, Stengel S, Bruns T, et al. Candida albicans beta-glucan differentiates human monocytes into a specific subset of macrophages. *Front Immunol.* (2018) 9:2818. doi: 10.3389/fimmu.2018.02818
24. Ifrim DC, Joosten LAB, Kullberg BJ, Jacobs L, Jansen T, Williams DL, et al. Candida albicans primes TLR cytokine responses through a dectin-1/Raf-1-mediated pathway. *J Immunol.* (2013) 190:4129–35. doi: 10.4049/jimmunol.1202611
25. Baillie JK, Arner E, Daub C, De Hoon M, Itoh M, Kawaji H, et al. Analysis of the human monocyte-derived macrophage transcriptome and response to lipopolysaccharide provides new insights into genetic aetiology of inflammatory bowel disease. *PLoS Genet.* (2017) 13:e1006641. doi: 10.1371/journal.pgen.1006641
26. Byles V, Covarrubias AJ, Ben-Sahra I, Lamming DW, Sabatini DM, Manning BD, et al. The TSC-mTOR pathway regulates macrophage polarization. *Nat Commun.* (2013) 4:2834. doi: 10.1038/ncomms3834
27. Choo AY, Yoon SO, Kim SG, Roux PP, Blenis J. Rapamycin differentially inhibits S6Ks and 4E-BP1 to mediate cell-type-specific repression of mRNA translation. *Proc Natl Acad Sci USA.* (2008) 105:17414–9. doi: 10.1073/pnas.0809136105
28. Bekkering S, Blok BA, Joosten LA, Riksen NP, van Crevel R, Netea MG. *In vitro* experimental model of trained innate immunity in human primary monocytes. *Clin Vaccine Immunol.* (2016) 23:926–33. doi: 10.1128/CVI.00349-16
29. Saeed S, Quintin J, Kerstens HH, Rao NA, Aghajanirefah A, Matarese F, et al. Epigenetic programming of monocyte-to-macrophage differentiation and trained innate immunity. *Science.* (2014) 345:1251086. doi: 10.1126/science.1251086
30. Weichhart T, Costantino G, Poglitsch M, Rosner M, Zeyda M, Stuhlmeier KM, et al. The TSC-mTOR signaling pathway regulates the innate inflammatory response. *Immunity.* (2008) 29:565–77. doi: 10.1016/j.immuni.2008.08.012
31. Kelly B, O'Neill LA. Metabolic reprogramming in macrophages and dendritic cells in innate immunity. *Cell Res.* (2015) 25:771–84. doi: 10.1038/cr.2015.68
32. Meyer CU, Kurlemann G, Sauter M, Wiemer-Kruel A, Hahn A, Doganci A, et al. Inflammatory characteristics of monocytes from pediatric patients with tuberous sclerosis. *Neuropediatrics.* (2015) 46:335–43. doi: 10.1055/s-0035-1562925
33. Pai GM, Zielinski A, Koalick D, Ludwig K, Wang ZQ, Borgmann K, et al. TSC loss distorts DNA replication programme and sensitises cells to genotoxic stress. *Oncotarget.* (2016) 7:85365–80. doi: 10.18632/oncotarget.13378
34. Sager RA, Woodford MR, Mollapour M. The mTOR independent function of Tsc1 and FNIPs. *Trends Biochem Sci.* (2018) 43:935–7. doi: 10.1016/j.tibs.2018.09.018
35. Bzowska M, Nogiec A, Bania K, Zygmunt M, Zarebski M, Dobrucki J, et al. Involvement of cell surface 90 kDa heat shock protein (HSP90) in pattern recognition by human monocyte-derived macrophages. *J Leukoc Biol.* (2017) 102:763–74. doi: 10.1189/jlb.2MA0117-019R
36. Garcia-Valtanen P, Guzman-Genuino RM, Williams DL, Hayball JD, Diener KR. Evaluation of trained immunity by beta-1, 3 (d)-glucan on murine monocytes *in vitro* and duration of response *in vivo*. *Immunol Cell Biol.* (2017) 95:601–10. doi: 10.1038/icb.2017.13
37. Bermejo-Martin JF, Martin-Fernandez M, Lopez-Mestanza C, Duque P, Almansa R. Shared features of endothelial dysfunction between sepsis and its preceding risk factors (aging and chronic disease). *J Clin Med.* (2018) 7:400. doi: 10.3390/jcm7110400
38. Zeng H, Chi H. mTOR and lymphocyte metabolism. *Curr Opin Immunol.* (2013) 25:347–55. doi: 10.1016/j.coi.2013.05.002

Conflict of Interest: The authors declare that the research was conducted in the absence of any commercial or financial relationships that could be construed as a potential conflict of interest.

frontiers in Immunology

ORIGINAL RESEARCH
published: 12 August 2020
doi: 10.3389/fimmu.2020.01946

CD4 T Follicular Helper Cells Prevent Depletion of Follicular B Cells in Response to Cecal Ligation and Puncture

Matthew D. Taylor[1,2,3†], Mariana R. Brewer[1,2,3], Ana Nedeljkovic-Kurepa[3], Yihe Yang[4], Kalpana S. Reddy[4], Mabel N. Abraham[1,2,3], Betsy J. Barnes[5] and Clifford S. Deutschman[1,2,3]*

[1] The Division of Critical Care Medicine, Cohen Children's Medical Center, Northwell Health, New Hyde Park, NY, United States, [2] Department of Pediatrics, Zucker School of Medicine at Hofstra/Northwell, Hempstead, NY, United States, [3] Sepsis Research Lab, The Feinstein Institutes for Medical Research, Manhasset, NY, United States, [4] The Department of Pathology, Zucker School of Medicine at Hofstra/Northwell, Hempstead, NY, United States, [5] Institute of Molecular Medicine, Feinstein Institutes for Medical Research, Manhasset, NY, United States

OPEN ACCESS

Edited by:
Vladimir Badovinac, The University of Iowa, United States

Reviewed by:
Sergio Iván Valdés-Ferrer, Instituto Nacional de Ciencias Médicas y Nutrición Salvador Zubirán (INCMNSZ), Mexico
Cassiano Felippe Gonçalves-de-Albuquerque, Rio de Janeiro State Federal University, Brazil

***Correspondence:**
Matthew D. Taylor
mtaylor15@northwell.edu

†ORCID:
Matthew D. Taylor
orcid.org/0000-0003-2643-3050

Specialty section:
This article was submitted to Inflammation, a section of the journal Frontiers in Immunology

Received: *06 May 2020*
Accepted: *20 July 2020*
Published: *12 August 2020*

Citation:
Taylor MD, Brewer MR, Nedeljkovic-Kurepa A, Yang Y, Reddy KS, Abraham MN, Barnes BJ and Deutschman CS (2020) CD4 T Follicular Helper Cells Prevent Depletion of Follicular B Cells in Response to Cecal Ligation and Puncture. Front. Immunol. 11:1946. doi: 10.3389/fimmu.2020.01946

Recent studies have demonstrated that induction of a diverse repertoire of memory T cells ("immune education") affects responses to murine cecal ligation and puncture (CLP), the most widely – used animal model of sepsis. Among the documented effects of immune education on CLP are changes in T cell, macrophage and neutrophil activity, more pronounced organ dysfunction and reduced survival. Little is known, however, about the effects of CLP on B cell responses, and how these responses might be altered by immune education. Importantly, effective B cell responses are modulated by IL21 produced by $CD4^+/CXCR5^+/PD1^+$ T follicular helper (Tfh) cells. We examined the B cell population in control and immune educated mice 24 h and 60 days after CLP. Education alone increased Tfh cells. Twenty-four hours after CLP, Tfh cells were depleted. However, this reduction was less pronounced in immune educated mice than in controls and the percentage of CD4 T cells expressing a Tfh phenotype increased in the animals. CLP did not alter splenic architecture and decreased numbers of follicular, marginal, and germinal center B cells. CLP induced changes were not, however, noted following CLP in immune educated mice. At 60 days post – CLP, numbers of follicular, germinal center and marginal zone B cells were increased; this increase was more pronounced in immune educated mice. Finally, while CLP reduced the induction of antigen specific B cells in controls, this response was maintained following CLP in immune educated mice. Our data suggest that preexisting Tfh assists in rescuing the B cell response to CLP.

Keywords: cecal ligation and puncture, sepsis, long-term effects, B cells, T follicular helper cells, CD4 T cells, T cell memory, adaptive immunity

INTRODUCTION

In contrast to other aspects of the immune system, study of the B cell response to sepsis has been limited. Previous studies have shown little beyond a progressive depletion of B cells over time (1) while more recent work has demonstrated that mortality from sepsis is associated with impaired B-cell maturation (2). Sepsis-induced depression of the adaptive immune response has

been recognized for many years. However, a lack of data regarding the early B cell response represents an important gap in our understanding of this deadly disorder.

Investigation into the pathobiological underpinnings of sepsis have long relied on the use of animal models, most commonly cecal ligation and pucture (CLP) in mice and rats (3, 4). However, the use of this and other models of inflammatory disorders has been questioned based on a lack of correlation between genetic responses in mice and humans (5, 6). More recent studies on laboratory mice have identified immune deficiencies that may impact on their use as models of human disease. In contrast to patients and to pet store or "mice in the wild," laboratory mice lack a memory T cell compartment. This deficiency likely reflects limited exposure to antigenic stimulation in the pathogen-free facilities where lab mice are reared and maintained (7, 8). Several approaches to address this concern have been developed. For example, Huggins, et al. have used co-housing of pathogen free mice with "pet store" mice to increase the number of $TLR2^+$ and $TLR4^+$ phagocytes prior to challenge with Listeria monocytogenes (9) while Sjaastad et al., immunized mice with an MHC-II-restricted peptide following CLP to examine T cell-dependent B cell activation following (10). Along the same lines, we have addressed the contribution of preexisting T cell memory in the mice by inducing widespread T cell memory via administration of an anti-CD3ε activating (11). This procedure, termed "immune education," led to widespread increase in the numbers of CD4 and CD8 memory T cells. Additional experiments indicate that memory T cell expansion altered the response to CLP by enhancing innate immune responses, increasing organ dysfunction, and reducing survival (Taylor et al., unpublished data). In the experiments described here we detail the effects of immune education on B cell responses following CLP.

MATERIALS AND METHODS

Mice

C57Bl/6J male mice were obtained from the Jackson Laboratory and maintained in the animal facility at the Feinstein Institute for Medical Research. All animal studies were approved by the Institutional Animal Care and Use Committee and adhered to National Institutes of Health and Animal Research: Reporting of *in vivo* Experiments (ARRIVE) guidelines.

In vivo Immunization

A total of 50 μg of Ultra-LEAF Anti-mouse CD3ε Antibody (145-2C11, BioLegend, San Diego, CA, United States) and Ultra-LEAF isotype Armenian Hamster IgG control (HTK888, BioLegend) were administered to 11 week old mice through a retro-orbital venous sinus injection. Mice were then rested for 35 days to allow for T cell memory development and to ensure that no acute response remained. Details of the initial response to inoculation and of the T cell phenotype at 35 days following have been published separately (11). Briefly, anti-CD3ε treatment induces acute CD4 and CD8 T cell activation. The acute response resolves by day 5 following treatment. Initial inoculation causes an acute expansion of neutrophils, which resolves by 35 days post-treatment. Further, by 35 days following treatment, no acute effector CD4 or CD8 T cells remain, and there is an expansion of the CD4 central and effector memory T cell population and the effector memory CD8 T cell population in the spleen, liver, and lungs. The innate immune system is not altered at 35 days following anti-CD3ε treatment in unchallenged mice.

For antigen specific response experiments, 4-hydroxy-3-nitrophenylacetic acid (NP, 5 μg, Sigma Aldrich, St. Louis, MO, United States) was dissolved in PBS and injected into the peritoneum at the end of CLP surgery or into unoperated (T_0) mice at the same time.

Cecal Ligation and Puncture Procedure

Cecal ligation and puncture was performed on 16 week old mice under isoflurane anesthesia as previously described (12). Briefly, following exposure, the cecum was single ligated approximately 1cm from the tip and two 22-guage needle punctures performed in series. One millimeter of fecal content was expressed from the punctures. The incision was closed in layers and the mice were resuscitated with 50 mL/kg 0.9% NaCl. No antibiotics were given. Resuscitation was repeated at 24 and 48 h post-CLP/NP injection. Mice were euthanized at given time points after CLP with pentobarbital. The effects of organ dysfunction in this model parallel those noted in the Vienna Consensus Conference on Animal Models of Sepsis (4).

Historically, CLP as detailed in this work was associated with 50% mortality at 24 h. Further, when mice were examined with a clinical scoring system developed for CLP, educated mice appeared sicker than control mice (**Supplementary Figure S1**) (13).

Leukocyte Isolation

Spleens were obtained from euthanized mice and immediately weighed. Sections were taken for hematoxylin and eosin stain. The remaining splenic tissue was homogenization and filtered at 70 μm. Red blood cells were lysed and cells counts were obtained using a Countess II Automated Cell Counter (Thermo Fisher Scientific, Waltham, MA, United States).

Flow Cytometric Analysis

Immediately after suspension, cells were stained for flow cytometric analysis with LIVE/DEAD fixable viability dye (Life Technologies, Carlsbad, CA, United States) and the following antibodies: CD90.2, CD44, CD8a, CD4, CD62L, CD11a, CXCR5, PD1, CD69, B220, CD19, CD23, CD21/35, GL7, IgM, IgD, CD138, and CD93. NP-PE (Biosearch Technologies, Teddington, Middlesex, United Kingdom) was utilized to detect NP-specific cells. Full antibody details are available in **Supplementary Table S1**. All flow cytometric analysis was performed on a BD LSR Fortessa 16-color cell analyzer and analyzed using FlowJo software version 10 (BD Biosciences, San Jose, CA, United States). Gating Strategy for T cells is shown in **Supplementary Figure S2** and for B cells is shown in **Supplementary Figure S3**.

Cytokine Production Assays

To assess cytokine production in T cells, single cell suspensions were treated with anti-CD3 (5 μg/ml, Biolegend) and anti-CD28 (1.7 μg/ml, Biolegend) for 5 h in the presence of Brefeldin A (2 μg/ml, BD Biosciences, San Jose, CA, United States). An unstimulated control was analyzed alongside stimulation experiments to assess for background production (14).

Statistical Analysis

Animal data were analyzed using Student's two-tailed T test or using two-tailed analysis of variance with Dunnett's correction where appropriate [Prism 7.0; GraphPad or SAS Studio University Edition (SAS)].

RESULTS

CLP Differentially Depletes Splenic B Cell Subsets and Memory T Follicular Helper Cells

Previous studies demonstrated that CLP depleted B cells via apoptosis (1, 15). The effects of CLP on specific B cell subsets, however, is unknown. Therefore, we examined splenic B cells obtained at baseline (T_0) and at 24, 48, and 72 h post-CLP. Compared to unoperated (T_0) controls, total splenic B cell numbers were significantly lower at 48 and 72 h post-CLP (**Figure 1A**). This difference was noted in both mature ($CD93^-$, **Figure 1B**, left) and immature ($CD93^+$, **Figure 1B**, right) B cells. Because the majority of B cells in the spleen were mature, these cells made the largest contribution to the reduction in total B cells.

Mature B cells can be divided into either follicular (FO, $IgM^{lo}/CD21/35^{lo}$) or marginal zone (MZ, $IgM^{hi}/CD21/35^{hi}$) B cells. Germinal center (FO $GL7^+$) B cells are a subset of FO B cells that generate germinal centers and initiate mature antibody responses. Numbers of splenic FO, MZ and germinal center B cells were lower than T_0 at 24, 48, and 72 h post-CLP (**Figure 1C**). FO B cells are further categorized as FO I B cells, which are resistant to depletion during infection or FO II B cells, which that transit to the spleen following B cell depletion to replenish both MZ and FO B cells. This decrease equally affected both FO I B cells that are more resistant to depletion during infection and FO II B cells (**Supplementary Figure S4**) (16, 17).

At 24, 48, and 72 h post-CLP, T1 (early emigrant) immature splenic B cells (that normally mature to form FO and MZ B cells) were depleted (**Figure 1D**). Numbers of splenic T2 and T3 immature B cells, which develop from T1 B cells during maturation, were not affected by CLP (data not shown) (18).

At 72 h post-CLP the number of plasma cells (mature B cells that can make functional antibody) was significantly increased; changes were not noted at earlier time points (**Figure 1E**).

T follicular helper cells (Tfh, $CD90^+/CD4^+/PD1^+/CXCR5^+$) interact with FO B cells to promote an effective B cell response, germinal center formation, and antibody production. At 24, 48, and 72 h following CLP the number of splenic CD4 Tfh was lower than at T_0 (**Figure 1F**).

Immune Education Attenuates the CLP-Induced Decrease in Memory Tfh Cells

We next examined the effects of immune education (induction of a diverse memory T cell repertoire using an anti-CD3ε activating antibody, as previously described) (11) on the Tfh and B cell responses to CLP. Relative to controls, immune education significantly increased the number (**Figure 2A**) and percentage (**Figure 2B**) of CD4 T cells expressing the Tfh phenotype. In both control and immune educated mice, CLP decreased the number of CD4 Tfh cells/spleen and the percentage of CD4 cells expressing the Tfh phenotypes. The CLP-induced decrease in the number of Tfh cell was significantly greater in educated than in control mice (0.9×10^6 vs. 0.5×10^6 cells/spleen, **Figure 2A**) but the percentage change in both groups was similar (approximately 7%, **Figure 2B**) and CLP did not induce a different change in Tfh in educated or control mice. Thus, both before and at 24 h post-CLP, Tfh cells represented a significantly greater proportion of CD4 T cells in educated mice than in controls.

Interleukin-21 (IL21) produced by Tfh cells interacts with FO B cells to promote differentiation and germinal center formation. In both educated and control baseline mice, no IL21 was detected following *ex vivo* T cell receptor (TCR; CD3/CD28) stimulation of Tfh cells. Similarly, TCR stimulation of Tfh cells isolated from control mice 24 h post-CLP did not elicit IL21 production (**Figure 2C**). In contrast, TCR-stimulation induced Tfh cells isolated from immune educated mice 24 h post-CLP to produce IL21 (**Figure 2C**) – that is, IL21 production was noted in approximately 2% of Tfh cells (**Figure 2D**). These Tfh cells were predominantly $CD44^+/CD11a^+/CD62L^-$, consistent with a memory effector phenotype (**Figure 2E**).

Immune Education Alters CLP-Induced Changes in Splenic Architecture

When activated, Tfh cells promote a follicular B cell response and germinal center formation. Therefore, we examined the effects of the immune education–induced increase in Tfh cells on splenic architecture 24 h following CLP. Neither education alone nor CLP in control mice altered the weight of the spleen (**Figure 3A**). Relative to both baseline in educated mice prior to CLP and to post-CLP controls, CLP in educated mice increased splenic weight by 25% (**Figure 3A**). The CLP-induced splenomegaly in educated mice was associated with an increased number of germinal centers (**Figure 3B**) and an increase in the area of the spleen taken up by germinal centers (**Figures 3C,D** and **Supplementary Figure S5**).

Immune Education Increases CLP Induced FO B Cell Responses in the Spleen

We next examined the effects of immune education on CLP-induced changes in splenic B cell phenotypes detailed in **Figure 1**. T cell education had minimal effect on B cells prior to CLP

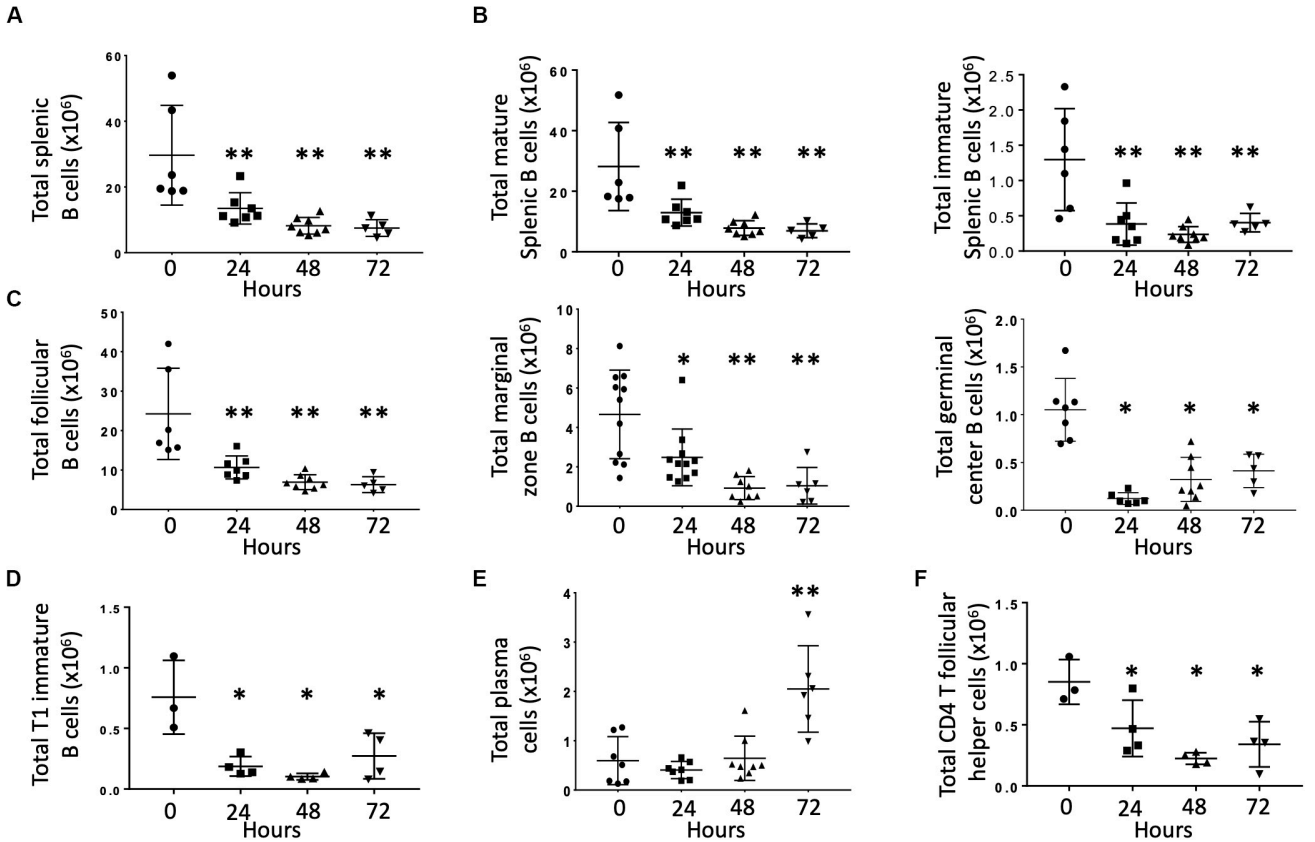

FIGURE 1 | Effects of CLP on total B cells and B cell subtypes in the spleen. C57Bl/6 laboratory mice underwent CLP and were euthanized at given timepoints. Data obtained using flow cytometry. Unmanipulated mice were used as T_0 controls. Each point represents results in an individual animal, central horizontal line indicates mean, upright, and inverted Ts indicate standard deviation, data representative of two independent experiments. $^*p < 0.05$, $^{**}p < 0.01$ for ** relative to T_0 using one-way ANOVA with Dunnett *post hoc* correction for multiple comparisons. **(A)** Total splenic B cells at given time post-CLP. Gating: FSC/SSC, singlets, Live, CD19+/B220+; *N* = 4–6/group. **(B)** Total mature (left) and immature (right) splenic B cells at given time post-CLP. Gating: FSC/SSC, singlets, Live, CD19+/B220+, CD93; *N* = 4–6/group. **(C)** Total follicular, marginal zone, and germinal center B cells per spleen at given time post-CLP. Gating: Follicular B cells: FSC/SSC, singlets, Live, $CD19^+/B220^+$, $CD93^-$, $B220^+/CD138^-$, $IgM^{lo}/CD21/35^{lo}$; Germinal center: FSC/SSC, singlets, Live, $CD19^+/B220^+$, $CD93^-$, $B220^+/CD138^-$, $IgM^{lo}/CD21/35^{lo}$, $GL7^+$; Marginal zone: FSC/SSC, singlets, Live, $CD19^+/B220^+$, $CD93^-$, $B220^+/CD138^-$, $IgM^{hi}/CD21/35^{hi}$; *N* = 5/group for Follicular, 3–4/group for germinal center B cells, 4–10 for marginal zone. **(D)** Total T1 transitional immature B cells per spleen at given time post-CLP. Gating: FSC/SSC, singlets, Live, $CD19^+/B220^+$, $CD93^+$, $IgM^{hi}/CD23^-$; *N* = 3–4/group. **(E)** Total plasma cells per spleen at given time post-CLP. Gating: FSC/SSC, singlets, Live, $CD19^+/B220^+$, $CD93^-$, $B220^+/CD138^+$; *N* = 3–4/group. **(F)** Total splenic CD4 T follicular helpers in the spleen at given time post-CLP. Gating: FSC/SSC, singlets, Live, $CD90^+/CD4^+$, $PD1^+/CXCR5^+$; *N* = 3–4/group.

(**Figure 4A**). In contrast to the reduction in total B cells observed 24 h post-CLP in control mice (**Figures 1A**, **4A**), CLP did not alter total B cell numbers in immune educated mice (**Figure 4A**). Similarly, while CLP in control mice reduced the number of FO B cells (**Figure 1C**), no such change was noted 24 h post-CLP in educated mice (**Figure 4B**). In contrast, immune education did not alter the CLP-induced decrease in MZ B cells (**Figures 1C**, **4C**). While the number of FO I B cells in control animals was not changed, in immune educated mice the number of FO I cells present 24 h post-CLP was greater than in control mice (**Figure 4D**). However, CLP reduced the number of FO II B cells in controls but not in educated mice (**Figure 4D**). The combined effects of CLP on FO I and FO II B cells accounted for the overall difference in the response of FO B cells observed 24 h post-CLP in educated mice (**Figures 4B,D**). The number of germinal center B cells in both control and educated mice was equally reduced 24 h post-CLP (**Figure 4E**) while neither CLP nor immune education affected the number of splenic plasma cells (**Figure 4F**).

B cell activation through antigen recognition is associated with upregulation of the surface marker CD69 (19). T cell education had no effect on the number of FO or MZ B cells expressing CD69 prior to CLP (**Figure 4G**). Following CLP, the number of $CD69^+$ FO B cells in control mice was not altered. In contrast, CLP induced an increase in $CD69^+$ FO B cells in educated mice, indicating increased activation (**Figure 4G**). When MZ B cells were examined for CD69 expression, CLP induced a similar increase in $CD69^+$ MZ B cells compared to baseline numbers in baseline mice, but immune education had no effect on activation of these cells (**Figure 4G**).

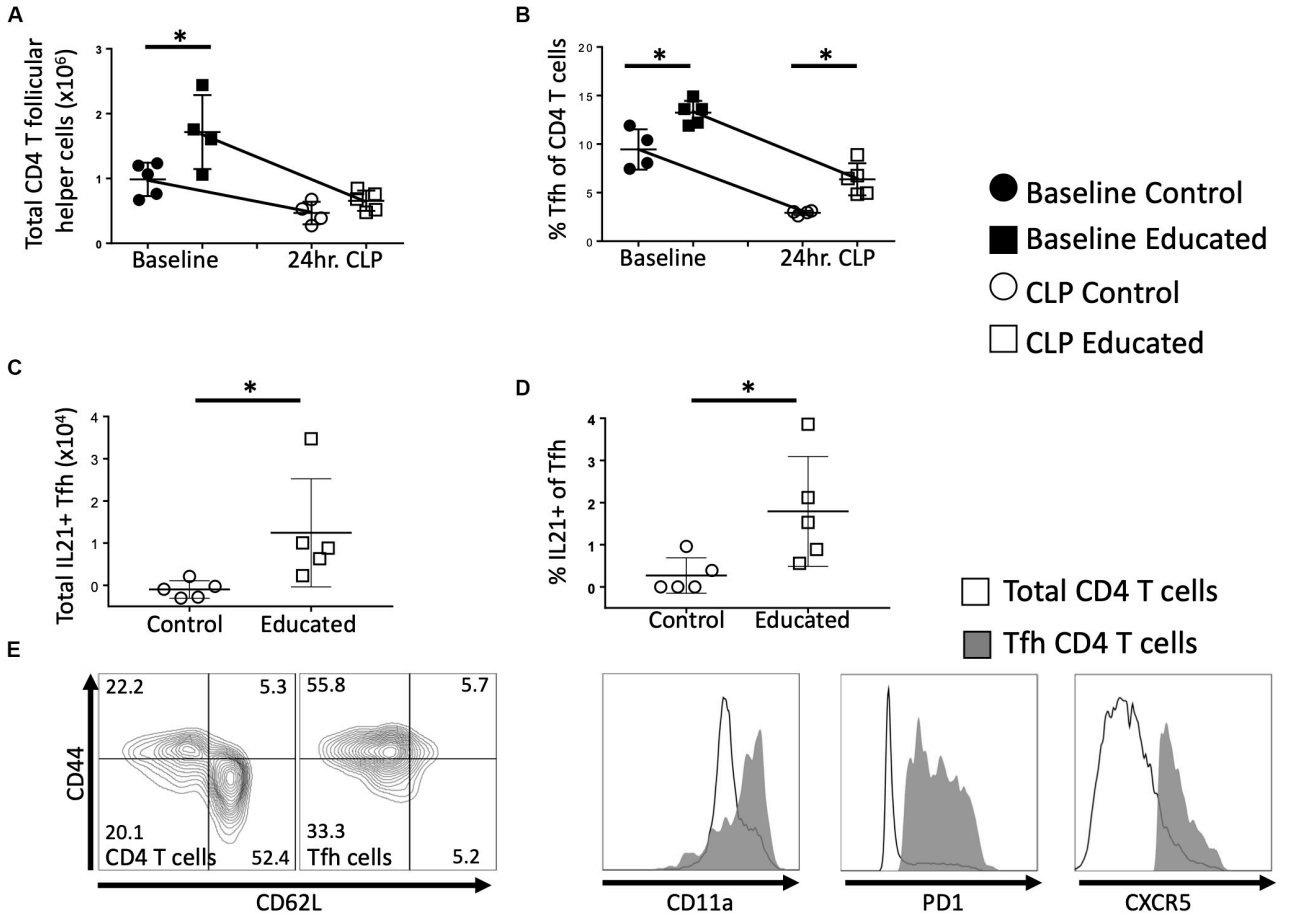

FIGURE 2 | Effects of immune education on splenic CD4 T follicular helper cell response to CLP. C57Bl/6 laboratory mice were injected with anti-CD3ε or isotype control antibody. Thirty five days later mice were euthanized (T_0) or subjected to CLP. Mice subjected to CLP were euthanized at 24 h and T follicular helper T cells were analyzed using flow cytometry. Each point represents results in an individual animal, central horizontal line indicates mean, upright and inverted Ts indicate standard deviation, data representative of two independent experiments. Filled circles – T_0 in control mice; Filled square – T_0 in immune educated mice; Open circle – 24 h post-CLP in control mice; Open square – 24 h post-CLP in immune educated mice. Data analyzed using two-way ANOVA with Sidak's *post hoc* correction for multiple comparisons. *, significantly different from value in control mice at same time point; *$p < 0.05$. **(A)** Total number of CD4 T follicular helper cells per spleen. Gating: FSC/SSC, singlets, Live, $CD90^+/CD4^+$, $PD1^+/CXCR5^+$; $N = 4–5$/group. **(B)** Percentage of CD4 T cells with T follicular helper cell phenotype. Gating: FSC/SSC, singlets, Live, $CD90^+/CD4^+$, $PD1^+/CXCR5^+$; $N = 4–5$/group. **(C)** Total number of IL21-producing T follicular helper cells per spleen. Cells stimulated *ex vivo* with CD3/CD28 for 5 h in the presence of Brefeldin A. Numbers represent percent above background. Gating: FSC/SSC, singlets, Live, $CD90^+/CD4^+$, $PD1^+/CXCR5^+$, $IL21^+$; $N = 4–5$/group. **(D)** Percentage of IL21 – producing T follicular helper cells per spleen. Cells stimulated *ex vivo* with CD3/CD28 for 5 h in the presence of Brefeldin A. Numbers represent percent above background. Gating: FSC/SSC, singlets, Live, $CD90^+/CD4^+$, $PD1^+/CXCR5^+$, $IL21^+$; $N = 4–5$/group. **(E)** Flow cytometric plot demonstrating CD44/CD62L phenotype of Tfh compared to all CD4 T cells, along with CD11a, PD1, CXCR5 histograms. Line represents all CD4 T cells, Gray represents Tfh. Representative of 5 replicates.

CD4 T Cell Memory Causes Persistent Alteration in the B Cell Response 60 Days Post-CLP

Sjaastad et al. have demonstrated that CLP attenuated the Tfh and FO B cell response to specific antigens (10). This decreased response persisted for at least 30 days following CLP. We have shown that immune education induced prior to CLP altered the acute response to CLP by (1) increasing the percentage of CD4 T cells expressing the Tfh phenotype (**Figure 2B**), (2) increasing IL21 production (**Figures 2C,D**) by Tfh cells, (3) increasing germinal center formation (**Figures 3B,C**), and increasing the number of splenic follicular B cells (**Figure 4B**). The effects of immune education, and specifically of the pre-existing presence of a substantial number of Tfh cells, on the long-term immune response to CLP is unknown. We therefore examined B cell responses 60 days after CLP in control and immune educated mice. Results are detailed in **Figure 5**. At this more remote time point, splenic weight in both control and immune educated mice was similarly increased (**Figure 5A**). The total number of splenic B cells increased relative to T_0 and 24 h post-CLP numbers but the increase in educated mice was significantly greater than in controls (**Figure 5B**). A similar response was noted in splenic follicular (**Figure 5C**) and germinal center cells (**Figure 5D**) as

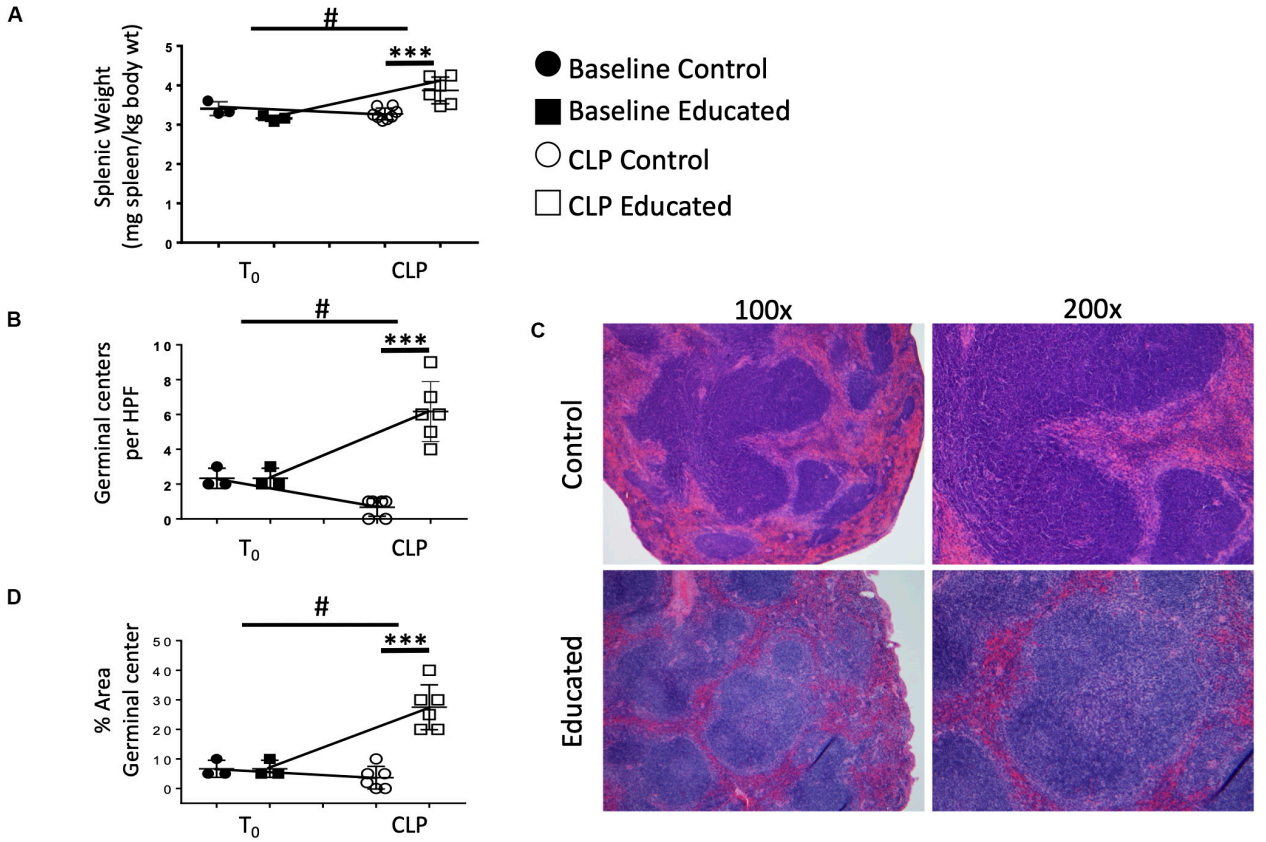

FIGURE 3 | Effects of immune education splenic size and splenic germinal center formation 24 h post-CLP. C57Bl/6 laboratory mice underwent education or treatment with isotype control antibody. Thirty-five days later mice were euthanized (T_0) or subjected to CLP. Mice subjected to CLP were euthanized 24 h later. Spleens were weighed immediately *ex vivo* and normalized to pre-CLP body weight. Spleens were fixed and stained with hematoxylin and eosin and analyzed for germinal center formation by blinded pathologists. Each point represents results in an individual animal, central horizontal line indicates mean, upright and inverted Ts indicate standard deviation, data representative of two independent experiments. Filled circles – T_0 in control mice; Filled square – T_0 in immune educated mice; Open circle – 24 h post-CLP in control mice; Open square – 24 h post-CLP in immune educated mice. Data analyzed using two-way ANOVA with Sidak's *post hoc* correction for multiple comparisons. $^{***}p < 0.001$, significantly different from value in control mice at same time point; $^{\#}p < 0.05$, slope of line connecting T0 mean and mean 24 h post-CLP significantly different than slope of line for control mice. **(A)** Splenic weight normalized to pre-CLP body weight. *N* = 3/group. **(B)** Germinal centers per high power field. *N* = 6/group. **(C)** Hematoxylin and eosin stain of the spleen visualized at 100× or 200× revealing germinal centers. Representative of 6 slides each. **(D)** Percent area covered by germinal centers in the spleen. *N* = 6/group.

well as in splenic plasma cells cell (**Figure 5E**). Marginal B cells were increased relative to T_0 and 24 h post-CLP numbers but, as seen in **Figure 4C**, there was no difference in marginal B cells between educated and control mice at 60 days (**Figure 5F**).

Education Increases the Antigen-Specific B Cell Response to CLP

Immune education induced general changes to the B cell response to CLP (**Figure 4**). However, the effects of CLP on specific B cell responses to known antigen present at the time of CLP in the presence of educated Tfh are unknown. Therefore, we administered 5 μg 4-hydroxy-3-nitrophenylacetic acid or vehicle into the peritoneum of control and educated mice at the time of CLP to mimic antigen introduction at the time of insult. Results were compared to what was observed 7 days after a similar injection was given to unoperated mice. Compared to mice administered NP but not subjected to CLP, NP-specific B cells could not be detected in animals not exposed to NP. Seven days following CLP, the number of NP-specific B cells in control mice was significantly lower than that measured in control animals subjected to injection only (**Figure 6A**). In contrast, the number of NP-specific B cells was maintained in educated mice following CLP. A similar result was noted in NP-specific FO B cells (**Figure 6B**, left), while NP-specific MZ B cells were not maintained in educated mice (**Figure 6B**, right).

DISCUSSION

The data presented here examine the B cell response to CLP in a murine model that includes a broad repertoire of memory T cells ("immune educated mice"). This particular component of adaptive immunity is not present when CLP is performed on standard laboratory (control) mice (7), and constitutes an important deficiency in this most commonly – used model of

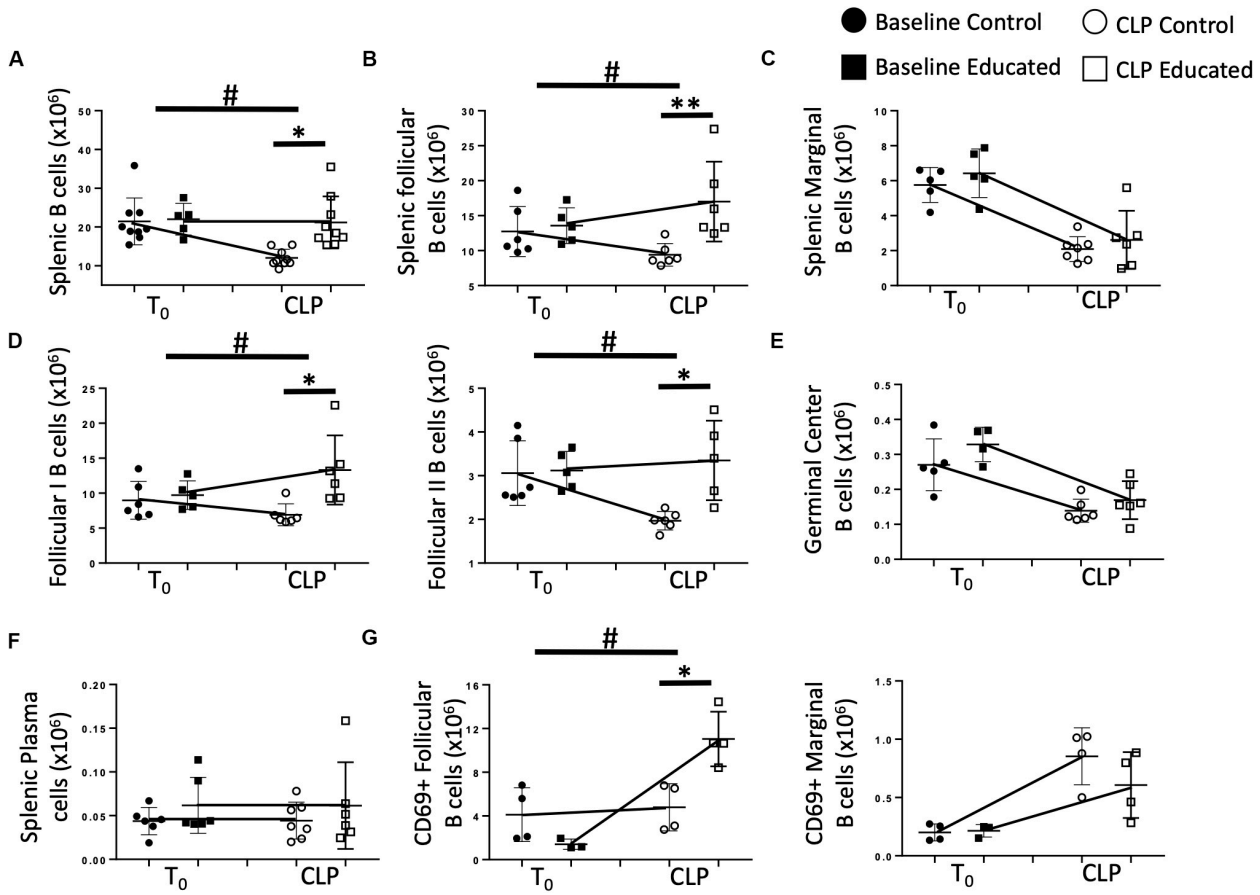

FIGURE 4 | Effects of immune education on B cell populations 24 h post-CLP. C57Bl/6 laboratory mice underwent education or treatment with isotype control antibody. Thirty-five days later mice were euthanized (T_0) or subjected to CLP. Mice subjected to CLP were euthanized 24 h later. Spleens were homogenized and B cell populations were analyzed using flow cytometry. Each point represents results in an individual animal, central horizontal line indicates mean, upright and inverted Ts indicate standard deviation, data representative of two independent experiments. Filled circles – T_0 in control mice; Filled square – T_0 in immune educated mice; Open circle – 24 h post -CLP in control mice; Open square – 24 h post-CLP in immune educated mice. Data analyzed using two-way ANOVA with Sidak's *post hoc* correction for multiple comparisons. $^{*}p < 0.05$, significantly different from value in control mice at same time point; $^{\#}p < 0.05$, slope of line connecting mean at T_0 to mean value 24 h post-CLP significantly different than same line in control mice. **(A)** Total splenic B cells. Gating: FSC/SSC, singlets, Live, $CD19^+/B220^+$; $N = 5–9$/group. **(B)** Total follicular (Left) and marginal zone (Right) B cells per spleen. Gating: Follicular B cells: FSC/SSC, singlets, Live, $CD19^+/B220^+$, $CD93^-$, $B220^+/CD138^-$, $IgM^{lo}/CD21/35^{lo}$. $N = 5–6$/group. **(C)** Total marginal zone B cells per spleen. Gating: Marginal zone: FSC/SSC, singlets, Live, $CD19^+/B220^+$, $CD93^-$, $B220^+/CD138^-$, $IgM^{hi}/CD21/35^{hi}$. $N = 5–6$/group. **(D)** Total follicular I (left) and follicular II (right) B cells per spleen. Gating: Follicular I B cells: FSC/SSC, singlets, Live, $CD19^+/B220^+$, $CD93^-$, $B220^+/CD138^-$, $IgM^{lo}/CD21/35^{lo}$, IgD^+/IgM^{lo}. Follicular II B cells: FSC/SSC, singlets, Live, $CD19^+/B220^+$, $CD93^-$, $B220^+/CD138^-$, $IgM^{lo}/CD21/35^{lo}$, IgD^+/IgM^{mid} $N = 5–6$/group. **(E)** Total germinal center B cells per spleen. Gating: FSC/SSC, singlets, Live, $CD19^+/B220^+$, $CD93^-$, $B220^+/CD138^-$, $IgM^{lo}/CD21/35^{lo}$, $GL7^+$; $N = 5–6$/group. **(F)** Total plasma cells per spleen. Gating: FSC/SSC, singlets, Live, $CD19^+/B220^+$, $CD93^-$, $B220^+/CD138^+$; $N = 7$/group. **(G)** Total CD69 + follicular (left) and CD69 + marginal (right) B cells per spleen. Gating: Follicular B cells: FSC/SSC, singlets, Live, $CD19^+/B220^+$, $CD93^-$, $B220^+/CD138^-$, $IgM^{lo}/CD21/35^{lo}$, $CD69^+/IgM^+$. Marginal B cells: FSC/SSC, singlets, Live, $CD19^+/B220^+$, $CD93^-$, $B220^+/CD138^-$, $IgM^{hi}/CD21/35^{hi}$, $CD69^+/IgM^+$ $N = 3–4$/group.

human sepsis (3, 4). Our data demonstrate that the presence of T cell memory altered several aspects of the acute response to CLP, most notably increasing induced IL21 production by Tfh cells indicating increased functionality. Increased functionality, in turn, reversed the CLP-induced decrease in splenic B cell populations noted in control animals, enhancing FO B cell and germinal center development. Further, B cell activation, as indicated by CD69 expression, was increased in the presence of T cell memory. While CLP diminished the response to a specific antigen in control mice, the response was preserved in immune educated animals. This finding indicates that memory Tfh cells may be required for antigen-specific responses in the presence of inflammation. Most importantly, the effects of immune education on B cell maturation were still present 60 days after CLP. Thus, a mature B cell response may contribute to differences in both short – and long – term abnormalities between control and immune educated mice. Further, the results suggest that T cell memory, in part via its effect on B cell development, plays an important role in the pathogenesis of human sepsis.

Little is known concerning the effects of preexisting T cell memory on the acute response to CLP. Tfh assist FO B cells in converting from short-lived, naïve IgM^+/IgD^+ B cells to

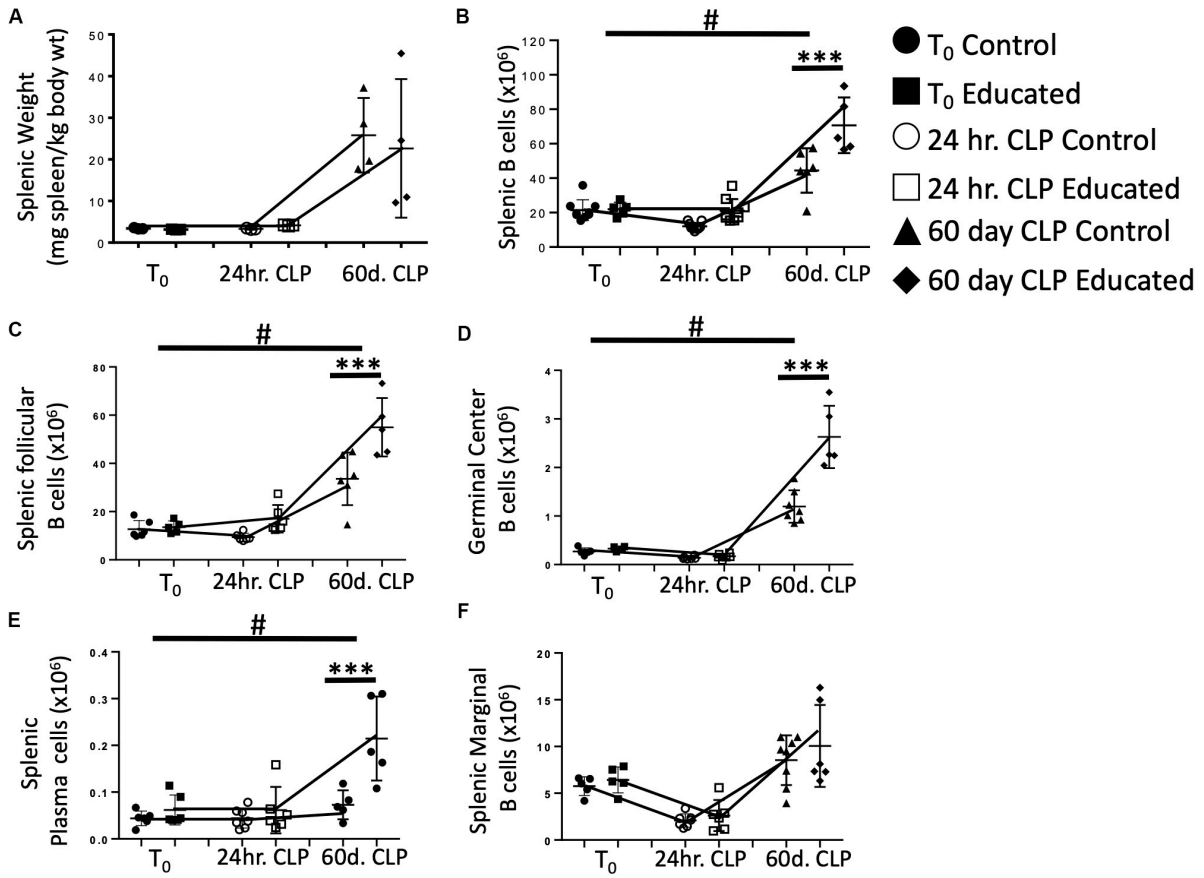

FIGURE 5 | Effects of immune education on Splenic Weight and B cell populations at T_0, 24 h and 60 days post-CLP. C57Bl/6 laboratory mice underwent education or treatment with isotype control antibody. Thirty-five days later mice were euthanized (T_0) or subjected to CLP. Mice subjected to CLP were euthanized 24 h (24 h CLP) or 60 days (60 days CLP) later. Spleens were weighed and homogenized and B cell populations were analyzed using flow cytometry. Each point represents results in an individual animal, central horizontal line indicates mean, upright and inverted Ts indicate standard deviation, data representative of two independent experiments. Filled circles – T_0 in control mice; Filled square – T_0 in immune educated mice; Open circle – 24 h post-CLP in control mice; Open square – 24 h post-CLP in immune educated mice. Data analyzed using two-way ANOVA with Sidak's *post hoc* correction for multiple comparisons. #, slope of line connecting T_0 mean and mean 24 h post-CLP significantly different than slope of line for control mice. $^{***}p < 0.001$, significantly different from value in control mice at same time point; $^{\#}p < 0.05$, slope of line connecting mean at T_0 to mean value 24 h post-CLP significantly different than same line in control mice. **(A)** Splenic weight normalized to pre-CLP body weight. *N* = 4/group. **(B)** Total splenic B cells. Gating: FSC/SSC, singlets, Live, $CD19^+/B220^+$; *N* = 3–4/group. **(C)** Total follicular B cells. Gating: Follicular B cells: FSC/SSC, singlets, Live, $CD19^+/B220^+$, $CD93^-$, $B220^+/CD138^-$, $IgM^{lo}/CD21/35^{lo}$; *N* = 4/group. **(D)** Total germinal center B cells. Gating: FSC/SSC, singlets, Live, $CD19^+/B220^+$, $CD93^-$, $B220^+/CD138^-$, $IgM^{lo}/CD21/35^{lo}$, $GL7^+$; *N* = 4/group. **(E)** Total plasma cells. Gating: FSC/SSC, singlets, Live, $CD19^+/B220^+$, $CD93^-$, $B220^+/CD138^+$; *N* = 4/group. **(F)** Total marginal zone B cells. Gating: FSC/SSC, singlets, Live, $CD19^+/B220^+$, $CD93^-$, $B220^+/CD138^-$, $IgM^{hi}/CD21/35^{hi}$; *N* = 4/group.

long-lived, memory B cells and plasma cells that can efficiently produce antibodies to assist the body in preventing recurrent infection. FO B cells that receive Tfh assistance are able to induce antibody class-switching with increased antibody affinity to both extracellular and intracellular pathogenic antigens. Without T cell help, only low affinity antibodies can be produced and class-switching is limited. Considering that most adult humans have a significant Tfh compartment prior to a septic event, the effect of pre-existing Tfh on the B cell response must be considered. Recent clinical data supports that decreased circulating Tfh at sepsis onset in human subjects correlates with decreased B cell maturation during sepsis and decreased survival (2).

Murine CLP has long been the animal model of choice for human sepsis (3, 4). There are, however, two commonly voiced concerns about this approach. First, based on immunologic and genetic differences, some have opined that differences between CLP and human sepsis are too profound for translation of findings from mice to men (5). Second, improved acute care has identified a cohort of sepsis survivors who have significant long-term health problems. To date, murine equivalents of these late or persistent abnormalities have not been well-characterized or investigated. The data presented here is pertinent to both concerns, emphasizing that addressing the first issue is required to address the second.

In previous work we have used an anti-CD3ε antibody to induce a broad repertoire of memory T cells in C57Bl/6 mice (11). The result has been a significant change in the response to CLP (Taylor et al., unpublished data). The findings presented

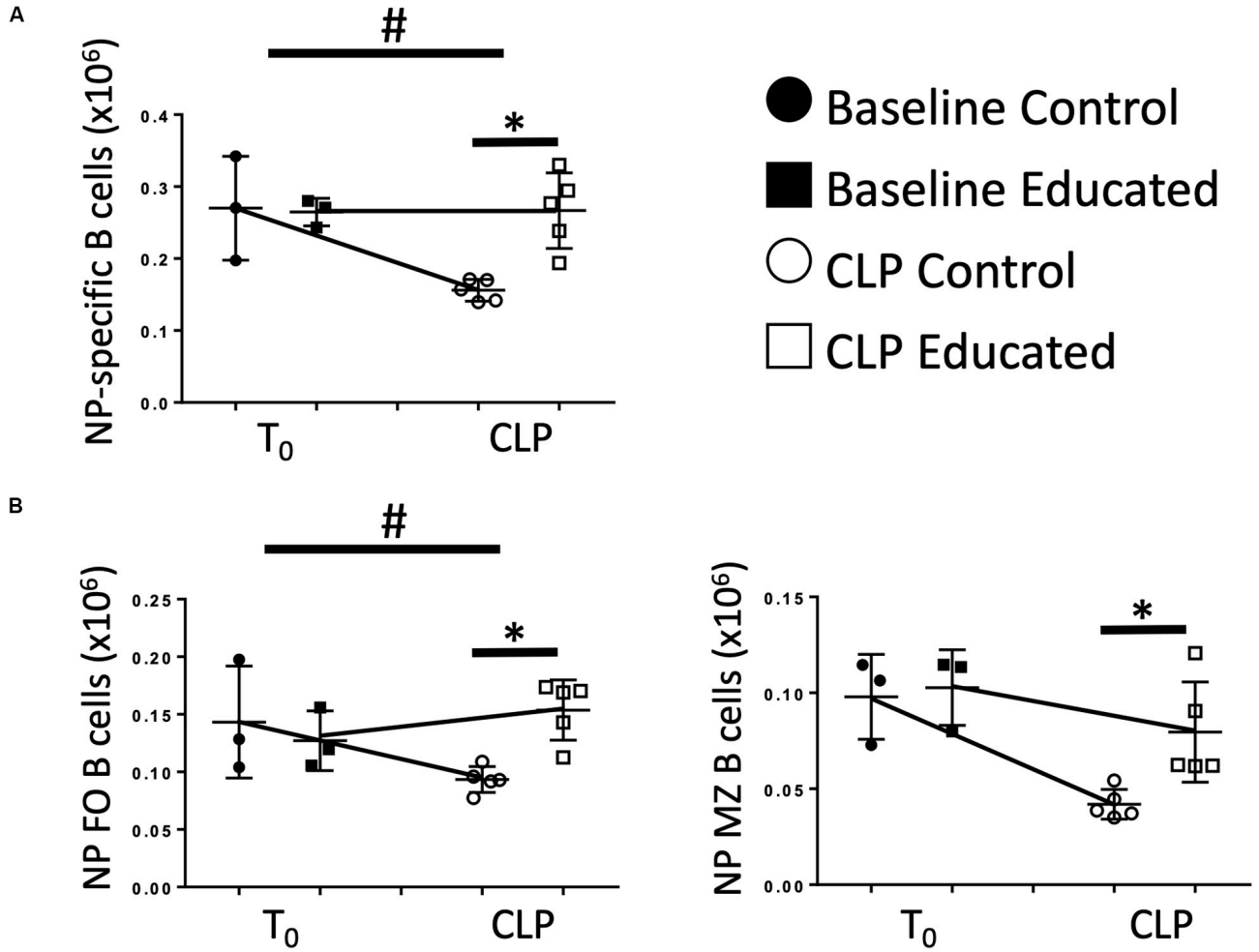

FIGURE 6 | Effects of immune education on NP-specific B cell populations. C57Bl/6 laboratory mice underwent immune education or treatment with isotype control antibody. Thirty-five days later were treated with intraperitoneal 4-hydroxy-3-nitrophenylacetic acid (NP), 5 μg suspended in PBS (T_0) or subjected to CLP and treated with NP (7 days CLP). Mice were euthanized 7 days later. Spleens were homogenized and B cell populations were analyzed using flow cytometry. Each point represents results in an individual animal, central horizontal line indicates mean, upright and inverted Ts indicate standard deviation, data representative of two independent experiments. Filled circles – T_0 in control mice; Filled square – T_0 in immune educated mice; Open circle – 24 h post-CLP in control mice; Open square – 24 h post-CLP in immune educated mice. Data analyzed using two-way ANOVA with Sidak's *post hoc* correction for multiple comparisons. $^{*}p < 0.05$, significantly different from value in control mice at same time point; $^{\#}p < 0.05$, slope of line connecting T_0 mean and mean 24 h post-CLP significantly different than slope of line for control mice. **(A)** Total splenic NP-specific B cells per spleen. Gating: FSC/SSC, singlets, Live, $CD19^+/B220^+$, $CD19^+/NP^+$; $N = 5–9$/group. **(B)** Total NP-specific follicular (Left) and marginal zone (Right) B cells per spleen. Gating: Follicular B cells: FSC/SSC, singlets, Live, $CD19^+/B220^+$, $CD19^+/NP^+$, $CD93^-$, $B220^+/CD138^-$, $IgM^{lo}/CD21/35^{lo}$, Marginal Zone B cells FSC/SSC, singlets, Live, $CD19^+/B220^+$, $CD19^+/NP^+$, $CD93^-$, $B220^+/CD138^-$, $IgM^{hi}/CD21/35^{hi}$; $N = 5–6$/group.

here further characterize the role of T cell memory in the response to CLP. Specifically, our findings demonstrate that the presence of memory Tfh cells, which has not been examined in either CLP or in human sepsis, is an essential component in the activation of B cells responses. These findings may have direct clinical relevance. Many years ago, Meakins et al., observed that a failure to resolve anergy was a poor prognostic factor in septic surgical and trauma patients (20). It is difficult to assess the ability of B cells to form antibody following an inflammatory insult. However, our findings indicate that an inadequate Tfh response limits B cell receptor signaling and maturation. One potential consequence of a lack of Tfh cells would be an acceleration of B cell apoptosis (21, 22), a finding present at autopsy in patients with fatal sepsis (1). Supporting this explanation is a recent prospective cohort study of sepsis patients indicating activation-associated cell death is a major driver of B cell lymphopenia in sepsis; preexisting Tfh may increase the apoptotic threshold of activated B cells, partially rescuing the B cell response (23).

Our data indicate that the acute CLP-induced decrease in mature B cell numbers was reversed 60 days following the procedure. The fact that this increase was more greater in immune educated mice likely reflects increased functionality by memory Tfh cells.

Our findings may also have relevance to what has been viewed as a major limitation of CLP – the use of laboratory mice (5, 6). Translation of results from CLP to human sepsis has been poor. It has been noted that, in contrast to humans, lab mice lack a memory T cell compartment (7, 8). Our group has developed a method of inducing widespread T cell memory through administration of an anti-CD3ε activating antibody. This "education" leads to widespread CD4 and CD8 T cell memory induction. This approach altered the response to CLP in a manner that enhances features consistent with sepsis – a more pronounced innate immune response, more profound organ dysfunction and decreased survival (Taylor, et al., unpublished data). The importance of the effects of immune education on CLP-induced changes in B cell numbers is unclear. However, it reverses acute depression of B cell responses that follows CLP. The augmentation of this early response to CLP indicates that perhaps a major component of the early response to sepsis has been neglected and that T cell memory may have important effects on the long-term responses to CLP and sepsis.

More importantly, the remaining B cells in the spleen that are not eliminated during the sepsis response, while low in number, may be mounting an effective antibody response that could play an important role in protective immunity. When examined, there was no difference in total IgG levels in the serum of mice at any time point (data not shown), indicating that the immune response at the cellular level may not be reflected in changes in total immunoglobulin repertoire, but instead, may represent alteration in specific B cell clones as demonstrated by an NP-specific B cell response with introduction of antigen. Addition of Tfh may help refine the B cell response and allow for antibody recognition of different epitopes that cannot be recognized without T cell help.

The Tfh memory response is understudied in CLP and could be an important target in future treatment of sepsis as a way to modulate the B cell response in a more effective manner. Tfh modulation may represent a target for preventing post-sepsis immunosuppression in the future.

DATA AVAILABILITY STATEMENT

The raw data supporting the conclusions of this article will be made available by the authors, without undue reservation.

ETHICS STATEMENT

The animal study was reviewed and approved by Institutional Animal Care and Use Committee of the Feinstein Institutes for Medical Research of Northwell Health.

AUTHOR CONTRIBUTIONS

MT performed all experiments, analyzed the data, and wrote the manuscript. MB, AN-K, and MA assisted in cecal ligation, puncture procedure, animal handling, data analysis, and writing the manuscript. YY and KR performed histological slide preparation and analysis, and assisted in writing the manuscript. BB assisted in experimental design, analysis of data, and writing. CD supervised and assisted in experimental design, analysis of data, and writing. All authors contributed to the article and approved the submitted version.

FUNDING

MT received funding from the NIH NIGMS K08GM132794 and Thrasher Research Fund Early Career Award 14734. CD received funding from the NIH NIGMS R01GM121102.

SUPPLEMENTARY MATERIAL

The Supplementary Material for this article can be found online at: https://www.frontiersin.org/articles/10.3389/fimmu.2020.01946/full#supplementary-material

FIGURE S1 | Murine Sepsis Score comparing control and immune educated mice following CLP. C57Bl/6 laboratory mice underwent education or treatment with isotype control antibody. Thirty-five days later mice were subjected to CLP and monitored daily for clinical scoring using the murine sepsis score. Data as mean ± standard deviation, $*p < 0.001$ for treatment effect over time by mixed effects modeling. Representative of two independent experiments. $N = 5$/group.

FIGURE S2 | Gating Strategy for Tfh cells. Splenic T cell populations shown from educated mouse 24 h following CLP without TCR stimulation for all except cytokine staining, which is shown following TCR stimulation.

FIGURE S3 | Gating Strategy for B cells. Splenic B cell populations shown from educated mouse 24 h following CLP (18).

FIGURE S4 | Effects of CLP on total B cells and B cell subtypes in the spleen. C57Bl/6 laboratory mice underwent CLP and were euthanized at given timepoints. Data obtained using flow cytometry. Unmanipulated mice were used as T_0 controls. Data as mean ± standard deviation, $*p < 0.05$, $**p < 0.01$ for spleen compared to T_0 by one-way ANOVA with Dunnett correction for multiple comparisons. Total follicular I (left) and follicular II (right) B cells per spleen at given time post-CLP. Gating: Follicular I B cells: FSC/SSC, singlets, Live, $CD19^+/B220^+$, $CD93^-$, $B220^+/CD138^-$, $IgM^{lo}/CD21/35^{lo}$, IgD^+/IgM^{lo}. Follicular II B cells: FSC/SSC, singlets, Live, $CD19^+/B220^+$, $CD93^-$, $B220^+/CD138^-$, $IgM^{lo}/CD21/35^{lo}$, IgD^+/IgM^{mid} $N = 3$–4/group.

FIGURE S5 | Effects of immune education on splenic germinal center formation in the spleen following CLP. C57Bl/6 laboratory mice underwent CLP and were euthanized at 24 h. Spleens were fixed and stained with hematoxylin and eosin and analyzed for germinal center formation by blinded pathologists. Photos are representative of two independent experiments. **(A)** Germinal center as indicated by red circle with central paling in white pulp of spleen. **(B)** Hematoxylin and eosin stain of the spleen in control and educated mice 40× magnification. Representative of 6 slides each.

TABLE S1 | Antibodies used for this manuscript.

REFERENCES

1. Boomer JS, To K, Chang KC, Takasu O, Osborne DF, Walton AH, et al. Immunosuppression in patients who die of sepsis and multiple organ failure. *JAMA*. (2011) 306:2594–605.
2. Duan S, Jiao Y, Wang J, Tang D, Xu S, Wang R, et al. Impaired B-Cell maturation contributes to reduced B Cell numbers and poor prognosis in sepsis. *Shock*. (2020) 54:70–7.
3. Wichterman KA, Baue AE, Chaudry IH. Sepsis and septic shock–a review of laboratory models and a proposal. *J Surg Res*. (1980) 29:189–201. doi: 10.1016/0022-4804(80)90037-2
4. Osuchowski MF, Ayala A, Bahrami S, Bauer M, Boros M, Cavaillon JM, et al. Minimum quality threshold in pre-clinical sepsis studies (MQTiPSS): an international expert consensus initiative for improvement of animal modeling in sepsis. *Infection*. (2018) 46:687–91.
5. Seok J, Warren HS, Cuenca AG, Mindrinos MN, Baker HV, Xu W, et al. Genomic responses in mouse models poorly mimic human inflammatory diseases. *Proc Natl Acad Sci USA*. (2013) 110:3507–12.
6. Warren HS, Tompkins RG, Moldawer LL, Seok J, Xu W, Mindrinos MN, et al. Mice are not men. *Proc Natl Acad Sci USA*. (2015) 112:E345.
7. Beura LK, Hamilton SE, Bi K, Schenkel JM, Odumade OA, Casey KA, et al. Normalizing the environment recapitulates adult human immune traits in laboratory mice. *Nature*. (2016) 532:512–6.
8. Abolins S, King EC, Lazarou L, Weldon L, Hughes L, Drescher P, et al. The comparative immunology of wild and laboratory mice, Mus musculus domesticus. *Nat Commun*. (2017) 8:14811.
9. Huggins MA, Sjaastad FV, Pierson M, Kucaba TA, Swanson W, Staley C, et al. Microbial exposure enhances immunity to pathogens recognized by TLR2 but increases susceptibility to cytokine storm through TLR4 sensitization. *Cell Rep*. (2019) 28:1729–43.e1725.
10. Sjaastad FV, Condotta SA, Kotov JA, Pape KA, Dail C, Danahy DB, et al. Polymicrobial sepsis chronic immunoparalysis is defined by diminished Ag-specific T cell-dependent B cell responses. *Front Immunol*. (2018) 9:2532. doi: 10.3389/fimmu.2018.02532
11. Taylor MD, Brewer MR, Deutschman CS. Induction of diverse T cell memory through antibody-mediated activation. *Eur J Immuno*. (2020). doi: 10.1002/eji.202048570. [Epub ahead of print].
12. Abcejo AS, Andrejko KM, Raj NR, Deutschman CS. Failed interleukin-6 signal transduction in murine sepsis: attenuation of hepatic glycoprotein 130 phosphorylation. *Crit Care Med*. (2009) 37:1729–34.
13. Shrum B, Anantha RV, Xu SX, Donnelly M, Haeryfar SM, McCormick JK, et al. A robust scoring system to evaluate sepsis severity in an animal model. *BMC Res Notes*. (2014) 7:233. doi: 10.1186/1756-0500-7-233 doi: 10.1186/1756-0500-7-233
14. Taylor MD, Burn TN, Wherry EJ, Behrens EM. CD8 T Cell memory increases immunopathology in the perforin-deficient model of hemophagocytic lymphohistiocytosis secondary to TNF-alpha. *Immunohorizons*. (2018) 2:67–73. doi: 10.4049/immunohorizons.1800003
15. Hotchkiss RS, Tinsley KW, Swanson PE, Schmieg RE, Hui JJ, Chang KC, et al. Sepsis-induced apoptosis causes progressive profound depletion of B and CD4+ T lymphocytes in humans. *J Immunol*. (2001) 166:6952–63.
16. Cariappa A, Tang M, Parng C, Nebelitskiy E, Carroll M, Georgopoulos K, et al. The follicular versus marginal zone B lymphocyte cell fate decision is regulated by aiolos, Btk, and CD21. *Immunity*. (2001) 14:603–15.
17. Martin F, Oliver AM, Kearney JF. Marginal zone and B1 B cells unite in the early response against T-independent blood-borne particulate antigens. *Immunity*. (2001) 14:617–29.
18. Allman D, Pillai S. Peripheral B cell subsets. *Curr Opin Immunol*. (2008) 20:149–57.
19. Zimmermann M, Rose N, Lindner JM, Kim H, Gonçalves AR, Callegari I, et al. Antigen extraction and B Cell activation enable identification of rare membrane antigen specific human B cells. *Front Immunol*. (2019) 10:829. doi: 10.3389/fimmu.2019.00829
20. Meakins JL, Pietsch JB, Bubenick O, Kelly R, Rode H, Gordon J, et al. Delayed hypersensitivity: indicator of acquired failure of host defenses in sepsis and trauma. *Ann Surg*. (1977) 186:241–50.
21. Kil LP, de Bruijn MJ, van Nimwegen M, Corneth OB, van Hamburg JP, Dingjan GM. Btk levels set the threshold for B-cell activation and negative selection of autoreactive B cells in mice. *Blood*. (2012) 119:3744–56.
22. Baumjohann D, Preite S, Reboldi A, Ronchi F, Ansel KM, Lanzavecchia A, et al. Persistent antigen and germinal center B cells sustain T follicular helper cell responses and phenotype. *Immunity*. (2013) 38:596–605. doi: 10.1016/j.immuni.2012.11.020
23. Shankar-Hari M, Fear D, Lavender P, Mare T, Beale R, Swanson C, et al. Activation-associated accelerated apoptosis of memory B cells in critically Ill patients with sepsis. *Crit Care Med*. (2017) 45:875–82.

Conflict of Interest: CD is a consultant for Enlivex Therapeutics Inc, Jerusalem, Israel.

The remaining authors declare that the research was conducted in the absence of any commercial or financial relationships that could be construed as a potential conflict of interest.

frontiers in Immunology

ORIGINAL RESEARCH
published: 12 August 2020
doi: 10.3389/fimmu.2020.01786

Polymicrobial Sepsis Impairs Antigen-Specific Memory CD4 T Cell-Mediated Immunity

*Frances V. Sjaastad[1], Tamara A. Kucaba[2], Thamotharampillai Dileepan[3,4], Whitney Swanson[2], Cody Dail[5], Javier Cabrera-Perez[1,6], Katherine A. Murphy[2], Vladimir P. Badovinac[7,8,9] and Thomas S. Griffith[1,2,4,10,11]**

[1] Microbiology, Immunology, and Cancer Biology Ph.D. Program, University of Minnesota, Minneapolis, MN, United States, [2] Department of Urology, University of Minnesota, Minneapolis, MN, United States, [3] Department of Microbiology and Immunology, University of Minnesota, Minneapolis, MN, United States, [4] Center for Immunology, University of Minnesota, Minneapolis, MN, United States, [5] Medical Student Summer Research Program in Infection and Immunity, University of Minnesota, Minneapolis, MN, United States, [6] Medical Scientist Training Program, University of Minnesota, Minneapolis, MN, United States, [7] Interdisciplinary Graduate Program in Immunology, University of Iowa, Iowa City, IA, United States, [8] Department of Pathology, University of Iowa, Iowa City, IA, United States, [9] Department of Microbiology and Immunology, University of Iowa, Iowa City, IA, United States, [10] Masonic Cancer Center, University of Minnesota, Minneapolis, MN, United States, [11] Minneapolis VA Health Care System, Minneapolis, MN, United States

OPEN ACCESS

Edited by:
Vandana Kalia, University of Washington School of Medicine, United States

Reviewed by:
Adrian Piliponsky, Seattle Children's Research Institute, United States
Stefanie Barbara Flohé, Essen University Hospital, Germany

***Correspondence:**
Thomas S. Griffith
tgriffit@umn.edu

Specialty section:
This article was submitted to Immunological Memory, a section of the journal Frontiers in Immunology

Received: *26 February 2020*
Accepted: *03 July 2020*
Published: *12 August 2020*

Citation:
Sjaastad FV, Kucaba TA, Dileepan T, Swanson W, Dail C, Cabrera-Perez J, Murphy KA, Badovinac VP and Griffith TS (2020) Polymicrobial Sepsis Impairs Antigen-Specific Memory CD4 T Cell-Mediated Immunity. Front. Immunol. 11:1786. doi: 10.3389/fimmu.2020.01786

Patients who survive sepsis display prolonged immune dysfunction and heightened risk of secondary infection. CD4 T cells support a variety of cells required for protective immunity, and perturbations to the CD4 T cell compartment can decrease overall immune system fitness. Using the cecal ligation and puncture (CLP) mouse model of sepsis, we investigated the impact of sepsis on endogenous Ag-specific memory CD4 T cells generated in C57BL/6 (B6) mice infected with attenuated *Listeria monocytogenes* (Lm) expressing the I-A^b-restricted 2W1S epitope (Lm-2W). The number of 2W1S-specific memory CD4 T cells was significantly reduced on day 2 after sepsis induction, but recovered by day 14. In contrast to the transient numerical change, the 2W1S-specific memory CD4 T cells displayed prolonged functional impairment after sepsis, evidenced by a reduced recall response (proliferation and effector cytokine production) after restimulation with cognate Ag. To define the extent to which the observed functional impairments in the memory CD4 T cells impacts protection to secondary infection, B6 mice were infected with attenuated *Salmonella enterica*-2W (*Se*-2W) 30 days before sham or CLP surgery, and then challenged with virulent *Se*-2W after surgery. Pathogen burden was significantly higher in the CLP-treated mice compared to shams. Similar reductions in functional capacity and protection were noted for the endogenous OVA_{323}-specific memory CD4 T cell population in sepsis survivors upon Lm-OVA challenge. Our data collectively show CLP-induced sepsis alters the number and function of Ag-specific memory CD4 T cells, which contributes (in part) to the characteristic long-lasting immunoparalysis seen after sepsis.

Keywords: sepsis, immune suppression, CD4 T cells, memory, IFN-gamma

INTRODUCTION

The importance of a functional immune system for overall health is dramatically illustrated by individuals with immune system defects being highly susceptible to serious and often life-threatening infections. States of immune deficiency can be congenital (e.g., impaired T and/or B cell development) or acquired [e.g., HIV infection, iatrogenic (post-organ transplant) immune suppression, or surgery/trauma]. Studies interrogating the events leading to acquired immunodeficiency are done with the goal of designing treatment modalities to restore immune system function and reduce the susceptibility to infection.

Sepsis causes millions of deaths annually worldwide (1). Defined as a systemic inflammatory response syndrome during a disseminated infection (2, 3), early stages of sepsis are marked by a potentially fatal hyperinflammatory state driven by proinflammatory cytokines (4–6). Concurrent with this hyperinflammation is system-wide transient loss of multiple immune cell types that decreases the ability of the septic host to respond to the primary infection or secondary nosocomial infection. Advancements in critical care medicine have improved survival rates of patients following the initial sepsis-inducing injury (7–10), where acute death from sepsis is no longer the major cause of mortality for these patients. Currently, ∼70% of sepsis-related deaths occur after the first 3 days of the disorder as the result of a secondary infection, with many patient deaths occurring weeks and months later (11). Interestingly, the sepsis-induced lymphopenia is transient, and the once hyperinflammatory immune response transitions to a prolonged immunosuppressive state even though the cellular composition of the immune system numerically returns to normal. In fact, the prolonged immune suppression that develops after a septic event is now considered a leading reason for the extended period of increased susceptibility to pathogens normally handled by the immune system in healthy individuals (11, 12).

CD4 T cells are among the immune cells significantly depleted during the acute stage of sepsis (13), but gradually recover during the immunosuppressive phase (14). CD4 T cells support the function of a variety of immune cells needed to mount a productive and protective immune response (15), and perturbations in the CD4 T cell compartment can dramatically affect overall immune system fitness. The ability to develop and sustain memory cells after infection or immunization is a hallmark of adaptive immunity and basis for protective vaccination against infectious disease (16, 17). Memory CD4 T cells possess several important features that distinguish them from naïve CD4 T cells. First, there are increased numbers of memory CD4 T cells compared to precursors, providing better coverage and a more rapid cellular response during re-challenge. Memory CD4 T cells have experienced cell-intrinsic "programming" changes that allow for rapid expression of effector cytokines, chemokines, and cytotoxic molecules. Additionally, memory CD4 T cells establish residence in both lymphoid and non-lymphoid tissues (18, 19). Finally, the number of memory CD4 T cells present at the end of the contraction phase of a primary response is maintained for the life of the host (20). Maintenance of memory CD4 T cell responses over time is a dynamic process, depending on subsequent encounters with either cognate or non-related Ag/infections that have the potential to change their phenotype and function (15). Similar to the primary response, the magnitude of a memory CD4 T cell response directly correlates with the quantity and quality of memory CD4 T cells present at the time of re-challenge. Thus, changes in composition and function of naive and memory CD4 T cells can result in impaired immunity and increased susceptibility to subsequent infections (21, 22). The present study took advantage of our ability to track the number and function of endogenous Ag-specific memory CD4 T cells in the wake of a septic event [using the cecal ligation and puncture (CLP) model of polymicrobial sepsis]. Our data demonstrate sepsis leads to dramatic and transient decline in pre-existing memory CD4 T cell numbers, with sustained functional impairments, which contribute to the overall increased susceptibility to secondary infections in sepsis survivors.

MATERIALS AND METHODS

Mice

Female C57BL/6 mice (8-weeks old) were purchased from the National Cancer Institute (Frederick, MD). Female pet store mice were purchased from local pet stores in the Minneapolis-St. Paul, MN metropolitan area. All mice were housed in AALAC-approved animal facilities at the University of Minnesota at the appropriate biosafety level (BSL-1/BSL-2 for SPF B6 mice, and BSL-3 for cohoused B6 and pet store mice). SPF B6 and pet store mice were cohoused at a ratio of 8:1 in large rat cages for 60 days to facilitate microbe transfer (23, 24). In all experiments, including those using cohoused mice, mice were age-matched. Experimental procedures were approved by the University of Minnesota Institutional Animal Care and Use Committees and performed following the Office of Laboratory Animal Welfare guidelines and PHS Policy on Human Cancer and Use of Laboratory Animals.

Cecal Ligation and Puncture (CLP)

Sepsis was induced by CLP (25). Briefly, mice were anesthetized using isoflurane (2.5% gas via inhalation). The abdomen was shaved and disinfected with 5% povidone-iodine antiseptic. Bupivacaine (6 mg/kg s.c.) was then administered at the site where a midline incision was made. The distal third (∼1 cm) of the cecum was ligated with 4–0 silk suture and punctured once with a 25-g needle to extrude a small amount of cecal content. After returning the cecum to the abdomen, the peritoneum was closed via continuous suture and the skin was sealed using surgical glue (Vetbond; 3M, St. Paul, MN). Post-operative analgesia and fluid resuscitation occurred at the conclusion of surgery and the following 3 days in the form of meloxicam (2 mg/kg) in 1 ml saline. Mice were monitored daily for weight loss and pain for at least 5 days post-surgery. To control for non-specific changes from the surgery, sham mice underwent the same laparotomy procedure excluding ligation and puncture.

Experimental Pathogens and Infections

C57BL/6 mice were immunized with attenuated *Listeria monocytogenes*-2W1S (Lm-2W1S) or Lm-OVA (10^7 CFU i.v.) or attenuated *Salmonella enterica* serovar Typhimurium strain BRD509-2W1S (*Se*-2W1S; AroA$^-$; 10^6 CFU i.v.) 30 days before sham or CLP surgery to generate memory CD4 T cells. In some experiments, mice received a second infection with attenuated Lm-2W1S (10^7 CFU i.v.), virulent Lm-OVA (10^4 CFU i.v.), or virulent *Se*-2W1S (10^3 CFU i.v.). In experiments where mice received a secondary virulent Lm-OVA bacterial challenge, mice were depleted of CD8 T cells by injecting 100 μg anti-CD8 mAb (clone 2.43) i.v. 3, 2, and 1 days prior to secondary infection. In experiments where mice received a secondary virulent *Se*-2W1S bacterial infection, some of the mice were depleted of CD4 T cells by injecting 800 μg of anti-CD4 mAb (clone GK1.5) i.v. 7 days before and 400 μg i.v. 4 and 3 days before challenge. To measure the clearance of the secondary infection of virulent Lm-OVA or virulent *Se*-2W1S, livers and spleens were removed 3 or 7 days post-infection, respectively, placed in 0.2% IGEPAL solution (Sigma-Aldrich), and homogenized. Serial dilutions of the homogenate were plated on tryptic soy broth agar containing 50 μg/ml streptomycin (for Lm-OVA) or 100 μg/ml streptomycin (for *Se*-2W1S), which restricted bacterial growth to the streptomycin-resistant Lm-OVA or *Se*-2W1S used for secondary infection. Bacterial colonies were counted after 24 h incubation at 37°C (26–28).

Enrichment and Analysis of Ag-Specific CD4 T Cells

I-A^b-specific tetramers containing 2W1S (EAWGALANWAVDSA) or $OVA_{323-339}$ (ISQAVHAAHAEINEAGR) were used to identify Ag-specific CD4 T cells (29–31). Briefly, I-A^b β-chains containing the 2W1S or $OVA_{323-339}$ epitopes covalently linked to the I-A^b β-chain were produced in Drosophila melanogaster S2 cells. 2W1S:I-A^b or $OVA_{323-339}$:I-A^b monomers were then biotinylated and made into tetramers with streptavidin-phycoerythrin (SA-PE; Prozyme). To enrich for Ag-specific CD4 T cells, tetramers (10 nM final concentration) were then added to single cell suspensions in 300 μl tetramer staining buffer (PBS containing 5% FBS, 2mM EDTA, 1:50 normal mouse serum, and 1:100 anti-CD16/32 mAb). The cells were incubated in the dark at room temperature for 1 h, followed by a wash in 10 ml ice cold FACS Buffer. The tetramer-stained cells were then resuspended in 300 μl FACS Buffer, mixed with 25 μl of anti-PE mAb-conjugated magnetic microbeads (StemCell Technologies), and incubated in the dark on ice for 30 min. The cells were washed, resuspended in 3 ml cold FACS Buffer, and passed through an EasySep Magnet (StemCell Technologies) to yield the enriched tetramer positive population. The resulting enriched fractions were stained with a cocktail of fluorochrome-labeled mAb (see below). Cell numbers for each sample were determined using AccuCheck Counting Beads (Invitrogen). Samples were then analyzed using a Fortessa flow cytometer (BD) and FlowJo software (TreeStar Inc., Ashland, OR). The percentage of 2W1S:I-A^{b+} or $OVA_{323-339}$:I-A^{b+} events was multiplied by the total number of cells in the enriched fraction to calculate the total number of 2W1S:I-A^b- or $OVA_{323-339}$:I-A^b–specific CD4 T cells.

In vivo peptide stimulation was used to determine Ag-specific CD4 T cell cytokine production, as previously described (31–34). Briefly, infected mice were injected i.v. with 100 μg of the 2W1S or $OVA_{323-339}$ peptides (synthesized by Bio-Synthesis, Louisville, TX). After 4 h, spleens were harvested in media containing 10 μg/ml brefeldin A. The resulting cell suspensions were fixed, permeabilized, and stained with anti-IFNγ, -TNF, and -IL-2 mAb.

Flow Cytometry

To assess the expression of cell surface proteins, cells were incubated with fluorochrome-conjugated mAb at 4°C for 30 min. The cells were then washed with FACS buffer. For some experiments, the cells were then fixed with PBS containing 2% paraformaldehyde. In procedures requiring intracellular staining, cells were permeabilized following surface staining using the transcription factor staining kit (Tonbo), stained for 1 h at 20°C with a second set of fluorochrome-conjugated mAb, and suspended in FACS buffer for acquisition. The fluorochrome-conjugated mAb used in both surface and intracellular stainings were as follows: Dump gate: APC-Cy7 CD11b (clone M1/70; Tonbo), APC-Cy7 CD11c (clone N418; Tonbo), APC-Cy7 B220 (clone RA3-6B2; Tonbo), APC-Cy7 F4/80 (clone BM8.1; Tonbo), Ghost Red 780 viability dye (Tonbo). Surface staining: BV650 CXCR5 (clone L138D7; BioLegend), Brilliant Violet 510 CD44 (clone IM7; BioLegend), redFluo 710 CD44 (clone IM7; Tonbo), Brilliant Violet 711 CD8 (clone 53-6.7; BioLegend), Brilliant Ultra Violet 395 Thy1.2 (clone 53-2.1; BD Biosciences)—used as an alternative to CD3 for gating T cells, Brilliant Ultra Violet 496 CD4 (clone GK1.5; BD Biosciences), Alexa Fluor 647 CD49d (clone R1-2; BD Biosciences), FITC CD11a (clone M17/4; eBioscience), PE-Cy7 CD11a (clone M17/4; eBioscience). Intracellular staining: Alexa Fluor 488 Foxp3 (clone FJK-15S; Invitrogen), PE-Cy7 Tbet (clone 4B10; BioLegend), PE Bcl6 (clone K112-91; BD Biosciences), BV650 IFN-γ (clone XMG1.2; BD Biosciences), APC IFN-γ (clone XMG1.2; eBioscience), PE-Cy7 IL-2 (clone JES6-5H4; BioLegend), APC TNF-α (clone MP6-XT22; BioLegend), PE TNF-α (clone MP6-XT22; BioLegend), PE-Cy7 IL-2 (clone JES6-5H4; BioLegend). Gating and fluorescence thresholds were determined using fluorescence minus one (FMO) controls.

Statistical Analyses

Data shown are presented as mean values ± SEM. GraphPad Prism 8 was used for statistical analysis, where statistical significance was determined using two-tailed Student *t*-test (for 2 individual groups, if unequal variance Mann-Whitney *U*-test was used) or group-wise, one-way ANOVA analyses followed by multiple-testing correction using the Holm-Sidak method, with $\alpha = 0.05$. $^*p < 0.05$, $^{**}p < 0.01$, $^{***}p < 0.005$, and $^{****}p < 0.001$.

RESULTS

The Number of Pre-existing Memory CD4 T Cells Fluctuate After Sepsis

Septic patients have reduced delayed-type hypersensitivity (DTH) responses, marked by a failure to respond to skin testing with Ag to which previous exposure is known to have occurred (35–37). DTH responses are driven in large part by

memory CD4 T cells—even though other immune cells such as CD8 T cells and antigen presenting cells (APCs) participate in the response—and DTH can be used as an assessment of overall immune system fitness (38). To more directly and rigorously interrogate the long-term consequences of sepsis on memory CD4 T cells, we used a protocol where an endogenous, Ag-specific memory CD4 T cell population was generated by infection with attenuated *Listeria monocytogenes* engineered to express the I-A^b-restricted peptide 2W1S (Lm-2W1S) 30 days before performing sham/CLP surgery (**Figure 1A**). We also employed a peptide:MHC II (I-A^b) tetramer-based approach to identify the endogenous 2W1S-specific CD4 T cells before and after sham/CLP surgery. Initially, spleens were harvested from naïve mice and mice at 7, 14, and 28 days post-infection to document the expansion, contraction, and establishment of memory 2W1S-specific CD4 T cells (**Figure 1B**). The majority of memory 2W1S-specific CD4 T cells adopted a Th1 (Tbet$^+$) phenotype (**Figure 1C**), but some cells upregulated Foxp3 suggesting their differentiation into regulatory T cells (**Figure 1D**).

Sham or CLP surgery was performed on the remaining mice 30 days post-infection, and the number of total and 2W1S-specific CD4 T cells in the spleen were determined 2, 7, 14, and 28 days post-surgery by flow cytometry (**Figure 2A**). Our version of the CLP model results in ∼20% mortality within the first 4 days after surgery (**Figure 2B**). Despite this low overall mortality, the mice that underwent CLP show dramatic reductions in number of total CD4 T cells and 2W1S-specific memory CD4 T cells at 2 days post-surgery that gradually recovered by day 30 (**Figures 2C,D**), which is consistent with our previous data (39–42). Interestingly, the numerical recovery of the Foxp3$^+$ 2W1S-specific memory CD4 T cells occurred by day 7 post-CLP, while it took longer for the number of Tbet$^+$ 2W1S-specific memory CD4 T cells to return to sham levels (**Figures 2E,F**). Collectively, these data show pre-existing memory CD4 T cells experience a transient reduction in number during CLP-induced sepsis.

Loss and Recovery of Ag-Experienced Memory CD4 T Cells in Septic "Dirty" Mice

Most preclinical sepsis research done to date has used specific pathogen-free (SPF) mice, which possess an immune system equivalent to that of neonatal humans (23). The vaccinations and infections experienced over a lifetime shape the immune system so rapid and protective functional responses can occur during new microbial encounters. Recently, we investigated the effect of sepsis on standard SPF B6 mice cohoused for 60 days with microbially-experienced "dirty" pet store mice (24). Cohousing laboratory SPF mice with pet store mice permits physiological pathogen transfer and matures the murine immune system to more closely resemble that seen in adult humans (23). To determine the effect of sepsis on multiple memory CD4 T cell populations generated following environmental pathogen/commensal exposure, we performed sham or CLP surgery on cohoused B6 mice age-matched to their SPF counterparts (**Figure 3A**). Cohousing increases the frequency of circulating memory CD44^{hi} CD4 T cells (compared to age-matched SPF mice; **Figure 3B**), and the number of total CD4 T cells and CD44^{hi} memory CD4 T cells dramatically decline 2 days after CLP surgery (**Figures 3C,D**). We extended this analysis of the memory CD4 T cell compartment using a second, more-stringent phenotyping to identify true "Ag-experienced" memory CD4 T cells based on the upregulation of CD11a and CD49d (43). The cohoused mice showed a significant reduction in number of Ag-experienced (CD11$^+$CD4d$^+$) and naïve (CD11a$^-$CD49d$^-$) CD4 T cells in the spleen 2 days after CLP that returned to sham levels by day 30 (**Figures 3B–E**), indicating entire CD4 T cell compartment is susceptible to sepsis-induced numerical reduction. Thus, the data in **Figures 2**, **3** collectively show memory CD4 cells initially elicited by infection undergo a significant, but transient, numerical reduction in secondary lymphoid organs following CLP-induced sepsis.

Recall Response to Cognate Ag by Pre-existing Memory CD4 T Cells Is Reduced After Sepsis

Data in **Figure 2** show 2W1S-specific memory CD4 T cells numerically recover by day 30 post-sepsis. This result would suggest this population of Ag-specific memory CD4 T cells has returned to normal. However, the ability of pre-existing memory CD4 T cells to proliferate, accumulate, and exert effector functions after a second encounter with cognate Ag in the post-septic host has not been rigorously defined. Thus, we first examined the ability of this population of Ag-specific CD4 T cells to proliferate in response to cognate Ag recognition during secondary pathogen encounter. To do this, B6 mice were immunized with attenuated Lm-2W1S 30 days before sham or CLP surgery. The mice were then infected a second time with attenuated Lm-2W1S on day 2 or 30 after surgery. Total numbers of 2W1S-specific CD4 T cells in the spleen were determined before and after the second Lm-2W1S infection (**Figure 4A**). When infected on day 2 post-surgery, the 2W1S-specific CD4 T cells had significantly reduced proliferative capacity compared to sham-treated mice (**Figure 4B**). Specifically, the number of 2W1S-specific CD4 T cells in the sham-treated mice expanded 44-fold during the 7 days after secondary infection, but only 6-fold in the CLP-treated mice. However, when challenged on day 30 post-surgery, the proliferative capacity of the 2W1S-specific memory CD4 T cells in CLP-treated mice had nearly recovered to what was found in sham mice (**Figure 4C**). These data indicate the ability of Ag-specific memory CD4 T cells to proliferate during a recall response to cognate Ag (such as during a secondary infection) is only transiently reduced following sepsis.

To examine the effector function of the 2W1S-specific memory CD4 T cells at 2 and 30 days post-surgery, we used *in vivo* peptide restimulation where the Lm-2W1S-immune mice were injected i.v. with 2W1S peptide (27, 31–34). This technique permits the evaluation of cytokine production by Ag-specific (tetramer$^+$) CD4 T cells with almost no background staining. Spleens were harvested 4 h after 2W1S peptide injection and processed for flow cytometry to determine the frequency and number of cytokine-producing 2W1S-specific memory CD4 T

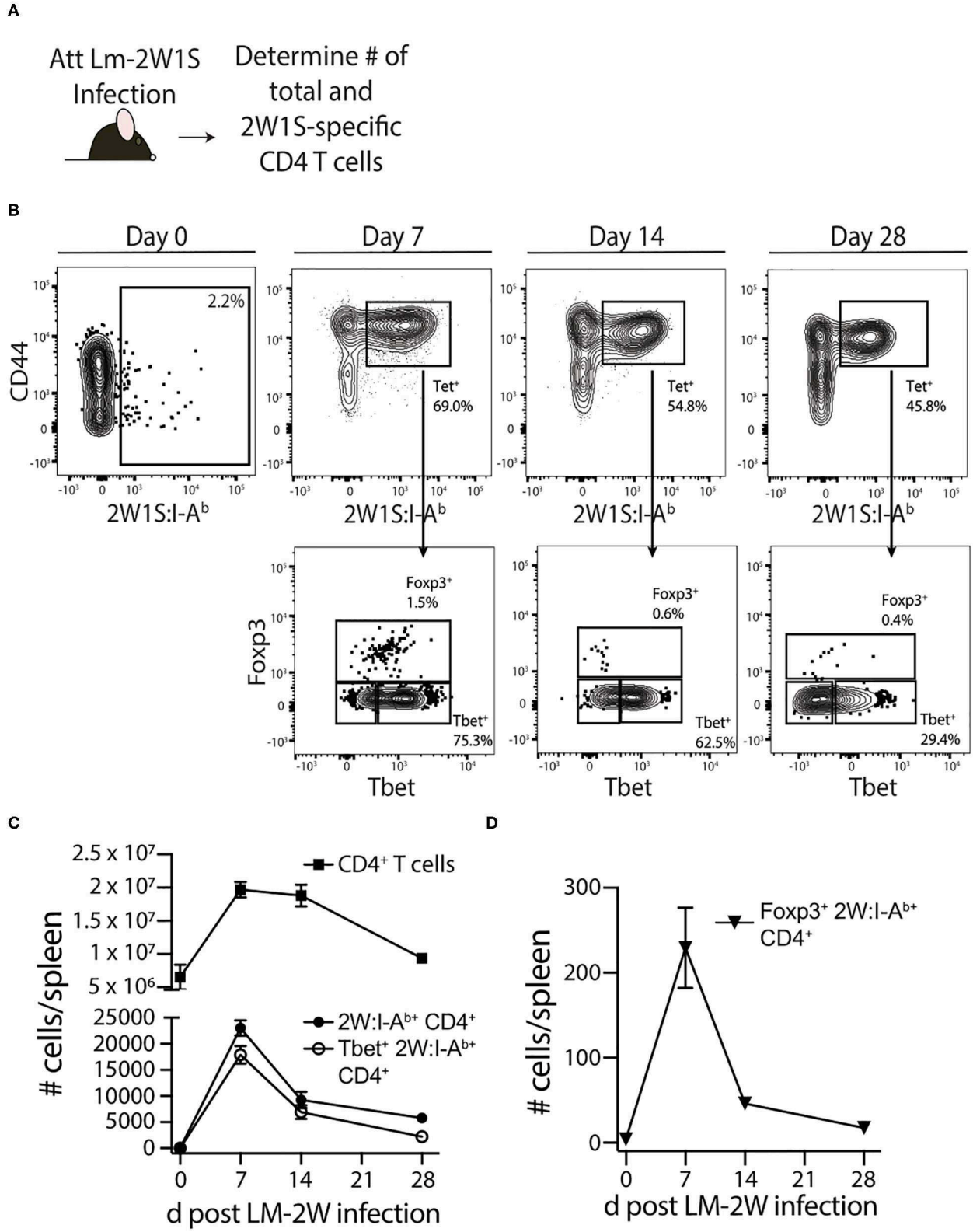

FIGURE 1 | Generation of Ag-specific memory CD4 T cells following attenuated *Listeria monocytogenes*-2W1S infection. **(A)** Experimental design—B6 mice were immunized with attenuated *Listeria monocytogenes*-2W1S (10^7 CFU i.v.). The number of 2W1S-specific CD4 T cells were determined before and after infection.

(Continued)

FIGURE 1 | (B) Representative flow plots show the gating strategy used to identify 2W1S:I-A^{b+} cells first identified as being $CD3^+$ and $CD4^+$. From the $tetramer^+$ gate, cells expressing the transcription factors Tbet (Th1 phenotype) or Foxp3 (regulatory T cell phenotype) were then identified. Positive and negative gating determined using FMO controls. The number of **(C)** total CD4 T cells, 2W1S-specific CD4 T cells, $Tbet^+$ 2W1S-specific CD4 T cells, and **(D)** $Foxp3^+$ 2W1S-specific CD4 T cells in the spleen was determined 7, 14, and 28 days after attenuated LM-2W1S infection. Data shown are representative from 3 independent experiments, with at least 3 mice/group/time point in each experiment.

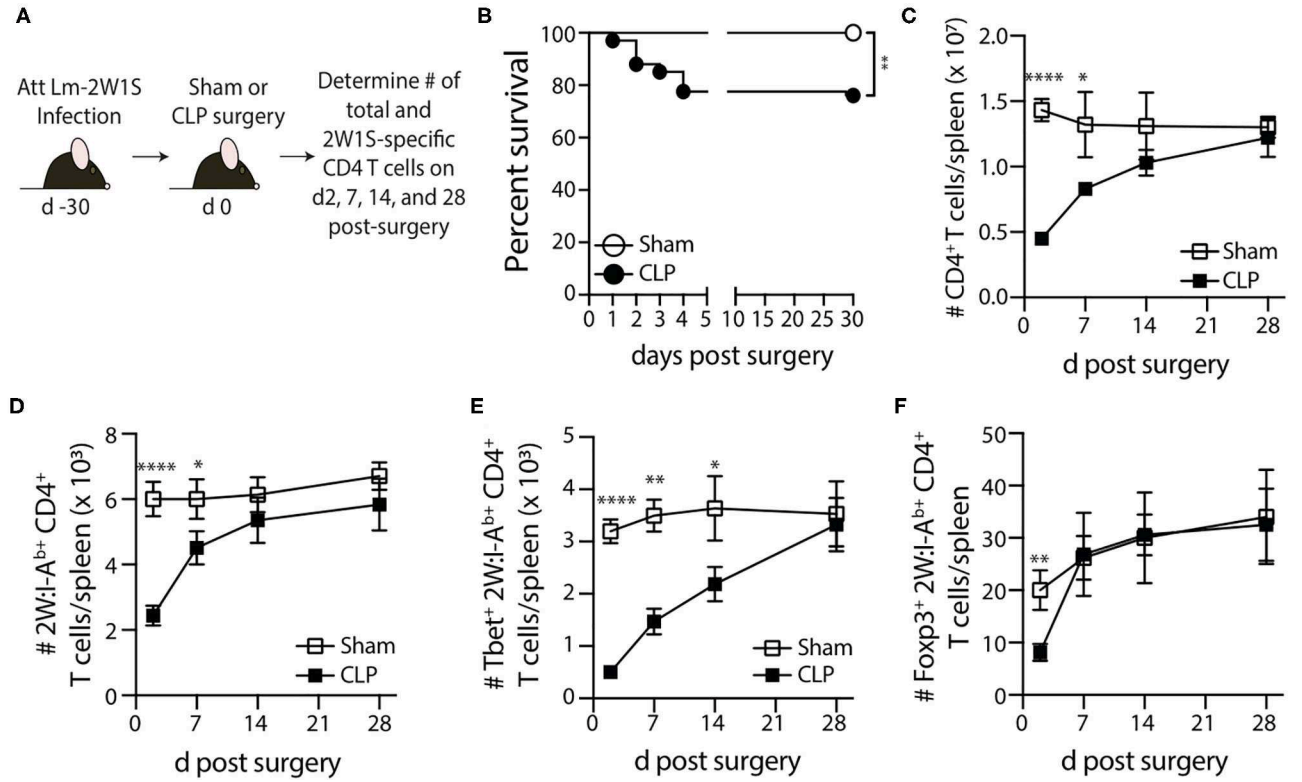

FIGURE 2 | Loss and recovery of 2W1S-specific memory CD4 T cells following CLP-induced sepsis. **(A)** Experimental design—B6 mice were immunized with attenuated *Listeria monocytogenes*-2W1S (10^7 CFU i.v.) 30 days before sham or CLP surgery. The number of 2W1S-specific CD4 T cells were determined after surgery. **(B)** Survival of LM-2W-infected B6 mice after sham and CLP surgery ($n = 29$ sham; $n = 67$ CLP). The number of **(C)** total CD4 T cells and **(D)** 2W1S-specific CD4 T cells in the spleen was determined 2, 7, 14, and 28 days after sham or CLP surgery by flow cytometry. In addition, the 2W1S-specific CD4 T cells were subtyped based on **(E)** Tbet (Th1 phenotype) and **(F)** Foxp3 (regulatory T cell phenotype) expression. Data shown are cumulative from 3 independent experiments, with at least 3 mice/group/time point in each experiment. $^*p \leq 0.05$, $^{**}p \leq 0.01$, $^{***}p \leq 0.005$, and $^{****}p \leq 0.001$.

cells. Lm infection primarily generates a Th1 response (44), therefore we identified the 2W1S-specific CD4 T cells making IFNγ, TNF, and IL-2 (**Figures 5A,B**). It is important to note the gating strategy employed permits the identification and analysis of bona fide memory CD4 T cells using 2W1S:I-A^b tetramers that helps us determine the "per cell" capacity of those cells to produce cytokines. Similar to what was observed with the reduction in proliferative capacity seen 2 days post-CLP-induced sepsis, the frequency and number of single or multi-cytokine producing 2W1S-specific memory CD4 T cells ($IFN\gamma^+$-, $IFN\gamma^+TNF^+$-, and $IFN\gamma^+TNF^+IL\text{-}2^+$) was significantly reduced at 2 days post-surgery (**Figures 5C,D**) and remained reduced 30 days after CLP. Interestingly, when we looked at the 2W1S-specific memory CD4 T cells only making IL-2 30 days after CLP surgery, the frequency and number of $IL\text{-}2^+$ 2W1S-specific memory CD4 T cells was similar to that seen in sham-treated mice (**Figures 5E,F**). This data is consistent with that in **Figure 4**, where we saw a restoration in proliferative capacity at day 30 post-CLP. Together, these data indicate prolonged impairment in the ability of the 2W1S-specific memory CD4 T cells to produce cytokines critical for pathogen clearing immunity when re-stimulated in an Ag-specific manner, despite recovery of cell numbers, and proliferative capacity (by day 30).

Sepsis Impairs Memory CD4 T Cell-Mediated Immunity to Infection

Our data show 2W1S-specific memory CD4 T cells numerically recover by 30 days after CLP surgery, but their ability to produce effector cytokines after re-stimulation remains blunted, suggesting a potential lesion in protective capacity following re-infection. To test this, we wanted to challenge post-septic mice with a virulent pathogen. Our experiments thus far have

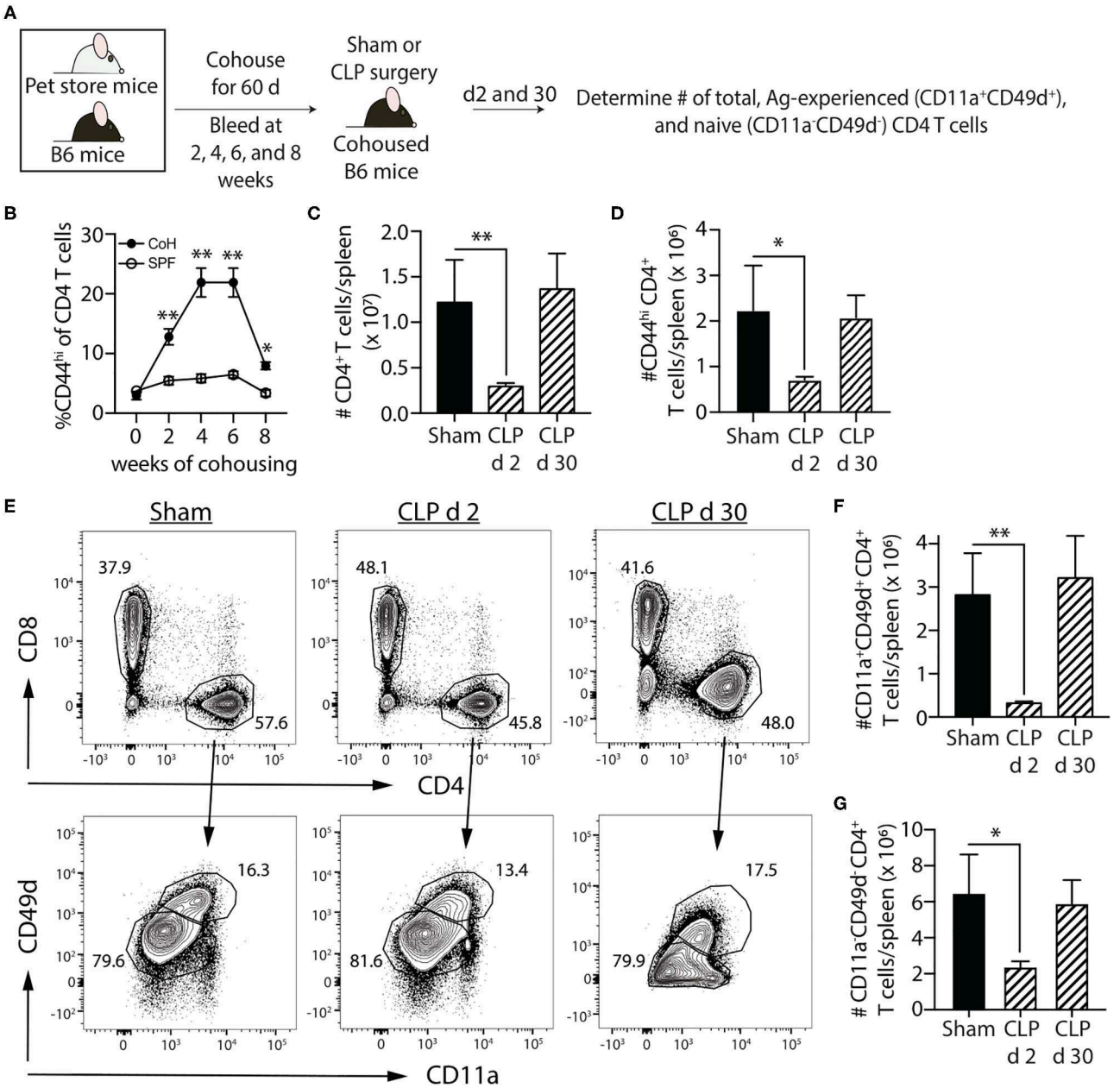

FIGURE 3 | Sepsis induces transient loss in number of pre-existing "Ag-experienced" CD4 T cells in microbially-experienced "dirty" mice. **(A)** Experimental design—SPF B6 mice were cohoused with pet store mice for 60 days to permit microbe transfer and immune system maturation. **(B)** Age-matched SPF and cohoused (CoH) mice were bled prior to and at 2, 4, 6, and 8 weeks after cohousing to determine the frequency of $CD44^{hi}$ CD4 T cells. **(C–G)** Sham or CLP surgery was performed on cohoused B6 mice. The number of total, $CD44^{hi}$, $CD11a^{+}CD49d^{+}$ "Ag-experienced," and $CD11a^{-}CD49d^{-}$ naive CD4 T cells in the spleen was determined 2 and 30 days post-surgery by flow cytometry. **(E)** Representative flow plots show gating strategy. Positive and negative gating determined using FMO controls. The number of **(C)** total, **(D)** $CD11a^{+}CD49d^{+}$, and **(E)** $CD11a^{-}CD49d^{-}$ CD4 T cells was determined. Data shown are representative of 2 independent experiments, with at least 4 mice/group in each experiment. $^{*}p \leq 0.05$ and $^{**}p \leq 0.01$.

used attenuated Lm-2W1S to generate a trackable population of endogenous memory Ag-specific CD4 T cells; however, no virulent form of Lm-2W1S exists. Therefore, in the following experiments we employed two different murine models of infection using virulent bacterial strains. It is important to note that while the bacteria strains selected are pathogens not typically found in human septic patients, their use as experimental pathogens is well-established and modification to express known $I\text{-}A^{b}$-restricted epitopes allow us to examine distinct, Ag-specific CD4 T cell responses after CLP. In the first model, we generated 2W1S-specific memory CD4 T cells by infecting mice with attenuated *Salmonella enterica* engineered to express the 2W1S

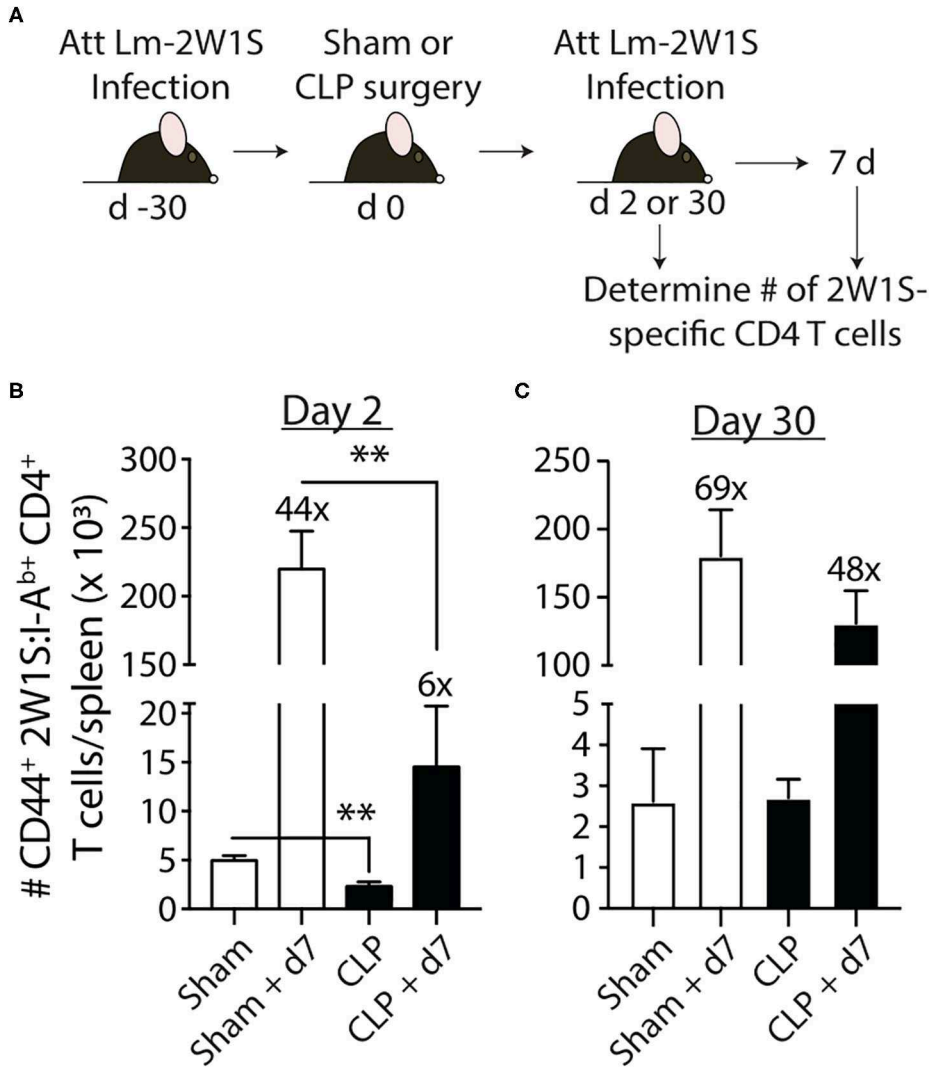

FIGURE 4 | Sepsis impairs the recall response by pre-existing 2W1S-specific memory CD4 T cells to cognate Ag. **(A)** Experimental design—B6 mice were immunized with attenuated *L. monocytogenes*-2W1S (10^7 CFU i.v.) 30 days before sham or CLP surgery. The mice were given a second infection with attenuated *L. monocytogenes*-2W1S (10^7 CFU i.v.) **(B)** 2 or **(C)** 30 days after surgery. Total number of 2W1S-specific CD4 T cells in the spleen was determined the day of and 7 days after the second LM-2W1S infection (10^7 CFU i.v.). The fold increase in cell numbers at day 7 post-secondary infection is indicated. Data shown are representative of 2 independent experiments, with 4 mice/group in each experiment. $^{**}p \leq 0.01$.

epitope (*Se*-2W). *Salmonella*-2W1S infection stimulates a robust Ag-specific CD4 T cell response (33, 45) because the bacteria replicate in the phagosomes of dendritic cells and macrophages—the location of peptide:MHC II complex formation (28, 46–49). Moreover, mice immunized with *Salmonella*-2W1S demonstrate protective immunity to a secondary infection with virulent *Salmonella* (45). To confirm the importance of *Salmonella*-specific memory CD4 T cells in the protection to virulent *Salmonella* infection, some of the *Se*-2W-infected mice were depleted of CD4 T cells (using the anti-CD4 mAb GK1.5) prior to a second infection of virulent *Se*-2W (**Figure 6A**). CD4 T cell-replete mice infected with attenuated *Se*-2W had significantly lower pathogen burdens after secondary virulent *Se*-2W infection compared to the CD4 T cell-depleted mice (**Figure 6B**), and had pathogen burdens comparable to that seen in naïve mice only infected with virulent *Se*-2W. We then performed sham or CLP surgery on a separate cohort of mice infected with attenuated *Se*-2W 30 days prior to surgery. On days 2 or 30 after surgery, all groups were infected with virulent *Se*-2W. Splenic bacterial titers were determined 7 days after virulent *Se*-2W infection, revealing higher burdens in the CLP-treated mice regardless of early or late secondary challenge (**Figures 6C,D**).

In the second model, naïve mice were infected with attenuated Lm engineered to express OVA (Lm-OVA) to elicit OVA_{323}-specific memory CD4 T cells (50). We tested the ability of the OVA_{323}-specific memory CD4 T cells to provide protection

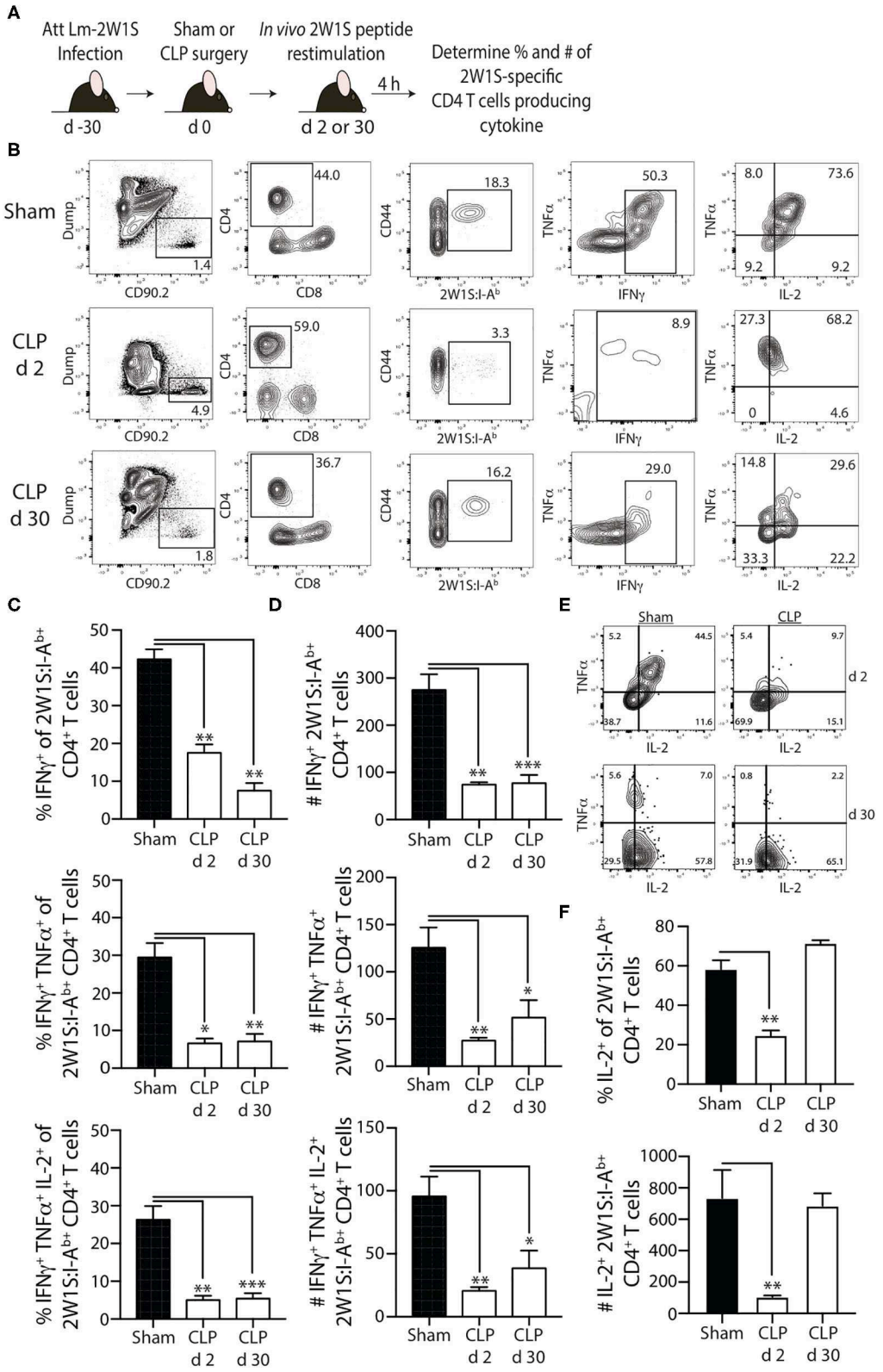

FIGURE 5 | Sepsis impairs the ability of 2W1S-specific memory CD4 T cells to produce effector cytokines after *in vivo* cognate Ag restimulation. **(A)** Experimental design—B6 mice were immunized with attenuated *L. monocytogenes*-2W1S (10^7 CFU i.v.) 30 days before sham or CLP surgery. Mice were injected with 2W1S

(Continued)

FIGURE 5 | peptide (100 μg i.v.) 2 or 30 days after surgery to restimulate the 2W1S-specific memory CD4 T cells. Spleens were harvested 4 h later, and the frequency and number of IFNγ$^+$, IFNγ$^+$TNFα$^+$, and IFNγ$^+$TNFα$^+$IL-2$^+$ 2W1S-specific CD4 T cells was determined by flow cytometry. **(B)** Representative flow plots of intracellular IFNγ, TNFα, and IL-2 detection in CD44^{hi}2W1S:I-A^{b+} CD4 T cells after *in vivo* peptide restimulation. Plots show cells gated from 2W:I-A^b-enriched CD4 T cells from sham- or CLP-treated mice. Positive and negative gating determined using FMO controls. Frequency **(C)** and number **(D)** of CD44^{hi}2W1S:I-A^{b+}-specific CD4 T cells in the spleen producing IFNγ, IFNγ/TNFα, and IFNγ/TNFα/IL-2. **(E)** Representative flow plots of intracellular IL-2 detection in CD44^{hi}2W1S:I-A^{b+} CD4 T cells after *in vivo* peptide restimulation. Plots show cells gated from 2W:I-A^b-enriched CD4 T cells from sham- or CLP-treated mice. Positive and negative gating determined using FMO controls. **(F)** Frequency and number of CD44^{hi}2W1S:I-A^{b+}-specific CD4 T cells in the spleen producing IL-2. Data shown are representative of 2 independent experiments, with at least 4 mice/group in each experiment. *$p \leq 0.05$, **$p \leq 0.01$, and ***$p \leq 0.005$.

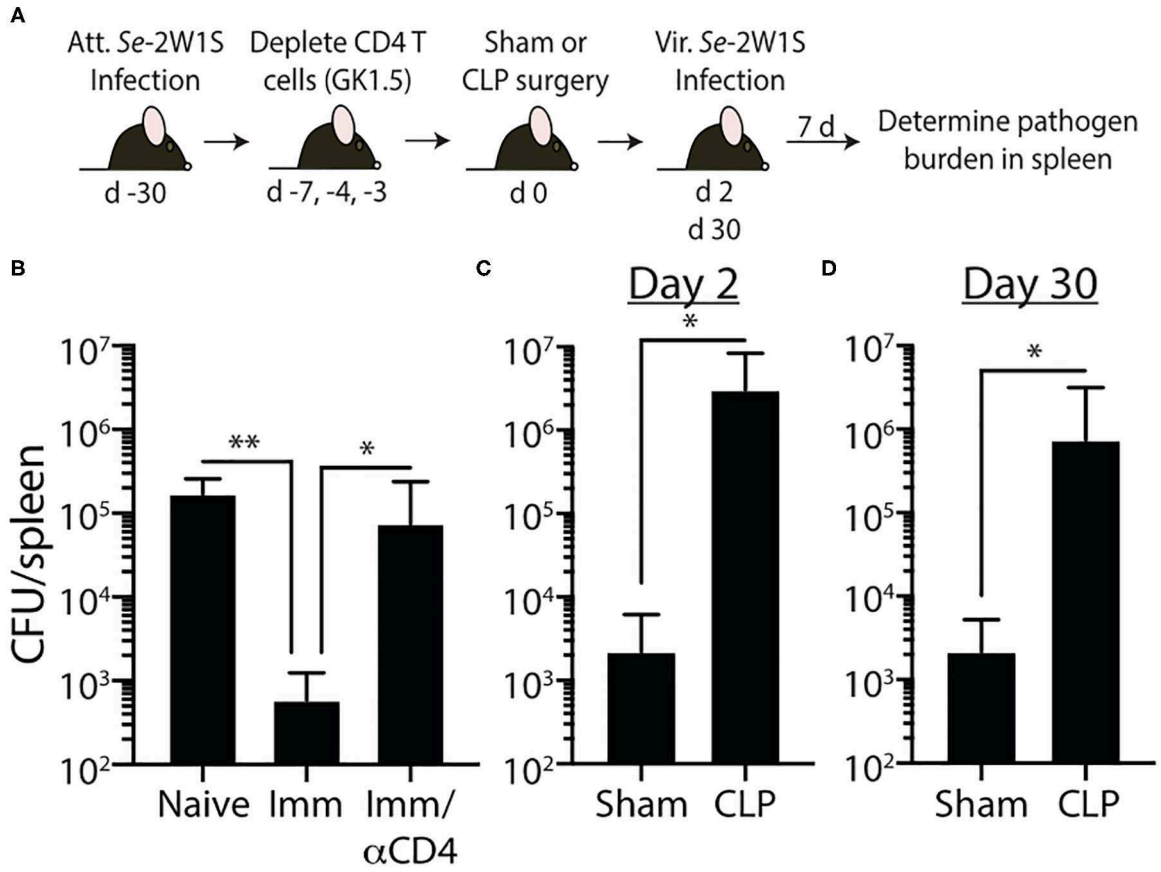

FIGURE 6 | Impaired 2W1S-specific memory CD4 T cell-mediated immunity to secondary *Salmonella*-2W1S infection after CLP-induced sepsis. **(A)** Experimental design—B6 mice were immunized with attenuated *Salmonella enterica* strain BRD509-2W1S (*Se*-2W1S; AroA$^-$; 10^6 CFU i.v.) 30 d before sham or CLP surgery. **(B)** One group of mice (Imm/αCD4) was depleted of CD4 T cells by injecting anti-CD4 mAb GK1.5 i.v. (800 μg on day -7, and 400 μg on days −4 and −3) before second infection with virulent *Salmonella*-2W1S (10^3 CFU i.v.). Bacterial titers in the spleen were determined 7 days later. **(C–D)** In separate cohorts of attenuated *Se*-2W1S infected mice, sham or CLP surgery was performed. These mice were then challenged with virulent *Se*-2W1S (10^3 CFU i.v.) **(C)** 2 or **(D)** 30 days after surgery. Bacterial titers in the spleen were determined 7 days later. Data shown are representative of 3 independent experiments, with at least 5 mice/group in each experiment. *$p \leq 0.05$, **$p \leq 0.01$.

against a secondary Lm-OVA infection after sepsis induction. The adaptive immune system does not confer protection against primary Lm infections after CLP (51). CD8 T cells play prominent roles in controlling and eradicating secondary infections by intracellular pathogens that mainly localize to the cytosol of the infected cell, such as *L. monocytogenes* (52), due to the efficient production of peptide:MHC I complexes by the infected cell. However, Lm-specific CD4 T cells can provide sufficient protection to infection even in the absence of CD8 T cells (53–55). Thus, to focus on the memory CD4 T cell-mediated clearance of Lm-OVA, CD8 T cells were depleted using anti-CD8 mAb (clone 2.43) prior to performing sham of CLP surgery (**Figures 7A,B**). Two days later the mice were infected with virulent Lm-OVA, after which pathogen burden in the liver and spleen was determined. A separate group of naïve, CD8-depleted mice were infected with virulent Lm-OVA for reference. As expected, we saw substantially reduced Lm-OVA burden in both the liver and spleen compared to infected naïve

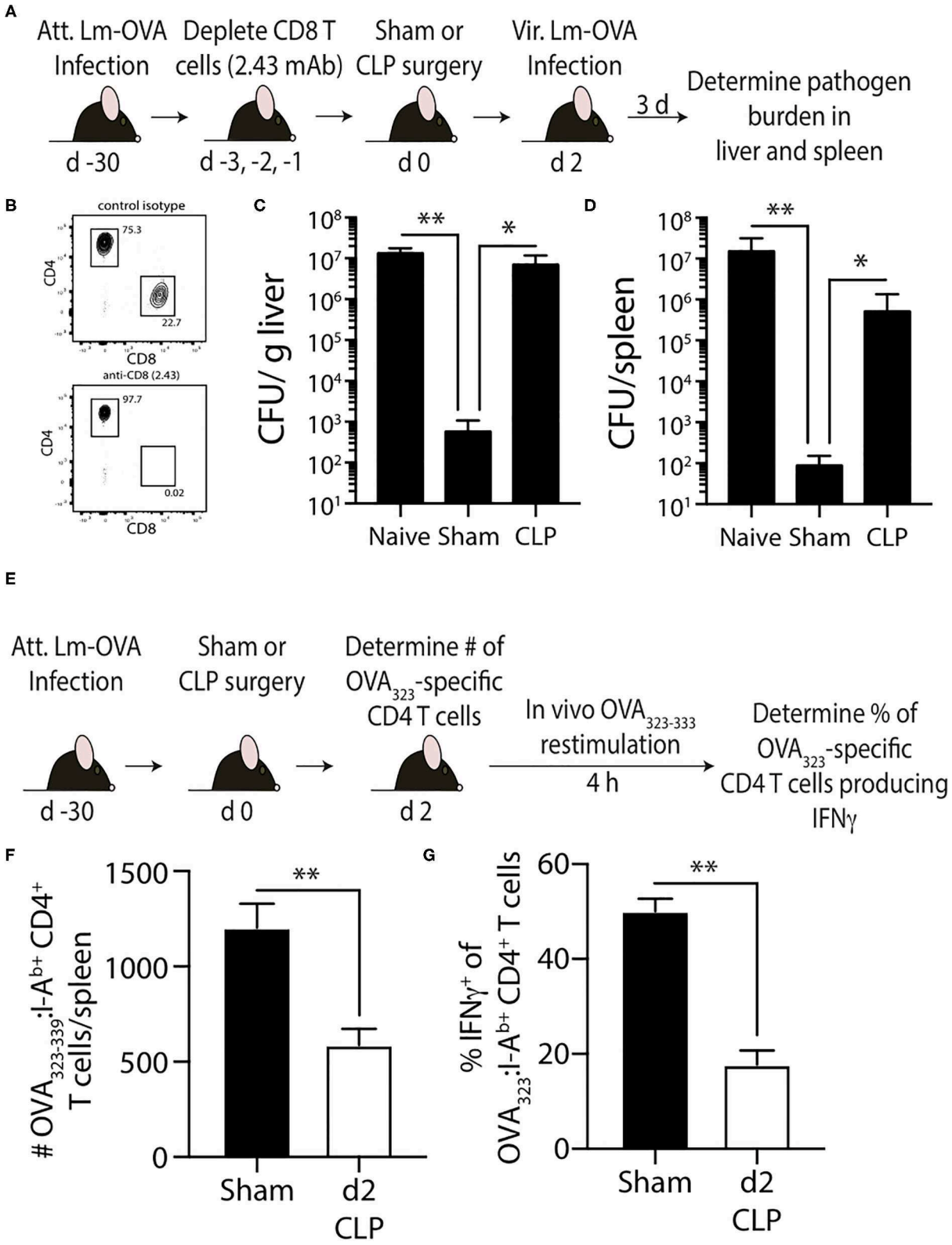

FIGURE 7 | Effect of sepsis on $OVA_{323-339}$-specific memory CD4 T cells. **(A)** Experimental design—B6 mice were infected with attenuated *L. monocytogenes*-OVA (LM-OVA; 10^7 CFU i.v.) 30 d before sham or CLP surgery. Mice in the naïve, sham, and CLP groups were depleted of CD8 T cells by injecting 100 μg anti-CD8 mAb

(Continued)

FIGURE 7 | (clone 2.43) i.v. 3, 2, and 1 days prior to surgery. **(B)** A small amount of blood was collected from the anti-CD8 mAb-treated mice on the day of surgery and staining for CD4 and CD8 T cells. Representative flow plots show the extent of CD8 T cell depletion compared to a reference mouse injected with a control isotype mAb. **(C,D)** The mice were infected with virulent LM-OVA (10^4 CFU i.v.) 2 days after surgery. Bacterial titers in the liver and spleen were determined 3 days post-vir LM-OVA infection. Data shown are representative of 2 independent experiments, with at least 5 mice/group in each experiment. $^*p \leq 0.05$ and $^{**}p < 0.01$. **(E)** Experimental design—B6 mice were infected with attenuated *L. monocytogenes*-OVA (LM-OVA; 10^7 CFU i.v.) 30 d before sham or CLP surgery. **(F)** On day 2 post-surgery, the number of $OVA_{323-339}$-specific memory CD4 T cells in the spleen were determined. **(G)** A separate cohort of mice were injected with $OVA_{323-339}$ peptide (100 μg i.v.) 2 days after surgery to restimulate the $OVA_{323-339}$-specific memory CD4 T cells. Spleens were harvested 4 h later, and the frequency of $IFN\gamma^+$ $OVA_{323-339}$-specific CD4 T cells was determined by flow cytometry. Data shown are representative of 2 independent experiments, with at least 5 mice/group in each experiment. $^{**}p < 0.01$.

mice (**Figures 7C,D**). In contrast, the Lm-OVA burdens were dramatically higher in the CLP-treated mice compared to sham mice. To better understand the cause for this reduced protection, we examined the impact of sepsis on the number and function of the OVA_{323}-specific memory CD4 T cells (**Figure 7E**). Just as seen with the 2W1S-specific memory CD4 T cells, CLP-induced sepsis led to a significant reduction in OVA_{323}-specific memory CD4 T cell numbers and ability to produce IFNγ after *in vivo* restimulation (**Figures 7F,G**). Together, the data in **Figures 5**, **6** show the sepsis-induced long-lasting changes in Ag-specific memory CD4 T cell pools that ultimately impact the ability of the host to properly respond to pathogen re-infection.

DISCUSSION

Sepsis causes millions of deaths annually (1, 56, 57), and the incidence of sepsis has increased dramatically in recent decades. Understanding the cellular mechanisms that contribute to sepsis-induced immunosuppression is critical for developing effective therapies and improving the survival and quality of life for septic patients. CD4 T cells have the unique flexibility of functioning in an array of immunological settings due to their ability to differentiate into a variety of phenotypic subsets based on the inflammatory milieu produced at the time of primary Ag encounter (58, 59). Clinical data show considerable reduction in number of circulating CD4 T cells (along with other lymphocyte populations) in sepsis patients of all ages (13, 60–62) and at the time of high pathogen burden (63, 64). Moreover, reports of decreased effector CD4 T cell function in critically ill sepsis patients date back to the 1970's with data showing impaired DTH reactions (35). These observations and the fact that DTH is mediated in large part by CD4 T cells (65) bring into question to what extent memory CD4 T cells are numerically and functionally affected by sepsis. However, most (if not all) of the previous studies examined the effect of sepsis on the CD4 T cell compartment in sum, which has the potential to mask some of the unique characteristics of individual Ag-specific populations (34). In contrast to these previous publications, the present study took advantage of pathogens engineered to express defined CD4 T cell epitopes to stimulate the generation of bona fide memory CD4 T cells and reagents to identify and quantitatively and qualitatively evaluate endogenous Ag-specific memory CD4 T cells that have experienced a septic event. As a complement to the experiments using conventional laboratory mice infected with a known experimental pathogen to generate Ag-specific memory CD4 T cells, our "dirty" mouse model allowed us to investigate how multiple populations of memory CD4 T cells are affected during sepsis in an animal with a more adult human-like immune system (23, 24, 66). Together, the experimental model systems used provided a unique means by which sepsis-induced immunoparalysis of memory CD4 T cells was evaluated.

One area of sepsis research that has received considerable attention recently deals with the idea that sepsis may differentially affect naïve and memory T cells. Indeed, there is data to suggest memory CD8 T cells are more resistant to radiation-induced apoptosis than naive cells (67). Cellular apoptotic mechanisms induced by extrinsic (i.e., death receptor) and intrinsic (i.e., mitochondrial) pathways have been suggested to be major contributors to the numerical reduction in total CD4 and CD8 T cells following sepsis (68), but the definitive molecule responsible for initiating lymphocyte apoptosis during sepsis has yet to be indentified. Regardless of the mechanism by which sepsis-induced lymphopenia occurs, studies from a number of laboratories using proven experimental infection models for eliciting Ag-specific memory T cells indicate circulating Ag-experienced memory CD8 T cells are equally susceptible to sepsis-induced attrition as naïve CD8 T cells (26, 69–71). In addition, the circulating memory CD8 T cells exhibit profound impairment in effector functionality (e.g., decreased Ag sensitivity, proliferative capacity, cytokine production, and inability to clear secondary infections) following a septic event (72). The numerical and functional decrease in circulating memory CD8 T cells is not, interestingly, reciprocated in tissue-resident memory CD8 T cells after a moderate sepsis insult that leads to <10% mortality (71). The number of tissue-resident memory CD8 T cells is maintained after sepsis, as well as their ability to produce effector cytokine after re-stimulation. In contrast to the aforementioned similar attrition of naïve and memory CD8 T cells after sepsis, it was recently suggested by Xie et al. that $CD44^{hi}$ CD8 T cells in "memory mice" (generated via *Listeria* and LCMV infection) exhibited significant attrition after CLP while this was not the case for naïve $CD44^{lo}$ CD8 T cells (73). It was surprising to see that CLP sepsis did not lead to a reduction in $CD44^{lo}$ CD8 T cells, as such a reduction has been noted in other papers (14, 39, 40, 74–77). Moreover, these authors examined the bulk CD8 T cell compartment, even though peptide:MHC I tetramers were available to identify LCMV-specific CD8 T cells. The authors also detected increased expression of CD25, PD-1, and 2B4 on the memory CD8 T cells, but did not perform any studies to directly determine if and/or how these proteins may be altering T cell sensitivity to sepsis-induced attention. Needless to say, additional data

is needed to conclusively determine the extent of naïve and memory CD8 T cells sensitivity to CLP-induced apoptosis and the potential role played by intrinsic factors (e.g., CD25, PD-1, 2B4, and other proteins) in regulating this sensitivity.

Fewer studies have examined the effect of sepsis on Ag-experienced memory CD4 T cells compared to what has been done for memory CD8 T cells, driving our interest in the current set of experiments. Contrary to the increased susceptibility of memory $CD44^{hi}$ CD8 T cells (vs. naïve $CD44^{lo}$ CD8 T cells) to sepsis-induced apoptosis suggested by Xie et al. (73), data presented by these authors suggested $CD44^{hi}$ CD4 T cells were not more sensitive to attrition during sepsis compared to $CD44^{lo}$ CD4 T cells. As with their CD8 T cell data, the CD4 T cells were examined at the bulk (non-Ag-specific) level. Some of the data presented herein are consistent with the data by Xie et al., but there are some important differences in our study that are worth noting. First, our data show CLP-induced sepsis results in a transient numerical reduction of 2W1S-specific memory CD4 T cells (current study), while 2W1S-specific naive CD4 T cells suffer from prolonged numerical reduction (34). Second, while the numerical reduction was transient, the inability of the 2W1S-specific memory CD4 T cells to produce cytokines upon peptide restimulation was evident out to day 30 post-CLP, similar to what was observed in naïve cells (34). Cytokine "help" from CD4 T cells is a hallmark of this population of immune cells, and the prolonged dysfunction in cytokine production may contribute the generalized immunoparalysis seen during sepsis. Furthermore, the *in vivo* peptide restimulation assay used is a more physiological way of activating the desired Ag-specific population via MHC II presentation of peptide Ag (31–34). Third, despite their reduced ability to produce cytokines at day 30-post-sepsis, 2W1S-specific memory CD4 T cells were surprisingly able to expand upon Ag re-encounter 30 days after CLP to nearly sham levels. It is important to note that the accumulation/expansion of Ag-specific effector CD4 T cells upon Ag re-encounter is dependent on the rate of proliferation (leading to an increase in cell accumulation) and rate of death (decrease in accumulation). We did not measure either of these parameters; however, impairment is clearly seen in day 2 septic mice undergoing secondary challenge since the fold-expansion in numbers from pre-challenge level was significantly diminished (6x compared to 44x—see **Figure 4**). It is reasonable to suggest that the reduction in accumulation of memory CD4 T cells following a second encounter with cognate Ag to be due to decreased per-cell proliferation, increased death, or both. Together, our data show the 2W1S-specific memory population is similarly prone to the initial sepsis-induced depletion and prolonged inability to produce important inflammatory cytokines compared to their naïve counterparts. However, unlike naïve 2W1S-specific CD4 T cells, Ag-experienced memory 2W1S-specific CD4 T cells quickly recover numerically, as well as their ability to proliferate in response to a secondary infection. It remains to be determined how sepsis affects the number and function of tissue-resident memory CD4 T cells. Moreover, the different recovery rates between the memory and regulatory $Foxp3^{+}$ CD4 T cell populations could suggest additional time-dependent mechanisms that control the ability of sepsis survivors to respond to secondary infection. There have been a few reports specifically looking at the role of regulatory $Foxp3^{+}$ CD4 T cells in sepsis (78–80), and while these data hint at the participation of this CD4 T cell subset in sepsis-induced immune suppression additional evaluation is needed to better define how regulatory CD4 T cells are maintained and function in the post-septic host.

Our data collectively show CLP-induced sepsis results in a transient numerical reduction and long-term functional deficits of Ag-specific memory CD4 T cells, which contributes to the characteristic long-lasting immunoparalysis seen after sepsis and reduced protection to secondary infection. Secondary infection after sepsis, acquired while in the hospital or after discharge, is a leading cause of sepsis mortality (81–84). Lungs, blood stream, surgical site/soft tissue, and urinary tract are the most sites of secondary infection in septic patients, with *Pseudomonas* spp., *Staphylococcus* spp., *Candida albicans*, *E. coli*, and *Enterococcus* spp. being common secondary infection microbes (85). We recognize that the experimental pathogens used in this study (to establish either the primary or secondary infection) are not the "typical" pathogens found in sepsis patients. We chose to use *Listeria* and *Salmonella* for the following reasons: (1) both are well-established model pathogens for examining the immune response to bacteria, where attenuated strains are available for generating memory T cells and virulent strains are available to assess the protective capacity of the memory T cells; (2) *Listeria* and *Salmonella* infection stimulates a robust Ag-specific CD4 T cell response because the bacteria replicate in the phagosomes of dendritic cells and macrophages—the location of peptide:MHC II complex formation; and (3) the recombinant *Listeria* and *Salmonella* strains express known I-A^{b}-restricted epitopes. Future studies could include engineering recombinant *P. aeruginosa*, *S. aureus*, and/or *S. pneumonia* to express the 2W1S (or some other) epitope that will enable testing of the 2W1S-specific memory CD4 T cell response in CLP-treated mice given a secondary infection with a clinically-relevant pathogen after recovery from the initial septic event. It is also important to note that while our study exclusively examined the *in vivo* function of memory CD4 T cells after sepsis, other publications have shown the environment is also a critical factor in sepsis-induced suppression of T cells (86). Following sepsis, a number of CD4 T cell extrinsic factors have been found to suppress the activity of CD4 T cells, including the reduced APC function and TNF signaling (79, 86). Sepsis also leads to dysfunction of the innate immune system, including impaired bacterial clearance by neutrophils, leading to increased susceptibility to *P. aeruginosa* and *S. aureus* (51, 87). Future studies could investigate the extent to which sepsis impairs innate immune responses, especially those related to trained innate immunity, in microbially-experienced mice containing a high frequency of Ag-experienced memory T cells.

In summary, our experiments have uncovered differences in recovery and function within the endogenous memory CD4 T cell compartment compared to what has been detected at the "bulk" CD4 T cell level. The data presented here

will serve as the foundation for a number of future studies examining the behavior of endogenous, Ag-experienced memory CD4 T cells in the septic host, as well as methods of reversing the immunoparalysis typically observed within this population of immune cells vital to overall immune system fitness.

DATA AVAILABILITY STATEMENT

All datasets generated for this study are included in the article/supplementary material.

ETHICS STATEMENT

This animal study was reviewed and approved by University of Minnesota Institutional Animal Care and Use Committees.

AUTHOR CONTRIBUTIONS

FS, TK, TD, WS, CD, JC-P, KM, and TG performed experiments and analyzed data. VB and TG provided input on the research design. FS, VB, and TG wrote and edited the manuscript. All authors read and approved the submitted version.

FUNDING

This work was supported by National Institutes of Health grants R01GM115462 (TG), R01AIGM113961 (VB), R35GM134880 (VB), T32CA009138 (FS), T32AI007313 (FS and JC-P), T35AI118620 (CD), and a Veterans Administration Merit Review Award (I01BX001324; TG). This work was also supported in part by NIH P30 CA77598 utilizing the Masonic Cancer Center, University of Minnesota Flow Cytometry shared resource.

REFERENCES

1. Shankar-Hari M, Phillips GS, Levy ML, Seymour CW, Liu VX, Deutschman CS, et al. Developing a new definition and assessing new clinical criteria for septic shock: for the third international consensus definitions for sepsis and septic shock (Sepsis-3). *JAMA*. (2016) 315:775–87. doi: 10.1001/jama.2016.0289
2. Brun-Buisson C, Doyon F, Carlet J, Dellamonica P, Gouin F, Lepoutre A, et al. Incidence, risk factors, and outcome of severe sepsis and septic shock in adults. A multicenter prospective study in intensive care units French ICU Group for Severe Sepsis. *JAMA*. (1995) 274:968–74. doi: 10.1001/jama.1995.03530120060042
3. Levy MM, Fink MP, Marshall JC, Abraham E, Angus D, Cook D, et al. 2001 SCCM/ESICM/ACCP/ATS/SIS international sepsis definitions conference. *Intensive Care Med.* (2001) 29:530–8. doi: 10.1007/s00134-003-1662-x
4. Hotchkiss RS, Nicholson DW. Apoptosis and caspases regulate death and inflammation in sepsis. *Nat Rev Immunol.* (2006) 6:813–22. doi: 10.1038/nri1943
5. Rittirsch D, Flierl MA, Ward PA. Harmful molecular mechanisms in sepsis. *Nat Rev Immunol.* (2008) 8:776–87. doi: 10.1038/nri2402
6. Hotchkiss RS, Monneret G, Payen D. Sepsis-induced immunosuppression: from cellular dysfunctions to immunotherapy. *Nat Rev Immunol.* (2013) 13:862–74. doi: 10.1038/nri3552
7. Sasser SM, Varghese M, Joshipura M, Kellermann A. Preventing death and disability through the timely provision of prehospital trauma care. *Bull World Health Organ.* (2006) 84:507. doi: 10.2471/BLT.06.033605
8. Probst C, Pape HC, Hildebrand F, Regel G, Mahlke L, Giannoudis P, et al. 30 years of polytrauma care: an analysis of the change in strategies and results of 4849 cases treated at a single institution. *Injury*. (2009) 40:77–83. doi: 10.1016/j.injury.2008.10.004
9. Probst C, Zelle BA, Sittaro NA, Lohse R, Krettek C, Pape HC. Late death after multiple severe trauma: when does it occur and what are the causes? *J Trauma*. (2009) 66:1212–7. doi: 10.1097/TA.0b013e318197b97c
10. Gentile LF, Cuenca AG, Efron PA, Ang D, Bihorac A, Mckinley BA, et al. Persistent inflammation and immunosuppression: a common syndrome and new horizon for surgical intensive care. *J Trauma Acute Care Surg.* (2012) 72:1491–501. doi: 10.1097/TA.0b013e318256e000
11. Hotchkiss RS, Monneret G, Payen D. Immunosuppression in sepsis: a novel understanding of the disorder and a new therapeutic approach. *Lancet Infect Dis.* (2013) 13:260–8. doi: 10.1016/S1473-3099(13)70001-X
12. Jensen IJ, Sjaastad FV, Griffith TS, Badovinac VP. Sepsis-induced T cell immunoparalysis: the ins and outs of impaired T cell immunity. *J Immunol.* (2018) 200:1543–53. doi: 10.4049/jimmunol.1701618
13. Hotchkiss RS, Tinsley KW, Swanson PE, Schmieg RE Jr, Hui JJ, Chang KC, et al. Sepsis-induced apoptosis causes progressive profound depletion of B and CD4+ T lymphocytes in humans. *J Immunol.* (2001) 166:6952–63. doi: 10.4049/jimmunol.166.11.6952
14. Unsinger J, Kazama H, Mcdonough JS, Hotchkiss RS, Ferguson TA. Differential lymphopenia-induced homeostatic proliferation for CD4+ and CD8+ T cells following septic injury. *J Leukoc Biol.* (2009) 85:382–90. doi: 10.1189/jlb.0808491
15. Pepper M, Jenkins MK. Origins of CD4(+) effector and central memory T cells. *Nat Immunol.* (2011) 12:467–71. doi: 10.1038/ni.2038
16. Kaech SM, Wherry EJ, Ahmed R. Effector and memory T-cell differentiation: implications for vaccine development. *Nat Rev Immunol.* (2002) 2:251–62. doi: 10.1038/nri778
17. Harty JT, Badovinac VP. Shaping and reshaping CD8+ T-cell memory. *Nat Rev Immunol.* (2008) 8:107–19. doi: 10.1038/nri2251
18. Schenkel JM, Masopust D. Tissue-resident memory T cells. *Immunity*. (2014) 41:886–97. doi: 10.1016/j.immuni.2014.12.007
19. Beura LK, Fares-Frederickson NJ, Steinert EM, Scott MC, Thompson EA, Fraser KA, et al. CD4(+) resident memory T cells dominate immunosurveillance and orchestrate local recall responses. *J Exp Med.* (2019) 216:1214–29. doi: 10.1084/jem.20181365
20. Taylor JJ, Jenkins MK. CD4+ memory T cell survival. *Curr Opin Immunol.* (2011) 23:319–23. doi: 10.1016/j.coi.2011.03.010
21. Condotta SA, Cabrera-Perez J, Badovinac VP, Griffith TS. T-cell-mediated immunity and the role of TRAIL in sepsis-induced immunosuppression. *Crit Rev Immunol.* (2013) 33:23–40. doi: 10.1615/CritRevImmunol.2013006721
22. Cabrera-Perez J, Condotta SA, Badovinac VP, Griffith TS. Impact of sepsis on CD4 T cell immunity. *J Leukoc Biol.* (2014) 96:767–77. doi: 10.1189/jlb.5MR0114-067R
23. Beura LK, Hamilton SE, Bi K, Schenkel JM, Odumade OA, Casey KA, et al. Normalizing the environment recapitulates adult human immune traits in laboratory mice. *Nature*. (2016) 532:512–6. doi: 10.1038/nature17655
24. Huggins MA, Sjaastad FV, Pierson M, Kucaba TA, Swanson W, Staley C, et al. Microbial exposure enhances immunity to pathogens recognized by TLR2 but increases susceptibility to cytokine storm through TLR4 sensitization. *Cell Rep.* (2019) 28:1729–43.e5. doi: 10.1016/j.celrep.2019.07.028
25. Rittirsch D, Huber-Lang MS, Flierl MA, Ward PA. Immunodesign of experimental sepsis by cecal ligation and puncture. *Nat Protoc.* (2009) 4:31–6. doi: 10.1038/nprot.2008.214
26. Duong S, Condotta SA, Rai D, Martin MD, Griffith TS, Badovinac VP. Polymicrobial sepsis alters antigen-dependent and -independent memory CD8 T cell functions. *J Immunol.* (2014) 192:3618–25. doi: 10.4049/jimmunol.1303460
27. Cabrera-Perez J, Babcock JC, Dileepan T, Murphy KA, Kucaba TA, Badovinac VP, et al. Gut microbial membership modulates CD4 T cell reconstitution and function after sepsis. *J Immunol.* (2016) 197:1692–8. doi: 10.4049/jimmunol.1600940

28. Goldberg MF, Roeske EK, Ward LN, Pengo T, Dileepan T, Kotov DI, et al. Salmonella persist in activated macrophages in T cell-sparse granulomas but are contained by surrounding CXCR3 ligand-positioned Th1 cells. *Immunity*. (2018) 49:1090–102.e7. doi: 10.1016/j.immuni.2018.10.009
29. Moon JJ, Chu HH, Pepper M, Mcsorley SJ, Jameson SC, Kedl RM, et al. Naive CD4(+) T cell frequency varies for different epitopes and predicts repertoire diversity and response magnitude. *Immunity*. (2007) 27:203–13. doi: 10.1016/j.immuni.2007.07.007
30. Moon JJ, Chu HH, Hataye J, Pagan AJ, Pepper M, Mclachlan JB, et al. Tracking epitope-specific T cells. *Nat Protoc*. (2009) 4:565–81. doi: 10.1038/nprot.2009.9
31. Pepper M, Pagan AJ, Igyarto BZ, Taylor JJ, Jenkins MK. Opposing signals from the Bcl6 transcription factor and the interleukin-2 receptor generate T helper 1 central and effector memory cells. *Immunity*. (2011) 35:583–95. doi: 10.1016/j.immuni.2011.09.009
32. Pagan AJ, Pepper M, Chu HH, Green JM, Jenkins MK. CD28 promotes CD4+ T cell clonal expansion during infection independently of its YMNM and PYAP motifs. *J Immunol.* (2012) 189:2909–17. doi: 10.4049/jimmunol.1103231
33. Nelson RW, Mclachlan JB, Kurtz JR, Jenkins MK. CD4+ T cell persistence and function after infection are maintained by low-level peptide:MHC class II presentation. *J Immunol.* (2013) 190:2828–34. doi: 10.4049/jimmunol.1202183
34. Cabrera-Perez J, Condotta SA, James BR, Kashem SW, Brincks EL, Rai D, et al. Alterations in antigen-specific naive CD4 T cell precursors after sepsis impairs their responsiveness to pathogen challenge. *J Immunol.* (2015) 194:1609–20. doi: 10.4049/jimmunol.1401711
35. Meakins JL, Pietsch JB, Bubenick O, Kelly R, Rode H, Gordon J, et al. Delayed hypersensitivity: indicator of acquired failure of host defenses in sepsis and trauma. *Ann Surg.* (1977) 186:241–50. doi: 10.1097/00000658-197709000-00002
36. Brown R, Bancewicz J, Hamid J, Patel NJ, Ward CA, Farrand RJ, et al. Failure of delayed hypersensitivity skin testing to predict postoperative sepsis and mortality. *Br Med J.* (1982) 284:851–3. doi: 10.1136/bmj.284.6319.851
37. Meakins JL, Christou NV, Bohnen J, Maclean LD. Failure of delayed hypersensitivity skin testing to predict postoperative sepsis and mortality. *Br Med J.* (1982) 285:1207–8. doi: 10.1136/bmj.285.6349.1207-a
38. Vissinga C, Nagelkerken L, Zijlstra J, Hertogh-Huijbregts A, Boersma W, Rozing J. A decreased functional capacity of CD4+ T cells underlies the impaired DTH reactivity in old mice. *Mech Ageing Dev.* (1990) 53:127–39. doi: 10.1016/0047-6374(90)90065-N
39. Gurung P, Rai D, Condotta SA, Babcock JC, Badovinac VP, Griffith TS. Immune unresponsiveness to secondary heterologous bacterial infection after sepsis induction is TRAIL dependent. *J Immunol.* (2011) 187:2148–54. doi: 10.4049/jimmunol.1101180
40. Condotta SA, Rai D, James BR, Griffith TS, Badovinac VP. Sustained and incomplete recovery of naive CD8+ T cell precursors after sepsis contributes to impaired CD8+ T cell responses to infection. *J Immunol.* (2013) 190:1991–2000. doi: 10.4049/jimmunol.1202379
41. Condotta SA, Khan SH, Rai D, Griffith TS, Badovinac VP. Polymicrobial sepsis increases susceptibility to chronic viral infection and exacerbates CD8+ T cell exhaustion. *J Immunol.* (2015) 195:116–25. doi: 10.4049/jimmunol.1402473
42. Sjaastad FV, Condotta SA, Kotov JA, Pape KA, Dail C, Danahy DB, et al. Polymicrobial sepsis chronic immunoparalysis is defined by diminished Ag-specific T cell-dependent B cell responses. *Front Immunol.* (2018) 9:2532. doi: 10.3389/fimmu.2018.02532
43. Mcdermott DS, Varga SM. Quantifying antigen-specific CD4 T cells during a viral infection: CD4 T cell responses are larger than we think. *J Immunol.* (2011) 187:5568–76. doi: 10.4049/jimmunol.1102104
44. Kotov DI, Kotov JA, Goldberg MF, Jenkins MK. Many Th cell subsets have fas ligand-dependent cytotoxic potential. *J Immunol.* (2018) 200:2004–12. doi: 10.4049/jimmunol.1700420
45. Benoun JM, Peres NG, Wang N, Pham OH, Rudisill VL, Fogassy ZN, et al. Optimal protection against Salmonella infection requires noncirculating memory. *Proc Natl Acad Sci USA*. (2018) 115:10416–21. doi: 10.1073/pnas.1808339115
46. Hess J, Ladel C, Miko D, Kaufmann SH. Salmonella typhimurium aroA- infection in gene-targeted immunodeficient mice: major role of CD4+ TCR-alpha beta cells and IFN-gamma in bacterial clearance independent of intracellular location. *J Immunol.* (1996) 156:3321–6.
47. Monack DM, Mueller A, Falkow S. Persistent bacterial infections: the interface of the pathogen and the host immune system. *Nat Rev Microbiol.* (2004) 2:747–65. doi: 10.1038/nrmicro955
48. Johanns TM, Ertelt JM, Lai JC, Rowe JH, Avant RA, Way SS. Naturally occurring altered peptide ligands control Salmonella-specific CD4+ T cell proliferation, IFN-gamma production, and protective potency. *J Immunol.* (2010) 184:869–76. doi: 10.4049/jimmunol.0901804
49. Johanns TM, Ertelt JM, Rowe JH, Way SS. Regulatory T cell suppressive potency dictates the balance between bacterial proliferation and clearance during persistent Salmonella infection. *PLoS Pathog.* (2010) 6:e1001043. doi: 10.1371/journal.ppat.1001043
50. Marzo AL, Vezys V, Williams K, Tough DF, Lefrancois L. Tissue-level regulation of Th1 and Th2 primary and memory CD4 T cells in response to Listeria infection. *J Immunol.* (2002) 168:4504–10. doi: 10.4049/jimmunol.168.9.4504
51. Delano MJ, Thayer T, Gabrilovich S, Kelly-Scumpia KM, Winfield RD, Scumpia PO, et al. Sepsis induces early alterations in innate immunity that impact mortality to secondary infection. *J Immunol.* (2011) 186:195–202. doi: 10.4049/jimmunol.1002104
52. Condotta SA, Richer MJ, Badovinac VP, Harty JT. Probing CD8 T cell responses with *Listeria monocytogenes* infection. *Adv Immunol.* (2012) 113:51–80. doi: 10.1016/B978-0-12-394590-7.00005-1
53. Brocke S, Hahn H. Heat-killed *Listeria monocytogenes* and *L. monocytogenes* soluble antigen induce clonable CD4+ T lymphocytes with protective and chemotactic activities *in vivo*. *Infect. Immun.* (1991) 59:4531–9. doi: 10.1128/IAI.59.12.4531-4539.1991
54. Harty JT, Schreiber RD, Bevan MJ. CD8 T cells can protect against an intracellular bacterium in an interferon gamma-independent fashion. *Proc Natl Acad Sci USA*. (1992) 89:11612–6. doi: 10.1073/pnas.89.23.11612
55. Bhardwaj V, Kanagawa O, Swanson PE, Unanue ER. Chronic Listeria infection in SCID mice: requirements for the carrier state and the dual role of T cells in transferring protection or suppression. *J Immunol.* (1998) 160:376–84.
56. Vincent JL, Marshall JC, Namendys-Silva SA, Francois B, Martin-Loeches I, Lipman J, et al. Assessment of the worldwide burden of critical illness: the intensive care over nations (ICON) audit. *Lancet Respir Med.* (2014) 2:380–6. doi: 10.1016/S2213-2600(14)70061-X
57. Cohen J, Vincent JL, Adhikari NK, Machado FR, Angus DC, Calandra T, et al. Sepsis: a roadmap for future research. *Lancet Infect Dis.* (2015) 15:581–614. doi: 10.1016/S1473-3099(15)70112-X
58. Le Gros G, Ben-Sasson SZ, Seder R, Finkelman FD, Paul WE. Generation of interleukin 4 (IL-4)-producing cells *in vivo* and *in vitro*: IL-2 and IL-4 are required for in vitro generation of IL-4-producing cells. *J Exp Med.* (1990) 172:921–9. doi: 10.1084/jem.172.3.921
59. Hsieh CS, Heimberger AB, Gold JS, O'garra A, Murphy KM. Differential regulation of T helper phenotype development by interleukins 4 and 10 in an alpha beta T-cell-receptor transgenic system. *Proc Natl Acad Sci USA*. (1992) 89:6065–9. doi: 10.1073/pnas.89.13.6065
60. Chen X, Ye J, Ye J. Analysis of peripheral blood lymphocyte subsets and prognosis in patients with septic shock. *Microbiol Immunol.* (2011) 55:736–42. doi: 10.1111/j.1348-0421.2011.00373.x
61. Gouel-Cheron A, Venet F, Allaouchiche B, Monneret G. CD4+ T-lymphocyte alterations in trauma patients. *Crit Care*. (2012) 16:432. doi: 10.1186/cc11376
62. Inoue S, Suzuki-Utsunomiya K, Okada Y, Taira T, Iida Y, Miura N, et al. Reduction of immunocompetent T cells followed by prolonged lymphopenia in severe sepsis in the elderly. *Crit Care Med.* (2013) 41:810–9. doi: 10.1097/CCM.0b013e318274645f
63. Baker CC, Miller CL, Trunkey DD, Lim RC Jr. Identity of mononuclear cells which compromise the resistance of trauma patients. *J Surg Res.* (1979) 26:478–87. doi: 10.1016/0022-4804(79)90037-4
64. Hansbrough JF, Bender EM, Zapata-Sirvent R, Anderson J. Altered helper and suppressor lymphocyte populations in surgical patients. A measure of postoperative immunosuppression. *Am J Surg.* (1984) 148:303–7. doi: 10.1016/0002-9610(84)90459-8

65. Uzzaman A, Cho SH. Chapter 28: Classification of hypersensitivity reactions. *Allergy Asthma Proc.* (2012) 33(Suppl. 1):S96–99. doi: 10.2500/aap.2012.33.3561
66. Hamilton SE, Badovinac VP, Beura LK, Pierson M, Jameson SC, Masopust D, et al. New insights into the immune system using dirty mice. *J Immunol.* (2020) 205:3–11. doi: 10.4049/jimmunol.2000171
67. Grayson JM, Harrington LE, Lanier JG, Wherry EJ, Ahmed R. Differential sensitivity of naive and memory CD8+ T cells to apoptosis *in vivo*. *J Immunol.* (2002) 169:3760–70. doi: 10.4049/jimmunol.169.7.3760
68. Hotchkiss RS, Osmon SB, Chang KC, Wagner TH, Coopersmith CM, Karl IE. Accelerated lymphocyte death in sepsis occurs by both the death receptor and mitochondrial pathways. *J Immunol.* (2005) 174:5110–8. doi: 10.4049/jimmunol.174.8.5110
69. Unsinger J, Mcglynn M, Kasten KR, Hoekzema AS, Watanabe E, Muenzer JT, et al. IL-7 promotes T cell viability, trafficking, and functionality and improves survival in sepsis. *J Immunol.* (2010) 184:3768–79. doi: 10.4049/jimmunol.0903151
70. Serbanescu MA, Ramonell KM, Hadley A, Margoles LM, Mittal R, Lyons JD, et al. Attrition of memory CD8 T cells during sepsis requires LFA-1. *J Leukoc Biol.* (2016) 100:1167–80. doi: 10.1189/jlb.4A1215-563RR
71. Danahy DB, Anthony SM, Jensen IJ, Hartwig SM, Shan Q, Xue HH, et al. Polymicrobial sepsis impairs bystander recruitment of effector cells to infected skin despite optimal sensing and alarming function of skin resident memory CD8 T cells. *PLoS Pathog.* (2017) 13:e1006569. doi: 10.1371/journal.ppat.1006569
72. Danahy DB, Strother RK, Badovinac VP, Griffith TS. Clinical and experimental sepsis impairs CD8 T-cell-mediated immunity. *Crit Rev Immunol.* (2016) 36:57–74. doi: 10.1615/CritRevImmunol.2016017098
73. Xie J, Chen CW, Sun Y, Laurie SJ, Zhang W, Otani S, et al. Increased attrition of memory T cells during sepsis requires 2B4. *JCI Insight*. (2019) 4:e126030. doi: 10.1172/jci.insight.126030
74. Hotchkiss RS, Swanson PE, Knudson CM, Chang KC, Cobb JP, Osborne DF, et al. Overexpression of Bcl-2 in transgenic mice decreases apoptosis and improves survival in sepsis. *J Immunol.* (1999) 162:4148–56. doi: 10.1097/00024382-199806001-00219
75. Hotchkiss RS, Chang KC, Swanson PE, Tinsley KW, Hui JJ, Klender P, et al. Caspase inhibitors improve survival in sepsis: a critical role of the lymphocyte. *Nat Immunol.* (2000) 1:496–501. doi: 10.1038/82741
76. Inoue S, Unsinger J, Davis CG, Muenzer JT, Ferguson TA, Chang K, et al. IL-15 prevents apoptosis, reverses innate and adaptive immune dysfunction, and improves survival in sepsis. *J Immunol.* (2010) 184:1401–9. doi: 10.4049/jimmunol.0902307
77. Unsinger J, Kazama H, Mcdonough JS, Griffith TS, Hotchkiss RS, Ferguson TA. Sepsis-induced apoptosis leads to active suppression of delayed-type hypersensitivity by CD8+ regulatory T cells through a TRAIL-dependent mechanism. *J Immunol.* (2010) 184:6766–72. doi: 10.4049/jimmunol.0904054
78. Cavassani KA, Carson WFT, Moreira AP, Wen H, Schaller MA, Ishii M, et al. The post sepsis-induced expansion and enhanced function of regulatory T cells create an environment to potentiate tumor growth. *Blood*. (2010) 115:4403–11. doi: 10.1182/blood-2009-09-241083
79. Stieglitz D, Schmid T, Chhabra NF, Echtenacher B, Mannel DN, Mostbock S. TNF and regulatory T cells are critical for sepsis-induced suppression of T cells. *Immun Inflamm Dis.* (2015) 3:374–85. doi: 10.1002/iid3.75
80. Rimmele T, Payen D, Cantaluppi V, Marshall J, Gomez H, Gomez A, et al. Immune cell phenotype and function in sepsis. *Shock*. (2016) 45:282–91. doi: 10.1097/SHK.0000000000000495
81. Hall MW, Knatz NL, Vetterly C, Tomarello S, Wewers MD, Volk HD, et al. Immunoparalysis and nosocomial infection in children with multiple organ dysfunction syndrome. *Intensive Care Med.* (2011) 37:525–32. doi: 10.1007/s00134-010-2088-x
82. Otto GP, Sossdorf M, Claus RA, Rodel J, Menge K, Reinhart K, et al. The late phase of sepsis is characterized by an increased microbiological burden and death rate. *Crit Care*. (2011) 15:R183. doi: 10.1186/cc10332
83. Goldenberg NM, Leligdowicz A, Slutsky AS, Friedrich JO, Lee WL. Is nosocomial infection really the major cause of death in sepsis? *Crit Care*. (2014) 18:540. doi: 10.1186/s13054-014-0540-y
84. Daviaud F, Grimaldi D, Dechartres A, Charpentier J, Geri G, Marin N, et al. Timing and causes of death in septic shock. *Ann Intensive Care*. (2015) 5:16. doi: 10.1186/s13613-015-0058-8
85. Zhao GJ, Li D, Zhao Q, Song JX, Chen XR, Hong GL, et al. Incidence, risk factors and impact on outcomes of secondary infection in patients with septic shock: an 8-year retrospective study. *Sci Rep*. (2016) 6:38361. doi: 10.1038/srep38361
86. Strother RK, Danahy DB, Kotov DI, Kucaba TA, Zacharias ZR, Griffith TS, et al. Polymicrobial sepsis diminishes dendritic cell numbers and function directly contributing to impaired primary CD8 T cell responses *in vivo*. *J Immunol.* (2016) 197:4301–11. doi: 10.4049/jimmunol.1601463
87. Robertson CM, Perrone EE, Mcconnell KW, Dunne WM, Boody B, Brahmbhatt T, et al. Neutrophil depletion causes a fatal defect in murine pulmonary *Staphylococcus aureus* clearance. *J Surg Res.* (2008) 150:278–85. doi: 10.1016/j.jss.2008.02.009

Conflict of Interest: The authors declare that the research was conducted in the absence of any commercial or financial relationships that could be construed as a potential conflict of interest.

Advantages of publishing in Frontiers

OPEN ACCESS
Articles are free to read for greatest visibility and readership

FAST PUBLICATION
Around 90 days from submission to decision

HIGH QUALITY PEER-REVIEW
Rigorous, collaborative, and constructive peer-review

TRANSPARENT PEER-REVIEW
Editors and reviewers acknowledged by name on published articles

Frontiers
Avenue du Tribunal-Fédéral 34
1005 Lausanne | Switzerland

Visit us: www.frontiersin.org
Contact us: frontiersin.org/about/contact

REPRODUCIBILITY OF RESEARCH
Support open data and methods to enhance research reproducibility

DIGITAL PUBLISHING
Articles designed for optimal readership across devices

FOLLOW US
@frontiersin

IMPACT METRICS
Advanced article metrics track visibility across digital media

EXTENSIVE PROMOTION
Marketing and promotion of impactful research

LOOP RESEARCH NETWORK
Our network increases your article's readership